Modern Approaches in Solid Earth Sciences

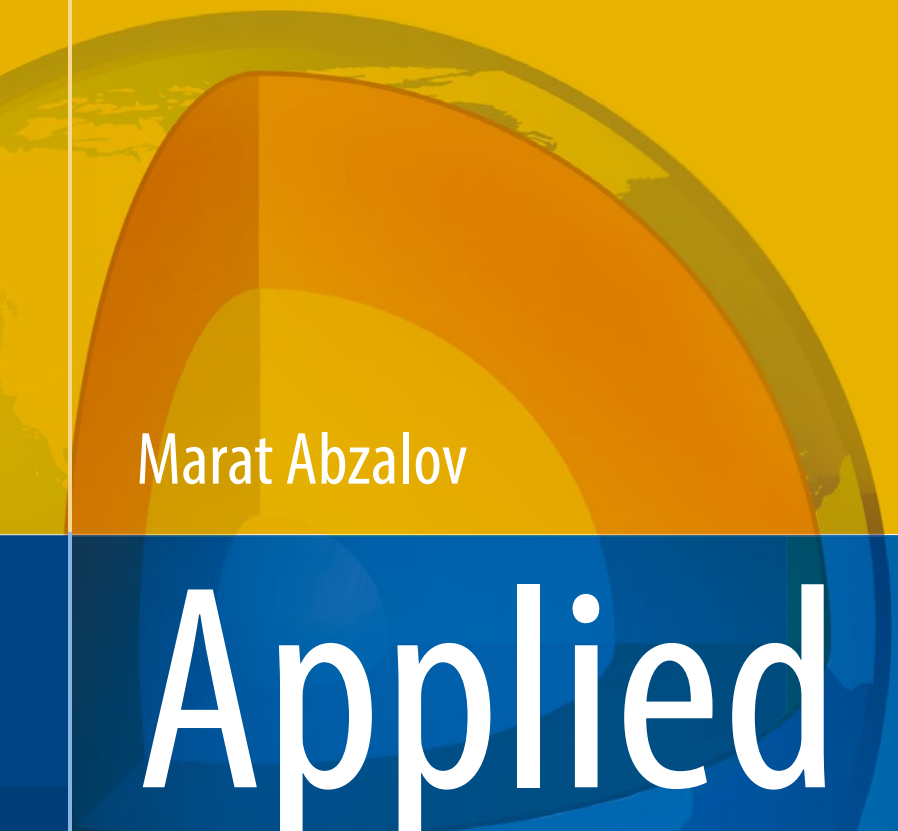

Marat Abzalov

Applied Mining Geology

EXTRAS ONLINE

Springer

Modern Approaches in Solid Earth Sciences

Volume 12

More information about this series at http://www.springer.com/series/7377

Marat Abzalov

Applied Mining Geology

Springer

Marat Abzalov
MASSA geoservices
Mount Claremont
WA, Australia

Centre for Exploration Targeting (CET)
University of Western Australia
Crawley, WA, Australia

Responsible Series Editor: F. Pirajno

Additional material to this book can be downloaded from http://extras.springer.com.

ISSN 1876-1682 ISSN 1876-1690 (electronic)
Modern Approaches in Solid Earth Sciences
ISBN 978-3-319-39263-9 ISBN 978-3-319-39264-6 (eBook)
DOI 10.1007/978-3-319-39264-6

Library of Congress Control Number: 2016943190

Printed on acid-free paper

This Springer imprint is published by Springer Nature
The registered company is Springer International Publishing AG Switzerland

To my family,
Svetlana, Aygul and Shamil,
for their help, patience and love

About the Author

Dr Abzalov is a geologist with 35 years of experience. He obtained a PhD in geology studying nickel deposits in Russia and Fennoscandia and undertook additional postgraduate studies in applied mathematics at Murdoch University, Australia, and geostatistics in Fontainebleau, France. In his long and diverse geological career, he has fulfilled different roles in research, exploration and mining geology, including senior management positions at WMC Resources, Rio Tinto and BOSS Resources.

With diverse commodity and geographic experience, with the projects encompassing five continents and different deposit types shown on the map, Dr Abzalov has demonstrated skills in greenfields, brownfields and mathematical geological modelling. Using an innovative approach of geostatistically assisted 3D structural modelling, he has led WMC Resources to the successful resource growth at Olympic Dam and Cliffs deposits. He was also instrumental in the discovery of the uranium resources in Jordan.

Dr Abzalov is an adjunct geoscientist at the Centre for Exploration Targeting, the University of Western Australia, and is successfully sharing his practical work in the mining industry with academic research. In 2015, he was awarded the Dani Krige's Gold Medal by SAIMM for his novel geostatistical method LUC (localised uniform conditioning).

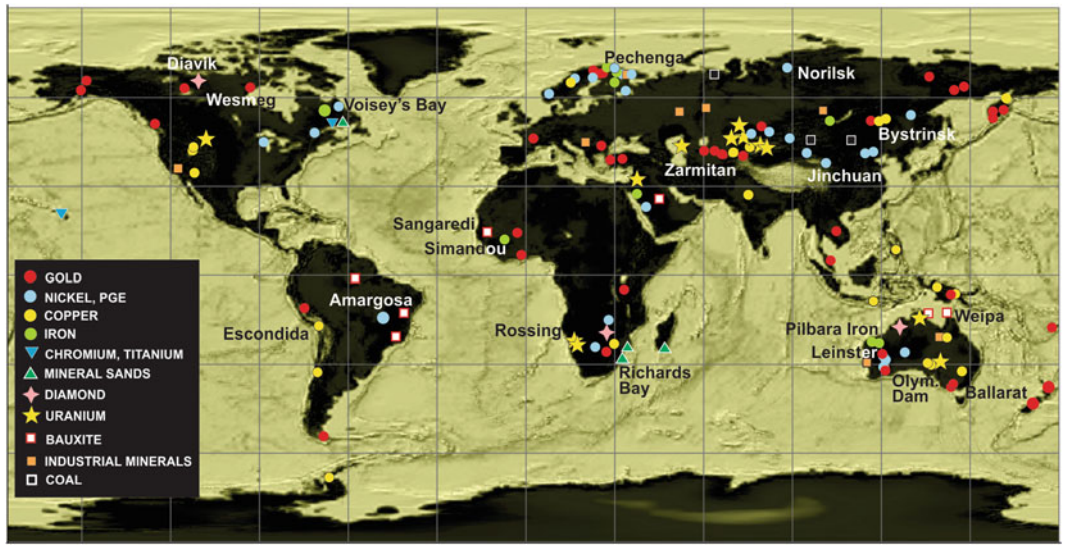

World map showing location of the geological projects studied by Dr M. Abzalov

Acknowledgements

I express my sincere gratitude to the copyright holders of the originals of many figures and tables reproduced in this book for the permission to use them. In particular, I would like to acknowledge the following organisations:

The Australasian Institute of Mining and Metallurgy (AusIMM) for permission to reprint in the book the figures and tables earlier published by the book's author in the *AusIMM Monograph 23* (2014) and the proceedings of the AusIMM conferences, including 'Ore body knowledge and strategic mine planning' (2004) and 'Heavy minerals conference' (2011).

The *Applied Earth Science (AES)* journal and the publisher Taylor and Francis (www.tandfonline.com) for permission to reprint in the book, a material earlier published by the book's author in the journal's several issues, particularly *AES* (2014) 123/2, *AES* (2013) 122/1 and *AES* (2010) 119/3.

The Canadian Institute of Mining, Metallurgy and Petroleum (CIM) for permission to reprint some materials published by the book's author in the issues of *Exploration and Mining Geology* journal (2009) 18/1–4 and (2008) 17/3–4.

The *Mathematical Geology* (*MG*) journal and the publisher Springer for permission to reproduce the description of the LUC technique and reprint the diagrams, published by the book's author in *MG* (2006) 38/4.

The Society for Mining Metallurgy and Exploration (SME) for permission to reprint the diagrams published in the monograph *Underground Mining Methods: Engineering Fundamentals and International Case Studies*.

The book has benefited from numerous discussions with my friends and colleagues in the mining industry, including geologists and mining engineers of WMC Resources, Rio Tinto, BOSS Resources, BHP Billiton, Newcrest, Harmony, Vale, Jordanian Uranium Mining Company and Anglo Gold Ashanti and also geoscientists from the different universities and research institutes.

I am also grateful to R. Minnitt, R. Reid, S. Masters and anonymous reviewers of Springer for their critical reading of the manuscript and many useful comments. I am in particular indebted to my family, Svetlana, Aygul and Shamil, for their enormous support through all my career.

Contents

Introduction 1

Mining geology is a specialised area of applied geological sciences that historically evolved as a support for operating mines and for evaluating mining projects. The main objective of mining geology is to provide detailed geological information, and undertake technical and economic studies to evaluate a mining project. When mining commences, mine geologists provide geological support to the operation, ensuring cost effective extraction of the valuable minerals and their accurate separation from the waste rocks. In addition to detailed understanding of the geology of the mining project area, they also provide accurate estimation of the spatial distribution of the economically valuable minerals and quantitative estimation of the geological characteristics that control mining and processing methods and operational costs.

Thus, modern mining geology represents an interface between different disciplines, including structural geology, petrography, stratigraphy, geochemistry, mining geophysics, sampling theory, mathematical statistics, geostatistics, mining engineering, rock mechanics, mineral economics and computer sciences. Because of the multifaceted nature of mining geology, and the variety of the scientific disciplines involved in the daily routines of mine geologists, the theoretical foundations and principles of mining geology have been adopted from the related disciplines and adjusted to the needs of mining geology.

The specific nature of the mining geology, which supports technical and economic valuation of the mining projects and ensures their sustainable expoitation based on optimal mine production plans, has dictated the needs for special techniques. These include accurate 3D geological modelling of the mineral deposits as well as quantitative determination of the geological characteristics, which are used as a basis for technical and economic assessment of the mining operations and optimisation of mine production.

The practical importance of mining geology and it's specific subject have dictated the needs for a specialised handbook, which would contain comprehensive overviews of mining geology techniques, and at the same time explain their underlying theoretical concepts. Rapid and intensive advances in software and computer technology means that the comprehensive description of mining geology produced by Peters (1987), almost 30 years ago does not fully represent the modern discipline of mining geology. More recently published textbooks for appraisal of mineral deposits (Annels 1991; Sinclair and Blackwell 2002) are mainly focused on resources and reserves estimation and do not cover many of the other important aspects of mine geology.

The current book is intended to fill the existing gap, and overviews the operational principles of modern mining geology. The ultimate goal of this book is to be a practical manual for geologists

M. Abzalov, *Applied Mining Geology*, Modern Approaches in Solid Earth Sciences 12,
DOI 10.1007/978-3-319-39264-6_1

working at the mines or studying and developing mining projects therefore book contains description of the various techniques and practical recommendations of effectively using them. The description is supported by exercises and computer scripts, developed by the author to assist in the application of the proposed methods. To facilitate the application of the computer scripts, they are presented either as Visual Basic macrocodes built into Excel spreadsheets or, as Fortran codes.

The book discusses mining project evaluation procedures with a focus on the deposit geology and estimation of resources, which are the prime responsibility of the mine geology teams. The book includes descriptions of several commodities, namely gold, iron ore, uranium, bauxites and mineral sands based on the authors personal observations summarised here together with published best-practice case studies. The mine and project geologists can reference the practical approaches and techniques presented in this book when developing projects or optimising mine geology procedures. The book also includes a brief review of the main mining and metallurgical (modifying) factors applied for the conversion of resources to reserves.

References

Annels AE (1991) Mineral deposit evaluation, a practical approach. Chapman and Hall, London, p 436

Peters WC (1987) Exploration and mining geology, 2nd edn. Wiley, New York, p 706

Sinclair AJ, Blackwell GH (2002) Applied mineral inventory estimation. Cambridge University Press, Cambridge, p 381

Part I

Mine Design, Mine Mapping and Sampling

Mining Methods

2

Abstract

A brief description of the most common mining methods is provided in this chapter together with the main terms used by mine personnel, illustrating them with photos and diagrams. Description is limited to an introductory level and uses a basic lexicon which will be understandable for the junior mine geologists. Aspects of mining methods selection in both, open pit and underground mining operations, depend on key environmental and economic factors including:

- Geological characteristics of the ore body, including the geotechnical competency of host rocks and the spatial distribution of ore and waste
- Depth of the ore body and thickness of the cover material
- Production rates and mine life
- Available technologies and comparative costs

In addition, 'unconventional' mining methods, including *in-situ* leach (ISL) and dredging of unconsolidated sediments, are briefly introduced.

Keywords

Mining • Open pit • Underground • ISL • Mining technology

Mine geologists, mining engineers and other mining personnel regularly communicate with each other in regard to mine planning, production and ore grade control. This specialised working environment dictates that all personnel, including the mine geologists, clearly understand and are fluent with respect to mining terminology, mining technologies and mining equipment.

A brief description of common mining methods and terms used by mining personnel are introduced in this chapter and are illustrated with photos and diagrams. The description is limited to a level representing recommended basic lexicon for mine geologists. More detailed explanations of commonly used mining methods can be found in Hamrin (1982, 2001); Brady and Brown (2004).

Mining method selection is a dependent on several key environmental and economic factors such as:

M. Abzalov, *Applied Mining Geology*, Modern Approaches in Solid Earth Sciences 12,
DOI 10.1007/978-3-319-39264-6_2

- Geological characteristics of the ore body, including spatial distribution of ore and waste rocks and their geotechnical competency
- Depth of the ore body and cover material
- Production rates and mine life
- Technology availability and comparative costs

Mining methods are traditionally grouped into open pit and underground mining. This subdivision will be followed in this chapter. In addition, a brief introduction is made to 'unconventional' mining methods, including *in-situ* leach (ISL) and dredging of unconsolidated sediments.

2.1 Open Pit Mines

Open pit mining is a process of fully opening an ore body and excavating it from the topographic surface (Fig. 2.1). The open pit is mined using steps, called benches (Fig. 2.1a). A bench is a horizontal slice of an open pit which is mined as a unit. Bench heights typically vary from 2 to 30 m (Table 2.1), with smaller benches generally reserved for selective mining and larger benches for bulk mining. The bench can be further subdivided into flitches if more selective mining is needed.

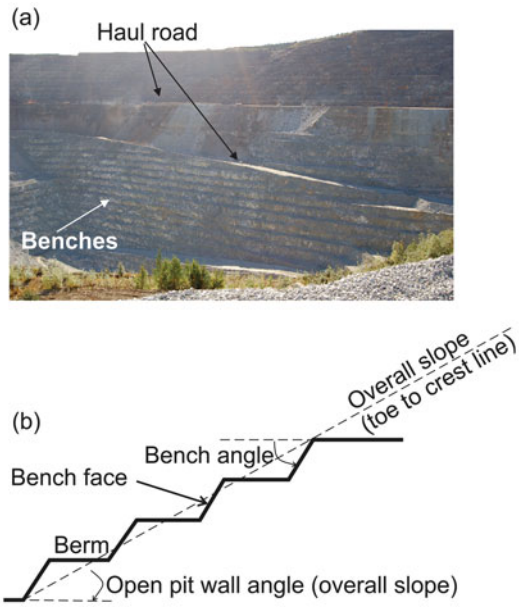

Fig. 2.1 Layout of the open pit: (**a**) general view of the open pit at the Fort Knox gold mine, Alaska; (**b**) cross-section through the pit wall

The excavating process in open pit mines result in cone-shaped volume in which the bench area becomes progressively smaller as the pit deepens with the walls formed by cascading benches (Fig. 2.1a). The flat surface of the bench remaining on the pit wall is called the berm (Fig. 2.1b). The berms create safe zones in case of rocks spalling away from the walls and also used for developing the haul roads (ramp) which are needed for accessing the bottom of the pit (Fig. 2.1a).

The slope of the pit wall is described by the two angles: the overall pit wall angle and the angle of the individual bench faces or batters (Fig. 2.1b). Both angles are important characteristics of open pits and together with the berm width and the bench height they control the safety and economics of the open pit mining. They largely depend on geotechnical characteristics of the rocks and equipment selection. The more geotechnically competent the wall rocks the steeper the pit slope can be.

The depth of the modern open pits varies from several tens of metres to more than a kilometre (Table 2.1). Pit depth depends on the geometry of the ore body and the overall economics of the project for which the overall pit wall angle remains one of the most important controlling factors.

Another common term in open pit mining is a parameter called 'stripping ratio'. It is estimated as a ratio of the tonnes of waste in the pit to the tonnes of ore (2.1.1). A disadvantage of this parameter is that it does not take into account the value of a metal or mineral mined therefore another parameter (2.1.2) can be used to account for this limitation of the conventional stripping ratio.

$$\text{Stripping ratio} = \text{Tonnes of waste} \,/\, \text{Tonnes of ore} \quad (2.1.1)$$

$$\text{Stripping index} = \text{Stripping ratio} \,/\, \text{Average ore grade} \quad (2.1.2)$$

Table 2.1 Characteristics of the selected open pits (Compiled by M. Abzalov using information collected at the visited mines)

Mine	Country	Deposit type	Depth	Bench height	Strip ratio[a]
Bingham Canyon	USA	Copper-porphyry stockwork	1200 m (in 2008)	15 m, in places 30 m	
Escondida	Chile	Copper-porphyry stockwork		15 m	
Argyle	Australia	Diamond-bearing lamproite pipe		15 m	2.6 : 1
Yandi	Australia	Pisolitic iron-ore	70 m (final pit)	10 m	1 : 3
Rossing	Namibia	Uranium, alaskite hosted	300 m (interim pit)	15 m	2 : 1
Taparko	Burkina Faso	Orogenic gold		5 m	7 : 3
Bissa	Burkina Faso	Orogenic gold	240 m (final pit)	12 m (flitches 2 – 2.5 m)	3 : 2
Geita	Tanzania	Orogenic gold, BIF hosted		10 m	8 : 1
Tarkwa	Ghana	Gold-bearing conglomerates and sandstones		6 m (2 – 3 m flitches)	

[a]estimated using the final pit design

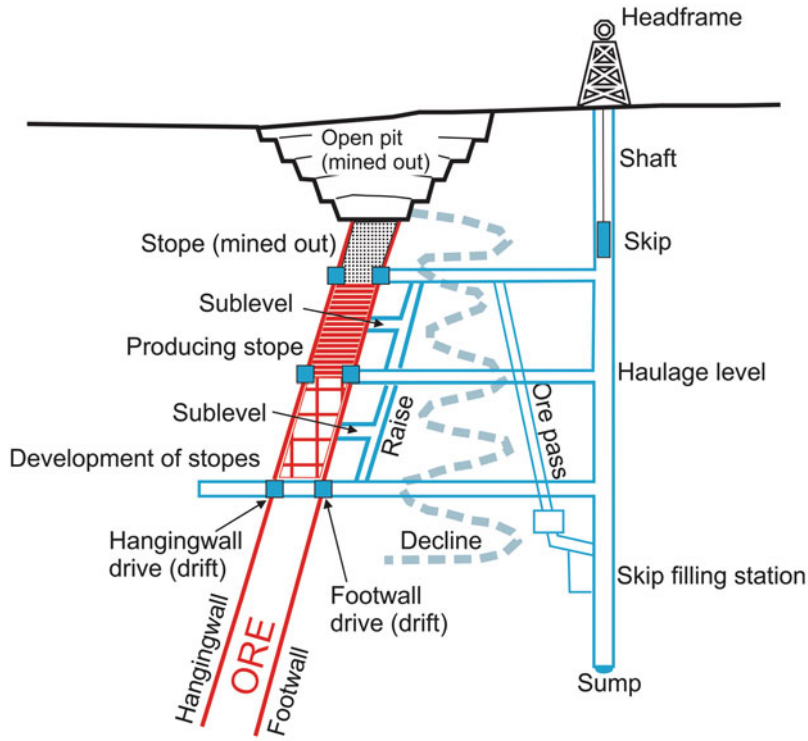

Fig. 2.2 General layout of an underground mine, generalised after Hamrin (1982, 2001)

2.2 Underground Mines

Underground mines are used for accessing and exploiting ore bodies that are generally not exposed on surface and due to technical or economic reasons cannot be mined by open pit methods. The infrastructure of underground mines is more complex than that of the open pits. A typical layout of an underground mine is shown on the Fig. 2.2.

A main feature of an underground mine is a shaft, which is a vertical or subvertical access to the underground workings or an inclined tunnel, called a decline. Both types of developments, shaft and decline, can be present in the same mine (Fig. 2.2). In the rugged terranes the concealed ore bodies can be accessed from the slope of the

hills using horizontal or gently declining tunnels, called an adit. The surface entrance to decline or adit is called a portal.

After accessing the ore body, underground workings are continued on successive horizontal planes, referred to as levels. Each level being a system of related underground workings located on the same horizontal plane. The underground workings include production stopes and mine development infrastructure for transportation of the broken ore to the surface for processing. Between the main development levels a mine can have sublevels, which are usually needed for more effective drill and blast control. Levels and sublevels are connected by inclined underground openings called ramps and also by the vertical opening, including raises and winzes. The main elements of the underground infrastructure are shown on the Fig. 2.2 and explained below.

- Drive or drift is a horizontal or nearly horizontal underground opening developed on the underground levels along the strike of ore body. The drives are subdivided into hangingwall (located at the upper ore-waste contact, 'hanging' above the ore body) and footwall (located at the lower ore-waste contact, at the 'foot' of the ore body) drives. A footwall drive is also commonly called an ore drive.
- A crosscut is a horizontal underground tunnel intersecting the ore body across its strike. The crosscuts are usually developed to connect the drives with the area in which stoping occurs.
- A raise is underground opening driven upward.
- A stope is an underground excavation made by removing ore from the host rocks. Development of stopes often starts from blasting a slot, which is a steeply dipping to vertical excavation at one boundary of the ore body. Mining then continues by blasting rings or slides of the orebody into the slot.
- A pillar is block of ore or barren rock left intact in the mined out stope or between two stopes to act as a mean of support. It required to provide structural integrity to the stoping process and prevent the stope walls from collapsing. Pillars may be removed after stopes are mined out, but some pillars may be left in place permanently.
- A draw point is a place from which the ore is extracted from the stope and loaded onto trucks or conveyors for further transportation.
- An ore pass is a steeply dipping underground opening for passing ore from one level to another under gravity. The ore is loaded through the chutes, which are the loading arrangements that utilise gravity. Important element of the ore loading and transportation system is a coarse steel grating, called a grizzly, for screening out oversize rock fragments.
- A winze is a small vertical excavation which can be developed in underground mines by driving it downward from one level to another, or it can be driven from a surface to a level.

The specific nature of an underground mining environment has led to the development of specialised machinery designed for effective operation in the tightly constrained spaces of the underground mines. This includes specialised machinery used for drilling of the blast holes in the underground development or production workings. A common variety are Jumbo drilling rigs, which may have one or two beams (Fig. 2.3a). For very selective mining, miners use hand held drilling equipment called air-legs (Fig. 2.3b).

Another standard underground machine is a load-haul-dump machine or simply LHD (Fig. 2.3c) used for loading the broken ore from the draw points of the stopes and tramming (hauling) it to the nearest ore pass or loading a truck. The crushed ore is transported to the surface (hoisted) either by the underground dump trucks through the decline or by the shaft's skips (Fig. 2.2).

One of the key responsibilities of the mine geologists is accurate mapping of all underground openings. This is mainly done by mapping the overhead surface of the underground excavation, called back of the drives and crosscuts. This is coupled with a systematic mapping of the drives faces.

The natural strength of the rocks is not always sufficient for safe excavation of the rock mass in the underground mines. In order to prevent a

Fig. 2.3 Examples of the underground machineries and equipment: (**a**) two beams Jumbo; (**b**) air leg; (**c**) LHD truck; (**d**) underground working supported by meshing and rock bolting (RB)

collapse of the rocks in the underground workings they must be strengthened and reinforced using the common roof support techniques of rock bolting and wire meshing (Fig. 2.3d).

In the case of extremely loose rocks the overhead surface and the side walls of the drives can be reinforced by the spraying a fluid cement or cement fibre mixing onto the rock surface. A method commonly referred to as shotcreting. A newly developed technique is to use thin spray-on liners which prevent the small fragments from dislodging and thereby holding the larger fragments in place.

Mining infrastructure significantly changes depending on the mining method. Mining techniques are commonly subdivided into selective and bulk mining methods. Selective methods generally extract lower tonnages but allow greater selectivity between ore and waste, which minimises dilution and mining loses and ensures the maximum ore recovery. Typically, selective mining used for extracting the narrow vein-type reefs. Bulk mining methods are fully mechanised allowing the excavation of large volumes of ore. These techniques enable high production rates in underground mines, but are less effective in separating ore and waste so are preferentially used in extracting massive ore bodies.

2.2.1 Underground Selective Mining Methods

Narrow steeply dipping veins are usually mined using cut-and-fill and shrinkage stoping methods, which allow highly selectively excavation of the ore while minimising dilution by the waste material.

2.2.1.1 Cut-and-Fill Method

The principles of cut-and-fill mining are shown in Fig. 2.4. The method is designed for selective mining of the steeply dipping veins, in particular for the narrow high-grade ore bodies.

The method removes the ore in horizontal slices, starting from the bottom undercut and

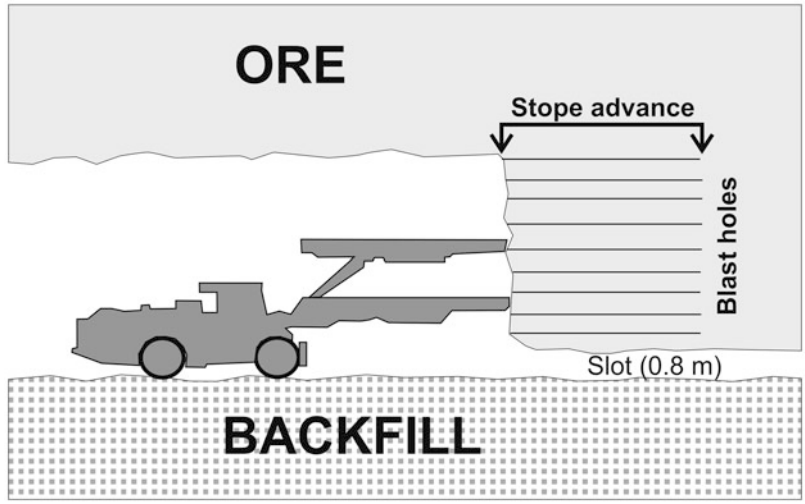

Fig. 2.4 Cut-and-fill mining procedure

advancing upward on a backfilled base (Fig. 2.4). Every slice is mined by drilling and blasting the face after which the broken ore (muck) is removed from the stope. The process is repeated until the entire slice (lift) is excavated along the strike of ore body. When the lift is mined out the resultant void is backfilled by waste rocks or, most commonly, by sand tailings or by sand-cement mixture. The backfill acts to support the stope walls and it also used as a working platform for equipment to mine the next slice (Fig. 2.4).

Drilling of the stope face can be done by either a Jumbo or an air-leg, depending on the thickness of the ore-body and the permissible external dilution.

2.2.1.2 Shrinkage Stoping

Shrinkage stoping is another highly selective mining method designed for mining narrow steeply dipping veins. Similarly to cut-and-fill method, shrinkage stoping starts from the bottom of the ore body and advances upward excavating the ore in horizontal slices (Fig. 2.5). However, the key difference is that the broken ore is not removed completely from the shrinkage stope. Approximately 60 % of the broken ore is left in the stope where it is used as a working platform for mining the next slice of the ore. The broken ore remaining in the stope, also serves as a support for the stope walls.

Shrinkage stoping is highly selective and cost effective mining method. However, its application is limited to the steeply dipping regular ore bodies in the very stable host rocks. Regular shape of the ore body is also important for effective use of this technique.

2.2.2 Underground Bulk Mining Methods

Where the ore body is large, massive and has regular shape, selective mining is not necessary nor desirable from a cost perspective. The ore body can be efficiently mined in large volumes and with higher productivity using larger underground equipment and the bulk mining methods. There are several methods for bulk underground mining, the most common being block caving, long hole open stoping, sublevel open stoping, sublevel caving and vertical-crater-retreat.

2.2.2.1 Block Caving

Block caving is a large-scale production technique applicable to homogeneous ore bodies of large dimensions and most commonly steep to vertical ore bodies. Block caving is regarded as one of the most productive and lowest cost underground mining methods and as such is often applied to low grade ore bodies.

The method uses gravity force in conjunction with internal rock stress which leads to fracturing of the rocks and eventually breaks them into small enough pieces which can be extracted

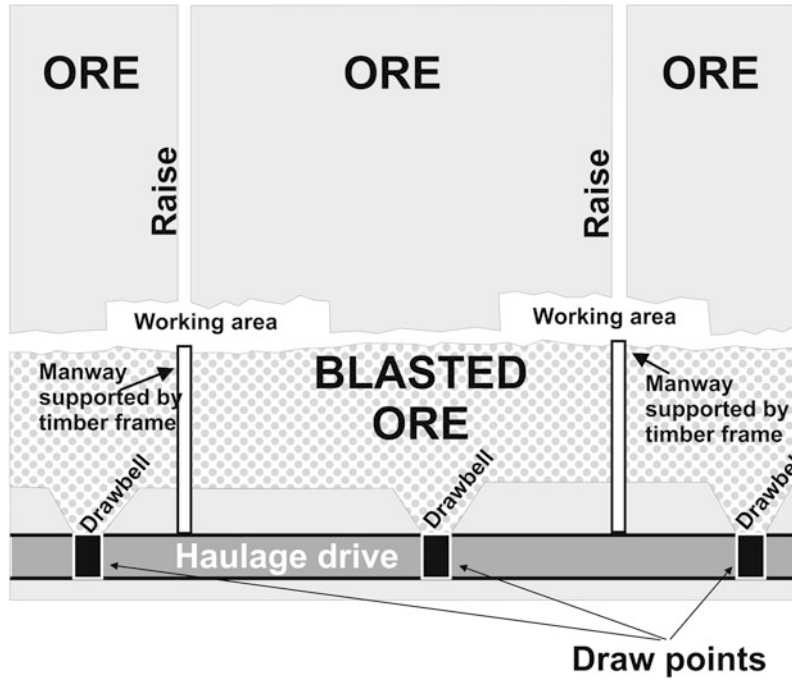

Fig. 2.5 Shrinkage stoping

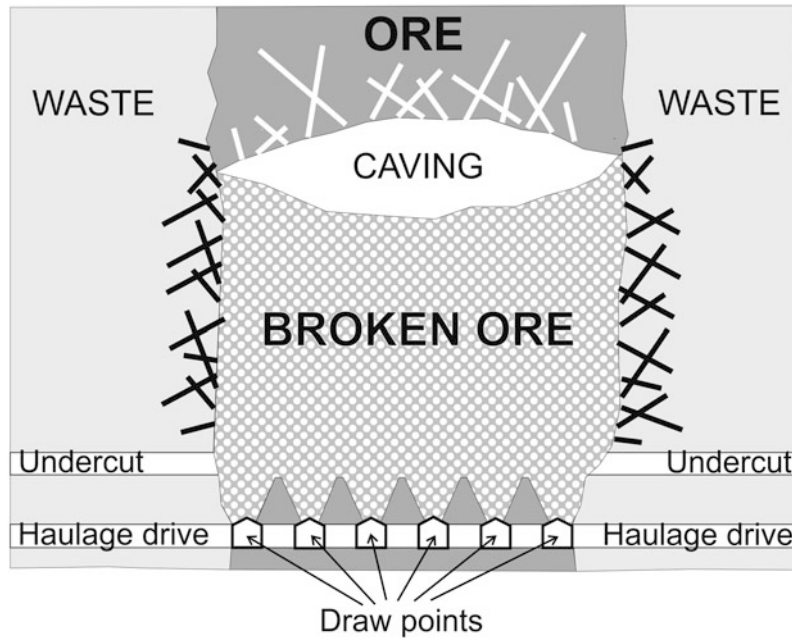

Fig. 2.6 Block caving, generalised after Hamrin (1982, 2001)

from draw points by LHD's (Fig. 2.6). The term 'block' refers to the entire volume of the ore which is prepared for excavation as a single block (Fig. 2.6).

Caving is induced by undercutting of a block. This is made by blasting the narrow ore slice located underneath of a block and removing of the blasted ore (Fig. 2.6). This creates a void beneath the block (undercut) and leaves the overlaying rock mass unsupported. As a consequence of removal this support the rocks fracturing, which was induced by the undercut blasting, starts spreading through the entire block due to the gravity force. The rock mass in a block

Table 2.2 Block cave mines

Mine	Country	Deposit type
El Teniente	Chile	Copper-porphyry stockwork
Andina	Chile	Copper-porphyry stockwork
Salvador	Chile	Copper-porphyry stockwork
Northparkes	Australia	Copper-porphyry stockwork
San Manuel	USA	Copper-porphyry stockwork
Tongkuangyu	China	Copper-porphyry stockwork
Freeport	Indonesia	Copper-porphyry stockwork
Henderson	USA	Molybdenum-porphyry stockwork
Palabora	South Africa	Copper-iron-gold carbonatite
Flinsch	South Africa	Diamond bearing kimberlite pipe
Premier	South Africa	Diamond bearing kimberlite pipe
Kimberley	South Africa	Diamond bearing kimberlite pipe

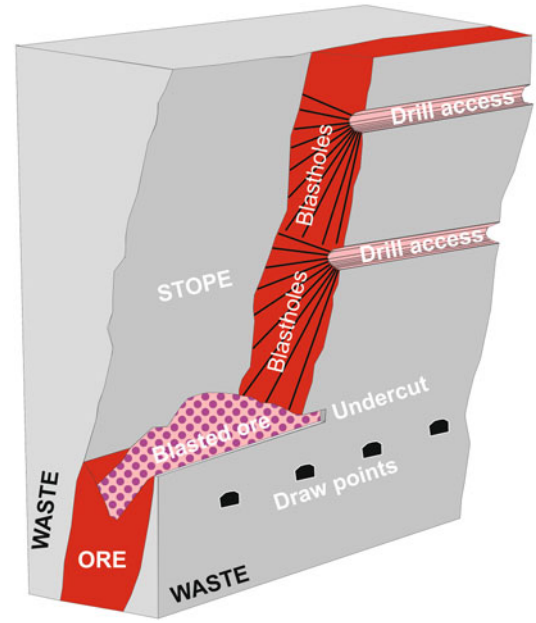

Fig. 2.7 Sublevel open stoping, generalised after Hamrin (1982, 2001)

breaks into small pieces which falls to the bottom of a stope (cave) where they are extracted through draw points (Fig. 2.6).

Application of the block caving technique is limited to the large ore bodies preferably of a shape of a vertical cylinder and characterised by a favourable hydrolic radius (Brady and Brown 2004). The success of the method hinges on the understanding of the fracturing process and capability of the broken ore to flow to the extraction points. In particular, it is essential that hanging-wall of a stope is allowed to subside. Another condition for the ore body to be amenable for block cave mining is the capability of the rock mass for breaking into small pieces by the rock stress and gravity. All three conditions are rarely met therefore the method is used only for certain type of deposits, most commonly these are copper and molybdenum porphyry deposits and diamond-bearing kimberlite pipes (Table 2.2). The block caving is also used for mining some large iron-ore deposits.

2.2.2.2 Sublevel Open Stoping

When block caving is not suitable for mining the ore body but its large size is still favourable for large scale production the methods like bighole open stoping and sublevel open stoping (SLOS) can be considered. Both methods subdivide the ore body into several large stopes. Each of the stopes are mined either using sublevels (sublevel open stoping) or as a single large void (bighole open stoping). The latter is merely a scaled-up variant of the sublevel open stoping and used when geometry of the ore body and the rock conditions allows to use the larger underground openings.

The basic principles of this group of the methods is explained using the sublevel open stoping (SLOS) as an example (Fig. 2.7). The SLOS stopes are distributed along the strike of ore body with the pillars left between the stopes to support the hanging wall. Pillars are normally shaped as vertical beams and distributed across the entire ore body. Horizontal sections of the ore, known as crown pillars, are also left to support the mine workings above the producing stope.

The stopes are developed using the sublevel drives which are prepared inside the ore body between the main levels (Fig. 2.7). The blast holes are drilled from the sublevel drives distributed as a tight fan pattern covering the whole stope. The ore is broken by firing the blast holes on the

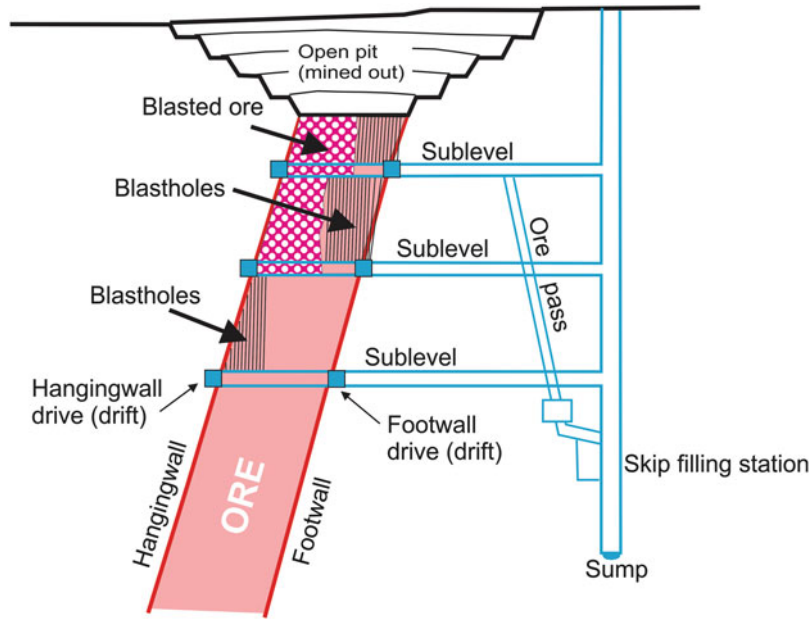

Fig. 2.8 Sublevel caving, generalised after Hamrin (1982, 2001)

same cross-sections, usually referred to a firing ring. The SLOS mining advances in a horizontal direction, usually along the strike of the ore body, by drilling of the next firing ring, charging the blast holes and blasting them (Fig. 2.7).

The broken ore is removed by LHD from the draw points distributed along the stope bottom (Fig. 2.7). The recovery of the ore from the stopes is facilitated by trough shaped bottom of the stope (Fig. 2.7). This technique creates large open voids, in particular in a vertical direction. In order to prevent their collapsing after the ore was recovered the stopes are normally backfilled.

The method is used for steep dipping ore bodies and require stable rocks in the hangingwall and footwall of the stope and also competent ore. Irregular shape of the ore body and uneven contacts are undesirable because this can lead to excessive dilution of the ore. The same comments is related to internal waste distributed inside of the ore body. The SLOS method doesn't allow to separate internal waste from the valuable material therefore everything inside the drilled pattern is recovered as an ore. Therefore, geologists reporting the ore reserves must make a correction for the internal and external dilution.

2.2.2.3 Sublevel Caving

Sublevel caving is another method available for mining of the large steeply dipping ore bodies (Fig. 2.8). This technique uses sublevels developed through the entire ore body at regular intervals. On each sublevel a system of the drives and crosscuts is developed following a geometrically systematic layout. The drives are developed along the footwall and hangingwall of the ore body and joined by series of the parallel and regularly distributed crosscuts (Fig. 2.8).

Production of the sublevel caves is made by drilling the long blastholes into the hangingwall from the sublevel crosscuts. The long blastholes are charged and blasted to generate a controlled caving when hangingwall fractures and collapses following the cave. Ground on the top of the ore body must be permitted to subside.

The ore body can be mined by retreating from the hangingwall to footwall, which is referred to as transverse sublevel caving (Fig. 2.8), or, conversely, retreating the stopes along the strike of ore body. The latter approach is used if the thickness of the ore body is not suitable for transverse sublevel caving technique.

The rock mass must be stable enough to allow the sublevel drives to remain open with a limited

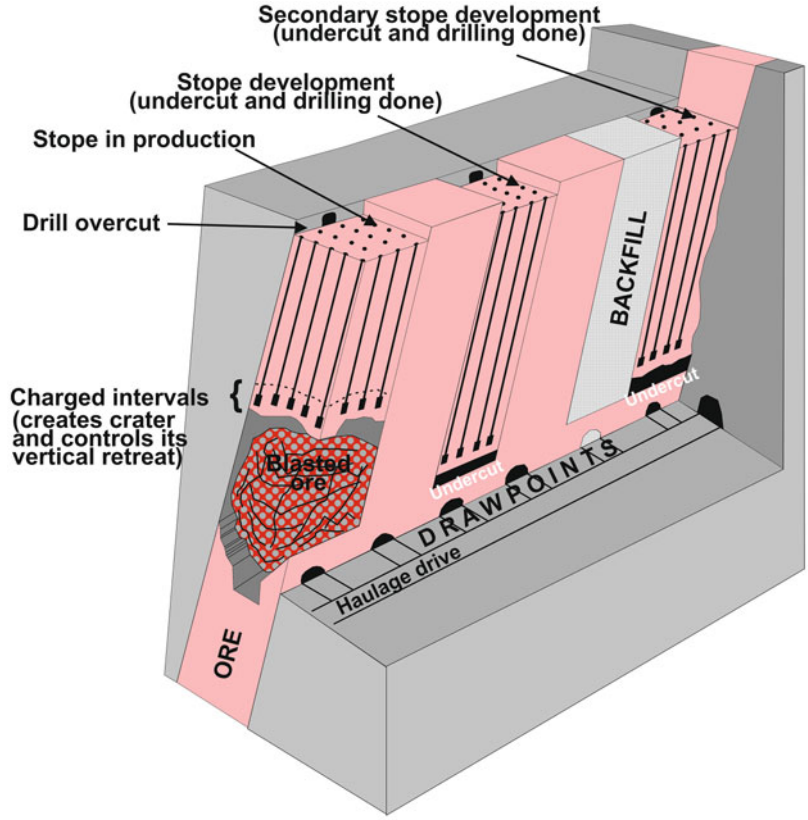

Fig. 2.9 *Vertical* crater retreat mining, generalised after Hamrin (1982, 2001)

support, usually a local rock bolting and meshing of the most unstable areas. It general, the method can be used instead of the SLOS technique if the rock mass competence is insufficient for open stoping.

2.2.2.4 Vertical Crater Retreat

Vertical crater retreat method (VCR) is used at the deposits that have competent steeply dipping ore hosted by the competent wall rocks (Fig. 2.9). The ground conditions in general is similar to that of the SLOS method, however the VCR is technically simpler and allows to achieve a large production rate commonly at lower production costs.

The method is based on the crater blasting which is made by firing the large diameter blast holes drilled downward from the overcut developed on the top of a stope (Fig. 2.9). The blast holes are charged by explosives which is placed into the short sections of the holes which is referred to as crater charge. The explosive is positioned in the each hole at the same distance above the open surface (Fig. 2.9). The blasting loosens the ore slice of ore creating a crater which is vertically retreated. Ore is continuously extracted from the draw points together with rigorous recording of the blasting progress in each hole.

2.2.3 Mining of the Gently Dipping Ore Bodies

The methods which were described above are designed for steeply dipping ore bodies. Mining of the horizontal and gently dipping ore bodies require different approach, which includes continues support for the large overhead surfaces exposed during mining of the flat stopes. The different methods are available for mining of the flat-bedded deposits. Two of them, room-and-pillar and longwall mining, are described in the section below.

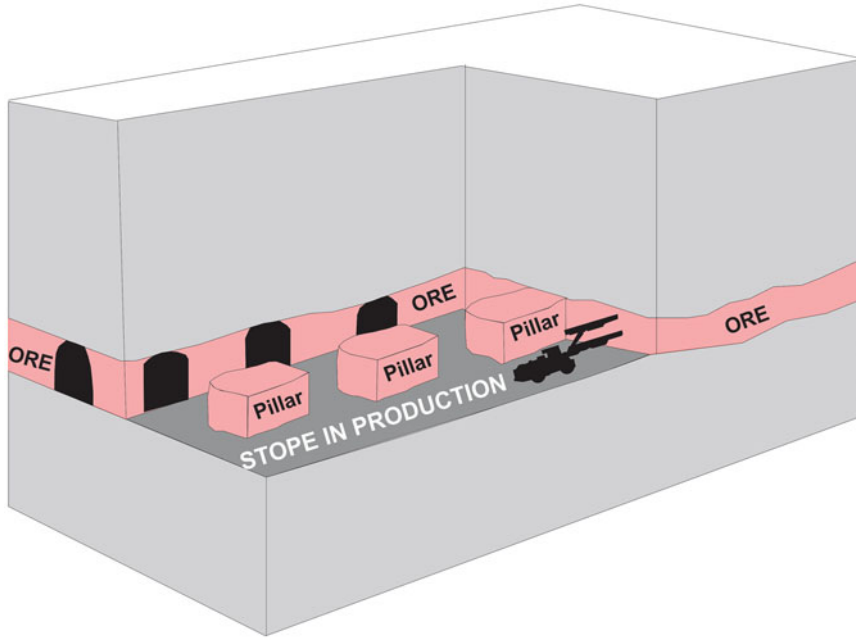

Fig. 2.10 Room-and-pillar methods, generalised after Hamrin (1982, 2001)

2.2.3.1 Room-and-pillar Method

The room-and-pillar method is used for mining flat bedded deposits using the flat open stopes. Hangingwall of such stopes extends for large areas and therefore have to be prevented from collapsing by leaving pillars, which support the hangingwall of the stopes (Fig. 2.10). In order to minimise the mining losses the pillars are usually left where low-grade material or internal waste present in the ore. In case if the ore grade material has been left in the pillars it is unrecoverable and therefore mine geologists have to exclude these volumes from the ore reserves. The flat ore body and large open areas allows to establish several production areas with an easy communication between different sites. These factors make the room-and-pillar method a highly efficient system for recovery ore from the flat beds.

2.2.3.2 Longwall Mining

Narrow gently dipping ore bodies of a uniform thickness can also be mined using longwall mining technique. The ore is extracted from a long straight front using system of the long flat stopes (Fig. 2.11a). The method was found in particular efficient for mining of the coal seams hosted in the soft sedimentary rocks. Excavation of such deposits does not require blasting and can be fully mechanised. The large length of the working faces allows to use conveyor belts for haulage of the ore. The method also allows the hangingwall to collapse at some distance behind the working face which decreases the mining costs

In South Africa the technique was adapted for mining reef-type gold deposits, where gold is distributed in the thin beds of the quartz conglomerates, usually less than 1 m thick (Fig. 2.11b). Some of the mines are deep and therefore roof is supported by the pillars made of concrete or timber.

2.3 Unconventional Mining

Extraction of minerals from the host rocks not always made by digging of the open pits or sinking shafts. Some minerals are extracted by dissolving them directly in their host rocks (*in situ*) therefore the exploitation technique is referred to as *in situ* leach (ISL). This unconventional

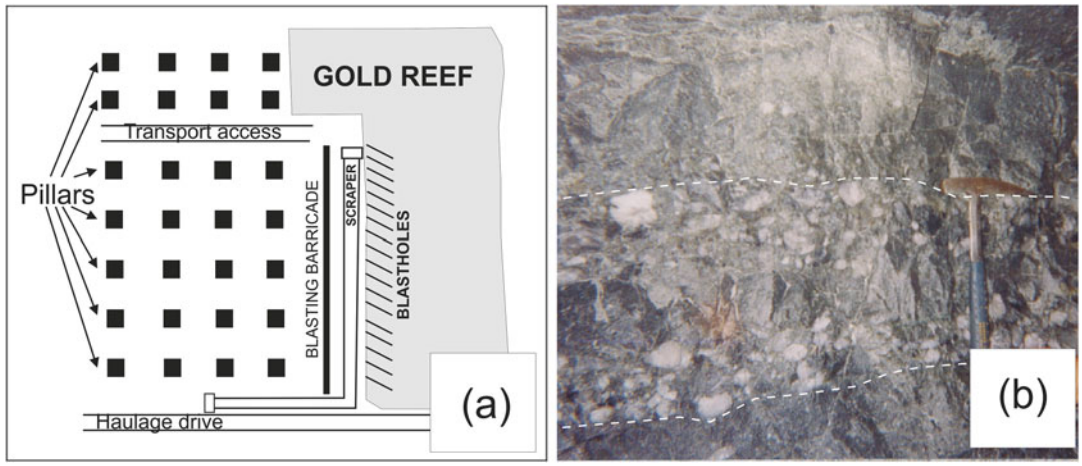

Fig. 2.11 Longwall mining, generalised after Hamrin (1982, 2001): (**a**) plan showing general layout of the longwall stope; (**b**) gold reef mined by longwall method in South Africa

mining approach is broadly used for extraction of the dissolvable minerals hosted in the water permeable rocks. In particular, this is the main production method for the sandstone hosted uranium deposits (Abzalov 2012).

Another technique, included into the group of unconventional mining method is dredging, which is also not a mining technology *senso stricto*. In the mining industry, this method is used for exploitation of the mineral sand deposits. A brief description of these methods is given below.

2.3.1 *In situ* Leach (ISL) Technique

In situ leach (ISL) technology is used for exploitation different types of the deposits, however, the most sophisticated version of the ISL technology was developed for mining uranium from the weakly lithified sandstones. The method is based on dissolving the uranium minerals directly in their host rocks by reactive solutions injected through the drill holes distributed along the regular pattern (Abzalov 2012). Solutions dissolve uranium minerals directly in the host rocks and are then pumped to the surface through the extraction drill holes (Fig. 2.12a). The pregnant solutions are collected on the surface and supplied to the processing plant where uranium is extracted.

A significant advantage of the ISL operations over conventional mining is their low capital and production costs. The favourable economics of the ISL technology coupled with a specific technical characteristics of the method allow to use it for mining the low grade deposits hosted in the unconsolidated sands at the depth up to 600 m below surface, which cannot be mined by conventional methods (Abzalov 2012).

The method is based in its entirety on the drilling and therefore the surface disturbance at the ISL operations is minimal (Fig. 2.12b). This is another advantage of the ISL technologies in comparison with the conventional mining methods. All these features have made the ISL technology a favourable option for exploitation of the sandstone hosted uranium deposits (Abzalov 2012) and for mining some industrial minerals (e.g. salt, potash).

2.3.2 Dredging of the Mineral Sands

Dredging is a process of excavation of the bottom sediments from the water basins. The prime objective of the method was not mining as, primarily, the technique was designed for maintaining the waterways navigable. Later, the technique found its application in mining, where it has become used for excavation diamond from the

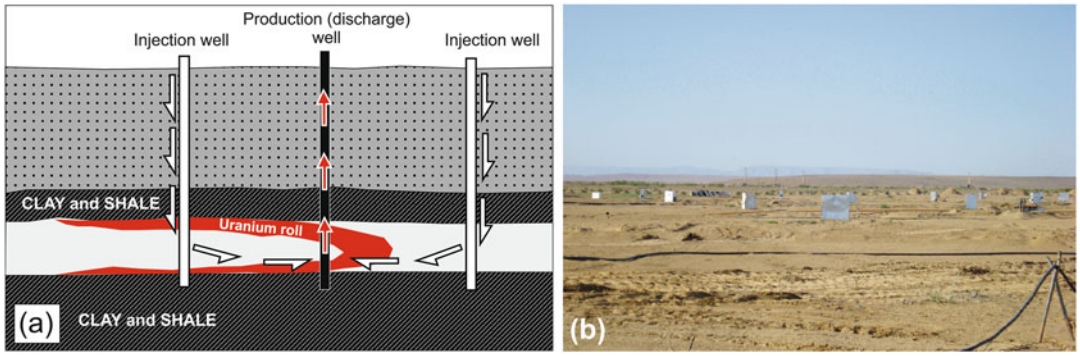

Fig. 2.12 *In situ* leach uranium mining: (**a**) principles of the technique; (**b**) production field at the Budenovskoe mine, Kazakhstan

Fig. 2.13 Dredging at the Richards Bay titanium sands deposit, South Africa

off-shore marine placer deposits, gold placers at the river beds and for mining the mineral sands deposits. The latter requires the mineralised strata, to be, at least partially, below the water table (Fig. 2.13). In that case the mineral sand dunes can be mined by dredging using the system of the artificial basins (dredge ponds). The excavated sands are pumped in slurry to concentrator floating at the same pond where the dredge is. The heavy minerals are separated from the barren sand and clay which are back filled to the pond behind the dredge.

References

Abzalov MZ (2012) Sandstone hosted uranium deposits amenable for exploitation by *in-situ* leaching technologies. App Earth Sci 121(2):55–64

Brady BHG, Brown ET (2004) Rock mechanics for underground mining. Kluwer Academic Publishing, New York, p 628

Hamrin H (1982) Choosing an underground mining method. In: Hustrulid WA (ed) Underground mining methods handbook. AIME, New York, pp 88–112

Hamrin H (2001) Underground mining methods and applications. In: Hustrulid WA, Bullock RL (eds) Underground mining methods: engineering fundamentals and international case studies. Society for Mining Metallurgy and Exploration, Littleton, pp 3–14

Mine Mapping

3

Abstract

Geological mapping remains one of the most important methods of recording mine geology, in particular for delineating geological structures and accurately locating geological contacts. This activity is important for understanding favourable geological features controlling distribution of the economic minerals which is essential for accurate exploitation of the deposits. Principles of the mine mapping and the most common tools are discussed in this chapter.

Keywords

Toe method • Digital technologies • Photogrammetry • SIROVISION • LIDAR

3.1 Mine Mapping Principles

Before commencing the mining project and for effective geological support of the operating mines the basic mine geology procedures should be summarised as concise guidelines. Procedures should include:

- Geological mapping / logging tools and procedures (log sheets, electronic devices)
- Features to be mapped and logged:
  - geological characteristics
  - geotechnical data capturing
  - quality of recovered samples
  - drilling / sampling techniques
- Data flow management
- Presentation of the mine mapping data
  - cross sections
  - longitudinal projections (longsections)
  - level plans
- Control of the captured data quality
- Sampling and assaying protocols and samples quality control
- Database administration

Geological mapping is routinely undertaken through all stages of the mining projects evaluation and continues at the operating mines. In the past, the tools available for recording geological data in the mines were almost entirely limited to compass and measuring tape (Peters 1987). Observations were plotted onto scaled paper in the field. After non-expensive digital cameras became routinely available they became an integral part of the geological mapping in

M. Abzalov, *Applied Mining Geology*, Modern Approaches in Solid Earth Sciences 12,
DOI 10.1007/978-3-319-39264-6_3

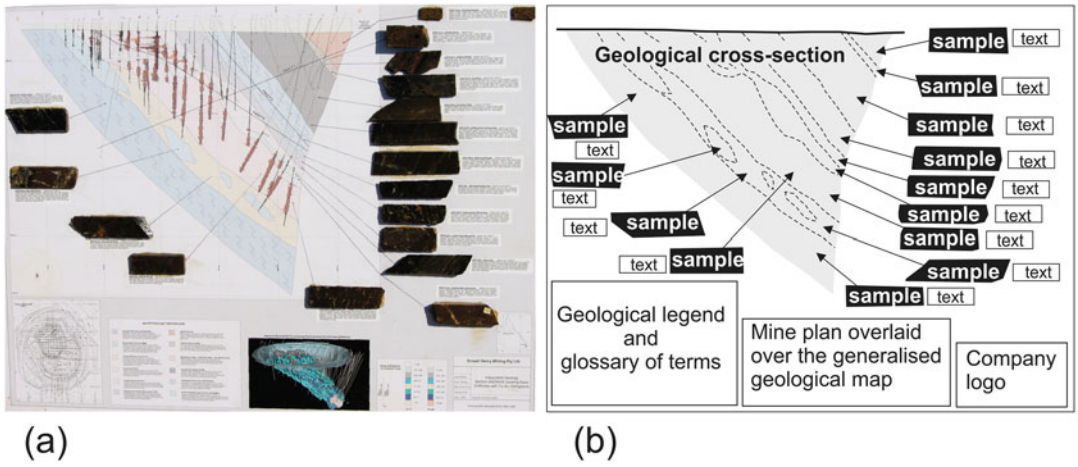

Fig. 3.1 Samples of the main rocks arranged as a display board (rock atlas): (**a**) example of a display board used at the Ernest Henry mine, Australia; (**b**) generalised layout of a rock sample collection, which is the suggested template for rock display boards

the modern mines. Digital technologies and computers have changed the whole procedure of the mine mapping which became an interactive process between direct observations in the field and desktop mapping using georeferenced digital photos plotted on the relevant mine faces, such as open pit benches or underground workings. The georeferenced digital photos and directly observed and recorded in the filed geological features, strike and dip of the geological contacts, faults, shears, lineation, cleavage, axial plans of the folds and other structures, are combined and interpreted together to produce a digital geological map of the mine. Concept of map has changed too, which now has become a construction of a digital 3D geological model rather than a construction of the 2D interpretations which dominated mine mapping in the past.

Scale of the mine mapping varies approximately from 1:500 to 1:2000 depending on mining selectivity, reserves definition parameters and grade control practices. The common approach is to record the field observations at a scale larger than the final geological map, which often is represented as a simplified geologic map of entire mine. The certain parts of the mine can be of a special interest requiring more detailed mapping, these documented at the large scale, up to 1:200. Depending on the chosen scale, the mappable units need to be determined. For example, the vein swarm is shown differently on the maps of 1:200 and 1:2000 scales. The maps of 1:200 scale allow to document and plot each vein composing the veins swarm, whereas on the smaller scale maps, such as 1:2000, the individual veins may not be distinguishable and the veins swarm will be shown as a zone of veining.

To ensure consistency in geological documentation made by different geologists it is necessary to document the mapping principles as concise guidelines describing rock types distributed at the mine, their characteristics and other geological features requiring documentation by mapping geologists. The ore bodies, main faults and folds are usually named and their specific features are described in the guidelines to simplify identifying these features in the field. It is also a good practice to supplement the guidelines by the rock atlas, also known as a rock board (Fig. 3.1) which should include photos of the main rock types. The guidelines and rock atlas are used for training geologists and also can be taken to field and used as a practical field manual by geologists mapping mine and logging drill holes.

3.2 Mapping Open Pit Mines

Geological features in the open pit mines are best observed and recorded at the pit faces and in particular along the bench toes where geological features exposed on the face above the broken

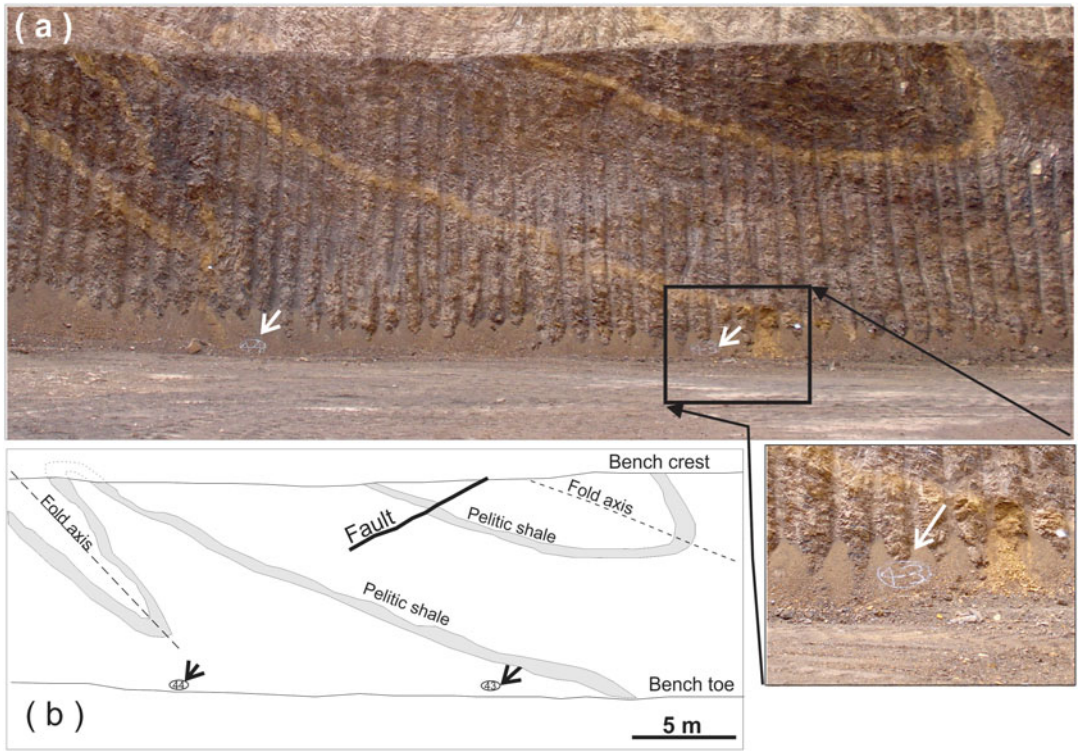

Fig. 3.2 Mapping rock faces at the Brookman iron ore open pit mine, Australia: (**a**) face of the bench with the control points marked by white paint (denoted by *arrows*) on the rocks exposed at the bench toe; (**b**) Geological interpretation based on the visual observations on the face and photo documentation. Geological features have been digitised from the photo

rocks (Fig. 3.2a). Observed geological features are accurately recorded on the base maps using surveyed control points, which are marked by paint on the pit faces or on the broken rock at the toe (Fig. 3.2a) and their exact location is marked on the base maps. The mapping sheets should also display the pit infrastructure, in particular toes and crests of the benches, which used as background data helping accurately plot observed geological features on the base map (Fig. 3.2b).

The toe method allows to map the open pit levels as a record of a successively retreating toe positions (Fig. 3.3). The map in this case represents a single horizontal plan and all contacts are shown with their true strike direction. The map can be further improved by adding the data collected during grade control sampling of the blast holes. Blast holes are usually drilled at distances of 5–10 m between them and accurately located by the mine surveyors, which provides a unique opportunity of recording high density information on rock types and their grades (Abzalov et al. 2010). Combination of toe mapping and blast holes documentation allows to produce the detailed geological maps of the mine levels (Fig. 3.4).

Mapping sheets are currently replaced by electronic data capturing devices, such as electronic mapping tablet (Fig. 3.5). Digital capturing of the data allows direct uploading information onto computers and therefore expedites construction of the digital 3D models. Nevertheless, the disadvantage of this approach is that it's more standardised and less flexible than traditional mapping on the paper sheets, being constrained by a scale of the map, format and chosen legend. The limitation of the direct mapping onto electronic devices can be overcome if to supplement electronic mapping with a conventional field notepad.

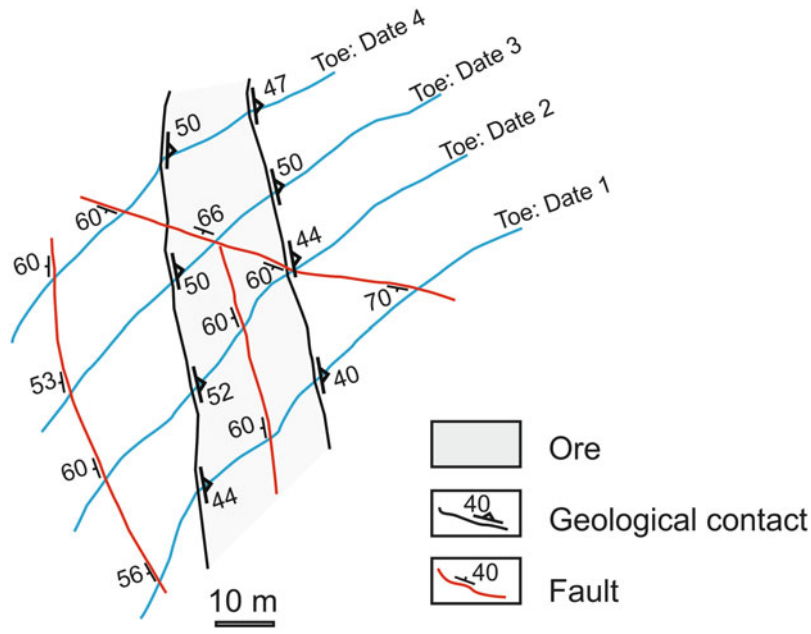

Fig. 3.3 Example of open pit mine geology documented by the toe method and plotted on one level

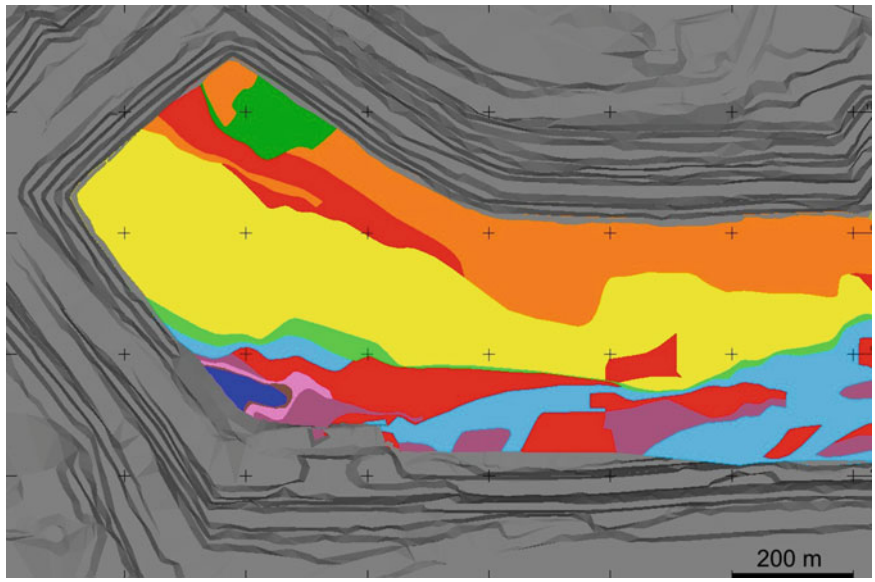

Fig. 3.4 Bench 15 of the Rossing uranium open pit in Namibia mapped by combination of the toe method and blast holes documentation. *Colours* denote different rock types

The latter will be used for recording additional data such as the areas of a special interest and the various geological observations that cannot be plotted on an electronic tablet because of scale restrictions or other technical or logistical limitations of the electronic tablets. These features can be sketched in the notepad and then used together with electronically captured features and digital photos to produce a geological map and 3D model of the mine. Therefore, the good practice is to use field geological notepad in conjunction with electronic mapping devices.

Fig. 3.5 Electronic tablet and note pad used for open pit mapping at the Escondida copper mine, Chile

Geological features that are recorded along the bench toe can be extended onto entire face. This approach is similar to documentation of the vertical cliffs during regional geological survey and it's particularly useful for recording steeply dipping geological features.

When this approach is used for geological mapping of the pits it is a good practice to make a photo of the entire wall first and to sketch the main geological features prior to commencing a detailed mapping of the faces (Fig. 3.6). After that, the pit face is usually represented as the sets of segmented vertical sections and each mapped separately. The mapped faces should contain the marked and surveyed reference points for accurately locating observed features (Fig. 3.2).

A good practice is to use a photo of each mapped segment with a level of details matching the chosen mapping scale. The photos should be georeferenced which significantly improve quality of the map allowing precisely locate observed features by their direct digitising from the photos. The best results achieved when photos are georeferenced and draped on digital model of the pit shell. This technique closely reproduces on the computer screens a 3D look of the pit faces at the time of their mapping (Fig. 3.7). Main geological features can be digitised directly from the photos draped onto digital surfaces and this ensures accurate location of the mapped features. The minor details are added in the field, including the accurate diagnostics of the rocks and measured attitude of the structural elements

3.3 Mapping of Underground Mines

Geological mapping in underground mines is more challenging then surface mapping because of lacking the perspective view available in the open pit mines (Fig. 3.6). On the contrary to pit mapping the mapping underground mines represents the sets of spatially separated observations with variable level of details and reliability which eventually the geologist need to correlate and assemble into a single map (Fig. 3.8). Geologists mapping the underground mines are rarely having an opportunity to see the whole picture before the map is completed.

The limitation can be partially overcome by using available surface maps that can provide a general geological context showing the dominant structural patterns and geometry of the mineralised zones. The large scale surface maps, when they available, help better understand and correlate geological features observed in different locations of the underground mine workings

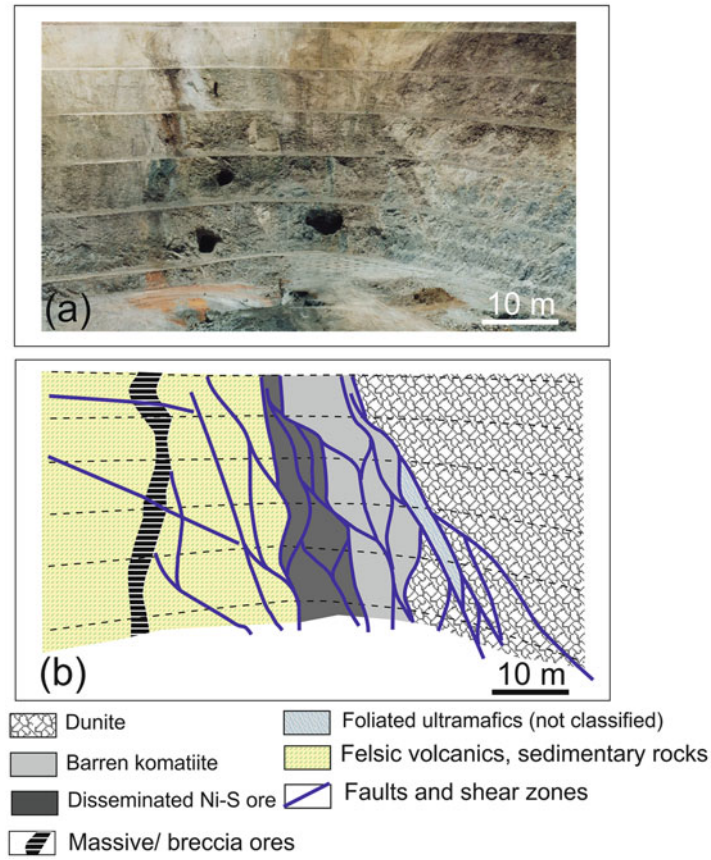

Fig. 3.6 Perseverance nickel-sulphide open pit, Australia: (**a**) photo of the pit wall; (**b**) geological interpretation of the data shown on the photo made by this book's author

however don't fully overcome the limitations of lacking of a perspective views in underground environments.

Another serious problem encountered by mining geologists mapping underground mines is the difficulties in diagnostics of the rock characteristics which look differently under dim lights of the head lamps in the underground workings. Dust covering underground surfaces and muddy smears on the walls are another obstruction often faced by mining geologists. Therefore prior to mapping surfaces in underground mines they are thoroughly washed by geologists.

Geological features are recorded on the special mapping sheets usually made of water resistant paper and containing the printed grid lines (Fig. 3.9). The sheets prepared for mapping should include the outlines of the underground workings copied from the detailed engineering maps (Fig. 3.9). The sheets during mapping are kept in a special sheet holder which also equipped by a made of a waterproof material a pencil and scale sheath attached onto a front cover of the sheet holder (Fig. 3.10).

Equipment used by geologists for underground mapping in addition to traditional geological items, such as compass, geological pick, digital camera and hand lens also include measuring tapes, usually one 20 or 30 m long and another small pocket tape, preferably 5 m long and made of metal for measuring vertical sizes, two or three cans of spray paint of the different colours, and powerful electric torch. The latter is particularly important for mapping the backs of the drives because illumination of the cap lumps usually is too dim for observing geological features at the distance 4–6 m, a common height of the drifts and declines in the modern mines.

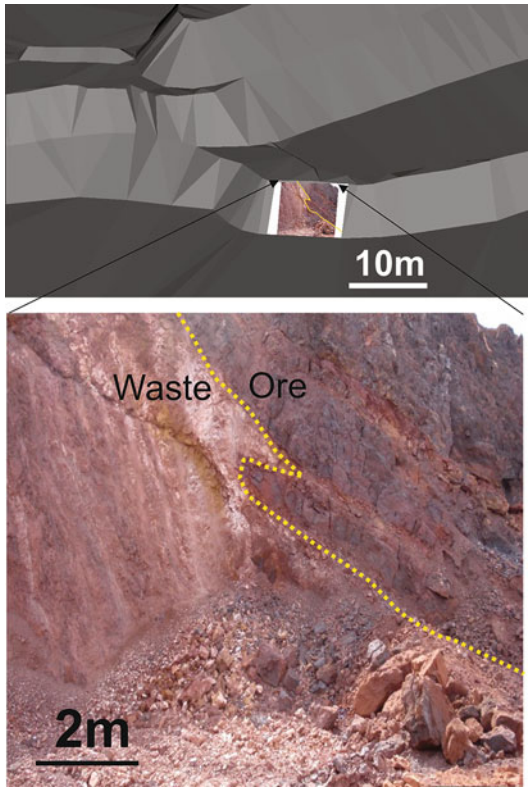

Fig. 3.7 Photo of the open pit face georeferenced and draped onto the digital pit model Tom Price iron-ore mine, Australia

Surfaces that are most suitable for mapping in the underground environments include freshly cut faces of the ore drifts and backs of the drifts (Fig. 3.11). Side walls of the underground workings are also mapped in particular when they developed across the strike of the ore body (Fig. 3.11). Depending on geometry of the mineralisation and geological complexity decision should be made which surface require main attention and most detailed mapping. In many nickel-sulphide mines in Western Australia the preferred approach is mapping the backs of the drives and cross-cuts (Fig. 3.8), supplemented by mapping walls of selected cross-cuts in the geologically most important areas containing critical information for correct geological interpretation.

Gently dipping structures are best exposed on the walls of the underground drives (Fig. 3.12). In that case, the due emphasis should be made on documentation geology exposed along the walls.

Mapping backs and walls require marking the reference points on the walls of the underground workings. The marks are usually painted in 2 m with a 10 m intervals highlighted. Depending on the mapping scale the marks can be drawn at the different distances, up to 1 m on areas requiring a most detailed mapping (Fig. 3.12). The marks are best to start from survey stations located on the backs of the workings, which are accurately surveyed and therefore are the optimal for using as a starting reference points in underground mapping. The surveying stations are firmly attached to the backs of workings by surveyors who usually screw them into holes drilled by portable electric drill using diamond drill bits. To measure distance from the survey station to the marks on the walls it is necessary to attach to the station a string with weight on the its end and then measure distance to the reference mark from the weight projected to the floor of the working.

Faces of the ore drifts are mapped and sampled regularly when they developed through mineralisation (Fig. 3.13). Mapping them is particularly important when drifts are developed along the narrow steeply dipping ore bodies. In that case the mapping of the faces provides vital information for accurately designing the mining stops, planning the mine production and to control quality of the excavated ore.

Faces are surveyed each time after the underground workings drive has been advanced by blasting therefore precise location of the mapped surface can be obtained from surveyors. Nevertheless, it is a good practice to backup surveyed location of the mapped faces by recording their distance from a nearest surveying station.

It is a common practice that before mapping faces and walls of the drifts the geological contacts are marked by spray paint (Fig. 3.13). Usually 2–4 different colours are used for denoting different features. It is impractical to use more colours as this causes unnecessary complication of the mapping process.

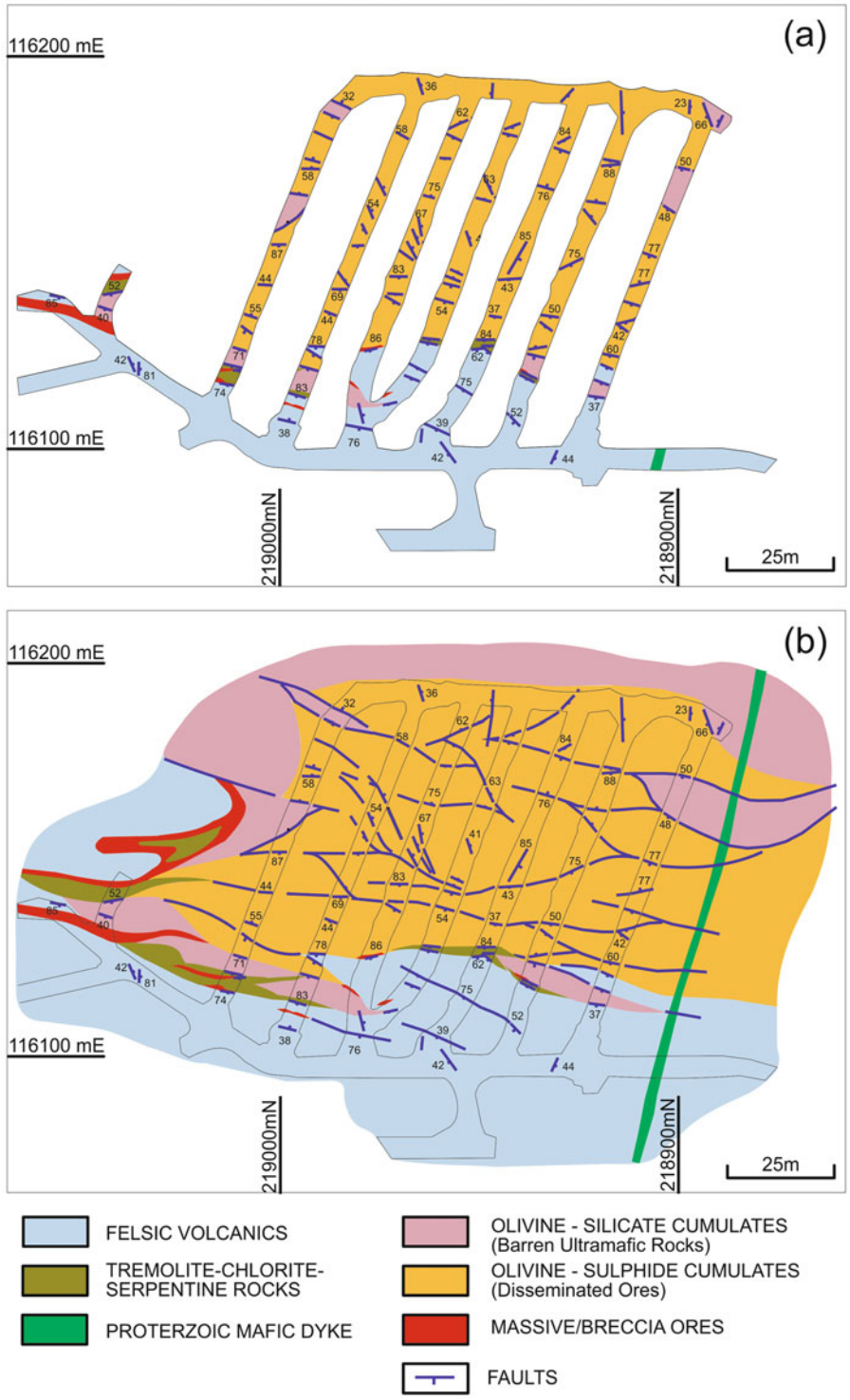

Fig. 3.8 Level 10075 of the Perseverance nickel-sulphide mine, Leinster, Australia, mapped by the current author: (**a**) field documentation of the geological features observed at the backs of the underground drives and cross cuts; (**b**) geological map compiled using underground mapping records and drill hole data

Fig. 3.9 Mapping sheet prepared for geological mapping at the Perseverance nickel-sulphide underground mine, Leinster, Australia. Outlines of the mine workings were copied from engineering maps. Lenses of the massive sulphide ore (coloured in *purple* tabular and lenticular bodies) were copied from the ore reserves model

Mapping in underground mines can be significantly improved by using the georeferenced digital photos. Procedures of using digital cameras for geological mapping in underground mines are similar to using to their application for geological mapping of the open pits (Fig. 3.7). Main difference is that GPS techniques are not applicable for georeferencing the photos made in underground.

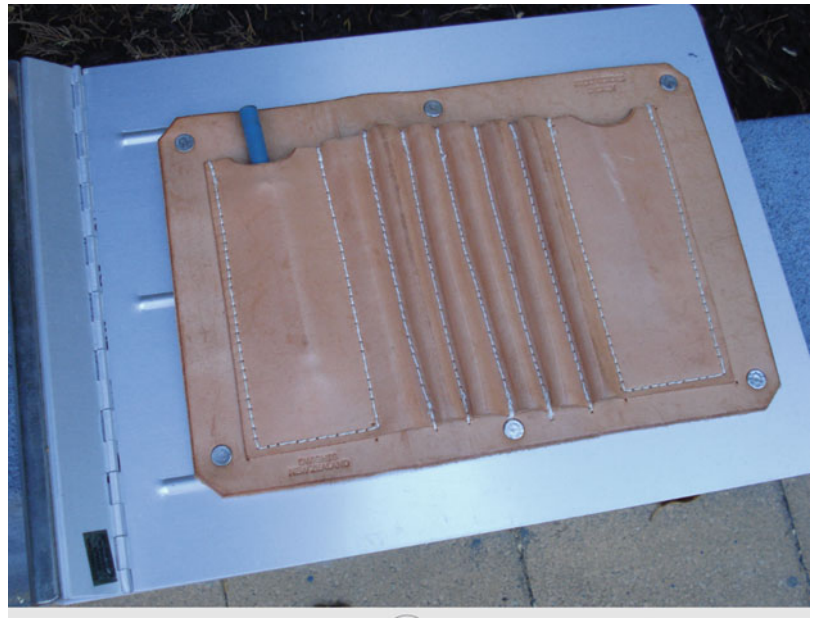

Fig. 3.10 Mapping sheets holder with attached pencils sheath for underground mapping

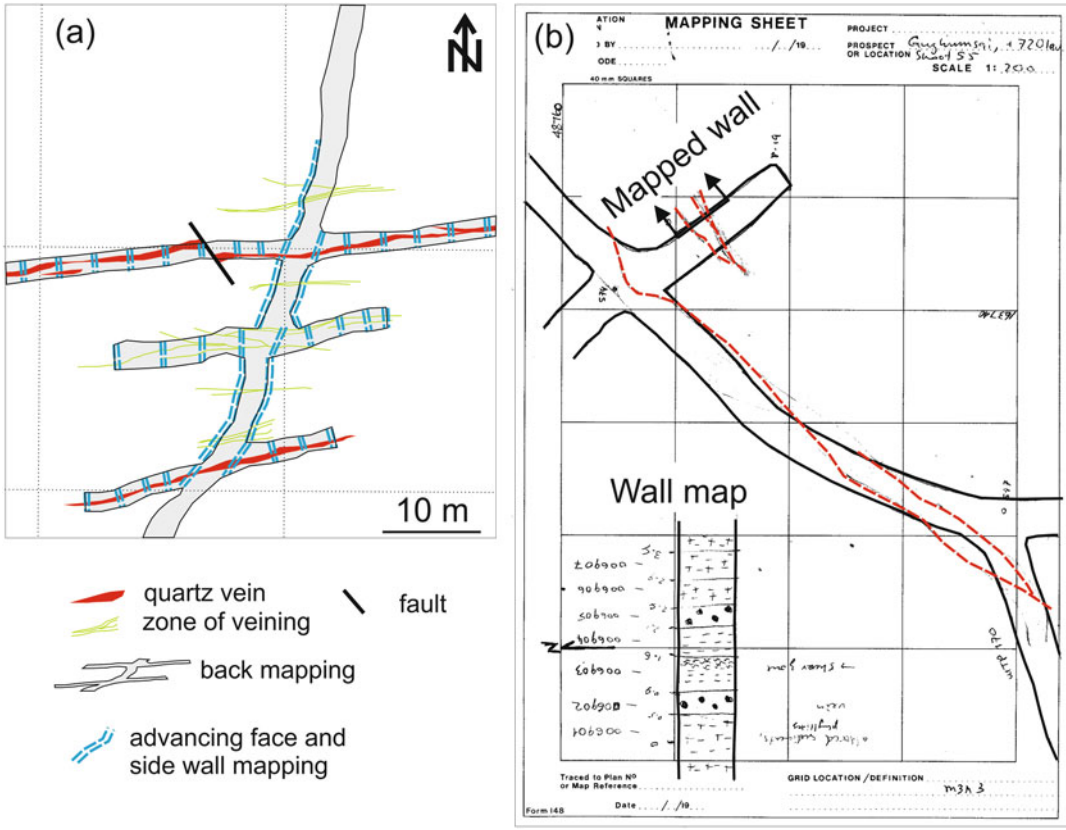

Fig. 3.11 Underground mapping in the Zarmitan gold mine, Uzbekistan (Abzalov 2007): (**a**) map sheet showing back mapping results and location of the mapped faces and side walls; (**b**) field mapping sheet showing the mapped cross-cut

Fig. 3.12 Mapping walls of the underground drive at the Bullen mine, Norseman, Australia

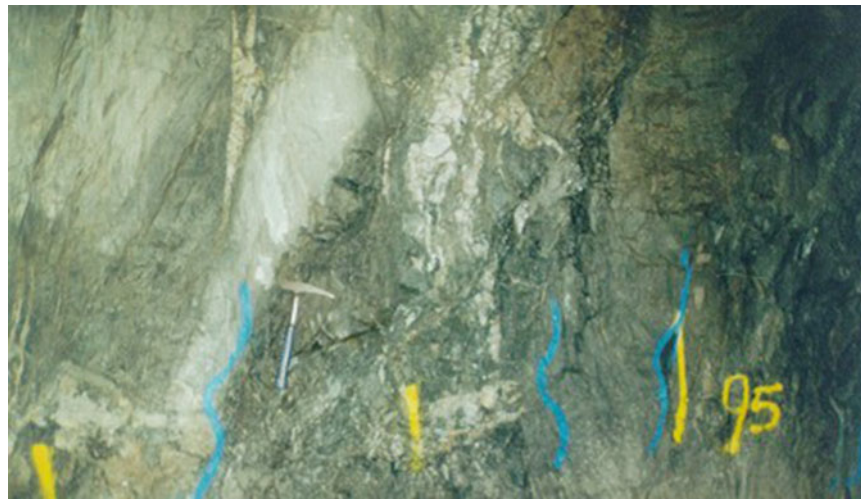

Fig. 3.13 Face mapping at the Ballarat gold mine, Australia. *Yellow* marks are reference points drawn in 1 m distance, *blue* lines denote contacts of the quartz veining zones

The photos can be accurately located only by determining location of the painted reference marks relative to surveying stations. Therefore, it is important that reference marks are clearly visible on a photo and their location has been determined before the mapped face was blasted away, shotcreted or became inaccessible.

Depending on available software the photos can be draped on digital model of the corresponding surfaces or simply posted onto planes whose positions approximately coincide with the surface displayed on the photo (Fig. 3.14). Geological contacts can be digitised directly from these images. Accurate location of the image when it

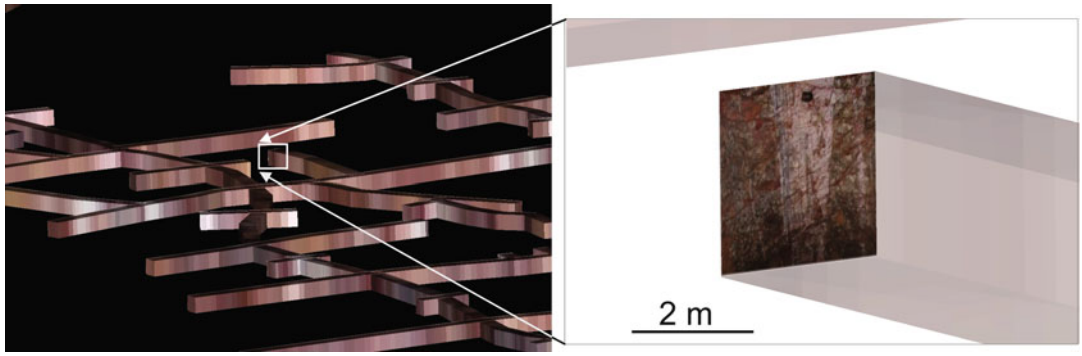

Fig. 3.14 3D digital model of the underground workings at the Zarmitan gold mine, Uzbekistan. Insert shows a photo of the face of underground drive that was georeferenced and draped on corresponding plane of the 3D model

is draped onto corresponding plane allows to obtain the accurate 3D position of the geological features that was exposed on the studied face.

3.4 Mapping Using Digital Photogrammetry and Laser Technologies

Conventional mapping, discussed in previous sections has a serious limitation of being time consuming and labour intense. These limitations impose a serious disadvantage for using in the modern mines characterised by a high production and development rates requiring quick capturing of the geological and geotechnical information from exposed faces before they have been blasted away or shotcreted. Another issue encountered during conventional mapping is that some parts of the mine containing the vital information can be inaccessible for mapping because of safety or logistical reasons. In order to overcome these limitations, the modern mining industry is actively introducing the remote data capturing devices and desk-top mapping techniques. A simplistic version of this approach is using digital photos of the faces, georeferencing them using control points whose location was accurately surveyed and draping then on the digital models of corresponding them mine surfaces that are mapped (Figs. 3.7 and 3.14). The more sophisticated versions of the remote mapping require special devices for capturing and processing data. The last decade there have been enormous advance in the technologies for characterisation the rock faces using remote data capturing technologies. Currently, the most common methods are photogrammetry and laser mapping which allows to collect information on a rock face from a distance to a studied face. The same technologies produce a digital 3D surface model rendering the studied face, called Digital Terrain Model (DTM).

3.4.1 Mapping Mining Faces Using Photogrammetry

The most common approach currently used for remote mapping of the mine faces is a photogrammetry (Atkinson 1996; McGlone 2004). This approach uses pairs of digital photos of the same object taken from the different locations and known as a stereo pair (Fig. 3.15). Using triangulation of the studied object P(x,y,z) and two digital images pL(u,v) and pR(u,v) the angles between them can be measured and position in space of the point P(x,y,z) can be determined given that position of the camera for each image, orientation and focal length of the camera for each image are known (Fig. 3.15).

An important characteristic of photogrammetry is that the accuracy of 3D measurements can be varied and configured by changing geometry of the stereo system (Fig. 3.15). While, for a given camera, the coverage is directly related to the focal length of the lens and the distance from the area being mapped, the accuracy is de-

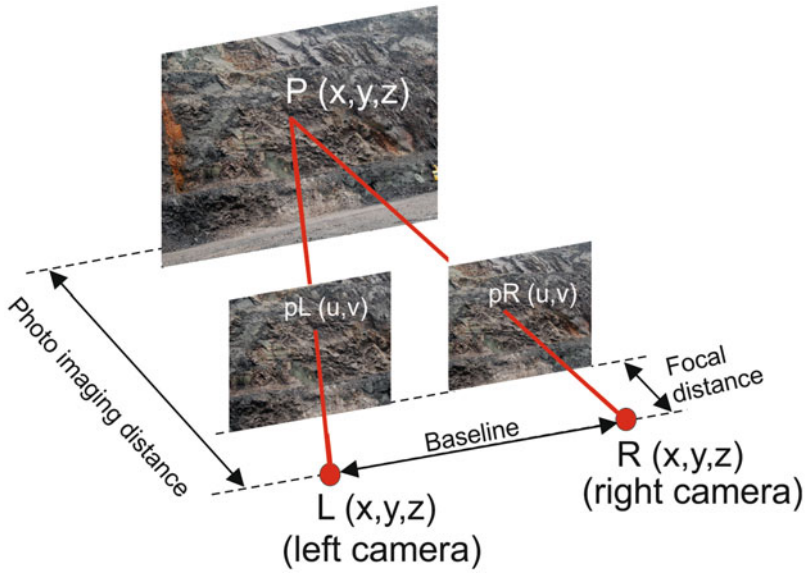

Fig. 3.15 Sketch explaining the principals of stereoscopic image pair used for photogrammetric survey of the rock faces. Based on Atkinson (1996) and McGlone (2004)

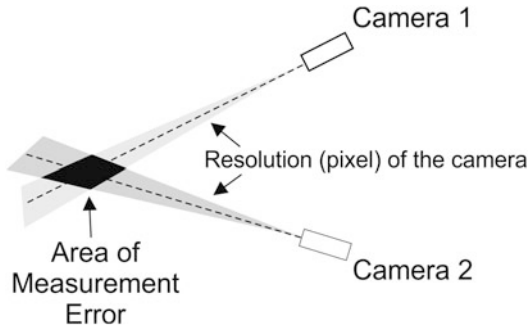

Fig. 3.16 Measurement error in stereo photogrammetry

pendent on a number of parameters that interact in a non-linear manner. The practically one of the most important parameters is the distance between cameras (Fig. 3.16). When it decreases the measurement error increases dramatically. Increasing the distance between cameras relative to their distance to object makes error ellipse more circular, improving the depth accuracy.

Technology of creating accurate 3D measurements of studied object from pair of the matching 2D images is not new and for a long time was known in geological applications as aerial photo stereo pairs. This technology is a routine approach for generating topographic terrain maps and also commonly used for preliminary interpretation of the terrain geology. Despite of being known for long time and commonly used in regional geological surveys this technology only recently was introduced into mining industry. It was pioneered by Australia's Commonwealth Scientific and Industrial Research Organisation (CSIRO) which together with Datamine have developed a SIROVISION system representing first commercially available photogrammetric device supplemented with data processing software.

Another system currently used for photogrammetric documentation of the mine faces is ADAM technology (Birch 2006). When applied correctly the photogrammetric technology permits to achieve exceptionally high resolution of the photographed mine surfaces with accuracy in the order less than 1 cm (Birch, written communication). The reported accuracy of depth measurements by ADAM technology at the Mount Newman iron ore mine in Australia was 10–20 cm when working range of taking stereo photos was 0.7–1.2 km. The same technology has produced map with accuracy of varying from 1 to 2 cm and the ground pixel size of 1.5×1.5 cm when photos was taken from a distance of 50 m from studied face.

The optimal working procedures for generating 3D maps from a pair of images are as follows. At first, the chosen site needs to be prepared for photomapping including a washing

of the mine faces. If safety and logistic permits it is a good practice to mark and survey the control points which will be used for verification the surface model generated by photogrammetric technology. The control points should be chosen in such manner that ensures their location as close as possible to the centre of the overlapping pair of stereo images.

Camera positions and physical layout of the data acquisition process need to be determined and ensured that it is feasible for a given camera and lens configuration. As a rule of thumb the ratio $\left(\frac{\text{Separation between cameras}}{\text{Distance from cameras to mine face}}\right)$ should be within the range from 1/6 to 1/8. Camera should be used with tripod equipped with spirit level for ensuring the horizontal and non-tilted position. Prior to taking photos the following measurements need to be obtained:

- The 3D coordinates (absolute or relative) of the camera at the time each image is acquired need to be accurately determined;
- Three orientations of the camera need to be measured each time when image was acquired: (a) the azimuth of the optical axis of the camera. Stereo photographs should be taken with as little convergence as possible, ideally with the photos of all images made by cameras aligned in parallel. Convergence in the order of 10° is likely to result in large error in 3D map caused by poor matching of the stereo pairs; (b) the dip of the axial plan of the camera (zero-degree elevation is horizontal, ninety degrees elevation is vertically up); (c) the tilt of the camera. The tilt of the camera should be zero if possible;
- The focal length of the camera lens usually determined during lens calibration;
- From camera specifications it is necessary to obtain the image format including number of rows and columns of pixels and the pixel size.

The obtained data are processed using commercially available software, which conventionally used for construction digital surfaces. File structure and processing procedures vary depending on chosen software however their basic principles and main steps are the same: firstly, the pair of stereo images needs to be matched and then built-in algorithm will calculate coordinates of each pixel using above mentioned geometric principles (Fig. 3.15). As an outcome of this process each pixel will be assigned a 3D coordinates and then the surface can be presented as wireframe (triangulated mesh) model (Fig. 3.17a). Infilling the wireframe with the pixels recorded by digital photography produces the textured 3D photographic image of the surface closely reproducing the actual look of that face at the time when photo was made (Fig. 3.17b).

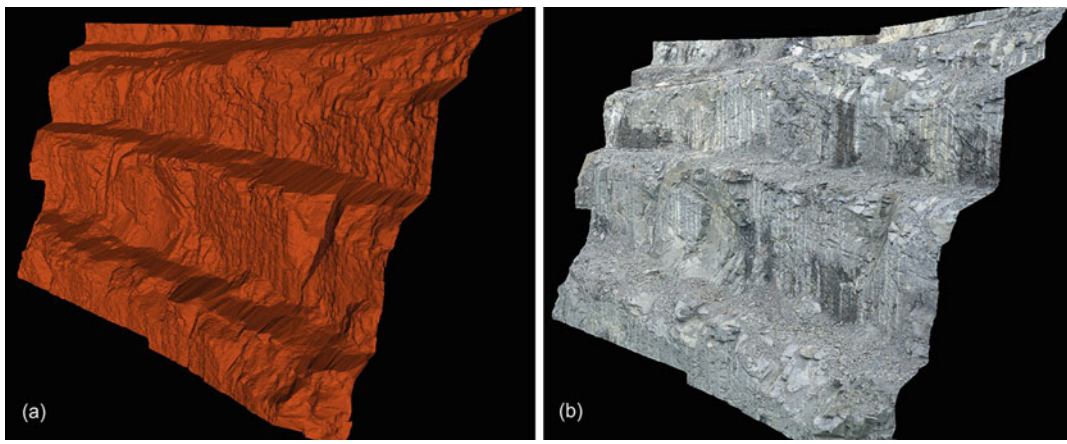

Fig. 3.17 3D photographic image of the pit wall obtained using SIROVISION technology (Courtesy of Datamine). Bench height 10 m: (**a**) wireframe; (**b**) wireframe model infilled by pixels of the photographic image

Fig. 3.18 Detailed 3D image of part of the underground drift (8 m long) recorded using ADAM photogrammetric technology, Diavik diamond mine, Canada

In the mining environment the photogrammetric technology initially was introduced into open pit operations (Fig. 3.17) and later it was successfully implemented for mapping underground mines (Fig. 3.18).

3.4.2 Remote Mapping of the Mines Using Laser

Three dimensional laser scanning of the mining faces is another powerful technology for remotely characterisation of geological and geotechnical features of the rocks exposed on the mining faces (Kemeny et al. 2003, 2006). The system is similar to ordinary radar, however it utilises the speed of light by sending out narrow pulses of the beam of light rather then a broad radio waves used by conventional radars. The laser radar technology is usually referred as LIDAR, which is abbreviation for Light Detection and Ranging scanner. LIDAR instrument (Kemeny et al. 2006) is a compact portable device combining laser emitter and receiver. It sends out high frequency laser pulses and capture reflection. The measurements are based on trigonometric calculations of the distances between LIDAR instrument and object reflecting the beam.

Frequency of sending pulses is 530–1500 nm, that allows to accumulate more than one million reflected points during less than 15 min of survey, a usual duration of a single scan. Instrument operates at the ranges varying from several meters to several 100 m, up to 1 km, with an accuracy of the measured coordinates within the range of 2–10 mm (Kemeny et al. 2006). Density of the captured reflecting points is so high that scanned surface is looking as the actual photographic image of the surface. Next step is to generate a triangulated mesh from captured points. This is done by special software designed for processing large data files, containing millions of the registered points which need to be georeferenced into a real world coordinates and then generating a digital model of the scanned surface by triangulating the recorded points and creating 3D digital mesh.

Further application of the digital model depends on the objective of the LIDAR survey. The triangulated mesh (wireframe) can be analysed to determine the fracture density, preferred orientation of the discontinuities, can be used for accurate estimation of the mined out voids for reconciliation with the reported mine production.

3.5 Optimisation of the Mine Mapping Procedures

It is important to remember that although remote scanning of the faces using photogrammetry or laser technologies significantly expedites the mapping process and increases accuracy of determining the location of the mapped features in 3D space it's not eliminates the needs for geological observations and documentation the rocks characteristics. Geological and geotechnical mapping in the modern mines should include conventional mapping when mine geologist observes and records geological features exposed on the excavated faces and uses remote mapping approaches for documenting the large areas.

Both approaches have their strengths and weaknesses. New technologies designed for remote scanning of the rock faces are practically irreplaceable for mapping inaccessible sites such as mined out stopes, walls of the old pits, slopes of the ponds at the dredging operations, ore stockpiles and waste dumps. When applied for mapping pit benches the remote mapping approach has one advantage in comparisons with a conventional mapping as it generates an accurately located image of entire bench (Fig. 3.17) whereas direct geological observations and measurements are limited to the bench toes (Fig. 3.3). The limitations of the remote mapping techniques applied in the mines is similar to that encountered in the regional surveys, as different geological features can look similar on the photo stereo pairs and images generated by laser scanning. Therefore, visual inspection of the key areas, diagnostics of the rocks and structural features is still necessary and this require mining geologists to check and verify maps generated by interpreting remotely captured images. Another disadvantage of the remote documentation of the rock masses is that it requires special equipment, software and trained personnel for operating and all of these can be a serious limitation at the small operations with a limited budget.

Summarising strengths and weaknesses of the both approaches, it is obvious that remote mapping cannot eliminate the needs for conventional geological documentation of the mining faces. However, at the contemporary mines the proportions between remote mapping technologies and conventional mapping approaches are steadily changing in favour of remote mapping leaving conventional mapping for detailed studies of the key areas that are most important for correct interpretation of the overall geological patterns and understanding relationships between different geological features. In parallel with mapping faces mining geologists need to sample them for characterisation the rocks and quantitative estimation grade of the ore bodies exposed on the mapped faces.

Characterisation of the rocks should start from compilation of the representative collection of the rocks distributed at the given operation and documenting their mineralogical and chemical composition, textures, and visual characteristics that can be used for the rocks diagnostics (Fig. 3.1). In order to facilitate interpretation of the geological features and diagnostics of the rocks on the remotely mapped images it is important to include into the rock atlas the representative examples of the remotely mapped rock faces showing the different rocks, alteration zones, discontinuities and geological contacts. All geological features that captured by remote mapping devices should be shown as they look on the captured images and then clearly identified and explained on the geological map supplementing the photo of the given face.

Field mapping procedures should be a combination of two approaches, remote mapping and conventional mapping. Remote mapping approaches can vary from detailed photogrammetric documentation, if company budget permits, to a simple digital photography that georeferenced and draped onto wireframe model of the mine walls (Figs. 3.7 and 3.14). A combined approach, including desk-top interpretation and digitising geological features from georeferenced digital photos and conventional mapping of the geological features exposed on the mine faces, allows more accurate geological documentation at the increased overall speed of mapping. In fact, using georeferenced digital photography together with

Table 3.1 Mine mapping check list

Activity	Example
Mapping and logging procedures are available and geologists are trained	
Rock collection (rock library) available and geologists are trained	Fig. 3.1
General overview highlighting the geometry of the ore bodies and main structures is available	Fig. 3.6
Sites chosen for mapping are exposed and can be safely accessed	Fig. 3.2
Mapping surfaces are clean and if necessary washed	Figs. 3.2, 3.12, and 3.13
Mapping scale is chosen and matching needs of the mine production and quality control	Fig. 3.8
Reference points are marked on surfaces. Density of observations should match the mapping scale	Figs. 3.12 and 3.13
Location of the reference points is obtained from surveyors or determined by GPS	
Mapping sheets with print out grid is available	Fig. 3.9
Mining infrastructure and exposed mining faces are printed onto mapping sheets	Figs. 3.9 and 3.11
Field equipment is obtained and is optimal for the given mapping tasks	Fig. 3.10
Faces are photographed and photos are georeferenced using reference points[a]	Fig. 3.7
Preliminary geological interpretation of the photographed rock faces is made in office[a]	Fig. 3.7
Field observations made and recorded onto mapping sheets and georeferenced photos[a]	Fig. 3.3
Observed features are digitised in 3D space and available for updating 3D geological model[a]	Figs. 3.8 and 3.19

[a]remote mapping technologies, such as photogrammetry can be used at this stage

conventional mapping brings field data capturing and desk-top mapping approaches closer to each other making a gap between them narrower. It is also important to remember that mapping is an interactive process. Rock faces after they have been remotely scanned and documented need to be visited for clarification geological features, resolving a possibly controversial interpretations of the remote mapping results and making the control measurements to verify desk-top interpretations.

Check list summarising main steps and activities required for assuring good quality and safe mapping geological features at the operating mines is presented in the Table 3.1. The same check-list is applicable for advanced exploration sites where pilot mining has been commenced as part of the detail evaluation of the mining project (e.g. bankable feasibility study).

The next step is to compile the geological maps and cross sections from numerous records made in the different parts of the mine and often with different level of the details. At this stage all available data are used, including geological records of the mining faces, documentation of the surface outcrops, drill holes and mining geophysics.

Eventually, based on mapped data and interpreted level maps and cross sections a coherent 3D geological model of the deposit is constructed (Fig. 3.19). The 3D models are built using special mining software and used for estimation resources and reserves of the mining projects and estimating the mine production plans. The models are regularly updated because of operating mine provides new and more detailed information that allows to revise the earlier made model, extend the ore-bodies and often significantly changes the interpretations. Compilation of the mine geology data, construction of the 2D sections and plans and generating 3D models will be discussed in details in the following chapters of the book.

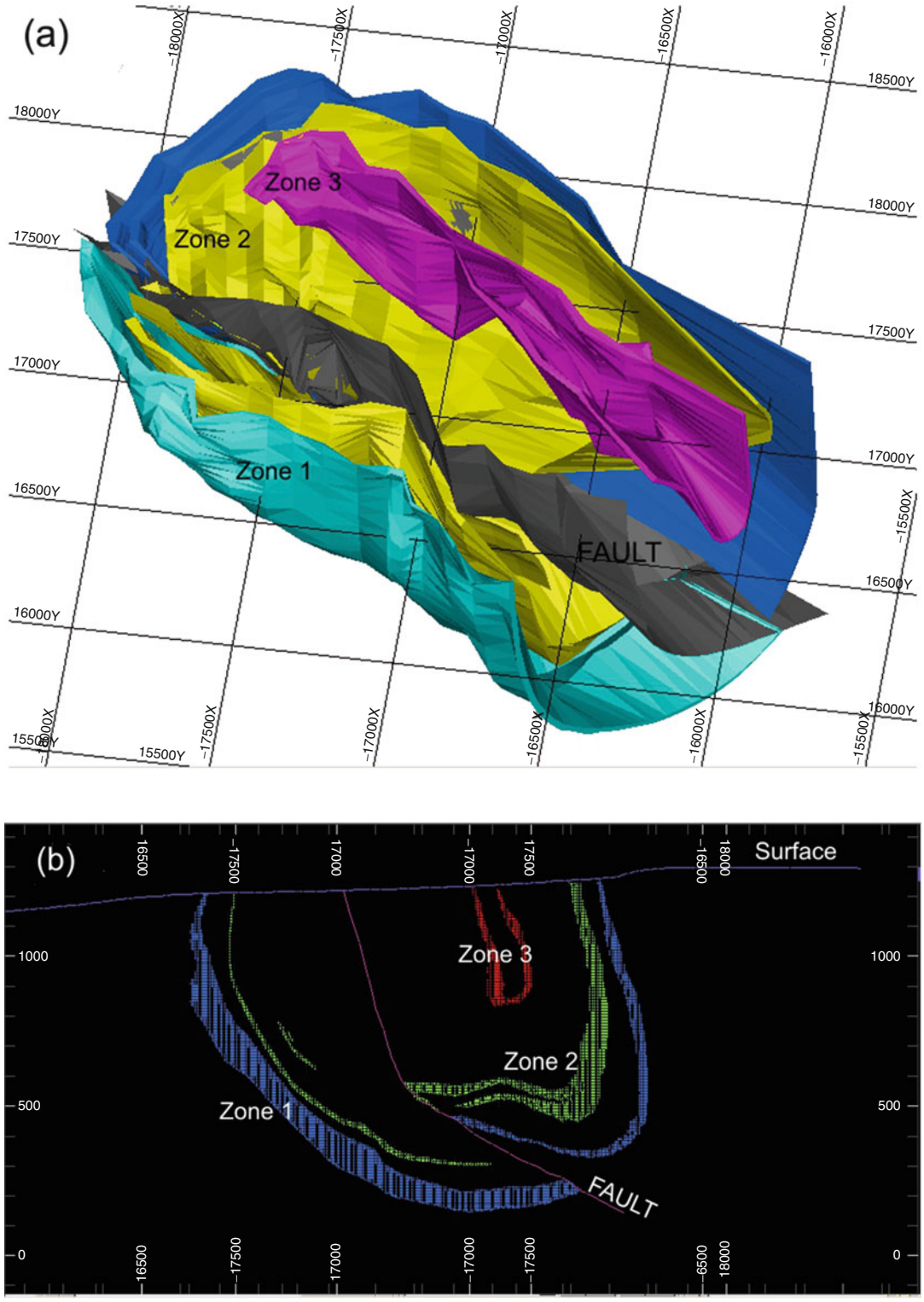

Fig. 3.19 Taezhnoe iron-ore deposit, Russia: (**a**) 3D geological model showing magnetite mineralisation (Zones 1, 2 and 3) and main fault. Topographic surface removed; (**b**) cross section through 3D model

References

Abzalov MZ (2007) Granitoid hosted Zarmitan gold deposit, Tian Shan belt, Uzbekistan. Econ Geol 102(3):519–532

Abzalov MZ, Menzel B, Wlasenko M, Phillips J (2010) Optimisation of the grade control procedures at the Yandi iron-ore mine, Western Australia: geostatistical approach. Appl Earth Sci 119(3):132–142

Atkinson KB (1996) Close range photogrammetry and machine vision. Whittles, Caithness, p 384

Birch JC (2006) Using 3 DM analyst mine mapping suite for rock face characterisation. In: Tonon E, Kottenstette J (eds) Laser and photogrammetric methods for rock face characterisation. Golden, Colorado

Kemeny J, Mofya E, Handy J (2003) The use of digital imaging and laser scanning technologies for field rock fracture characterisation. In: Culligan J, Einstein H, White A (eds) Proceedings of soil and rock America 2003 – 12th Pan American conference on soil mechanics and geotechnical engineering and the 39th US rock mechanics symposium. Massachusetts Institute of Technology, Cambridge, pp 117–122

Kemeny J, Turner K, Norton B (2006) LIDAR for rock mass characterisation: hardware, software, accuracy and best practices. In: Tonon F, Kottenstette J (eds) Laser and photogrammetric methods for rock face characterisation. Golden, Colorado

McGlone C (ed) (2004) Manual of photogrammetry, 5th edn. American Society for Photogrammetry and Remote Sensing, Bethesda, Maryland, p 1168

Peters WC (1987) Exploration and mining geology, 2nd edn. Wiley, New York, p 706

Drilling Techniques and Drill Holes Logging

4

Abstract

Modern mines use different sampling data, coming from drill holes, trenches, samples collected from the rock faces exposed in the mine workings and the grade control data. Among all various sampling techniques, drilling remains the main method for acquiring samples for the appraisal of the mining projects and extensively used at the operating mines.

Keywords

Drill hole • Core recovery • Orientated core • RC • Air core • Sonic • Auger

One of the key responsibilities of the mine geologists is to provide quantitative geological characteristics of the ore bodies and their host rocks. This is made by systematic sampling of the deposits with the total number of collected samples often in the order of the hundreds of thousands (Annels 1991; Sinclair and Blackwell 2002). Using these data geologists generate a detailed 3D interpretation of the deposits supplemented with quantitative assessment of the technical and economic parameters of a mining projects.

Modern mines use different sampling data, coming from drill holes, trenches, samples collected from the rock faces exposed in the mine workings and the grade control data. Among all various sampling techniques, drilling remains the main method for acquiring samples for the appraisal of the mining projects and extensively used at the operating mines. Thus, description of the mine sampling started with review of the drilling methods.

4.1 Drilling Methods

The available drilling equipment varies in a wide range of technologies and functional characteristics (Chugh 1985; Hartley 1994) which differ depending on the methods of breaking rocks, types of the drill bits and the modes of transportation of the rock cuttings to surface which is necessary for clearing holes during drilling (Table 4.1).

According to the hole making action the drilling techniques can be subdivided as follows:

- if drilling uses hammering (percussion) or rotation method for breaking rocks

M. Abzalov, *Applied Mining Geology*, Modern Approaches in Solid Earth Sciences 12,
DOI 10.1007/978-3-319-39264-6_4

Table 4.1 Common drilling methods used in the mining industry

		Hole making methods						
		Hammering			Rotation (turning action)			Sonic (high frequency vibration)
		Top hammer	Downhole hammer	Cable	Rotary	Hydraulic	Auger	
Hole Clearing Methods	Mechanical			Cable drilling	Diamond core		Auger (Short flight, Hollow, Backet)	Sonic drilling
	Fluid (Direct)	Open hole percussion (e.g. Blast holes)	Open hole percussion (e.g. Rotary Air Blast)		Tricon drilling	Tricon drilling with down-hole turbine		
	Fluid (Reverse)		Reverse Circulation Percussion (RC)		Tricon drilling using of reverse circulation of drilling fluids			

- whether hole making action is driven by air, hydraulic, electrical or mechanical means
- mode of transferring mechanical force to the drill bit that can be a cable or string of the drill pipes
- The hole clearing approaches includes the following main groups:
  - whether the hole is cleared mechanically or by flushing fluids
  - fluid flushing techniques are subdivided on the methods that use air and methods based on flushing holes by a drill mud.

Each of the groups can have the further subdivisions depending on drill bit types, fluid circulation modes, and if the drilling tool (e.g. hammer) is located on surface or down hole on the rock face.

The current chapter will overview the most common techniques currently used in the mining industry. These are mainly diamond core drilling and different non-core drilling methods based on percussion technologies, including standard open hole percussion and reverse circulation (RC) methods. Diamond core drilling recovers samples as a solid core of the rocks and is one of the most important methods for obtaining good quality geological information about buried mineralisation. Percussion drilling techniques, which are commonly used for grade control at the operating mines (Abzalov et al. 2010), recovers samples as small rock cuttings. The percussion samples are less informative than diamond core but this is offset by higher drilling rates and significantly lower costs. Reverse Circulation percussion (RC) drilling method is commonly used in the mining industry for infill drilling of earlier delineated mineralisation and for grade control at some open pit mines (Abzalov et al. 2010). The basic principles of these drilling technologies are overviewed in the current chapter and presented together with practical recommendations regarding efficient geological documentation of the holes and their sampling procedures.

For a long time percussion drilling methods have been the main technique used for appraisal mineralisation hosted in weekly lithified or non-consolidated sediments (Abzalov and Mazzoni 2004; Abzalov and Bower 2009). However, these techniques are currently replaced by methods based on sonic and vibrating technologies (Oothoudt 1999). Sonic drilling is currently used for definition of reserves and planning production at the deposits comprised by the non-consolidated sands, such as alluvial gold or heavy mineral sands (Abzalov et al. 2011).

Methods such as auger and tricon drilling are less common in the mining industry however auger drilling is used as routine techniques at some bauxite mines and tricon drilling is a main drilling method at the uranium operations utilising in-situ leach exploitation technology. These techniques and their application in mining geology are also discussed in the current chapter.

4.2 Diamond Core Drilling

Diamond drilling is a technique that uses the drill bits (Fig. 4.1) impregnated by diamond crystals (Cumming and Wicklund 1980; Chugh 1985). The diamonds used are fine to micro-fine industrial grade diamonds which are set within a metallic matrix of varying hardness.

The drill bit is threaded onto the core barrel and attached onto a bottom of a hollow drill

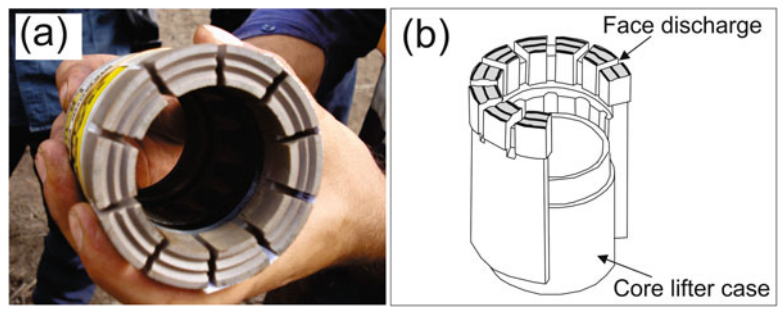

Fig. 4.1 Diamond drill bits: (**a**) photo of the diamond drill bit; (**b**) sketch showing interior design of the drill bit

Fig. 4.2 Diamond core at the Pilanesberg mine, Bushveld Complex, Republic of South Africa

rod string. Because of the opening at the end of the diamond bit (Fig. 4.1a) it cuts a cylindrical shaped solid column of rock, called drill core, (Fig. 4.2) which moves up into the tubular drill rod (pipe) as drilling progresses downward. Design of the drill bits includes a core lifter assembly which allows to retain the core collected in the internal pipe during drilling (Fig. 4.1b). The drill core after it was recovered from hole is placed in the core trays, special boxes for storing the drill core (Fig. 4.2).

Diamond drilling can be performed from surface or underground workings (Fig. 4.3). Surface drill rigs vary in size from large, truck-mounted or track crawlers rigs (Fig. 4.3a), capable of drilling 2000 m deep holes, to small man transportable rigs. The small rigs are convenient for exploration in the rigid terrains where access is almost entirely restricted to helicopter, however they are uncommon in mining operations where surface drilling is usually done using powerful truck-mounted rigs. Design of modern diamond core drill rigs has allowed for the drilling of holes at different angles, from vertical to horizontal, however the most practical dip angles at surface drilling are 60–80°.

Underground rigs are smaller in size than typical surface rigs and usually they are mounted on the skids and driven by electric motors (Fig. 4.3b). Such design is important for the underground drill rigs which are used for drilling from small and confined drill cuddies developed in the underground workings at the operating mines and exploration shafts. The limited choices of the available drill sites are compensated by ability of the underground rigs to drill in a wide range of the drilling angles varying from approximately vertical up to vertical down (Fig. 4.3b).

Penetration during diamond drilling is achieved by rotation of the drill rod with attached diamond bit on the end which allows cutting the rock at the bit face and advancing through them as the cutting progresses. The drill bits used in the mining industry have different sizes allowing to obtain a drill core from 20 to 165 mm in diameter (Hartley 1994). The most common drill bits are listed in the Table 4.2. The most

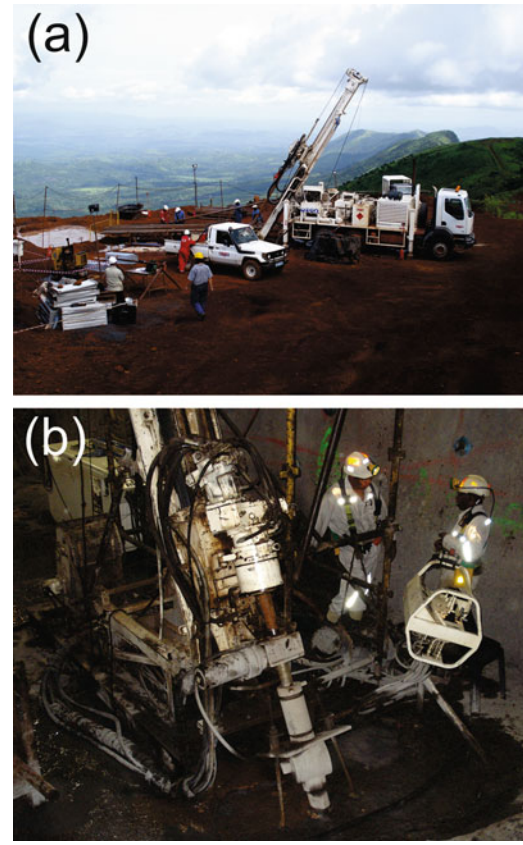

Fig. 4.3 Diamond core drilling: (**a**) surface drilling using truck mounted drill rig, Simandou iron-ore project, Guinea; (**b**) underground drilling, skid mounted rig, Palabora Cu-mine, Republic of South Africa

Table 4.2 Standard diamond drill sizes

	Standard			Wireline		
	Index	Hole diameter (mm)	Core diameter (mm)	Index	Hole diameter (mm)	Core diameter (mm)
North American	XRT	30	19			
	EX	38	22			
	AX	48	31	AQ	48	27
	BX	60	42	BQ	60	36
	NX	76	55	NQ	76	48
	HX	96	74	HQ	96	63
				PQ	123	85

	North American equivalent (approximate)	Hole diameter (mm)	Core diameter (mm)	
			Thin bits	Thick bits
Metric System	EX	36	22	–
	AX	46	32	28
		56	42	34
	BX	66	52	44
	NX	76	62	54
		86	72	62
	HX	101	–	75
		116	–	90
		131	–	105
		146	–	120

practical and commonly used in the mining geology applications are drill bits of NQ, HQ and PQ size.

Technology of diamond drilling requires pumping water from a drill rig on a surface through the drill rods to the drill bit on the rock face. It facilitates cutting rocks by applying a hydraulic pressure to the drill bit. This water is also needed to cool the bit during drilling. Diamond drill rigs are equipped with a special assembly including drill head and water swivel that are used for directing water to the drill rod string. From this assembly, water is pumped down to the drill bit where it escapes through the channels on the bit face (Fig. 4.1) and travels back to the surface along the space outside of the drill rods and between the drill hole wall. Continuous pumping of water down the hole and circulation of it back to surface is needed for cleaning the hole by the removal of fines and cuttings and also to provide lubrication to the drill string and reduce torque. It is also important for hole stability. Depending on ground conditions, special additives can be added to pumped water to create a more viscous and heavier drill mud which is needed for drilling through fractured, highly porous and unstable rocks.

Core, which is collected in the core barrel, is recovered on surface either by 'standard' or 'wireline' techniques. Standard technique requires that everything to be pulled out of the drill hole, which is laborious and time consuming procedure. The 'wireline system' was designed to overcome limitations of the 'standard' core recovering technique and it enables the core to be retrieved without pulling the rods and core barrel from the hole. The name 'wireline' is given because system uses a wire rope for delivering the inner tube which during drilling is located inside of the core barrel and captures and retains the drilled material.

Diamond drilling is an expensive process and the core is the final product. Drillers must wash and clean core before placing it into core tray. Drill crew must ensure that core is placed into the trays in the correct sequence as it comes out of the tube, and that the orientation of the core is not mixed up

The depth intervals drilled should be measured for each core run and clearly recorded on to the core blocks (Fig. 4.4). Care should be taken

Fig. 4.4 Examples of core blocks marked and placed by drillers into core trays. The core blocks denote the depth where core was taken and also can contain the notes of the measured lengths of drilled interval and recovered core

to assure that core blocks are placed correctly as they are main reference to the drilled depth where samples are taken. Each core tray is also marked by drillers, ensuring that project name, hole number, drilled depth, sequential number of core tray and drilling date are clearly recorded on at least on two sides of the core tray. It should be remembered that the way core is presented by the drill crew in the core trays is an indication of the care and professionalism of that crew.

Mine geologists, supervising the drilling, should review recovered core, with special attention to the sequence in which core was placed into core trays. It is a good practice to verify depths marked by drillers on the core blocks by marking the whole core at 1 m intervals and checking the depth and recovery recorded by drillers with the same values measured by geologists (Fig. 4.5).

4.2.1 Core Quality and Representativeness

Quality of the geological information obtained from diamond drilling directly depends on quality and representativeness of the drill core. Examples of poor quality drill core which can produce non-representative and potentially biased samples are shown on the Fig. 4.6. It is important to remember that after core has been extracted from the hole it cannot be improved therefore geologist should rigorously monitor the drilling performance and when necessary request a drilling crew to modify their drilling parameters.

The most common criterion used in mining industry for assessing quality of the drill core is measuring the amount of core loss. It is traditionally reported as core recovery representing a ratio of length of the recovered core to the nominal

Fig. 4.5 Drill core reviewed and logged by a mine geologist at Ranger uranium mine, Australia. The marked line denotes apical points of a bedding along which the core shell be cut for sampling

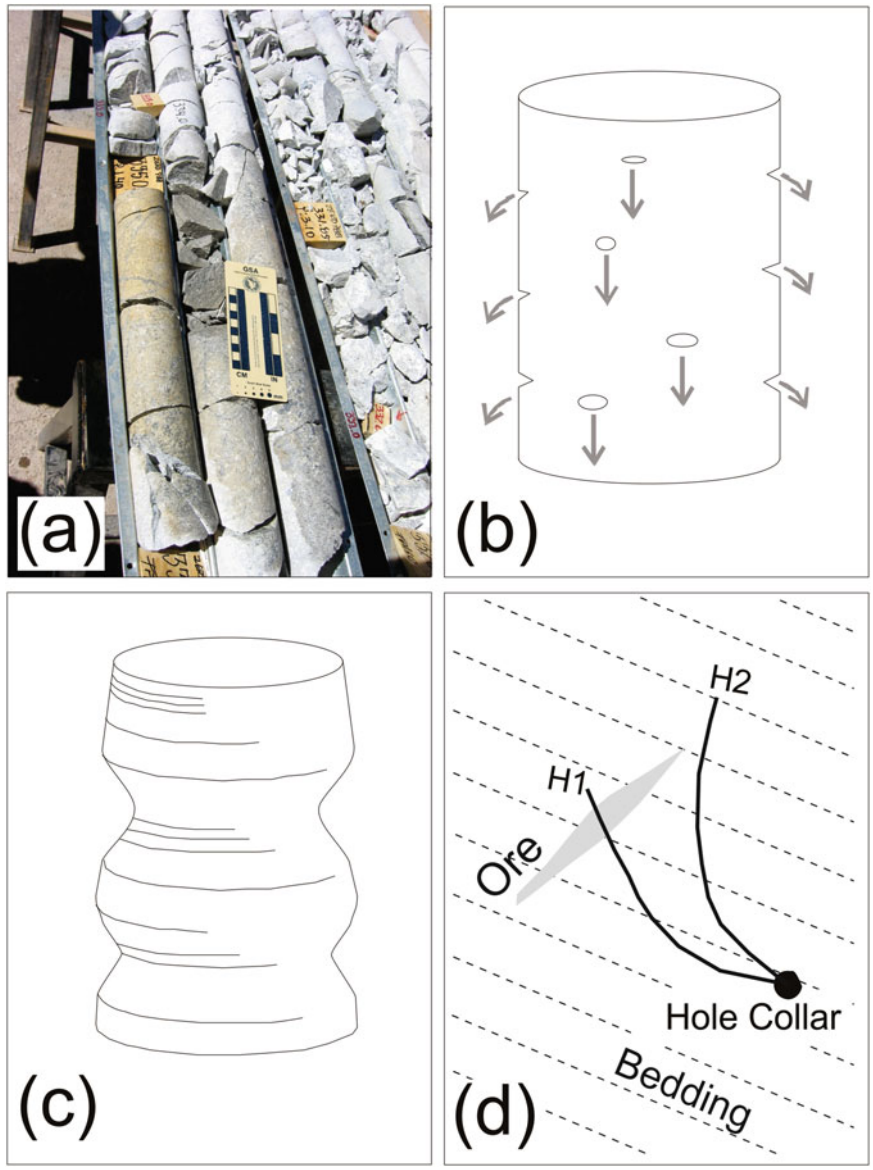

Fig. 4.6 Examples of the suboptimal quality diamond core samples which can produce a biased assay results: (**a**) alternating of a solid sections of drill core (100 % recovery) with broken material collected from fractured rocks (recovery significantly less than 100 %); (**b**) sketch showing the drill core where mineral grains have been plucked from the core surface; (**c**) sketch of the drill core with excessively grinded surface; (**d**) sketch (plan view) showing an examples of correct and suboptimal orientation of the drill hole. Hole (H1) allows for azimuth change due to bedding and therefore intersects a drilling target (mineralisation) at the angle close to 90º. Hole (H2) commences aimed directly at target with no consideration for deviation due to bedding, its longer and intersects target at high angle which is likely to prohibits a collecting good representative sample

length of the core that had to be recovered. The recovery is expressed as percentage. The values less than 100 % imply that some core was lost during drilling. For example, recovery reported as 70 % means that approximately 30 % of the core was lost during drilling. Poor core recovery is the main source of sampling errors in diamond drilling. When recovery is less than 100 % the

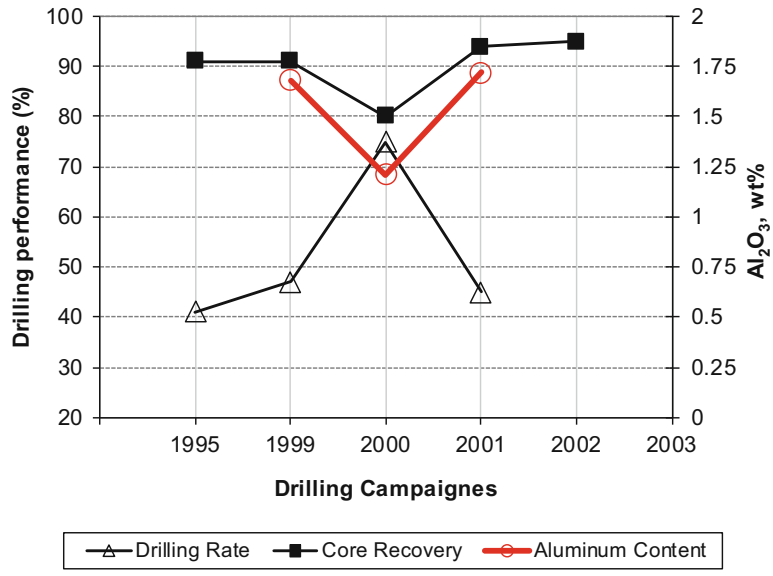

Fig. 4.7 Diagram showing relationships between increased drilling rate, poor core recovery and sample bias, iron ore mine, Australia

material is usually lost disproportionally to their actual distribution in the drilled rocks. Such samples are likely to be biased. The poor core recovery means a less reliable core sample, and the higher likelihood that the sample assays are biased. In some cases the reported recovery exceeds 100 %. One of the common errors causing "swelling" of the core is incorrect documentation of the drill core runs by the drillers.

An example presented on the Fig. 4.7 shows the relationship between poor core recovery and sample biases. At this iron ore mine the Al_2O_3 is a metallurgically deleterious component therefore it is important to accurately estimate its content in the ore. During the project review it was noticed that Al_2O_3 assays of the drill core samples collected in year 2000 were significantly lower than Al_2O_3 values obtained at the other years (Fig. 4.7). It was suspected that Al_2O_3 assays of the 2000 samples were biased. Special investigation has revealed that year 2000 drilling campaign was characterised by significantly lower core recovery than in other years (Fig. 4.7). It was well known that in this deposit the Al_2O_3 was accommodated mainly in the clay minerals. Therefore, when a poor recovery of the core was identified it became clear that biased Al_2O_3 assays are most likely caused by the preferential losses of clay minerals which have been washed away from core because of excessively high drilling rate. Drilling twin holes has confirmed this interpretation (Abzalov 2009).

Washing away a soft material before it was captured in the core barrel is not the only cause of the core losses during drilling. Poor core recovery can also be cause by core drops which often happen when drilling through intensely fractured and friable rocks. The main reason for core drops is that core is not properly held in the inner tube and therefore drops to the bottom of the drill hole when inner tube is extracted to surface. To prevent an excessive core loss a triple tube diamond drilling technologies are used (Hartley 1994).

Another common reason for core loss is core jamming in the core barrel. In this case the core barrel opening is blocked therefore the rocks are not entering the core barrel and are subsequently ground away as drilling progresses. It should be remembered that all cases of core losses, no matter what have caused them (Fig. 4.6), significantly downgrading quality and representativeness of the core samples. Core losses often lead to the biased assay results.

Given the importance of core recovery it should be rigorously documented by drillers and geologists. Most common technique of measuring core recovery is simple and based on

measuring the ratio of length of recovered core to nominal length of the drilled interval (4.1.1).

$$\text{CORE RECOVERY (\%)} = 100 \frac{\text{CORE LENGTH (cm)}}{\text{DRILLED INTERVAL (cm)}} \quad (4.2.1)$$

The technique is easy to apply when core recovered as the chain of solid cylinders (Figs. 4.2 and 4.5). On the contrary, if core was recovered as broken fragments (Fig. 4.6a) the accurate measurement of its length becomes nontrivial task. In that case driller is usually pushing fragments in the core tray trying to approximately rebuild shape of the core cylinder and then measuring the length. Such measurements cannot be used as quantitative estimate of the core recovery and should be treated only as an indicative assessment of a magnitude of the core losses.

In order to accurately measure the core recovery it should be estimated as a ratio of the masses and expressed as percentage. The mass of recovered material is divided to a theoretical mass of the 100 % recovered core (4.1.2). Application of this procedure requires weighting the recovered material (M) and measuring the dry bulk density (ρ) of the drilled rocks. Theoretical mass is calculated assuming that 100 % recovery implies that core has a perfectly cylindrical shape, whose volume is easily estimated geometrically, knowing the nominal diameter of the drill core (d) and length of the drilled interval. Theoretical mass is then obtained simply as a product of the measured dry bulk density (ρ) and a geometrically calculated volume (4.1.2).

$$\text{CORE RECOVERY (\%)} = 400 \frac{\text{M}}{\rho\ \pi\ \text{d}^2\ \ [\text{DRILLED INTERVAL (cm)}]} \quad (4.2.2)$$

Where:

M – measured core mass (grams);
ρ – dry bulk density of the core material (g/cm^3);
d – nominal diameter of the core (cm);
π – constant, 3.14.

The method produces more accurate results than estimating core recovery by measuring the length of the recovered core, however it also has limitations. The main disadvantage of this method is the necessity to know exactly the dry bulk density (ρ) of the core material. This limitation can be overcome by measuring density of the drilled rocks in a field. In practice, many mines are using in-house devices for measuring rock densities which are usually installed at the core storage facilities. Rock densities are measured regularly when core is cut and samples collected for assaying. More detailed explanation of the rock density measuring devices will be presented in the Chap. 7 of the book.

Another limitation of the technique based on weighing recovered core is the possible difficulties in accurately measuring the weight of core. When drilled rocks are porous, fractured or friable the recovered core is impregnated by drilling fluids which introduces errors in the measured weights and estimating core recovery. This limitation can be overcome by estimating recovery as ratio of the volumes (4.1.3). The volume of the recovered rocks is divided by a theoretical volume of the core cylinder, whose diameter equals to a nominal diameter of the drill core and length is the drill run. This approach does not require knowledge of the drilled rocks density, however, an accurate measurement of volume of the broken material is not a trivial task.

$$\text{CORE RECOVERY (\%)} = 400 \frac{\text{V}}{\pi\ \text{d}^2\ \ [\text{DRILLED INTERVAL (cm)}]} \quad (4.2.3)$$

Where:

V – measured core volume (cm^3);
d – nominal diameter of the core (cm);
π – constant, 3.14.

Drilled interval, in all of the above mentioned approaches (4.2.1, 4.2.2, and 4.2.3) is estimated from core blocks marked by drillers (Fig. 4.4). When all core recovered at the single run is broken an average recovery rate is measured for the entire drilled interval (Fig. 4.8a). On the con-

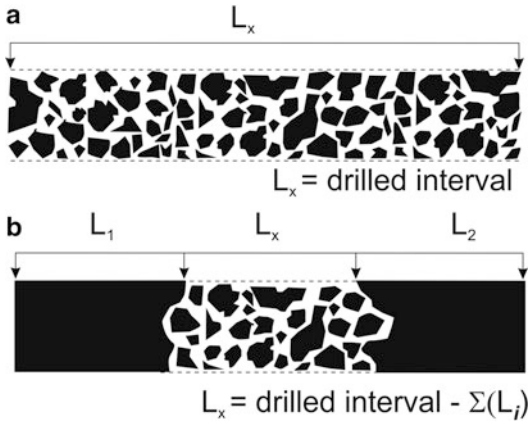

Fig. 4.8 Sketch explaining measurement of the core length: (**a**) case when all core recovered at the single drilling run was broken; (**b**) core was recovered as intercalation of the lengthy solid blocks and broken zones. In both cases the 'drilled interval' was measured by drillers as penetration of the drill rods and recorded on the core blocks (Fig. 4.4)

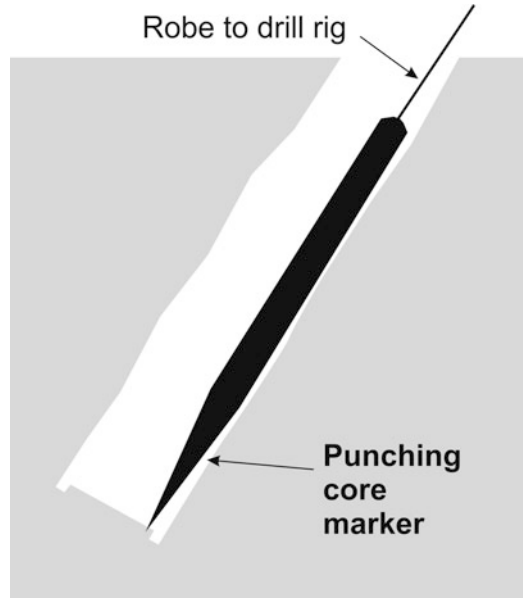

Fig. 4.9 Sketch explaining procedure of marking core by punching it by spear-like chisel that leaves indent on the core surface

trary, if core was recovered as a mixture of solid and broken intervals the recovery rates should be calculated for solid core and broken intervals separately (Fig. 4.8b) and they also sampled separately (Pitard 1993).

Core losses can be prevented or at least minimised by using appropriate drilling equipment and adjusting drilling parameters for the given rock types. Representativity and quality of the drill core also depends on the angle at which a target is drilled (Fig. 4.6d). The higher angle the less representative is drill core. Deviation of hole from its initial direction depends on geological conditions which should be taken into account when setting the drill rig. Therefore, communication between geologists and drillers is important for obtaining good quality core samples. This is particularly important for core drilling in the underground mines where choice of the available drill sites is limited and therefore several holes often drilled as a fan from one drill cuddy.

It should be remembered that poor quality drill core is not always expressed in low recovery values. Plucking crystals from core surface during drilling (Fig. 4.6b) and excessive grinding of the core (Fig. 4.6c) can also cause core sample biases. These types of core defects cannot be identified by measuring core recovery, in particular estimating it as a ratio of a core length to a drilled interval, however they can be easily diagnosed by a visual core inspection. Therefore, procedures of the core quality review should include visual inspection of the core by geologists and measuring core recovery. Linear recovery approach (4.2.1) should be verified by the more accurate estimations based on ratios of the recovered to theoretical core masses (4.2.2).

4.2.2 Orientated Core

Orientated core is a procedure of marking it in the core barrel before it is broken and extracted to surface. The mark allows orientating the core to its *in situ* location after core was removed from a hole (Chugh 1985; Hartley 1994). This technique has a broad range of geological and geotechnical applications but is particularly useful in mining environments requiring a high degree of accuracy in delineation of the ore reserves and designing the production stopes.

The core is usually marked by a spear-like chisel (Fig. 4.9) called 'core marking punch'

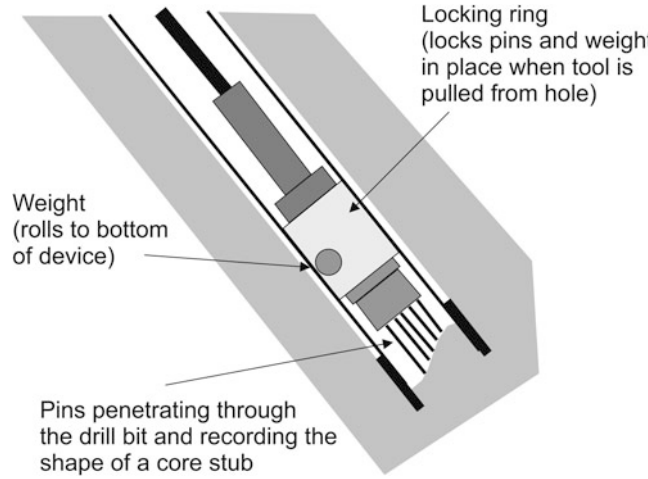

Fig. 4.10 Sketch explaining principles of the Craelius core orientator

(Hartley 1994). The 'core marking punch' has a sharp and hard end that leaves indent on a core face. This is achieved by lowering it down the hole on a wire and then dropped so that it leaves a mark on a core surface on the lower side of the hole face (Fig. 4.9). The method does not work well if the rocks are very soft and not suitable for very hard rocks also. Conversely, the pencil marker can be used instead of sharp tip at the spear end. Pencil marker uses the same spear-like metal bar, but the steel tip is replaced by a pencil holder. The pencil marker overcomes a problem of the marking very hard rock however is still ineffective with soft rocks.

Both of these methods, core marking punch and pencil marker, have a low accuracy. Another limitation of these techniques is that they can work only in a limited range of the dip angles and not applicable in vertical holes and also cannot be effectively used in the horizontal or upward inclined holes.

Another common core marking technique is known as 'Craelius core orientator' (Hartley 1994). It is a small free moving barrel that has several steel pins protruding through the drill bit and taking shape of the upper surface of the core (Fig. 4.10). The orientator is inserted into the inner tube of the core barrel and firmly attached to the upper edge of the core lifter. The design of the orientator allows to clearly define its orientation in the core baller when steel pins are protruded through the drill bit (Fig. 4.10).

When the core barrel is lowered to the bottom of the hole the steel pins taking positions that fits to profile of the top of the core. In other words, the steel contact pins taking the positions which is a footprint of the core surface. At these positions the contact pins will be locked and protected from displacements by detaching orientator from the core lifter and lifting it from the rock surface. After core has been removed from the core barrel it can be orientated to its *in situ* position by matching pins profile to the upper end of the core. The low side of the hole is identified from a steel ball whose position denote the low side of the orientator at the time when the contact pins have taken the snap shot of the core surface (Fig. 4.10).

Design of the Craellius core orientator allows it to be used in dipping, upward inclined and horizontal holes. It can be used even in vertical holes if drill string has been oriented (Chugh 1985). It also overcomes limitations of the conventional core markers and produces accurate mark on soft core. However, its ineffective when core surface is flat and smooth.

Other core orientating techniques, including tools based on residual magnetism of the drill core or direct alignments of the drill rods (Chugh 1985; Hartley 1994), are less common and are not reviewed in this section.

The oriented core after it is recovered from the core barrel should be reviewed by a geologist who finds the lowermost point on the top face

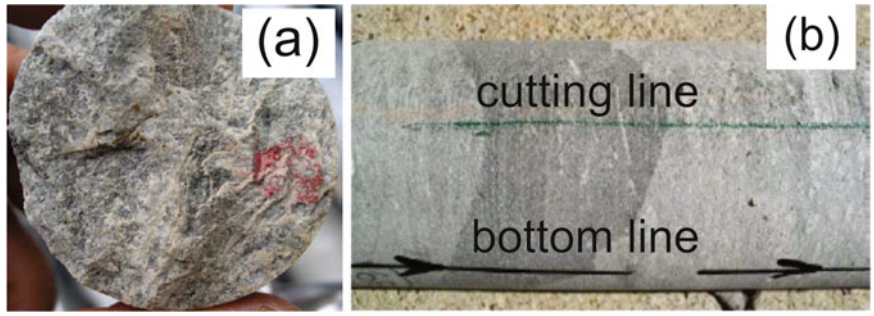

Fig. 4.11 (**a**) Mark on the core surface left by punching core marker; (**b**) line denoting the bottom of the drill core (*bottom line*) which position was reconstructed from a mark left by core orientator and then marked on the core surface by geologist during logging hole. *Barbs* denote down-hole direction

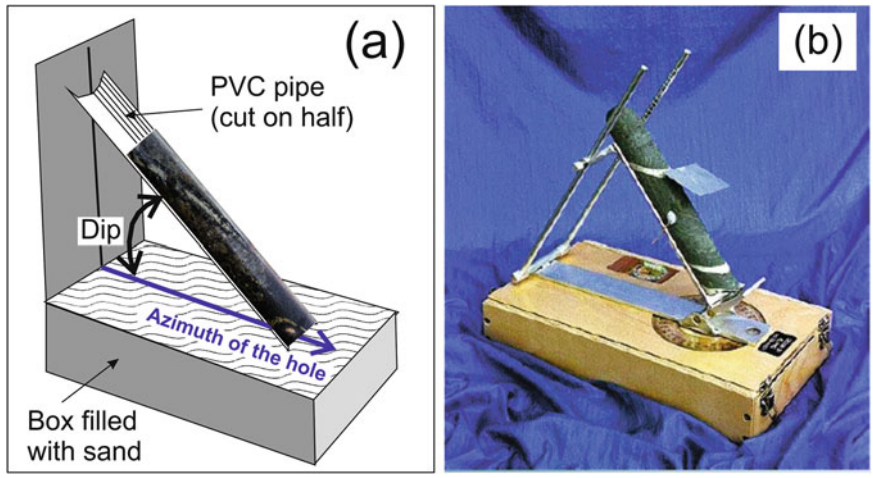

Fig. 4.12 Devices for placing orientated core in its true position corresponding to that of the surveyed dip and azimuth of the drill hole: (**a**) orientating core using half of PVC pipe and box with sand; (**b**) commercially available core orientating kit equipped with built-in inclinometers allowing accurate measurements of the geological structures

of the core as it is identified by a core orientator (e.g. Fig. 4.11a) and then marks the reference line on the core surface (Fig. 4.11b). The reference line is usually a bottom line of the core which is deduced from an orientator. Special care should be taken by geological personnel marking the bottom line of the core as this line will be the main reference used in all further measurements of orientations of the geological structures. This is usually done using a special frame, made from a v-rail (angle iron) which should be long enough to hold a multiple core runs. The same frame can be used for geotechnical documentations, in particular for systematic measurements of the fracture densities.[1]

When the bottom line is marked, the orientations of the geological structures can be measured. There are two ways to do this. The first approach requires placing the recovered core in its true in-situ orientation and directly measuring strike and dip of the geological structures from core in the same way as geologist taking structural measurements of the outcrops (Fig. 4.12). In order to use this approach the core should

[1] Geotechnical documentation is described in Chap. 6.

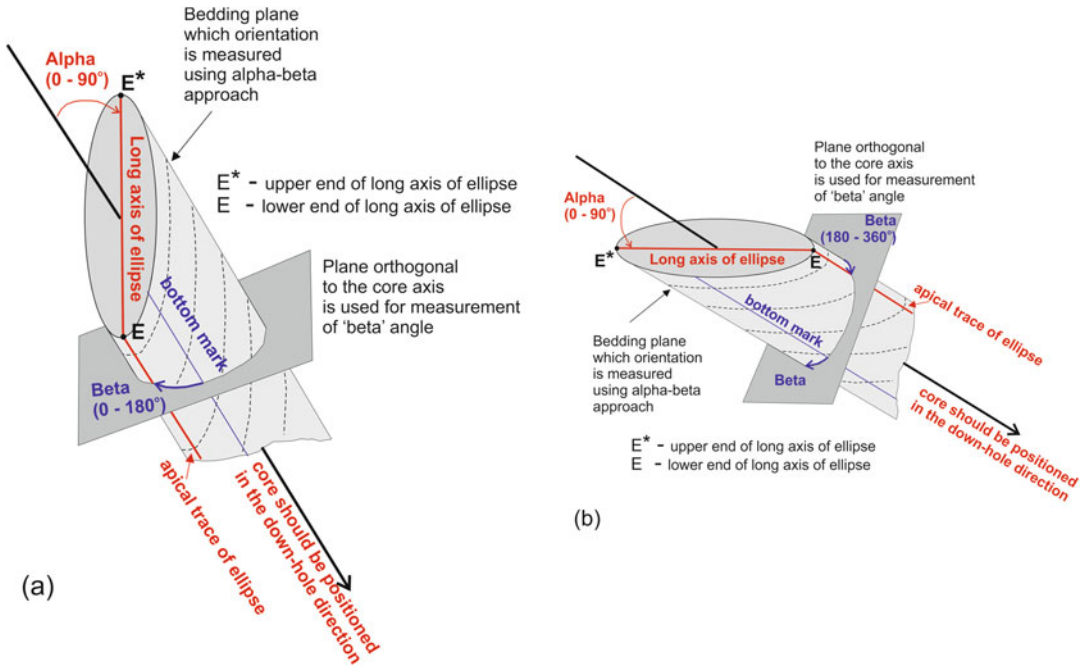

Fig. 4.13 Alpha and beta angles of the planar geological structure (e.g. bedding plane) identified on the drill core. *Bottom line* is a reference line denoting the lowermost side of the core: (**a**) case when beta angle is less than 180°; (**b**) case when beta is between 180° and 360°

be placed in a specially designed core holders. Equipment used for this task varies from a simple box filled with sand (Fig. 4.12a) to a specially designed core orientating kits (Fig. 4.12b). The latter is often referenced as 'rocket launcher'. The core should be placed in the core holder, usually made from angle aluminium. Core should be located with the bottom reference line accurately at the bottom of the core holder. After that the core holder is oriented in the direction corresponding to surveyed dip and azimuth of the drill hole and structural measurements can be directly taken.

An alternative technique includes measurement of the critical angles between studied geological structure, core axis and reference marks on the core. Two angles, conventionally called alpha and beta (Fig. 4.13), are the main features which are most commonly measured when the 'critical angles' approach is used (Annels and Hellewell 1988; Marjoribanks 2007):

- alpha – is the acute angle between the core axis and the studied planar geological structure, the values change from 0 to 90°;
- beta – is the angle between the reference (bottom) line of the core and line denoting the dip direction of the studied structure. It is measured clockwise from the bottom line and holding the core as it was drilled, in other words looking toward the base of the hole. The values of the beta angle vary from 0 to 360°.

Strike and dip of the geological structures is deduced from the measured alpha and beta values by plotting them on to stereographic projection for calculating a true geological orientation. Geometric meaning of the alpha and beta angles and their relationships with the strike and dip of the studied structure are shown on the Fig. 4.14.

Procedure of plotting alpha and beta angles is as follows (Annels and Hellewell 1988; Marjoribanks 2007).

1. Mark on the stereonet (Fig. 4.14) a point representing the azimuth and dip (inclination) of the drill hole measured at the depth where the alpha and beta measurements are

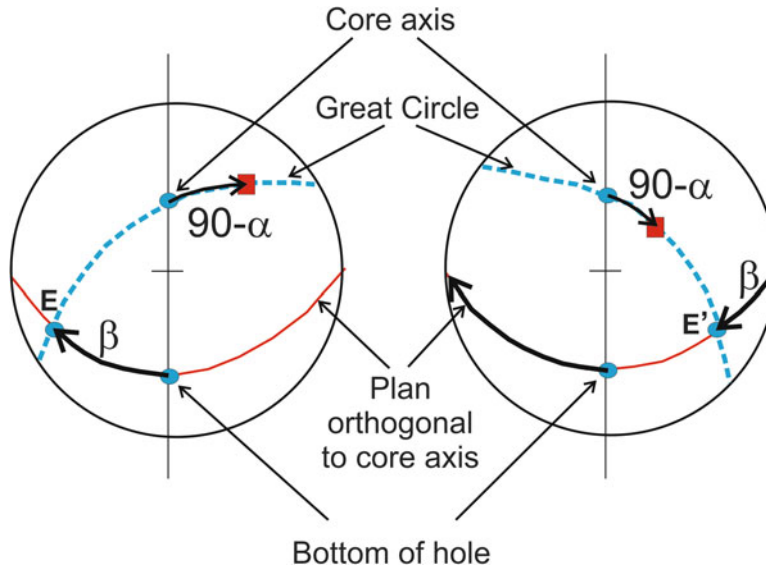

Fig. 4.14 Stereographic plotting of the alpha and beta angles measured on the oriented core

undertaken. It is labelled 'core axis' on the stereo net.

2. Plot the vertical plane passing through the core axis. This is the main reference plan denoted on the diagrams (Fig. 4.14) as straight line passing through the 'core axis' and the centre of the net.
3. Plot the plane normal to the core axis. This is second reference plan denoted on the Fig. 4.14 as 'plan orthogonal to core axis'.
4. Where these two reference planes intersect is point, representing the 'bottom of hole'. This is the point from which the angle beta was measured (Fig. 4.13).
5. Using the printed graticules of the net, measure the beta angle along the reference plan denoted as 'plan orthogonal to core axis'. Measurement on the stereonet is made in a clockwise direction from the 'bottom of hole' point (Fig. 4.14) like it was measured on the drill core (Fig. 4.13).
6. If the beta angle lies between 0 and 89°, or between 271 and 360°, then the point marked on to the net is E. If beta lies between 91 and 269°, then point E* is plotted on the net. In the special case where beta is exactly 90 or 270° then both E and E* will plot on the net, at diametrically opposite points of its circumference.
7. By rotating the overlay over the stereonet, locate the great circle that contains the point denoting the core axis and E (or E*). Only one great circle will be found which passes through the two points. Trace this onto the overlay.
8. Measure the angle 90–α along the great circle traced on to the stereonet's overlay. Measurement starts from the point denoting the core axis direction away from point E. If point E* the net, then the angle 90–α must be plotted from core axis toward the point E*. If both E and E* appear on the net, which is happening when angle beta is equal 90° or 270°, then either construction is acceptable.
9. The new point, found by measuring the angle 90–α along the great circle is the pole to the planar structure measured in the core. This point should be clearly marked on the stereonet's overlay, and the structural parameters (strike and dip of the planar geological structure) deduced from this point and entered into computer for further structural analysis.

Dip and strike of the geological structure can also be mathematically deduced from alpha and beta measurements (Zimmer 1963).

4.2.3 Logging Diamond Core Holes

Quality of drilling and obtained information depends on rigour that was applied to planning drill holes, supervising drilling and documentation of results. Documentation should not be limited to recording the basic characteristics of a hole, such as core recovery or surveyed coordinates, and has to include different auxiliary information, including drilling characteristics and technical parameters of a hole, rig type, drill bits, drilling dates and names of the drill masters. The auxiliary information is important for diagnostic of the causes of suboptimal drilling results and poor core recovery. For diagnostic purpose the drilling results often need to be grouped and analysed selectively by drilling campaigns or drilling crews therefore documentation should include the data that can be used for the selective data analysis. A checklist of the main categories of data that should be recorded for diamond hole is summarised in the Table 4.3.

After drilling is completed the hole should be surveyed and recovered core logged and sampled. Logging of the drill core is one of the most common types of geological activity as this often is the only direct geological information about rocks located hundreds meters below surface. However, logging core for mining geology needs differs from other geological applications. In general, it is more detailed and requires quantitative measurements of structures, contacts and geotechnical characteristics of the rocks.

Another specific feature of the core logging for mining geology applications is the amount of drilling which escalates when a mining project reaches feasibility stage. Maintaining production at the operating mines also requires large amounts of infill drilling for delineation of ore bodies and replenishing exploited reserves. This is why the amount of drilling at the operating mines usually exceeds the number of holes drilled for scientific or exploration purposes by orders of magnitude (Table 4.4).

Given the amount of drilling at the operating mines it is almost inevitable that at the operating mines holes are logged by different geologists who often differ in their skills and practical experiences. In order to maintain fast logging rates and assure consistency between different geologists the logging procedures should be standardised and supported by documentation templates, pre-printed log forms and operational guidelines. Example of the log form is shown on the Fig. 4.15. It is important that the log form contains a column for graphical presentation of the geological data. A good practice is to

Table 4.3 Check list for documentation of the diamond drill holes

Activity	Example/Reference
Dates when hole drilling was started and finished has been recorded	
Drilling equipment and parameters are recorded	
Name of the drill captain is documented	
Name of the geologist(s) supervised drilling and logged core are documented	
Collar of the drill hole has been surveyed and documented	Section 8.1
Downhole survey has been completed, results reviewed and documented	Section 8.2
Core blocks denoting the drilled intervals have been checked and verified	Figure 4.4
Core reviewed and damaged surfaces documented	Figure 4.6
Core recovery estimated and recorded	Section 4.2.1
Geological logging completed	Figure 4.15
Core photographed	Figure 4.16
Geotechnical logging completed	Chapter 6
Sampling intervals are marked and the sample numbers assigned	Section 4.2.4
Core photo documentation completed	Figure 4.17
Drill hole handed over to sampling team	

Table 4.4 Amount of the drill hole data used for evaluating mining project and at the operating mines

Deposit type	Property name, country	Mine status	Year of the data collection	Drilling type	Number of drill holes	Total drilled metres	Number of samples	Average length of a sample (m)
Cu-U-Au-Ag	Olympic Dam, Australia	Mine	2003	Core	8,280	1,636,256	812,556	1.5
Copper-porphyry	Northparkes, Australia	Mine	2005	Core	106	54,692	29,241	1.4
Ni-sulphides	Perseverance, Australia	Mine	2002	Core	1,155	62,537	43,338	1.4
	West Masgrave, Australia	Project	2003	Core	134	31,287	16,802	1.0
Fe oxide	West Angeles, Australia	Mine	2004	Core	5,483	343,473	166,167	2.0
	Pic de Fon (Simandou), Guinea	Project	2007	Core	56	7,474	2,479	2.8
	Yandi, Australia	Mine	2005	RC	594	30,378	30,164	1.0
	Mesa, Australia	Project	2005	RC	1,420	46,178	20,455	2.0
	Nummuldi E-F, Australia	Project	2004	RC	281	29,654	14,589	2.0
Uranium	Rossing, Namibia	Mine	2006	Core	441	37,257	28,264	1.3
	Ranger, Australia	Mine	2005	Core	619	95,896	62,357	1.0
Orogenic gold	Gladstone (Norseman), Australia	Project	2000	RC	887	47,105	30,338	1.3
	Victor (St.Ives), Australia	Mine	1998	Core	1,728	184,002	124,137	0.9
	Emu (Agnew), Australia	Mine	1998	Core	2,315	106,790	106,533	1.1
	Meliadine, Canada	Project	2001	Core	327	70,306	27,184	1.0
Ti- sands	Fort Daufin, Madagascar	Project	2005	Vibracore	1523	27,104	17,807	1.5

use 2–4 columns for separately documenting observed features and interpretation. In some cases it is also necessary to separately record primary characteristics of the rocks and superimposed alteration or metamorphic fabrics (Fig. 4.15). The current author found it also useful to document ore textures into separate column rather than mixing it with the host rock graphic logs. It is strongly recommended that holes are logged using the same geological legend that is used for the mine mapping (Fig. 3.1).

Unfortunately conventional graphic logging of the drill holes is rarely used in contemporary mines where it replaced by digital data capturing and recording of geological information directly entered to the palm-top computers. Electronic logging is fast and helps to quickly enter the logged information to mine planning software. Many of the digital logging devices have built-in procedures for diagnostic errors in assigned depth intervals or sample numbers and this is another important advantage of the digital logging. However, digital logging has some important limitations in comparisons with conventional graphical logging on the paper log-sheets (Fig. 4.17). The most serious is that digital logging represents a serious simplification in comparison with a conventional graphical documentation of the drill holes. The author's experience shows that core logging practice currently has been converted in the mining industry to a simple entering the rock codes (Fig. 4.17) into the palm-top computers. This simplification means many details that could be observed and documented

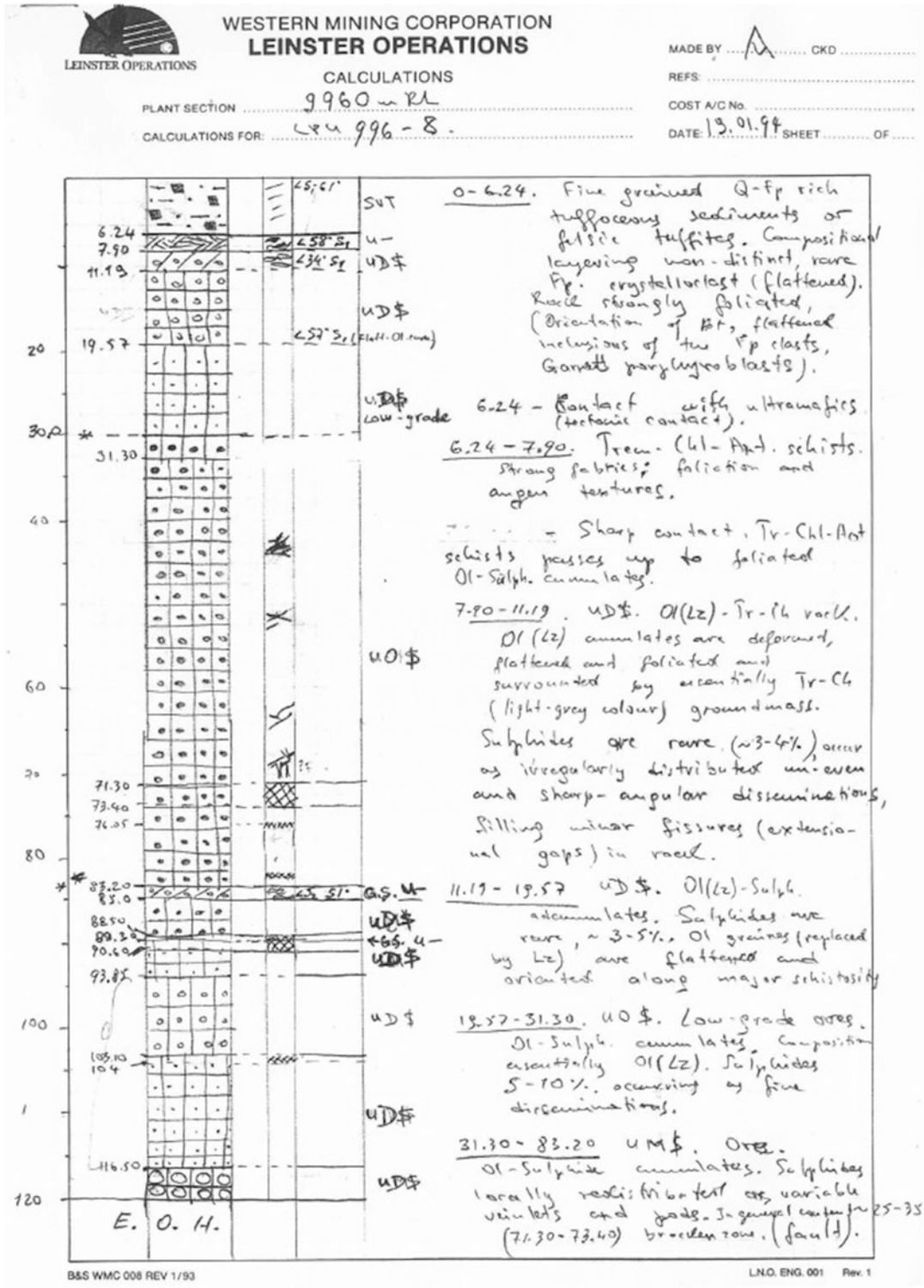

Fig. 4.15 Example of the graphic core logging by recording data onto pre-printed log form, Perseverance Ni-sulphide mine, Australia

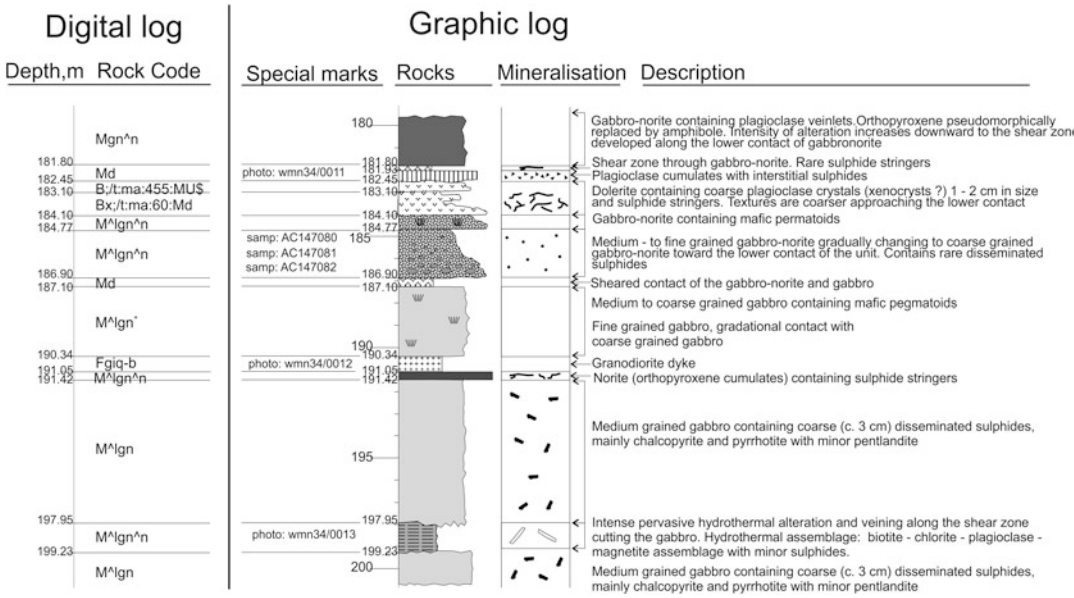

Fig. 4.16 Comparison of the electronic log with a more conventional geological documentation of the same drill core

Fig. 4.17 Frame holding four digital cameras of high resolution used for photographing core at the Escondida copper mine, Chile

using a conventional approach are simply missing. It is also inflexible leaving fewer opportunities for geologists to document and highlight important geological features than would be possible if the conventional graphic logging was used (Fig. 4.17).

Comparison of electronic logging (entering digital codes into electronic tables) with conventional documentation, made using graphic logging and descriptions of the observed geological features, is shown in Fig. 4.17. The same hole has been independently logged by the experienced

geologists, using both, the conventional graphic logging approach and electronic techniques. It is clear (Fig. 4.17) that the amount of detail captured on the graphic log noticeably exceeds that of the digital recording of the rock codes. Simplification of geological documentation can lead to incorrect geological interpretations and the eventual consequence of this can be incorrectly estimated potentials or missed opportunities. Therefore, digital data should not eliminate needs for conventional geological documentation which are made on paper log sheets and field note pads which are traditionally stored in the fireproof cabinets or can be scanned and saved as pdf files.

Another advantage of creating drill hole sections as part of the routine logging holes is the ability to quickly compare field logs made by different geologists and identify inconsistencies in documented geological features. Draft cross sections of the drilled deposits can also be easily created in the field by simple copying and pasting images from the graphic log sheets. This approach allows validation of logs and interpretation of geology directly in the field, while drill core is still on the core racks allowing the correction of geological interpretations if inconsistencies in the geological logs have been identified. This is practically impossible to do when geological features are recorded only as the digital codes entered into a single spread sheet or several interlinked tables. Understanding and utilising this coded data requires decoding and most likely needs extra time for correcting typing errors, inconsistent diagnostics and incomplete documentation geological features (Abzalov 2014a) which will delay graphical representation of the data.

In general, both systems, digital records of data and graphical logs, have their own applications and are not mutually exclusive. Numerical information, such as the down hole depth of the geological contacts, sampling intervals and corresponding them sample numbers, alpha and beta angles (Fig. 4.13), core recovery (Fig. 4.8), hole diameter, geotechnical parameters, are best recorded directly into electronic tables. Qualitative information, including geological descriptions, rock types and textures, mineralisation styles, special comments, interpretations made in the field, should be recorded into graphic log sheets (Figs. 4.15 and 4.16). Supplementing digital geological documentation of the holes by graphical logs on the paper sheets will slow down the logging process, however it will be compensated by better quality and detail of the geological documentation and improved consistency of the geological interpretations.

Common practise in the modern mining industry is to photograph all core for future studies and auditing. Core is usually photographed before it was cut for sampling but after it was logged and marked (Fig. 4.5) because the marked contacts and the depth intervals help with correlation of features observed on the photographs with logged information. Equipment used for photographing core varies from a simple digital camera to special devices, when three or four high resolution cameras installed on a special frame allowing non-distorted photos of the core (Fig. 4.17). Each photo should contain a reference to hole number, core tray and drilled interval. In cases where a mine geology team does not use conventional graphical logs the high quality core photographs can partially overcome this limitation therefore it is important that mine geology team uses appropriate photographic equipment. Some geological features can be particularly important for correct geological interpretations therefore they should be photographed separately and usually at short distances for accurate representation of the rock textures and other important features.

4.2.4 Sampling Diamond Core

When drill core sampling is planned it should be remembered that part of the core should be retained for verification of the logging and sampling results. Retaining a representative part of core is also needed for formal audits of the mine reserves validity. Therefore, it is a common practice to split core and sample only one part of it, returning the second part to core trays.

The most common approach is to cut core in half (Fig. 4.18). Sampling quarter or one third of

the core is also used for evaluation of mineral deposits although it is less common. In some cases it is necessary to sample the whole core. In that case a good practice is to cut a narrow segment of core which will be retained in the core trays and used for auditing (Fig. 4.18). Conversely, instead of cutting narrow segment the small representative core samples can be collected at regular intervals. However, this approach is less practical because it destroys the continuity of the core.

A cutting line should be drawn by permanent marker and colour should be different to that of the reference line marked for orientated core studies (Fig. 4.11b). Down hole direction should be shown by barbs (Fig. 4.19) or arrows (Fig. 4.5). It is important that the reference line marked for orientated core studies always remains on the half of core that is left in the box. When bedding traces can be observed on the core the cutting line should be drawn along the apical points of bedding (Fig. 4.19).

General rules of sampling core are as follows:

- Samples should be taken to geological contacts.
- Minimum and maximum sample length should be determined according to sampling protocol determined for the given mineralisation.
- It is a good practise to maintain length of the samples as close as possible to average, which is an optimal sample size for a given style of mineralisation and sampling protocol. Examples of the average drill core sample lengths are listed in the Table 4.4.
- Broken intervals should be sampled separately of solid core intervals (Fig. 4.8b) if this not compromise minimum allowed sample length.

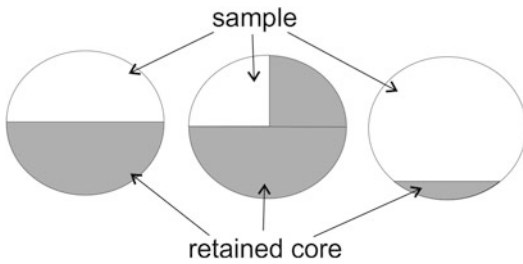

Fig. 4.18 Core sampling approaches that allow retention of part of core for further studies

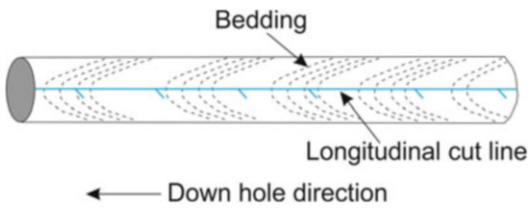

Fig. 4.19 Sketch explaining principle of cutting core along the longitudinal line of core drawn through the apical points of bedding

4.3 Open Hole Percussion Drilling

Percussion drilling and rotary percussion are fundamentally different from diamond core drilling because it creates small rock chips instead of solid core. Percussion drilling operates by a drill bit repeatedly striking the rock face and crushed rocks are transported to surface through hole annulus or drill rods (Fig. 4.20). The drilling provides less geological information than diamond core drilling, but this is offset by significantly higher drilling speed and lower cost.

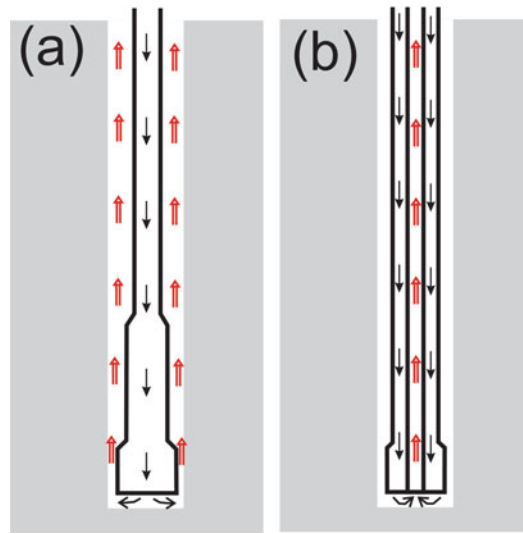

Fig. 4.20 Sketch illustrating fluid circulation approaches: (**a**) direct; (**b**) reverse

There are many varieties of percussion drilling techniques which differ depending on the method of application of the force to the drill bit and mode of transportation of the rock chips to surface (Hartley 1994). Depending on construction of the drill rig and hardness of the drilled rocks percussion drilling can use different drill bits, which can be in a shape of rock chisel, blade, roller bits or flat head cylindrical hammer with tungsten carbide buttons. Blade or roller bits are used in soft rocks whereas rock chisel and hammer are preferred in hard ground.

Two types of drilling, open hole percussion (Fig. 4.20a) and reverse circulation (Fig. 4.20b), are the most common methods after diamond core drilling that extensively used for mining geology applications. The open hole percussion method is operated by air blown down to the rock face through the centre of the drill rod and the crushed rocks are removed from hole along the gap (annulus) between exterior of the drill rod and the wall of the hole (Fig. 4.20a). This method is susceptible to contamination and is inefficient in wet ground, however low drilling costs making it an attractive when project development requires a rapid drilling of a large amount of shallow holes.

Open hole percussion drilling is commonly used for drilling exploration holes and referenced as rotary air blast (RAB). In the operating open pit mines the most common application of the open hole percussion technique is for drilling the blastholes which are sampled by mining geologists for grade control purposes. The practice of using this drilling technique for mining geology applications and its limitations are discussed in the current section using the blast holes as an example. Reverse circulation drilling (Fig. 4.20b) will be reviewed in the next section.

Fig. 4.21 Drilling blastholes using truck mounted open hole percussion drill rig, Yandi iron-ore mine, Western Australia

4.3.1 Sampling Blastholes for Grade Control Purpose in the Open Pits

The most common use of the open hole percussion drilling for mining geology applications is sampling blast hole cuttings for grade control purpose in the open pit mines (Abzalov et al. 2007) and collecting rock cuttings generated from the holes drilled by 'Jambo' in the underground mines. The blastholes are usually drilled in the open pit benches using truck mounted open hole percussion drill rigs (Fig. 4.21). The holes are drilled as regularly distributed patterns fully covering the exploited ore body and their host rocks in the open pit bench (Figs. 4.22 and 4.23). Grids can be square, rectangular or parallelogram. Spacing between blastholes is usually less than 10 m and their depth approximately matches the heights of the mining benches. A good spatial coverage of the mining area by the blastholes and their tight spacing make them a very convenient media for grade control purpose as close spacing between blastholes is convenient for accurate definition of the ore-waste boundary. A tight sampling grid also provides sufficiently detailed grade distribution information to characterise the excavated ore parcels.

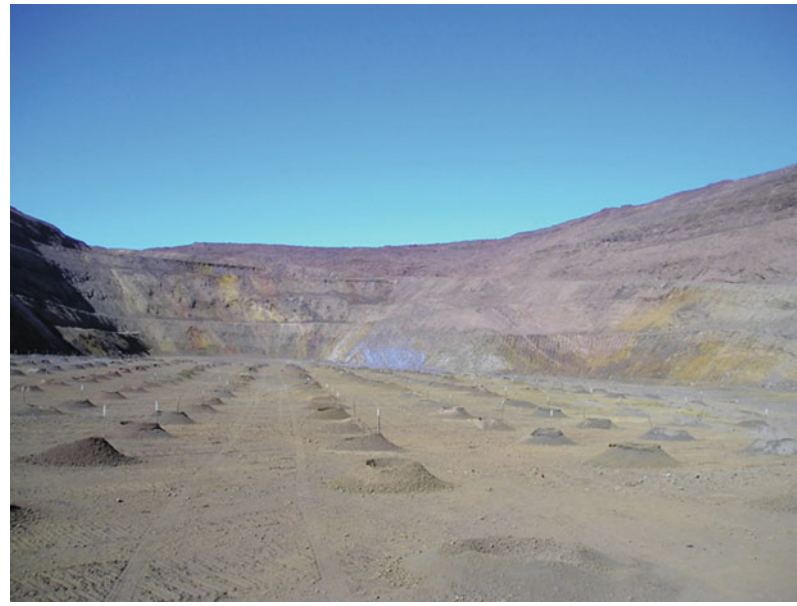

Fig. 4.22 Blastholes drilled in the West Angelas iron-ore mine, Western Australia

Fig. 4.23 Blastholes in the Ernest Henry Cu-Au mine, Queensland, Australia

Sampling of blasthole cuttings is a low cost procedure as it does not require any additional drilling or expensive sampling devices, which is another reason for its extensive use for grade control purpose at the open pit mines. However, it is important to note that blastholes are primarily drilled for breaking the hard rocks by firing explosives loaded to these holes, and they not designed for obtaining accurate and representative samples of the drilled rocks. Therefore, sampling of the blastholes is not a flawless process and contains several areas of serious concern.

The sources of the errors associated with blasthole sampling can be subdivided in two main groups: errors caused by drilling blast holes and errors related to suboptimal practices of collecting samples from the blasthole cones.

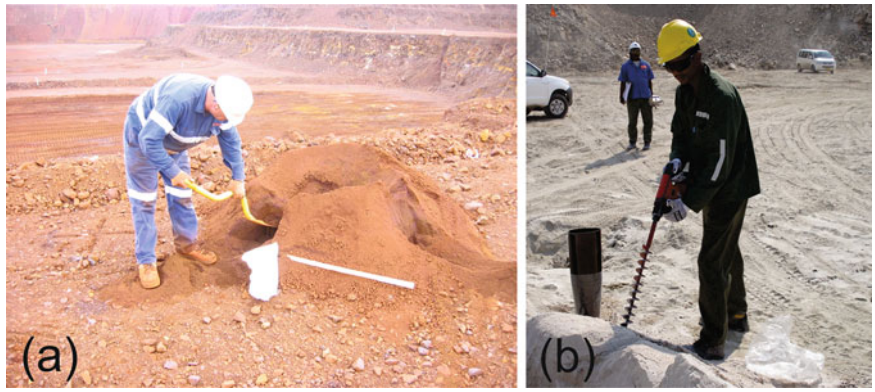

Fig. 4.24 Blasthole cone sampling for grade control purpose: (**a**) sampling by shovel, Yandi iron-ore mine, Western Australia; (**b**) sampling by hand held auger drill, Rossing uranium mine, Namibia

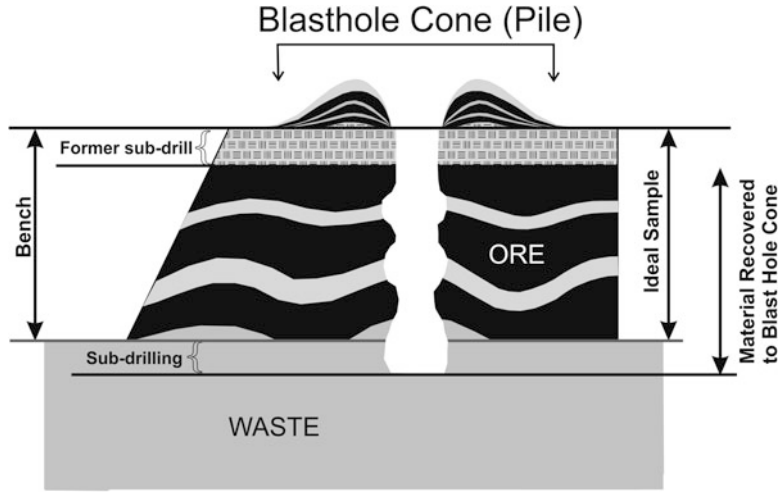

Fig. 4.25 Schematic section drawn through the blasthole

The common practice of sampling blastholes consists of collecting crushed rock fragments from the blasthole cones (Fig. 4.24). Samples can be collected by shovel (Fig. 4.24a), scoop, hand-held auger drills (Fig. 4.24b), or special devices allowing to split sample during drilling. Unfortunately, none of the currently used techniques can produce the fully representative and accurate blasthole samples. Fundamental issues associated with use of blastholes for grade control have been reviewed by Pitard (2005) and briefly explained below (Fig. 4.25).

The former sub-drill is another source of sampling errors. It is composed by broken rocks left on the top of the bench. This material is poorly recovered in the blasthole drilling therefore upper part of the bench is usually poorly presented in the samples.

The rigs used for drilling blastholes are not designed for sampling and consequently they are not equipped with proper sample catching devices. Procedures of blasthole drilling and the rigs design is such that material can be lost after the particles have been removed from the hole. This mainly affects the fugitive fine particles which are escaping along the drill rods however, the drilled material can be also selectively washed away when blastholes are drilled below water table. Particles can be also lost during retrieving a drill rod, or lost in fractures during drilling. Preferential loss of material, together with caving in the hole (Fig. 4.25), contamination of the

samples and drill cuttings falling back to the hole can cause significant bias in the assayed grades. In general, all these factors can lead to the material recovered from the blast hole and left on the surface as a blasthole cone being non-representative for the drilled bench and can be initially biased due to drilling related factors.

Rock particles can be unevenly distributed across the blasthole cone (Fig. 4.25), due to segregation factor. Therefore, bias or poorly repeatable assay results can be caused by using suboptimal sampling devices or poor sampling practices, in particular if samples are taken as the point samples. The commonly used approaches for collecting the sampling increments from the blasthole cone, in particular spearing by PVC pipe or sampling by a scoop or shovel, will likely fail to collect a complete column representative of all levels. Bottom of the pile, where the coarse fragments are often segregated, is often poorly represented in such samples (Fig. 4.26). Difficulties in collecting a sample where all layers are correctly represented is one of the most serious problem in blasthole sampling leading to their significant biases (Pitard 2005).

Fig. 4.26 Example of the blasthole sampling when *bottom* of the pile is not correctly represented in the collected sample

The simplicity of the method, good spatial coverage, low cost and efficiency of implementation are the main reasons why blasthole sampling is a very popular grade control technique in the open pit mines despite of the suboptimal samples quality. Representativeness of the blasthole samples can be partially improved by using correct sampling procedures or special devices (Fig. 4.27).

General principles of collecting representative sample from the blast hole cone (pile) are as follows.

1. Samples are better collected by a special instrument, such as hand held auger drill, allowing easy penetration through the entire pile (Figs. 4.24b). To ensure a good representativeness of the sample for the entire pile it should be collected by several increments which are distributed around the pile (Fig. 4.27). Pitard (2005) has suggested that most representative samples of the blast hole cone are obtained when increments are collected following the radial distribution pattern (Fig. 4.27).
2. It is important to assure that all layers of the pile, including that at the very bottom, are representatively sampled (Fig. 4.27).
3. A good practice is to collect larger sample and reduce it on site using transportable riffle splitter. This approach allows to obtain the samples correctly representing material recovered to the blast hole cones however unfortunately this technique is often ignored by mining geologists because of extra time required for grade control sampling.
4. When blastholes are drilled through highly heterogeneous material it can be necessary to use the special sampling devices, such as radial channel sampler (Fig. 4.28) proposed by Pitard (1993, 2005). The radial channels, usually two or three (Fig. 4.28), are positioned at random around the cone, approximately on opposite sides from each other. Top material, approximately 3–4 cm belonging to the sub-

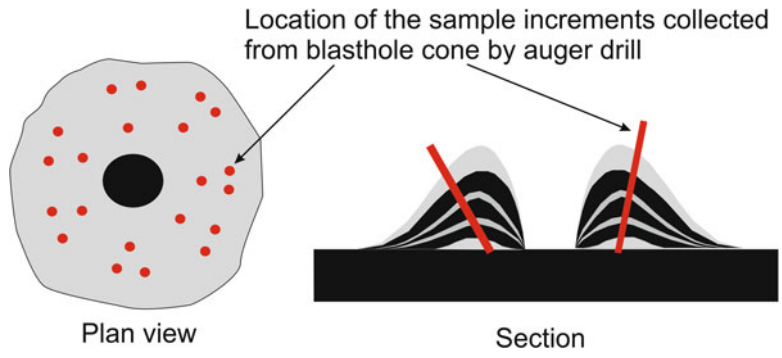

Fig. 4.27 Sketch explaining principals of blasthole sampling by hand held auger drill shown on the Fig. 4.24b

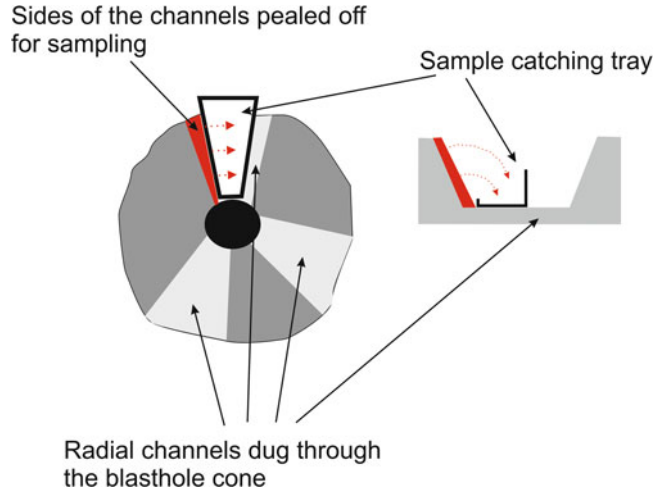

Fig. 4.28 Sampling blastholes by radial channels approach (Modified after Pitard (2005))

drill, should be carefully removed from parts of the cone prepared for sampling. Channels must be dug all the way to the ground and as close to the drilling hole as possible. Samples are collected by cutting along the side of the channels and peeling off into a special radial tray (Fig. 4.28). Each side of the channel should be sampled, therefore, the sample will be collected by four or six increments, depending on whether two or three channels are used for sampling. Minimum mass of increment depends on drilled bench and size of the sampled blasthole cone.

A practice shows that when blastholes are drilled through highly heterogeneous mineralisation the non-biased and repeatable blasthole assays can be only obtained by collecting large samples, often exceeding 20 kg in weight. In such cases the radial sampling device should be combined with a riffle splitter, allowing to correctly reduce the size of collected material to a practical size of a grade control sample, which is approximately 5–10 kg.

4.3.2 Use of 'Jumbo' Drilling for Delineation of Underground Stopes

In the underground mines the open hole percussion drilling can also be used for mining geology applications although it is less common than using blast holes for grade control in the open pit mines. In Western Australia the technique is used for delineating production stopes of the massive Ni-sulphide deposits. The ore body is intersected by the fan of the holes drilled using a 'Jumbo' from a footwall drive. Rock cuttings are collected regularly at 0.5 m intervals and contact

between the host rocks and massive sulphide ore is determined visually or using a hand held magnetometer. The samples containing sulphides and the wall rocks at their contacts are selected for assays and used for short term production plans. A similar approach is used in some gold mines in Australia although less successively because of poor repeatability of the gold assays.

4.4 Reverse Circulation (RC) Percussion Drilling

Reverse Circulation (RC) drilling overcomes limitations of the open hole percussion drilling which is prone to samples contamination. It uses the dual tube pipes (Figs. 4.29 and 4.30) allowing the high pressure air flow down the hole along the space between inner and outer tubes and to return sample cuttings along the inner tube. Separating flows of samples from high pressure air injecting down hole allows to obtain non contaminated samples as the rock cuttings are travelling inside the inner tube and at no time were in contact with the wall of the hole. The RC percussion technique used for drilling hard rocks uses drill bits in a shape of flat head cylinder with tungsten carbide buttons (Fig. 4.30c). RC rigs that are designed for drilling soft rocks usually use a smaller compressor and roller or blade instead of tungsten carbide drill bit.

RC drilling with downhole face sampling hammer (Figs. 4.29 and 4.30) is widely used in exploration and mine geology applications. In the operating mines this technique is commonly used for infill drilling, where it is often preferred to diamond core drilling by being cheaper and faster and yet producing good quality and representative samples. The technique can be classified as intermediate between open hole percussion at lower end and diamond core drilling at upper end producing a good quality samples at significantly lower cost than diamond drill core.

Modern RC rigs (Fig. 4.30a) that are used for drilling hard rocks, such as granite, volcanics, or metamorphic schists and gneisses, are equipped with a downhole face sampling hammer (Fig. 4.30c) which is activated pneumatically by compressed air. A piston of the hammer is striking top of the drill bit transferring the energy created to the rock face. Piston cycles from 1650 to 2000 beats per minute. The fast hammering motion is coupled with the rotation of the rods produced at the head swivel (Fig. 4.29) and these evenly crush rocks at the face being drilled. The rock chips are then removed from the face and brought to the surface through the

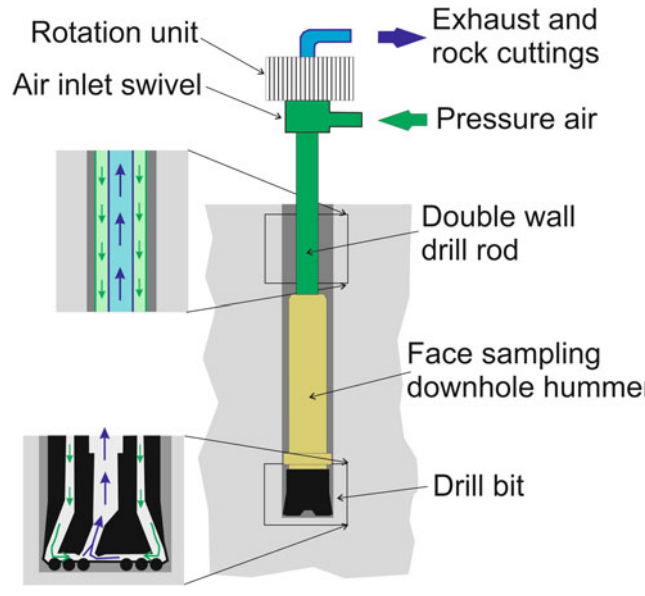

Fig. 4.29 Diagram of the principals of reverse circulation (RC) drilling showing air flow

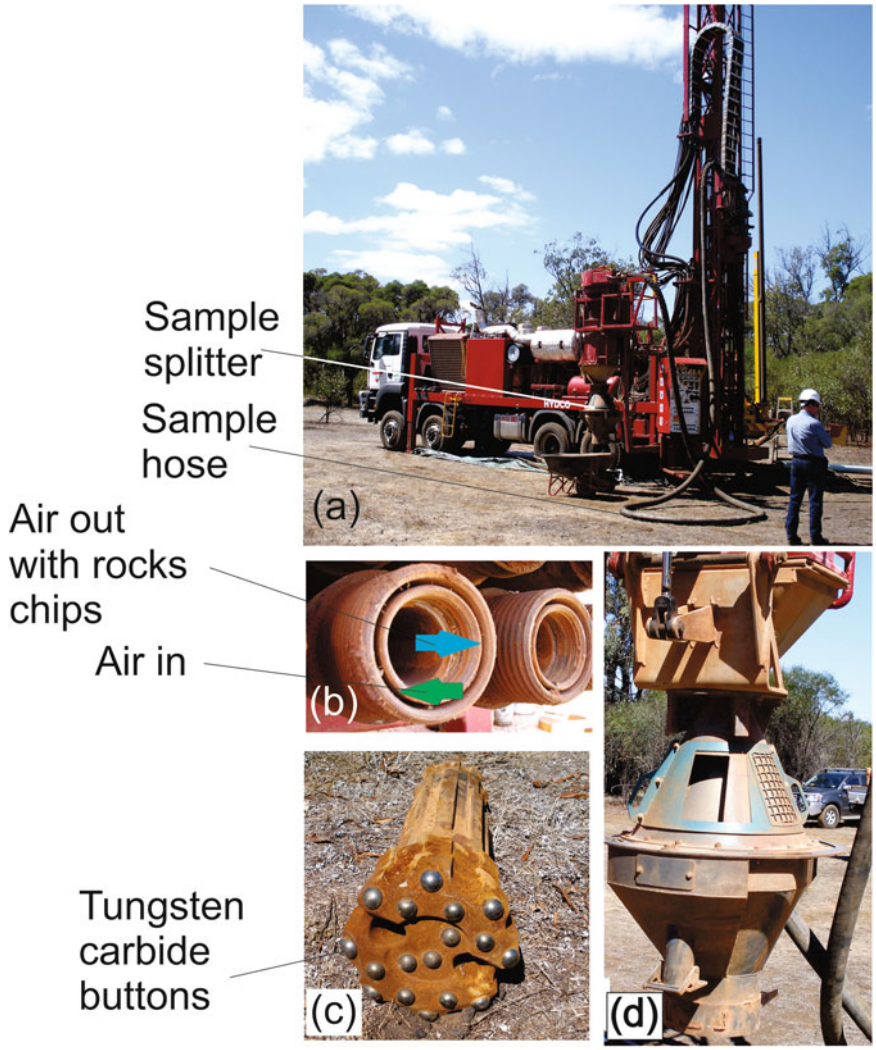

Fig. 4.30 RC drill rig: (**a**) general view of the RC drill rig operating in Western Australia; (**b**) double wall drill rod; (**c**) RC drill bit; (**d**) cone splitter for correctly reducing the samples size

inner tube (Fig. 4.29) where they are transported through the cyclone and sample splitting devices (Fig. 4.30d).

Modern RC rigs (Fig. 4.30a) allow to obtain a good quality samples from depths that were once only achievable for diamond drilling. At Kalgoorlie 'Super Pit' gold mine RC hole achieved a total depth of 822 m, which is the deepest RC hole so far drilled. Another common application of the RC technique is for grade control purpose at some open pit mines where it's preferred to blast holes sampling. Examples of RC drilling for grade control purpose include West Angeles Iron-ore and Murrin lateritic nickel open pits in Western Australia.

The method allows to achieve sample recovery of approximately 94–96 %. However, sample quality and representativeness can be marred by suboptimal drilling practices or specific conditions of the rocks drilled which are briefly described (Table 4.5).

Fine grained silty material can accumulate during drilling within the hammer forming a sticky putty-like material that clogs the internal

Table 4.5 RC drill sample errors

Error type	Error source	Mitigation
Contamination can occur when insufficient air is returning up in the inner tube	Worn inner tubes. Excess air escaping up the drill hole annulus	Weighing and documentation sample size. Regular inspection of the inner tubes
Contamination by a material scraped from the wall	Raising or lowering rods in a hole can cause scrapping material from the wall which falls to the bottom of the hole. Holes in soft ground and also inclined holes are particularly prone to this type of contamination	The material on the bottom of the hole should be discarded and sampling recommenced only after fresh rock is exposed. This precaution should be always taken when new rod is added to the drill string
	Use of blow back device to clear the inner tube also causes scraping material from the wall	
Contamination in the inner tube	When drilling sticky clay-rich formations the clay can build up in the inner tube obstructing the normal air flow and causing contamination of the samples	Weighing and documentation of sample size with particular attention if samples are wet; Regular inspection of the inner tubes
Contamination in the cyclone	Cyclones can selectively trap the rock cuttings because of the mechanical damages of the cyclone surfaces or their suboptimal design	Cyclones should be regularly checked, in particular after changing between wet and dry grounds. Do not hit the body of a cyclone to remove stuck sample
	Contamination because of poor cleaning cyclones after wet sticky samples	Check the internal surface and clean it regularly
Splitter generates non representative and/or biased samples	Incorrectly designed or mechanically damaged splitter can cause disproportional splitting of the different material types and/or losses of the fines	Regularly check and clean splitters; Duplicate samples should be regularly collected from splitter and assayed to monitor the samples repeatability (Abzalov 2008)

parts of the hammer. As a result of this the mechanical parts of hammer can seize up, resulting in the hammer stoping 'firing' and the sample not produced. The hammer also can stop firing when its parts become welded due to excessively high downhole temperature created during drilling. These and many other technical reasons (Table 4.5) can downgrade quality of the recovered samples therefore a rigorous monitoring of the drilling procedures and recovered samples is important.

4.4.1 Logging RC Holes

Documentation of RC holes (Table 4.6) in many aspects is similar to documentation of the diamond holes, with the main differences related to fact that RC samples are recovered as small rock chips compared with a solid cylindrical core recovered by diamond drilling. Because of this difference the RC holes are logged by collecting a small representative portion, 200–300 g from each sample, which is then washed by placing it in a sieve and petrographically logged using a hand lens (Fig. 4.31a, b). The logged material should be placed in a special container where it's retained for further reviews and auditing (Fig. 4.31c).

In order to assure consistency in diagnostic of the rocks and geological documentation it is recommended to create a collection of the main rock types by placing their representative rock chips into transparent jars with examples of their geological documentations. These materials should be included as a supplement to the rock library containing representative core samples, photos of the outcrops, chemical analysis and petrographic descriptions (Fig. 3.1).

Table 4.6 Check list for documentation of the RC holes

Activity	Example/reference
Dates when hole drilling was started and finished has been recorded	
Drilling equipment and parameters are recorded	
Name of the drill captain is documented	
Name of the geologist(s) supervised drilling and logged core are documented	
Collar of the drill hole has been surveyed and documented	Section 8.1
Downhole survey has been completed, results reviewed and documented	Section 8.2
Samples weights recorded and reconciled with theoretical weight of a sample assuming that hole diameter is constant and corresponds to a nominal size of a drill bit	
If downhole caliper survey has been completed and the density of the drilled rocks are known the sample weights are reconciled with actual geometry of the hole	
Rock chips are logged and stored	Figure 4.31
Samples collected, numbered and delivered to laboratory	

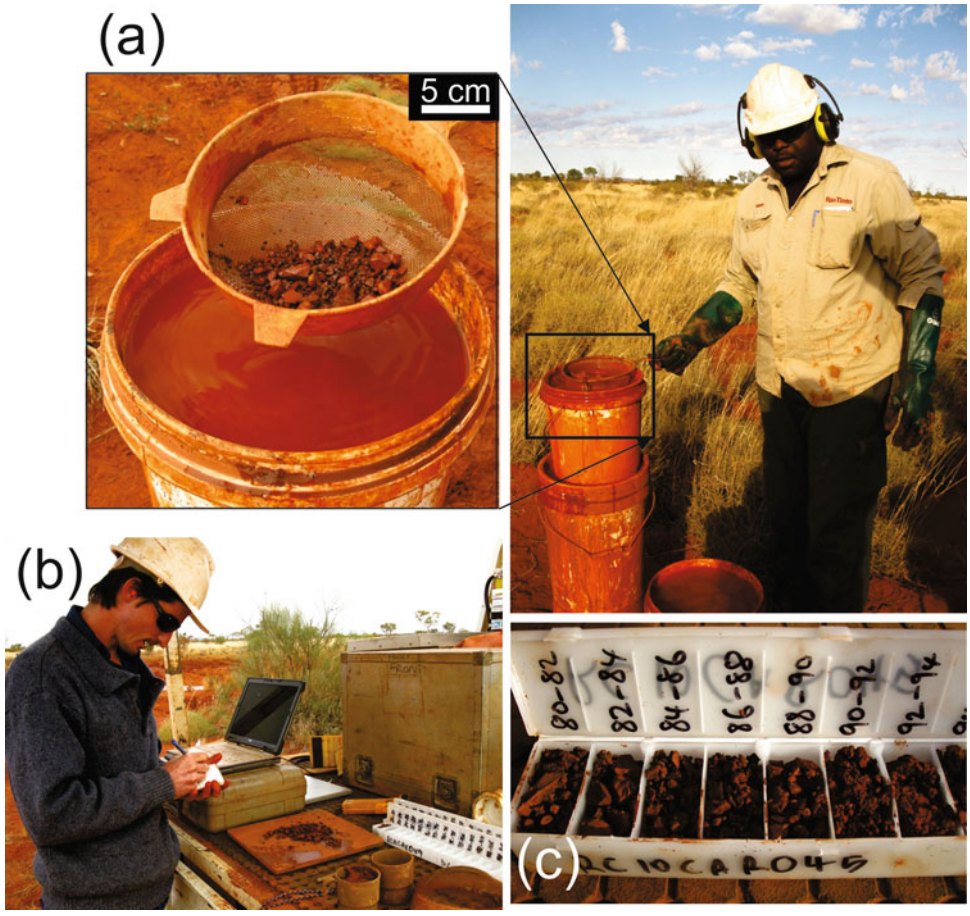

Fig. 4.31 Processing and documentation the rock chips recovered by RC drilling: (**a**) washing rock chips from clay and dust; (**b**) petrographic logging of the rock chips; (**c**) container for storing representative portion of the RC samples. Numbers denote the sampling intervals

The most difficult aspect of RC documentation is assessment of the drilling quality, in particular estimation of sample loss. The procedure requires accurate knowledge of the weight of the entire volume of the rock chips removed from the hole, volume of the excavated hole and density of the drilled rocks. Unfortunately, initial material that was recovered from RC hole is split in a sample divider (Fig. 4.30d) and rejects are discarded, therefore sample retained for laboratory assays represent only portion of the initially drilled material. Weighing of the laboratory sample is of a little use for assessing quality of the RC drilling because ratio between retained samples and rejected materials is highly variable. In order to overcome this limitation it's necessary to weigh all material removed from drill rig, including laboratory sample, duplicates and discarded rejects and then total weight of the material removed from the RC hole can be estimated as a sum of separately weighed increments.

It is important to remember that RC drilling produces samples which are highly variable in size caused by sample loss or possible caving of the drilled rocks related to their mechanical characteristics. Therefore, on the contrary to diamond drilling, correct estimation of RC sample recovery can not be based on a nominal diameter of the drill bit and should be based on correct estimation of the drilled volume by downhole calliper (Table 4.6).

The wet samples are collected without splitting therefore the entire sample can be weighed. However, weighing the wet samples is impractical therefore the right procedure should include delivery of the entire sample into laboratory, where it will be dried, weighed and then split for further processing.

4.4.2 Sampling RC Holes

Rock chips that are removed from the face by downhole hammer are transported through the inner tube of the drill rods (Fig. 4.30b) to the surface where they are captured in a cyclone and dropped down. The dry samples are dropped into a sample splitting device allowing reduction of sample size. Modern RC drill rigs are equipped with a cone splitter (Fig. 4.30d) for automatic reduction of the recovered material and producing homogeneous, representative and unbiased samples. The splitter is equipped with a cone that spins at approximately 30 rotations per minute allowing to obtain homogeneous, representative and unbiased eventual sample. The catchment reservoirs collect material as the cone spins. The collected sample passes down into funnels under the cone. Material from each catchment falls into buckets or bags which are used for separately collecting samples designated for assaying in the lab and retaining as duplicates. Remaining material is discharged down through the exhaust into the wheelbarrows and discarded to ground.

The splitter (Fig. 4.30d) can not correctly divide the wet samples. In such cases, when samples are wet they are dropped directly from the cyclone therefore the entire sample has to be collected and then dried, crushed and reduced in size (subsampled) in the lab.

Sampling wet samples is a tedious process. When the sample is represented by a thick soupy material, it should be collected into a polyweave bag instead of a plastic bag, so that water can be seeped out. In other cases, when samples were recovered as a thin soup, they are collected into plastic bags and water decanted after sediments have settled. Drilling clay rich formations below the water table can cause cyclones to be clogged up by a sticky mud. In that case, the material that stuck in the cyclone needs to be physically pushed into the plastic bag and the cyclone thoroughly cleaned prior to continuing drilling.

4.5 Sonic Drilling Technologies

Sonic drilling is a relatively new technique which became commercially available for mining industry needs since approximately mid 1980's (Oothoudt 1999). Sonic drilling (Oothoudt 1999) and its variations (Rotasonic, Minisonic, Sonicore, Resonatsonic and other similar terms with a common word sonic) is a technique based on a high frequency vibratory technology (Fig. 4.32)

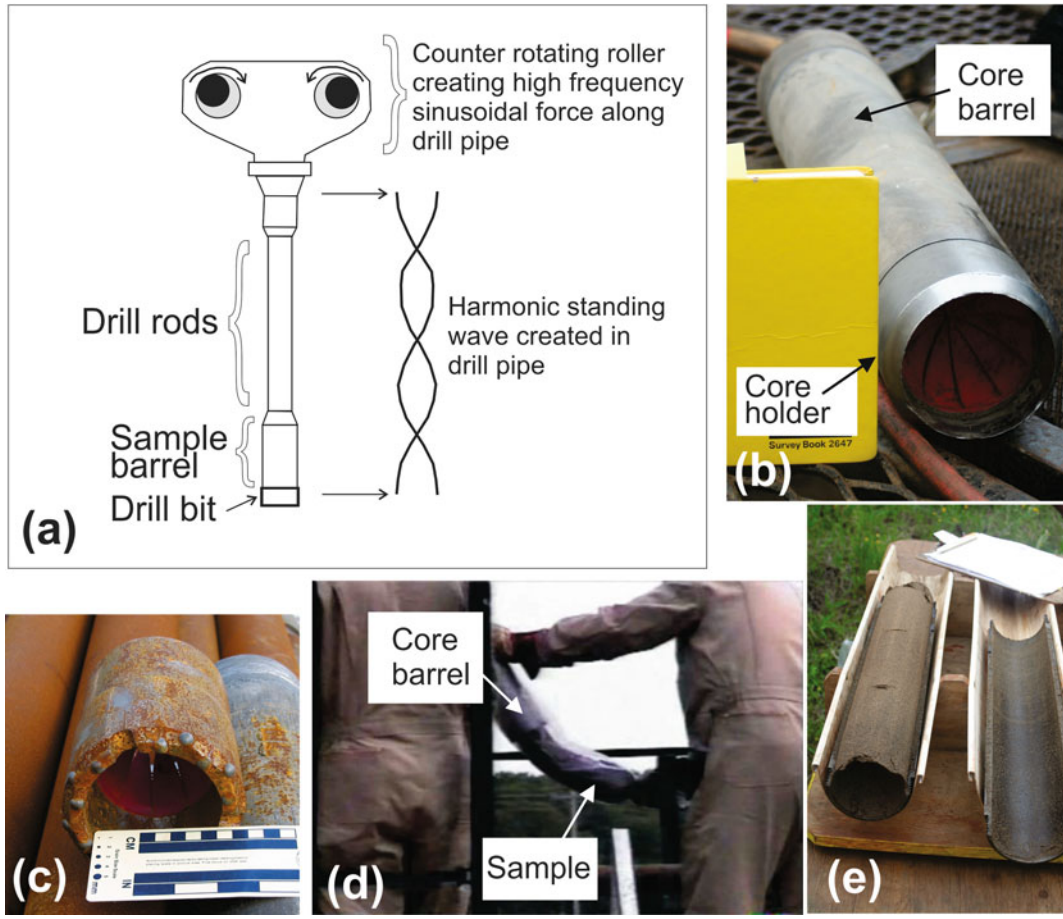

Fig. 4.32 Sonic drilling technology (Reprinted from (Abzalov et al. 2011) with permission of Australasian Institute of Mining and Metalllurgy). (**a**) sketch illustrating principals of sonic drilling; (**b**) core barrel with attached drill bit; (**c**) drill bit with tungsten carbide buttons designed for drilling soft sediments intercalating with hard pans; (**d**) recovery of sample from core barrel into plastic sleeve; (**e**) sand sample recovered into stainless steel split liner placed inside the core barrel

where the entire drilling string is vibrated with a frequency of 50–150 Hz or cycles per second. This frequency interval falls within the lower range of sound waves that can be detected by human ear, therefore the word sonic became a common term for describing this drilling technique. The differences between the previously mentioned drilling techniques are mainly related to rig designs (Fig. 4.33) and the methods of operation or down hole tools. Practical drilling rates and the hole diameters of the Sonic drill rigs are compared with other drilling techniques commonly used for drilling non-consolidated sediments (Table 4.7).

Sonic drill rigs are characterised by a specifically designed hydraulically powered drill head which generates oscillating high frequency vibratory force (Fig. 4.32a). The drill head uses two eccentric balanced weights (rollers) that counter rotate and they are arranged in such a way that creates a vibration at 0 and 180° of the rollers spinning. The sonic head is attached to drill pipe allowing the transfer of vibration through a core barrel to drill bit (Figs. 4.32b, c). The drill head is also equipped by an air spring that insulates a vibration from the drill rig.

The vibrating frequency is controlled by a driller who aims to achieve an optimum

Fig. 4.33 Sonic drill rigs: (**a**) track mounted *light* rig for drilling shallow holes, up to 30 m deep; (**b**) *heavy* duty rig allowing to drill holes more than 100 m deep

Table 4.7 Characteristics of the Sonic drill rigs

Rig type	Hole diameter (cm)	Drilling depth (m)	Mine/project
Minisonic	10.2	15.2	Fort Dauphin, Madagascar
	5.1	30.5	
Heavy Sonic	12	170	Richards Bay, South Africa

Reprinted from Abzalov et al. (2011) with permission of Australasian Institute of Mining and Metalllurgy

drilling rates when vibrating coincide with the natural resonate frequencies of the drill rod, a phenomenon known as a resonance. When resonance achieved the vibrational energy from the drill head is transferred to the drill bit and enhanced by a resonant drill string.

Sonic drilling is usually performed by track mounted rigs (Fig. 4.33) allowing their free moving on unconsolidated sands and the soft clay formations. Size of the rigs varies from small and light rigs, specifically designed for shallow drilling on the sand dunes (Fig. 4.33a) to large rigs (Fig. 4.33b) allowing drilling of deep holes, for testing targets located more than 100 m below surface (Table 4.7).

4.5.1 Strength and Weakness of the Sonic Drilling

The Sonic technique aims to collect representative undisturbed samples of non-consolidated sands (Figs. 4.32d, e) which are important for accurate estimation resources of the mineral sands deposits (Abzalov et al. 2011). All other conventional drilling techniques, including triple tube diamond, percussion and auger drilling, don't produce undisturbed samples, which limits their application for geological interpretations. Besides limited geological information obtained by the conventional drilling methods many of them also produce poorly repeatable and biased samples. In particular, it was noted that samples obtained by air core or reverse circulation drilling techniques can significantly underestimate grade of the valuable heavy minerals in the sand deposits (Fig. 4.34). Similarly biased results were also observed when auger and air core drilling was used for sampling heavy mineral sands in Mozambique (Abzalov and Mazzoni 2004; Abzalov 2009).

Sonic drilling is the only technique that allows to cost effectively obtain a continuous sample of the soft unlithified sedimentary formations. The diameter of Sonic drill holes (Table 4.8) allows to

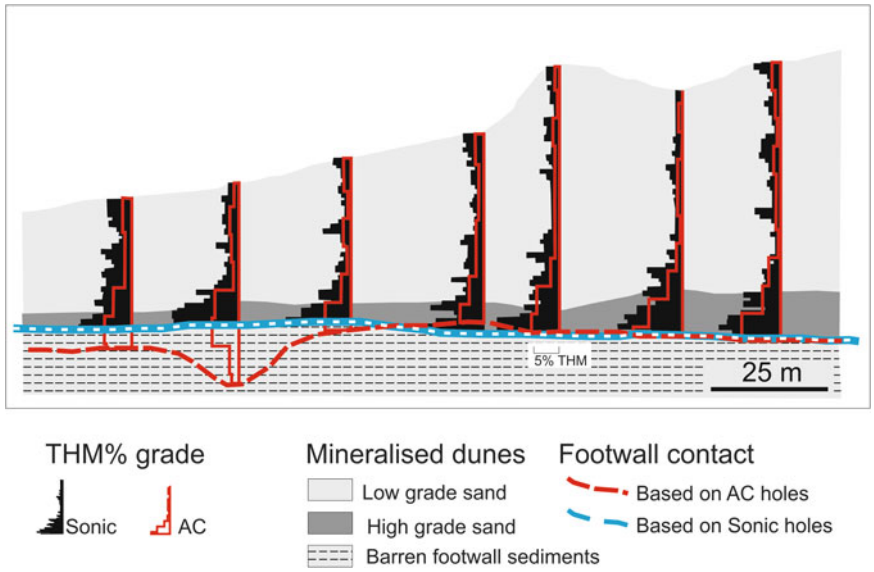

Fig. 4.34 Comparison of the Sonic and RC drilling in the Richards Bay mineral sands deposit, Africa (Reprinted from (Abzalov et al. 2011) with permission of Australasian Institute of Mining and Metalllurgy)

Table 4.8 Common errors of the Sonic core samples

Error Type	Error source	Mitigation
Sample losses	Sample lost when recovering from core barrel to plastic sleeve	Training and supervising drilling crew. Documenting sample weights
	Sample lost because of mechanical failure of the core catcher	Regularly review and if necessary replace drill bit and core catcher. Documenting sample weights
	Core catcher clogged up by clay preventing collecting a representative sample or causing loss by a sample being dropped from core barrel after it was lifted from the hole bottom	Use a split liner inserted into core barrel. Documenting sample weights
Drilling conditions	Poor recovery because of drilling through concreations or undurated layers	Use combination of sonic and rotary drilling approaches using tungsten carbide button drill bits
	Rising sediments in the drill hole after drill pipe has been removed. This is a natural diapirism which occurs in sands that situated under a high hydraulic pressure. The pressure difference pushes sands into the low pressure openings such as drill holes	Recording depth of the hole each time before withdrawing the drill pipe and when drilling recommenced. Review and adjust drilling procedures

obtain a large representative samples in amounts sufficient for comprehensive geochemical assays, geotechnical studies and metallurgical testwork. Sample integrity is significantly better than of the other techniques and possibility of sample contamination is minimised because samples are constantly contained within the core barrel and extruded into long plastic bags (sleeves) at the surface (Fig. 4.32d) or collected into core barrel liners (Fig. 4.32e).

The recognised benefits of obtaining a continuous core sample of unconsolidated sedimentary formations made the Sonic drilling a main method for evaluation mineral sands deposits. Its application varies from drilling twin holes for validation historic data (Mandena project,

Madagascar) (Abzalov 2009) to being used as the main drilling method for definition resources and reserves of the heavy mineral sands (Richards Bay deposit, Republic of South Africa). The technique is also used for environmental studies, requiring sampling of old tailing ponds, heap leach pads and overburden formations around the mines (Oothoudt 1999).

Review of the Sonic rigs' performance at several mines in Africa has revealed certain difficulties that can mar sample quality and representivity. It was noted that sampling errors can be caused by many factors, including drilling conditions, mechanical failure of equipment and suboptimal sampling practices. Most common errors and their mitigation procedures are summarised in the Table 4.8.

In general, it is important that sampling errors and possible sample losses are timely diagnosed therefore drilling should be supervised by experienced geologists. The project geologist, considering past experience if the site has been drilled before, should assess drilling conditions and envisage the technical difficulties the driller might have, which can compromise the integrity of the sample and result in poor sample recovery.

4.5.2 Logging and Sampling Sonic Drill Holes

Logging of Sonic core in general is similar to diamond core logging. The drill holes are usually logged by recording geological observations onto pre-printed paper log sheets which are now replaced by electronic tables loaded into handheld electronic instrument, such as a Pocket PC. The drill hole logging should be primarily focused on collection of the factual data, whereas interpretation and comments should be documented separately, usually in the different columns. Emphasis during logging Sonic core should be paid on accurate definition of the geological contacts, which are clearly discernible in the Sonic core (Fig. 4.35).

Each core sample should be photographed (Figs. 4.35a, b) and lithological units described with an emphasis on lithological characteristics of the sediments and sedimentary textures which often are clearly discernable on the Sonic core surface (Fig. 4.35c).

It is a good practice to summarise logging by drawing schematic section of the hole (Fig. 4.35a), noting what subjective assumptions have been made in the current interpretation and possible alternative interpretations. The core logging should be done at the drill rig site because geological contacts (Fig. 4.35b) and sedimentary textures (Fig. 4.35c) will be destroyed when samples are transported to a different location.

In order to assure consistency of the logging, the representative samples exhibiting features to be logged should be photographed and compiled as lithological atlas to be used as logging guide. When more than one geologist or technician are working within the project, rotating the fieldwork, and consequently logging drill holes, the different logs must be regularly compared and reviewed with all team members participating in comparative analysis. This procedure aims to enhance the consistency of the logging system, and must be recorded as such, including the name of geologists and technicians, hole and samples logged, date, differences found during the logging and respective actions to correct.

The routine sample quality control procedures should include documentation of the hole depth each time drilling is stopped and drill pipe has been withdrawn from the hole. Before recommencing drilling in that hole the depth should be measured again and two measurements compared and reconciled. If hydraulic swelling of sediments is noted then correction should be made to sampling intervals and, if necessary, the drilling procedures revised.

Recovered samples should be weighed in the field and all inconsistencies and possible sampling errors should be discussed with the drilling crew and recorded in the log sheets. The sample weights are recorded and should be used for sample recovery assessment. It is a good practice to enter sample weights into a spread sheet which will automatically recalculate to sample recovery for a given volume of Sonic core which is determined from a known diameter of the core

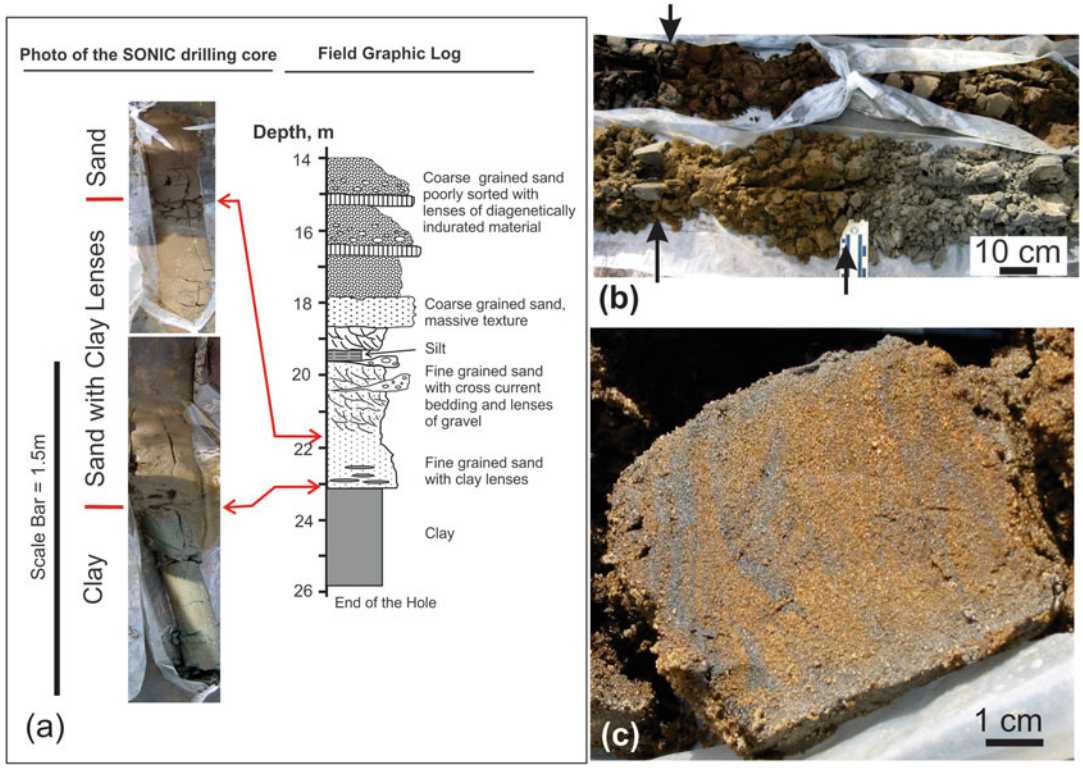

Fig. 4.35 Drill core of non-lithified sands recovered by sonic drilling at the Mandena Ti-sands project, Madagascar (Reprinted from (Abzalov et al. 2011) with permission of Australasian Institute of Mining and Metalllurgy). (**a**) sonic drill core and lithological log sheet documented in the field; (**b**) contacts between sedimentary beds are sharp and clearly discernable in core (marked by arrows); (**c**) close up view of drill core specimen of sands exhibiting cross-current bedding textures

barrel and drilling interval. Density of the sands should be also monitored by collecting samples using a split liner placed inside the core barrel (Fig. 4.32e). These samples are better suited for accurate measurement of the sands density because of their volume is more accurately measured then of conventional Sonic core samples recovered into the plastic sleeves.

4.6 Auger Drilling

Auger technique is used for drilling shallow holes in soft unconsolidated formations, mainly gold placers, bauxites and mineral sands deposits which located on the surface or concealed under shallow soft overburden.

Advantages of the auger method over other techniques available for shallow drilling in the soft formations is low drilling costs, high penetration rates and no contamination of samples by fluids. Therefore, the method is commonly applied for environmental and geotechnical studies at the mine sites and for drilling blast holes in the open pits, for example at the Sangaredi bauxite mine in Guinea. The method can also be used for definition resources of surficial mineralisation, however, quality of the auger samples is poorer in comparing with RC or Sonic drilling techniques therefore application of the auger technique for evaluation mining projects has currently decreased.

Auger drilling is subdivided into continuous flight auger (Fig. 4.36a), hollow auger, short flight auger, plate auger and bucket auger (Fig. 4.36b). Comparison of the different types of the auger drilling and their preferred operational environments are listed in the Table 4.9.

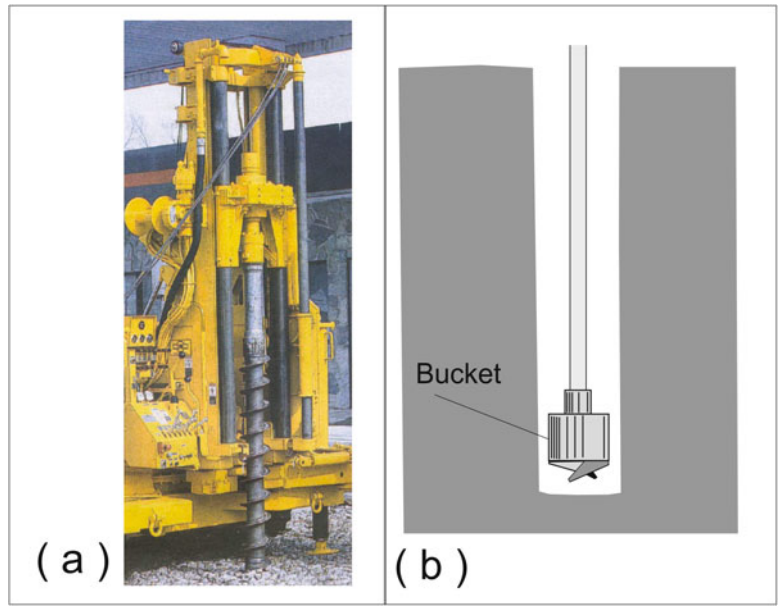

Fig. 4.36 Auger drilling techniques: (**a**) continuous flight auger; (**b**) sketch of the bucket auger

Table 4.9 Characteristics of the main types of the auger drilling

Drilling Method	Advantages	Disadvantages
Continuous Flight Auger	Low equipment cost	Suboptimal quality of samples
	Low operating cost	Special equipment is required for better quality samples
	Fast penetration	Will not drill below water table
Short Flight and Plate Auger	Drill large diameter holes	Water in hole washes cuttings from the auger flights
Bucket Auger	Drill large diameter holes	Limited depths of drilling
	Suitable for obtaining bulk samples for metallurgical tests	
	Can be used below water table and operates in mud filled holes	

Continuous flight augers allow to obtain a continuous sample of the drilled rocks. It is driven by a top-drive machine that rotates a special screw shaped drill pipe (Fig. 4.36a) that has a spiral ledge fixed to the exterior of the rods. The rocks are cut by a special drill bit at the end of the rod which can be in shape of blade that is used for drilling unconsolidated formations or by a tricon drill bit for drilling semi-consolidated rocks. Rock cuttings are removed from the bottom of the hole and carried to the surface moving up on the spiral ledge (helical flights) (Fig. 4.36a).

Hollow auger is a special version of the continuous flight auger which has a hollow centre tube for collecting sample. The drilling can be further modified by placing core barrel inside the hollow auger, which can be placed by a wireline system or using internal rod string.

Short flight, plate and bucket augers represent discontinuous sampling techniques. They all operate by entering a sampling catching device (Fig. 4.36b) into the hole, loading it with sample while it penetrates through the unconsolidated formations and then pulled out of the hole and

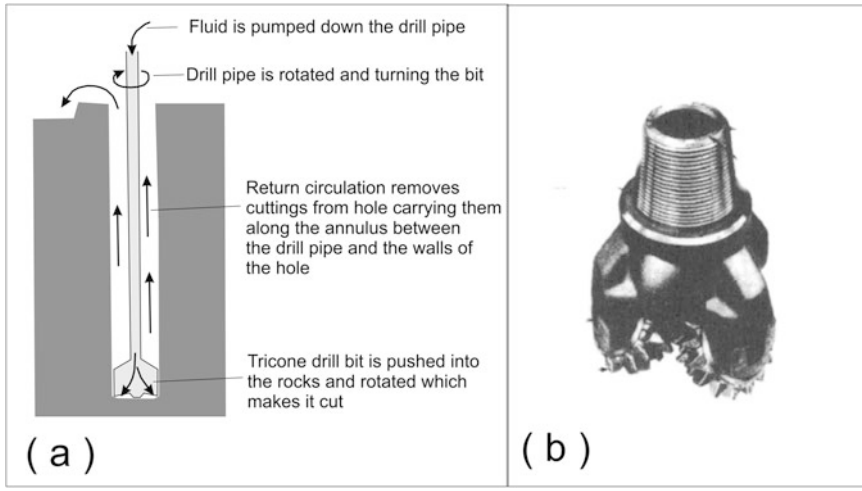

Fig. 4.37 (**a**) Sketch showing basic principles of the standard circulation tricone rotary drilling; (**b**) general view of the tricone drill bit

unloaded at the surface. The same operation repeated multiple times until hole reaches the desired depth.

4.7 Rotary Drilling Using Tricone Bit

Rotary drilling is a common term defining any form of drilling which makes a hole by rotating the drill bit located on the bottom of the drilling pipe (Eggington 1985). This section reviews, however, only a particular type of rotary drilling, a standard circulation rotary drilling (Fig. 4.37a) that uses tricone drill bits (Fig. 4.37b).

The drilling technique is commonly used for developing resources and drilling production holes at the sandstone-type uranium mines that are exploited by in-situ leach (ISL) technology (Abzalov et al. 2014). Uranium resources of the ISL-amenable projects are almost entirely based on down-hole geophysical logs therefore preference of drilling is given to standard circulation tricon rotary drilling characterised by low drilling costs and fast penetration rates. Sample quality is not important because a primary purpose of these holes is for downhole geophysical logging. Geophysical data are validated by drilling a small amount of twin holes (Abzalov 2009) which are usually drilled using a triple tube diamond core technique allowing to obtain representative samples (Abzalov et al. 2014)

Two different types of the rotary drilling are commonly used at the ISL operations:

- rotating the drill pipe by a rotary table which turns the pipe and allows it to slide through
- rotating the pipe by a hydraulically operated top-drive unit which is attached to drill pipe and moves up and down along the drill rig mast.

The drill bit can also be rotated by down hole turbine, however this technique is usually used in oil and gas industry and rarely applied in mining geology.

References

Abzalov MZ (2008) Quality control of assay data: a review of procedures for measuring and monitoring precision and accuracy. Exp Min Geol J 17(3–4): 131–144

Abzalov MZ (2009) Use of twinned drill – holes in mineral resource estimation. Exp Min Geol J 18(1–4):13–23

Abzalov MZ (2014a) Design principles of relational databases and management of dataflow for resource

estimation. In: Mineral resource and ore reserves estimation, AusIMM monograph 23, 2nd edn, Chapter 2: The resource database. AusIMM, Melbourne, pp 47–52

Abzalov MZ, Bower J (2009) Optimisation of the drill grid at the Weipa bauxite deposit using conditional simulation. In: Seventh international mining geology conference. AusIMM, Melbourne, pp 247–251

Abzalov MZ, Mazzoni P (2004) The use of conditional simulation to assess process risk associated with grade variability at the Corridor Sands detrital ilmenite deposit. In: Dimitrakopoulus R, Ramazan S (eds) Ore body modelling and strategic mine planning: uncertainty and risk management. AusIMM, Melbourne, pp 93–101

Abzalov MZ, Menzel B, Wlasenko M, Phillips J (2007) Grade control at the Yandi iron ore mine, Pilbara region, Western Australia: comparative study of the blastholes and RC holes sampling. In: Proceedings of the iron ore conference 2007. AusIMM, Melbourne, pp 37–43

Abzalov MZ, Menzel B, Wlasenko M, Phillips J (2010) Optimisation of the grade control procedures at the Yandi iron-ore mine, Western Australia: geostatistical approach. App Earth Sci 119(3):132–142

Abzalov MZ, Dumouchel J, Bourque Y, Hees F, Ware C (2011) Drilling techniques for estimation resources of the mineral sands deposits. In: Proceedings of the heavy minerals conference 2011. AusIMM, Melbourne, pp 27–39

Abzalov MZ, Drobov SR, Gorbatenko O, Vershkov AF, Bertoli O, Renard D, Beucher H (2014) Resource estimation of in-situ leach uranium projects. App Earth Sci 123(2):71–85

Annels AE (1991) Mineral deposit evaluation, a practical approach. Chapman and Hall, London, p 436

Annels AE, Hellewell EG (1988) The orientation of bedding, veins and joints in core: a new method and case history. Int J Min Geol Eng 5(3):307–320

Chugh CP (1985) Manual of drilling technology. Balkema, Rotterdam, p 567

Cumming JD, Wicklund AP (1980) Diamond drill handbook, 3rd edn. Smit, Toronto, p 547

Eggington HF (ed) (1985) Australian drillers guide, 2nd edn. Australian Drilling Industry Training Committee Ltd, Sydney, p 572

Hartley JS (1994) Drilling: tools and programme management. Balkema, Rotterdam, p 150

Marjoribanks RW (2007) Structural logging of drill core. Handbook 5. Australian Institute of Geoscientists, Perth, p 68

Oothoudt T (1999) The benefits of sonic core drilling to the mining industry. In: Tailing and mine waste'99: Proceedings of the sixth international conference on tailings and mine waste'99, Fort Collins, Colorado, USA, 24–27 January, pp 3–12

Pitard FF (1993) Pierre Gy's sampling theory and sampling practise, 2nd edn. CRC Press, New York, p 488

Pitard FF (2005) Sampling correctness – comprehensive guidelines. In: Proceedings – second world conference on sampling and blending. AusIMM, Melbourne, pp 55–66

Sinclair AJ, Blackwell GH (2002) Applied mineral inventory estimation. Cambridge University Press, Cambridge, p 381

Zimmer PW (1963) Orientation of small diameter core. Econ Geol 58(8):1313–1325

Sampling of the Mine Workings

5

Abstract

Collecting representative non-biased samples from rock faces and in particular sampling the broken ore is a non-trivial task which requires special sampling equipment and operational procedures. The current chapter overviews the most common techniques that mine geologists are using for sampling mine workings for delineating ore bodies, estimating reserves or need that samples to control grade and metallurgical characteristics of the excavated ore.

Keywords

Channel sampling • Trenching • Broken ore

Mining geology differ from exploration in a sense that exploited ore bodies are well exposed in the walls of the underground drives and the open pit benches allowing their systematic mapping and sampling in three dimensional space. The opportunity for systematic three dimensional sampling directly from the rock faces is rarely available for exploration geologists and therefore it represents one of the special areas of the mining geology where it became a routine task. Collecting representative non-biased samples from rock faces and in particular sampling the broken ore is a non-trivial task which requires special sampling equipment and operational procedures.

5.1 Sampling Rock Faces in the Underground Mines

Mineralisation can be exposed on the front faces of the underground drives, along the side walls and on the backs and floors. All these faces are suitable for sampling and choice depends on orientation of the mine workings relative to ore body and accessibility of the faces. For example, the good quality samples can be collected from the rocks exposed on the drive backs. In that case samples can be regularly distributed along the strike of ore body and represent a good supplement to the geological maps of

M. Abzalov, *Applied Mining Geology*, Modern Approaches in Solid Earth Sciences 12,
DOI 10.1007/978-3-319-39264-6_5

the underground drives facilitating geological interpretations and estimation of the ore reserves. The disadvantage of this approach is that it's one of the most complicated technically, time consuming and requires the special safety procedures because of working on a height. Sampling side walls is easier for implementation and commonly used for sampling cross cuts and raises, however is of a little use when ore drives are developed along the steeply dipping narrow mineralisation, such as quartz-gold lodes or massive sulphides.

Sites that are commonly sampled by mining geologists depending on mineralisation styles and the mine logistics are listed in the Table 5.1 and explained on the sketches (Fig. 5.1a, b).

5.1.1 Channel Sampling

Rocks exposed in the outcrops, trenches or walls of the mine workings are usually sampled by cutting narrow channels on the rock surface (Fig. 5.2). Channels are made by chisel and hammer (Fig. 5.2a) or diamond saw (Fig. 5.2b). Cutting by diamond saw is superior technique which produces samples of the significantly better quality than conventional sampling by chisel and hammer (Magri and McKenna 1986).

Channel sampling procedures are as follows.

1. Channels are cut through the entire ore body and extended to the wall rocks therefore entire length of the channels depends on the thickness of the studied mineralisation and can be tens of metres (Fig. 5.3).
2. Length of the individual samples varies from 10 cm to 100 cm depending on mineralisation style. Width of the channels is usually 5–10 cm and depth approximately 3–5 cm (Fig. 5.2), however depending on specific characteristics of the mineralisation, purpose of the sampling and cutting equipment the different depth and width can be used,
3. Location of the samples on the rock faces should be chosen in such a manner that allows to obtain a most representative samples for the given face (Fig. 5.3a). Channels are orientated at high angle to strike of the mineralisation, as close as possible to ninety degrees (Fig. 5.3a). However, it is important that mineralisation is sampled along the straight line from one contact to another therefore depending on location of the exposed contacts the channels can be cut at lower angles (Fig. 5.3b).
4. Channel samples are cut and sampled from lower part of channel into upward direction (Fig. 5.3c).
5. Samples should be taken to geological contacts which need to be clearly marked before sampling.
6. Channel width and depth should be constant along its entire length. Irregular shape of the channels usually caused by preferential carving of the certain material types (e.g. soft layers). It is a suboptimal sampling practice which leads to unrepresentative and potentially biased samples. Constant shape of the channel samples is rarely achieved when they are cut by chisel and hammer (Fig. 5.2a) and usually require using of the diamond saw (Fig. 5.2b).

5.1.2 Rock Chip Sampling

Another sampling approach, commonly used for sampling rock faces in the mines is known as rock chip sampling technique. The method is a systematic collection of the rock chips which are taken at the regular intervals along the straight line (Fig. 5.4a) or as a narrow band (Fig. 5.4b). In the latter case the rock chips are usually distributed as a rectangular grid. Points where rock chips should be collected can be marked on the rock faces before sampling. This extra step produces more representative samples because it minimises a potential sampling biases caused by subjective choices of a sampling spots by a sampler. Marking sampling spots is best made by using rope and knot approach.

The method is fast and inexpensive, but samples are less representative then channel samples. It is usually used for sampling uniformly distributed disseminated mineralisation where rock chip sampling approach produces representative samples.

Table 5.1 Choice of the rock faces for underground sampling

Walls of the mine workings		Application	Comments		Example
			Strength	Weakness	
Developing face of the ore drive		Narrow ore bodies fully exposed on the front face of the drive	Good exposure of the ore body which is convenient for channel or rock-chip sampling. Suitable practically for all types of mineralisation independently of the mining technologies	A limited accessibility of the developing faces, depending on a mine production schedule, is the main restraining factor of their use for mining geology purposes. The faces are usually mapped and sampled before or during drilling blast holes before they have been charged by explosives	Figs. 3.12 and 3.13
Side walls	Cross cut	Cross cuts are often used to delineate footwall and hangingwall of the steeply dipping mineralised zones	Side walls of the cross cuts intersecting the entire or part of the steeply dipping mineralisation are easily accessible and represents an optimal environment for detailed geological mapping and sampling	When ground conditions is poor the entire mine working, including the side walls, can be shotcreted	Figs. 3.11 and 5.1a
	Rise	Narrow and steeply dipping ore bodies delineated in the vertical direction by raises	Side walls of the raises developed along the dip of mineralisation are suitable for detailed geological mapping and sampling of the steeply dipping mineralisation	Sampling of the raises can me technically difficult and require special equipment	Fig. 5.1b
	Ore drive	Narrow flat laying ore body exposed on the side walls of the ore drive	Side walls of the drives are usually easily accessible for sampling and mapping	When ground conditions is poor the entire mine working, including the side walls, can be shotcreted	Fig. 3.12
Back	Ore drive	Narrow steeply dipping ore body exposed on the back of the ore drive	Ore-body exposed along it entire strike length allowing to study its continuity along the strike	Rarely used for sampling because of technical difficulties and safety issues. Access can be also restricted because of shotcreting or roof supporting materials	

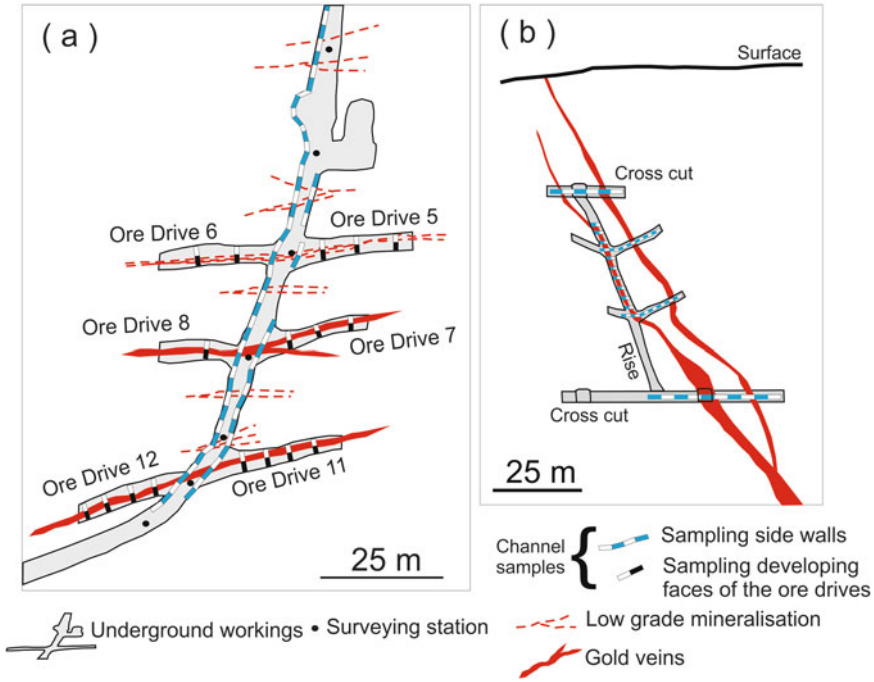

Fig. 5.1 Sampling rock faces exposed in the underground workings, Zarmitan gold mine, Uzbekistan: (**a**) plan view; (**b**) cross section

Fig. 5.2 Channel sampling of the exploration trench walls. Uranium deposit in central Jordan: (**a**) channel sampling using hammer and chisel; (**b**) channel sample cut by diamond saw

Rock chips are collected by geological pick and chisel or can be taken by hand held mechanical devices such as air-pick, hand held core drill, hand-held percussion drill or electric drills equipped with a drill cuttings catcher.

5.2 Sampling of the Broken Ore

Situations when mine geologists have to sample muck piles of broken ore are very common and includes sampling of the ore stock piles, conveyor

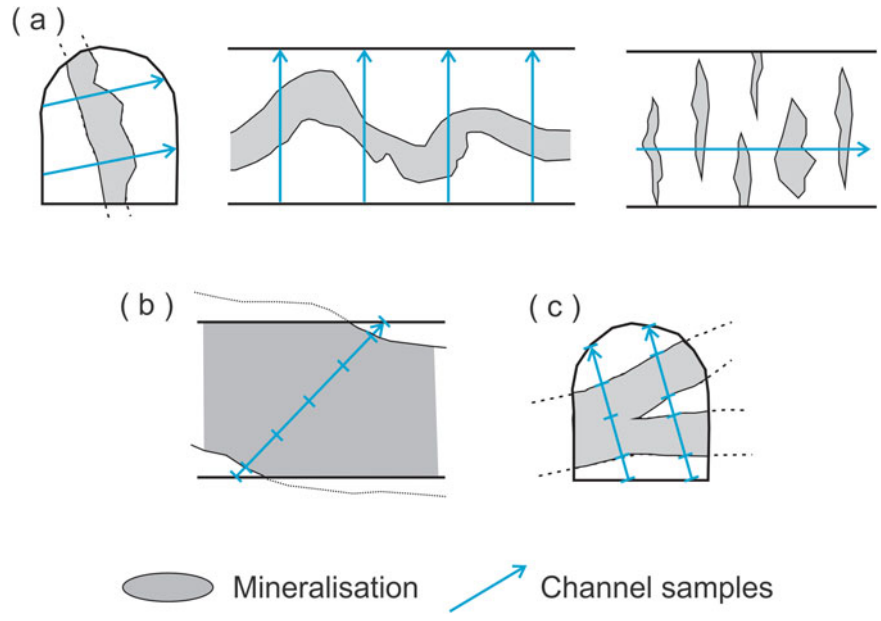

Fig. 5.3 General principals of the channel sampling: (**a**) orientation of the channels at right angle to mineralisation; (**b**) assuring that channel intersects *upper* and *lower* contacts of mineralised zone; (**c**) samples taken to geological contacts

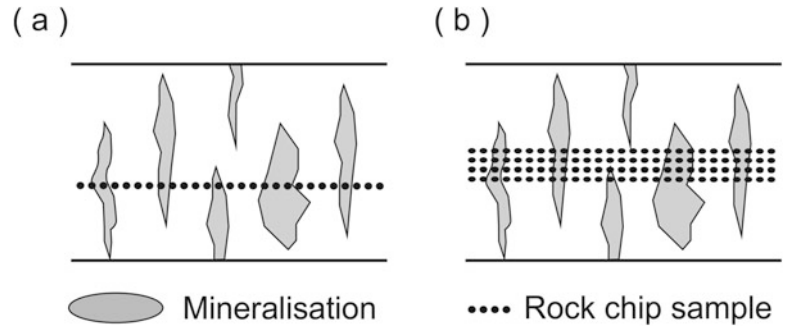

Fig. 5.4 Sketch explaining rock chip sampling: (**a**) sampling along the *straight line*; (**b**) sampling along the *rectangular grid* distributed as a *narrow band*

belts, tram cars and draw points of the underground stopes (Fig. 5.5). Sampling approach is known as grab sampling and involves collecting of the rock chips of 3–5 cm in size. Fragments are chosen at random and preferably throughout the entire surface of the pile. This approach is commonly used for ore grade control at the underground operations in particular at the mines which use block cave or sub-level cave mining technologies.

The task is extremely difficult because piles of the broken ore consist of fragments varying in the very wide range, from large boulders (Fig. 5.5), exceeding 1 m in diameter, to the fine debris, smaller then millimetre in size. Heavy and small fragments are segregated at the bottom of the piles which is difficult to access for sampling therefore that material not adequately represented in the samples. This problem is practically unresolvable and usually leads to poorly repeatable and often biased samples. Given suboptimal quality of the grab sampling of the muck piles this approach is used only when no other sampling means are applicable.

Samples representativeness can be partially improved if sampling is made by robe and knot method and supplemented by mapping of the muck piles. Main objective of the muck pile

Fig. 5.5 Broken ore at the draw point of the underground stope at the Northparkes copper mine

mapping is to determine proportions between ore and waste which is used as geological control of the muck pile sampling results.

5.3 Trenching and Winzing

Trenching and winzing represent shallow excavations made with an aim to access near surface mineralisation covered by thin overburden. Trenches are used where overburden is less then 3 m (Fig. 5.6), winzes allow to access mineralisation at larger depth, up to 30 m. These techniques are usually applied at the detailed exploration stage when project has matured and

Fig. 5.6 Examples of trenching in mining industry: (**a**) exploration trench dug by dozer, Bystrynsky Cu-Au project, Siberia, Russia; (**b**) trench ripped by a dozer ripper at the bench of the open pit, Tarkwa gold mine, Ghana; (**c**) exploration trench dug by back-hoe, CJUP uranium deposit, Jordan

requires accurate estimation of the mineral resources based on detailed mapping and sampling of mineralisation (Fig. 5.6a). At that stage trenches and winzes can also be used to obtain bulk samples from selected sites for metallurgical testwork.

In operating mines trenching is rarely used and applied mainly for detailed mapping and sampling of the open pit benches for grade control (Fig. 5.6b) or for collecting bulk samples when production poorly reconciles with reserves.

The trenches and winzes can be cut by hand (shovel) or mechanically. Commonly used equipment is as follows:

- Excavated by dozers (Fig. 5.6a)
- Dozer ripper (Fig. 5.6b)
- Back-hoe (Fig. 5.6c)
- Bucket excavator
- Ditch – Witch (Schwann 1987).

Choice of the excavating technique depends on thickness and hardness of overburden and also on terrain characteristics and the project logistics.

Trenches and winzes are mapped and sampled. Trenches are sampled from their floor. Winzes mapped and sampled at least on two mutually intersecting surfaces. When thickness and grade of mineralisation is highly variable then all four walls of the winzes are mapped.

Mapping trenches and winzes is similar to that used in the underground mines (Figs. 3.8 and 3.11). Samples are usually cut by diamond saw from the trench floor (Figs. 5.2b and 5.6c) and side walls of the winzes.

References

Magri EJ, McKenna P (1986) A geostatistical study of diamond-saw sampling versus chip sampling. J South Afr Inst Min Metall 86(8):335–347

Schwann BB (1987) The application of Ditch Witch sampling in oxidized open cut gold mines. In: Equipment in minerals industry, proceedings of exploration, mining and processing conference. AusIMM, Kalgoorlie branch, Kalgoorlie, pp 25–31

Geotechnical Logging and Mapping

6

Abstract

The most common types of the geotechnical data and the rock strength indexes (RQD, Q index) routinely compiled by the mining geologist are described with emphasis on the basic principles of geotechnical documentation of the drill core and the rock faces exposed on the mine walls.

Keywords

Rock strength • RQD • ESR • Q-index • Geotechnical mapping

Optimisation of underground openings and open pit slopes require systematic documentation of the different physical characteristics of the rocks which are commonly referred as geotechnical information (Vutukuri et al. 1974; Hudson and Harrison 1997; Brady and Brown 2004). The geotechnical information is obtained by drilling the specially designed geotechnical drill holes and also recorded in a process of geological mapping of the mines and in the drill core. The latter two tasks are commonly carried out by the mine geologists who are assisting the geotechnical engineers in collecting the geotechnical data.

This chapter describes the most common types of the geotechnical data routinely collected by the mining geologist with emphasis on the basic principles of geotechnical documentation.

Geotechnical data analysis is also briefly explained in this chapter, however, without going deeply into the rock mechanics. Theory of the mining rock mechanics and the rigorous mathematical foundations of that scientific discipline are beyond the scope of this chapter and can be found in the special textbooks (Vutukuri et al. 1974; Brady and Brown 2004).

6.1 Geotechnical Logging of the Drill Core

Diamond drill core is the most common source of geotechnical information at the mining projects therefore geotechnical documentation of the drill core has become one of the routinely undertaken tasks of the mine geologists. The geotechnical logging procedures are usually set by experienced geotechnical engineer and can significantly differ between the mines depending on a mineralisation style and mining method. For example, open pit mines require

M. Abzalov, *Applied Mining Geology*, Modern Approaches in Solid Earth Sciences 12,
DOI 10.1007/978-3-319-39264-6_6

Table 6.1 Geotechnical features recorded by mine geologists

Features		Reference to this book	Additional references
Core recovery		Sect. 4.2.1	
Drilling equipment and parameters		Table 6.2	
Rock strength	Intensity of the rock weathering	Sect. 6.1.2	
	Strength of individual rock fragments	Sect. 6.1.3	
Fractures	Rock quality designation index (RQD)	Sect. 6.1.4	Deere (1964, 1968)
	Rock structure rating	Sect. 6.1.5	
	Fragment frequency	Sect. 6.1.5	
	Number of structure sets	Sect. 6.1.5	
Characteristics of the fractures (separately by the structural sets)	Classification defects by strength	Sect. 6.1.5	
	Orientation of the fractures	Sect. 4.2.2	
	Planarity of fractures	Sect. 6.1.5	
	Roughness of the fracture walls	Sect. 6.1.5	
	Infill type	Sect. 6.1.5	
	Width	Sect. 6.1.5	
Rock density		Chap. 7	Lipton (2001) and Abzalov (2013)

rigorous documentation and analysis of the rock fractures whereas supporting in-situ leach (ISL) operations require systematic measurement and documentation of the porosity and permeability of the rocks that host mineralisation. The most commonly documented geotechnical parameters are shown in the Table 6.1 which can be used as a preliminary check-list ensuring that all geotechnical parameters are recorded for every diagnosed and logged geotechnical feature. Consistency in logging is facilitated by training the geologists in geotechnical documentation who should use geotechnical logging sheets and templates. These can be created using the geotechnical characteristics listed in the Table 6.1 which cover the commonly logged geotechnical parameters.

It is also a good practice to assign the codes to the observed geotechnical features, which together with their clear description in the logging sheets will allow selecting and grouping geotechnical characteristics for structural analysis and for their selective use in geotechnical model of the mine.

6.1.1 Drilling Parameters and Core Recovery

Drilling equipment and drilling parameters may carry important geotechnical information on drilled rock masses and should be recorded by drillers. Most common parameters that are recorded to facilitate geotechnical interpretations of the rock mass characteristics are shown in the Table 6.2.

Core recovery depends on the drilled ground conditions and drilling methodology and therefore carries important geotechnical information. It should be systematically recorded for every drilled hole.

6.1.2 Rock Weathering

Weathering is causing significant changes of the rock strengths therefore degree of rock weathering should be defined and documented by geologists. It is recommended to use classification of the residual regolith (Butt et al. 2000)

Table 6.2 Drilling parameters recorded as part of geotechnical logs

Drilling parameters	Explanation
Drill casing	The use of drill casing is required in a poor ground
Flushing return	Loss of flush return is an indication of cavities, fractures of permeable ground
Drilling rate	Drilling rates should be recorded by drillers and reviewed by geologists. Low drilling rate can indicate for highly fractured and/or very competent rocks. High drilling rates are indicative of a soft ground
Water level	Level when water first intersected is recorded and, if possible, inflow rates documented. Static level of water in the drill hole is determined and recorded
Hole diameter	Change of hole size because of drilling difficulties should be recorded by drillers and explained to geologists

Table 6.3 Definitions of rock strength

Classification	Explanation
Extremely strong	Specimen can only be chipped with a geological hammer
Very strong	Specimen requires many blows of a geological hammer to fracture it
Strong	Specimen requires more then one blow of a geological hammer to fracture it
Moderately strong	Cannot be scrapped or peeled by a pocket knife. Specimen can be fractured with a single firm blow of a geological hammer
Weak	Can be peeled by pocket knife with difficulty. Shallow indentations made with firm blows with point of a geological hammer
Very weak	Crumbles under firm blows with point of geological hammer. Can be peeled by a pocket knife
Extremely weak	Indented by thumbnail

for defining the types of weathered material. Site specific classification of the weathered material should be developed based on documented profile of the regolith developed in the project area.

6.1.3 Rock Strength

Strength of individual rock fragments is determined and described by mine geologists logging core. Usually rock strength is qualitatively defined in the field using field equipment, such as geological hammer, pocket knife and rock scratcher. Example of the field classification of the rock strengths used by the author at the Australian mines is presented in the Table 6.3. More detailed measurements of the rock strengths are made in laboratory (Brady and Brown 2004). The measurements are made on the rock specimens which are collected by the field geologists and they should be representative for the mapped rock types.

6.1.4 Rock Quality Designation Index (RQD)

Rock Quality Designation index (RQD) was developed by Deere (1964) and since then has become the standard technique in the mining industry for quantitative assessment of the rocks quality. This parameter is routinely documented by the mine geologists for rock mass classification which are used for estimating support requirements in the underground mining.

RQD is defined as the percentage of intact core pieces longer than 10 cm recovered during a single core run (6.1.1).

$$\text{RQD}\ (\%) = 100 \times \frac{\sum\left(\text{Length of core pieces} > 0.1\text{m}\right)}{\text{Total length of Core Run}} \tag{6.1.1}$$

Core should be not less than NQ size (48 mm core diameter), however HQ size (63 mm core

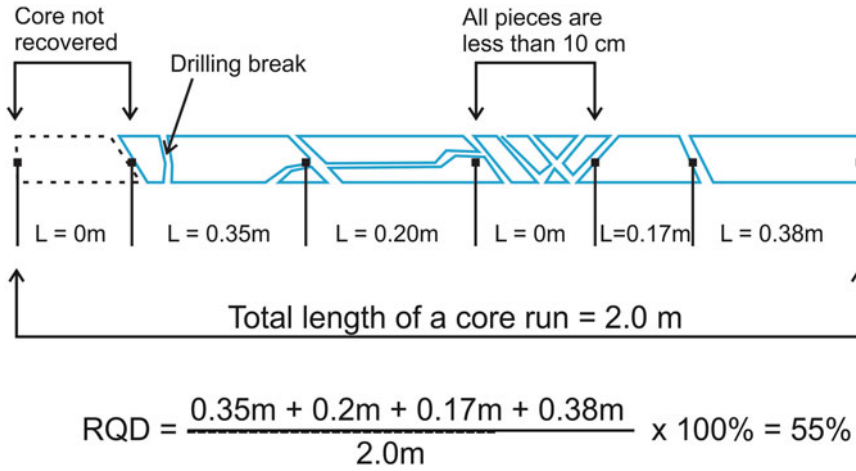

Fig. 6.1 Sketch explaining RQD measurements, generalized after Deere (1964, 1968)

diameter) and larger are preferred for RQD measurements.

RQD is directionally dependant parameter therefore its value can change depending on the drill hole orientation.

It is important that only natural fractures and fragments are used for calculation RQD. Fractures and fragments that have been induced by drilling or core handling processes should be excluded from RQD measurements (Fig. 6.1). All defects induced by drillers should be marked on the core to facilitate geotechnical logging and measurements.

Lost core should be considered as highly fragmented intervals, where all core pieces were less than 0.1 m, and they should be included in calculation of RQD (Fig. 6.1).

Measured RQD values are used for estimating the mean discontinuity spacing (Fig. 6.2) which are commonly used for calculation the rock mass classification indexes (Priest and Hudson 1981; Brady and Brown 2004).

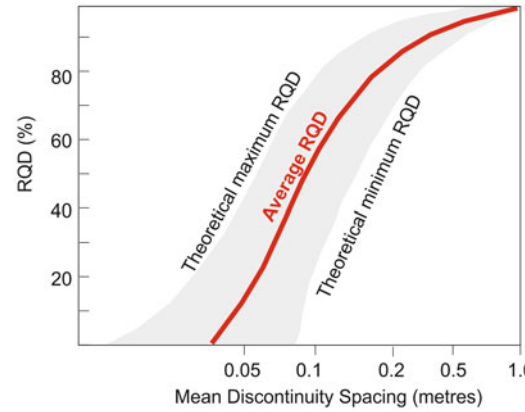

Fig. 6.2 Theoretical RQD vs. mean discontinuity spacing, generalized after Priest and Hudson (1981)

6.1.5 Natural Breaks

Natural breaks represent important geotechnical information and therefore their characteristics are thoroughly documented when core logged for geotechnical purposes. Natural breaks, also often referred as rock defects or discontinuities, can be open or sealed, and represent different geological phenomena, such as cleavage, bedding planes, joints, stress release fractures, faults, brittle shear zones, geological contacts, dykes, veins and many others. Geological nature of the defects should be clearly documented and explained in the logging guidelines where diagnostic features of each rock defect types are

concisely summarised. Type examples of each defect type should be photographed and included into logging manual.

Natural breaks should be unambiguously differentiated from the breaks induced during handling core after it was recovered from the core barrel therefore core handling procedures should include marking of the breaks which were made by drillers for fitting the drill core into core trays or accidental breaking of a long core. Defects, when logged for geotechnical purposes are classified by their strength. A common approach is to describe strength of the rock defects depending on degree of cementation of the rock fractures (Barton et al. 1974; Grimstad and Barton 1993).

Geotechnical modelling requires good understanding of preferred orientation of the rock defects. Orientation of the rock defects is measured on the orientated core, therefore, core orientation should be carried out on each core run in the geotechnical drill holes. Such holes usually located in the places which provide more detailed geotechnical information on the rock masses forming walls of the proposed open pits or underground stopes. It is important to remember that measurement of the defects orientation should be made before core was cut for assaying.

Geotechnical characteristics of the rock defects include description of the planarity (Fig. 6.3) and roughness of the breaks, which can change from slickensided type, when roughness is less than 0.1 mm, to very rough category, when roughness exceeds 5 mm (Barton et al. 1974; Grimstad and Barton 1993). Planarity represents the large scale undulations on a rock defect plane and roughness of the break surfaces characterises small scale irregularities on a defect plane.

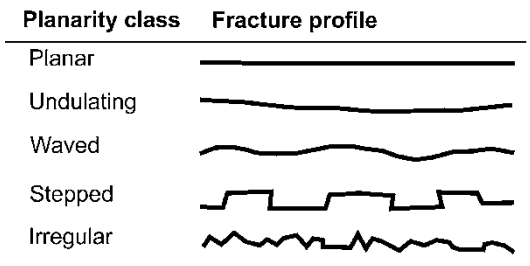

Fig. 6.3 Classification of the rock breaks

Minerals that are developed on the surface of the rock defects should be diagnosed and documented. Thickness of mineral infill developed on the rock defects is important geotechnical characteristics and it should be measured and recorded in millimetres.

6.2 Geotechnical Mapping

Geotechnical mapping of the rock faces includes collection of the same information which recorded during geotechnical core logging. However, several additional parameters can be observed on the rock faces and mapped, in particular, length of the discontinuities which is finite and can be measured on the rock faces. Length is measured along strike of discontinuity and in the down dip direction.

Discontinuities can be terminated to other defects, including faults, shear zones and joints or fading in the rocks. The type of termination of each end of the defect should be recorded on the map sheet. Spacing between discontinuities is another parameter which is difficult to measure in a drill core but is relatively easy to deduce from rock faces. It is measured as the perpendicular distance between two defects of the same set. Another important geotechnical parameter that is preferably documented in the mine workings is water seepage. This parameter is used in the rock mass classification schemes (Grimstad and Barton 1993; Hudson and Harrison 1997; Brady and Brown 2004).

Characteristics which observed in the drill core and mapped on the rock faces should be compared and reconciled. Some parameters, such as number of discontinuity sets and their geological types, usually more accurately defined on the rock faces. The discrepancies should be documented and taken into account when recorded geotechnical data analysed and geotechnical model is constructed.

6.3 Geotechnical Applications of Rock Mass Classification Schemes

Results of the geotechnical studies are used by the mine design specialists for estimating the optimal parameters of the mine excavation, including the pit slope in the open pit mines and size and shape of underground workings. Based on the geotechnical data the requirements for the roof support of the underground workings is determined together with definition of the optimal support methods and parameters of the rockbolting and shotcreting. This is usually made using a detailed information on in situ stresses, rock mass properties and planned excavation sequence.

When the detailed information is not available, in particular at the early stages of the mine development, approximate estimates can be made using a rock mass classification scheme. Using geotechnical documentation of the drill core and the rock faces mine geology team can construct a 3D geotechnical model of the mine, showing composition and characteristics of a rock mass as determined by the chosen rock mass classification scheme. The model provides an initial estimate of support requirements, and to provide estimates of the strength and deformation properties of the rock mass.

The most widely used rock mass classification schemes are Rock Mass Rating (RMR) proposed by Bieniawski (1973) and Q-index (Barton et al. 1974; Grimstad and Barton 1993). Both systems include geological, geometric and the main governing rock engineering parameters incorporating them into a single quantitative value characterising the rock mass quality. Thus, the estimated indexes provide a basic guidance for geotechnical assessment of the mine designs. In practice, the both systems provide similar results and often used together, as a single classification system arranged as a binary diagram where Q and RMR indexes represents diagram axes (Bieniawski 1993).

In order to demonstrate the principles of the rock mass classification for the mine geologists definition of the Q index is shown below.

Q index is calculated using equality (6.3.1). The geotechnical parameters used in calculations are explained in the Table 6.4. Application of the estimated Q-index for estimating of the support categories is made using classification diagrams (Fig. 6.4). Simplicity of using rock mass classification indexes made them routinely used tools in the mining industry, however, it should be remembered that use of these systems as the sole design tool cannot be supported on scientific grounds therefore the classification indexes shell be used as approximate guidance only.

$$Q = \frac{RQD}{Jn} \times \frac{Jr}{Ja} \times \frac{Jw}{SRF} \tag{6.3.1}$$

Table 6.4 Parameters for estimation Q – system (Barton et al. 1974; Grimstad and Barton 1993)

Parameter	Description	Value
RQD (rock quality designation)	Excellent	90–100
	Good	75–90
	Fair	50–75
	Poor	25–50
	Very poor	0.25
Jn (joint set number)	Massive	0.5
	One set	2
	One set random	3
	Two sets	4
	Two sets random	6
	Three sets	9
	Three sets random	12
	Four or more sets, 'sugar cube'	15
	Crushed rock	20
Jr (joint roughness number)	Noncontinuous joints	4
	Rough stepped	4
	Rough undulating	3
	Smooth stepped	2
	Smooth undulating	2
	Rough planar	1.5
	Slick undulating	1.5
	Smooth planar	1
	Slick planar	0.5
	Filled discontinuities	1
Ja (joint alteration number)	Unfilled joints	
	Healed joints	0.75
	Staining only, no alteration	1
	Slightly altered	2
	Silty or sandy coating	3
	Clay coating	4
	Filled joints	
	Sand or crushed rock filling	4
	Stiff clay filling, less than 5 mm thick	6
	Soft clay filling, less than 5 mm thick	8
	Swelling clay filling, less than 5 mm thick	12
	Stiff clay filling, more than 5 mm thick	10
	Soft clay filling, more than 5 mm thick	15
	Swelling clay filling, more than 5 mm thick	20

(continued)

Table 6.4 (continued)

Parameter	Description	Value
Jw (joint water factor)	Dry, inflow less than 5 l/min	1
	Medium water inflow	0.66
	Large inflow, unfilled joints	0.5
	Large inflow, filled joints with washout	0.33
	Large inflow, filled joints, high transient inflow	0.2-0.1
	Large inflow, filled joints, high continuous inflow	0.1-0.05
SRF (stress reduction factor)	Loose rocks with clay-filled discontinuities	10
	Loose rocks with open discontinuities	5
	Shallow depth, less than 50 m	2.5
	Rock with clay-filled discontinuities	2.5
	Rock with light unfilled discontinuities, medium stress	1

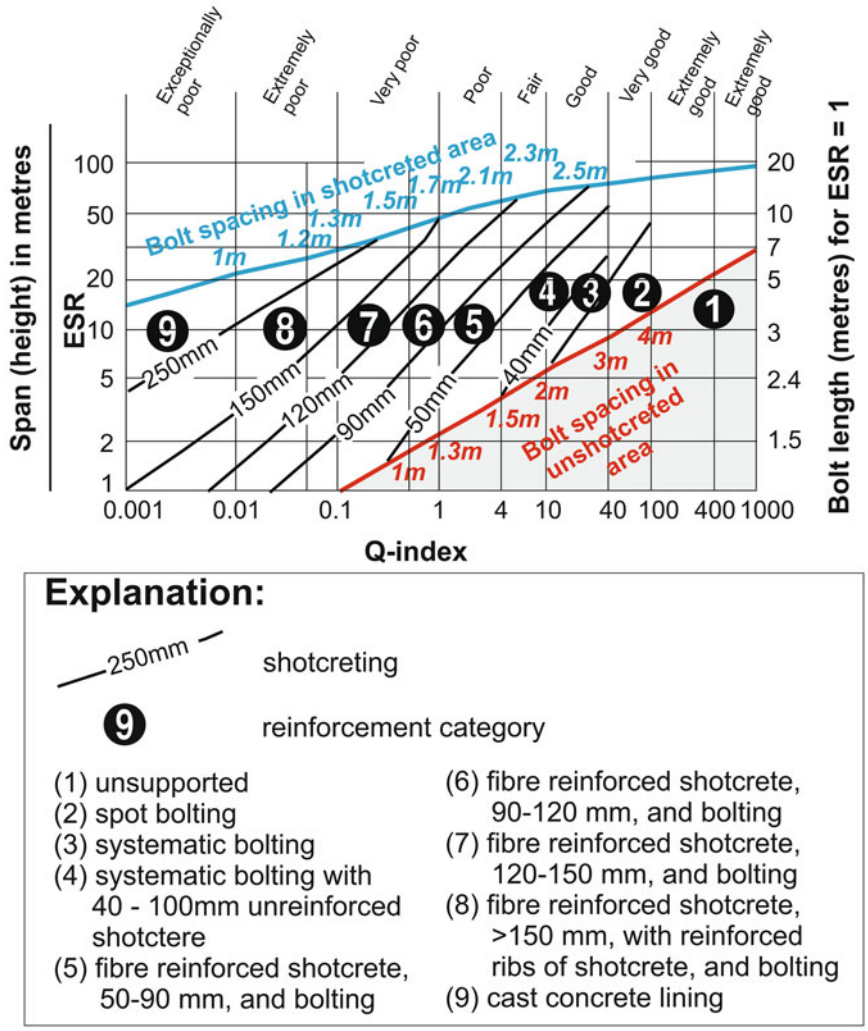

Fig. 6.4 Estimating support requirements using Q-index (Grimstad and Barton 1993). ESR (excavation support ratio) is explained in the Table 6.5

Table 6.5 Definition of the ESR (generalised after Barton et al. 1974)

Type of excavation	ESR
Temporary mine openings	3–5
Permanent mine openings (e.g. access drive for large openings)	1.6
Storage caverns (access declines, surge chambers)	1.3
Portals, intersections of the underground drives	1
Railway stations	0.8

References

Abzalov MZ (2013) Measuring and modelling of the dry bulk density for estimation mineral resources. Appl Earth Sci 122(1):16–29

Barton N, Lien R, Lunde J (1974) Engineering classification of rock masses for the design of tunnel support. Rock Mech 6:189–236

Bieniawski ZT (1973) Engineering classification of jointed rock masses. Trans S Afr Inst Civ Eng 15(12):335–344

Bieniawski ZT (1993) Classification of rock mass for engineering: the RMR system and future trends. In: Hudson J (ed) Comprehensive rock engineering. Pergamon, Oxford, 3:553–573

Brady BHG, Brown ET (2004) Rock mechanics for underground mining. Kluwer Academic Publishing, New York, p 628

Butt CRM, Lintern MG, Anand RR (2000) Evolution of regolith and landscapes in deeply weathered terrain – implications for geochemical exploration. Ore Geol Rev 16:167–183

Deere DU (1964) Technical description of rock cores for engineering purposes. Rock Mech Rock Eng 1(1):17–22

Deere DU (1968) Geological considerations. In: Stagg KG, Zienkiewicz OC (eds) Rock mechanics in engineering practice. Wiley, London, pp 1–20

Grimstad E, Barton N (1993) Updating the Q-system for NMT. In: Kompen R, Opsahl OA, Berg KR (eds) Proceedings International conference sprayed concrete – modern use of wet mix sprayed concrete for underground support. Norwegian Concrete Association, Oslo, pp 46–66

Hudson JA, Harrison JP (1997) Engineering rock mechanics. An introduction to the principles. Pergamon, Amsterdam, p 444

Lipton IT (2001) Measurement of bulk density for resource estimation. In: Edwards AC (ed) Mineral resource and ore reserve estimation – the AusIMM guide to good practice. AusIMM, Melbourne, pp 57–66

Priest SD, Hudson JA (1981) Estimation of discontinuity spacing and trace length using scanline surveys. Int J Rock Mech Min Sci Geomech Abstr 18(3): 183–197

Vutukuri VS, Lama RD, Saluja SS (1974) Handbook on mechanical properties of rocks: series on rock and soil mechanics, v2, n1. Trans Tech Publication, Bay Village, p 280

Dry Bulk Density (DBD) of Rocks

7

Abstract

The dry bulk density (DBD) is determined as dry mass of a rock (i.e. excluding natural moisture) per unit of actual *in situ* rock volume, including porosity. Despite of an obvious importance of the density for accurate estimation of resources and reserves it is often overlooked and receives significantly less attention then assayed metal grades. In this chapter the commonly used DBD measurement methods applied for the different material types, including competent non-porous rocks, weathered and porous rocks, soft partially cemented sediments and unconsolidated free flowing sands, are briefly described and their strengths, weakness and the main error sources are explained. It is shown that the bigger challenge is construction of an accurate 3D model of the rock densities distribution at the studied deposit.

Keywords

DBD • Rock density • CoreLok • Sand replacement method

Estimation of Mineral Resources and Ore Reserves require three parameters, volume, grade and the bulk density of the rocks that contain minerals of interest. Tonnage of any geological objects is obtained by multiplying its volume by density of the rocks which need to be accurately determined as part of the project study.

Grade of mineralisation is usually reported as ratio of metal or mineral of interest to unit weight. For example, grade of gold, silver and platinum mineralisation is reported as grams/tonne (g/t), diamond deposit grade is determined as carats/tonne (c/t) and for most of the metalliferous deposits grade is reported as weight percentage (wt.%). The sample assays and mineralisation grades are determined on a dry weight basis therefore rock densities which applied for estimation mineral resources and ore reserves are determined as dry bulk density, commonly referred as DBD (Abzalov 2013). In the past, the dry bulk density of the rocks was commonly referred as SG (specific gravity). However, the term SG incorrectly represents the nature of the measured rock densities and therefore is not recommended for using.

The dry bulk density (DBD) is determined as dry mass of a rock (i.e. excluding natural moisture) per unit of actual *in situ* rock

M. Abzalov, *Applied Mining Geology*, Modern Approaches in Solid Earth Sciences 12,
DOI 10.1007/978-3-319-39264-6_7

volume, including porosity. The commonly used DBD measurement methods are explained in this chapter, emphasising that methods differ depending on the material types, such as the competent non-porous rocks, weathered and porous rocks, soft partially cemented sediments and unconsolidated free flowing sands.

7.1 Types of the Rock Densities Used in the Mining Industry

Choice of the optimal methods for measuring the rock densities and thorough quality control assuring that samples are representative for the studied deposit are important for obtaining accurate model of the rocks densities of the deposit.

Most commonly the DBD values are used by the mine geologists for different mine geology applications. The DBD measurement procedures are chosen in accordance with the official standards and guidelines (AS1289.5.3.1 2004; AS2891.9.1 2005).

Some mining operations require measurements of *in situ* bulk density representing the natural *in situ* density of a rock inclusive of the water and gases within the rock pores. This is particularly important for reporting coal reserves (Preston and Sanders 1993) and usually obtained by detailed measurements of density, porosity, moisture and coal quality.

In situ bulk density can also be applied for reconciliation reserves *vs*. mine production. However, in practice, when *in situ* bulk density is needed for mine geology applications other than definition of coal reserves, it is obtained by adding the natural rock moisture to the dry tonnage of ore reserves and therefore only dry bulk density measurement techniques are reviewed in the book.

7.2 Dry Bulk Density Measurement Techniques

The dry bulk density of the geological samples is determined by dividing the dry mass of sample by its volume (7.2.1.). The dry mass in the most cases is obtained by drying sample for approximately 24 h at 110 °C and then weighing it at an accurate electronic balance.

$$\text{DBD}\left(\text{g}/\text{cm}^3\right) = \frac{\text{Dry Mass of Sample (g)}}{\text{Volume of Sample (cm}^3\text{)}} \quad (7.2.1)$$

Accurately determining volume of the sample is technically more challenging process. The volume is usually estimated using the water displacement technique which is based on Archimedes' principle (Abzalov 2013). The method includes weighing sample immersed in the water and therefore when applied to porous rocks or soft friable materials an additional preparation of the samples is needed, mainly coating or sealing of the dry sample by wax or plastic. The coating is not required for competent non-porous rocks.

Depending on the material types the density measurement techniques are subdivided into three groups: (i) competent and non-porous rocks; (ii) porous rocks and/or semi-soft rocks; (iii) soft non-consolidated sediments, such as free flowing sands.

7.2.1 Competent Non-porous Rocks

A dry bulk density of a good quality drill core can be determined by dividing its dry mass determined by weighing sample in air after it was dried by volume of a drill core.[1] This approach requires cutting a core at right angle to the core length and estimating average length and diameter of the core from several measurements. The method is simple and does not require special equipment; however, its application is limited to the samples having geometrically accurate shapes. It's not applicable when shape of the samples irregular or samples represented by several rock chips, therefore this technique is rarely applied and bulk volume of the solid non-porous rocks is measured using a water displacement technique. The method requires weighing sample in air, after

[1] $V = \pi\ R^2\ L$, where $\pi = 3.14$, R – radius of a circular base of a cylindrical drill core, L – length of core cylinder.

it was dried, and then in a water. Dry bulk density is estimated using formula (7.2.2).

$$\mathrm{DBD}\left(\mathrm{g}/\mathrm{cm}^3\right) = \frac{\mathrm{M_S}}{\left(\frac{\mathrm{M_S} - \mathrm{M_{SW}}}{\rho_{\mathrm{WATER}}}\right)} \quad (7.2.2)$$

where: M_S – dry mass of a sample in air (after sample was dried for approximately 24 h at 110 °C);

M_{SW} – mass of a sample in water;

ρ_{WATER} – water density, approximately 1 g/cm^3;

The mass of a sample in water (M_{SW}) is determined by placing the rock chips in a wire basket suspended from a balance and immersed in water (Fig. 7.1) and measured at two steps, first by weighing the empty basket immersed in a water (M_1) and then by weighing basket with a rock specimens immersed in a water (M_2). The final mass (M_{SW}) is determined by subtracting weight of an empty basket immersed in water (M_1) from the weight of basket holding the rock chips in water (M_2).

A variation of this method involves weighing an entire container of water with a sample holding basket firmly attached to container (Abzalov 2013). The procedure requires the water container is weighed twice, once when wire basket is empty and second time the same container and basket with a rock sample placed in it. Dry bulk density is estimated using formula (7.2.3).

$$\mathrm{DBD}\left(\mathrm{g}/\mathrm{cm}^3\right) = \frac{\mathrm{M_S}}{\left(\frac{\mathrm{M_{(C+B+SW)}} - \mathrm{M_{(C+B)}}}{\rho_{\mathrm{WATER}}}\right)} \quad (7.2.3)$$

where: M_S – dry mass of a sample in air (after sample was dried for approximately 24 h at 110 °C);

M_{C+B+SW} – mass of a water container with an immersed basket holding rock specimen;

M_{C+B} – mass of a water container with an immersed empty basket;

ρ_{WATER} – water density, approximately 1 g/cm^3.

Both approaches are reliable and allow to obtain an accurate estimate of the dry bulk density of the rocks. However, weighing samples in a basket suspended from electronic balance (Fig. 7.1) is used more often because of better ergonomics and all measurements can be performed using one balance. The method is simple, does not require special equipment and can be easily implemented at the mine sites and exploration camps. Dry bulk density measurement facilities are usually installed at the core farms and the density is measured at the same time when core cut for assaying. In many op-

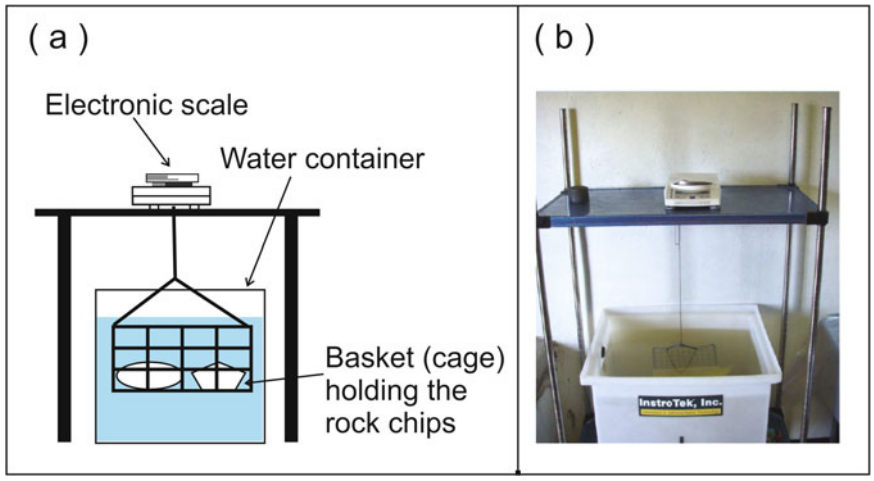

Fig. 7.1 Weighing samples in a basket suspended from a balance to water: (**a**) sketch explaining principles of the method; (**b**) electronic balance with attached wire basket used for weighing rock samples at the Simandou iron-ore project, Guinea

erations (Olympic Dam, Perseverance) the same rock specimens that collected for metal assays are also used for density measurements. The procedures are as follows:

- Drill hole logged, drill core photographed, sample intervals are marked and sample numbers assigned;
- Samples cut and placed in the trays for drying;
- Dry bulk density measured using water displacement method;
- Samples are placed in sample bags and ready for shipment to analytical lab.

Simplicity of the method does not eliminate possibility for errors. The most common sources of errors are as:

- Sample was not properly dried before weighing in air;
- Balance/scale was not properly calibrated;
- Contamination of a wire basket by rock chips from previous measurements;
- Physical or chemical characteristics of sample were changed when it was dried or immersed in water. This can happen if samples tend to disintegrate in water or temperature which used for drying samples was too high.

Quality of density measurements is usually controlled by check measurements of the selected samples in the reputable laboratory, preferably in the same lab where samples assayed for metal contents. Check measurements should be performed for every sample batch and in total 5–10 % of original measurements should be checked and confirmed by the laboratory tests.

7.2.2 Porous and Weathered Rocks

The water displacement method described in the previous section is not suitable when samples are clay-rich or represented by intensely weathered rocks. In general it can to be used when samples are represented by porous rocks or tend to disintegrate when immersed in water. Such samples need to be coated with wax after drying and before immersing in water (Lipton 2001; Abzalov 2013).

The procedure of measuring the dry bulk density of such materials is explained in AS2891.9.1 (2005) and briefly summarised below:

- Samples are dried at a temperature that not destructive for sample. If necessary, it can be a room temperature. The drying at low temperatures is facilitated by placing samples under current of air;
- Dry mass (M_S) is determined by weighing samples in air;
- Determine density of the wax;
- The sample is completely sealed by coating it with hot paraffin wax and then cooled to a room temperature;
- Sample is weighed again in air to determine the mass of a sample coated by wax (M_{S+WAX});
- Immerse the coated sample in water for 1 h;
- Transfer sample to a wire basket suspended from a balance to water (Fig. 7.1a). Weigh sample and subtract the weight of a basket to determine the weight of the coated sample in water ($M_{S+WAX\ IN\ WATER}$);
- Calculate dry bulk density of a sample using Eq. (7.2.4).

$$\mathrm{DBD}\left(\frac{\mathrm{g}}{\mathrm{cm}^3}\right) = \frac{M_S}{\left(\frac{M_{S+WAX} - M_{S+WAX\ IN\ WATER}}{\rho_{WATER}}\right) - \left(\frac{M_{S+WAX} - M_S}{\rho_{WAX}}\right)} \tag{7.2.4}$$

where: M_S – dry mass of a sample in air;
M_{S+WAX} – mass of sample coated with wax and weighed in air;
$M_{S+WAX\ IN\ WATER}$ – mass of sample coated in wax and immersed in water;
ρ_{WAX} – density of wax;
ρ_{WATER}- water density, approximately 1 g/cm^3.

The method is labour intensive and can be very time consuming mainly because of slow drying process at low temperatures. Alternatively, to competent non-porous rocks the density of porous rocks is usually determined on a single hand specimen as it is not practical to coat with wax a sample which represented by several rock chips. Usually a specimen that used for dry bulk density measurement is 10–15 cm in size which

Fig. 7.2 CoreLok device for vacuum-sealing samples in the polymer bags

is relatively small and therefore it is important to assure that the specimen is representative for studied rock type. Coating with wax is another common source of error, as it is difficult to effectively seal highly porous rocks with wax. On the other hand coating with wax is also making the specimens unsuitable for further analysis or repeat measurements of density for quality control purpose therefore accuracy and reproducibility of the measured density should be controlled by testing the duplicate samples.

Alternative approach for sealing porous and friable materials is based on vacuum-sealing of samples in polymer bags (Fig. 7.2). The procedure was developed for testing asphalt mixes and is known as 'CoreLok'.

Density measurement procedure is as follows:

- Dry sample and measure its dry mass (M_S) in air;
- Measure mass (M_{BAG}) and density (ρ_{BAG}) of polymer bag;
- Vacuum-seal sample in polymer bag (Fig. 7.2);
- The sealed sample is weighed again in air (M_{S+BAG}). This is a control measurement as weight of sealed sample should be equal to sum of its dry mass and polymer bag ($M_{S+BAG} = M_S + M_{BAG}$);
- Place the sealed sample to a wire basket suspended from a balance to water (Fig. 7.1a) and measure mass of the sample immersed in water ($M_{S+BAG\ IN\ WATER}$). Correction should be made for weight of a basket;
- Calculate dry bulk density of a sample using equation (7.2.5).

$$\mathrm{DBD}\left(\mathrm{g}/\mathrm{cm}^3\right) = \frac{M_S}{\left(\frac{M_{S+BAG} - M_{S+BAG\ IN\ WATER}}{\rho_{WATER}}\right) - \left(\frac{M_{BAG}}{\rho_{BAG}}\right)} \tag{7.2.5}$$

where: M_S – dry mass of a sample in air

M_{BAG} – mass of sample sealed in bag and weighed in air

M_{S+BAG} – mass of sample sealed in bag and weighed in air

$M_{S+BAG\ IN\ WATER}$ – mass of sealed sample in water

ρ_{BAG} – density of the polymer bag

ρ_{WATER} – water density, approximately 1 g/cm^3.

The CoreLok methodology has an advantage over conventional coating with wax:

- CoreLok measurements are not dependent on mix specific calibrations;
- Different sample sizes and shapes can be used including rock chips;
- Method is suitable practically for all types of geological materials, including one that can be destroyed in water;
- Samples remain dry and uncontaminated and suitable for further testing purposes and control measurements of dry bulk density;
- Sealing process is fast and usually takes 2–3 min.

The method can also be used for determination porosity of the rocks, which can be estimated as difference between dry bulk density of the rock

and its maximum density inferred from mass of a submerged sample when it is saturated with water (M_{SAT}). The mass of a sample saturated with water is obtained by opening bag under water, usually by cuttingthem or piercing by knife. Porosity is estimated using equality (7.2.6). The variables are the same as in (7.2.5), except (M_{SAT}), which is mass of submerged sample in a polymer bag and saturated with water.

$$\mathrm{Por}\,(\%) = 100\mathrm{x}\frac{\dfrac{M_S}{\left(\dfrac{M_{S+BAG}-M_{SAT}}{\rho_{WATER}}\right)-\left(\dfrac{M_{BAG}}{\rho_{BAG}}\right)}-\dfrac{M_S}{\left(\dfrac{M_{S+BAG}-M_{S+BAG\ IN\ WATER}}{\rho_{WATER}}\right)-\left(\dfrac{M_{BAG}}{\rho_{BAG}}\right)}}{\dfrac{M_S}{\left(\dfrac{M_{S+BAG}-M_{SAT}}{\rho_{WATER}}\right)-\left(\dfrac{M_{BAG}}{\rho_{BAG}}\right)}} \tag{7.2.6}$$

The Por(%) is a measure of open porosity as isolated voids can not be saturated by water, therefore it tends to underestimate the actual porosity and should be treated as indicative measure.

Dry bulk density of weathered rocks can also be determined in field using 'Sand replacement method' (AS1289.5.3.1 2004). This is a field measurement technique, not a laboratory measurement and it's designed to measure *in situ* density. The method involves digging a small cylindrical hole, approximately 300–400 cm^3 in volume and 150–200 mm in diameter depending on size of used equipment (Fig. 7.3). The hole is filling with sand of a uniform grain size and known density. Dry bulk density of a studied rock is estimated from measured dry weight of a material excavated from the hole and the volume of a hole, which is deduced from a volume (amount) of sand that was poured to fill the hole.

Equipment for 'sand replacement method' includes (Fig. 7.3) a plastic container (bottle) having a funnel shaped bottom which is attached to a plastic cone. The device also equipped with valve located above the cone (Fig. 7.3) and is used to control sand flow when its running into the test hole. The assembled apparatus is placed on a flat metal tray which is fixed into ground through four small corner holes. The central hole in the tray, approximately 150–200 mm in diameter (Fig. 7.3), is used as a pattern for digging a test hole in the studied rocks and also for pouring sands into the hole.

Procedure for measuring in situ dry bulk density is as follows:

- Density of the sand (ρ_{SAND}) that used in the experiment should be thoroughly calibrated

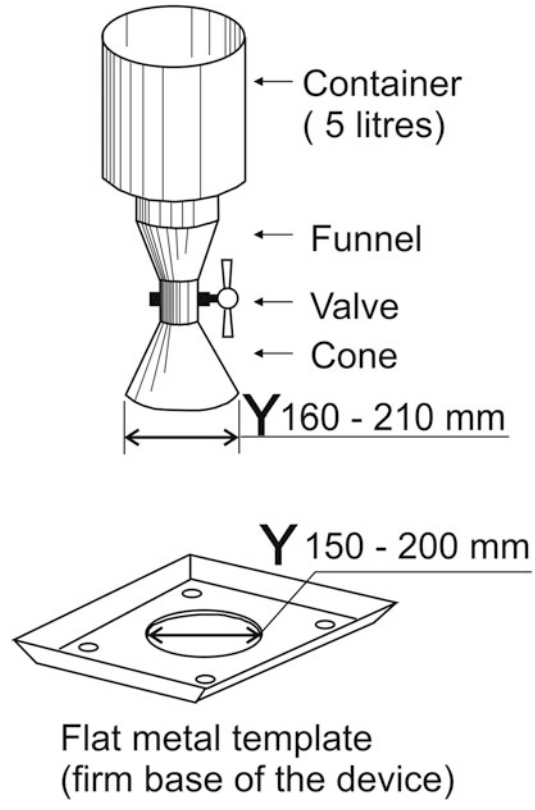

Fig. 7.3 Equipment for pouring sand, sand replacement method

using the same sand pouring devise (Fig. 7.3). It is important that each new batch of sand should be calibrated;
- In a test site, this is usually a mine bench, the flat place should be found and cleaned from compacted or disturbed material;
- Fix the tray into the place using four corner holes (Fig. 7.3);
- Dig a cylindrical hole using an opening in the middle of the tray as a template constraining the diameter of the dug hole. The test hole should not extend underneath of the template rim. The depth of the hole should be approximately the same as width of the tray;
- Collect all material that was dug from the hole and place it plastic bag, trying to prevent the moisture loss. Weigh the filled bag and determine the raw (wet) mass of a sample (M_{SW}) by subtract the weight of the bag. It is a good practice to prepare and weigh the sample bags in office before field tests. Allocated sample numbers and determined weights of the bags should be written on the front sides of the bags and recorded in the log books;
- Fill the container with sand having uniform grain size and known (calibrated) density (ρ_{SAND}). Weigh the bottle filled with sand (M_1);
- Attach the valve and cone to the container, invert it and place on top of the template. Slowly open the valve and fill the hole with a sand;
- When the hole is filled, which is determined by sand has stopped running, the valve should be closed and the device removed from the template. It is important that sand is not compacted into the test hole;
- Container with remaining sand is weighed again (M_2);
- Wet bulk density is calculated using Eq. (7.2.7).

$$\text{Wet Bulk Density } \left(\text{g}/\text{cm}^3\right) = \frac{\rho_{SAND} \times M_{SW}}{(M_1 - M_2 - M_3)} \tag{7.2.7}$$

where: M_{SW} – wet mass of a sample in air;
M_1 – the mass of sand and container before experiment;
M_2 – the mass of remaining sand and container after experiment;
M_3 – the mass of sand that filled the pouring cone on the metal tray. It's usually measured before digging the hole;
ρ_{SAND} – calibrated density of the sand that used for experiment;

- In order to estimate the dry bulk density all recovered material should be taken to laboratory and dried at approximately 100 °C to determine the dry mass of sample in air (M_S). After that, the dry bulk density is easily calculated using (7.2.8). The moisture can be calculated as ratio between dry and wet masses.

$$\text{DBD } \left(\text{g}/\text{cm}^3\right) = \frac{\rho_{SAND} \times M_S}{(M_1 - M_2 - M_3)} \tag{7.2.8}$$

The method is robust and produces accurate density estimates of soft and porous materials. The errors can be introduced if operational procedures not carefully followed, in particular, the main sources of errors are:

- Compaction of the sand in the test hole;
- Failure to keep sand dry;
- Inaccurate calibration of the sand density;
- Uneven surface where template was installed;
- Losses of material when it's transferred from the hole to plastic bag or further to laboratory for determining dry weight. Additional errors can be introduced by improper subsampling of material extracted from the test hole, in particular when sample is represented by coarse fragments of the different sizes and fines. Therefore drying the whole original sample and weighing it for determining the dry bulk density (7.2.8) is a preferred approach;
- Method can be applied only to horizontal rock surface exposed at the outcrops or mine workings and is not practical for using with the thick or steeply dipping ore bodies.

7.2.3 Non-consolidated Sediments

Measuring dry bulk density of the soft non-consolidated sands is particularly challenging because of difficulties in obtaining undisturbed representative samples, assuring that sampled sediments have not been accidently compacted during sampling. Sand replacement method may not be applicable too, because the dug voids tend to collapse when the technique (Fig. 7.3) is applied to free flowing sands. The problem can be partially overcome by using a metal cylinder with both ends open which is pressed into sands and used as a casing frame. Sediments inside of the cylinder are collected by a scoop and dried to determine a dry mass (M_S). Volume of the hole is calculated from a known internal diameter of the cylinder and the measured depth of a dug hole. Alternatively, when bottom of the hole is uneven, the volume can be determined by a sand replacement method (Fig. 7.3).

Limitations of this technique are the same as that of the sand replacement method. In particular, the method is not applicable when thickness of the studied mineralisation is several tens of metres and deep parts of the deposit can not be accessed by exploration pits or winzes.

A personal experience of the author in heavy mineral sands deposits (Abzalov and Mazzoni 2004; Abzalov 2009; Abzalov et al. 2011) shows that Sonic drilling is the most practical approach for obtaining undisturbed sample of sands located deeply below surface. The samples can be used for density measurements, in particular if drilling equipment included stainless steel split liner placed inside the core barrel (Fig. 4.32e). This technique proved to be particularly effective for definition resources of the heavy minerals sands at the Richards Bay deposit, where thickness of mineralised dunes in places reaching 170 m (Abzalov et al. 2011).

7.3 Spatial Distribution of the Rock Density Measurements

The important question is – how many density measurements need to be taken to assure that tonnage of the ore bodies and their host rocks are accurately estimated. Review of the current practices has shown that number of the dry bulk density (DBD) samples varies from less than 200 to several thousands and has reached 739,972 at the one reviewed mines (Table 7.1).

The proportion of the DBD samples to the samples collected for estimation of the metal grades varies from 5 % to 96 %. Even similar mines can significantly differ by amount of the DBD measurements (Table 7.1). For example, 4984 samples have been collected at Mesa-A iron-ore mine, located at the Pilbara region of the Western Australia. These represent 24 % of the total number of samples assayed for estimation the deposit grade. For comparison, at the West Angeles iron-ore mine, located in the Pilbara region, density was measured on 103,740 samples, which is 62 % of the total assayed samples at the deposit.

Significant differences (Table 7.1) in quantities of the density measurements indicate that at present the DBD sampling programs are designed subjectively. Rationale for choosing samples quantity and their spatial distribution is not clearly defined and the associated risks are not quantified.

Inconsistencies in the rock density measurements and in the modelling of their spatial distributions indicate that current DBD measurement programmes are set without estimation errors in the rock density models and, what is particularly important, without quantification of their impact on the resource classification categories. This limitation can be overcome if DBD values are modelled geostatistically, in the same manner as the metal grades of the mineral deposit (David 1977; Journel and Huijbregts 1978; Goovaerts 1997; Chiles and Delfiner 1999). This allows creating the non-biased 3D models of the studied variables and estimates the model uncertainties (estimation errors) which are used for non-subjective classification of the mineral resources (Royle 1977; Blackwell 1998; Dielhl and David 1982; Arik 1999; Abzalov and Bower 2009; Abzalov 2013).

Using the geostatistical approach the optimal distances between DBD samples have been determined for several deposits (Figs. 7.4 and 7.5).

Table 7.1 Comparison of the density (DBD) measurements with total number of the assayed samples (Abzalov 2013)

Deposit type	Number of the drill holes	Number of assay samples	Number of samples for the rock density measurements	Density (t/m^3)	COV[a] of density	Metal, mineral	Average grade	COV[a] of the grade
Nickel sulphide, high grade disseminated	1155	43,258	40,121	2.95	0.15	Ni,%	1.46	1.10
Nickel sulphide, low-grade disseminated	134	16,794	14,301	2.97	0.07	Ni,%	0.25	2.29
Iron Oxide Copper Gold	8280	812,556	739,972	3.27	0.16	Cu,%	1.24	1.32
Unconformity uranium	619	62,357	3035	2.70	0.03	U_3O_8,%	0.32	3.03
Copper porphyry	121	28,604	3362	2.73	0.02	Cu,%	0.55	1.05
Iron-ore, CID-type	1420	20,373	4984	2.56	0.14	Fe,%	48.14	0.28
						Al_2O_3,%	5.50	0.73
						SiO_2,%	14.27	1.20
Iron-ore, BIF derived	5458	166,167	103,740	2.57	0.15	Fe,%	52.08	0.25
						Al_2O_3,%	5.20	1.14
						SiO_2,%	12.02	1.18
Orogenic gold	327	27,184	2535	2.83	0.03	Au,g/t	1.47	6.44
Diamond, kimberlite pipe	13	184	177	2.78	0.03	Diamond, c/t	4.99	0.42
Diamond, kimberlite pipe	20	442	248	2.13	0.17	Diamond, c/t	3.40	0.62

[a]COV (coefficient of variation) = standard deviation/mean

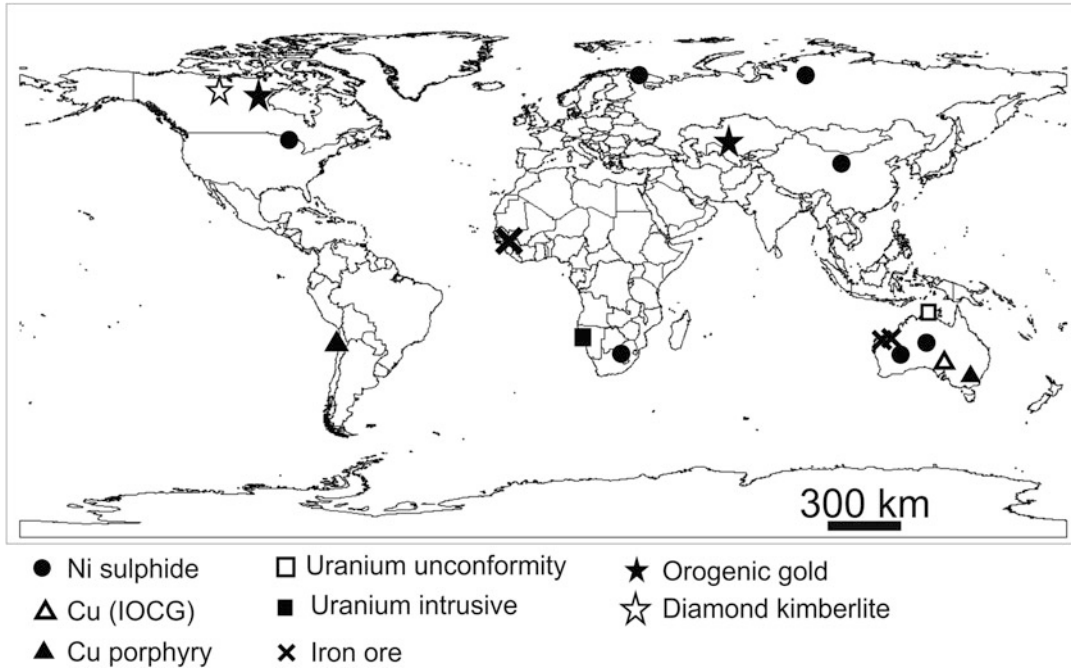

Fig. 7.4 Map showing deposits chosen for case studies of the rock density distributions

Estimation errors were deduced from the extension variance which is an average variogram value (F-function) when spatial distribution patterns of the data correspond to 'random stratified grid' (Abzalov 2013). Grid was considered optimal if the average density of the rocks at the deposit was estimated with an error of +/− 10 % (at 95 % CL). The classification criteria applied to the studied deposits are as follows (Abzalov 2013):

- Measured Resources (Proved Reserves) include mineralisation for which tonnage and grade of a panel representing a quarterly production is estimated with uncertainty of ±10 % error with approximately 95 % confidence (2 standard deviations);
- Indicated Resources (Probable Reserves) include mineralisation for which tonnage and grade of a panel representing annual production was estimated with uncertainty of ±10 per with approximately 95 % confidence (2 standard deviations).

Based on the geostatistical models (Abzalov 2013) the uncertainties (estimation errors) of the ore reserves have been estimated for the rock densities and the metal grades and plotted versus corresponding them sampling distances (Fig. 7.6). The diagrams (Fig. 7.6) clearly show that estimation errors of the rock densities are consistently lower than of the metal contents suggesting that accurate estimation of the rock densities for classification ore reserves can be made using considerably less samples than needed for modelling the metal grades at the same deposits (Fig. 7.6; Table 7.2). The data presented in the Table 7.1 indicate that some mining projects tend to collect unnecessarily large amount of the DBD samples.

The geostatistically optimal proportions between chemical assays and the DBD measurements shown in the Table 7.2 can be used as approximate guide for choosing sampling grids at the early stages of exploration. However, it should be noted that estimates presented in the Table 7.2 are only approximate and therefore can not be directly applied for classification mineral

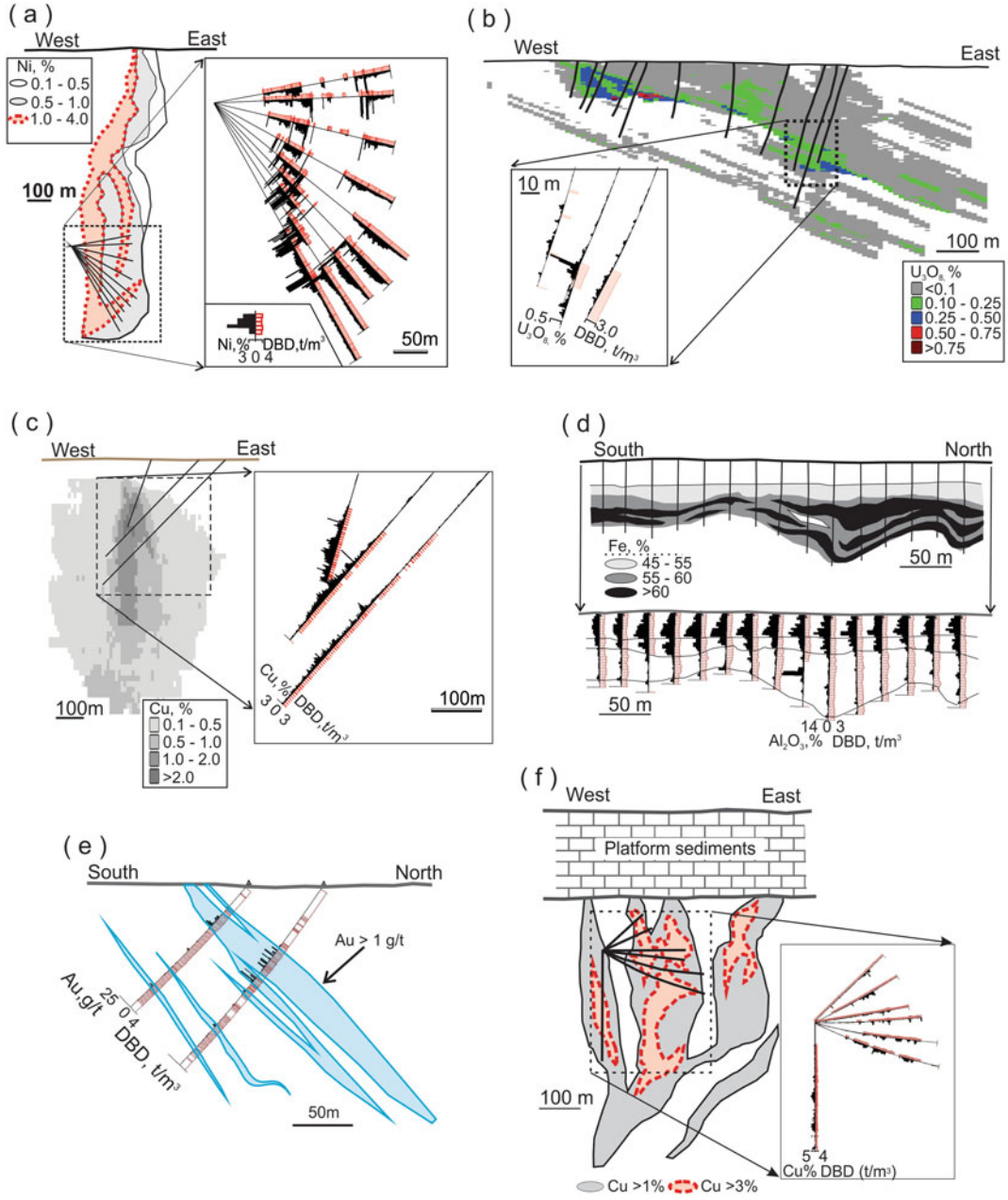

Fig. 7.5 Cross-sections of the selected deposits showing distribution of dry bulk density (t/m3) and the metal grades assayed on drill hole samples. Reprinted from (Abzalov 2013) with permission of Taylor-Francis Group: (**a**) Perseverance Ni-sulphide deposit, Australia; (**b**) Ranger unconformity type uranium deposit, Australia; (**c**) Northparkes Cu-porphyry deposit, Australia; (**d**) West Angeles BIF-derived iron-ore deposit, Australia; (**e**) Meliadine orogenic gold, Canada; (**f**) Olympic Dam IOCG-type copper-gold-uranium deposit, Australia

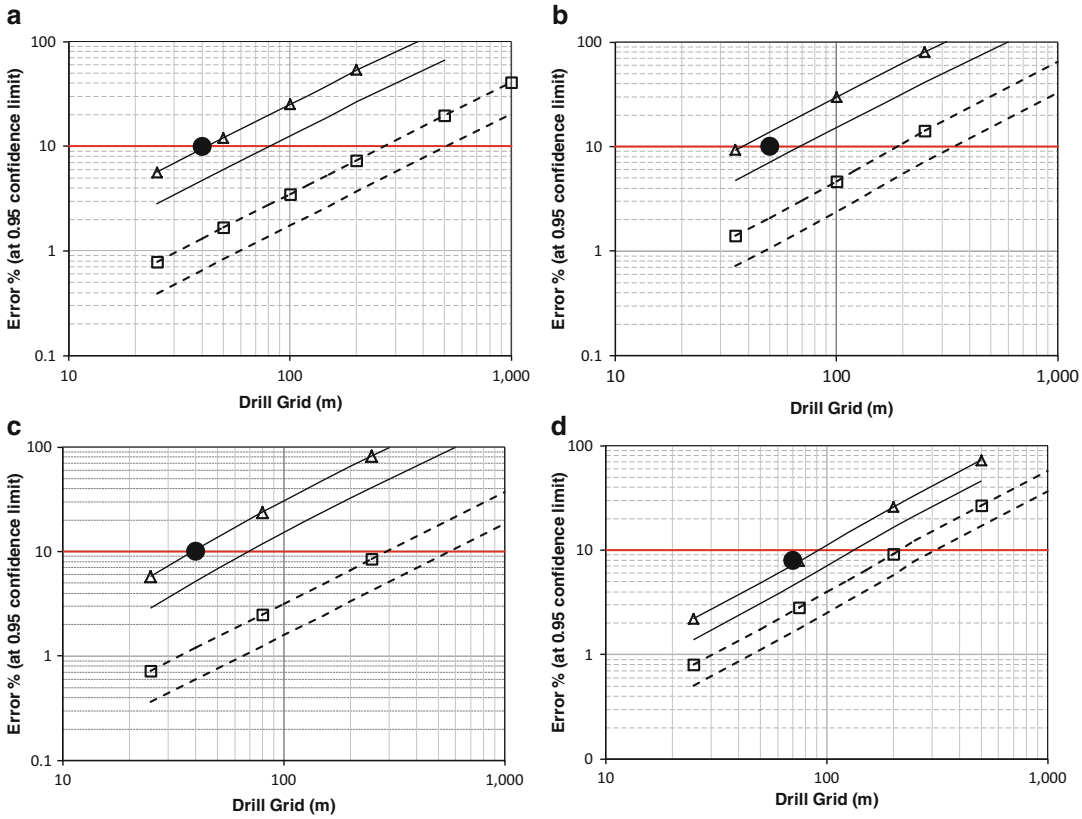

Fig. 7.6 Estimation errors at different sampling grids. Reprinted from (Abzalov 2013) with permission of Taylor-Francis Group: (**a**) high-grade Ni-sulphide deposits (Fig. 7.5a); (**b**) unconformity uranium (Fig. 7.5b); (**c**) Cu porphyry (Fig. 7.5c); (**d**) BIF derived iron ore (Fig. 7.5d); (**e**) orogenic gold (Fig. 7.5e); (**f**) CID type iron ore; (**g**) low-grade Ni-sulphide; (**h**) IOCG type (Fig.7.5f)

resources. Classification requires more work which is commonly made at the more advanced stages of exploration using stochastic simulation or another special geostatistical techniques (Royle 1977; Dielhl and David 1982; Goovaerts 1997; Blackwell 1998; Chiles and Delfiner 1999; Arik 1999; Abzalov and Mazzoni 2004; Abzalov and Bower 2009).

The same approach can be used for determining optimal number of the DBD measurements for the grade control purposes (Abzalov 2013). Grade control is performed at the operating mines by additional infill drilling or sampling the blast holes which are assayed for economically valuable metals and the deleterious components. However, rock densities are rarely measured at this stage and therefore tonnage of the mined ore is determined using the rock densities measured during the resource definition drilling. Optimal number of the DBD measurements for grade control purposes have been estimated assuming that objective of the grade control is accurate estimation of the daily ore production (Abzalov 2013). Results are summarised in the Table 7.2 which shows that geostatistically optimal grids for measuring the rock densities commonly lay between chemical assay grids needed for estimation proved and probable reserves.

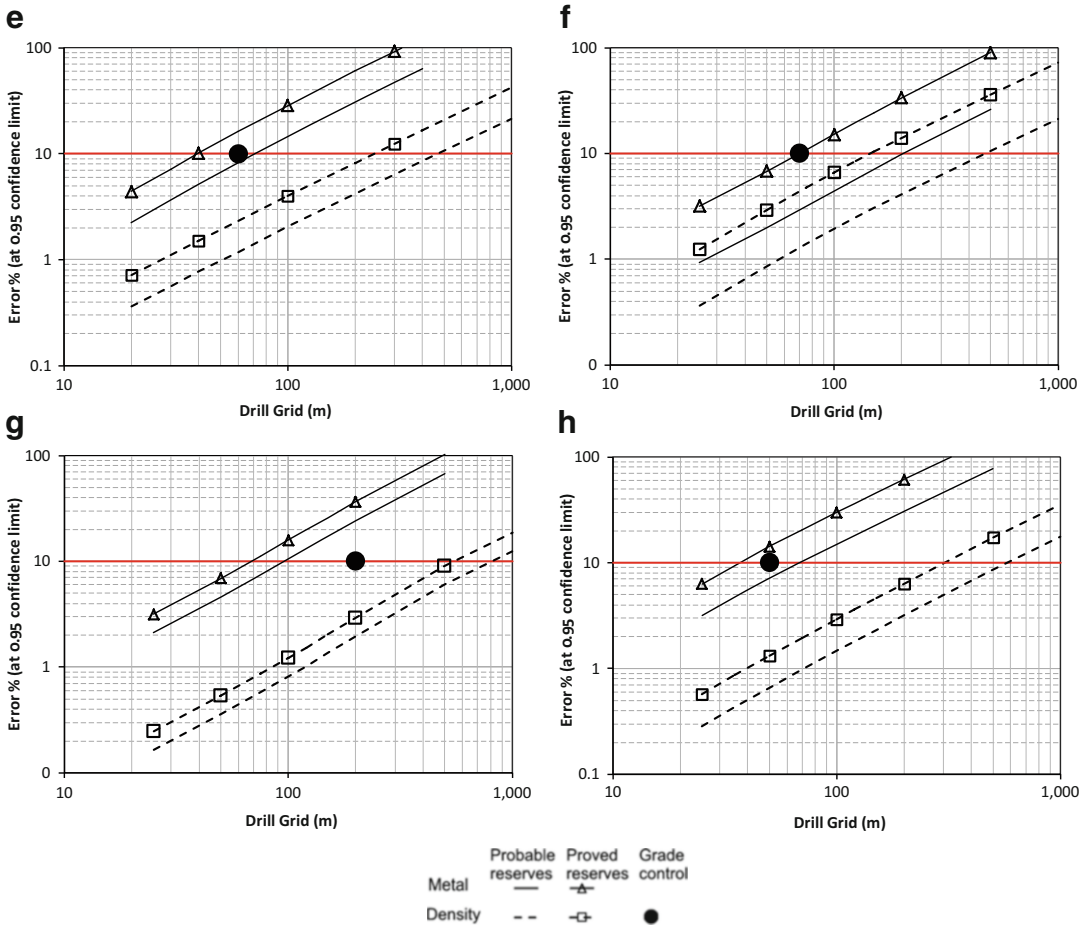

Fig. 7.6 (continued)

Table 7.2 Geostatistically estimated optimal sampling grids for estimation reserves and for the production grade control (Abzalov 2013)

	Metal grade		DBD		
Deposit type	Proved reserves	Probable reserves	Proved reserves	Probable reserves	Grade control
Ni sulphide (high grade)	40 × 40	80 × 80	250 × 250	500 × 500	40 × 40
Ni sulphide (low grade)	70 × 70 (month)	100 × 100 (quarter)	500 × 500 (month)	800 × 800 (quarter)	200 × 200
IOCG	35 × 35	70 × 70	300 × 300	550 × 550	50 × 50
Unconformity uranium	35 × 35	70 × 70	175 × 175	350 × 350	50 × 50
Cu-porphyry	40 × 40	80 × 80	300 × 300	550 × 550	40 × 40
Iron ore (BIF derived)	80 × 80 (month)	150 × 150 (quarter)	200 × 200 (month)	300 × 300 (quarter)	70 × 70
Iron ore (CID)	70 × 70 (month)	200 × 200	150 × 150 (month)	500 × 500	70 × 70
Au orogenic	40 × 40	70 × 70	250 × 250	450 × 450	60 × 60

References

Abzalov MZ (2009) Use of twinned drill – holes in mineral resource estimation. Exp Min Geol J 18(1–4):13–23

Abzalov MZ (2013) Measuring and modelling of the dry bulk density for estimation mineral resources. App Earth Sci 122(1):16–29

Abzalov MZ, Bower J (2009) Optimisation of the drill grid at the Weipa bauxite deposit using conditional simulation. In: Seventh international mining geology conference. AusIMM, Melbourne, pp 247–251

Abzalov MZ, Mazzoni P (2004) The use of conditional simulation to assess process risk associated with grade variability at the Corridor Sands detrital ilmenite deposit. In: Dimitrakopoulus R, Ramazan S (eds) Ore body modelling and strategic mine planning: uncertainty and risk management. AusIMM, Melbourne, pp 93–101

Abzalov MZ, Dumouchel J, Bourque Y, Hees F, Ware C (2011) Drilling techniques for estimation resources of the mineral sands deposits. In: Proceedings of the heavy minerals conference 2011. AusIMM, Melbourne, pp 27–39

Arik A (1999) An alternative approach to resource classification. In: Proceedings of the 1999 computer applications in the mineral industries (APCOM) symposium. Colorado School of Mines, Colorado, pp 45–53

AS1289.5.3.1 (2004) Australian standard, methods of testing soils for engineering purposes. Method 5.3.1: soils compaction and density tests – determination of the field density of a soil – sand replacement method using a sand-cone pouring apparatus. Standards Australia International, Sydney, pp 12

AS2891.9.1 (2005) Australian standard, methods of sampling and testing asphalt. Method 9.1: determination of bulk density of compacted asphalt – waxing procedure. Standards Australia International, Sydney, pp 8

Blackwell G (1998) Relative kriging error – a basis for mineral resource classification. Exp Min Geol 7(1–2):99–105

Chiles J-P, Delfiner P (1999) Geostatistics: modelling spatial uncertainty. Wiley, New York, p 695

David M (1977) Geostatistical ore reserve estimation. Elsevier, Amsterdam, p 364

Dielhl P, David M (1982) Classification of ore reserves/resources based on geostatistical methods. CIM Bull 75(838):127–135

Goovaerts P (1997) Geostatistics for natural resources evaluation. Oxford University Press, New York, p 483

Journel AG, Huijbregts CJ (1978) Mining geostatistics. Academic, New York, p 600

Lipton IT (2001) Measurement of bulk density for resource estimation. In: Edwards AC (ed) Mineral resource and ore reserve estimation – the AusIMM guide to good practice. AusIMM, Melbourne, pp 57–66

Preston KB, Sanders RH (1993) Estimating the *in situ* relative density of coal. In: Australian coal geology, vol 9. AusIMM, Melbourne, pp 22–26

Royle AG (1977) How to use geostatistics for ore reserve classification. World Min, February, 52–56

Data Points Location (Surveying)

8

Abstract

Errors in the data points coordinates, which can be made during surveying or transfer of the data, can significantly mar efficiency of the mining operations and downgrade categories of the estimated resources and reserves. Therefore, it is important that surveying procedures are thoroughly monitored by the geological teams and quality of the data points location regularly checked and verified.

Geological teams evaluating mining projects and working at the operating mines need to assure that all the data points are located accurately, this includes drill holes (collar and down-hole surveys), trench and surface samples and also rock faces which were chosen for mapping.

Keywords

DTM • DGPS • Down-hole survey • Gyroscopic (Gyro)

Surveying is performed by the certified surveyors, therefore it is not a *senso stricto* task for the mine geologists. However, it is discussed here because the mine geologists are the main clients for surveying teams, they request the surveyors to pick up the data points and utilise the obtained data for construction 3D geological and mineral resource models, which are used for updating mine development plans and the production schedules.

It is important that errors in the data points coordinates, which can be made during surveying or transfer of the data, can significantly mar efficiency of the mining operations and downgrade categories of the estimated resources and reserves. Therefore, it is important that surveying procedures are thoroughly monitored and quality of the data points location regularly checked and verified, the tasks usually assigned to the mine geologists. Geological teams evaluating mining projects and working at the operating mines need to assure that all the data points are located accurately, this includes drill holes (collar and down-hole surveys), trench and surface samples and also rock faces which were chosen for mapping.

Control of the data points is usually made by comparing different sets of data. This can be different types of data or their different generations. It is also a common procedure to control survey

M. Abzalov, *Applied Mining Geology*, Modern Approaches in Solid Earth Sciences 12,
DOI 10.1007/978-3-319-39264-6_8

quality by repeating measurements using different equipment. The most common approaches which are used for verification coordinates of the surveyed data points, quantification of the diagnosed errors and for estimating their impact onto the mineral resources are described in this chapter.

8.1 Surface Points Location

The surveyed points located on the surfaces of the rocks, which can be topographic surface or mine excavations, are usually validated by comparing their surveyed Z coordinates with the Z* values derived from the digital model of the topographic surface, commonly referred as Digital Terrane Model (DTM) (Fig. 8.1). The good practice is to present results as the histograms of the estimated errors (Fig. 8.2) and plot the errors on the maps with a DTM topography shown as a background (Fig. 8.2). The most common factors causing differences between surveyed elevations (Z) and matching them Z* values derived from the DTM surface are as follows:

- Errors of the surveyed coordinates;
- Incorrect DTM surface, due to modelling algorithm, data density, errors in raw data;
- Mixed surveyed point numbers;
- Mixed X and Y coordinates of the surveyed points;
- Use of different grid systems and the conversion errors
- Typing errors or data have been changed during electronic transfer.

Simplicity of the method (Fig. 8.1) and utilisation of the existing sets of data allow to apply this method as a routine test for quick screening of the survey data immediately after completion of the survey. The difference between Z and Z* values indicates for presence of the errors in the recorded coordinates and this will trig a special investigation of the surveying procedures. Example of successful application of this test is shown on the Fig. 8.2. The large difference between Z coordinates of the drill hole collars reported by surveyors and corresponding them Z* values derived from the digital terrane model have trigged the special investigation which have found that topographic surface has been overly smoothed by surveyors. Instead of digital model of the topographic surface the method can use the mine surfaces, which can be open pit benches and the underground excavations.

However, it should be noted that the proposed approach (Fig. 8.1) addresses only the Z coordinate and this is the main limitation of the technique. It also does not allow exact diagnostic of the error sources therefore the method should be considered as a preliminary check of the surveyed data quality which not eliminating the needs for more detailed quality control procedures.

8.2 Down-Hole Survey

Drill holes, which remain the main tools for sampling of the mineral deposits and estimation their resources and reserves, need to be accurately located using the down hole surveying instruments. The instruments, most commonly used in exploration and mine geology, are as follows:

- Magnetic survey instruments. These instruments, which usually referred as single shot or

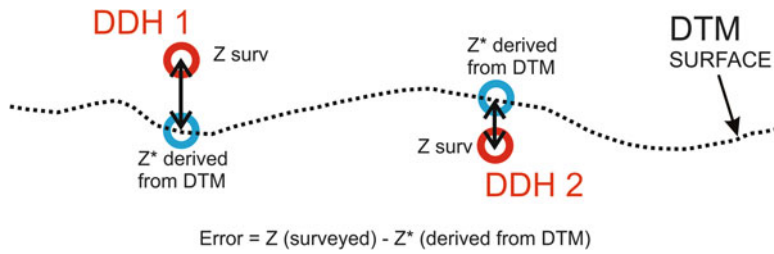

Fig. 8.1 Sketch explaining relationships between Z coordinates of surveyed data points (*red dots*) and matching them Z* values derived from the points projection onto the digital model of the topographic surface (DTM)

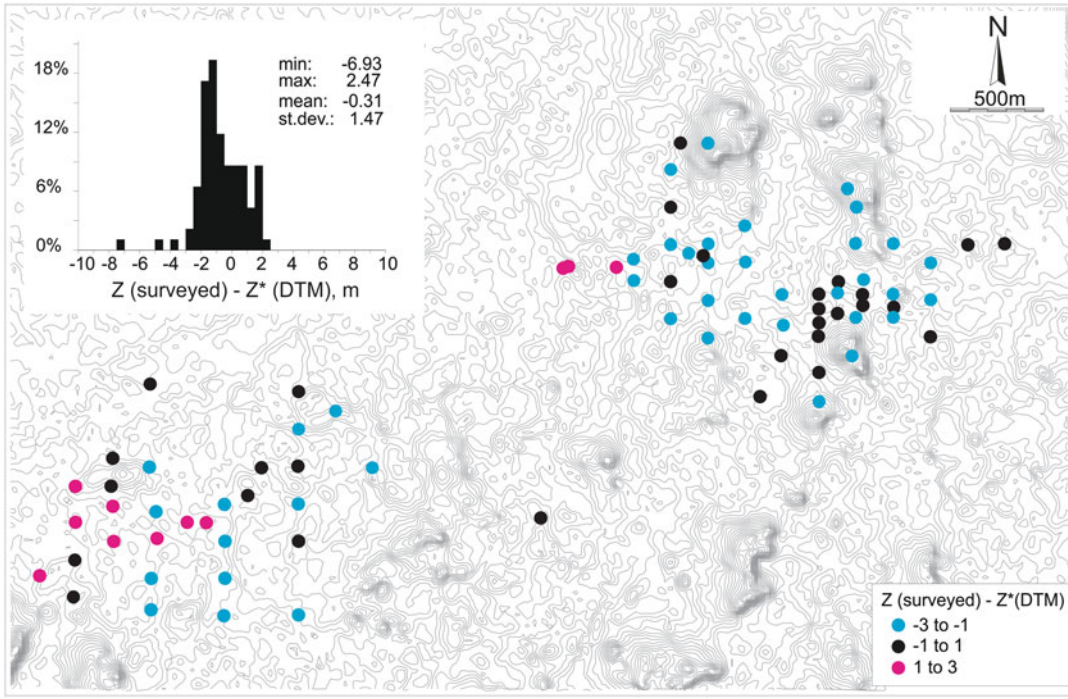

Fig. 8.2 Surveying errors (Z surveyed – Z* DTM, m) presented as the histogram and map. Topographic surface is shown on the background. West Musgrave Ni-sulphide project, Australia

multi shot down hole survey cameras, measure direction of the drill hole based on magnetic principles. Inclination (dip) of the hole is determined by gravimetric measurement;

- Optical non-magnetic instruments (e.g. Reflex Maxibor). It uses optical measurements for recording of direction changes and gravimetric measurements of dip changes;
- Gyroscopic instruments. The instrument is uses the gyroscopic principles for estimation of the true azimuth.

Optical and gyroscopic instruments have advantage over the magnetic instruments because they are not affected by ferromagnetic materials therefore can be used in magnetically disturbed rocks. Magnetic instruments are unsuitable if the host rocks contain magnetic minerals, in particular magnetite, and produce highly erratic results. Comparison of the drill hole paths surveyed by multi shot magnetic camera with the coordinates obtained using Gyro instrument are shown on the Fig. 8.3. The drill hole coordinates based on the magnetic down hole survey were shifted by more than 30 m in comparison with the Gyro survey results (Fig. 8.3). The erratic measurements were caused by magnetic disturbance due to presence of the magnetite mineralisation and could occur even at the shallow holes, 150–200 m deep, if the magnetite rich layers present in the drilled sequence.

The optical and gyroscopic survey measurements also can be used inside of the drill rods, which is in particular important when drilled rocks are soft and therefore unsuitable for using instrument in the open hole. This is another advantage of these instruments over more conventional magnetic cameras.

Although optical and gyroscopic instruments in general produce better results than magnetic cameras (Nordin 2009) none of the surveying

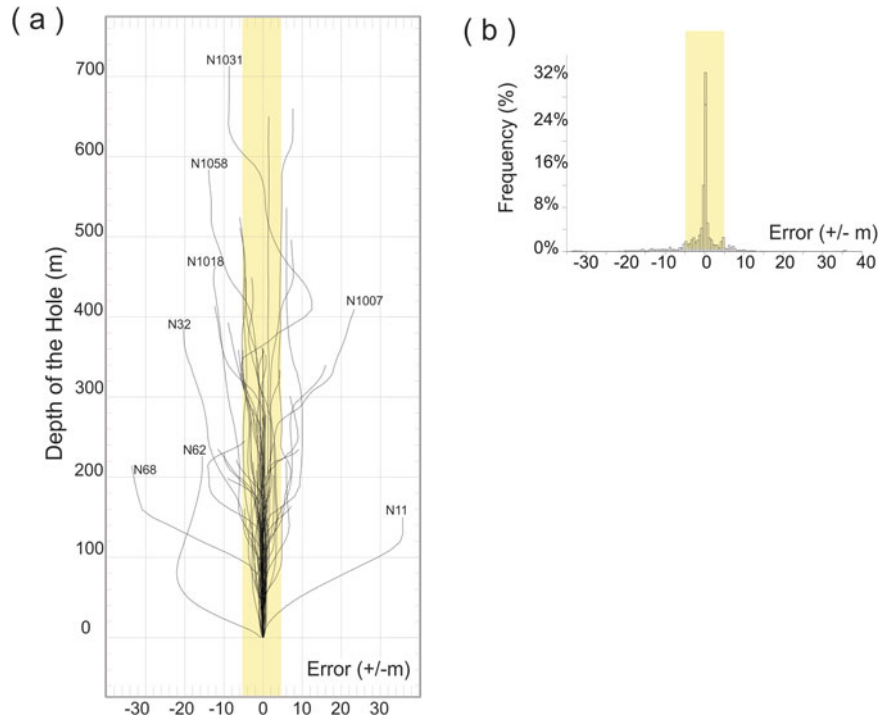

Fig. 8.3 Diagrams showing the differences (errors) between the magnetic multi shot survey camera and the Gyro down hole survey, West Musgrave Ni-sulphide project, Australia: (**a**) deviations of the drill hole path deduced from the magnetic survey in comparison with the Gyro based drill hole coordinates; (**b**) histogram of the survey errors

instruments can guarantee that survey results are accurate. In order to assure the quality of the down hole survey the instruments need to be regularly checked, their errors estimated and calibrated depending on a hole depth and orientation. In addition, the down hole survey results should be systematically verified by the alternative measurements. In particular, it is a good practice to survey the holes twice. The first measurements are made when instrument inserted into a hole and moving in the down a hole direction, second readings are taken when instrument is retrieved from the hole.

Nordin (2009) has suggested a practical procedure for calibrating instruments and estimating their errors which can be used routinely at the operating mines and also applicable for mining projects. The proposed procedure is based on using a long PVC as an artificial drill hole. In his study, Nordin (2009) has used 389.6 m long pipe which was laid down along the slope of the hill. Vertical difference between start and end of the pipe was 44 m. The pipe was clamped to the concrete blocks to assure that it is not shifted during experiment. Location of the pipe was accurately surveyed to produce true trace of the hole. The artificial hole can be used for comparison different instruments and calibrating their errors. It is noted (Nordin 2009) that down hole survey error cumulative and deviation of the surveyed hole trace from the true path increases with the down a hole distance. Using of artificial hole allows to calibrate down hole survey errors as a function of the distance from the drill hole collar. The estimated errors can be plotted as the error ellipses around the drill hole intersections on the longitudinal projections of the ore body or their plans (Fig. 8.4).

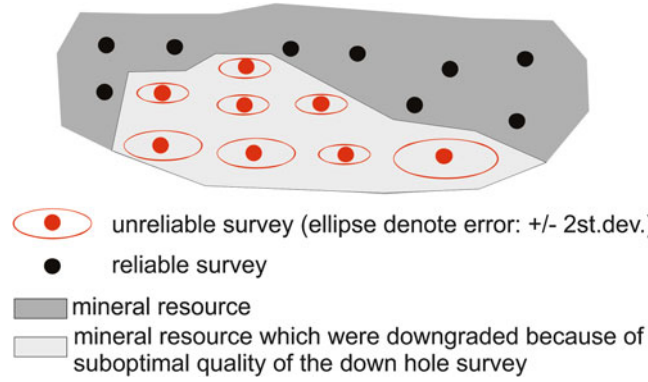

Fig. 8.4 Schematic presentation of the longitudinal view of the ore body showing impact of the down hole survey quality onto the mineral resource categories

Survey results which are characterised by a large error are unreliable and should be clearly presented on such plans (Fig. 8.4). It is likely, that the large down hole survey errors will lead to downgrading category of the mineral resources.

Reference

Nordin W (2009) The effect of downhole survey uncertainty on modelled volume. In: 7th international mining geology conference. AusIMM, Melbourne, pp 81–84

Part II

Sampling Errors

Introduction to the Theory of Sampling

9

Abstract

Theoretical background of sampling errors explained including detailed analysis of the types of the errors and the factors causing them. A special attention is paid to Fundamental Sampling Error (FSE) which can be estimated and used for establishing optimal sampling procedures (sampling protocols) at the studied project.

Keywords

TOS • Precision • Accuracy • Fundamental sampling error • Sampling protocol • Nomogram

The fundamental cause of the sampling errors is heterogeneity of the sampled materials which is used as an underlying concept in the Theory of Sampling (TOS) (Gy 1979; Pitard 1993). The more heterogeneous is the sampled material the more difficult is to obtain representative sample and infer characteristics of the geological object from samples. Intuitive look on relationships between degree of the heterogeneity of the sampled mineralisation and representativeness of sample is shown on the Fig. 9.1.

9.1 Types of Sampling Errors

Sampling errors are traditionally determined in terms of precision and accuracy of the data (Fig. 9.2). Precision, or repeatability, is a measure of how close are sample values to each other (Fig. 9.2) and accuracy is a measure of how close is sample value to the true grade (Fig. 9.2). Both of these parameters have to be estimated and strictly monitored during evaluation of the mineral deposits and their eventual exploitation.

These errors can be generated at any stage of samples extraction, preparation and their eventual analytical assaying. Example of sampling protocol (i.e. sample preparation flow sheet) and possible errors associated with each stage of material comminution and reduction are shown on the Fig. 9.3.

In the current study the sampling errors are grouped by their types and factors causing errors (9.1.1).

$$\text{TOTAL ERROR} = \text{Err. 1st Group} + \text{Err. 2nd Group} + \text{Err.3rd Group} \quad (9.1.1)$$

M. Abzalov, *Applied Mining Geology*, Modern Approaches in Solid Earth Sciences 12,
DOI 10.1007/978-3-319-39264-6_9

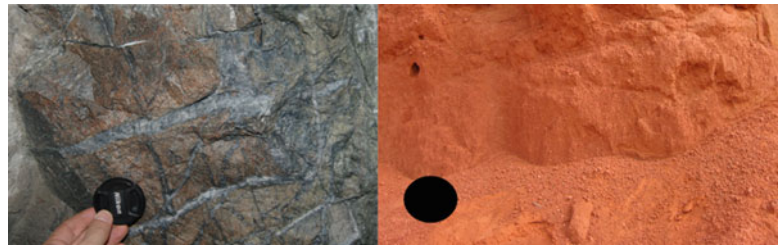

Fig. 9.1 Intuitive look on relationships between sample size, heterogeneity of the sampled materials and sampling error

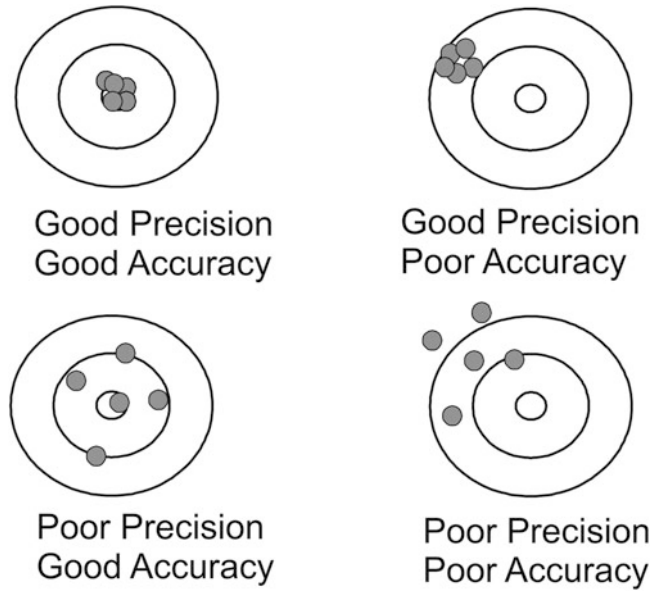

Fig. 9.2 Sketch explaining precision and accuracy of the data

Where:

Err.1st Group – is the sampling errors related to a sampling protocol;
Err.2nd Group – is the group of errors related to sampling practise;
Err.3rd Group – analytical and instrumental errors occurred at the assaying stage.

The first group includes errors related to sampling protocol. An example is poor repeatability of the sampling results caused by disproportionately small size of the samples in comparing with degree of heterogeneity of material. Main error of this type is known as Fundamental Sampling Error (Gy 1979). It is always present and can not be fully eliminated as it is related to intrinsic characteristics of the sampled material, such as mineralogy and texture of mineralisation. The Fundamental Sampling Error (FSE) can be minimised through optimisation of the sampling protocols. The first group also includes Grouping-Segregation error representing a complementary part of the FSE being a consecutive of the distribution heterogeneity of the material (Pitard 1993).

The errors associated with implementation of the protocol are combined into second group, in other words these are the errors related to sampling practices. Second group includes delimitation, extraction, preparation and weighing errors. These errors are caused by incorrect extraction of the samples from a lot,[1] their suboptimal preparation procedures and incorrect analytical measurements. Human errors, such as mixed sample numbers, can also be included to this group. These type errors can be minimised by upgrading practices of the samples extraction and preparation, which usually needs an improvement of

[1]Lot – batch of material assumed to be a single entity from which the samles are taken.

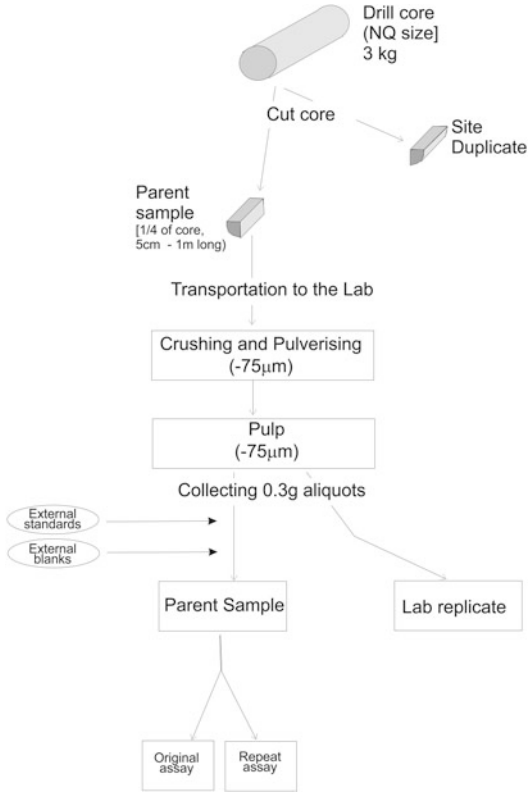

Fig. 9.3 Example of sampling protocol, gold project, Canada

the quality control procedures and often require equipment upgrading.

The third group includes various analytical and instrumental errors occurred during the analytical operations (Gy 1979) such as assaying, moisture analysis, weighing the aliquots, density analysis. These errors are considered in the current study separately from the two first groups because of the different factors causing them.

9.2 Fundamental Sampling Error

Fundamental Sampling Error (FSE) is error related to constitutional heterogeneity of the sampled material. It depends on shape and size of the particles which constitutes the sampled material, size at which the critical components are liberated and also on mineralogy and density of gangue (non-valuable minerals) and valuable components (ore minerals). It is the only error which can be theoretically determined as it directly related to the constitutional characteristics of the sampled materials.

9.2.1 Theoretical Background

The best known theoretical approach for estimating the FSE is that of the 'Sampling Theory of the Particulate Materials' which was proposed by Gy (1979) and further developed by Pitard (1993) and Francois-Bongarcon (1991, 1993, 1998, 2005). The theory states that FSE, representing precision of the samples expressed as their relative variance, can be estimated as follows:

$$\sigma^2_{FSE} = fgcld^3_N \left(\frac{1}{M_S} - \frac{1}{M_L}\right) \qquad (9.2.1)$$

where,

σ^2_{FSE} – Fundamental Sampling Error

f – shape factor. This parameter represents geometry of the particulate materials. It is dimensionless factor varying from 0, when particles are ideal cubes, to 1, when they represented by ideal spheres. Most types of mineralisation have shape factor varying in a narrow range from 0.2 (gold or mica flakes) to 0.5 (isometric grains).

g – granulometric factor, which is also called a particle size distribution coefficient or size range factor. This factor is dimensionless and taking into account the fact that fragments do not have the same size (d). If all fragments have had exactly the same size the factor (g) would be equal to 1. This theoretically is possible only in the ideal case when studied material is perfectly sorted. In practice it is never happening, therefore the (g) factor is less than one and can be as small as 0.1 when particles shows a wide range of distribution. Default values of (g) factor are summarised in the Table 9.1. In mining industry, the value of 0.25 is usually used as default value as it suites for the most types of mineralisation and

Table 9.1 Default values of the granulometric factor (Pitard 1993)

Type	Explanation	Default (g) value
Non sorted material	Output of jaw crusher	0.25
Sorted material	Material between two consecutive screen openings	0.55
Naturally sorted material	Grains, e.g. rice	0.75

corresponds to case when 95 % of particles passing the nominal mesh size.

d_N – a nominal particle size in centimetres. This is size (diameter) of a mesh retaining upper 5 % of particles.

M_S – mass of sample in grams.

M_L – mass of lot in grams.

c – mineralogical composition factor expressed as g/cm^3.

$$c = \left(\frac{1 - t_L}{t_L}\right) \times (\rho_M \ (1 - t_L) + \rho_G \ t_L) \tag{9.2.2}$$

where:

t_L – absolute grade of a lot expressed as decimal proportions of ore mineral, it changes from 0 to 1 (e.g. 1 g/t = 0.000001), ρ_M – specific gravity of ore minerals, ρ_G – specific gravity of gangue.

The formula (9.2.2) can be simplified (Francois-Bongarcon 1998) and represented by it's concise version (9.2.3).

$$c = \left(\frac{1 - t_L}{t_L}\right) \times \left(\frac{\rho_M \times \rho_G}{\rho}\right) \tag{9.2.3}$$

In Eq. (9.2.3) (ρ) denotes the average specific gravity of mineralisation at the given grade (t_L), other variables are the same as in (9.2.2).

For low-grade ores, a mineralogical factor (c) can be further simplified and approximated as ratio of density of the mineral of interest by the average grade of the studied material:

$$c = \frac{\rho_M}{t_L} \tag{9.2.4}$$

Mineralogical factor (c) relates the sampling variance given by formula (9.2.1) to the grade of mineralisation (lot) being sampled. Francois-Bongarcon and Gy (2001) have noted that any use of a formula and the sampling nomogram derived from is relevant only to the grade level at which it is established.

l – liberation factor, estimated as ratio of liberation size to a nominal particle size (9.2.5).

$$l = \left(\frac{d_L}{d_N}\right)^A \tag{9.2.5}$$

where: d_N – a nominal particle size in centimetres, d_L – liberation size in centimetres, representing a liberation diameter of a mineral of interest, A – exponent.

Substituting liberation factor (l) to equality defining FSE it becomes (9.2.6):

$$\sigma^2_{FSE} = fgc\left(\frac{d_L}{d_N}\right)^A d_N^3 \left(\frac{1}{M_S} - \frac{1}{M_L}\right) \tag{9.2.6}$$

If the exponent (A) is expressed as ($3-\alpha$) the FSE formula becomes (9.2.7)

$$\sigma^2_{FSE} = fgc\left(\frac{d_L}{d_N}\right)^{3-\alpha} d_N^3 \left(\frac{1}{M_S} - \frac{1}{M_L}\right) \tag{9.2.7}$$

which, after reduction of (d_N^3) becomes (9.2.8)

$$\sigma^2_{FSE} = f \ g \ c \ d_L^{3-\alpha} d_N^{\alpha} \left(\frac{1}{M_S} - \frac{1}{M_L}\right) \tag{9.2.8}$$

Product of ($f \ g \ c \ d_L^{3-\alpha}$) is known as sampling constant (Francois-Bongarcon 1993; De Castilho et al. 2005) and usually is denoted as (K).

$$K = f \ g \ c \ d_L^{3-\alpha} \tag{9.2.9}$$

Substituting sampling constant (K) to equality (Eq. 9.2.8) leads to formula of FSE (9.2.10).

$$\sigma^2_{FSE} = K d_N^{\alpha} \left(\frac{1}{M_S} - \frac{1}{M_L} \right) \quad (9.2.10)$$

The value of exponent (α) changes depending on (d_N). When (d_N) is smaller than liberation size (d_L) the exponent (α) is equal 3. Above the liberation size (d_L) the exponent (α) can be smaller, within the range from 1 to 3.

Formula (9.2.10) can be simplified by removing the ratio ($\frac{1}{M_L}$) which becomes negligibly small when mass of a lot (M_L) is significantly larger than sample mass (M_S). Removing ($\frac{1}{M_L}$) ratio from equation of FSE (9.2.10) leads to concise version of FSE formula (9.2.11)

$$\sigma^2_{FSE} = \frac{K \, d_N^{\alpha}}{M_S} \quad (9.2.11)$$

Parameters (K) and (α) can be calibrated experimentally (Francois-Bongarcon 1993, 2005, Francois-Bongarcon and Gy 2001) which make equality (9.2.10) and its concise version (9.2.11) practically most convenient tools for experimental definition of the FSE.

9.2.2 Experimental Calibration of the Sampling Constants

Sampling constants can significantly differ even between deposits of the similar mineralisation types. For example, at the lode gold deposits K-constant values vary from 1 to more than 10,000 (Table 9.2). Thus, in order to accurately estimated FSE the sampling constants need to be obtain using special calibration experiments.

Several techniques have been proposed (Gy 1979; Pitard 1993; Francois-Bongarcon 1993, 2005; Bartlett and Viljoen 2002; Minkkinen and Paakkunainen 2005; De Castilho et al. 2005; Minnitt et al. 2007) for experimental determination of the deposit specific values of the (K) and (α) constants.

The most common approaches are the technique developed by Francois-Bongarcon (2005), representing a modified version of the 'sampling tree experiment' (Francois-Bongarcon 1993), and 'heterogeneity test' of Pitard (1993). '30-Pieces Experiment' developed by Francois-Bongarcon (1993) has many similarities to above mentioned 'heterogeneity test' (Pitard 1993) representing a simplified version of it. All these experiments require collection of the special samples which are collected, processed and analysed following special procedures which are described in the current section of the book. When samples for special calibration experiments are not available the sampling constants can be approximately estimated from the available drill core samples (Francois-Bongarcon 1993).

9.2.2.1 Modified Sampling Tree Experiment (MSTE)

'Sampling Tree Experiment' was first proposed by Francois-Bongarcon (1993) and then modified (Francois-Bongarcon 2005). This modified technique represents analysis of the series of the duplicate samples (Fig. 9.4) cut from a lot at various comminution degrees (Table 9.3) allowing to experimentally obtain the (K) and (α) parameters of the Fundamental Sampling Error (9.2.11).

Theoretical background of this method is as follows. Firstly, the formula 9.2.11 can be logarithmically transformed to the equality (9.2.12):

$$\mathrm{Ln}\left(M_S \sigma^2_{FSE}\right) = \alpha \, \mathrm{Ln}\,(d_N) + \mathrm{Ln}(K) \quad (9.2.12)$$

According to this expression the values of Ln ($M_S \sigma^2_{FSE}$) are plotted against the particle sizes [Ln (d_N)] as a straight line because the

Table 9.2 Range of the K-constant values determined at the gold deposits

Degree of complexity	Range of the K-constant values	Deposit (reference)
Low level of complexity	1–100	Mulatos, Kidston, Musselwhite (Sketchley 1998)
Middle level of complexity	100–500	Meliadine (Abzalov and Humphreys 2002a)
		Zarmitan (Abzalov 2007)
High level of complexity	>500, can exceed 10 000	Big Bell, Dome (Sketchley 1998)

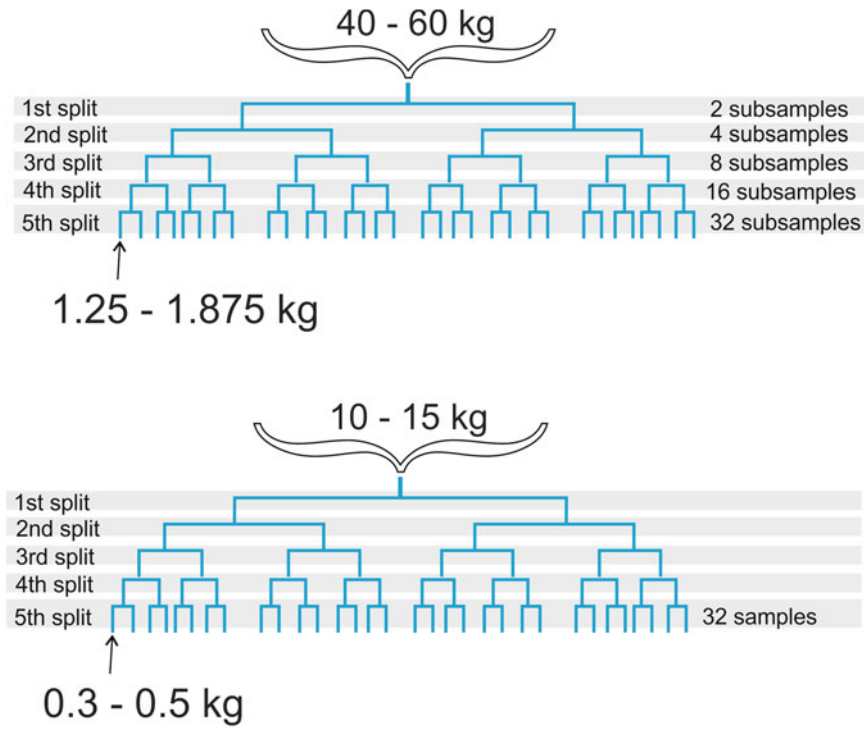

Fig. 9.4 Flow sheet of the 'Modified Sampling Tree Experiment' (MSTE). The shown binary sampling tree is applied to each of the four nominal size fractions (Table 9.3)

Table 9.3 Examples of the nominal particle sizes (cm) of the samples at the "Modified Sampling Tree Experiment"

		Sampling series					
		First	Second	Third	Forth	Elements of interest	Reference
Deposit type	Orogenic Gold	2.5	0.3	0.1	0.05	Au, As	a, b
	Ni-S: Komatiitic-type	3	1	0.5	0.1	Ni, Cu, As	b
	Cu-Au-U: IOCG-type	2.5	0.5	0.1	0.05	Cu, U, Au, S	b
	U: unconformity-type	2.5	1	0.1	0.01	U	b
	Bauxite	3	1	0.5	0.1	Al_2O_3, SiO_2, Fe, LOI	b
	Iron ore: Banded Iron Formation (BIF) -derived	3	1	0.5	0.1	Al_2O_3, SiO_2, Fe, LOI, P	b
	Cu-Au: porphyry-type	2.5	1	0.1	0.05	Cu, Mo, Au, As	b

LOI loss on ignition
Data used: a – (Minnitt et al. 2007), b – Abzalov M (unpublished data)

equality (9.2.12) represents equation of the line ($Y = AX + B$). Tangent of the angle between this line and the abscise axis (A) is equal to exponent (α) in the equality (9.2.12) and constant (B) is equal to Ln(K). The objective of the 'MSTE' is to deduce parameters (A) and (B) of a linear function describing relationships between ($M_S\sigma^2_{FSE}$) values and the particle sizes (d_N). In

practise, to infer parameters of a linear function $\mathrm{Ln}\left(M_S\sigma^2_{FSE}\right) = \alpha\,\mathrm{Ln}\,(d_N) + \mathrm{Ln}(K)$ it is sufficient to experimentally obtain several point which are plotted onto diagram $\mathrm{Ln}\,(M_S\sigma^2_{FSE})$ vs. $\mathrm{Ln}(d_N)$ and then a linear function is inferred by a suitable best fit algorithm.

'MSTE' method is based on collecting a representative sample of 40–60 kg which then dried, successively crushed and split following the flow sheet shown on the Fig. 9.4. The nominal particle sizes for the four groups of subsamples depend on mineralogy and textures of the mineralisation.

Examples of the particle sizes that have been used at the 'MSTE' are shown in the Table 9.3. The values in the Table 9.3 can be used for reference when 'MSTE' is planned; however, the best practise is to determine experimentally the sample weight and the nominal particle size of each sampling series. Procedure of the 'Modified Sampling Tree Experiment' is as follows (Fig. 9.4; Table 9.3):

- Representative sample of 40–60 kg is collected and dried;
- The whole sample is crushed at jaw crusher to a nominal size of 95 % passing the mesh size chosen for Series 1 (Table 9.3);
- One-quarter of the sample (lot) is split out and forms the first subsampling series;
- Remaining material is crushed to a nominal size of 95 % passing the mesh size chosen for Series 2 (Table 9.3);
- One-third of these secondary crushed material is split out and forms the second subsampling series;
- Remaining two fractions are recombined and crushed to a nominal size of 95 % passing the mesh size chosen for Series 3 (Table 9.3);
- The crushed material is split by riffle splitter onto two equal subsamples, one of them split out and forms the third subsampling series;
- The remaining material is crushed to a nominal size of 95 % passing the mesh size chosen for Series 4 (Table 9.3);
- Using a riffle splitter each of these portions is now split into 32 sub-samples (Fig. 9.4).

This approach produces 4 groups of 32 samples. Each group includes samples of the same nominal size of the particles and approximately of the equal weight. Two of samples are recommended (Minnitt et al. 2007) to use for granulometric analysis and remaining 30 samples are assayed and used for statistical inference of the (K) and (α) parameters.

Example of the experimentally obtained assay values of the four series of subsamples (Minnitt et al. 2007) is shown in the Table 9.4.

Table 9.4 Processing of the 'MSTE' assays

	Sampling series			
	1	2	3	4
Size (cm)	2.5	0.3	0.1	0.05
Sample average weight	340.07	385.47	385.47	316.1
1	12.96	12.08	12.76	11.42
2	14.8	11.82	13.38	13.96
3	11.86	12.08	14.24	11.08
4	11.94	12.16	13.4	12.34
5	9.56	12.88	13.14	12.98
6	10.38	12.42	12.54	11.86
7	15.76	11.76	12.72	12.32
8	17.94	12.78	12.28	12.4
9	9.88	11.32	14.28	13.04
10	5.44	11.8	12.52	13.22
11	9.54	12.74	12.78	12.28
12	14.1	12.9	13.9	12.16
13	10.28	10.86	12.4	11.62
14	12.78	12.34	13.04	12.04
15	10.78	12.24	11.36	13.24
16	14.12	12	12.74	12.76
17	9.92	12.18	13.2	12.18
18	10.3	14.04	14.18	12.04
19	24.26	12.76	12.5	12.86
20	8.78	12.56	12.98	12.78
21	6.66	14.9	13.16	12.66
22	9.98	13.4	13.94	12.5
23	13.3	12.94	13.1	12.22
24	16.48	11.28	14.44	12.4
25	s29.4	12.1	11.6	12.18
26	11.68	12.96	12.7	12.44
27	9.52	14.4	13.2	11.92
28	13.46	15.7	12.94	12.58
29	20.14	12.98	12.66	12.72
30	12.64	13.97	13.26	12
Mean	12.95	12.68	13.04	12.41
Variance	24.38	1.15	0.53	0.34

Parameters (K) and (α) are estimated as follows:

- Determine average sample weight for each of the four sub-sampling series;
- Determine mean grade and variance for each series;
- Calculate the relative variances (i.e. Relative Variance = Variance / Mean);
- Calculate logarithms of the nominal particle sizes Ln(d_N) and the logarithms of the products of the relative variances multiplied by the average weight of the samples in a given series Ln ($M_S\sigma^2_{RELATIVE}$);
- Plot four sampling series onto Ln ($M_S\sigma^2_{RELATIVE}$) vs. Ln(d_N) diagram (Fig. 9.5) and infer (α) and (K) parameters from a linear regression equation fitted to the experimental points. Constant (α) is slope of regression fitted to experimental points (Fig. 9.5) and sampling constant (K) is equal to ($M_S\sigma^2_{FSE}$) value corresponding to 1 cm particles.

Exercise 9.2.2.a Calculate sampling constant (K) of the FSE Eq. (9.2.11) using the assays obtained by the 'Sampling Tree Experiment' applied to gold ore. Data for the exercise are available in the file Exercise 9.2.2.a.xls in the Appendix 1.

9.2.2.2 30-pieces Experiment

Another calibration method is known as '30-pieces experiment'. It was proposed by Gy (1979) and has been further revised by Francois-Bongarcon (1993). This experiment is less time consuming and easier for implementation as it requires only 30 assays of chosen samples.

Procedure of this experiment is as follows. 30 pieces of rock approximately of the same size are taken at random from volume of the crushed geological material. It is important to assure that all pieces of the lot are easily accessible during sampling which means have an equal probability to be collected. All pieces are assayed and weighed so that accurate assay and mass values obtained for each of 30 pieces. Relative variance of the grade values is calculated directly from 30 assays. This value represents a FSE (σ^2_{FSE}) at the given nominal particle size (d_N) because the conditions of experiment has eliminated contributions of all other sampling error types. Average mass (M_S) is also obtained during experiment as all 30 pieces are weighed prior to assaying.

Using these parameters the sampling constant (K) can be calculated by substituting the experimentally obtained parameters into equality 9.2.13 which is derived from definition of the FSE (9.2.11). Application of this method requires assigning a default value for (α), in practice it is taken as 1.5.

$$K = \frac{\sigma^2_{FSE}\, M_S}{d_N^{\alpha}} \tag{9.2.13}$$

Where: d_N – is nominal particle size in centimetres. It is calculated from average diameter ($d_{AVERAGE}$) of all 30 pieces which is converted to a nominal particle size by dividing it on a corresponding granulometric factor (g) in the power of 1/3 (9.2.14).

$$d_N = \frac{d_{AVERAGE}}{g^{1/3}} \tag{9.2.14}$$

σ^2_{FSE} – is calculated as variance of all 30 assay values;

M_S – average mass of the analysed pieces (in grams).

Exercise 9.2.2.b Calculate sampling constant (K) of the FSE Eq. (9.2.11) using methodology of the '30-pieces experiment' (Francois-Bongarcon 1993). Data for this exercise were collected at the operating Au-Ag-U mine and saved into the file 'Exercise 9.2.2.b.xls' (Appendix 1).

30 pieces of ore of approximately the same size have been collected from crushed ore stock pile and assayed. Average grade of these pieces is 8.29 g/t, average mass 2889 g and relative variance 9.41. The density of the studied ore is 3.0 g/cm^3. It is assumed that exponent (α) is equal to 1.5.

To calculate the constant (K) it is necessary to estimate the nominal particle size (d_N). Firstly, we need to calculate the average volume of 30 pieces of ore, which is equal 2889/3.0 = 963 cm^3. Assuming that this is a sphere we can

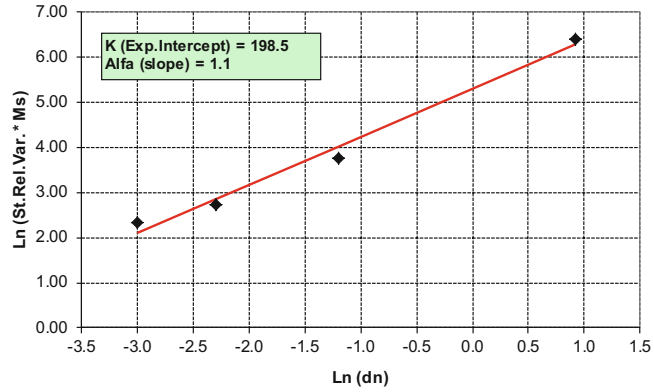

Fig. 9.5 Experimental calibration of the sampling constants (K) and (alfa) applied to the gold mineralisation

calculate diameter using trigonometric definition of a sphere volume (Sphere Volume = $4/3\ \pi$ Radius^3). In our case it gives diameter of 12.25 cm. This is an average volume of the 30 analysed pieces. In order to calculate nominal particle size the average volume is divided by ($g^{1/3}$) where (g) is a granulometric factor and for most types of mineralisation it is equal 0.25 corresponding to case when 95 % of particles passing the nominal mesh size.

Dividing average volume of 12.25 cm by ($0.25^{1/3}$) gives the nominal particle size (d_N) equal to 19.45 cm. Substituting obtained values to equality (9.2.13) gives the following result

$$K = \frac{9.41 \times 2889}{19.45^{1.5}} = 316.9$$

9.2.2.3 Heterogeneity Test

The 'Heterogeneity Test', proposed by Pitard (1993), consists in extracting of a certain number of the fragments, collected one by one at random from the coarsest size fraction of the studied material and their further statistical analysis. It is recommended (Pitard 1993) to collect approximately 50 samples when major components are studied, and more than 100 for trace elements, such as gold and other noble metals. Every of these individual samples are made from individual pieces, usually 30 fragments per each sample. Each of the collected pieces is washed, dried, weighed, and each of them assayed individually.

Based on the experimentally determined grade, mass and volume of all individual pieces the 'Constant Factor of Constitution Heterogeneity' denoted (Pitard 1993) as (IH_L) can be calculated using equality (9.2.15)

$$IH_L = g\sum_{i=1}^{N}\left[\frac{(a_i - A_B)^2}{A_B^2} \times \frac{m_i^2}{\sum_{i=1}^{N} m_i}\right] \tag{9.2.15}$$

where, N is a total number of collected fragments in a batch,

(a_i) and (m_i) are the grade and a mass of (i) piece, respectively, (g) is a granulometric factor, which is equal to 0.25, and (A_B) is weighted average grade of a single piece in a batch (9.2.16)

$$A_B = \frac{1}{\sum_{i=1}^{N} m_i}\sum_{i=1}^{N} a_i m_i \tag{9.2.16}$$

The factor (IH_L), which is experimentally estimated using the 'Heterogeneity Test', is directly related to the sampling constant (K) of interest (Pitard 1993) (9.2.17).

$$\sigma_{FSE}^2 = \frac{K\, d_N^3}{M_S} = \frac{IH_L}{M_S} \tag{9.2.17}$$

Based on the relationships between (IH_L) and the constant (K) the eventual formula for estimation the sampling constant (K) is obtained (9.2.18)

$$K = \frac{IH_L}{d_N^3} = \frac{g\sum_{i=1}^{N}\left[\frac{(a_i - A_B)^2}{A_B^2} \times \frac{m_i^2}{\sum_{i=1}^{N} m_i}\right]}{d_N^3} \tag{9.2.18}$$

9.2.2.4 Calibration of the Sampling Constants Using Drill Hole Data

Unfortunately, special experimental tests are not always available, in particular at the early stages of the mine project evaluation. However, establishing correct sampling procedures is in particular important at this stage as biased and non-representative sampling can lead to incorrect decisions and eventually cause significant financial losses. This problem can be partially overcome by approximate estimation of the sampling constants using available drill hole samples and applying methodology of 30-piece experiment (Francois-Bongarcon 1993). This approach allows to estimate one experimental point for the graphical fitting of the FSE.

Procedure of this experiment is as follows. At first step of this experiment is to calculate the volume of a drill hole sample and deduce the diameter of a sphere whose volume is equal to the average volume of the analysed drill hole samples. The estimated average diameter is further converted to a nominal size (d_N) by dividing it on ($g^{1/3}$) value (9.2.14).

To plot this single experimental point on the calibration diagram (Fig. 9.5) the $U = \text{Ln}\left(M_S\sigma_{FSE}^2\right)$ value is obtained by taking a natural logarithm of a product of estimated mass of a drill hole sample and estimated relative variance of the samples grades. When experimentally determined masses of the drill hole samples are not available they are calculated by multiplying the estimated average sample volume by specific gravity of the studied material.

Assuming that exponent (α) of the FSE equation is equal to 1.5 for the given material the sampling constant (K) can be deduced from the equality $K = \frac{\sigma_{FSE}^2 M_S}{d_N^{\alpha}}$.

9.2.3 Sampling Nomogram

Variance of the fundamental sampling error (FSE) can be graphically expressed as a function of sample weight (M_S) and the nominal particle size (d_N). Diagram representing relationships between these parameters is called nomogram (Fig. 9.6). This is achieved by plotting the FSE vs. the given sample mass (Pitard 1993; Francois-Bongarcon 1993). For practical reasons all values are plotted on the nomogram in the logarithmic coordinates (Fig. 9.6).

On this diagram (Fig. 9.6) the crushing and grinding stages, which do not contribute to sampling variance, are represented by vertical lines. The sample reduction stages, when a smaller sample is extracted from a larger sample, in other words a sample mass reduction at constant rock particle size, are represented on the diagram as a path along the straight lines of a slope −1. The actual position of the line depends on particle size (d_N) and also sampling constants (α) and (K) therefore only one line can be constructed for each sub sampling stage at the given sample particle size (d_N). Every stage when particle size reduced (i.e. comminution) is lowering the FSE and therefore it is represented on the nomogram by vertical line which extended until it intersects a new straight line of slope −1 corresponding to a new particle size. Combination of the vertical and diagonal segments corresponding to all stages of the sampling protocol graphically visualises the entire sample preparation protocol. Each stage contributing to the overall precision error is clearly represented on the nomogram and this allows to use this diagram as an effective tool for assessment, control and improvement of the sampling procedures.

To facilitate interpretation of this diagram a certain values of the acceptable precision errors can be shown. A common practice is to draw line corresponding to 10 % relative error, or in other words the relative variance equal to 0.01 (Fig. 9.6). This threshold is known as P.Gy's safety line (Gy 1979). All suboptimal sample preparation stages which FSE exceeds the chosen threshold are easily diagnosed on the nomograms.

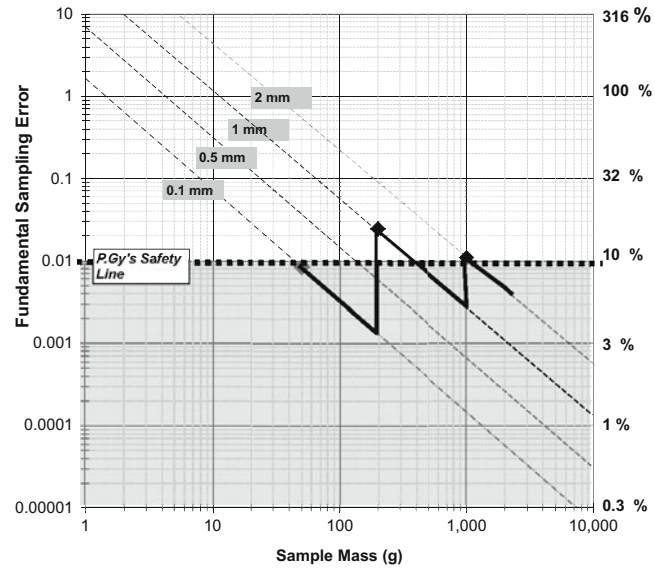

Fig. 9.6 Sampling nomogram, gold deposit, Canada

Example presented on the Fig.9.6 shows that largest FSE introduced at second subsampling stage when 200 g of sample is collected from a pulp grinded to −0.5 mm. This stage introduces approximately 20 % precision error whereas first sub-sampling, when 1 kg was split from the material crushed to −1 mm causes a smaller error, less than 10 %. Final stage when 50 g aliquot was collected from a 200 g pulp pulverised to −0.1 mm is also characterised by less than 10 % of FSE. Based on this nomogram it is obvious that improvement of the sampling protocol should be focused on optimisation of the stage 2, which can be easily achieved by collecting larger subsample, approximately 500 g.

Exercise 9.2.3.a Construct sampling nomogram and estimate FSE of the Ni-Cu mineralisation.

Optimise the sampling protocol using sampling nomogram.

Use attached file 'Exercise 9.2.3.a.xls' (Appendix 1).

9.3 Grouping – Segregation Error

This section briefly describes the Grouping-Segregation error which is generated by small scale distribution heterogeneity and reflects the differences in the content of a metal of interest between groups of fragments (increments) collected at the very small intervals (Pitard 1993). Examples of Grouping – Segregation error includes separation of the fine particles from larger fragments when they discharged from the sampling devices or conveyor belts (Fig. 9.7a). Another example of a possible error caused by segregation factor is accumulation of the heavier and smaller particles at the bottom of blast hole cones (Fig. 9.7b). This can be gold grains or sulphide minerals liberated from a gangue. Segregation can also be caused by different physical or chemical properties of the sampled materials, including magnetic or electrostatic properties, moisture content, adhesiveness (Pitard 1993).

The Grouping-Segregation error by definition is a function of two factors, grouping factor (f_G) and segregation factor (f_S), both being a consequence of the small scale distribution heterogeneity of the material.

$$\sigma^2_{GS} = f_G f_S \sigma^2_{FSE} \tag{9.3.1}$$

Grouping factor in practise is characterises the size of the increments (i.e. fragments) making up the sample. A segregation factor characterises the amount of increments. Both of these factors are dimensionless and can not be dissociated from each other.

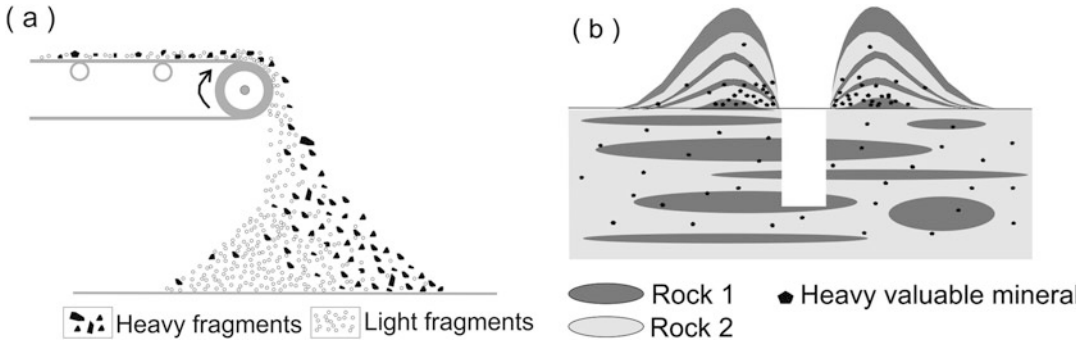

Fig. 9.7 Examples of segregation of the rock fragments: (**a**) segregation of the *heavy* and *lighter* fragments at the discharge from conveyor belt (Modified after Pitard (1993)); (**b**) uneven distribution of the fragments in the blast hole cones caused by segregation of the smaller and heavier fragments and their accumulation at the bottom of the cone

The above made definition (9.3.1) implies that Grouping-Segregation error is directly related to the Fundamental Sampling Error (9.3.1) and therefore has been assigned here to the first group of errors (9.1.1). However, this error differs from the Fundamental Sampling Error because in addition to dependence on the sampling protocol, being controlled by the value of fundamental error (σ^2_{FSE}), the Grouping-Segregation error also occurs as a consequence of the suboptimal implementation of the sampling protocol. For example, Grouping-Segregation error can be generated by insufficient homogenisation of the material prior to sampling.

The Grouping-Segregation error can't be theoretically estimated, however, in practice, it can be minimised if factors causing this error are well understood. Pitard (1993) has pointed out that grouping factor can be minimised by taking as many and as small increments as practically possible, assuming that all aspects of extraction and preparation of these increments is carried out correctly. Practical implication of this finding is that when selecting a riffle splitter preference should be given to that with a more riffles. When collecting samples by randomly chosen fragments, as a rule of thumb, the sample should be made of at least 30 increments (Pitard 1993). The same rational applies to choice of the rotary splitter. To minimise the grouping-segregation error it is necessary to assure that sample was collected by at least 30 cuts from the lot.

Segregation factor is more difficult to minimise, and many geologists working on the alluvial gold deposits and the heavy mineral sands are familiar with this phenomenon. The only method which can be applied in practice is to homogenise material prior to sampling. Unfortunately, often this is not practically possible or at least not economically viable. In many instances, a minimisation of the segregation factor requires changing of the sampling equipment. For instance, it is well recognised (Abzalov 2009; Abzalov et al. 2011) that air-core samples collected from the ilmenite-bearing sands are often biased because of a large value of segregation factor affecting these samples. Elimination of this bias requires changing air-core drilling method to a more efficient type allowing to minimise segregation of the ilmenite in the drill samples. Eventually, air-core technique has been replaced by a sonic drilling.

When strong segregation effect present in the blast hole cones (Fig. 9.7b) conventional blast hole sampling procedures become unsuitable for grade control purposes. To minimise the errors caused by segregation factor it was recommended (Pitard 2005) to use a sampling device which is radial in plan view. Blast holes should be sampled (Pitard 2005) by taking several increments positioning them at random around the pile.

9.4 Errors Related to the Sampling Practices

This group includes delimitation, extraction, preparation and weighing errors, which occur as a result of incorrect extraction of the samples from a lot and their suboptimal preparation procedures. In other words, the errors included in this group are not directly related to the sampling protocol but on the contrary they are associated with practical implementation of protocol. Simple meaning of this statement is that having the best possible protocol does not guarantee that your samples will be accurate and repeatable as this requires that protocol should be implemented in a such practical way that eliminates, or at least minimises, the errors related to sampling practices which are described here as Group 2 errors. The common example of these type errors is contamination of the laboratory samples during their preparation. Contamination of the samples caused by incorrect preparation procedures can completely destroy integrity of the samples and all efforts to obtain the samples with the lowest possible fundamental error will be wasted.

Delimitation error occurs when not all material in the sampled lot has equal probability to be selected to the sample (Gy 1979; Pitard 1993, 2005). The very common situation leading to delimitation errors is sampling of the piles of crushed material, which can be blast hole cone (Fig. 9.8), crushed ore at the draw points of the underground stopes or the ore stockpiles. The bottom of the piles is often poorly represented in sample causing the biased results due to delimitation error (Fig. 9.8).

Extraction error is the result of a sampling tool which is selectively taking fragments, therefore these errors also known as sample recovery errors because they are caused by selective sampling systems (Pitard 1993). This type of errors can be frequently observed in geological exploration and mining geology applications. One of the common examples of extraction error is a preferential caving of the soft material, when drilled hard rocks containing clay pods (Abzalov et al. 2010).

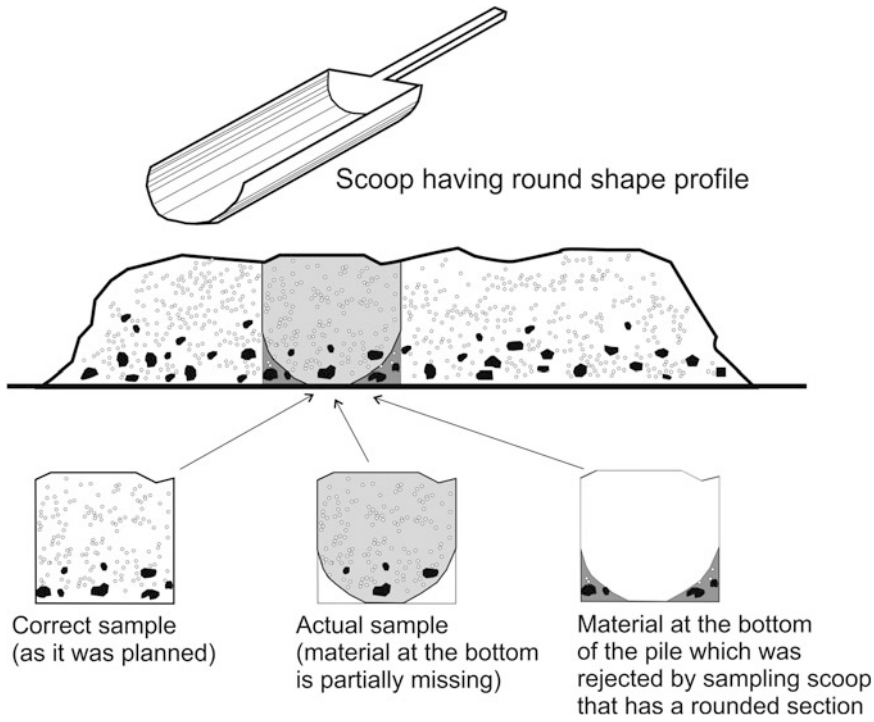

Fig. 9.8 Example of delimitation error caused by sampling the blast hole cone by a scoop having round shape profile

Preferential losses of the material often occur during drilling or sample preparation. In particular, this can be loss of the fugitive fine particles escaping along the drill rods. Another example of this error is washing away sandy and clay material from blast hole samples. Sampling of the blast hole cones by incorrectly designed auger drills, which rejects large fragments is another type of extraction error often occurring in geological applications. In all these cases the extraction error can cause significant biases of the analytical results. It is important to note that having correct equipment does not guarantee high quality results because inappropriate use of equipment can also lead to significant extraction error. Example shown on the Fig. 9.9 demonstrates an extraction error caused by incorrect use of riffle splitter which is quickly fed on one side. Such approach leads to disproportional distribution of the fragments and segregation of heavier particles on one side.

Preparation error is the changes of chemical or physical characteristics of the material caused by its crushing, grinding, pulverising, homogenising, screening, filtering, drying, packaging and transportation. These errors are taking place during the processing of the samples, and include contamination of the samples, preferential losses and alteration of sampled material. For example, in the blast holes some portion of the drill cuttings is falling back to the hole which can be a source of the sample biases due to preparation error.

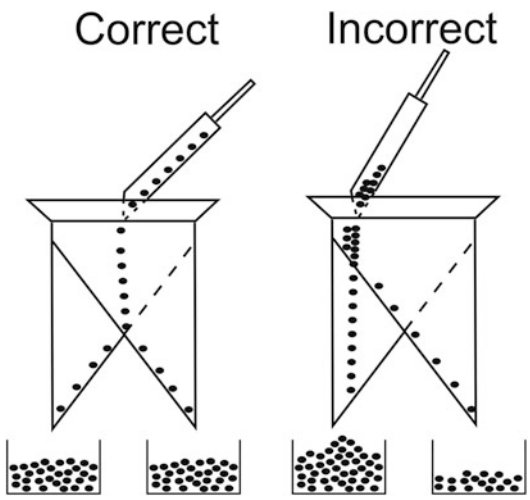

Fig. 9.9 Examples of extraction error caused by incorrectly used riffle splitter (Modified after Pitard (1993))

Weighing error is the error which is introduced by weightometers and scales. The author has observed a case when the laboratory has been equipped with the state of art analytical equipment including robotic XRF instrument, whereas in the sample preparation stage the very old, out of date and poorly calibrated scales have been used, entirely eliminating all benefits of having high precision analytical instrument.

Second group also includes different types of human errors, such as mixing sample numbers, transcript errors, and incorrect instrument readings. These errors, except the cases of a deliberate fraud, are accidental by their nature and can create extremely erratic values, abnormally high or low in comparison with the true sample grades. When such extreme values are present, these accidental-type human errors can be easily recognised by presence of the outliers on the scatter-diagrams where sample duplicates are plotted against the original samples (Fig. 9.10).

9.5 Instrumental Errors

This group includes errors related to various analytical and instrumental measurements during weighing of the final aliquots and their assaying. Typical example of these type errors is the instrumental drifts causing the biased assays. It also can be incorrect calibration of the instruments. The instrumental errors also include those which are caused by use of the out-of-date equipment, in particular if it is characterised by poor detection limits.

Special case of the instrumental errors is represented by incorrectly chosen analytical techniques, which is suboptimal for given type of mineralisation and/or grade ranges. For example, fire assay with atomic absorption finish is used for low-grade gold mineralisation, whereas high grade gold is better assayed by fire assay with gravimetric finish. Application of the atomic absorption finish to high grade gold samples can lead to their incorrectly determined grades because of instrumental error.

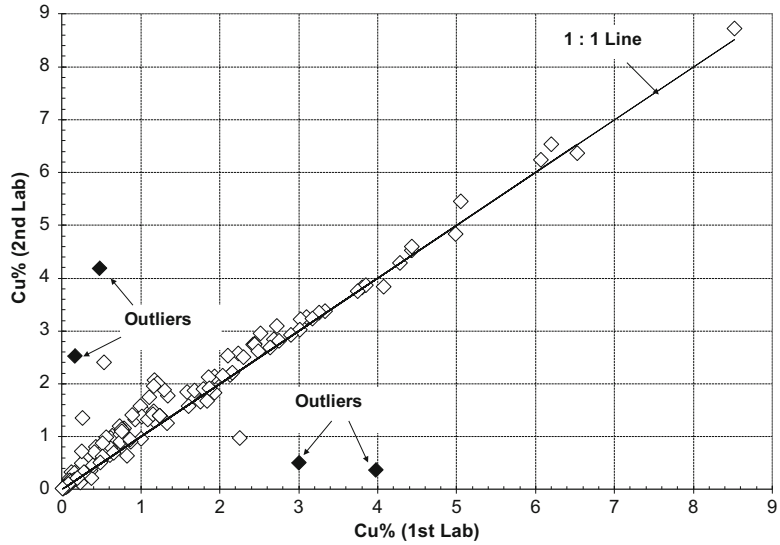

Fig. 9.10 Scatter-diagram of the Cu grades determined in the drill core samples and their duplicates. Cu-Au bearing skarn, Russia. All data, except several outliers, are compactly distributed along the 1:1 line indicating a good repeatability of the sample grades. Several erratic results (outliers) have been caused by mixing the sample numbers in the lab

References

Abzalov MZ (2007) Granitoid hosted Zarmitan gold deposit, Tian Shan belt, Uzbekistan. Econ Geol 102(3):519–532

Abzalov MZ (2009) Use of twinned drill – holes in mineral resource estimation. Exp Min Geol J 18(1–4):13–23

Abzalov MZ, Humphreys M (2002) Resource estimation of structurally complex and discontinuous mineralisation using non-linear geostatistics: case study of a mesothermal gold deposit in northern Canada. Exp Min Geol J 11(1–4):19–29

Abzalov MZ, Menzel B, Wlasenko M, Phillips J (2010) Optimisation of the grade control procedures at the Yandi iron-ore mine, Western Australia: geostatistical approach. App Earth Sci 119(3):132–142

Abzalov MZ, Dumouchel J, Bourque Y, Hees F, Ware C (2011) Drilling techniques for estimation resources of the mineral sands deposits. In: Proceedings of the heavy minerals conference 2011. AusIMM, Melbourne, pp 27–39

Bartlett HE, Viljoen R (2002) Variance relationships between masses, grades, and particle sizes for gold ores from Witwatersrand. J South Afr Inst Min Metall 102(8):491–500

De Castilho MV, Mazzoni PKM, Francois-Bongarcon D (2005) Calibration of parameters for estimating sampling variance. In: Proceedings – second world conference on sampling and blending. AusIMM, Melbourne, pp 3–8

Francois-Bongarcon D (1991) Geostatistical determination of sample variance in the sampling of broken ore. CIM Bull 84(950):46–57

Francois-Bongarcon D (1993) The practise of the sampling theory of broken ore. CIM Bull 86(970):75–81

Francois-Bongarcon D (1998) Error variance information from paired data: application to sampling theory. Exp Min Geol J 7(1–2):161–165

Francois-Bongarcon D (2005) Modelling of the liberation factor and its calibration. In: Proceedings second world conference on sampling and blending. AusIMM, Melbourne, pp 11–13

Francois-Bongarcon D, Gy P (2001) The most common error in applying 'Gy's formula' in the theory of mineral sampling, and the history of the liberation factor. In: Edwards A (ed) Mineral resources and ore reserve estimation – the AusIMM guide to good practise. AusIMM, Melbourne, pp 67–72

Gy P (1979) Sampling of particulate materials, theory and practice. Developments in Geomathematics 4. Elsevier, Amsterdam, p 431

Minkkinen P, Paakkunainen M (2005) Direct estimation of sampling variance from time series measurements – comparison to variographic analysis. In: Proceedings – second world conference on sampling and blending. AusIMM, Melbourne, pp 39–44

Minnitt RCA, Rice PM, Spangenberg C (2007) Part 2: Experimental calibration of sampling parameters K and alfa for Gy's formula by the sampling tree method. J South Afr Min Metall 107:513–518

Pitard FF (1993) Pierre Gy's sampling theory and sampling practise, 2nd edn. CRC Press, New York, p 488

Pitard FF (2005) Sampling correctness – comprehensive guidelines. In: Proceedings – second world conference on sampling and blending. AusIMM, Melbourne, pp 55–66

Sketchley DA (1998) Gold deposits: establishing sampling protocols and monitoring quality control. Exp Min Geol 7(1–2):129–138

Quality Control and Assurance (QAQC) 10

Abstract

The chapter provides a detailed review of the modern principles and techniques applied in mining industry to assure the samples quality and their appropriateness for evaluation of the mineral deposits. This group of techniques is traditionally referenced as Quality Assurance – Quality Control system and often called by acronym 'QAQC'. In general, QAQC procedures consist of monitoring accuracy and precision of analytical results, controlling the samples contamination, timely diagnostics of the sample errors and identification the error sources.

Keywords

QAQC • Precision • Accuracy • Standards • Sampling protocol • CV%

10.1 Accuracy Control

This section overviews the methods used in the modern mining industry to assure that samples are accurate. It overviews the criteria of diagnostic the sample biases and identification their possible causes (Leaver et al. 1997; Sketchley 1998). A particular emphasis is made on the common statistical techniques applied for quantification samples accuracy (Kane 1992; ISO Guide 1989; CANMET 1998).

Accuracy of samples is usually monitored by including samples with known grade to the assayed samples batch. The samples with *a priori* known grade are called standard samples or simply standards. They can be obtained from commercial laboratories where standards have been prepared and assayed rigorously following the appropriate procedures (Kane 1992) and results statistically certified. The best practice is to prepare standards from material mineralogically similar to that of the studied mineralisation; these are called the matrix matched standards.

A possible contamination is controlled by inserting the blank samples. Blanks are the samples where grade of a metal of interest is negligibly low, usually below detection at the given laboratory. It is a common practise to make the blank samples from barren quartz.

Standards and blanks are called reference materials and used for detection a possible sample biases and quantification the accuracy errors. Leaver et al. (1997) have suggested to define a reference material as 'a substance for which one or several properties are established sufficiently

M. Abzalov, *Applied Mining Geology*, Modern Approaches in Solid Earth Sciences 12,
DOI 10.1007/978-3-319-39264-6_10

well to calibrate a chemical analyser or to validate a measurement process.' A reference material is classified as certified reference material (CRM) if it was issued and certified by agencies, such as Canadian Centre for Mineral and Energy Technology (CANMET), the National Institute of Standards and Technology and other governmental agencies, whose technical competency is internationally recognised (Leaver et al. 1997).

Standard samples alone cannot identify biases introduced at different stages of sample preparation. Alternative approach to control samples accuracy is to assay the samples duplicates in the external laboratory which has an authority to act as an independent auditor. Certain strength of this technique is the fact that it allows detecting the errors introduced at the sample preparation stage which often can not be recognized by use of the reference materials. It is a good practice when at least 5 % of the total analysed duplicates, including pulp duplicates and coarse rejects, is analysed in the reputable external laboratory.

10.1.1 Statistical Tests for Assessing Performance of the Standard Samples

Accuracy of laboratory analyses is assessed by statistical tests (Kane 1992; ISO Guide 1989; CANMET 1998) which largely is based on comparison of the arithmetic mean of the replicate analyses of a certified standard against its certified mean. This statistical test of the assay accuracy should be supported by the estimation of the standard deviation of the replicate analyses of the standard samples, as poor precision of the standard sample assays (i.e. S_W is excessively large) can prohibit reliable detecting of the analytical biases. The statistical tests of the standard samples repeatability can be based on replicate assays of a certified standard in one laboratory or, conversely, inter laboratory (Round Robin) analyses.

10.1.1.1 Estimation Accuracy by Repeat Analyses of the Certified Standards, Single Laboratory

The most common situation is when one or several certified standard samples have been included in a batch of samples and analysed together in the same laboratory. In such case when several repeat assays of a given standard sample is available the analytical accuracy is assessed using statistical test (10.1.1). If this condition is satisfied the analytical results are considered acceptable with regard to accuracy.

$$|m - \mu| \leq 2\sqrt{\sigma_L^2 + \frac{S_W^2}{n}} \qquad (10.1.1)$$

where:

μ – certified mean of a given standard sample;
σ_L – standard deviation of a given standard samples certified for the between-laboratories case;
m – arithmetic mean of the replicate analyses of this certified standard sample in the assay batch;
S_W – estimated within-laboratory standard deviation of the replicate analysis of the standard sample included in assay batch;
n – number of replicate assays of a given certified standard in analytical batch.

The base formula (10.1.1) can be simplified as the usual empirical relationships is $\sigma_L \approx 2\ S_W$ (CANMET 1998). Consequently, for large ($n > 10$) number of replications the above condition (10.1.1) can be simplified as follows (ISO Guide 33):

$$|m - \mu| \leq 2\,\sigma_L \qquad (10.1.2)$$

Certified value of the between-laboratory standard deviation (σ_L) of the reference materials not always available. If this is the case,the condition

of the accuracy acceptance can be further simplified (CANMET 1998):

$$|m - \mu| \leq 4\,S_W \tag{10.1.3}$$

Exercise 10.1.1.a A certified standard of iron-ore was used for assessing accuracy of analytical method used in a studied laboratory. Certified characteristics of the standard sample are as follows:

60.73 % Fe – (μ) certified mean of the standard;
0.09 % Fe – (σ_C) certified within-laboratory standard deviation of the standard;
0.20 % Fe – (σ_L) certified between-laboratory standard deviation of the standard.

This certified standard material has been included in a single assay batch and analysed 10 times. The obtained results were as follows: 60.94, 60.99, 61.04, 61.06, 61.06, 61.09, 61.10, 61.14, 61.21, 61.24.

Based on these results can the given method be considered as accurate as required.

Arithmetic mean (m) of the replicate analyses of the given certified standard is 61.09 % Fe and their estimated standard deviation (S_W) is 0.092 % Fe.

Substituting these values to equality (10.1.3) gives the following result:

$$|61.09 - 60.73| = 0.36\%\text{Fe} \leq (0.092\%\text{Fe} \times 4 = 0.368\%\text{Fe})$$

This result shows that analytical method is accurate (unbiased) as required.

10.1.1.2 Estimation Accuracy by Repeat Analyses of the Certified Standards, Different Laboratories

When exploration samples have been analysed in (p) several different laboratories, the overall accuracy of the analytical results can be tested using statistical condition (10.1.4):

$$|m - \mu| \leq 2\sqrt{\frac{S_{LM}^2 + \frac{S_W^2}{k}}{p}} \tag{10.1.4}$$

where:

μ – certified mean of a given standard sample;
m – arithmetic mean of the replicate analyses of this certified standard sample in the assay batch;
S_W – estimated within-laboratory standard deviation of the replicate analyses of the standard samples;
S_{LM} – estimated between-laboratory standard deviation of the replicate analyses of the standard samples;
$k = \frac{n}{p}$, is a ratio of total numbers of replicate analysis (n) of certified standards to a number of laboratories (p) participating in Round Robin test.

Exercise 10.1.1.b A certified standard of iron-ore was used for assessing the within laboratory precision using the Round Robin analysis. Certified characteristics of the standard sample are as follows:

60.73 % Fe – (μ) certified mean of the standard;
0.09 % Fe – (σ_C) certified within-laboratory standard deviation of the standard;
0.20 % Fe – (σ_L) certified between-laboratory standard deviation of the standard.

Round Robin test was performed using 34 laboratories ($p = 34$) and 110 analyses ($n = 110$) of the standard samples have been obtained. Ratio of total numbers of analysis to number of participating laboratories is $k = \frac{110}{34} = 3.24$. Results of Round Robin test were as follows:

60.71 % Fe – (m) estimated mean of the standard;
0.10 % Fe – (S_W) estimated within-laboratory standard deviation of the standard;
0.06 % Fe – (S_{LM}) estimated between-laboratory standard deviation of the standard.

Substituting the corresponding values to equality (10.1.4) we will obtain

$$|m-\mu| \;=|60.71-60.73| \;=0.020$$

$$2\sqrt{\frac{S_{LM}^2+\frac{S_W^2}{k}}{p}}=2\sqrt{\frac{0.06^2+\frac{0.10^2}{3.24}}{34}}$$

$$=2*0.014=0.028$$

$$|m-\mu|=0.020\le 2\sqrt{\frac{S_{LM}^2+\frac{S_W^2}{k}}{p}}=0.028.$$

This result shows that analytical method is accurate (unbiased) as required.

10.1.1.3 Estimation Accuracy by a Single Assay of the Certified Standard

Repeat assays of the certified standards may not be available in a single analytical batch, which often can contain only one standard sample. When repeat assays of certified standards are not available, the above mentioned statistical tests (10.1.1, 10.1.2, 10.1.3, and 10.1.4) are inapplicable. In such case, when decision on the analytical accuracy should be made using a single value (X) of the certified standard, the commonly used statistical test is as follows (Kane 1992; ISO Guide 1989; CANMET 1998):

$$|X-\mu| \;\le\; 2\,\sigma_C \qquad (10.1.5)$$

where:

X – assayed value of the certified standard;
σ_C – certified within-laboratory standard deviation of the standard;
μ – certified mean of a given standard sample.

10.1.1.4 Within Laboratory Analytical Precision, Single Laboratory Case

This is the most common situation when multiple analyses of a certified standard have been made in the same laboratory. These data can be used for estimation of analytical precision of laboratory. Analytical precision is acceptable if results of the replicate analysis of the certified standards assayed in this laboratory satisfy the statistical test (10.1.6) (ISO Guide 33):

$$(S_W/\sigma_C)^2 \;\le\; \frac{\chi^2_{(n-1);\,0.95}}{n-1} \qquad (10.1.6)$$

where:

S_W – standard deviation of the replicate analysis of the standard;
σ_C – the certified value of the within-laboratory standard deviation of the standard;
$\chi^2_{(n-1);\,0.95}$ – critical value of 0.95 quartile ($\alpha = 0.05$) of the (χ^2) distribution at (n−1) degrees of freedom, where (n) is the number of replicate analysis of the standard.

In practise, at least three repeat analysis of the certified standards should be available for this test (CANMET 1998).

Exercise 10.1.1.c A certified standard of iron-ore was used for assessing precision of analytical method used in a studied laboratory. Certified characteristics of the standard sample are as follows:

60.73 % Fe – (μ) certified mean of the standard;
0.09 % Fe – (σ_C) certified within-laboratory standard deviation of the standard.

This standard has been analysed ten times. Estimated standard deviation (S_W) of these replicate analyses is 0.092%Fe. Substituting these values to statistical formula (10.1.6) gives:

$$(S_W/\sigma_C)^2 \;=\; \frac{0.092^2}{0.09^2}=1.04;$$

$$\frac{\chi^2_{(n-1);\,0.95}}{n-1}=\frac{\chi^2_{9;\,0.95}}{9}=1.88.$$

Empirical ratio of the variances $(S_W/\sigma_C)^2$ is less than the corresponding them table value $(\frac{\chi^2_{(n-1);\,0.95}}{n-1})$. Thus, the test result confirms that analytical precision of the method is statistically valid.

10.1.1.5 Assessment of the Analytical Precision Using Round Robin Analysis of a Certified Standard Sample

When the same certified standard sample has been analysed in several different laboratories (Round Robin test) a within-laboratory analytical precision can be estimated using the equality (10.1.7).

$$(S_W/\sigma_C)^2 \quad \leq \quad \frac{\chi^2_{p(k-1);\,0.95}}{p\,(k-1)} \qquad (10.1.7)$$

where:

S_W – estimated standard deviation of the replicate analysis of the standard;
σ_C – the certified value of the within-laboratory standard deviation of the standard;
$k = \frac{n}{p}$, is a ratio of total numbers of replicate analysis (n) of certified standards to a number of laboratories participating in Round Robin test (p);
$\chi^2_{p(k-1);\,0.95}$ – critical value of 0.95 quartile ($\alpha = 0.05$) of the (χ^2) distribution at $p(k-1)$ degrees of freedom.

Exercise 10.1.1.d A certified standard of iron-ore was used for assessing the within laboratory precision using the Round Robin analysis. Certified characteristics of the standard sample are as follows:

60.73 % Fe – (μ) certified mean of the standard;
0.09 % Fe – (σ_C) certified within-laboratory standard deviation of the standard;
0.20 % Fe – (σ_L) certified between-laboratory standard deviation of the standard.

Round Robin test was performed using 34 laboratories ($p = 34$) and 110 analyses ($n = 110$) of the standard samples have been obtained. Ratio of total numbers of analysis to number of participating laboratories is $k = \frac{110}{34} = 3.24$.

Round Robin test has returned the following values:

60.67 % Fe – (m) estimated mean of the standard;
0.10 % Fe – (S_W) estimated within-laboratory standard deviation of the standard;
0.06 % Fe – (S_{LM}) estimated between-laboratory standard deviation of the standard.

Substituting the corresponding values to equality (10.1.7) we will obtain

$$(S_W/\sigma_C)^2 \quad = \quad (0.10/0.09)^2 = 1.23$$

$$\frac{\chi^2_{p(k-1);\,0.95}}{p\,(k-1)} = \quad \frac{\chi^2_{76;\,0.95}}{76} = 1.28\,.$$

In other words, the empirical ratio of the variances $(S_W/\sigma_C)^2$ is less than the corresponding them table value ($\frac{\chi^2_{p(k-1);\,0.95}}{p(k-1)}$), which indicates that applied method is precise as required.

10.1.1.6 Between Laboratories Precision

The between laboratories precision can be assessed indirectly using the equality (10.1.8). Precision is considered satisfactory if this equality is true.

$$\frac{S^2_W + kS^2_{LM}}{\sigma^2_C \;+\; \sigma^2_L} \quad \leq \quad \frac{\chi^2_{(p-1);\,0.95}}{(p-1)} \qquad (10.1.8)$$

where:

σ_C – certified value of within-laboratory standard deviation of reference standard;
σ_L – certified value of between-laboratory standard deviation of reference standard;
S_W – estimated standard deviation of the replicate analyses of the standard samples;
S_{LM} – estimated between-laboratory standard deviation of the replicate analyses of the standard samples;
$k = \frac{n}{p}$, is a ratio of total numbers of replicate analysis (n) of certified standards to a number of laboratories participating in Round Robin test (p);
$\chi^2_{(p-1);\,0.95}$ – critical value of 0.95 quartile ($\alpha = 0.05$) of the (χ^2) distribution at $(p-1)$ degrees of freedom.

Exercise 10.1.1.e The same Round Robin results described in Exercise 10.1.1.d can be used for between laboratories assessment of the preci-

sion of analytical method. In this case a between-laboratories precision is assessed using the statistical test (10.1.8). Substituting certified parameters and results of the Round Robin analyses to this equality we obtain:

$$\frac{S_W^2 + kS_{LM}^2}{\sigma_C^2 + \sigma_L^2} = \frac{0.10^2 + 3.24 * 0.06^2}{0.09^2 + 3.24 * 0.20^2} = 0.1573$$

$$\frac{\chi^2_{(p-1);\,0.95}}{p-1} = \frac{\chi^2_{33;\,0.95}}{33} = 1.$$

Empirical ratio of the variances is less than the corresponding them table value indicating that analytical method is precise as precise as those used in the certification of the standard.

10.1.2 Statistical Tests for Assessing the Data Bias Using the Duplicate Samples

The bias in the analytical data can be estimated using the duplicate samples assayed in the reputable external laboratory (10.1.9).

$$\overline{\Delta}_{RE}(\%) = 100\frac{\left[\sum_i^N \left(a_i - b_i\right)\right] /N}{m_a} \tag{10.1.9}$$

where:

$\overline{\Delta}_{RE}$ (%) is a bias value normalised to mean of the original sample assays and expressed as a percentage;

a_i original sample, assayed in the first laboratory;

b_i duplicate sample, assayed in reputable external laboratory;

m_a is a mean of the original sample assays;

N – number of duplicate samples.

Eremeev et al. (1982) have suggested to estimate statistical significance of the bias detected using equality 10.1.9. The proposed approach (Eremeev et al. 1982) is based on comparing of experimentally calculated t-student value (t_{EXP}) with the corresponding theoretical value $t_{(p-1);\,0.95}$, determined for a given degrees of freedom $(p-1)$ and confidence interval ($\alpha = 0.95$). Bias is statistically insignificant if the equality (10.1.10) is correct.

$$t_{EXP} \leq \frac{t_{(N-1);\,0.95}}{N-1} \tag{10.1.10}$$

where:

$$t_{EXP} = \frac{|\Delta_{AVR}|\sqrt{N}}{\sqrt{\sum_i^N [(a_i - b_i) - \Delta_{AVR}]^2 / (N-1)}}$$

Δ_{AVR} – is absolute bias, determined as mean of difference between original and duplicate sample assays $\left[\sum_i^N \left(a_i - b_i\right)\right]$ /N;

$t_{(p-1);\,0.95}$ – critical value of 0.95 quartile ($\alpha = 0.05$) of the (t) distribution at (p-1) degrees of freedom.

10.1.3 Diagnostic Diagram: Pattern Recognition Method

This method is based on a fact that specific types of analytical problems have recognisable patterns on the special types of the diagrams. The different distribution patterns of the analytical results are indicative of the error sources and types.

The pattern recognition technique is most effective when applied to certified standards (Leaver et al. 1997; Sketchley 1998; Abzalov 2008). The assayed values of the certified standards are plotted onto the diagram on a batch/time basis (Fig. 10.1). Good quality analysis will be characterised by a random distributions of the data points around the certified mean value on this diagram (Fig. 10.1a) and the 95 % of the data points will lie within two standard deviations of the mean and only 5 % of assays can lie outside the interval of two standard deviations from the mean. It is essential that the same number of samples should occur above and below mean.

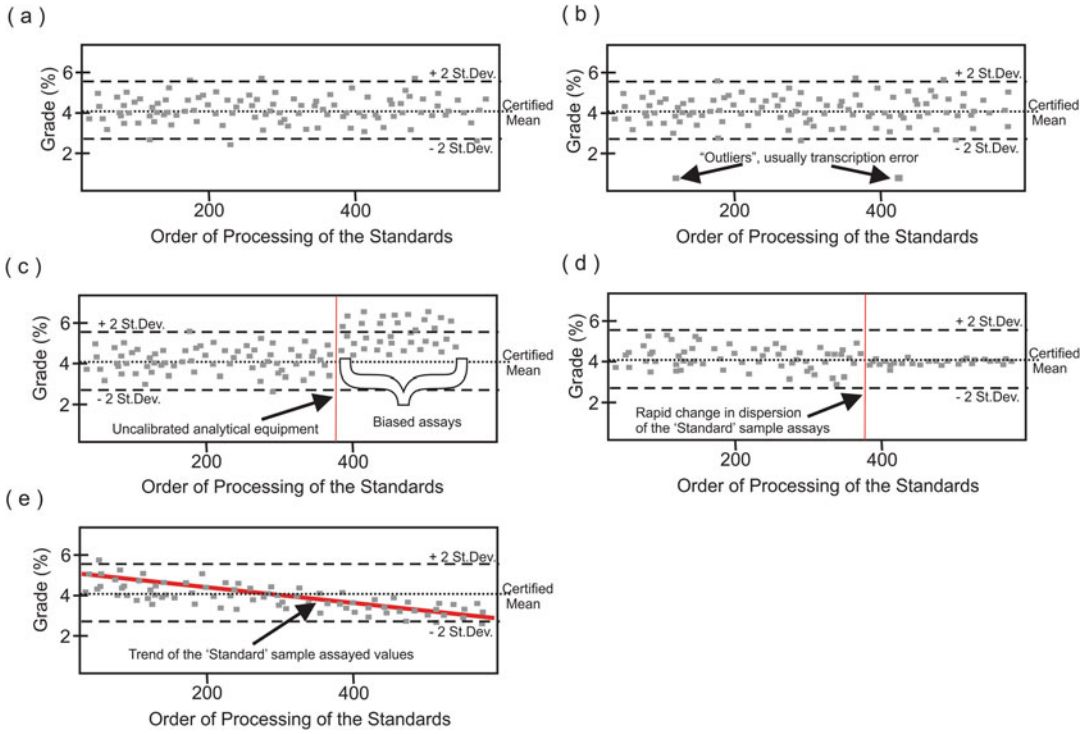

Fig. 10.1 Schematic diagrams showing quality control pattern recognition method (Reprinted from (Abzalov 2008) with permission of the Canadian Institute of Mining, Metallurgy and Petroleum): (**a**) accurate data, statistically valid distribution of the standard values; (**b**) presence of 'outliers' suggesting transcription errors; (**c**) biased assays; (**d**) rapid decrease in data variability indicating for a possible data tampering; (**e**) drift of the assayed standard values

In some cases the grades of the standard samples significantly differ from their certified values (Fig. 10.1b). Presence of such 'outliers' is most likely indicate for the data transcription errors (Abzalov 2008). This feature does not imply data bias but nevertheless indicate for a poor data management suggesting the possible random errors in the database.

Data bias is easily recognisable by a consistent shift of a standard sample assays (Fig. 10.1c). Usually this occurs because of failed equipment calibration or can be caused by changed analytical procedures in the lab.

Less common distribution pattern is when dispersion of the standard sample grades rapidly decreases (Fig. 10.1d). Such decrease in the standards variability is commonly interpreted (Sketchley 1998) as indicative of the data tampering.

Accurate analyses are also characterised by lack of systematic data trends on grade vs. order of analysis diagrams. Trends can be recognised by a systematic increase ore decrease the assayed values of the standards (Fig. 10.1e). Another commonly used criteria for identification of the possible trends are such distributions when two successive points lie outside the two standard deviations or four successive points lie outside the one standard deviation (Leaver et al. 1997).

A systematic drift of the assayed standard values usually indicates for a possible instrumental drift. Alternatively, it can be also caused by degradation of the standard samples. Author of the current paper is familiar with cases when characteristics of the standard samples have degraded in comparison with their certified values because of inappropriate storing conditions of the standards when they were kept in the large jars

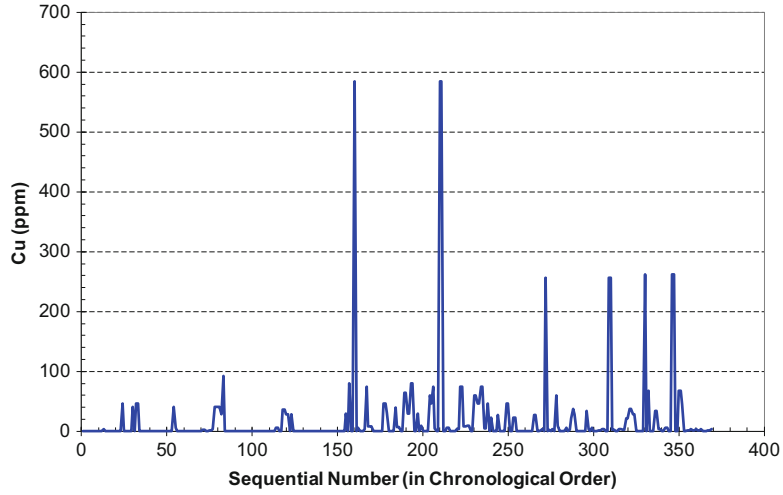

Fig. 10.2 Grade of blank samples plotted vs. order of their analysis. Resource definition programme at the Ni-Cu project, Western Australia

and have not been protected against vibrating due to operating equipment.

Blank assays are also presented on the grade vs. order of analysis diagram (Fig. 10.2) and arranged in the same manner as the assays of the standard samples. The main purpose of using blanks is to monitor laboratory for a possible contamination of samples which mainly is caused by insufficiently thorough cleaning of equipment.

The blank samples are usually inserted after high grade mineralisation samples and if equipment have not been properly cleaned the blank samples will easily detect it by showing increased grades of the metal of interest (Fig. 10.2).

Exercise 10.1.3 Construct the standard samples diagnostic diagram using the data in the excel file Exercise 10.1.3.xls (Appendix 1). The file contains built-in Visual Basic script (Standards) to be used with this exercise. Provide your interpretation of the obtained results. Use the macro code (Exercise 10.1.3.xls) with the data from your project.

10.2 Precision Control

Precision of the samples is monitored by using matching pairs of samples. These are the pairs of samples which are processed in a similar manner allowing their comparative analysis. The differences between the assayed values of sample and it's duplicate is caused by errors associated with sample preparations and assaying. Precision error is mathematically deduced from differences between matching pairs of data, and is usually represented as variance of the assayed values normalised to the means of the corresponding pairs of the data (Abzalov 2008).

10.2.1 Matching Pairs of Data

Sample duplicates represent the most common type of the matching pairs of data. Duplicate sample is merely another sample collected from the same place and following the same rules as used for collecting the initial (original) sample. This is the main approach used in mining industry to monitor the samples precision. In practise, the duplicate sample can be a second blast hole sample collected from the same blast hole cone or another half of the drill core. It also can be a duplicate sample collected at a particular stage of the sampling protocol, such as coarse rejects after crushed material has been split using an appropriate sample reducing devise or second aliquot collected from the same pulverised pulp. When sampling protocol includes several stages of comminution and subsampling the duplicate samples it is a good practise to take duplicate samples at each subsampling stage.

Preparation procedure and analysis of the duplicate samples should be the same as used for their original samples. The duplicate sample can be analysed in the same laboratory as original or can be send to different laboratory for interlaboratory control. When duplicates are analysed in the same laboratory where original samples were assayed the variations of the results allows estimate the precision errors incurred at the particular stage of the sampling protocol which is represented by a given duplicates. When duplicate samples are processed in a different laboratory it is a common practise to choose an internationally recognised laboratory with audited and approved quality. In this case interlaboratory analysis of the duplicates samples allows assessing both, precision and accuracy, errors of the samples assayed in the tested laboratory.

Another type of the matching data pairs are twin holes. This technique is not a precision control method and is mainly used for verification of the previous drilling results. It will be described separately in the next chapter of the book.

10.2.2 Processing and Interpretation of Duplicate Samples

The precision error is quantified from the paired data through assessing the scatter of the data points with corrections for their deviation from $y = x$ line. The different methods are available for estimation precision error from the paired data (Garrett 1969; Thompson and Howarth 1973, 1976, 1978; Howarth and Thompson 1976; Bumstead 1984; Shaw 1997; Francois-Bongarcon 1998; Sinclair and Blackwell 2002; Abzalov 2008). The most common methods are based on the assumption of linear relationships between sampling and analytical errors and concentration of the assayed metals (Thompson and Howarth 1973, 1976, 1978; Howarth and Thompson 1976; Bumstead 1984; Shaw 1997). Francois-Bongarcon (1998) has extended this principle to the more complex relationships described by a quadratic model. Special type of a linear model is reduced major axis (RMA) (Sinclair and Bentzen 1998; Davis 2002; Sinclair and Blackwell 2002). This technique is applicable to linear cases when different sets of paired data exhibit systematic differences (bias). Pitard (1998) has suggested a special diagnostic diagram, relative difference plot (RDP), which can be used for detailed analysis of the causes of poor data precision or sample biases. All these methods have been reviewed by Abzalov (2008) and compared by applying to the same sets of the duplicated pairs of samples collected in operating mines and mining projects.

10.2.2.1 Method of Thompson – Howarth

This method was developed in early 70th (Thompson and Howarth 1973, 1976, 1978; Howarth and Thompson 1976) and since then became a popular technique for duplicated data analysis in the mining industry.

It uses assumption that precision error is normally distributed and the variation of the samples precision, represented as standard deviation of the duplicated data (S_C), can be expressed as a linear function of the samples concentration (C) and the standard deviation at zero concentration (S_0) (10.2.1).

$$S_C = S_0 + K\,C \tag{10.2.1}$$

Relative precision (P_C) at the given concentration (C) can be determined using the equality (10.2.2) which represent precision at one standard deviation confidence level.

$$P_C = S_C\,/C \tag{10.2.2}$$

Precision at one standard deviation confidence level is chosen for consistency with other precision estimates, which are discussed below.

Substituting (S_C) in equality 10.2.2 by it's definition presented in equality 10.2.1 and multiplying by 100 to represent relative precision error as percentage have led to the final formula (10.2.3).

$$P_C = 100\ [(S_0\,/C) + K] \tag{10.2.3}$$

where:

P_C – precision at concentration C;
S_0 – standard deviation at zero concentration;

K – precision at concentrations well above the detection limit (asymptotic precision).

Modification of the equality 10.2.3 for a case, when precision (P_C) is equal to 1 (i.e. 100 % variation at confidence level of two standards deviation) leads to expression 10.2.4 which allows to determine practical detection limit (C_d).

$$C_d = 2\,S_0 \,/\, (1 - 2K) \qquad (10.2.4)$$

C_d – practical detection limit, is defined as the concentration where the precision (P_C) equals 1 at the two standard deviations confidence level. Laboratory detection limit is usually lower than practical detection limit, which includes sampling and analytical errors.

The parameters (S_C) and (K) can be calculated empirically from available data pairs and then used in 10.2.3 for quantification of the samples precision. Two approaches have been proposed (Thompson and Howarth 1973, 1976, 1978; Howarth and Thompson 1976) for experimental calculation of (S_0) and (K) parameters.

First approach, has been proposed (Thompson and Howarth 1973, 1976, 1978), to use when 50 or more duplicated results are available. Procedure of calculating (S_0) and (K) parameters in this case are as follows (Thompson and Howarth 1976, 1978):

Using (N > 50) of the data pairs (a_i) and (b_i) ($i = 1,2,\ldots N$) the means of the data pairs $(a_i + b_i)/2$ and their absolute differences $|a_i - b_i|$ should be calculated.

All data are sorted in increasing order of their mean grades.

Data pairs are subdivided on the groups of 11 results. The last group, if it contains less than 11 records, should be ignored.

The average value of the pairs means and the median value of the absolute differences are calculated for each group of data.

Median values are plotted as function of the group means and regression line is fitted to experimental points (Fig. 10.3).

Parameters (S_0) and (K) are derived from that diagram. Slope of regression line represents (K) parameter and (S_0) is equal to a value of regression function at zero mean. Practice shows that fitting regression lines to so few points commonly leads to peculiar, or even impossible, results. For example, a negative intercept with y-axis.

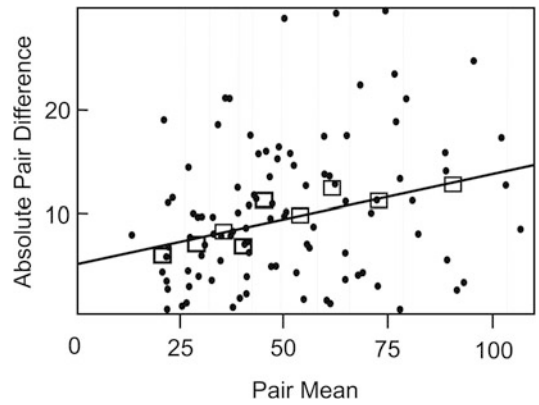

Fig. 10.3 Absolute difference vs. mean of data pairs, applied when >50 data pairs available. Vertical lines separate groups of 11 records. *Open squares* denote the experimental points calculated for each group of 11 records. X-value of a square corresponds to the average value of the pair means and Y-value corresponds to median of the absolute differences of the data pairs in a group. *Bold solid line* is regression line fitted to experimental points

Second method (Thompson and Howarth 1973, 1976, 1978) is used when number of duplicated samples is insufficient for reliable estimation of (S_0) and (K) parameters. Usually, it is the case when number of available data pairs varies from 10 to 50.

This is graphical method which consists of construction of the precision control chart (Fig. 10.4). Construction of this diagram starts from specifications of the precision parameters in the equality (10.2.1). Using the chosen specifications, the (d_{90}) and (d_{99}) values are calculated using the formulas (10.2.5 and 10.2.6) (Thompson and Howarth 1973, 1976):

$$d_{90} = 2.326\ (S_0 + K\,C) \qquad (10.2.5)$$

$$d_{99} = 3.643\ (S_0 + K\,C) \qquad (10.2.6)$$

The (d_{90}) and (d_{99}) are plotted over the practical range of the sample grades on the precision control chart (Fig. 10.4). The calculated (d_{90})

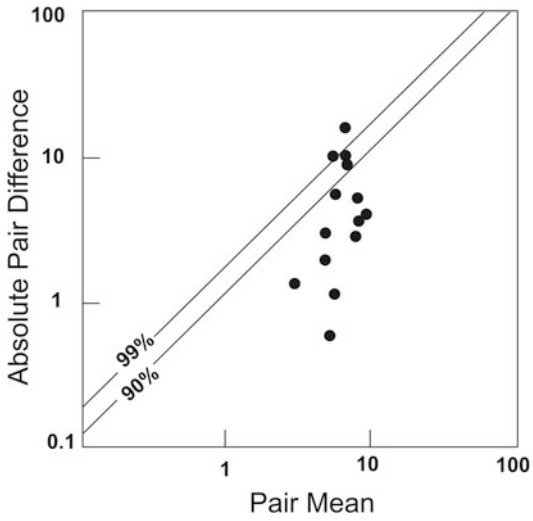

Fig. 10.4 Precision control chart, applied when <50 data pairs available

and (d_{99}) functions represent 90th and 99th percentiles of the absolute differences between duplicated data. These differences are expressed as function of the sample grades, assuming normal distribution of the errors.

Thompson and Howarth (1978) have suggested to use 10 % precision as a default value for general geochemical studies. In this case the (d_{90}) and (d_{99}) percentile lines are calculated for ($S_C = 0.05$ C) specification.

Next step is to calculate using available data pairs (a_i) and (b_i) ($i = 1,2,\ldots N$) the pair means $(a_i + b_i)/2$ and their absolute differences $|a_i - b_i|$. These calculated values are also plotted on the precision control chart. Precision of the duplicated data complies with specification if approximately 90 % of the data points are plotted below the line (d_{90}) and 99 % fall below (d_{99}) line.

In practice, use of the Thompson-Howarth approach to quantifying precision should be preceded by construction of a conventional scatter-diagram plotting the duplicate sample grades vs. their original values. This diagram should be investigated for possible features, such the data bias, non-linear distribution of the precision errors and presence of the different statistical subpopulations. All this factors deteriorates application of the Thompson-Howarth technique.

Exercise 10.2.2.a Estimate samples precision by Thompson and Howarth method. Data for this exercise are presented in the attached Excel file Exercise 10.2.2.a.xls (Appendix 1). The file contains the built-in Visual Basic scripts (TH-1 and TH-2) to be used with this exercise.

10.2.2.2 Relative Precision Error

This group of methods includes various estimators (Table 10.1) based on calculation of the absolute differences between original and duplicate samples and normalising (dividing) them by the mean grades of corresponding data pairs (Bumstead 1984; Shaw 1997; Roden and Smith 2001; Stanley and Lawie 2007a).

Stanley (2006) has shown that absolute difference between paired data is directly proportional to standard deviation ($|a_i - b_i| = \sqrt{2} \times$ Standard Deviation) and consequently the various measurements representing ratio of the absolute differences between paired data to the means of the corresponding pairs (Table 10.1) are directly proportional to coefficient of variation (CV%[1]) (10.2.7).

$$\begin{aligned} \mathrm{CV\%} &= 100\% \times \frac{\text{Standard Deviation}}{\text{Mean}} \\ &= 100\% \times \frac{|a_i - b_i| \,/\sqrt{2}}{\frac{a_i + b_i}{2}} \end{aligned} \tag{10.2.7}$$

Average CV% can be calculated from the (N) pairs of the duplicated samples (10.2.8).

$$\begin{aligned} \mathrm{CV\%_{AVR}} &= 100\% \times \sqrt{\frac{1}{N}\sum_{i=1}^{N}\frac{\sigma_i^2}{m_i^2}} \\ &= 100\% \times \sqrt{\frac{2}{N}\sum_{i=1}^{N}\left(\frac{(a_i - b_i)^2}{(a_i + b_i)^2}\right)} \end{aligned} \tag{10.2.8}$$

Hence, such statistics as AMPD (10.2.9) and HARD (10.2.10), commonly used by geoscien-

[1]For consistency with other measurements coefficient of variation (CV) (one standard deviation divided by mean) is expressed as percentage (CV%)

Table 10.1 Measures of Relative Error based on absolute difference between duplicated data pairs

Conventional name of the error estimator	Single duplicate pair formula	Reference	Comments
AMPD	$\text{AMPD} = 200\% \times \frac{\lvert a_i - b_i \rvert}{(a_i + b_i)}$	Bumstead (1984)	This estimator is also known as MPD (Roden and Smith 2001) or ARD (Stanley and Lawie 2007a)
HARD	$\text{HARD} = 100\% \times \frac{\lvert a_i - b_i \rvert}{(a_i + b_i)}$	Shaw (1997)	HARD is simply the half of the corresponding AMPD

where (a_i) is original sample and (b_i) is its duplicate

tists, represent nothing else but products of CV% by constants ($\sqrt{2}$) and ($\frac{\sqrt{2}}{2}$) respectively (Stanley and Lawie 2007a).

$$\text{AMPD} = 100 \times \frac{|a_i - b_i|}{(a_i + b_i)/2} = \sqrt{2} \times \text{CV}\% \tag{10.2.9}$$

$$\text{HARD} = 100 \times \frac{|a_i - b_i|}{(a_i + b_i)} = \frac{\sqrt{2}}{2} \times \text{CV}\% \tag{10.2.10}$$

Stanley and Lawie (2007a) have rightfully noted that using such statistics like AMPD and HARD, which are directly proportional to coefficient of variation, offer no more information than the CV itself.

10.2.2.3 Geostatistical Approach of the Duplicate Samples Analysis

Alternative approach in estimating precision of analytical data involves calculation of various geostatistical measures of the spatial correlation, in particular different variants of variograms. Garrett (1969) has suggested to calculate variance between original samples and their duplicates by lognormally transforming their assay values and then applying formula of the lognormal variogram (10.2.11). This approach did not find application in practice.

$$\sigma^2_{\text{GAR}} = \frac{1}{2N} \sum_{i}^{N} [\ln(a_i) - \ln(b_i)]^2 \tag{10.2.11}$$

Approach developed in the former USSR (Eremeev et al. 1982) is based on grouping data by the grade classes and calculating precision errors (S_R %) separately for each grade class. To obtain a reliable estimation of sample precision, it is recommended to analyse at least 30 data pairs for each grade class (Eremeev et al. 1982). Where samples have been assayed in the different laboratories, the data are grouped and analysed separately for each laboratory.

Precision error (S_R %) is calculated within each grade class as ratio of the standard deviation of the duplicated data to the mean of all data within a given grade class (10.2.12).

$$\begin{aligned} S_R\% &= 100\% \times \frac{S}{\overline{C}} \\ &= 100\% \times \frac{\sqrt{\sum_{i}^{N} \left(a_i - b_i\right)^2 / 2N}}{\left[\left(\sum_{i}^{N} a_i\right) + \left(\sum_{i}^{N} b_i\right)\right] / 2N} \end{aligned} \tag{10.2.12}$$

where (N) is number of sample pairs, (a_i) is the first sample and (b_i) is the duplicate sample of the (i) pair.

It is noteworthy that equality (10.2.12) is the square root of the relative variogram[2] applied to the duplicated samples and expressed as percentage.

[2]Conventional formula (Goovaerts 1997) of the relative variogram is as follows $\gamma_R(h) = \frac{1}{2N} \sum_{i=1}^{N} \frac{[Z(x_i) - Z(x_i + h)]^2}{m^2}$, where Z(x) is a value of variable (Z) at the location (x), (h) is a vector separating $Z(x)$ from $Z(x_i + h)$ points and (m) is mean of the variable [Z(x)]

F. Pitard has suggested (pers. comm.) to calculate relative variance (σ^2_{FP}) of the matching pairs of the data, (a_i) and (b_i), using formula (10.2.13) presented below.

$$\sigma^2_{FP} = \frac{1}{2N}\sum_{i}^{N}\left(\frac{a_i - b_i}{\frac{a_i + b_i}{2}}\right)^2 = \frac{2}{N}\sum_{i}^{N}\left(\frac{a_i - b_i}{a_i + b_i}\right)^2 \quad (10.2.13)$$

The formula (10.2.13) is known in geostatistics as a pair-wise[3] relative variogram (Goovaerts 1997) and it is particularly useful for variables characterised by strongly skewed statistical distributions and when outliers present.

Average precision error is easily deduced from equality (10.2.13) by taking the square root of the relative variance and multiplying by 100 % to represent the precision error as a percentage at one standard deviation (10.2.14)

$$P_{FP}\% = 100\% \times \sqrt{\sigma^2_{FP}} \quad (10.2.14)$$

However, it is easy to see that when pair-wise relative variogram is applied to duplicated samples it simply measures the relative variance of the paired data. The square root of this value is equal to average coefficient of variation. Hence, the two approaches, one that uses the coefficient of variation and the second that uses a geostatistical approach based on the application of a pair-wise relative variogram for measuring precision error are identical because both are based on calculating the average relative variance of the paired data (10.2.15).

$$\mathrm{CV_{AVR}}\,(\%) = P_{FP}\,(\%) = 100 \times \sqrt{\frac{2}{\mathrm{N}}\sum_{\mathrm{i=1}}^{N}\left(\frac{(a_i - b_i)^2}{(a_i + b_i)^2}\right)} \quad (10.2.15)$$

[3]Conventional formula (Goovaerts 1997) of the pair-wise relative variogram: $\gamma_{\mathrm{PWR}}\,(\mathrm{h}) = \frac{1}{2\mathrm{N}}\sum_{\mathrm{i=1}}^{N}\frac{[\mathrm{Z}\,(\mathrm{x_i}) - \mathrm{Z}(\mathrm{x_i} + \mathrm{h})]^2}{\left[\frac{\mathrm{Z}\,(\mathrm{x_i}) + \mathrm{Z}\,(\mathrm{x_i} + \mathrm{h})}{2}\right]^2}$, where Z(x) is a value of variable (Z) at the location (x) and (**h**) is a vector separating $Z(x)$ from $\mathrm{Z}\,(\mathrm{x_i} + \mathrm{h})$ points

10.2.2.4 Partitioning of the Precision Error

Francois-Bongarcon (1998) analysed sampling and analytical precision by subdividing the total precision error into components. The practical recommendation of that study was to use formula 10.2.16 for estimating precision variance if the data represent different grade classes. Error at one standard deviation is estimated using 10.2.17:

$$\sigma^2_{\mathrm{DFB}} = 2\ Var\left[\frac{(a_i - b_i)}{(a_i + b_i)}\right] \quad (10.2.16)$$

$$P_{DFB}\,(\%) = 100 \times \sqrt{\sigma^2_{DFB}} \quad (10.2.17)$$

Calculation of other components of the global variance is beyond the scope of the current review and can be found in the above mentioned paper of Francois-Bongarcon (1998).

10.2.2.5 Reduced Major Axis

This is a linear regression technique which takes into account errors in two variables, original samples and their duplicates (Sinclair and Bentzen 1998; Davis 2002; Sinclair and Blackwell 2002). This technique minimises the product of the deviations in both the X- and Y- directions. This, in effect, minimises the sum of the areas of the triangles formed by the observations and fitted linear function (Fig. 10.5). The general form of the reduced major axis (RMA) is as follows (10.2.18):

$$b = W_0 + W_1 a \pm e \quad (10.2.18)$$

where (a_i *and* b_i) are matching pairs of the data, (a_i) denotes a primary samples plotted along X axis and (b_i) is duplicate data, plotted along the Y axis. (W_0) is Y-axis intercept by the RMA linear model, (W_1) is the slope of the model to X-axis, (e) standard deviation of the data points around the RMA line.

The parameters (W_0, W_1 and e) estimated from the set of the matching pairs of data (a_i and b_i), plotted along X-axis and Y-axis, respectively. The slope of RMA line (W_1) is estimated as ratio of standard deviations of the values (a_i and b_i) (10.2.19).

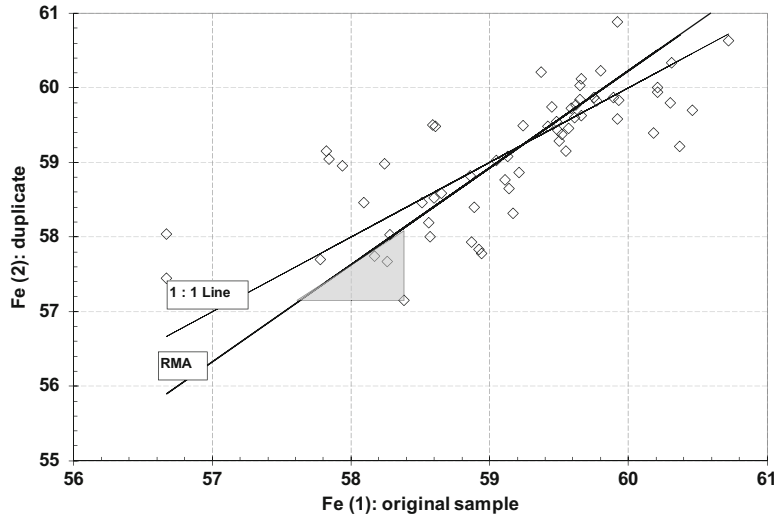

Fig. 10.5 Scatter-diagram and the RMA model (*thick line*) fitted to paired Fe grades of the blast hole samples. 1:1 line (*fine*) is shown for reference. *Grey* triangle shows an area formed by projection of the data points and RMA line. RMA technique minimises the sum of the areas of the all triangles

$$A_1 = \frac{\text{St.Dev}\,(b_i)}{\text{St.Dev}\,(a_i)} \tag{10.2.19}$$

Intercept of the RMA model with Y axis is estimated as follows:

$$W_0 = Mean\,(b_i) - W_1 Mean\,(a_i) \tag{10.2.20}$$

RMA model allows quantifying the errors between matching data pairs. Dispersion of the data points about the RMA line (S_{RMA}) is estimated using 10.2.21.

$$S_{RMA} = \sqrt{\left[2\,(1-r)\left(Var\,(a_i) + Var\,(b_i)\right)\right]} \tag{10.2.21}$$

Error on Y-axis intercept (S_0) is estimated using (10.2.22) and the error on the slope (S_{SLOPE}) is estimated using (10.2.23).

$$S_0 = St.Dev\,(b_i) \sqrt{\left[\frac{(1-r)}{\mathrm{N}}\right]\left[2 + \left(\frac{Mean\,(a_i)}{St.Dev\,(a_i)}\right)^2 (1+r)\right]} \tag{10.2.22}$$

$$S_{SLOPE} = \frac{\text{St.Dev}\,(b_i)}{\text{St.Dev}\,(a_i)}\sqrt{\frac{(1-r^2)}{\mathrm{N}}} \tag{10.2.23}$$

Where:

(r) is correlation coefficient between (a_i and b_i) values;
(N) is the number of the data pairs;
(*Var*) are variances of the (a_i and b_i) values.

The relative precision error ($P_{RMA}(\%)$)[4] can be estimated from the RMA model:

$$P_{RMA}\,(\%) = 100 \times \frac{\sqrt{\frac{S^2_{RMA}}{2}}}{\frac{\left(\sum_i^N a_i\right) + \left(\sum_i^N b_i\right)}{2N}} \tag{10.2.24}$$

Exercise 10.2.2.b Calculate RMA and estimate relative variances using attached Excel file Exercise 10.2.2.b–d.xls (Appendix 1) containing the Visual basic scripts.

10.2.2.6 Relative Difference Plot

Relative difference plot (RDP) has been suggested Pitard (1998) as graphic tool for diagnostics of the factors controlling precision error. The method is based on estimation the differences between matching pairs of the data which are

[4]For consistency with other estimates discussed in this section the ($P_{RMA}(\%)$) value is estimated at 1 standard deviation and expressed as percentage.

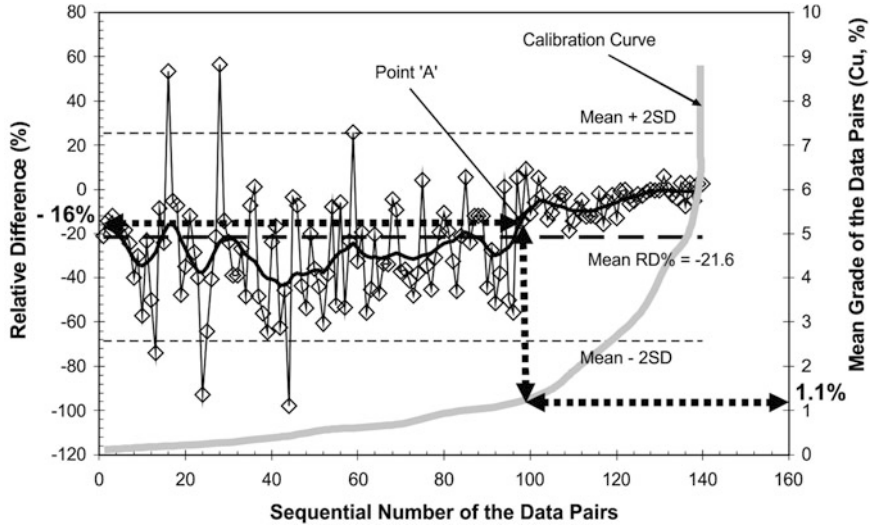

Fig. 10.6 Relative Difference Plot (RDP) showing Cu(%) grades of duplicated drill core samples, Cu-project, Russia (Reprinted from (Abzalov 2008) with permission of the Canadian Institute of Mining, Metallurgy and Petroleum). *Open symbols* (*diamond*) connected by fine tie-lines are RD(%) values calculated from matching pairs of data (i.e., original sample and duplicate). Average RD(%) value (*thick dashed line*) and + 2SD values (*fine dashed lines*) are shown for reference. The *solid line* is a smoothed line of the RD(%) values calculated using a moving windows approach. The 'Calibration Curve' sets the relationship between RD% values on the primary y-axis, the sequential number of the data pairs plotted along the x-axis and the average grades of the data pairs plotted on the secondary y-axis

normalised to the means of the corresponding pairs of the data (10.2.25).

$$\text{RD (Relative Differnce) \%} = \frac{1}{\text{N}}\sum_{i}^{N}\left[100 \times \frac{(a_i - b_i)}{(a_i + b_i)/2}\right] \quad (10.2.25)$$

where (a_i) and (b_i) are the matching pairs of the data and N is the number of pairs.

Calculated RD(%) values are arranged in increasing order of the average grades of the data pairs and then RD(%) values are plotted against sequential numbers of the pairs whereas the calculated average grades of the data pairs are shown on the secondary y-axis (Fig. 10.6).

A more traditional approach would be to plot RD(%) values against the average grades of the data pairs. However, in that case diagnostic ability of this diagram is marred by uneven distribution of the data between grade intervals and plotting RD(%) values against sequential numbers of the data pairs allows to overcome this problem. Link between average grades of the data pairs and their sequential numbers are established by adding 'Calibration curve' to the RDP diagram (Fig. 10.6).

Relative difference values of the data pairs usually exhibit a large range of variations; therefore, interpretation of this diagram can be facilitated by applying the moving window technique to smooth the diagram (Fig. 10.6).

The example in Fig. 10.6 is based on data collected from a massive Cu-sulphide project in Russia. Construction of this diagram as explained in details in Abzalov (2008, 2011) and is briefly summarised here. At the project approximately 140 core duplicate samples have been analysed in an external reputable laboratory as part of the technical due diligence. The results, when plotted on an RDP diagram (Fig. 10.6), show that copper assays of low grade samples (Cu < 1.1 %) are biased. Assayed values have significantly underestimated the true copper grade of those samples. Another feature revealed by this diagram is that low grade samples (Cu < 1.1 %) exhibit exces-

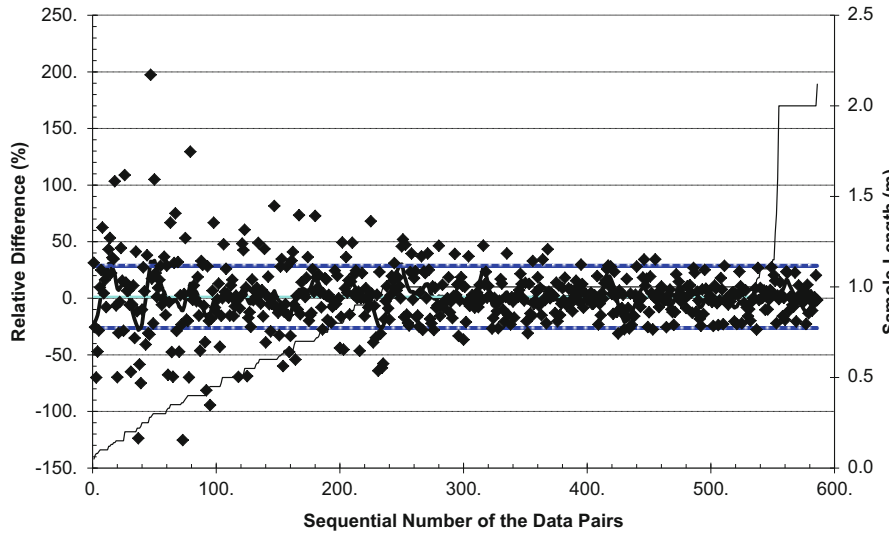

Fig. 10.7 Cu% grades of the duplicated drill hole samples plotted on the RDP diagram. RD% values are arranged by length of the samples

sively large precision error which is not shown by higher grade samples (Cu >1.1 %). These findings have triggered a special investigation of the laboratory procedures, with a particular emphasis on differences between high-grade and low-grade samples.

The RDP diagram can be used for testing the impact onto data precision the different factors, for example sample size, core recovery, depth of the samples collection. In that case the RD% values are arranged according to a factor under investigation. On the Fig. 10.7 the RD% values are plotted against the sequential number of the samples arranged by their sizes (i.e. length of the sampling interval). The diagram (Fig. 10.7) shows that small samples, less than 0.5 m in length, are characterised by approximately twice as larger precision error than samples of 1 m in length.

Exercise 10.2.2.c Construct RDP diagram using attached Excel file Exercise 10.2.2.b–d.xls (Appendix 1) containing the Visual basic codes.

10.3 Comparative Analysis of the Statistical Estimation Methods

The statistical methods for estimating precision have been compared by applying them to the same set of duplicate sample analyses (Abzalov 2008, 2009). Data for this study were obtained from operating mines and mining projects, including published data (Abzalov and Both 1997; Abzalov 1999, 2007; Dominy et al. 2000; Roden and Smith 2001; Abzalov and Humphreys 2002a,b; Sinclair and Blackwell 2002; Abzalov and Mazzoni 2004; Abzalov and Pickers 2005; Abzalov et al. 2010) and unpublished reports.

All errors are estimated as relative standard deviations and expressed as percentages (Table 10.2). The Thompson and Howarth method (Thompson and Howarth 1973, 1976, 1978; Howarth and Thompson 1976) has been applied to the average grades of the datasets to make the estimates by this method comparable to other estimates.

Table 10.2 Samples precision: case studies of the operating mines and projects

Mineralisation type/deposit	Metal	Grade range	Average	No of sample pairs	Correlation	P th% (10.2.3*)	CV% (10.2.8)	AMPD (10.2.9)	P dfb% (10.2.17)	P rma% (10.2.24)	Sample type
Orogenic gold, coarse grained, USA	Au (g/t)	0.1–1206	89.6	36	0.92		74.5	105.4	75.5	105.2	Repeat channel samples
Archean gold, medium and coarse grained, Canada	Au (g/t)	0.03–50	4.3	201	0.71	34.4	47.2	66.7	46.6	110.1	1st (Coarse) split
	Au (g/t)	0.01–355	1.3	4209	0.98	15.3	24.5	34.6	24.5	132.2	Pulp duplicates
Copper-silver veins, Canada	Ag (g/t)	2–393	72.31	42	0.98		15.3	21.7	15.5	21.1	Channel vs. blast hole samples
	Cu (%)	0.01–0.97	0.16	42	0.99		13.5	19.2	13.5	12.0	
Native Cu-mineralisation	Cu (%)	1.17–1.51	1.37	10	−0.55		9.6	13.6	10.1	14.5	Pulp duplicate
Cu-Au porphyry, Australia	Cu (%)	0.0001–4.83	0.10	4707	0.99	5.7	14.1	20.0	14.1	30.3	Field duplicate
	Au (g/t)	0.0005–7.01	0.05	4784	0.95	18.6	41.7	59.0	41.7	157.7	
	Cu (%)	0.0002–5.3	0.4	6346	0.98	1.9	10.5	14.8	10.5	25.3	Pulp duplicate
	Au (g/t)	0.02–276	0.8	14346	1.00	4.4	17.1	24.2	17.0	26.6	
Cu-Mo porphyry, USA	Cu (%)	0.003–14.4	1.45	398	1.00	1.4	7.1	10.0	7.1	3.9	1st (Coarse) split
	Mo (%)	0.005–1.14	0.03	398	1.00	4.0	14.2	20.0	14.2	14.2	
	Cu (%)	0.015–9.6	1.43	346	1.00	0.9	2.5	3.6	2.5	1.8	Pulp duplicate
	Mo (%)	0.005–0.315	0.03	346	1.00	2.7	11.5	16.3	11.5	7.3	
Iron Ore, Deposit 1, Pilbara, Australia	Fe (%)	50.63–67.37	62.2	228	0.94	0.6	1.4	2.0	1.4	1.9	Field duplicate
	Al_2O_3 (%)	0.19–7.38	2.06	228	0.92	5.8	12.4	17.5	12.3	26.3	
	SiO_2 (%)	0.7–26.0	3.45	228	0.95	7.1	13.7	19.3	13.7	30.1	
	LOI (%)	0.83–10.95	4.89	228	0.98	2.2	4.9	6.9	4.9	7.2	
Iron Ore, Deposit 2, Pilbara, Australia	Fe (%)	1.84–67.3	51.27	8088	1.00	0.6	2.2	3.0	2.1	1.8	Field duplicate
	Al_2O_3 (%)	0.11–50.66	5.7	8088	1.00	2.3	6.9	9.8	6.9	7.7	
	SiO_2 (%)	0.68–95.96	12.56	8088	1.00	2.3	7.0	9.9	6.9	6.8	
	LOI (%)	0.34–26.03	7.38	8088	1.00	1.4	2.5	3.5	2.5	3.2	

(continued)

Table 10.2 (continued)

Mineralisation type/deposit	Metal	Grade range	Average	No of sample pairs	Correlation	P th% (10.2.3*)	CV% (10.2.8)	AMPD (10.2.9)	P dfb% (10.2.17)	P rma% (10.2.24)	Sample type
Iron Oxide hosted Cu-Au mineralisation, Australia	Au (g/t)	0.0005–41.3	0.74	1522	0.93	12.5	25.3	35.7	25.2	163.6	1st (Coarse) split
Cu-Au-Fe skarn	Cu (%)	0.003–12.3	0.91	806	1.00	2.6	8.7	12.4	8.5	6.3	Field duplicate
	Au (g/t)	0.05–35.24	1.39	616	0.99	10.9	20.7	29.2	20.6	25.7	
Ni-Cu-PGE-sulphides, Australia	Ni (%)	0.0001–6.82	0.345	587	0.97	12.1	22.1	31.3	22.2	59.9	Field duplicate
	Cu (%)	0.0001–4.86	0.22	586	0.95	14.6	21.8	30.8	21.8	70.3	
	Co (%)	0.0001–0.16	0.0125	586	0.96	9.4	14.5	20.5	14.5	52.2	
	Pd (ppm)	0.005–2.46	0.08	323	0.96	12.3	29.4	41.5	29.1	57.8	
	Ni (%)	0.0001–5.4	0.17	961	1.00	1.2	11.0	15.6	11.0	5.3	Pulp duplicate
	Cu (%)	0.0001–15.8	0.18	961	1.00	1.4	4.2	5.9	4.2	4.5	
	Co (%)	0.0001–0.175	0.0788	961	1.00	1.7	7.5	10.6	7.5	5.9	
	Pd (ppm)	0.001–1.26	0.109	836	0.97	3.9	17.7	25.1	17.8	26.3	
Detrital Ilmenite sands, deposit 1, Africa	Total heavy minerals (%)	0.7–26.2	7.48	539	0.89	5.4	17.7	25.0	17.7	24.7	Field duplicate
Detrital Ilmenite sands, deposit 2, Africa	Total heavy minerals (%)	2.4–19.3	8.96	27	0.96		8.1	11.5	8.1	13.9	Field duplicate

(Reprinted from (Abzalov 2008) with permission of the Canadian Institute of Mining, Metallurgy and Petroleum)

*P th% error has been estimated at average (arithmetic mean) grade of the paired data

CV% – Coefficient of Variation (%). This estimator is recommended as a universal measure of relative precision error in the mine geology applications (Abzalov 2008)

LOI– loss on ignition

Comparison of the results in Table 10.2 shows that precision errors produced by the Thompson-Howarth technique are consistently the lowest among all the reviewed methods. These results are not surprising because they reflect the assumption in the Thompson-Howarth method that measurement errors are normally distributed (Thompson and Howarth 1973, 1976, 1978; Howarth and Thompson 1976). Based on this assumption, the method uses the median value of absolute differences of the data pairs for calculation of precision error, and this inevitably produces biased results when errors are not normally distributed. To overcome this problem, Stanley (2006) suggested a modification to the Thompson-Howarth method that calculates the root mean squares of the absolute pair differences instead of their medians. This alternative approach (Stanley 2006; Stanley and Lawie 2007b) is a more robust estimator in comparison to the conventional Thompson-Howarth method because it does not require a normality assumption. However, this modification is likely to be more sensitive to outliers, and should therefore be rigorously tested in order to better understand its possible limitations when applied to various geological materials.

A second group of estimators include AMPD and other similar statistical methods (Table 10.1), which are based on calculation of the absolute differences between the original and duplicate samples normalised by the mean grades of the data pairs (Bumstead 1984; Shaw 1997; Roden and Smith 2001). Relative errors obtained from this approach are proportional to coefficients of variation (Stanley 2006; Stanley and Lawie 2007a) and represent nothing more than the product of the coefficient of variation (CV) and a constant. Hence, the various statistics included in this group (e.g., AMPD, HARD) offer no more information than the coefficient of variation itself ($CV_{AVR}(\%)$) which is suggested to use as a universal measure of the relative precision error (Stanley and Lawie 2007a; Abzalov 2008, 2014).

The approach suggested by Francois-Bongarcon (1998) calculates the ratio of the difference between the paired data to their sum ($\frac{(a_i-b_i)}{(a_i+b_i)}$) and then estimates variance of this complex variable. Results of this method are similar to the average coefficient of variation $CV_{AVR}(\%)$ (Table 10.2). However, formula (10.2.16) seems to be unnecessarily complicated in comparison to the conventional $CV_{AVR}(\%)$ approach (10.2.8).

The RMA method consists of the calculation of the RMA line and related parameters and is particularly useful for identifying bias between paired data (Sinclair and Bentzen 1998; Davis 2002; Sinclair and Blackwell 2002; Abzalov 2008). This method can be used to calculate the precision error estimate from dispersion of the data points about the RMA function (10.2.24). However, the errors estimated from the RMA model ($P_{RMA}(\%)$) can significantly differ from $CV_{AVR}(\%)$ values (Table 10.2). These differences are likely due to sensitivities of the RMA model to the presence of outliers, which makes this technique inappropriate for strongly skewed distributions.

In summary, the author concurs with the proposal of Stanley and Lawie (2007a) that $CV_{AVR}(\%)$ be used as the universal measure of relative precision error. Based on numerous case studies, the appropriate levels of sample precisions are proposed for different types of deposits in Table 10.3, and it is suggested that these levels be used as approximate guidelines for assessing analytical quality.

It is important to remember that the values in Table 9.3, although based on case studies of the mining projects, may not be always appropriate because mineral deposits can significantly differ by the grade ranges, statistical distribution of the studied values, mineralogy, textures and grain sizes.

Later it was shown (Abzalov 2014) that because estimation of $CV_{AVR}(\%)$ is based on the same expression as pair-wise relative variogram therefore when it is used for estimating the samples precision the assay data variance can be directly compared with spatial (i.e. geological) variability of the studied variable.

Table 10.3 Best and acceptable levels of the precision errors proposed as reference for evaluating the mining projects

Mineralisation type / deposit	Metal	Best practise	Acceptable practise	Sample type
Gold, very coarse grained	Au (g/t)	20 (?)	40	Coarse rejects
Gold, coarse to medium grained	Au (g/t)	20	30	Coarse rejects
	Au (g/t)	10	20	Pulp duplicate
Cu-Mo-Au porphyry	Cu (%)	5	10	Coarse rejects
	Mo (%)	10	15	
	Au (g/t)	10	15	
	Cu (%)	3	10	Pulp duplicate
	Mo (%)	5	10	
	Au (g/t)	5	10	
Iron Ore, palaeochannel hosted goethitic mineralisation	Fe (%)	1	3	Field duplicate
	Al2O3 (%)	10	15	
	SIO2 (%)	5	10	
	LOI (%)	3	5	
Cu-Au-Fe skarn and iron-oxide associated Cu-Au	Cu (%)	7.5	15	Coarse rejects
	Au (g/t)	15	25	
	Cu (%)	5	10	Pulp duplicate
	Au (g/t)	7.5	15	
Ni-Cu-PGE sulphide deposit	Ni (%)	10	15	Coarse rejects
	Cu (%)	10	15	
	PGE	15	30	
	Ni (%)	5	10	Pulp duplicate
	Cu (%)	5	10	
	PGE (g/t)	10	20	
Detrital Ilmenite sands	Total Heavy Minerals (%)	5	10	Field duplicate

(Reprinted from (Abzalov 2008) with permission of the Canadian Institute of Mining, Metallurgy and Petroleum)

10.4 Guidelines for Optimisation of the Sampling Programmes

The current section summarises the sampling practices of the modern mining industry and incudes practical recommendations for design and implementation of the optimal sampling protocols and quality control procedures.

10.4.1 Planning and Implementation of the Sampling Programmes

Evaluation of the mineral deposits requires application the right sampling protocols assuring the good quality of the collected samples and supplementing it by the rigorous quality control procedures. It is highly recommended to implement the optimal sampling and quality control systems at the early stage of the project evaluation just after it has been realised that a discovered mineral occurrence warrants a detailed delineation and studies. At this stage, usually referenced as Order of Magnitude or Scoping study, the given deposit has to be systematically drilled and sampled, based on which the geological characteristics of the deposit will be quantified and the resources estimated. The biased or otherwise incorrectly data can lead to incorrectly assessed mining project causing the costly consequences. Delays in establishing good sampling protocols and implementing the rigorous quality control procedures is also not warranted as this can create the different data generations which often of a different quality. Author has observed numerous cases when the earlier obtained samples have been rejected at the pre-feasibility or feasibility

studies because the earlier samples were found of a suboptimal quality. Another common situation is when the more advanced stages of the project studies are delayed because of additional work needed to verify the earlier drilling results.

The first step is to design sample preparation procedures assuring that they are optimally suited for a studied mineralisation. The good starting point is to estimate Fundamental Sampling Error (FSE) and plot the proposed protocol on a sampling nomogram (Fig. 9.6). This approach allows to optimise such parameters like weight of the initial sample, particle sizes after each comminution stage and sizes of the reduced samples. Based on this study all stages of the samples preparation are clearly determined and parameters of the process are quantified. These parameters need to be considered choosing equipment for sample preparation. In particular, it is necessary to assure that capacity of equipment is matching to the proposed protocol.

Established sampling protocol needs to be documented. It is a good practice to represent it graphically, as the sample preparation flow chart and make it easily accessible for the geological team.

The next step after sampling protocol has been optimised is to add the quality control procedures. At this stage it is necessary to decide how many duplicates will be collected and how they are taken. It is also necessary to decide how many reference materials shell be inserted with each sample batch and develop procedures allowing to disguise the standards and blanks. The project management at this stage is making decision if they will develop the matrix matched standards, specially prepared for the studied mineralisation, or will be using commercially available certified standards.

QAQC procedures should be developed together with the new sampling programme and if the latter is modified, the associated QAQC map is often being changed too. It is a good practice (Abzalov 2008, 2011) to plot the quality control procedures directly on the sample preparation flow-chart. Such combined diagrams are useful practical tools helping to implement and administrate the QAQC procedures assuring that all sampling and preparation stages are properly controlled.

Finally, all procedures should be documented and personnel responsible for their implementation and control determined and instructed. It is necessary to assure that geological team, working at the mine or developing project, regularly reviews the QAQC results in order to timely diagnose the sampling errors. The author after reviewing many different mines found the most effective and practically convenient periodicity for the data quality review is when the QAQC results were checked by in every analytical batch and summary QAQC reports have been prepared for approval by chief geologist on the monthly basis. The monthly reports should contain several diagrams showing performance of the reference materials and duplicates. The most commonly used diagrams are (Abzalov 2008, 2011):

- standard samples diagnostic diagram (Fig. 10.1);
- diagram of the blank samples (Fig. 10.2);
- scatter-diagram of the duplicate samples showing RMA line and CV% (Fig. 10.5)
- RDP diagram (Fig. 10.6).

The calculated precision variances shell be compared with their acceptable levels. The levels of acceptable precision errors and deviation of the standards from their certified values should be clearly determined and documented as part of the QAQC procedures.

10.4.2 Frequency of Inserting QAQC Material to Assay Batches

Number of quality control samples and frequency of their insertion to analytical batches should be sufficient for systematic monitoring of the assays quality. Recommended quality control materials vary from 5 to 20 % (Garrett 1969; Taylor 1987; Vallee et al. 1992; Leaver et al. 1997; Long 1998; Sketchley 1998) depending on mineralisation type, location of the mining project and stage of the project evaluation. Brief overview of the different recommendations on frequency of insertion of the QAQC material is given below.

Garrett (1969) has recommended that approximately 10 % of geochemical samples should be controlled by collecting the duplicate samples. Taylor (1987) recommends that from 5 to 10 % of samples analysed by laboratory should be a reference material. Leaver et al. (1997) suggest to analyse one in-house reference material with every 20 assayed samples and also include to the same batch at least one certified standard.

Long (1998) has suggested that to control samples quality in the mining projects it is necessary to do as follows: at least 5 % of pulps should be checked by independent laboratory; 5 % of field and/or coarse rejects should have a second pulp prepared and analysed by the primary laboratory; every sample batch should include from 1 to 5 % of standard reference materials, such as certified standards and blanks. Good practise is to analyse at least 5 % of the duplicates in the different laboratory (Long 1998).

Sketchley (1998) has recommended that every sample batch submitted to analytical laboratory should include from 10 to 15 % quality control samples. In particular, every batch of 20 samples should include at least one standard, one blank and one duplicate sample (Sketchley 1998).

Guide to Evaluation of Gold Deposits (Vallee et al. 1992) recommends that at least 10 % of the determinations in an exploration or mining projects should be QAQC samples, including standards, blanks and duplicates.

Based on the review of above mentioned published QAQC procedures and numerous case studies by the current author (Abzalov and Both 1997; Abzalov 1998, 1999, 2007; Abzalov and Humphreys 2002a; Abzalov and Mazzoni 2004; Abzalov and Pickers 2005; Abzalov et al. 1997, 2010, 2015) it is suggested that reliable control of sample precision is achieved by using approximately 5–10 % of field duplicates, and 3–5 % of the pulp duplicates. Duplicate samples should be prepared and analysed in the primary laboratory.

In order to detect bias in analytical results, it is necessary to include 3–5 % of standard reference materials with every sample batch. A good practice is to use more than one standard, so that their values span the practical range of grades in the actual samples. However, standard samples alone cannot identify biases introduced at different stages of sample preparation. Anonymity of the standards is another issue, because standards can be easily recognised in the sample batches and be treated more thoroughly by laboratory personnel. To overcome this problem some duplicate samples should be analysed in an external, reputable laboratory as part of the accuracy control. It is suggested that at least 5 % of the total analysed duplicates, including pulp duplicates and coarse rejects, should be analysed in the reputable external laboratory.

10.4.3 Distribution of the Reference Materials

Standards should be inserted with such frequency that allows to constantly monitor the possible instrumental drifts and biases. In general, the best practice is to insert standards and blanks to every sample batch. Good practise is to use more than one standard, so that their values are bracketing the practical range of the grades in the actual samples. Distribution of the reference material within the batch should allow detecting possible biases of the results and at the same time these reference samples should remain anonymous.

10.4.4 Distribution of the Duplicate Samples

Practical recommendations on optimisation the duplicated sample analysis with a particular emphasis on the duplicates distribution in the analytical batches have been presented and discussed by many researchers (Thompson and Howarth 1978; Sketchley 1998; Vallee et al. 1992; Abzalov 2008). The basic rules of collecting of the duplicate samples are summarised below.

Duplicate samples should be chosen in such manner that all stages of data preparation are properly addressed and the precision errors associated with all sub-sampling stages are adequately estimated by the sample duplicates.

This means that sample duplicates should include field duplicates, coarse reject duplicates and the pulp duplicates (Long 1998). A special attention should be given to the field duplicates as they are mostly informative for estimation of the overall precision of samples. When rotary drilling is used, the field duplicates, which in this case are called "rig" duplicates, are collected from the sample splitting devices built-in to the drill rigs. These can be rotary, cone or riffle slitters. In case of diamond core drilling the field duplicates are represented by another portion of core. Field duplicates of the blast hole samples should be another sample, taken from the same blast hole cone as the original sample and following exactly the same procedures.

Coarse reject duplicates consist of material representing output from crushers. It often can be more than one type of coarse rejects when samples preparation requires several stages of crushing and splitting. In this case, coarse reject duplicates should be collected for each stage of crushing and/or grinding followed by sample reduction.

Operations, using large pulverisers, such as LM5, usually don't have coarse rejects as all collected sample is pulverised to affine pulp. In this case, it is extremely important to collect and analyse the field duplicates to understand the overall repeatability of the assayed results.

Collecting the sample duplicates it is necessary to remember that they should be identical to the sample which they are duplicating. Unfortunately, this is not always possible as the chemical or physical characteristics of the remaining material can be altered after sample has been collected or its amount is simply insufficient to make a representative duplicate. For example, if drill core is sampled by cutting a half core it is unwise to collect quarter core as a duplicate as this will produce a duplicate samples of a twice smaller weight than the original samples. Such duplicates are likely to produce a larger precision error than that of the original samples. Using all remaining second half of core as duplicate is also suboptimal practice as it breaches auditability of the data. The problem can be partially resolved if to take duplicate using the approach shown on the Fig. 10.8.

In case when all drill samples are assayed, the latter is a common case at the bauxite mines, the only possibility to assess precision of the drill samples is to use twin holes. However, it is necessary to account for the geological factor (Abzalov 2009).

It is important to assure that duplicate samples should be representative for the given deposit covering the entire range of the grade values, mineralisation types, and different geological units and have a good spatial coverage of the deposit. It is difficult to achieve the representativeness of the duplicates when they collected at random from the sample batches. Disadvantage of randomly selected duplicates is that most of them will represent the most abundant type of the rocks, usually barren or low-grade mineralisation. The ore grade and, in particular, high-grade intervals are often poorly represented in randomly chosen duplicates. They can also be non-representative regarding mineralisation types, their spatial distribution or grade classes. To meet these two conditions,

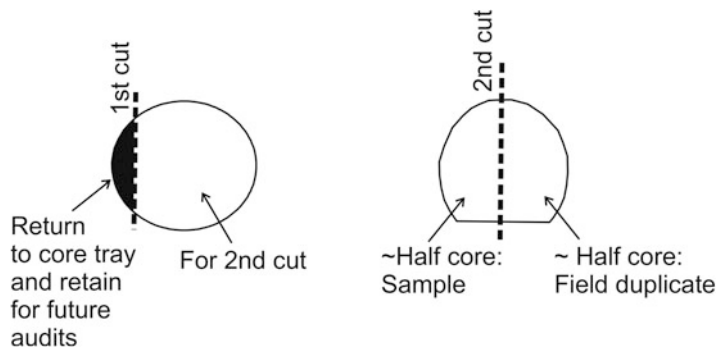

Fig. 10.8 Sketch explaining collection the duplicate drill core samples in case if routine samples represent the half of the core cut by diamond saw

a two-pronged approach is recommended: approximately half of the duplicates should be collected by a project geologist with instructions to ensure that they properly represent all mineralization styles and grade ranges, and that they spatially cover the entire deposit. The other half of the duplicates should be selected and placed at random in each assay batch.

The position of the sample duplicates in a given analytical batch should not be immediately after their original samples and also should not be systematically related to it. It is important that the original samples and their duplicates are included in the same analytical batch which will allow using them for within-batch precision studies.

Numbering of the duplicate samples should disguise them in the analytical batch. The duplicate samples should be taken through the same analytical procedure as the original sample.

References

Abzalov MZ (1998) Chrome-spinels in gabbro-wehrlite intrusions of the Pechenga area, Kola Peninsula, Russia: emphasis on alteration features. Lithos 43(3):109–134

Abzalov MZ (1999) Gold deposits of the Russian North East (the Northern Circum Pacific): metallogenic overview. In: Proceedings of the PACRIM '99 symposium. AusIMM, Melbourne, pp 701–714

Abzalov MZ (2007) Granitoid hosted Zarmitan gold deposit, Tian Shan belt, Uzbekistan. Econ Geol 102(3):519–532

Abzalov MZ (2008) Quality control of assay data: a review of procedures for measuring and monitoring precision and accuracy. Exp Min Geol J 17(3–4):131–144

Abzalov MZ (2009) Use of twinned drill – holes in mineral resource estimation. Exp Min Geol J 18(1–4):13–23

Abzalov MZ (2011) Sampling errors and control of assay data quality in exploration and mining geology. In: Ivanov O (ed) Application and experience of quality control. InTECH, Vienna, pp 611–644

Abzalov MZ (2014) Chapter 2: The resource database. Geostatistical criteria for choosing optimal ratio between quality and quantity of the samples: method and case studies. In: Mineral resource and ore reserves estimation, 2nd edn, AusIMM monograph 23. AusIMM, Melbourne, pp 91–96

Abzalov MZ, Both RA (1997) The Pechenga Ni-Cu deposits, Russia: aata on PGE and Au distribution and sulphur isotope compositions. Mineral Petrol 61(1–4):119–143

Abzalov MZ, Humphreys M (2002a) Resource estimation of structurally complex and discontinuous mineralisation using non-linear geostatistics: case study of a mesothermal gold deposit in northern Canada. Exp Min Geol J 11(1–4):19–29

Abzalov MZ, Humphreys M (2002) Geostatistically assisted domaining of structurally complex mineralisation: method and case studies. Geostatistically assisted domaining of structurally complex mineralisation: method and case studies. In: The AusIMM 2002 conference: 150 years of mining, Publication series No 6/02, pp 345–350

Abzalov MZ, Mazzoni P (2004) The use of conditional simulation to assess process risk associated with grade variability at the Corridor Sands detrital ilmenite deposit. In: Dimitrakopoulus R, Ramazan S (eds) Ore body modelling and strategic mine planning: uncertainty and risk management. AusIMM, Melbourne, pp 93–101

Abzalov MZ, Pickers N (2005) Integrating different generations of assays using multivariate geostatistics: a case study. Trans Inst Min Metall 114:B23–B32

Abzalov MZ, Brewer TS, Polezhaeva LI (1997) Chemistry and distribution of accessory Ni, Co, Fe arsenic minerals in the Pechenga Ni-Cu deposits, Kola Peninsula, Russia. Mineral Petrol 61(1–4):145–161

Abzalov MZ, Menzel B, Wlasenko M, Phillips J (2010) Optimisation of the grade control procedures at the Yandi iron-ore mine, Western Australia: geostatistical approach. Appl Earth Sci 119(3):132–142

Abzalov MZ, van der Heyden A, Saymeh A, Abuqudaira M (2015) Geology and metallogeny of Jordanian uranium deposits. Appl Earth Sci 124(2):63–77

Bumstead ED (1984) Some comments on the precision and accuracy of gold analysis in exploration. Proc AusIMM (289): 71–78

CANMET (1998) Assessment of laboratory performance with certified reference materials. CANMET Canadian Certified Reference Materials Project Bulletin, p 5

Davis JC (2002) Statistics and data analysis in geology, 3rd edn. Wiley, New York, p 638

Dominy SC, Annels AE, Johansen GF, Cuffley BW (2000) General considerations of sampling and assaying in a coarse gold environment. Trans Inst Min Metall 109:B145–B167

Eremeev AN, Ostroumov GV, Anosov VV, Berenshtein LE, Korolev VP, Samonov IZ (1982) Instruction on internal, external and arbitrary quality control of the exploration samples assayed in the laboratories of the ministry of geology of the USSR. VIMS, Moscow, p 106 (in Russian)

Francois-Bongarcon D (1998) Error variance information from paired data: application to sampling theory. Exp Min Geol J 7(1–2):161–165

Garrett RG (1969) The determination of sampling and analytical errors in exploration geochemistry. Econ Geol 64(5):568–569

Goovaerts P (1997) Geostatistics for natural resources evaluation. Oxford University Press, New York, p 483

Howarth R, Thompson M (1976) Duplicate analysis in geochemical practice: Part 2, examination of proposed method and examples of its use. Analyst 101: 699–709

ISO Guide 33 (1989) Uses of certified reference materials. Standards Council of Canada, Ontario, p 12

Kane JS (1992) Reference samples for use in analytical geochemistry: their availability preparation and appropriate use. J Geochem Exp 44:37–63

Leaver ME, Sketchley DA, Bowman WS (1997) The benefits of the use of CCRMP's custom reference materials. Canadian certified reference materials project. In: Society of mineral analysts conference. MSL No 637, p 16

Long S (1998) Practical quality control procedures in mineral inventory estimation. Exp Min Geol 7(1–2):117–127

Pitard FF (1998) A strategy to minimise ore grade reconciliation problems between the mine and the mill. In: Mine to mill. AusIMM, Melbourne, pp 77–82

Roden S, Smith T (2001) Sampling and analysis protocols and their role in mineral exploration and new resource development. In: Edwards A (ed) Mineral resources and ore reserve estimation – the AusIMM guide to good practise. AusIMM, Melbourne, pp 73–78

Shaw WJ (1997) Validation of sampling and assaying quality for bankable feasibility studies. In: The resource database towards 2000. AusIMM Illawara branch, Wollongong, Australia, pp 69–79

Sinclair AJ, Bentzen A (1998) Evaluation of errors in paired analytical data by a linear model. Exp Min Geol 7(1–2):167–173

Sinclair AJ, Blackwell GH (2002) Applied mineral inventory estimation. Cambridge University Press, Cambridge, p 381

Sketchley DA (1998) Gold deposits: establishing sampling protocols and monitoring quality control. Exp Min Geol 7(1–2):129–138

Stanley CR (2006) On the special application of Thompson-Howarth error analysis to geochemical variables exhibiting a nugget effect. Geochem Explor Environ Anal 6:357–368

Stanley CR, Lawie D (2007a) Average relative error in geochemical determinations: clarification, calculation and a plea for consistency. Exp Min Geol 16:265–274

Stanley CR, Lawie D (2007b) Thompson-Howarth error analysis: unbiased alternatives to the large-sample method for assessing non-normally distributed measurement error in geochemical samples: Geochemistry: Exploration. Environ Anal 7:1–10

Taylor JK (1987) Quality assurance of chemical measurements. Lewis Publishers, Michigan, p 135

Thompson M, Howarth R (1973) The rapid estimation and control of precision by duplicate determinations. Analyst 98(1164):153–160

Thompson M, Howarth R (1976) Duplicate analysis in geochemical practice: Part 1. Theoretical approach and estimation of analytical reproducibility. Analyst 101:690–698

Thompson M, Howarth R (1978) A new approach to the estimation of analytical precision. J Geochem Exp 9(1):23–30

Vallee M, David M, Dagbert M, Desrochers C (1992) Guide to the evaluation of gold deposits: Geological Society of CIM, Special Volume 45, p 299

Twin Holes

11

Abstract

Drilling twinned holes is a traditional technique used for verification of intersections of high-grade mineralization, testing of historic data, or confirmation of drillhole data during geological due diligence studies. Twinned holes can also be used for special tasks such as correcting earlier data that are recognized to be biased.

Successful implementation of the twinned-holes technique requires thorough planning. Experience suggests that good practice is to drill twinned holes no more than 5 m apart. Many unsuccessful twinned-holes programs could possibly have failed because the twinned holes have been drilled too far apart.

A formal, rigorous analysis of twinned-hole data is essential. Repeatability of sampling, analytical results, and bias must be analyzed and statistically quantified. The number of twinned holes required for conclusive statistical and geostatistical analysis can be as high as 20–30, in particular where the studied variables are characterized by high short-range (local) variability.

Keywords

QAQC • Twin holes • Due diligence

Drilling of twinned holes (i.e., drilling of a new hole, or "twin", next to an earlier drill hole) is a traditional technique used in exploration and mining geology for verification of mineralization grades. The importance of this technique is emphasized in the JORC Code, which specifically queries if twinned holes have been used for 'verification of sampling and assaying' (JORC 2012). However, the experience at various operating mines and in mining project studies shows that despite its practical importance and reasonable simplicity, the twinned holes approach is often misunderstood and not applied to full advantage in the mining industry. One of the most common myths is that drilling of twinned holes is inappropriate in geological environments characterized by large short range variability of grade. This and other prejudices have limited the wider

M. Abzalov, *Applied Mining Geology*, Modern Approaches in Solid Earth Sciences 12,
DOI 10.1007/978-3-319-39264-6_11

application of this useful technique. Such limitations seem to result from a lack of a clear description of principles of the method, and an absence of representative case studies in the technical literature. For example, the published guides on evaluation of mineral deposits (Peters 1987; Annels 1991; Vallee et al. 1992; Sinclair and Blackwell 2002) only briefly mention the twinned holes approach. This deficiency has been partially addressed in the recently published paper (Abzalov 2009) which briefly described the basic principles of the twinned holes technique and provided examples of its application. The findings of that study (Abzalov 2009) have been revised and presented in the current chapter. The examples described represent different stages in the appraisal of mineral deposits, ranging from scoping to feasibility studies and the grade control drilling at the operating mines. Deposit types include orogenic gold, mineral sands, bauxite, and banded iron formation (BIF) iron oxide deposits.

11.1 Method Overview

Twinned holes should be thoroughly planned, starting with a clear definition of the objectives of the study, and progressing to choices of the number of holes, their location, studied variables, and statistical procedures for treatment of the resulting data.

11.1.1 Objectives of the Twinned Holes Study

The most common application of twinned holes is for verification of grades reported by previous drilling. Usually, this involves verification of high-grade intersections, including an assessment of grade variability.

Another common objective of drilling twinned holes is to verify historic data. Such a need usually occurs where results from earlier drill holes are causing concerns either by being noticeably different to other drilling campaigns in the same area, or where poor quality of drilling has been revealed from previously documented parameters, such as core recovery. In some cases, historic data might be suspect (e.g., biased) because of suboptimal drilling technology or inappropriate drilling parameters. For example, air-core drilling of a mineral sands deposit might be biased, and the issue could be examined by twinning the historic air-core holes with sonic drill holes.

Verification of earlier drilled holes by twinning them with new holes is a common technique used by geological due diligence teams when reviewing third party projects (Gilfillan 1998). Drilling twinned holes becomes particularly important where the reviewed project is based on historical data that were collected without rigorously applied sampling quality control procedures, or where the relevant quality assurance/quality control (QAQC) documentation is lacking. Where bias of historic data has been proven, the data from twinned holes can be used for quantification of this bias, and integrated into the resource model using multivariate and/or non-stationary geostatistical methods for correcting the resource estimates (Abzalov and Pickers 2005). It is unlikely that the new resource or reserve estimates based on geostatistically corrected data will be accepted by a formal regulator, or publically reportable in compliance with reporting cods, such as JORC (2012), and/or financial institutions. However, such studies can provide a good quantification of the risk or upside potential of the project, and can demonstrate the economic benefits of additional infill drilling, or, in some cases, complete redrilling of the deposit.

The number and locations of twinned holes, drilling methods, and the tested variables are selected to accomplish the objectives of the proposed study. For example, if the purpose of drilling twinned holes is to verify high grade intersections, new holes should be drilled next to previous holes that reportedly intersected high grade mineralization. Conversely, if the objective is to test and statistically quantify a possible bias in historic data, the twinned holes should be drilled in such a manner that assures that a wide range of grades is tested, including both low- and high- grade mineralization. In this latter case, twinned holes should be distributed throughout the entire deposit, and the number of twinned holes should be sufficient for statistical analysis of the data.

11.1.2 Statistical Treatment of the Results

Statistical procedures applied to twinned hole data can vary depending on the objective of the study. In general, two main errors are assessed from the matching pairs of twinned holes: repeatability (precision) and bias. Repeatability of twinned holes can be quantified by the average coefficient of variation $CV_{AVR}(\%)$ of the paired data (10.2.8). Examples of application of this technique to twinned hole data are presented in Table 11.1. Average coefficient of variation values for the studied twinned holes vary from 0.9 to 51 %. They are usually larger for variables characterized by large nugget effects.

Bias of the data can be diagnosed by the graphic tools including Relative Difference Plot (RDP) and Reduced Major Axis (RMA) diagrams (Pitard 1998; Sinclair and Bentzen 1998; Abzalov 2008), and then assessed by statistical tests (Davis 2002). A common, and valid, approach is the conventional statistical *t*-test. Other useful diagnostic tools and statistical methods of estimation of precision and accuracy errors can be found in Vallee et al. (1992)) and Abzalov (2008). When bias in certain datasets has been diagnosed, it can be further studied by geostatistical methods (Abzalov and Pickers 2005).

11.1.3 Distance Between Twinned Holes

In general, twinned holes should be located as close as possible to the original holes to minimize the effects of short range variability in the studied variables. In many geological environments, in particular when studying gold deposits, it is impossible to avoid the nugget effect, and advance knowledge of that parameter is essential when comparing results of old and new drilling in a pair of twinned holes. In practice, most twinned holes, including those listed in the Table 11.1, are drilled at distances varying from 1 to 10 m from the original holes, depending on logistics of the drill sites, deposit type, mineralization style, and studied variables. A well-known example of a (negatively) successful twinned holes program is the confirmatory drilling done by Freeport-McMoRan at the Busang project of Bre-X Minerals Ltd. Fraud was revealed by seven twinned holes (Lawrence 1997). Each of the seven new holes was drilled only 1.5 m away from supposedly extensively gold mineralized holes, and all failed to substantiate the originally stated gold values (Lawrence 1997).

A study undertaken by Abzalov et al. (2010) at the Yandi iron-ore open pit has shown that $CV_{AVR}(\%)$ of Al_2O_3 grades estimated from matching pairs of blast holes and reverse circulation (RC) holes increase from 23.8 to 35.7 % when the distance between twinned holes increases from 1 m to 10 m. These results suggest that many unsuccessful twinned holes studies could have failed because twinned holes have been drilled too far apart.

The close distances of 1–1.5 m employed for twinned holes at Busang (Lawrence 1997) and at the Yandi mine (Abzalov et al. 2010) are likely to represent the special cases. At Busang, the confirmatory holes had to be as close as possible to the originals to satisfy technical due diligence considerations. Similarly, the large short range variability caused by the presence of irregularly distributed clay pods at the Yandi mine required very close spacing of twinned holes (Abzalov et al. 2010). In general, particularly when the studied variable has less spatial variation, the acceptable distance between twinned holes can be larger. However, personal experience of the author indicates that good practice is not to drill matching pairs of holes more than 5 m apart.

11.1.4 Drilling Quality and Quantity

When planning twinned drill holes it is necessary to remember that important decisions may have to be made based on a limited number of verification holes. Therefore, it is necessary to ensure that their quantity and quality are sufficient to make a conclusive decision. The number of twinned holes depends on the aim of the twinning program and the range of variation in the studied variables.

Table 11.1 Characteristics of the studied twinned holes projects

Twinned holes project	Drilling type: new vs. old	Number of twinned holes	Compared variable	Composited samples (number of matching pairs)	Mean values		Standard deviation		CV_{AVR} (%)	RMA parameters (y = ax + b)		Reference to diagram
					Old holes	New holes	Old holes	New holes		a	b	
Ti-sands project, Africa	Aircore vs. aircore	35	THM, %	3 m composite (669)	7.7	7.8	3.0	3.3	25.1	1.09 ± 0.03	−0.6 ± 0.3	Fig. 11.2
			THM, %	12 m composite (169)	7.7	7.8	2.3	2.5	15.1	1.07 ± 0.05	−0.4 ± 0.4	
			THM, %	Intersection	7.7	7.7	1.5	1.6	8.9	1.01 ± 0.1	−0.1 ± 0.8	
Ti-sands project, Africa	Diamond (triple tube) vs. aircore	8	THM, %	3 m composite (98)	9.4	11.9	5.0	5.7	30.3	1.1 ± 0.07	1.1 ± 0.7	Fig. 11.5
Ti-sands project, Madagascar	Sonic vs. vibracore	20	THM, %	1.5 m composites (201)	4.74	4.76	2.4	2.5	29.7	1.0 ± 0.05	−0.1 ± 0.3	Fig. 11.6
Orogenic gold, Canada	Diamond (NQ) vs. diamond (NQ)	5	Au, g/t	Intersection	7.9	8.9	11.6	15.0	51.2	1.3 ± 0.07	−1.2 + 0.9	Fig. 11.3
Iron ore deposit, Australia	RC vs. blast holes	40	Fe,%	Composited to bench	58.8	58.5	1.1	1.8	1.4	1.6 ± 0.15	−37.4 ± 8.6	
			Al_2O_3, %	Composited to bench	1.40	1.47	0.5	0.8	23.8	1.7 ± 0.27	−1.0 ± 0.4	
			SiO_2, %	Composited to bench	4.0	4.1	1.4	1.6	10.2	1.2 ± 0.09	−0.5 ± 0.4	
Iron ore deposit, Australia	Diamond (PQ) vs. RC	26	Fe,%	Intersection	51.3	51.3	2.5	3.5	3.2	1.4 ± 0.19	−21.5 ± 9.7	
			Al_2O_3, %	Intersection	5.1	4.8	0.6	1.0	19.0	1.3 ± 0.16	−2.5 ± 1.8	
			SiO_2, %	Intersection	9.3	9.7	3.3	4.4	15.9	1.6 ± 0.32	−3.4 ± 1.6	
Bauxite deposit, Australia	Aircore vs. aircore	13[a]	Al_2O_3, %	Intersection	49.9	49.9	4.0	4.4	1.9	1.1 ± 0.09	−4.5 ± 4.7	Fig. 11.7
			SiO_2, %	Intersection	14.9	15.1	6.3	7.0	9.7	1.1 ± 0.1	−1.5 ± 1.8	
			Thickness, m	Intersection	4.4	4.3	1.8	1.9	10.0	1.06 ± 0.09	−0.3 ± 0.4	
Bauxite deposit, Africa	Diamond vs. auger	62	Thickness, m	Intersection	9.5	7.6	2.9	2.3	25.1	0.8 ± 0.1	0.1 ± 1.1	

Notes: [a]Only part of the Weipa deposit and related twinned holes data were included in this study
CV_{AVR} (%) = average coefficient of variation of the paired data (10.2.8); *RMA* reduced major axis (Sinclair and Bentzen 1998); *THM* total heavy minerals
(Reprinted from (Abzalov 2009) with permission of the Canadian Institute of Mining, Metallurgy and Petroleum)

The studies that require 20–30 twinned holes are not uncommon (Table 11.1).

It is necessary to ensure that verification holes are of the best practically achievable quality. This often requires the use of a different drilling technique, commonly a more expensive one to that used for the previous drilling. For example, air core holes in mineral sands projects are preferably twinned by sonic drilling, auger holes in bauxite deposits by diamond core holes, and RC holes in coal deposits by PQ diamond core holes. It is important to realize that verification holes, even if they are drilled using the most up to date technology, can still produce biased and/or excessively variable results. For example, quality of confirmatory diamond drilling can be marred by poor core recovery, or sonic drilling can be adversely affected by self-injection of sands into core barrels caused by lithostatic pressure. The risks of incorrect twinned holes studies can best be minimized by optimising drilling parameters, for example using HQ or PQ drill bits for verification of NQ diamond holes, and adjusting drill mud and drilling rate to ensure the best possible core recovery. Twinned holes require more thorough monitoring by technical and geological personnel. In all cases, the sampling protocols and quality of assays in the verification holes should be rigorously monitored and documented (Abzalov 2011).

11.1.5 Comparison of Studied Variables

Prior to comparing assayed grades in the twinned holes it is necessary to compare geological logs, because the geological features are usually more continuous than grades (Sinclair and Bentzen 1998). Twinned holes are initially compared by mineralised intersections (Fig. 11.1a). Comparisons should not be limited to average grades of intersections, but should also include thicknesses and positioning of the contacts. The latter is particularly important when down hole contamination of the samples is suspected. Common

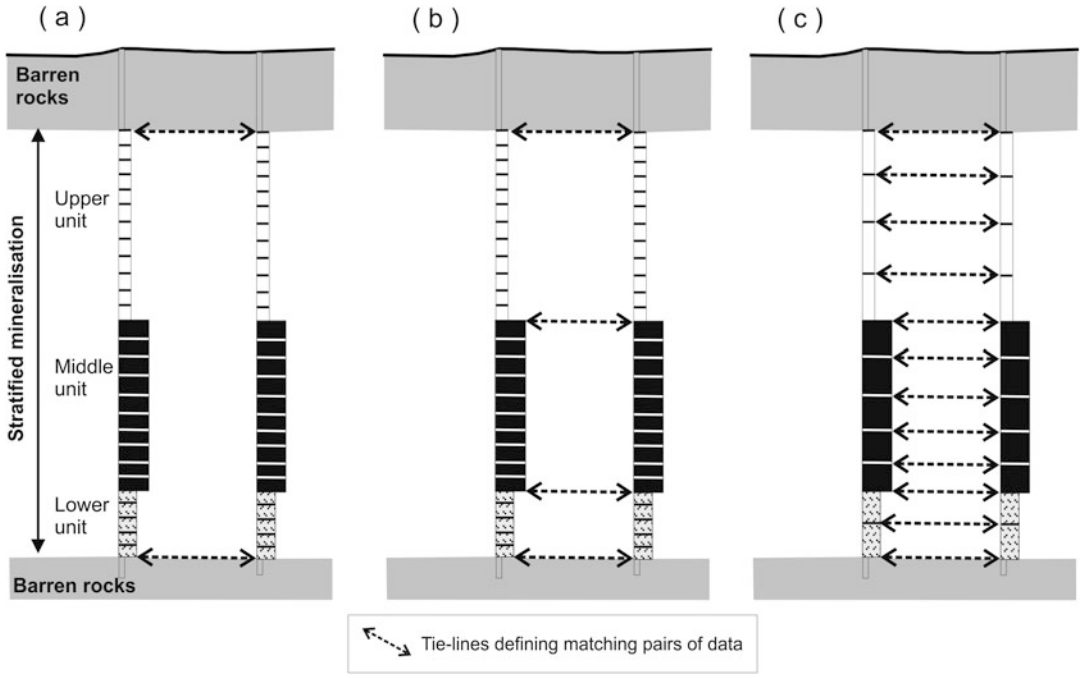

Fig. 11.1 Idealised diagram explaining various comparative approaches for twin holes data (Reprinted from (Abzalov 2009) with permission of the Canadian Institute of Mining, Metallurgy and Petroleum): (**a**) comparison by ore-grade intersections; (**b**) comparison by geological units; (**c**) comparison by matching individual samples

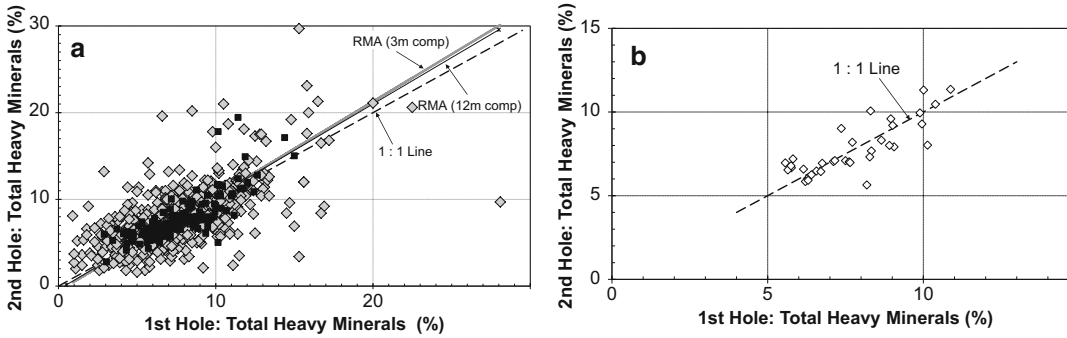

Fig. 11.2 Twinned holes study at a Ti-sands project, Africa (Reprinted from (Abzalov 2009) with permission of the Canadian Institute of Mining, Metallurgy and Petroleum): (**a**) scatter diagram comparing matching pairs between twin holes. Samples have been composited to 3 m (*grey symbols*) and 12 m intervals (*black symbols*), RMA = Reduced Major Axis; (**b**) scatter diagram comparing the same drill holes by the average grades of the mineralised intersections

examples include the use of auger drilling for evaluation of bauxite or heavy mineral deposits, or RC drilling in gold projects.

More detailed studies include comparison of twinned holes by matching intervals. Practically achievable outcomes are often obtained through grouping samples by geological units (Fig. 11.1b). This approach is particularly useful when twinned holes are drilled through stratified mineralization or regularly intercalated low- and high-grade zones.

In particular cases, for example when twinned holes are drilled through mineralization exhibiting gradational zoning, comparison can be made directly between samples where they are of an equal length; alternatively, comparisons may be made between equal length composites (Fig. 11.1c). Compositing of samples smooths away the impact of outliers and converts samples into common length data, which are necessary for geostatistical resource estimation (Sinclair and Blackwell 2002). In twinned holes analysis, when comparing variables with high statistical variation, grouping samples to larger composites is commonly necessary to minimize the noise exhibited by individual samples. It is important to ensure that samples are composited to geological boundaries.

An example of comparing twinned holes by composites of different lengths is shown in Fig. 11.2. In this project, compositing from 3 m to 12 m has significantly decreased data variance and scatter, and has decreased $CV_{AVR}(\%)$ from 25.1 to 15.1 % (Table 11.1, first example). Reduced Major Axis functions of two datasets of 3 m and 12 m composites are very similar (Fig. 11.2a, Table 11.1). When the same data were composited to ore grade intersections, $CV_{AVR}(\%)$ was further decreased to 8.9 % (Fig. 11.2b, Table 11.1).

11.1.6 Practice of Drilling Twinned Holes for Mining Geology Applications

It is important to note that the twinned holes approach does not replace other validation techniques, such as bulk sampling or comparative analysis of data from drilling campaigns related to different stages of infill drilling. Each of the validation methods has its specific areas of application.

Comparison of drill holes from different drilling campaigns is needed for validation of exploration data prior to resource/reserves estimation. This approach is most effective when different drilling generations evenly cover the same area, allowing their comparisons by global statistics. Such comparisons are usually made at a first stage of data testing, entirely based on data subsets extracted from a drill hole database.

When comparisons of the data generations reveal systematic differences, more detailed analyses are usually undertaken, including drilling of twinned holes.

Bulk samples are taken at the advanced stages of a mining project study and are used mainly for metallurgical test work. Another objective of the bulk sampling program is validation of reserve models by comparing estimated values in the block model with bulk sampling results (Annels 1991).

A twinned holes approach, representing the drilling of a relatively small amount of verification holes, is usually applied for quick and conclusive confirmation/refutation of high-grade intersections (e.g., the Bre-X Busang project), verifying historic data, and testing third party mining projects. Given the typically small number of verification holes drilled, it is necessary to thoroughly plan the program to ensure that the confirmatory holes are of the best practically achievable quality and value. They are often drilled using a more expensive, but more reliable, technique to that used for the previous drilling.

Quantity and quality of the twinned holes should be sufficient for a conclusive decision regarding confirmation of the variables of interest. Common practice is to drill several twinned holes. However, when studied variables are characterized by large short range variability, the number of twinned holes drilled may be significantly larger. The author has studied projects where 40–60 twin holes were drilled for the data verification purposes (Table 11.1).

Twinned holes should be located as close as possible to the original holes in order to minimize the effect of short range variability in the studied variables. Good practice in the twinned holes approach is to drill them no more than 5 m apart. In special cases, the distance between twinned holes may be as close as 1–1.5 m, as previously discussed in the Busang project where the imperative was to conclusively confirm or reject previous drilling results (Lawrence 1997). At the Yandi project, where the studied mineralization is characterized by large short range variability, comparative analysis of the matching pairs of blast holes and RC holes has shown that repeatability of the results significantly worsens when the distance between twinned holes increases from 1 m to 10 m (Abzalov et al. 2010). This result suggests that many apparently unsuccessful twinned hole studies could have failed because the twinned holes were drilled too far from the original holes.

Geological interpretation should be an important part of twinned holes analysis (Sinclair and Bentzen 1998). Geological information provides an important guide for choosing matching intervals in twinned holes, and facilitates interpretation of the data.

Comparison by mineralised intersections is the most practical approach for comparing twinned holes. Length-weighted average grades of the matching intersections and thicknesses of mineralisation are calculated and compared, and good practice is also to compare locations of the geological contacts determined by twinned holes. When the thickness of mineralisation is large, and in particular if the mineralisation has a zoned structure, it becomes necessary to compare twinned holes by geological units or samples grouped to equal length composites. Grouping samples to larger composites is commonly necessary to minimize the noise exhibited by samples taken at smaller intervals.

Statistical techniques used for analyses of twinned holes results are not different to other QAQC approaches (Vallee et al. 1992; Pitard 1998; Sinclair and Bentzen 1998; Stanley and Lawie 2007a; Abzalov 2008, 2011). Repeatability of the twinned holes results can be quantified by the average coefficient of variation. Bias in the data can be diagnosed by graphical tools, in particular RMA and RDP diagrams, and then assessed by statistical *t*-tests.

11.2 Case Studies

The above explained approach has been successfully used in twinned holes studies in many different deposit styles and commodities, including orogenic gold, mineral sands, base metals, bauxite, and iron ore. Objectives of the studies varied from confirmation of high-grade intersections at

gold deposits, to quantification and correction of bias in historic data.

The case studies below demonstrate that a popularly held belief that the twinned holes approach is impractical and/or inapplicable in geological environments characterized by large short-range variability is unjustified, and may commonly simply reflect prejudice rather than fact.

11.2.1 Gold Deposits: Confirmation of High-Grade Intersections

Confirmation of high grade intersections is essential in deposit styles characterized by high nugget effect of metal grades. It is particularly important where a deposit contains erratically distributed high-grade shoots (Vallee et al. 1992; Abzalov 1999, 2007; Abzalov and Humphreys 2002a). In such cases, confirmation of high-grade intersections must include two objectives. First, the high-grade assays returned by a previously drilled hole need to be verified, and, second, the geological significance and size of the high-grade shoot needs to be assessed and/or confirmed. The first task can be achieved by twinning the original hole with a new hole drilled as close as possible to the original hole. However, such closely located twinned holes do not allow proper assessment of the size of the shoot, and therefore do not fully accomplish the total objective for verification of high-grade zones.

The second part of the objective will require drilling several holes at different distances from the first high-grade intersection. These holes are not twinned holes *senso stricto* and represent a related technique, namely delineation of the high-grade zones by closely spaced step-out drilling. The difference between these cases is shown by Figs. 11.3 and 11.4.

The first case (Fig. 11.3) is represented by an orogenic gold deposit in Canada. The presence of high-grade zones was recognized by the project team, and were partly delineated by closely spaced infill drilling. However, because the project included several drilling campaigns, the project management elected to verify some of the earlier drilled high-grade holes by twinning them with the new holes (Table 11.1). Structural interpretations and close spaced drilling in the detailed study areas have shown that high-grade shoots have 50–70 m strike lengths and widths of approximately 25 m (Fig. 11.3a). Twinned holes were drilled within 1–5 m, and in some cases up to 10 m, from the original holes. This was considered acceptable given the prior knowledge of the structure of the gold lodes and dimensions of the high grade shoots (Fig. 11.3b). The twinned holes overall confirmed the previously reported grades, although significant variation ($CV_{AVR} = 51\,\%$) between twinned hole grades was revealed (Table 11.1). This level of variation was considered acceptable because the deposit is characterized by high short range variability. The relative nugget effect of the gold grade is approximately 40 %.

The second case (Fig. 11.4) was observed at an orogenic gold deposit in the Norseman-Kambalda greenstone belt, Western Australia. The first phase of resource definition drilling at this deposit delineated resources potentially viable for economic extraction by a conventional open pit mine. However, it was recognized that the main risk of incorrect estimation of the resources was related to results for two high-grade shoots, in particular one in the northern part of the deposit where the length-weighted average grade of a key drill hole intersection totalled 51.4 g/t. To mitigate this risk, additional drilling was undertaken. This high-grade zone was first confirmed by drilling a twin hole, which returned 41.9 g/t (Fig. 11.4), and after that, the extension of the high-grade shoot was studied by drilling several holes along the strike of mineralization.

Delineation holes, drilled at 15–20 m intervals, show that the high grade shoot extends less than 30 m along strike and is approximately half of this size in the across-strike direction (Fig. 11.4). When these findings were incorporated into the revised resource model it caused significant changes in the open pit design, production schedule, and project economics.

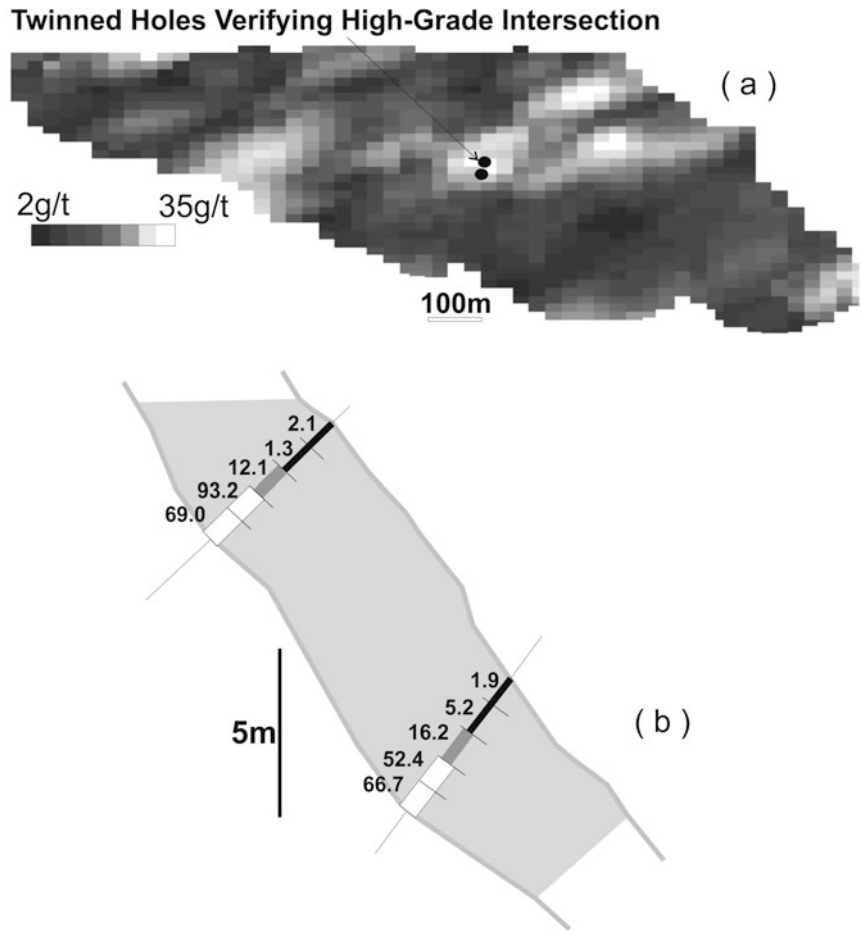

Fig. 11.3 Confirmation of high-grade intersections in an orogenic gold deposit by twinned holes (Reprinted from (Abzalov 2009) with permission of the Canadian Institute of Mining, Metallurgy and Petroleum): (**a**) long-section (*looking north*) showing location of the twin holes; (**b**) cross section (*looking west*) showing twin holes drilled through high-grade gold shoot. *Numbers* denote the sample grades (Au, g/t)

11.2.2 Twin Holes Studies in Iron Ore Deposits

During evaluation of an iron ore deposit in the Pilbara region of Western Australia, the quality of RC holes was tested by diamond holes of PQ core diameter. Results presented in Table 11.1 show that PQ holes have verified the RC drilling. The small differences between Al_2O_3 grades of the PQ core samples and the corresponding RC samples were statistically insignificant,[1] so the results from the RC drilling technique were accepted for the project feasibility study.

Another twinned holes study was undertaken at the Yandi open pit iron ore mine located in the eastern part of the Pilbara region (Abzalov et al. 2010). The grade control approach used at the mine was based on sampling of production blast holes on a 6 × 6 m spacing. An alternative approach of using RC holes distributed on a 25 m × 25 m grid was considered. In order to assess representativity of the blast hole samples they were initially compared with full blast hole cone grades, and with RC samples composited to bench heights. In total, six blast hole cones were processed. Comparisons revealed that blast

[1]Calculated *t*-values are 1.31 and 0.37 for Al_2O_3 and SiO_2, respectively. The critical value of *t*-distribution with 50° of freedom and at 5 % confidence limit is 2.01 (Davis 2002).

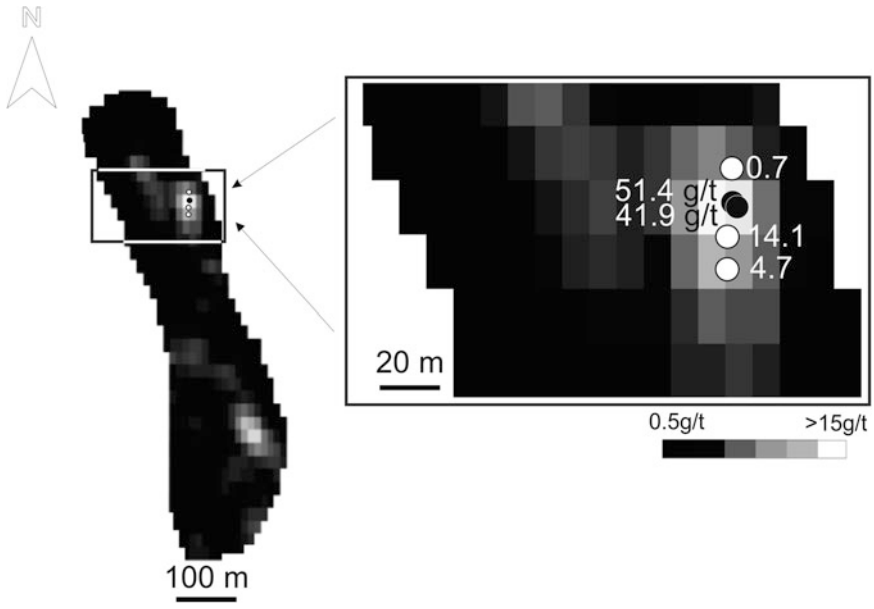

Fig. 11.4 Delineation by closely spaced step-out drilling of the high grade zones at an orogenic gold deposit, Norseman mine camp, Western Australia (Reprinted from (Abzalov 2009) with permission of the Canadian Institute of Mining, Metallurgy and Petroleum)

Table 11.2 Comparison of six full cone grades with corresponding blast hole and composited RC samples, Yandi iron ore mine, Australia (Abzalov et al. 2007, 2010)

	Fe, wt%	SiO_2, wt%	Al_2O_3, wt%
Full cone	58.18	6.38	1.14
Blast hole sample	58.59	6.16	1.06
RC sample	59.01	5.8	1.02

hole sample grades of Al_2O_3 and SiO_2 were slightly higher than their values in the full cone assays, whereas Fe grade was lower (Table 11.2). Comparison of the RC composites with full cone assays showed a similar trend; however, the magnitude of the differences was larger than that of the blast-hole samples (Table 11.2).

The study was continued by drilling additional RC holes that twinned blast holes. In total, 12 pairs of RC and blast holes were obtained. The new results showed similar relationships to those presented in Table 11.2, but with larger variability of the results. In order to investigate the causes of excessive variability between the twinned holes, all available pairs of RC (and/or diamond) holes and blast holes separated by a distance less than 1 m were recovered from the deposit drill holes database. RC holes were composited to bench heights and compared with the blast-hole grades. Results show that average blast hole grades are consistent with the RC (and/or diamond) grades when the distance between them is less than 1 m (Table 11.1). When the distance increases, the variations between grades of the matching pairs of holes also increases. Coefficients of variation of Al_2O_3 grade increased from 23.8 % at 1 m separation, to 30.1 % at 5 m, and 35.7 % at 10 m. Based on these results, it was concluded that use of RC drilling for grade control at this mine would not necessarily provide better results than blast hole samples, and, therefore, the grade control procedures remained unchanged (Abzalov et al. 2010).

11.2.3 Mineral Sands Deposits: Validation of Historic Drilling

Air core drilling is a common technique used for resource definition of heavy mineral sands deposits of ilmenite, rutile, zircon, and leucoxene. However, it is the author's experience that in some cases, depending on mineralogy of the deposit, depth of water table, clay content of the sands, and other factors, air core drilling can generate biased results by systematically underestimating the THM (total heavy minerals) grades of the mineral sands. The potential bias can be tested and quantified by drilling twin holes, historically using triple tube diamond core drilling and, more recently, by sonic drilling.

A case study for a Ti-sands project in Africa is presented in Fig. 11.5 and summarized in Table 11.1. Mineralisation is distributed between several stratigraphic units with combined thickness exceeding 100 m. Historic air-core holes were tested by twinning them with triple tube diamond core holes (Fig. 11.5a). All assays were composited to 3 m intervals. The matching pairs of samples are plotted on a scatter-diagram in Fig. 11.5b, and statistically analysed. Results clearly show that historic air core holes tend to underestimate THM grade. Bias of air core samples is clearly seen by the noticeable mismatch between the RMA line and the first bisect (1:1 line) of that diagram (Fig. 11.5b). This twinned holes analysis has revealed that, in addition to variations related to lithology and mineralogy of the mineral sands, the bias of the air core samples increases when sampled units are located below the water table.

Another example was taken from a Ti-sands project in Madagascar (Fig. 11.6, Table 11.1). The deposit was first drilled using a vibratory drill hole built in-house by the project team. At the feasibility stage, the quality of the data was validated with twinned holes drilled using a commercially available sonic drill rig. In this example, sonic drilling fully confirmed the stratigraphy and grades of the heavy mineral sands as earlier defined by the historic vibratory drilling (Fig. 11.6).

11.2.4 Bauxites: Use of Twin Holes as a Routine Control of Drilling Quality

In many bauxite deposits in Australia, Africa, and Asia, twinned holes are used as a routine quality control technique (Abzalov and Bower 2014). Besides conventional tasks such as diagnosis and quantification of the biases of assays, twinned holes are commonly used to verify thicknesses of bauxite seams and to assure accurate positioning of the upper and lower contacts of the bauxite (Fig. 11.7). The latter is necessary to assure good control of mining losses and dilution, because many bauxite ore bodies are narrow, with average thickness of less than 3 m.

When twinned holes are used as part of the routine QAQC procedures, the second hole is not drilled immediately after the first hole. This assures that twinned holes provide a good control of drilling quality, and supplement the traditional QAQC approaches (Abzalov 2008) based on duplicate samples and reference materials.

An example of twinned holes drilled at the Weipa bauxite deposit in Australia is shown in Fig. 11.7, where twinned holes fully confirm previous drilling results: estimated RMA functions of the studied variables coincide with the 1:1 line on scatter diagrams. It is also noted that thickness and SiO_2 are characterised by larger variability than Al_2O_3. Coefficients of variation of thickness and SiO_2 are 12.5 % and 9.7 %, respectively, whereas $CV_{AVR}(\%)$ of Al_2O_3 is 1.9 % (Table 11.1). These results are consistent with variography analysis of these variables. The Al_2O_3 variogram is characterized by a small nugget effect (10.5 %), whereas thickness and SiO_2 values exhibit large short range variability manifested by a large nugget effect on their variograms: 39.3 % and 24.4 %, respectively.

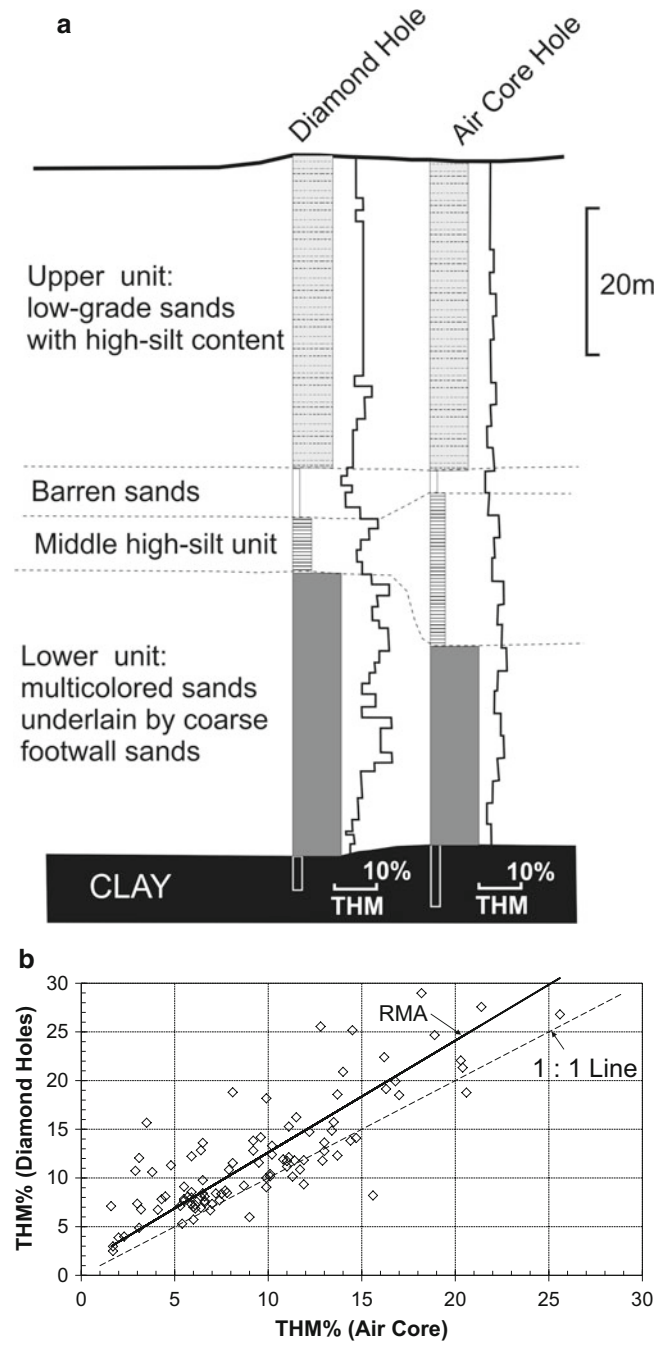

Fig. 11.5 Twinned holes approach applied to verify historic data at a Ti-sands project in Africa (*THM* total heavy minerals) (Reprinted from (Abzalov 2009) with permission of the Canadian Institute of Mining, Metallurgy and Petroleum): (**a**) air-core hole twinned by triple tube diamond drill hole; horizontal distance (less than 5 m) between twinned holes is not to scale; (**b**) Scatter diagram of the THM grades of diamond drill holes vs. air core holes (*RMA* reduced major axis)

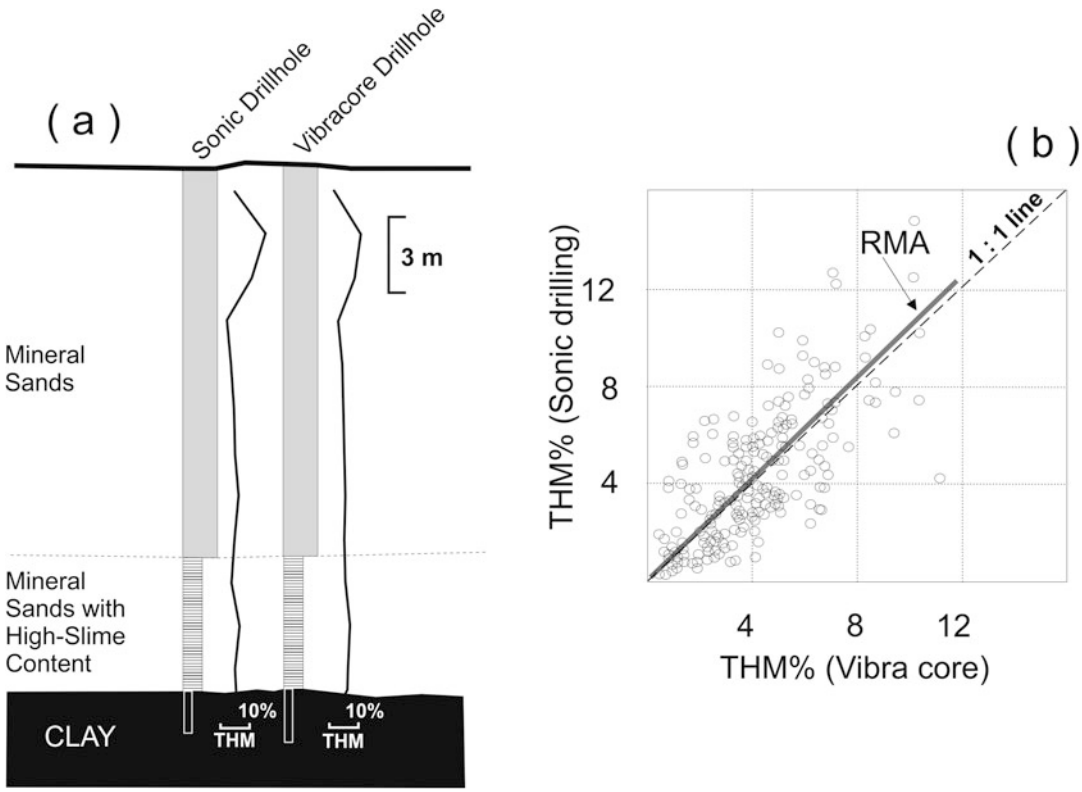

Fig. 11.6 Validation of historic exploration data by twinned holes, Ti-sands project, Madagascar (*THM* total heavy minerals) (Reprinted from (Abzalov 2009) with permission of the Canadian Institute of Mining, Metallurgy and Petroleum): (**a**) historic hole drilled using vibratory technology, twinned by sonic hole; (**b**) THM grades of sonic drill hole samples vs. samples from twinned vibratory holes (*RMA* reduced major axis)

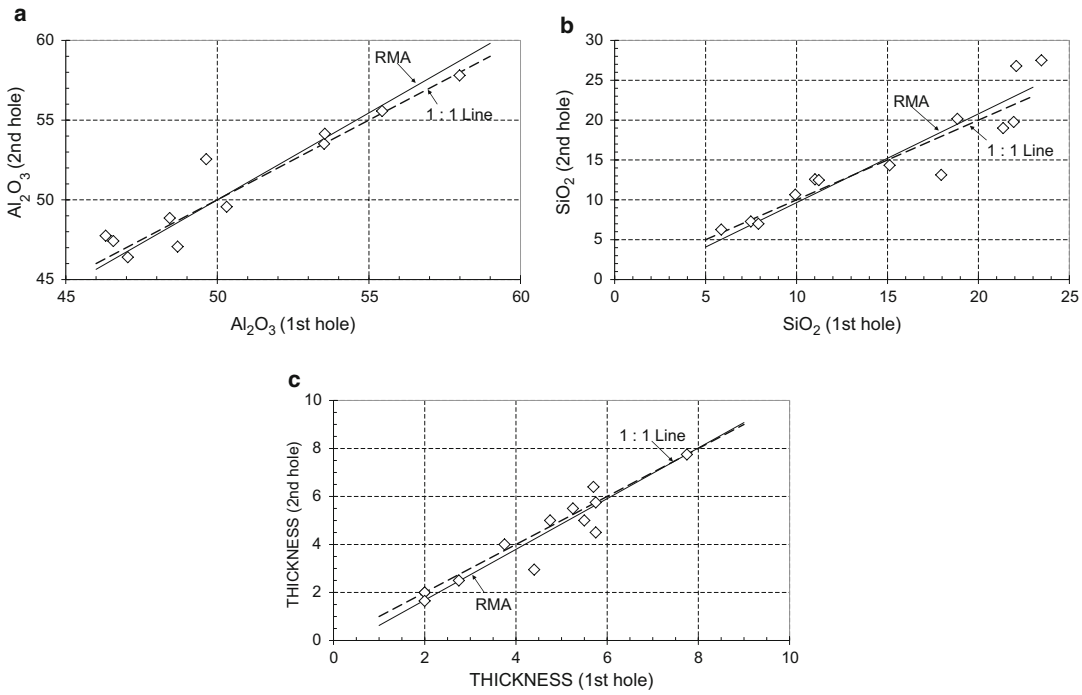

Fig. 11.7 Validation of grade and thickness of bauxite by twinned holes, Weipa deposit, Australia (*RMA* reduced major axis) (Reprinted from (Abzalov 2009) with permission of the Canadian Institute of Mining, Metallurgy and Petroleum): (**a**) Al_2O_3; (**b**) SiO_2; (**c**) Thickness (m)

References

Abzalov MZ (1999) Gold deposits of the Russian North East (the Northern Circum Pacific): metallogenic overview. In: Proceedings of the PACRIM '99 symposium. AusIMM, Melbourne, pp 701–714

Abzalov MZ (2007) Granitoid hosted Zarmitan gold deposit, Tian Shan belt, Uzbekistan. Econ Geol 102(3):519–532

Abzalov MZ (2008) Quality control of assay data: a review of procedures for measuring and monitoring precision and accuracy. Exp Min Geol J 17(3–4):131–144

Abzalov MZ (2009) Use of twinned drill – holes in mineral resource estimation. Exp Min Geol J 18(1–4):13–23

Abzalov MZ (2011) Sampling errors and control of assay data quality in exploration and mining geology. In: Ivanov O (ed) Application and experience of quality control. InTECH, Vienna, pp 611–644

Abzalov MZ, Bower J (2014) Geology of bauxite deposits and their resource estimation practices. Appl Earth Sci 123(2):118–134

Abzalov MZ, Humphreys M (2002) Resource estimation of structurally complex and discontinuous mineralisation using non-linear geostatistics: case study of a mesothermal gold deposit in northern Canada. Exp Min Geol J 11(1–4):19–29

Abzalov MZ, Pickers N (2005) Integrating different generations of assays using multivariate geostatistics: a case study. Trans Inst Min Metall 114:B23–B32

Abzalov MZ, Menzel B, Wlasenko M, Phillips J (2007) Grade control at the Yandi iron ore mine, Pilbara region, Western Australia: comparative study of the blastholes and RC holes sampling. In: Proceedings of the iron ore conference 2007. AusIMM, Melbourne, pp 37–43

Abzalov MZ, Menzel B, Wlasenko M, Phillips J (2010) Optimisation of the grade control procedures at the Yandi iron-ore mine, Western Australia: geostatistical approach. Appl Earth Sci 119(3):132–142

Annels AE (1991) Mineral deposit evaluation, a practical approach. Chapman and Hall, London, p 436

Code JORC (2012) Australaisian code for reporting of exploration results, mineral resources and ore reserves. AusIMM, Melbourne, p 44

Davis JC (2002) Statistics and data analysis in geology, 3rd edn. Wiley, New York, p 638

Gilfillan JF (1998) Testing the data—the role of technical due diligence. In: Ore reserves and finance seminar, Sydney, 15 June, 1998. AusIMM, Melbourne, pp 33–42

Lawrence MJ (1997) Behind Busang, the Bre-X scandal: could it happen in Australia? Aus J Min 12(134):33–50

Peters WC (1987) Exploration and mining geology, 2nd edn. Wiley, New York, p 706

Pitard FF (1998) A strategy to minimise ore grade reconciliation problems between the mine and the mill. In: Mine to mill. AusIMM, Melbourne, pp 77–82

Sinclair AJ, Bentzen A (1998) Evaluation of errors in paired analytical data by a linear model. Exp Min Geol 7(1–2):167–173

Sinclair AJ, Blackwell GH (2002) Applied mineral inventory estimation. Cambridge University Press, Cambridge, p 381

Stanley CR, Lawie D (2007) Average relative error in geochemical determinations: clarification, calculation and a plea for consistency. Exp Min Geol 16: 265–274

Vallee M, David M, Dagbert M, Desrochers C (1992) Guide to the evaluation of gold deposits: Geological Society of CIM, Special Volume 45, p 299

Database

12

Abstract

The main principles for the construction and administration of a relational database are explained coupled with practical recommendations for efficient data entry and database management. It has been shown that effective practices in the storage and manipulation of large volumes of data depend in equal measures on database software, supporting file structures, sound database administration practices and adherence to strict data-capture protocols in the field.

It is emphasized that the performance of a relational database can be downgraded by poor database administration practices, in particular the inefficient monitoring of field and office data flows.

Keywords

Relational database • Data flow • Metadata

Modern mining operations use a vast amount of different sampling data which need to be stored together in a database. A practical way of arranging the data is to distribute the information between several tables which are linked together using the key fields. This system is known as a relational database.

The databases currently used in the mining industry vary from relatively simple in-house developed systems to sophisticated packages, such as acQuire, that are specialised for mining industry needs. Despite differences in their complexity relational databases all have a common characteristic: they are designed for the effective storage and manipulation of large volumes of digital data carrying various types of information allowing easy access to the stored data.

This chapter discusses the main principles for the construction and efficient administration of a relational database for mining and exploration geology, emphasising that that the performance of a relational database can be downgraded by a poorly designed database structure.

It is also noted that a correct management of the data flow is an essential factor assuring that data transfer is flawless and data are not altered or lost due to suboptimal procedures of electronic data handling. The practical recommendations are made for efficient data entry and database management.

M. Abzalov, *Applied Mining Geology*, Modern Approaches in Solid Earth Sciences 12,
DOI 10.1007/978-3-319-39264-6_12

12.1 Construction of the Database

It is of particular importance to correctly set up the database structure from the beginning of the project. The sampling data should be stored in a way that will allow quick compilation of all information required for appraisal of the resources and reserves of a mineral deposit, preparing accurate mine plans and arranging the production quality controls.

In addition to main characteristics of the samples, it is necessary to store all auxiliary information, for example date of drilling and assaying, laboratory and analytical method, and many other characteristics of samples and details of the drilling campaigns which are important for easy and effective evaluation of the data. It is impossible to store all the variable information in one table, usually referenced as a 'flat table' by database administrators. Such a table would be excessively large and cumbersome. A practical way of arranging the data is to distribute the information between several tables which are linked together using certain key fields (Fig. 12.1). This system is known as a relational database (Codd 1990, Long 1998, Lewis 2001, Abzalov 2014a).

Based on personal experience the author suggests arranging the relational database as is shown in Fig. 12.1. The master table should contain drill hole number, sample interval, sample number and sample assay values and can contain additional characteristics of the sample such as core recovery. Drill hole numbers and sample numbers are used to link sample information in the master table to other tables containing drill hole information therefore project managers from the very beginning have to assure that these numbers are unique (Fig. 12.1). These additional tables include drill hole collar

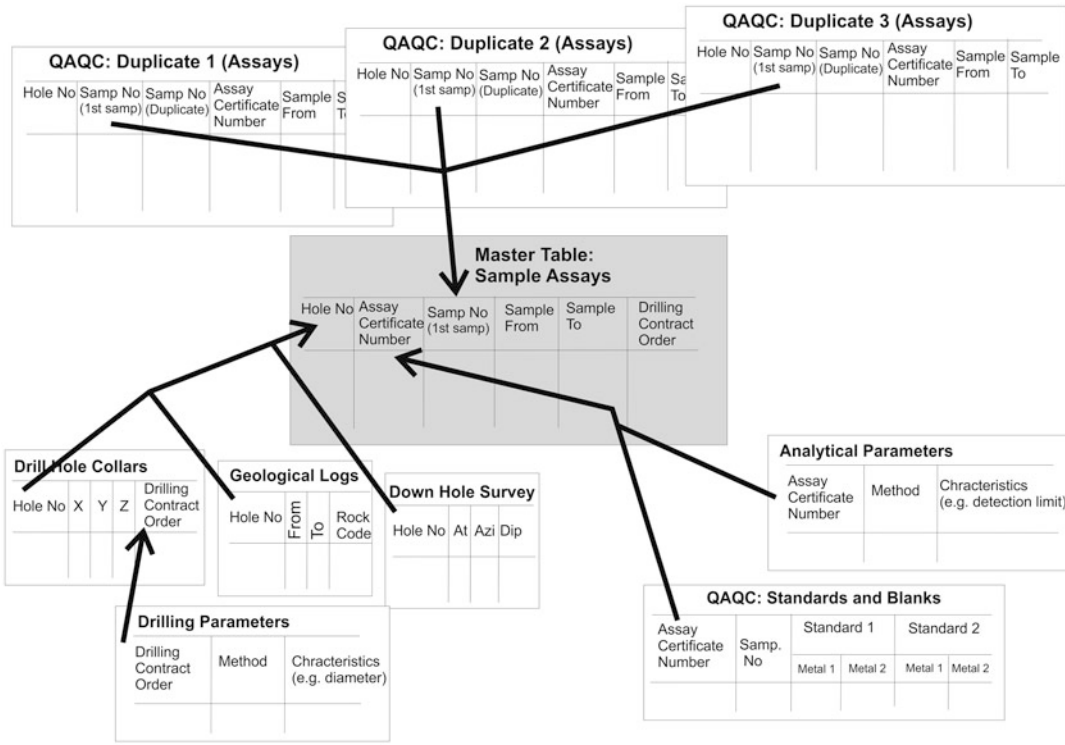

Fig. 12.1 Sketch explaining structure of the relational database. Different types of data are distributed between tables which are linked using the key fields (Reprinted from Abzalov 2014a with permission of Australasian Institute of Mining and Metalllurgy)

coordinates, down hole survey results and digital geological logs.

The four above mentioned tables encompass the main types of sampling data and they are used by most of the modern resource modelling softwares therefore the proposed structure (Fig. 12.1) allows flawless transfer of the data from the database to the specialised software. The structure proposed in Fig. 12.1 does not enlist all possible data types but rather shows main principles, with distribution of data between tables following the conventions accepted by most mining software. Additional data, for example geotechnical logs or digital geophysics, can be added as separate files linked to the master table by the designated keys.

It is important to assure that stored original data are not mixed with newly created values or derived data, such as X,Y,Z coordinates calculated for each sample. The fields containing values generated by the database software should be clearly identified.

Special attention should be paid for the appropriate storage of quality control data (QAQC) including various duplicate samples, repeat assays, standards and blanks (Long 1998, Sinclair and Blackwell 2002, Abzalov 2008). It is poor practise to store QAQC data in the master table with main samples. A more effective way is to store QAQC data in separate tables (Fig. 12.1), linking them to their corresponding assay batches by common key fields.

Good relational databases should not be limited to storing the data which are required for geological modelling and resource estimation. They should also include metadata or "data about the data". A vast amount of auxiliary information is usually received from the drilling contractors, field geologists and analytical laboratories, all which need to be systematically stored in the relational database. Long (1998) has suggested a practical way to store all additional information without making the database tables overly cumbersome. Most of the important auxiliary information are recorded at the headers of the data sheets, received from the personnel and laboratories undertaking drilling, documentation, sample collection and assaying. For example, almost all auxiliary information related to analytical techniques is usually reported at the header of assay certificate received from the laboratory. Entering this information into a separate table within the same relational database enables storage of all key facts related to analytical laboratory, technique, personnel and dates of analyses. This information is linked to the corresponding samples by a key field denoting the certificate's unique number. This key field should be added to the sample table as an additional column. In practice the combination of the date when the certificate was issued and the laboratory name can be used as the composite key.

Auxiliary information regarding drilling parameters, including type, date, drill company, rig type, drill bit diameter and the name of the driller are generally reported in the drilling contract orders. These can be stored in separate tables of the same relational database. These data are linked to the main table containing sample assays through a key field denoting the drill contract order (Fig. 12.1) and in some cases drill hole number. Depending on the amount of the auxiliary information the administrator of the database will elect whether to store data in separate tables or simply add several extra fields to the table containing coordinates of the drill hole collars. The same principles are used for storing surveying data and digital geological logs.

The relational database structure is flexible and allows for the situation where there may not be a relationship between all records in all tables. For example, a table containing drill hole collars can have more holes than are present in the assay table (Fig. 12.1). This may occur when some holes have failed to be completed, or when a project geologist has chosen not to sample some holes if they did not intersect mineralisation. The opposite situation may arise when records of the drill hole coordinates are missing, for example if they have not been surveyed. There are legitimate reasons why data may be missing from the database, however missing or incorrect data could be the result of data entry errors and poor database management. Although it is technically possible for relational databases to have mismatching records this practice is sub-

optimal and can cause considerable confusion when data is analysed. Therefore, from a practical point of view it is better to assure that the same hole numbers are recorded in all four main tables: sample assays, drill hole collars, down hole survey and geological logs (Fig. 12.1). In the case where some data are not available, as in the above-mentioned example, when a drill hole has not been sampled or logged, the hole can be represented in the corresponding tables by a single record indicating that this drill hole, from its collar to the bottom, does not have samples. It is also useful to add an additional column into the table containing the drill hole collars recording comments regarding any issues which occurred with the hole. Unexplained gaps in the data and a lack of documentation for the missing records can decrease confidence in the data, and cause concerns about the database management. This may even result in the need for additional formal data verification studies when the mining project is reviewed by external auditors.

12.2 Data Entry

Data can be entered to a centralised database manually from a key board or in electronic form. Currently it is a common practice to enter data electronically, and often electronic files are directly transferred to databases from the analytical laboratories and the digital data capturing devices, such as palm top computers used by the field geologists for the drill holes logging. Entering data by typing from the keyboard was the main approach before computers and user friendly software became routinely available in the industry, this happened in 1990s. Because of this the manual data entry from the key board became obsolete and rarely used in the modern mining industry.

12.2.1 Electronic Data Transfer

At present, electronic data transfer from digital devices is a preferred method of data entering to database. However, it is important to remember that this technique does not guarantee that data has been copied to database without errors. Good practice is when electronically transferred data are supplemented by printed hard copies of the laboratory assay sheets which can also be sent as the certified PDF files. Each time, when data has been transferred electronically the geological personnel should check the entered data and compare them with the PDF files received from laboratory or geological contractors. Check mechanisms should at least include comparisons of the elementary statistics, sums, means and variances, calculated by columns of the newly entered data and corresponding columns in the received files. Laboratories can change without notice the reporting units of the assayed metals, for example from 10^{-2} to 10^{-3}%. Entering such data without adjustment causes incompatible records in the database. Therefore, prior to data transfer their compatibility with that already stored in the database should be checked by a database administrator. The required auxiliary information can be derived from the headers of the analytical certificate therefore it is important to save the certificate headers in the database and link them to the corresponding samples as it has been shown on the diagram (Fig. 12.1). However, if this mistake has not been recognised at the time of the data entry it can be a time consuming and very costly exercise to find these incompatible data at the later stages.

All original files have to be saved as they have been received from the laboratory or contractors and carefully stored to assure auditability of the data. The latter is one of the key requirements for proper reporting of the mineral resources and ore reserves.

12.2.2 Keyboard Data Entry

Manual data entry is largely obsolete in the modern mining industry, being limited almost entirely to digitising old legacy data. When data are entered by typing them from a keyboard the likelihood of the typing errors is high (Fig. 12.2). Long (1998) has suggested that quality standard of the manual data entry is not more than one error per 10 000 key strokes. Less experienced data entry personnel can make significantly more

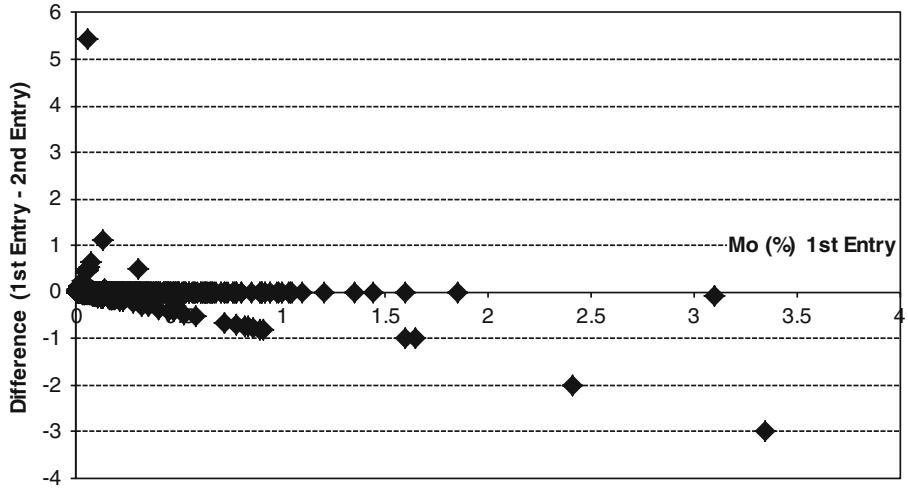

Fig. 12.2 Diagnostic diagram comparing the same data which were entered twice ('double entry' approach). Mo-porphyry project, Russia

errors. Special precautions need to be taken in order to assure that database is free of typing errors.

If data are entered manually, best practice is to enter data twice by two different individuals. The process is known as 'double entry procedure'. After data entry the independently entered sets of the data are compared, where the matching pairs of data are different this indicates data entry errors at one of the data sets. The comparisons is better to do by subtracting values of one set from another and plot the difference on a diagram vs. first entry (Fig. 12.2).

If data has been entered correctly the values in the both data sets will be identical and their difference will be equal to zero. Any other difference between two compared values, not equal zero, will indicate that there is a typing error in one of the data sets. These records need to be compared with the original assays and corrected. Rigorous application of this procedure allows to achieve a good quality database free of typing errors.

When reviewing databases compiled by manual data entry it is a good practice to compare approximately 5 % of the records in the database with their original values in the analytical sheets. This is in particular important if there are concerns that data have been entered without using a 'double entry' approach.

12.2.3 Special Values

Assay sheets can contain such values as TR, denoting traces of a given element, sign less than, <X, indicating that content of the analysed element is below detection limit X, signs of greater than a certain value, >X, are also encountered although they are less common than below detection limit values. Lost samples sometimes denoted as LS and not analysed samples as NA. All these values represent the special values which need to be properly managed in the databases. It is inconvenient to have the alpha-numeric records and text characters mixed up in the assay fields with numeric values therefore all special values are usually replaced by the numeric values. A common practice is to use special unambiguous codes which replace the special values in the corresponding assay fields (Long 1998).

Examples of the codes which were used at the gold project that was reviewed by author are shown in the Table 12.1. These codes allow preservation of all important information recorded in the original assay sheets and at the same time the values can be easily replaced by the more appropriate values for further data processing. The numeric codes, and the special values matching them, should be clearly documented, and all personnel instructed on their use.

Table 12.1 Numeric codes replacing the special values in the database of the gold project, Australia

Special value	Numeric code	Explanation
<0.1	−333.1	below detection limit of 0.1 g/t Au
<0.05	−333.05	below detection limit of 0.05 g/t Au
TR0.1	−555.1	trace values, at the detection limit of 0.1 g/t
0	−9990	Sample was intentionally not analysed because of a known Zero grade (barren rock)
NA	−9999	Not analysed sample, insufficient material or another technical reason
LS	−9991	Lost sample
>1000	−881000	Value above the upper limit of analysis of 1000 ppm

The author has audited a diamond mine where reserves were incorrectly overestimated because of their intentionally unsampled barren intervals have been erroneously interpreted as lost samples and high grade values have been extrapolated to the barren rocks.

A special attention should be paid to zero values. This is a most confusing value in the database which is difficult to manage. It is not clear if zero indicates that the assayed value was below detection limit or a given sample was not analysed. To use zero for denoting the values below detection limits is impractical as detection limits for a given element can change as a result of changing laboratory, upgrading laboratory procedures, updating equipment or changing laboratory. In general, zero values should be avoided in the database, meaning of all encountered zero values should be investigated and zeros replaced by an appropriate numeric codes (Table 12.1).

12.3 Management of the Data Flow

The author has seen many databases with good written procedures but nevertheless still containing incorrectly entered data. Analysis of the database management procedures at the numerous mines has allowed to conclude that main cause is inefficient management of the data flow. Unfortunately, many companies are leaving responsibility for database management to a database administrator. All data electronically transferred to central database and it is expected that administrator of the database undertakes a complete and rigorous check of the data quality assuring that they are error free. The problem with using this approach is that data are usually transferred to centralised database at a much larger volumes and speed than a database administrator can process even if they will be working around the clock. Consequence of this is almost always the same; the data are transferred directly to the database from the capturing devices and laboratories hoping that they will be checked and validated at a later stage. As a result of this a database will be 'infected' by errors requiring a special cleaning which can be time consuming and sometimes expensive exercises. The rule of thumb is that it takes four times as long to correct an error once it is in the database than it takes to prevent it getting into the database.

This problem, however, can be easily mitigated by adding one additional step to the data flow. The author suggests to shift responsibility for data checks and validation to senior project geologists responsible for drilling and sampling. The senior geologists at each site, prior to sending data to the centralised database have to collect all data from different sources, laboratories, field geologists, drilling contractors and assure that they are error free. They should also complete a preliminary QAQC analyses and only after this they authorise the transfer of the data to a database. Adding this very simple step can improve integrity of the database and save a lot of time which otherwise will be lost for cleaning the 'infected' databases.

Senior project geologists reviewing data before they are send to the database must also consider the sample sizes which should comply with the approved sampling protocols. This is

particularly important when sampling the drill core, as geologists are subjectively choosing the sampling intervals and can make them too small or excessively large.

Eventually, the data will have to be extracted from the database for estimation of the resources and reserves of the mineral deposit. In case of the mining projects the data are extracted for the special studies, such as conceptual study at the early stages of the project evaluation, pre-feasibility study when project maturing and finally for a bankable feasibility study. At the operating mines data are extracted from database every year for annual reports updating shareholders on the current status of reserves and resources.

To ensure that all information is used adequately an additional editing of data is needed. The author, based on a personal experience of extensive modelling of the geological resources, recommends that for every extracted element a new column should be created and denoted with a prefix 'FIN_' or 'USE_'. In this column all negative values used in the special codes (Table 12.1) should be replaced by a non-negative values. When several determinations exist for a certain element at the given sample the 'FIN_' column will contain a value which will be used for resource estimation. The way how values have been obtained at the 'FIN_' column should be clearly documented.

Finally, the file containing extracted data and new created fields should be saved on a separate back up disk, server or tape for auditing purpose. At this stage data are transferred to special mining software for estimation resources and reserves. Having data safely backed up ('frozen') on a separate device assures that all possible changes or errors introduced to data during resource estimation will not be incorrectly interpreted as the database issues.

12.4 Database Safety and Security

Database is a final storage for data collected by large teams of geologists, drillers, surveyors, mine workers, analytical personnel, data entry assistants, and many others and these data are basis for technical and economic evaluation of the deposits, design of the mine and making the important financial decisions. If data are accidentally lost they practically can not be restored therefore it is extremely important to store data safely and assure that the system is backed up.

A good practice is back up database every day at night shift and store back up copies separately in a fire proof place. In addition to this all entered data should be saved separately on the CDs which should be properly stored in a safe place and should be easily available for reviews and audits. The same is valid for extracted data, which also should be saved on the separate CDs as it was explained in the Sect 11.2.4. This is important to assure transparency of the data handling procedures and their auditability. Having daily data back-ups allows to minimise losses in case of technical accidents. If paper copies of the assay sheets have been received from the labs they also should be scanned and saved as PDF files and archived for audits.

References

Abzalov MZ (2008) Quality control of assay data: a review of procedures for measuring and monitoring precision and accuracy. Exp Min Geol J 17(3–4):131–144

Abzalov MZ (2014) Design principles of relational databases and management of dataflow for resource estimation. In: Mineral resource and ore reserves estimation, AusIMM monograph 23, 2nd edn, Chapter 2: The resource database. AusIMM, Melbourne, pp 47–52

Codd EF (1990) The relational model for database management, 2nd edn. Addison – Wesley Longman, Boston, p 567

Long S (1998) Practical quality control procedures in mineral inventory estimation. Exp Min Geol 7(1–2):117–127

Lewis RW (2001) Resource database: now and in the future. In: Edwards AC (ed) Mineral resource and ore reserve estimation – the AusIMM guide to good practice. AusIMM, Melbourne, pp 43–48

Sinclair AJ, Blackwell GH (2002) Applied mineral inventory estimation. Cambridge University Press, Cambridge, p 381

Part III

Mineral Resources

Data Preparation

13

Abstract

The data used for evaluation of the mining project can be of the different types and sizes and therefore can be unsuitable for estimation resources without special treatment, referred to as data preparation. The procedures of the data preparation carried prior to resource estimation are explained in this chapter.

Keywords

Composited samples • Optimal compositing • Top cut

Mine geologists routinely collecting and processing the significant amounts of the different types of samples, which need to be processed and validated before they can be used for the mining geology aplications.

13.1 Data Compositing

Samples collected for evaluation of a mineral deposit can significantly differ in size and therefore the data need to be regularised for estimating resources. The procedure is referred to as compositing of the drill hole data, because it implies grouping of the different samples into the composites which length is the same through the entire deposit (Fig. 13.1).

13.1.1 Data Coding

Samples are composited by the geological domains adjusting composites to the geological contacts. A common practise is to use one size of the composited samples in the deposit, however, in some cases the different sizes can be used at the different domains, for example for high-grade massive sulphide ore and low-grade disseminated sulphide mineralisation at the magmatic nickel-sulphide deposits. Thus, the compositing is made to the geological contacts and separately by the resource domains. In order to assure that these principles are rigorously followed samples are coded and the codes are used in the compositing algorithms for guiding the compositing procedures.

M. Abzalov, *Applied Mining Geology*, Modern Approaches in Solid Earth Sciences 12,
DOI 10.1007/978-3-319-39264-6_13

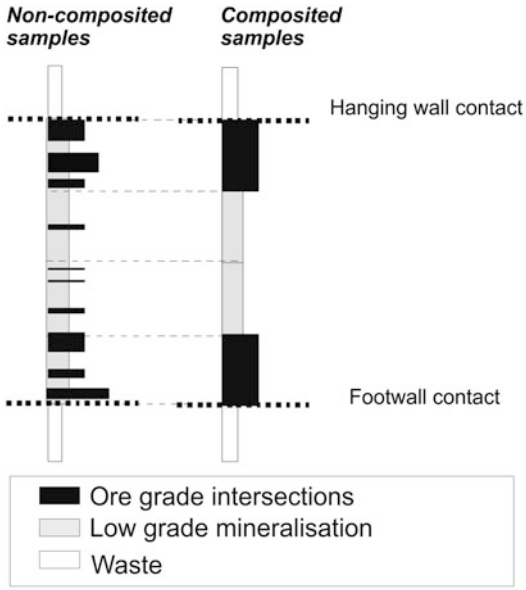

Fig. 13.1 Schematic diagram showing compositing of the drill hole samples

Data coding is the process of flagging the samples by the domain(s) in which they occur and it is done on raw samples, prior to compositing.

13.1.2 Compositing Algorithms

Approaches which are most commonly used for compositing the drill hole samples are known as 'fixed length compositing' and 'optimal length compositing' (Fig. 13.2). These methods are working as follows.

The fixed length compositing approach requires the composite length to be defined as a fixed value. The method is grouping samples and slicing them precisely at the defined composite length. The method also requires definition of the minimum composite length. This parameter is used to decide if the remaining part of a sample, or group of the samples, is retained or rejected. The remaining samples (or part of a sample), are composited and retained if their length larger than the minimum allowed length, and rejected if smaller. Thus it is possible for part or all of one or more samples to be excluded from the composite and this is a serious limitation of the fixed length compositing algorithm. The problem can be partially overcome if the residual samples, which length is smaller than minimum composite length is added to the last composite. Another issue of this method is highly skewed distribution of the composite lengths.

Example presented on the Fig. 13.2b shows the drill holes data composited to 5 m long composites using fixed length approach. Length of the original samples were 0.01–3.30 m (Fig. 13.2a). Compositing was made by setting a minimal composite length to 0.25 m, which was chosen in order to minimise the data losses. As a result of this approach the histogram of the composited samples lengths is characterised by presence of a long tail stretching from 5 to 0.25 m. Standard deviation of composite lengths is 0.79 (Fig. 13.2b) which is larger than variability of the original sample length which standard deviation is 0.60 (Fig. 13.2a) therefore the obtained composites are suboptimal for estimation resources using geostatistical methods.

The same data have been composited using optimal compositing algorithm (Fig. 13.2c). Optimal length compositing approach forces all samples to be included in one of the composites by adjusting the composite length, while keeping it as close as possible to defined composite length. Thus it overcomes the issues of rejected samples and does not leave long tails of the small composites. The histogram of the composites lengths is compact; the lengths vary from 3 to 7 m symmetrically around the mean length equal to 4.99 m. Standard deviation is 0.29 (Fig. 13.2c) which is a significant improvement in comparison with the 0.79 value of standard deviation of the composites created using fixed length compositing approach (Fig. 13.2b).

13.1.3 Choice of the Optimal Compositing Intervals

Choice of the optimal compositing length requires study of the sample length and distribution of the metal grades by length intervals. First of all it is necessary to study variation of the sample lengths which are presented as the histograms

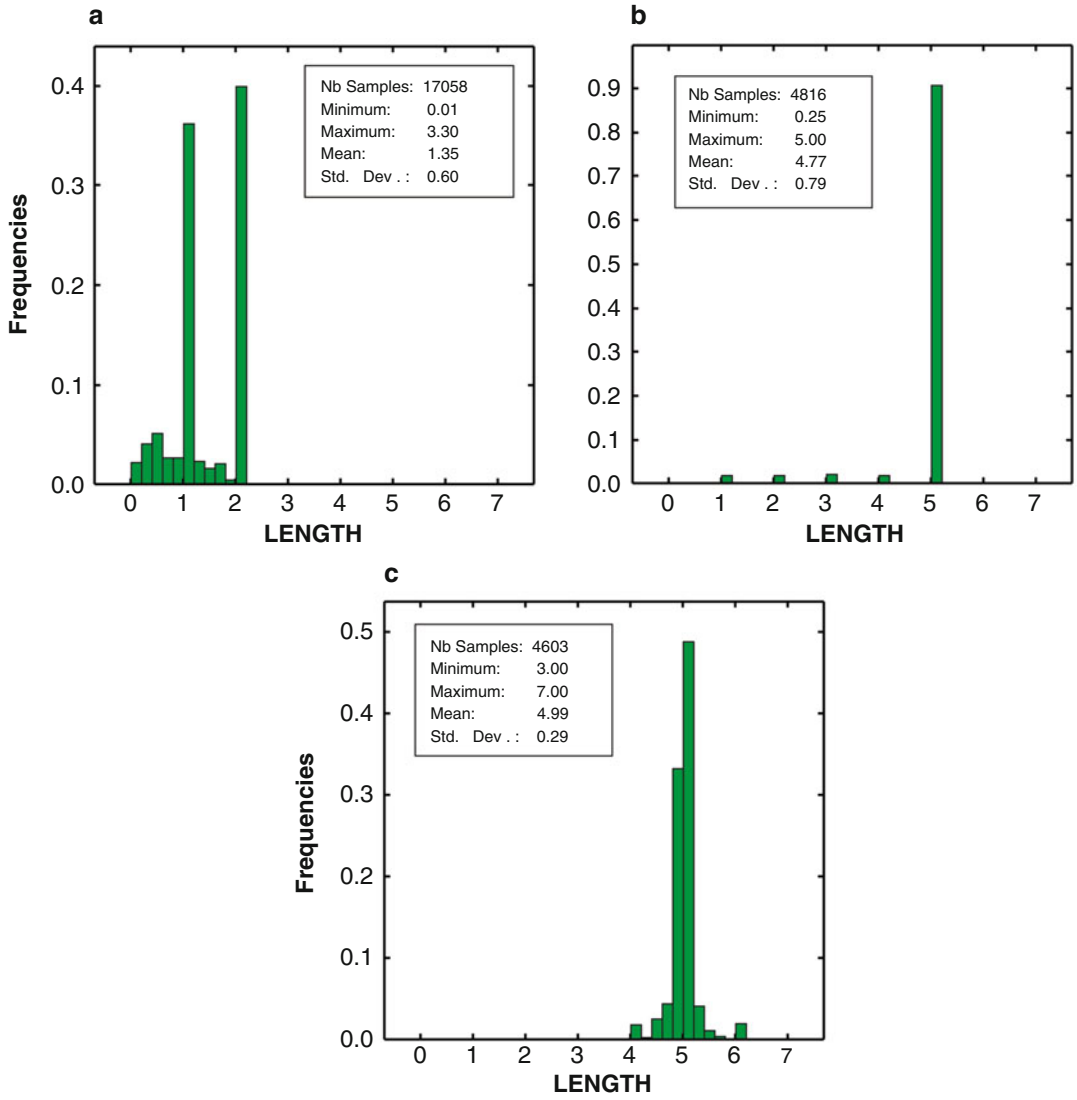

Fig. 13.2 Histogram of the drill hole sample lengths, Cu porphyry deposit, Australia: (**a**) original (non-composited) data; (**b**) composites generated using 'fixed length' technique. Composite length – 5 m, minimum composite – 0.25 m; (**c**) composites generated using 'optimal length' approach. Composite length is 5 m

(Fig. 13.2a). It is also useful for finding the optimal compositing sizes to study distribution of contained metal (grade x length) by the same ranges of the sample lengths which are used for construction of the sample length histogram.

The relationships between sample grades and their size should be studied for each sample type separately. The most common approach is by construction of the scattergrams by plotting sample grades against the sample length (Fig. 13.3).

The key points which should be considered when choosing the sample compositing size are as follows:

- The composite size should be larger than the average sample length. Decomposition of large samples into smaller composites is bad practice, because it creates unrealistically smooth spatial distribution of the metal

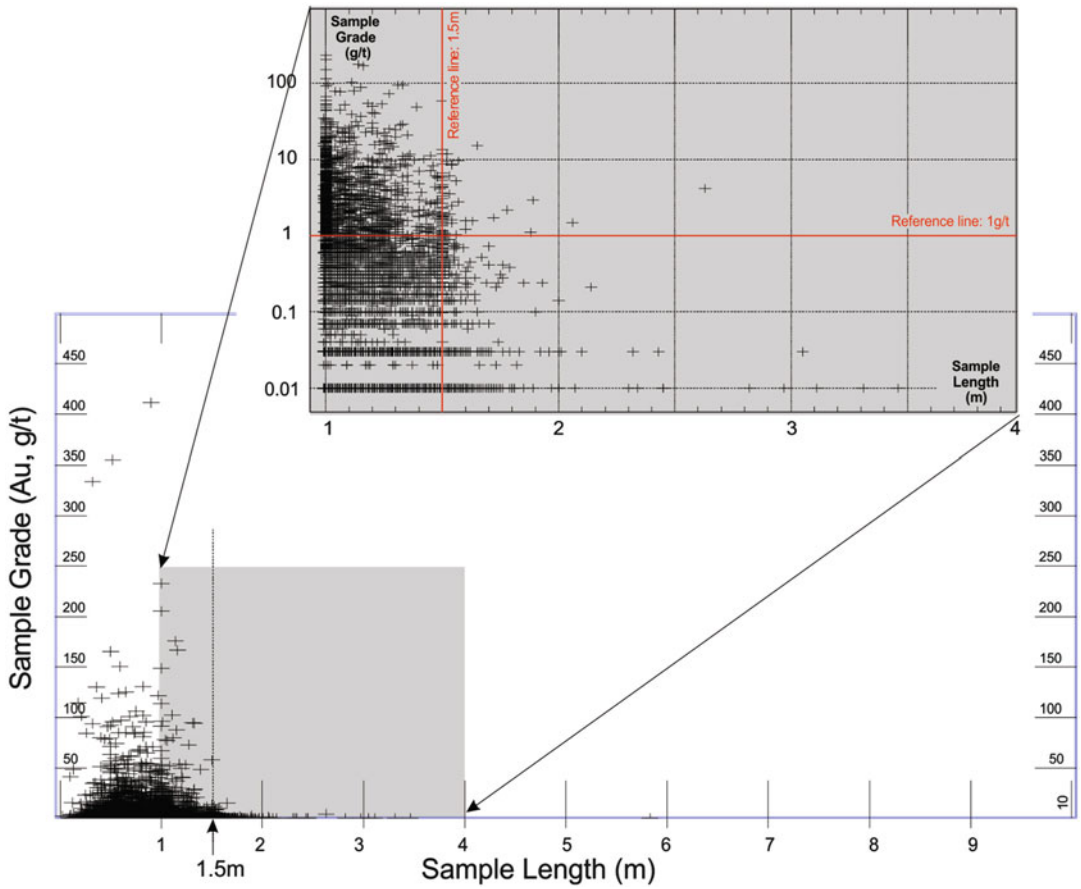

Fig. 13.3 Gold grade vs. sample lengths. Drill holes data, Meliadine gold project, Canada

grades which will be reflected in the variograms;
- The composite size should be approximately half of the block dimension used for Kriging model (Pan 1995);
- Compositing should not change the mean grade of the samples. Any major changes (>5 %) should be investigated;
- Compositing should not change the total sum of the contained metals (grade x length). Any major changes (>5 %) should be investigated.

13.1.4 Validating of the Composited Assays

To assure that compositing of the samples did not introduce the bias the composited data should be compared with non-composited (original) data. A good practical approach of validating the compositing procedures consists of calculating the contained metals by the drill hole intersections through mineralised domain and comparing results obtained from composited data with the original (non-composited) samples.

Three main parameters should be compared:

- length of the mineralised intersection (Fig. 13.4a);
- total contained metal (Fig. 13.4b);
- average grade (Fig. 13.4c).

When compositing is accurate all three parameters estimated from the composited data will be identical to estimates made using the original (non-composited) samples. The data points on the

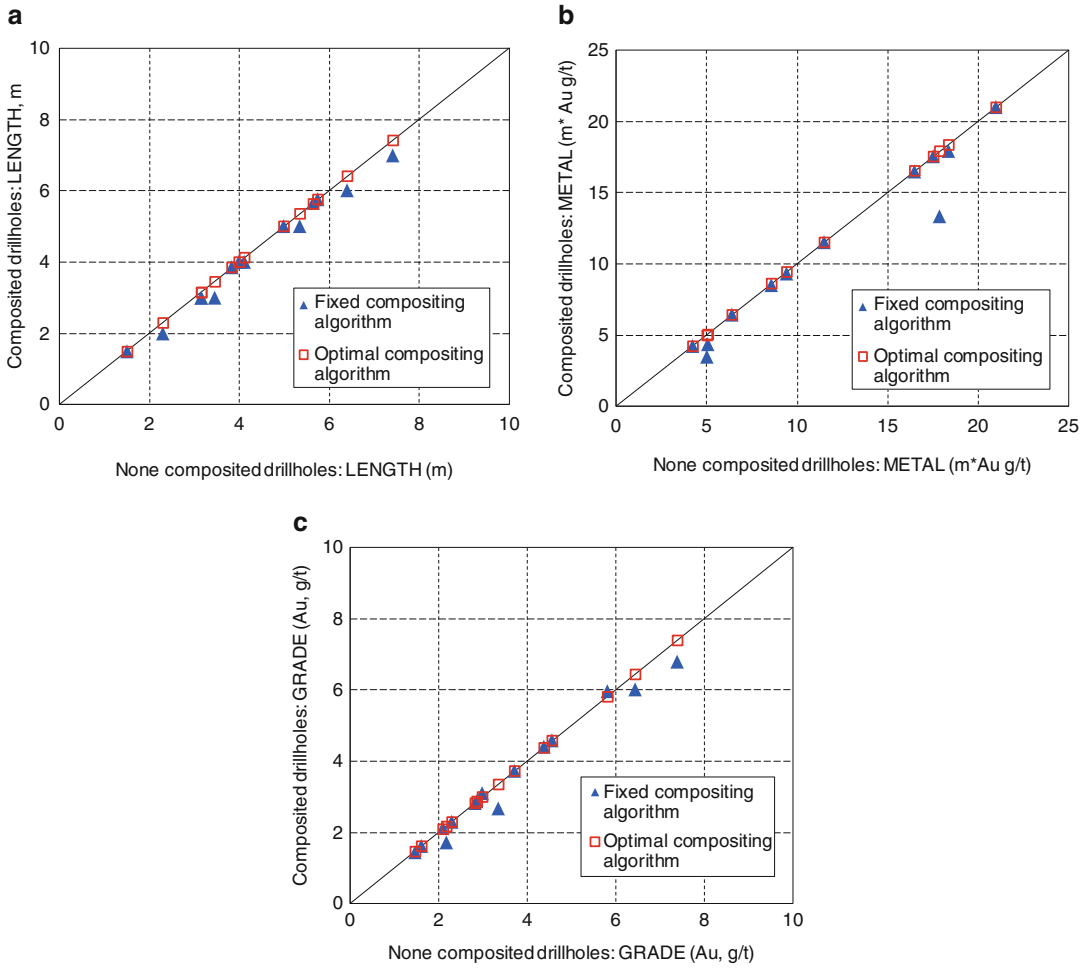

Fig. 13.4 Validating of the samples compositing by comparing mineralised intersections estimated using composited and none composited data: (**a**) length of mineralised intersection; (**b**) contained metal; (**c**) average grade

scatter diagrams are distributed along the 1:1 bisect (Fig. 13.4). Such relationships were obtained when optimal compositing algorithm was used (Fig. 13.4).

Deviation from the 1:1 on the diagram presenting the total length of mineralised intersections are caused by rejecting of the parts of samples which were smaller than the minimum composite size (Fig. 13.4a). Changes in the total intersection length can also cause metal losses (Fig. 13.4b) and eventually lead to incorrect estimation of the average grade of intersection (Fig. 13.4c). These are the common errors when fixed length composting is used.

13.2 High Grade Cut-Off

Highly skewed statistical distribution of the metals represents serious challenge for their resource estimation because of a risk of smearing of the high grade values which can cause overestimation of the resource grade. These characteristics are common for gold, diamond, platinum and uranium deposits. Their resources are estimated using special techniques, in particular geostatistical methods based on the grade indicators (Journel and Isaaks 1984) allowing to accurately model spatial distribution of the high grade values. When resources of these deposits are

estimated using conventional linear algorithms the anomalous assays have to be truncated in order to prevent excessive smearing of the high grade values. This is commonly called high grade cut-off, top cut or high grade capping. The thresholds for cutting the high grades are estimated statistically for each mineralised domain.

The most common approach for cutting the high grades at the gold deposits is to truncate them to the 95 percentile of the cumulative frequency diagram (Vallee et al. 1992). Alternatively, the high grades are cut to one of the following values:

- sum of the data mean and twice of the standard deviation
- four times of the mean value
- the point where the ragged tail starts on a grade histogram

Before applying the top cut it is necessary to ensure that all samples have the same volume support, therefore top cut is applied to the composited data. Optimisation of the high grade cut-off procedures is made empirically by comparing the estimates made using the different high grade cut-offs. At the operating mines the high grade cut-off parameters can be optimised by reconciling the estimated models against the grade control and production data. When these data not available the model is validated by comparing the estimated grades with the input drill hole data.

References

Journel AG, Isaaks EH (1984) Conditional indicator simulation: application to a Saskatchewan uranium deposit. Math Geol 16(7):685–718

Pan G (1995) Practical issues of geostatistical reserve estimation in the mining industry. CIM Bull 88: 31–37

Vallee M, David M, Dagbert M, Desrochers C (1992) Guide to the evaluation of gold deposits: geological society of CIM, Special vol 45, p 299

Geological Constraints of Mineralisation

14

Abstract

This chapter discusses the basic principles of the wireframing of the mineralised bodies and explains methods of the geological analysis. A particular emphasis is made on characterisation of the geological contacts, structural analysis of mineralisation and definition of the cut-off values for construction of the wireframes.

Keywords

Wireframe • Contact profile • Unfolding

Evaluation of the mining project is made by construction of the 3D computer model of the mineral deposit, accurately presenting the shape of the mineralised bodies, their spatial location and all geological, geotechnical and metallurgical characteristics which can impact the extraction of the valuable metals or minerals. The process starts from geological interpretation of a mineral deposit, understanding and collection all information required for 3D constraining of the mineralised bodies and it's culminated by construction their 3D geological model, colloquially referred as wireframe models.

Thus, wireframes are the end result of a process that has some specific criteria and objectives:

- Identify the key attributes for 3D modelling (these could be grades, rock type, mineralogy);
- Define what the domains are designed to represent and/or be used for resource estimation;
- Investigate the "internal structure" of the variable to be modelled (mosaic, diffusive);
- Define domaining criteria – this may be a simple grade threshold or defined by a combination of chemical and geological data;
- Contacts may be sharp or gradational;
- Code the data according to domains;
- Create 'domains' considering the all resource attributes;
- Test the domains, to assure that they meet the objectives and are geologically robust.

14.1 Introduction to Wireframing

The 3D geological models of the mineral deposits are routinely constructed by exploration and mining geologists using specialised computer programmes which constrain the volumes as the wireframes (Fig. 14.1a). The wireframes' triangles (Fig. 14.1b) are commonly rendered

M. Abzalov, *Applied Mining Geology*, Modern Approaches in Solid Earth Sciences 12,
DOI 10.1007/978-3-319-39264-6_14

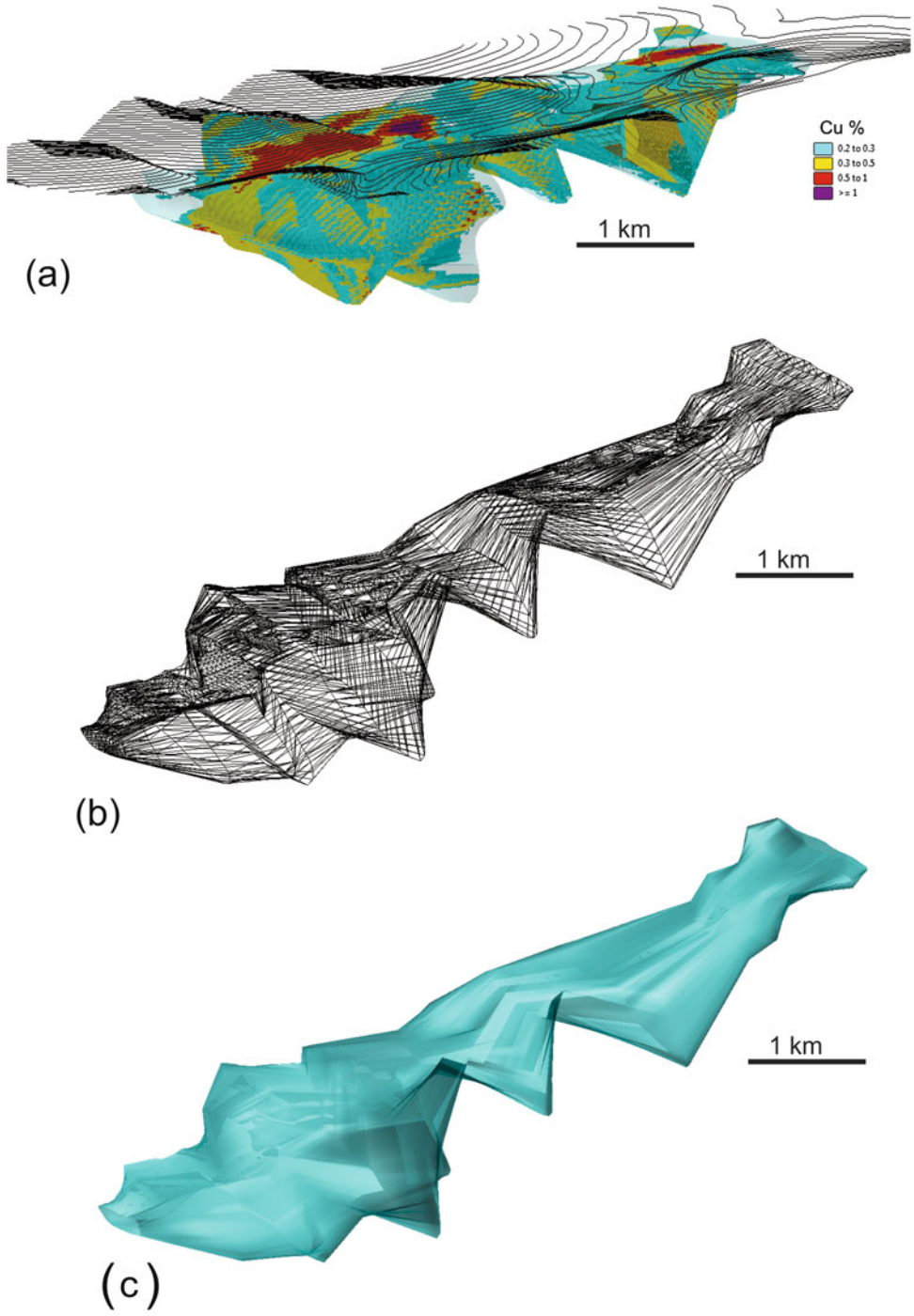

Fig. 14.1 Peschanka Cu-porphyry deposit, Russia: (**a**) 3D model of the deposit. Mineralisation is constrained at 0.4 % Cu; (**b**) wireframe model is presented as 3D lines; (**c**) wireframe model presented as the solid shell

and the model is visualised as the solid shells (Fig. 14.1c).

Wireframing procedures differ at the different computer packages however the main construction principles are the same: mineralisation is interpreted on the cross sections and the plans and contoured at a chosen cut-off, which is a contact of the mineralised rocks with the waste. Contacts are usually initially delineated on the 2D plans and then connected by the tie lines (also called tag strings) to create a 3D model (Fig. 14.1).

Construction of the wireframes, in particular joining the 2D interpretations by the tie lines, require using all available geological data and often facilitated by using of the geophysical data. Procedure of constraining mineralisation in 3D is as follows:

- Characterisation of the mineralisation contacts;
- Determining of a cut-off value for delineating the mineralised volumes;
- Geological interpretation of the deposit structure and delineation of mineralisation between data points;
- Review of the 3D deposit model assuring that it is compliant with the mineralisation style.

14.2 Characterisation of the Mineralisation Contacts

Contacts of mineralised bodies can be sharp and straight, or, alternatively, can be highly irregular, can be gradational and not related to the contacts of the host rocks. All these characteristics need to be studied and quantitatively estimated.

14.2.1 Contact Profile

Sharp or gradational type of contacts is deduced from the grade distribution profiles across the contact (Fig. 14.2). Sharp contacts are characterised by a rapid change of the mineralisation grade, which increases from barren to ore grade at the distance of several centimetres. Contacts of this type are usually geological by its nature

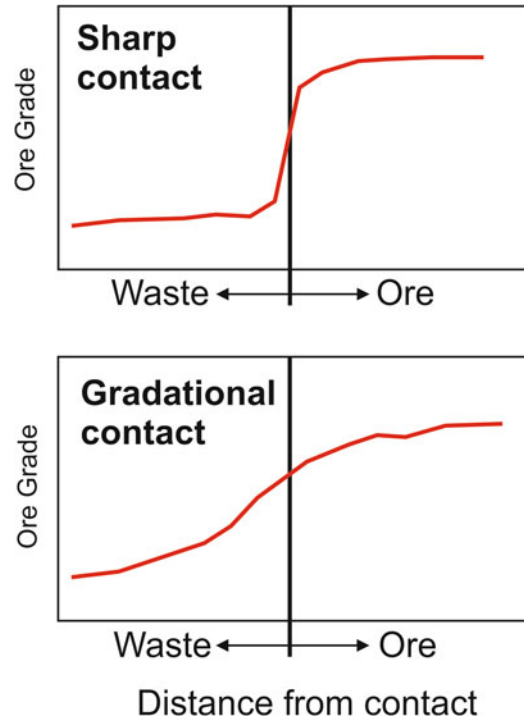

Fig. 14.2 Sketch explaining sharp and gradational contacts

and represents the contacts of the different rocks. The good examples are massive sulphide deposits where grade changes from barren at the host rocks to high grade in the massive sulphides immediately after crossing the contact. Gold veins also often have the sharp contacts, in particular, when gold-bearing vein not accompanied by halo of stringers and altered rocks (Fig. 14.3a).

Different type of the mineralisation contacts present at the deposits containing quartz stockworks (Fig. 14.3b) and disseminated mineralisation (Fig. 14.4). In these deposits mineralisation grade changes gradually forming gradational contact. These type contacts do not have the geological expressions and determined entirely from the grade profile which should be constructed through the contact zone and extended for several metres into the barren wall rocks.

Both type contacts can present at the same ore body. Disseminated sedimentary mineralisation often has gradational hanging wall contact and sharp footwall contact (Fig. 14.4). Similar distribution profiles occur at the magmatic deposits of

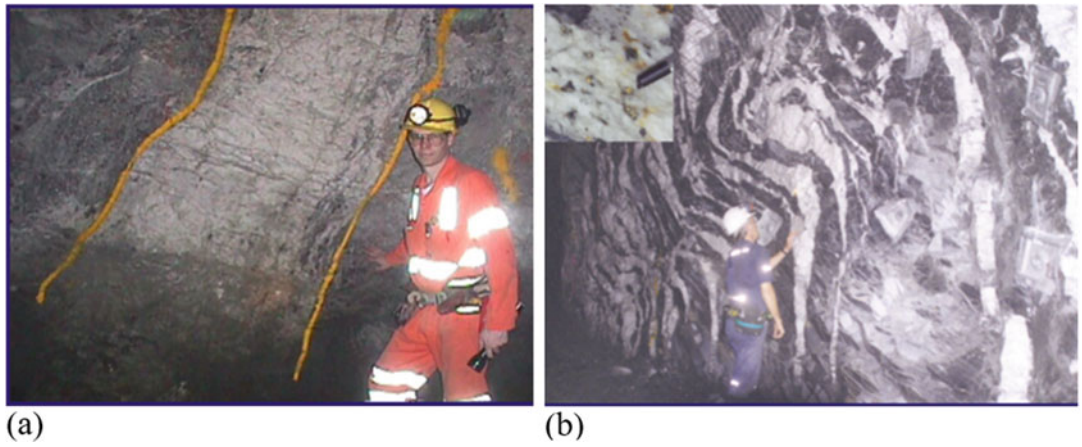

Fig. 14.3 Mineralisation contacts: (**a**) sharp contact of the gold vein, Bullen mine, Australia; (**b**) gradational contact of the gold stockwork at the Bendigo mine, Australia

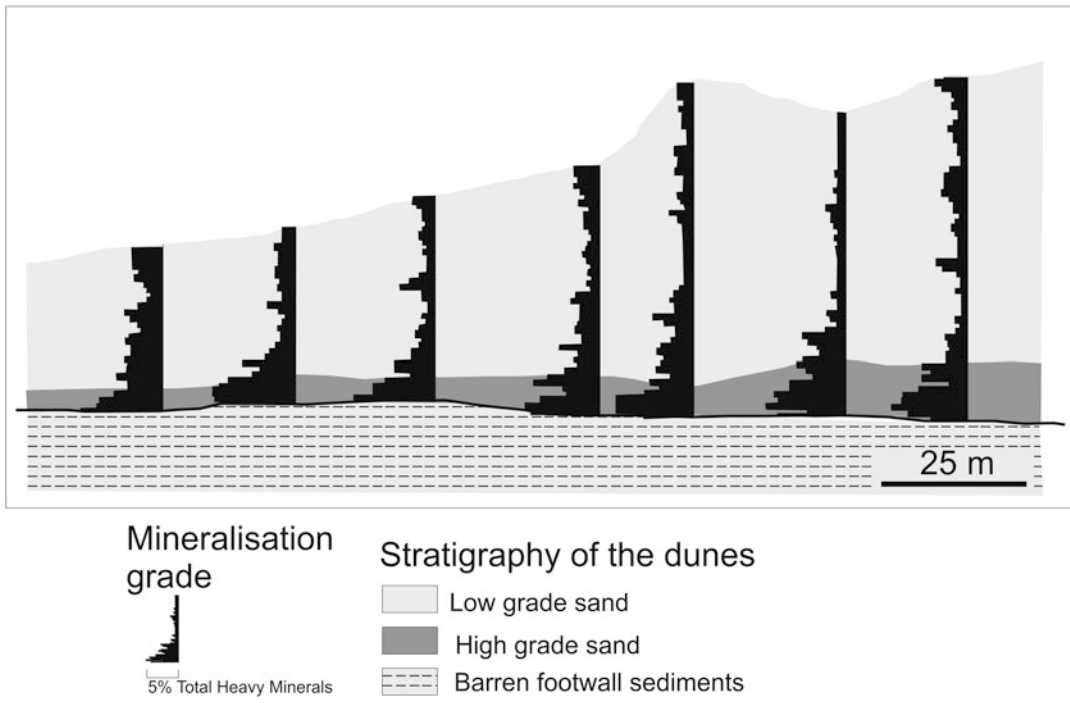

Fig. 14.4 Gradational hanging wall contact and sharp footwall contact, Richards Bay mineral sands deposit, Republic of South Africa

the disseminated nickel sulphide mineralisation. At these deposits upper contact of mineralisation is usually gradational and lower contact is sharp (Abzalov and Both 1997). Uranium rolls are also characterised by presence of the different types of contacts (Fig. 14.5). Front side of a roll has a diffused nature and contact on this side is gradational. The rear part of a roll is sharp and characterised by a rapid drop of uranium grade from several hundred ppm to below the detection limit.

The grade distribution profile can differ in the different parts of the deposit, at the different domains and even between the drill holes. There-

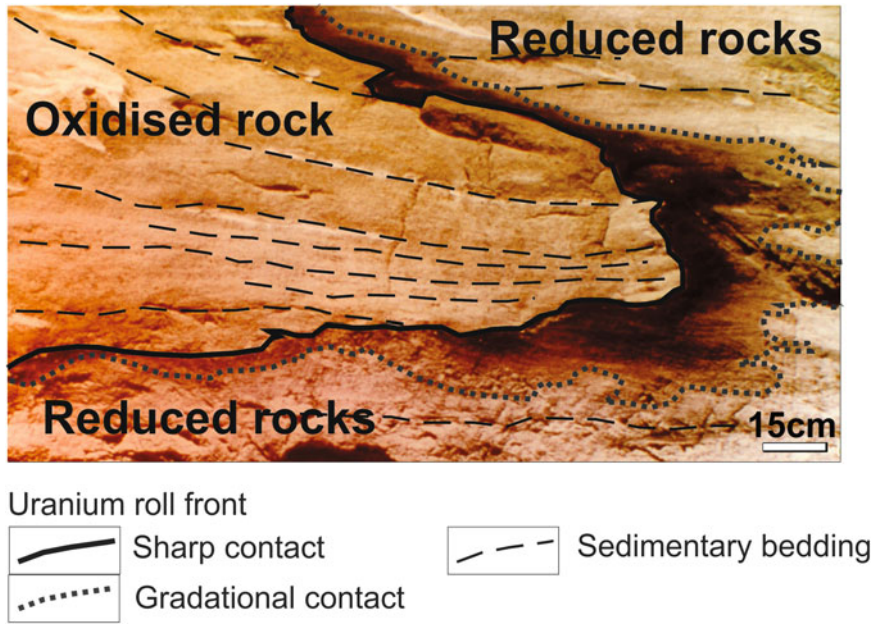

Fig. 14.5 Uranium roll from the Shirley basin, Wyoming, USA. *Dark colour* denotes high grade uranium mineralisation (Photo courtesy of O. Paulson)

fore, the practical approach for characterisation of the contact is as to calculate average profile by domains or ore bodies. Procedure of calculation is as follows:

- Geologist analyses grade distribution and identifies the contact in every drill hole applying the earlier chosen cut-off value;
- Samples are composited to the mineralisation contacts. Compositing should be made using optimal compositing algorithm;
- Composites are grouped by their location relative to the contact. Because length of the composited samples differs the composites are grouped by the sequential number of the composite relative to the contact (Fig. 14.6);
- Average grade is estimated for every group using the length weighted algorithm. Profiles are constructed for main commodities and the deleterious components;
- Contact profile is constructed by plotting of the estimated average grades against their distance from the contact. The distance is presented as a sequential number of the composites (Fig. 14.7a);
- It is a good practice to show on the diagram denoting the contact profile the number of samples used for estimation average grades. This is usually shown as a separate line on the contact profile diagram which is referred to a secondary Y axis (Fig. 14.7a);
- Statistics, such as variance and coefficient of variation, are estimated for every group and can be added to the diagram;
- In order to analyse consistency of the grade profile between the drill holes and estimate representativeness of the average profile it is useful to generate a second diagram where the average estimated profile is plotted together with the profiles deduced for each drill hole (Fig. 14.7b). Presenting individual profiles estimated by the drill holes allow to analyse representativeness of the average profile and to find the outliers (Fig. 14.7b).

Based on the contact type a geologist estimating the mineral resources is deciding to include samples outside of the contact for estimation of the grade or conduct estimation using exclusively the samples within the constrained domains. Approach, when estimation is conducted using exclusively the samples within the constrained domains is colloquially referred to as

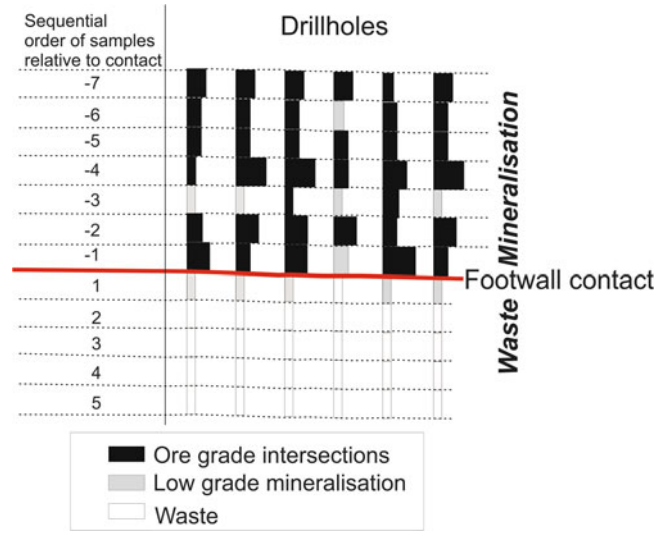

Fig. 14.6 Sketch explaining principles of the composites grouping by their sequential number relative to the contact

hard boundary approach. This method is usually applied to mineralisation characterised by sharp contacts, in particular, when high grade mineralisation located immediately at the contact with the barren host rocks. Alternative method, when estimation is made by a broader set of data, which includes samples outside of the domain contacts, is called soft boundary approach. This method is used when mineralisation exhibits the gradational contacts.

Exercise 14.2.1 Construction of a grade distribution profile through the contact using the Datamine programme. Data and Datamine macro code are contained in the file (Exercise 14.2.1.a.ZIP) available in the Appendix 1.

14.2.2 Determining of the Cut-Off Value for Constraining Mineralisation

Choice of the cut-off value for constraining mineralisation depends on the contacts type. Mineralisation with the sharp and geologically expressed contacts is constrained to their geological contacts (Fig. 14.3a).

Mineralisation with the gradational contacts is constrained at the assay values representing economically viable cut-off. At the early stage of exploration, the economic characteristics of the project are not accurately estimated therefore economic cut-off can not be confidently chosen. In this case it is helpful to analyse the cut-off values applied for constraining mineral resources at the similar deposits which are comparable by their logistics and geological parameters.

This is followed up by analysis of a spatial distribution of the grade and estimating the impact of changing cut-off on to the shape of the mineralised domains (Fig. 14.8). Using higher cut-offs creates small and discontinuous domains which are suboptimal for resource estimation. Therefore, mineralisation should be constrained at lower cut-off which creates a broader mineralised envelop encompassing all potentially economic domains.

Example presented on the Fig. 14.8 shows a gold mineralisation constrained at 0.3 g/t Au. This has allowed to apply geostatistical techniques for modelling spatial distribution of the gold grade and accurately estimate resources (Abzalov and Humphreys 2002a, b). Scoping study of the project has shown that economic cut-off at this deposit is 1.5 g/t Au assuming that mineralisation will be mined by open pit. This value was applied to the block grades and used for reporting resources (Fig. 14.8).

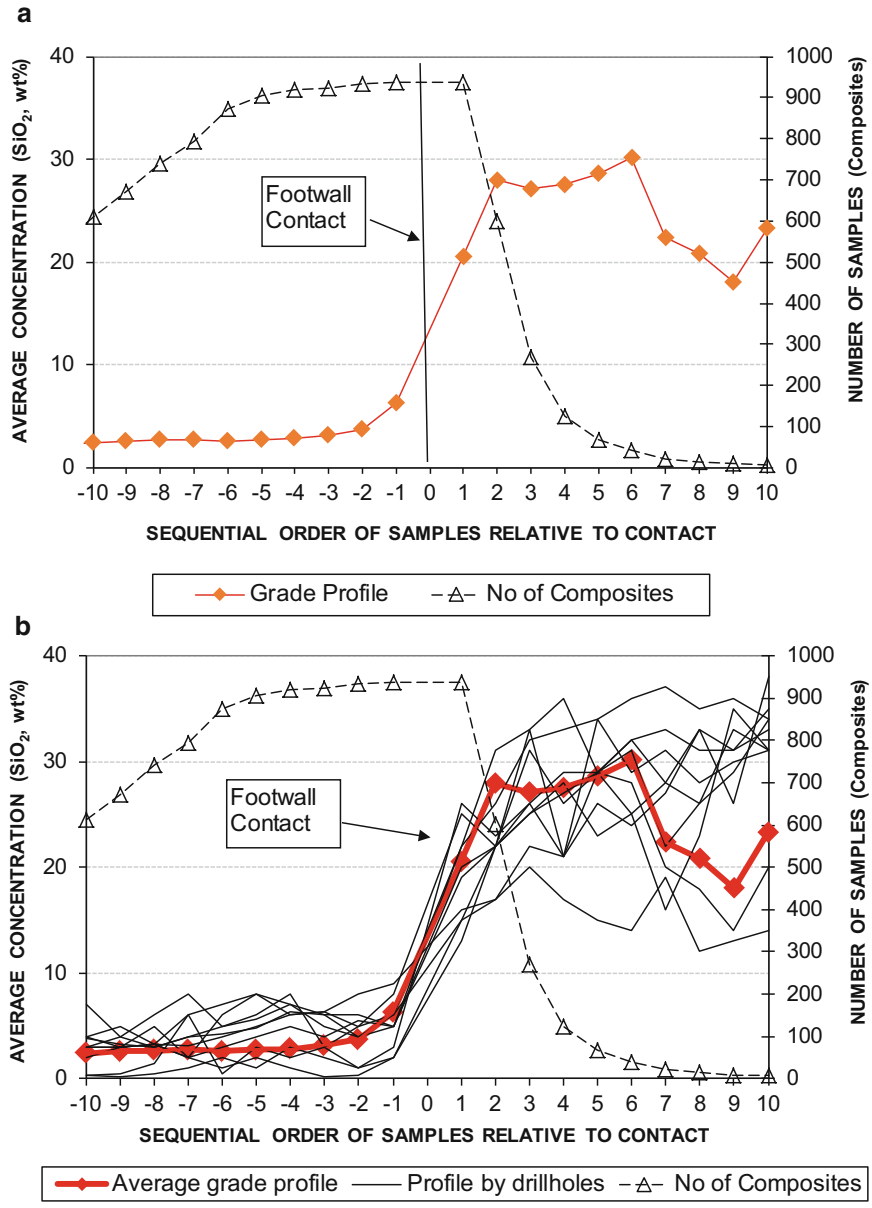

Fig. 14.7 Profile of the SiO_2% through the footwall contact at the mineral sand deposit, Madagascar: (**a**) average grade distribution profile; (**b**) grade profiles estimated and plotted by the drill holes

14.2.3 Contact Topography

Contacts can be either straight or irregular (Fig. 14.9a, b). Degree of the contact irregularity is independent of the contact type, sharp or gradational. Murrin Murrin lateritic nickel deposit is an example of the deposits with sharp contacts of mineralisation (Fig. 14.9b). Alternative example is polymetallic Olympic Dam deposit where mineralisation has gradational contacts (Fig. 14.10). In both cases the contacts shape is highly irregular.

The contacts are usually presented as topographic maps of the contact surfaces (Fig. 14.10).

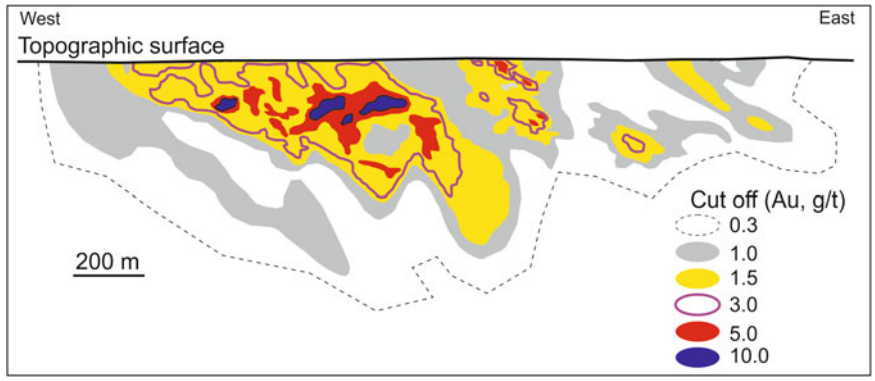

Fig. 14.8 Longsection of the lode 1000, Meliadine deposit, Canada (Abzalov and Humphreys 2002a)

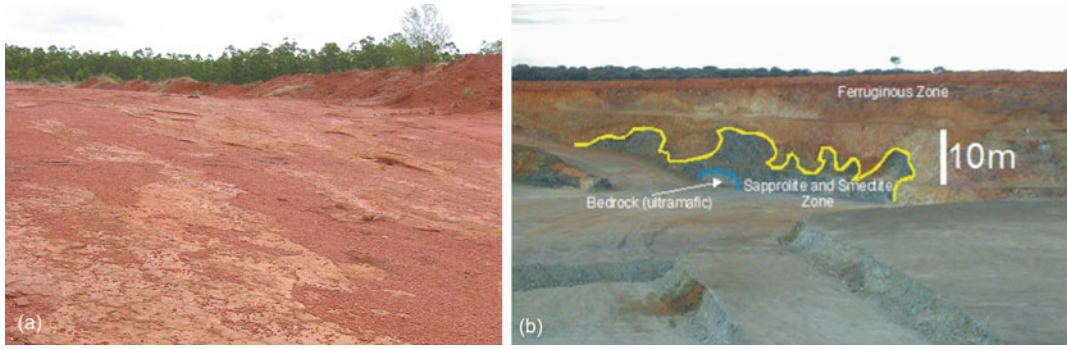

Fig. 14.9 Contact topography: (**a**) straight footwall contact of the Weipa bauxite deposit exposed after ore has been mined out, Australia; (**b**) highly irregular contact of lateritic Ni mineralisation exposed on the open pit wall, Murrin Murrin mine. Australia

The surface maps are generated separately for footwall and hanging wall of mineralisation and for each domain.

14.2.4 Uncertainty of the Contacts

Quantitative modelling of the contacts topography is important for estimation of the mining dilution and losses and therefore this is one of the key parameters for economic evaluation of the mining project. Uncertainty of the contacts depends on accuracy and spatial distribution of data which are used for constraining mineralisation. A common practice is to plot the points where exploration drill holes piercing the ore body contacts and estimate their distribution grid (Fig. 14.11). This allows to visually assess the reliability of the geological interpretation and identify the unreliable parts of the deposit requiring more drilling.

When project matures and advances to a final stages of evaluation a spatial continuity of the ore body contacts and degree of their irregularity are estimated geostatistically using conditional simulation technique (Goovaerts 1997; Abzalov and Bower 2009). The technique is based on generating several contact modes, which are mathematically equiprobable and therefore can be used for estimating uncertainty of the contacts (Fig. 14.12). The degree of the contacts uncertainty is used for estimating risks of excessive mining dilution or unforeseen mining losses (Abzalov and Bower 2009).

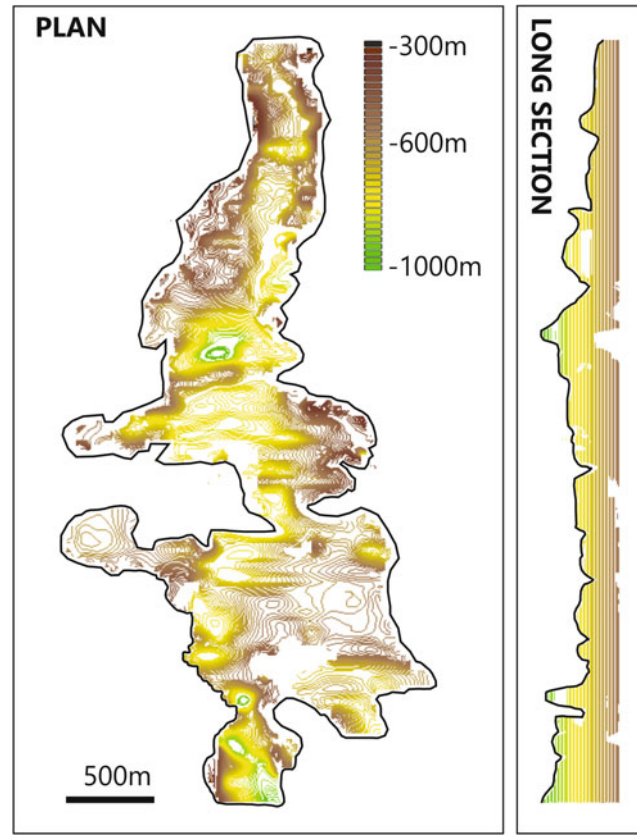

Fig. 14.10 Map showing footwall topography of the Olympic Dam deposit, Australia, constrained at 30$/t cut-off

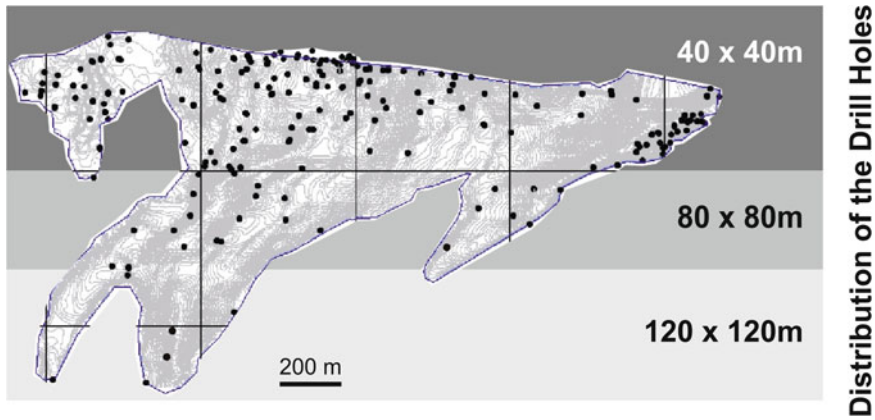

Fig. 14.11 Drill holes intersecting the contact of the kimberlite pipe (piercing points), Argyle diamond deposit, Australia

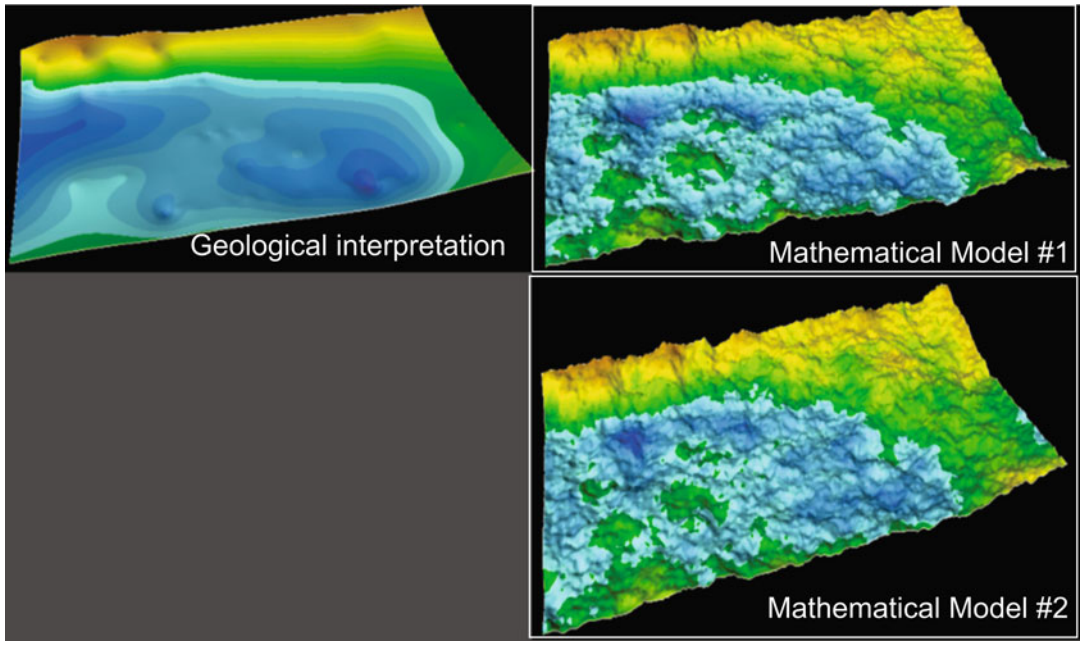

Fig. 14.12 Footwall contact of the tabular-type sandstone hosted uranium deposit, Kazakhstan. Geological interpretation and mathematically generated equiprobable models

14.3 Geometry and Internal Structure of the Mineralised Domains

Ore bodies are rarely homogeneous. Their internal structure commonly exhibits different degrees and types of zoning (Fig. 14.13a) and layering (Fig. 14.13b). Mosaic distribution of the high grade blocks is another common structural type usually observed when ore body is cut by post-mineral tectonic faults and also present at superficial uranium deposits (Fig. 14.13c). Many deposits have braided structures (Fig. 14.13d). This type is particularly common for alluvial deposits and for basal channel type sandstone hosted uranium deposits. The mineralisation at these deposits is distributed between several basal channels which are meandering forming a very complex braided structural pattern of the deposits (Fig. 14.13d). All these types can present in one deposit and even in one ore body which can be further complicated by folds and tectonic faults.

Accurate interpretation of the deposits structure and their correct representation in their resource models is extremely important. Mistakes in structural interpretations will lead to incorrect technical and economic evaluation of the projects, will propagate to mine plans and cause significant financial losses.

The risk is mitigated by using high quality data ensuring that their spatial distribution is appropriate for a given style of mineralisation (Fig. 14.11). Risks can be quantitatively estimated and in some cases mitigated by using the special mathematical algorithms which were developed for construction of the 3D models of the deposits, including geometry and internal structure of the domains (Abzalov and Humphreys 2002a, b; Strebelle 2002; Armstrong et al. 2011).

14.3.1 Unfolding

There are methods allowing to simplify a complex geometry of mineralisation. In particular unfolding of the folded tabular deposits by flattening the upper contact of the mineralised body (Fig. 14.14). The top flattening method of unfolding is relatively simple, its application does

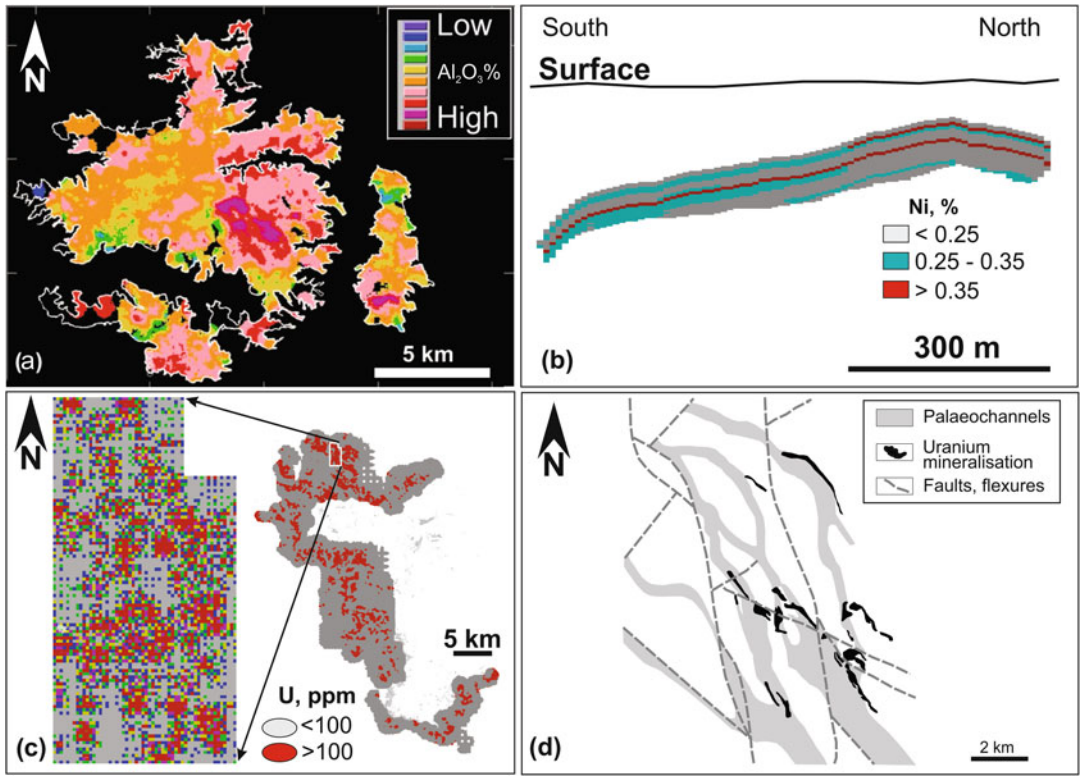

Fig. 14.13 Zoned structure of mineralised domains: (**a**) gradational zoning of the bauxite grade at the Gove deposit, Australia. Reprinted from (Abzalov and Bower 2014) with permission of Taylor-Francis Group; (**b**) layered distribution of the nickel-sulphide mineralisation, Babel deposit, Australia; (**c**) mosaic structure of uranium mineralisation at the CJUP deposit, Jordan; (**d**) braided structure of the basal channel hosted uranium mineralisation, Tortkuduk deposit, Kazakhstan (Reprinted from (Abzalov et al. 2014) with permission of Taylor-Francis Group)

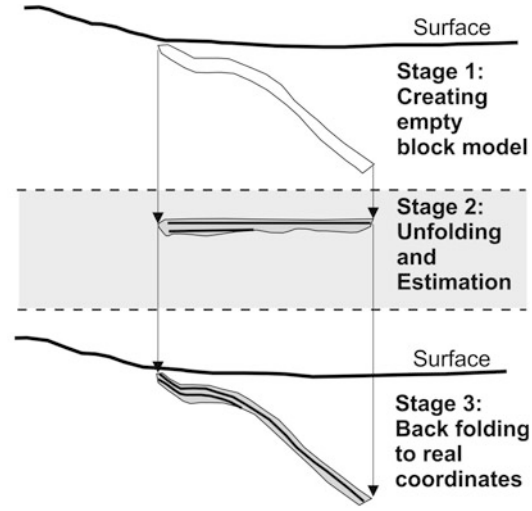

Fig. 14.14 Sketch explaining principles of unfolding a tabular ore body

not require a special mathematical trainings and therefore can be routinely used by the mine geologists. Principles of the approach are as follows:

- The mineralisation volume is constrained at the given cut-off and filled by the rectangular blocks. This is referred as empty block model. Stage 1 on the Fig. 14.14;
- Empty block model is unfolded. This is made by flattening the block model so that upper contact of the tabular body obtains a horizontal position. Stage 2 on the Fig. 14.14. The same unfolding parameters are used for unfolding the drill holes data which are used for geostatistical estimation performed in the unfolded environment;
- After block grades were estimated they are transferred back to their original space (back folded). This is referred as Stage 3 on the Fig. 14.14. In order to back transform the block model data their actual coordinates are kept as the block attributes when empty model has been transferred to unfolded space. Therefore, back folding is a simple procedure of changing the field name used for definition Z coordinates back to the original Z field.

The algorithm can be modified to bottom flattening or conversely the mineralised body can be flattened to its central (bisect) line.

A variation of this method includes unfolding of the tabular bodies using the equal thickness unfolding approach. This technique is used at the bauxite deposits in Australia (Abzalov and Bower 2014). Similar method, referred as proportional unfolding algorithm, is used with Plurigaussian simulation model (Bleines et al. 2013).

This approach (Fig. 14.14) cannot be used for unfolding of the tightly folded or meandering mineralisation. Unfolding of such mineralisation not always possible and usually is time consuming and requires special computer programmes. Such structures are commonly unfolded by unrolling (straightening) of the central line (bi-

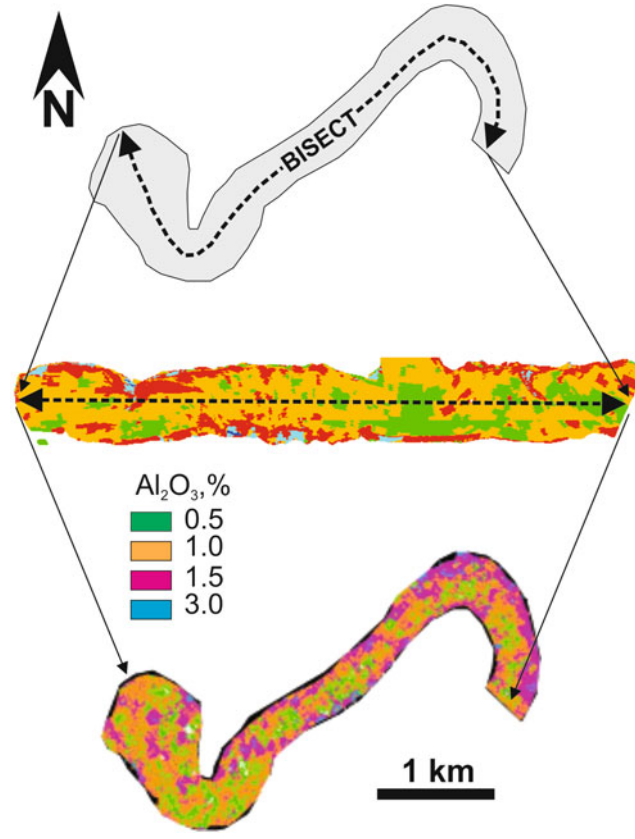

Fig. 14.15 Sketch explaining principles of the geological unfolding. Yandi iron ore mine, Australia

sect) of the mineralised seam maintaining its linear length and width of the mineralised domain which is estimated at right angle to the bisect (Fig. 14.15).

Exercise 14.3.1: Unfolding of the Folded Tabular Deposit Apply top flattening algorithm for unfolding the folded tabular deposit using the Fortran programme (Exercise 14.3.1.ZIP) which is available in the Appendix 1.

References

Abzalov MZ, Both RA (1997) The Pechenga Ni-Cu deposits, Russia: data on PGE and Au distribution and sulphur isotope compositions. Mineral Petrol 61(1–4):119–143

Abzalov MZ, Bower J (2009) Optimisation of the drill grid at the Weipa bauxite deposit using conditional simulation. In: Seventh international mining geology conference. AusIMM, Melbourne, pp 247–251

Abzalov MZ, Bower J (2014) Geology of bauxite deposits and their resource estimation practices. Appl Earth Sci 123(2):118–134

Abzalov MZ, Humphreys M (2002a) Resource estimation of structurally complex and discontinuous mineralisation using non-linear geostatistics: case study of a mesothermal gold deposit in northern Canada. Exp Min Geol J 11(1-4):19–29

Abzalov MZ, Humphreys M (2002b) Geostatistically assisted domaining of structurally complex mineralisation: method and case studies. Geostatistically assisted domaining of structurally complex mineralisation: method and case studies. In: The AusIMM 2002 Conference: 150 years of mining, Publication series No 6/02, pp 345–350

Abzalov MZ, Drobov SR, Gorbatenko O, Vershkov AF, Bertoli O, Renard D, Beucher H (2014) Resource estimation of *in-situ* leach uranium projects. Appl Earth Sci 123(2):71–85

Armstrong M, Galli A, Beucher H, Le Loc'h G, Renard D, Doligez B, Eschard R, Geffroy F (2011) Plurigaussian simulation in geosciences, 2nd edn. Springer, Berlin, p 149

Bleines C, Bourges M, Deraisme J, Geffroy F, Jeanne N, Lemarchand O, Perseval S, Poisson J, Rambert F, Renard D, Touffait Y, Wagner L (2013) ISATIS software. Geovariances Ecole des Mines de Paris, Paris

Goovaerts P (1997) Geostatistics for natural resources evaluation. Oxford University Press, New York, p 483

Strebelle S (2002) Conditional simulation of complex geological structures using multiple-point statistics. Math Geol 34(1):1–22

Exploratory Data Analysis

15

Abstract

The exploratory data analysis (EDA) is a final test of the data quality. EDA may provide insights that necessitate revisiting of the domaining and wireframing. Thus, EDA and domaining and wireframing are reiterative processes.

Unlike to a trivial QAQC of the assays the EDA is lacking of a mandatory study methods and a rigidly prescribed sequence of the study steps is also lacking. The methods, most commonly used at the EDA includes comparative statistical analysis of the data by types, exploration campaigns, geological characteristics and their spatial distributions which are needed for finding the optimal approaches for integrating different sets of data into a single and coherent set for their further analysis using geostatistical techniques.

Keywords

EDA • Declustering • Domaining • Data generations

The exploratory data analysis (EDA) is a final test of the data quality. It includes comparative statistical analysis of the data by types, exploration campaigns, geological characteristics and their spatial distributions which are needed for finding the optimal approaches for integrating different sets of data into a single and coherent set which will be used for geostatistical resource estimation.

Unlike to a trivial QAQC of the assays the EDA is lacking of a mandatory study methods and a rigidly prescribed sequence of the study steps is also lacking. On the contrary to QAQC of the assays, the EDA procedures and choice of the methods can significantly differ in the different projects depending on a project complexity, risks and sources of the data errors. Effectiveness of the EDA depends on experience and intuition of the specialists who analyse the data pursuing an aim of "unravelling the mysteries of a data set".

15.1 Objective of the EDA

Statistical data analysis is routinely performed by the mine geologists on the different sets of data. This includes the regularly performed compilations and analyses of the grade control

M. Abzalov, *Applied Mining Geology*, Modern Approaches in Solid Earth Sciences 12,
DOI 10.1007/978-3-319-39264-6_15

data, QAQC of the assays, reconciliation of the ore reserves with the mine production results and statistical analysis of the mineral resource database. The latter is a special task which is referred an Exploratory Data Analysis (EDA) and represents the final statistical tests of the data prior to estimation of the mineral resources. This is one of the most important tasks in the project evaluation process because a good understanding of the data sets is essential foundation for a good resource estimation (Tukey 1977).

Geologist undertaking the EDA need to be fluent in mathematical methods for detailed statistical characterisation of the data populations but also should have a deep knowledge of the studied deposits because the EDA requires grouping of the data into mineralised domains and subdividing them by the sample types, exploration campaigns, host rocks, geological structures, mineralogical characteristics of the ore, and other criteria, if they found important for accurate resource estimation.

15.2 Overview of the EDA Techniques

EDA is performed using traditional statistical techniques and also by special methods of the data analysis (Isaaks and Srivastava 1989; Davis 2002). Most common approach is to group data using one of the attributes, for example by a sample type, and then to apply statistical tests for comparison of the created groups. The statistical distribution of the data is visualised and groups compared using histograms and box-and-whisker plot (box plot) diagrams constructed for the data groups. Relationships between studied variables are investigated on the scatter diagrams and quantified using correlation and regression analysis. Statistical distributions of the data sets are compared using Q-Q and P-P plots.

Special EDA techniques includes wide range of the methods (Tukey 1977; Isaaks and Srivastava 1989; Davis 2002). Based on a personal experience of the author of this book some of the most commonly used methods are chosen and explained. Emphasis is made on spider-diagrams which are used for visualisation of the spatial data trends and is particularly efficient for comparison data generations and reconciliation of the block model versus the input data. Methods of the data declustering, Q-Q plot and box-and-whisker plot diagrams are also commonly used for EDA at the mining and exploration projects and therefore also briefly explained in the following sections.

15.2.1 Spider Diagram

This method is based on comparison of the mineralisation profiles created using different sets of data. The profiles are plotted together against the common coordinate points. The principles of the method are as follows (Fig. 15.1):

- the data are grouped into large panels drawn across the entire deposit;
- average is calculated for each panel and for all sets of data contained in a panel;
- estimated average values are plotted on a diagram against coordinates denoting the centre of the panel;
- a final diagram is commonly referred a spider-diagram. This is because of a complex pattern which is often exhibited by the diagram when different profiles are plotted together.

The method is easy to implement and it provides direct comparison of the studied data sets. Comparative analysis of the data profiles undertaken in a context with their spatial distribution patterns allows to identify biased samples, find suspicious anomalies and recognise erratic data behaviour.

15.2.2 Data Declustering

Statistical analysis of the geological data is complicated when density of sampling varies in the different parts of a deposit. Exploration strategy usually causing a preferential drilling in the higher grade areas whereas lower grade areas are less densely sampled (Fig. 15.2a). Construc-

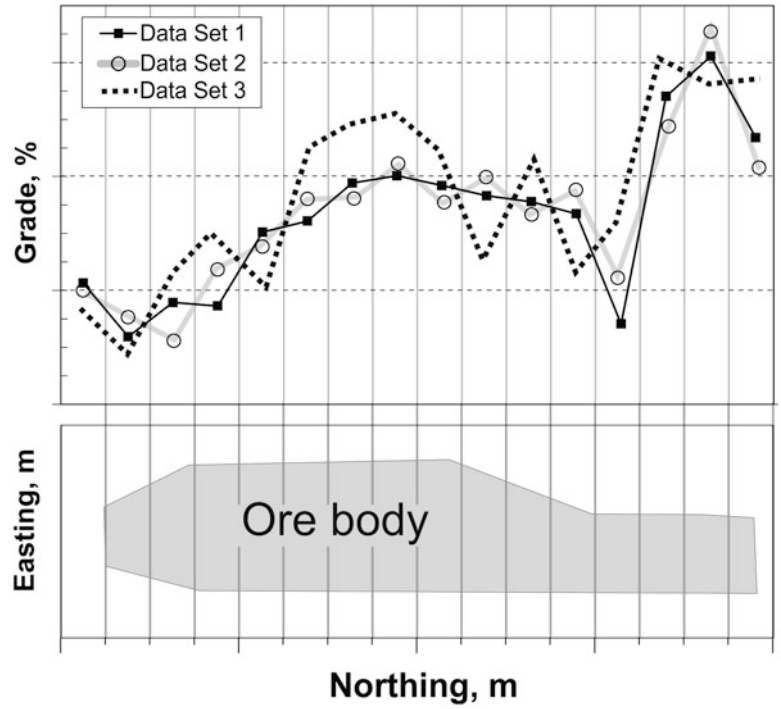

Fig. 15.1 Sketch showing three sets of data presented as spider-diagram

tion of the histograms and estimating mean and variance can be a futile exercise when data are strongly clustered with preferential distribution of the samples in high grade areas. Estimated mean of such data can significantly differ from exhaustive mean.

In order to overcome an influence of the data clusters all samples should be assigned the weights reflecting a degree of the data clustering. The samples distributed in the densely drilled areas receive smaller weights than samples from sparsely drilled areas and this moderates influence of the clustered data. Two declustering methods are most commonly used by the resource estimation practitioners, cell declustering and polygonal declustering (Isaaks and Srivastava 1989; Deutsch and Journel 1998).

Cell declustering approach divides a sampled area into rectangular blocks (cells). and declustering weights are estimated by the cells (Fig. 15.2b). For each cell the sum of the weights is normalised to one and the weights of the samples are estimated as ratio of one to number of samples in a cell. This value is further normalised to entire studied domain by dividing the obtained ratio by the total number of cells in the studied domain (15.2.1.). According to this procedure all samples in the same cell receive the same weight which is inversely proportional to the number of samples in the cell (Table 15.1; Fig. 15.2b).

$$\text{Sample Weight} = \frac{1\ /\text{Number of Samples in the Cell}}{\text{Total Number of Cells in the Studied Domain}} \tag{15.2.1}$$

Estimate obtained from the cell declustering method depends on the size of the cells. If cells are too small, then only one sample can fall into a cell and all samples will therefore have the weight equal to 1. Declustered mean estimated using these cells is the same as the mean of raw (non-declustered) data. Another extreme case is when cell is excessively large and equal to the entire sampled area. In this case all samples fall into one cell and therefore all samples will receive the same weight, equal to 1/total number of samples. The declustered mean estimated

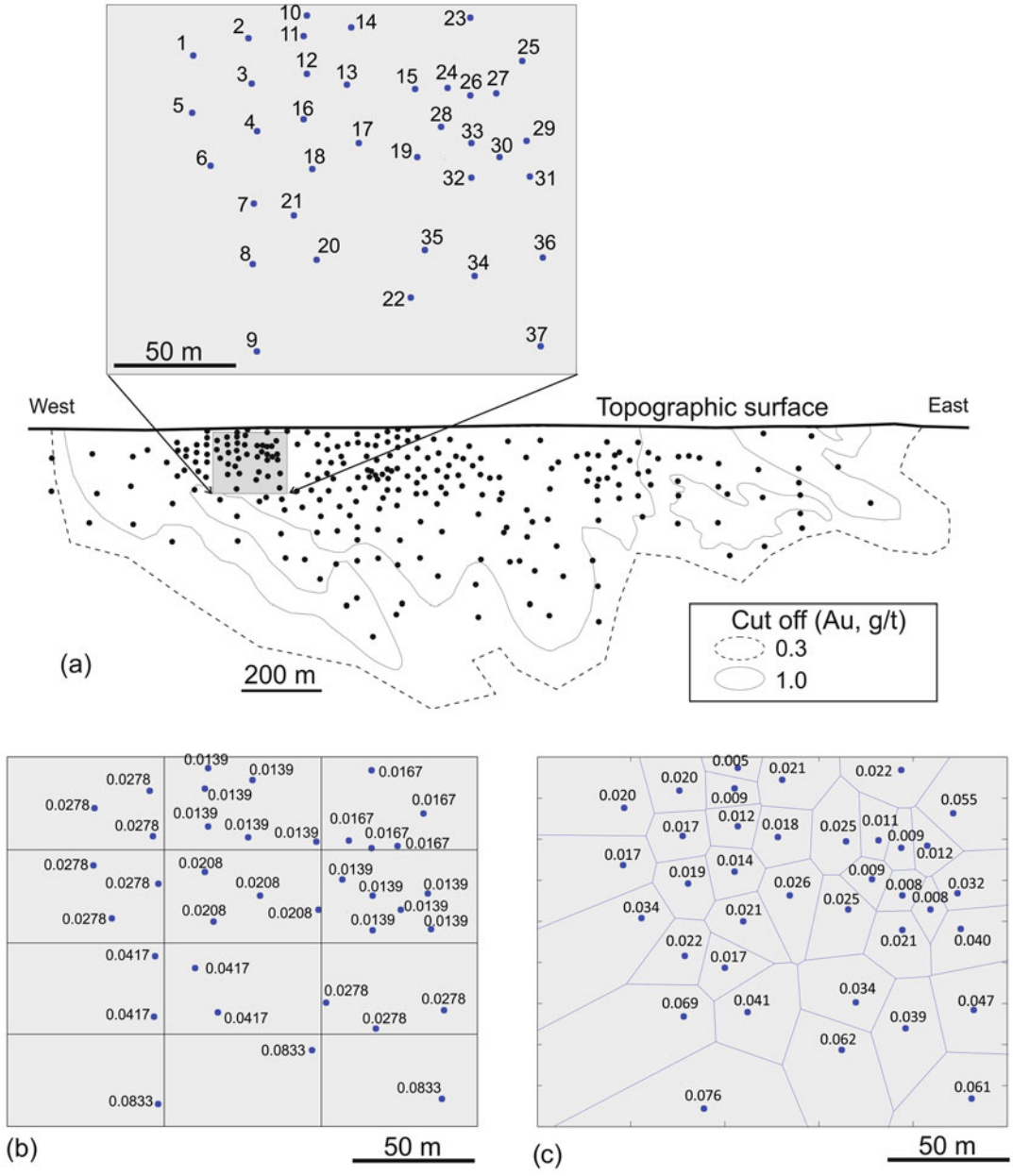

Fig. 15.2 Declustering methods applied to Meliadine gold deposit, Canada: (**a**) longsection of the lode 1000 showing distribution of the drill hole intersections. The drill hole numbers are the same as in the Table 15.1; (**b**) sample declustering weights estimated using cell declustering method; (**c**) sample declustering weights estimated using polygonal declustering method

using the extremely large cell is also equal to the mean of the raw data.

The appropriate size of the declustering cell is somewhere between these two extreme cases and the mean of the declustered data systematically differs from the raw data mean. If samples are clustered in the high grade areas their declustering will create lower estimate than mean of a raw data (Fig. 15.3a). Alternatively, if samples are clustered in the low grade parts of ore body, the

Table 15.1 Declustering weights for the data presented on the Fig. 15.2

Drill hole ID	Thickness of intersection (m)	Grade of intersection (Au, g/t)	Polygon declustering		Cell declustering		
			Area (m^2)	Weight, polygon declustering	Cell ID	Number of drillholes in the cells	Weight, cell declustering
1	1.52	8.03	848.88	0.020	1	3	0.0278
2	1.09	22.00	844.69	0.020		3	0.0278
3	2.48	1.00	706.59	0.017		3	0.0278
4	2.62	0.69	784.97	0.019	2	3	0.0278
5	13.52	2.83	734.58	0.017		3	0.0278
6	1.69	0.62	1453.17	0.034		3	0.0278
7	1.62	2.86	920.94	0.022	3	2	0.0417
8	5.00	0.97	2945.2	0.069		2	0.0417
9	22.82	1.00	3237.76	0.076	4	1	0.0833
10	2.34	6.00	226.13	0.005	5	6	0.0139
11	1.63	5.59	401.88	0.009		6	0.0139
12	0.27	1.62	516.58	0.012		6	0.0139
13	1.34	1.31	773.33	0.018		6	0.0139
14	1.40	36.28	876.78	0.021		6	0.0139
15	3.00	1.07	1046.21	0.025		6	0.0139
16	0.69	3.00	612.99	0.014	6	4	0.0208
17	1.78	8.31	1098.91	0.026		4	0.0208
18	0.58	2.86	885.35	0.021		4	0.0208
19	1.09	1.10	1081.11	0.025		4	0.0208
20	17.26	0.59	1734.45	0.041	7	2	0.0417
21	11.36	1.00	706.84	0.017		2	0.0417
22	1.50	1.90	2645.63	0.062	8	1	0.0833
23	1.12	1.07	917.46	0.022	9	5	0.0167
24	5.03	1.17	446.86	0.011		5	0.0167
25	8.07	0.93	2327.09	0.055		5	0.0167
26	1.14	1.00	376.31	0.009		5	0.0167
27	4.05	3.59	510.61	0.012		5	0.0167
28	3.81	0.66	400.66	0.009	10	6	0.0139
29	0.42	1.00	1374.61	0.032		6	0.0139
30	1.59	1.00	353.23	0.008		6	0.0139
31	0.60	25.38	1678.77	0.040		6	0.0139
32	5.23	0.69	900.98	0.021		6	0.0139
33	1.14	1.00	355.29	0.008		6	0.0139
34	0.95	0.86	1660.81	0.039	11	3	0.0278
35	2.00	1.17	1431.79	0.034		3	0.0278
36	1.38	5.72	2011.63	0.047		3	0.0278
37	2.91	1.00	2588.13	0.061	12	1	0.0833
Mean (raw data)			3.68				
Cell declustered mean			5.22	Declustering weights obtained using (15.2.1)			
Polygon declustered mean			4.94	Declustering weights obtained using (15.2.2)			

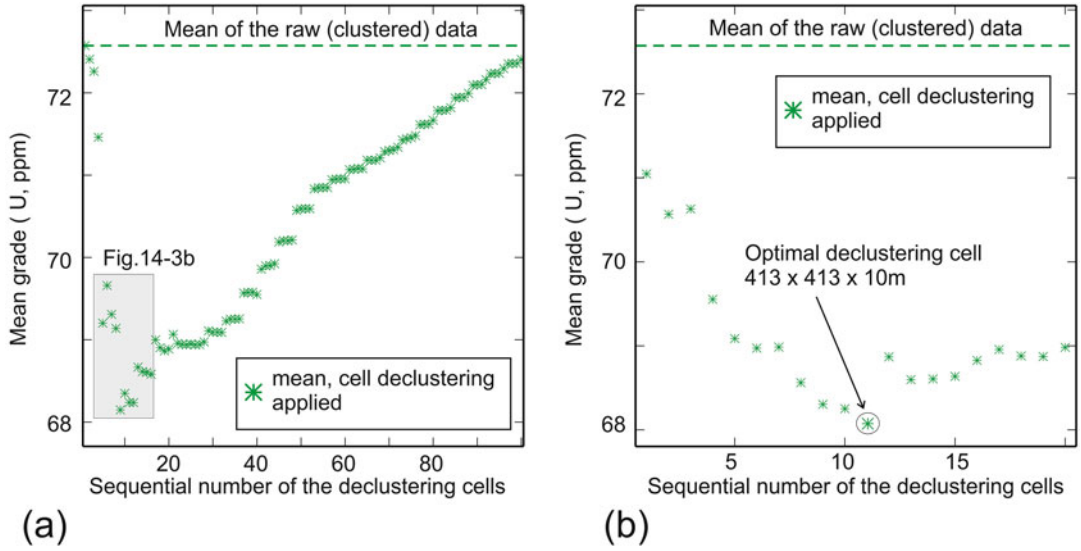

Fig. 15.3 Diagram showing relation between global declustered mean and the declustering cell size, which is denoted by the sequential number of a tested cell: (**a**) first test, cell sizes change from the smallest possible (one sample per cell) to a largest (entire sampled area); (**b**) second (detailed) test, cell sizes change in a small interval identified during the first test; contour map of the global declustered mean

declustering creates higher estimate than mean of a raw data. This behaviour is used to determine the optimal size of the declustering cell. It is found empirically by comparing estimates made using different declustering grids. Usually 20–100 grids are tested and the estimated means are plotted on a diagram versus corresponding them cells. In practice, the cells are arranged in the size increasing order and the estimated means are plotted versus sequential numbers of the cells. This approach assures that data points are evenly distributed along the abscissa axis of the diagram (Fig. 15.3). An optimal cell is chosen from a diagram by finding a pivotal value of the estimates. For the data clustered on the high grade areas this is the lowest declustered mean (Fig. 15.3). If samples are grouped on the low grade areas the optimal cell will corresponds to largest declustered mean. Procedure of finding an optimal cell usually includes two steps. Initially, the maximally wide range of sizes, spanning from the lowest possible to largest, are tested (Fig. 15.3a). After finding an inflection point on the diagram, the test is repeated over the narrow range of sizes covering the size indicated by the first set test and optimal cell size if deduced from the detailed diagram (Fig. 15.3b).

In some situations the binary diagrams (Fig. 15.3a, b) are insufficient for finding an optimal size of the declustering cells and geologist may choose to present relation between global declustered mean and the declustering cell size on the contour map (Fig.15.4). Advantage of the contour map over binary diagrams in that it allows to estimate effect on a global mean of the different sides of the declustering cells. This is obtained by changing east-west (X) and north-south (Y) dimensions of the cells and recording the global declustered mean for every combination of the XY sizes of the declustering cells (Fig. 15.4). Such maps are commonly constructed when drilling grid is anisotropic with broader space between samples in one direction, for example along the strike, and significantly closer in another, commonly across the strike.

Cell declustering method is most effective for the data sets which are preferentially clustered in a high or low grade areas and performs in particular well when samples are distributed following a pseudo regular grid. However, this is not always

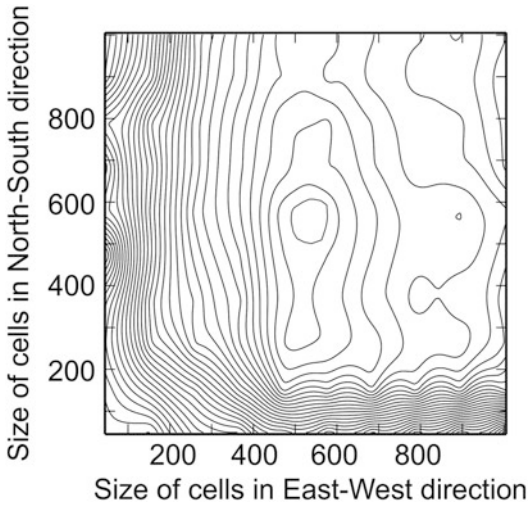

Fig. 15.4 Contour map showing relationship between global declustered mean and the declustering cell size, uranium project

the case. When data are distributed at random and regular grids are lacking the pivotal values may not present on the diagrams or contour maps therefore choice of the optimal cell size becomes problematic. In that case a different declustering method is needed. In particular, polygonal declustering method suites well for such data (Isaaks and Srivastava 1989).

The method is based on delineating a polygon of influence around each sample and estimating the area of each polygon (Fig. 15.2c; Table 15.1). Two methods are used for delineating the polygons (Annels 1991). First approach is called perpendicular bisectors method (Annels 1991). The polygons are constructed by drawing the bisectors at a right angle to the tie-lines linking adjacent samples. This technique was used for constructing the polygons mosaic shown on the Fig. 15.2c. Second technique is called angular bisectors (Annels 1991). The polygons are constructed by linking samples with tie-lines and then constructing angular bisectors between these lines to define a central polygon. Both methods produce the similar results.

The declustering using the polygonal method is made by estimating the areas of the polygons of influence and using them as the declustering weights. In practice, the sample weights are normalised by dividing the area of a polygon by a sum of the all polygons in the studied domain (15.2.2).

This method has advantage over the cell declustering method because it produces a unique estimate. However, the main disadvantage of the polygonal method it can not be adjusted to the deposit structure, whereas cell declustering method has this capability by adjusting the orientation and dimensions of the rectangular cells to better match the ore body structure.

$$\text{Sample Weight} = \frac{\text{Area of a Polygon Containing Samples}}{\text{Sum of the polygons in the studied domain}} \quad (15.2.2)$$

15.2.3 Q-Q Plots

EDA procedure commonly includes comparison of the statistical distributions of the different data sets. However, the studied data sets often have the different numbers of data therefore their direct comparison not always feasible. In such situations, when studied distributions differ by the number of data, they are compared using a diagram called Q-Q plot. On this diagram the quantiles of two distributions are plotted versus one another by using quantiles of a first distribution as the X-coordinate and quantiles of a second distribution will serve as Y-coordinates (Fig. 15.5).

When two distributions are identical their quantiles are equal and therefore plot on the Q-Q diagram as the straight line coincident with the bisect (X = Y line). Deviation from the bisect reveals the grade range where distributions ae different (Fig. 15.5).

15.2.4 Box-and-Whisker Plot (Box Plot)

Box-plot is a diagram specially devised (Tukey 1977) for EDA needs. The method allows pre-

senting the essential aspects of a sample distribution in a simple and concise form and therefore the technique is often used for the data analysis (Fig. 15.6).

The essence of the method is in presenting the data as a box and lines extending from the box, called "whiskers" (Tukey 1977). The box denotes the central 50 % of distribution. Lower limit of a box is set to 25th percentile of distribution and upper limit to 75th percentile (Fig. 15.6a). Median (50th percentile) is denoted as a straight line crossing the box (Fig. 15.6a).

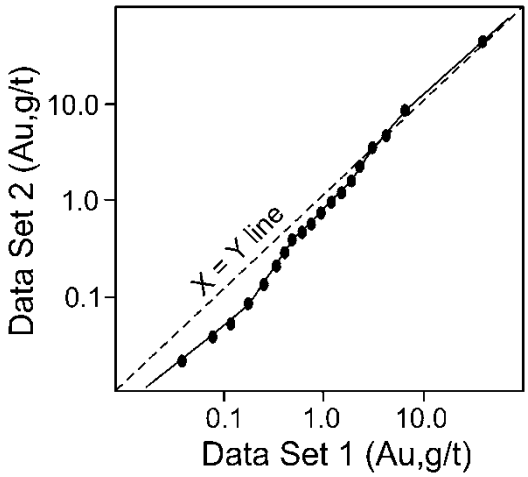

Fig. 15.5 Q-Q plot comparing two groups of the gold assays, Meliadine project, Canada

The lines extending from the box ("whiskers") usually extend to 5th and 95th percentiles and the data lying outside of these extremes are denoted as dotes (Fig. 15.6). The diagram also contains the arithmetic average (mean) which is denoted by a diamond (Fig. 15.6a) or cross (Fig. 15.6b).

The box-plot diagrams allow to visually compare the different data by plotting them together which allows quickly to find differences in their statistical distributions (Fig. 15.6b).

15.3 Grouping and Analysis of the Data

Different criteria for the data grouping is used for EDA analysis, depending on a project and data characteristics. Criteria most commonly used for data grouping are as follows:

- types of the data;
- exploration campaigns and the data generations;
- geological characteristics of samples.

15.3.1 Data Types

Resource estimation database commonly includes different types of data which can differ by quality or sample size (volume support)

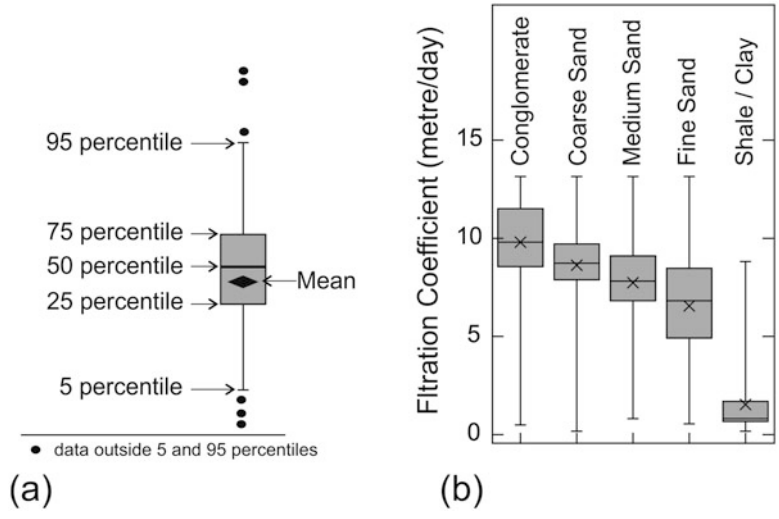

Fig. 15.6 Box-plot diagrams: (**a**) sketch explaining construction of the diagram; (**b**) box-plot diagrams showing permeability (filtration coefficient) of the different rocks at the Budenovskoe in-situ leach uranium project, Kazakhstan (Reprinted from (Abzalov et al. 2014) with permission of Taylor-Francis Group)

therefore combining them together for estimation resources not always possible or can require special geostatistical techniques (Abzalov and Pickers 2005). Examples of the different types of data commonly encountered at the resource databases are as follows: percussion, RC and diamond core drill holes at the iron ore deposits, auger and RC drilling at the bauxite deposits (Abzalov and Bower 2014), diamond core and RC drill holes at the gold and base-metal deposits, RC (air core) and Sonic drilling at the mineral sands deposits (Abzalov et al. 2011). At the operating open pit mines the resource databases can also include blast hole samples (Abzalov et al. 2010). Underground operations commonly use channel samples collected at the rock faces exposed in the underground drives which shell be combined for estimating resources and reserves with the drill hole samples.

Two cases need to be considered when several types of data were found in the resource estimation database:

- All types of data are of a good quality and suitable for estimation resources. Difference in their quality is insignificant;
- A certain type of data is unreliable. It can be the case when data bias as detected or certain type of data is characterised by excessively large variances causing poor repeatability of the results.

In the first case, when quality of the data is sufficient for estimating resources, it is necessary to check if the different types of samples can be grouped into a single set. The geostatistical methods require the samples to be of a similar size (equal volume support), therefore it is necessary to investigate if the different types of samples are complying with the equal volume support condition of the geostatistical methods. If samples of a different size are present, which is a common case when different types of drilling were used, the equal support is achieved by adjusting the length of the composited samples to the holes diameter. For example, at the Cu porphyry deposit in Australia, equal volume support was achieved by compositing diamond drill core samples into 5 m composites, and RC samples were composited into 4 m composites.

A more difficult situation is when one type of the data is unreliable. It is necessary to analyse spatial distribution of the suboptimal data, which can be evenly distributed through the deposit or concentrated in some areas (Fig. 15.7). The parts of the deposit which was explored using suboptimal techniques, often are excluded from the resources or their resource category is downgraded. Such situation was encountered at the Australian iron-ore projects where significant part of the deposit was excluded from the project resources because it was estimated using open hole percussion drilling which was found biased (Fig. 15.7).

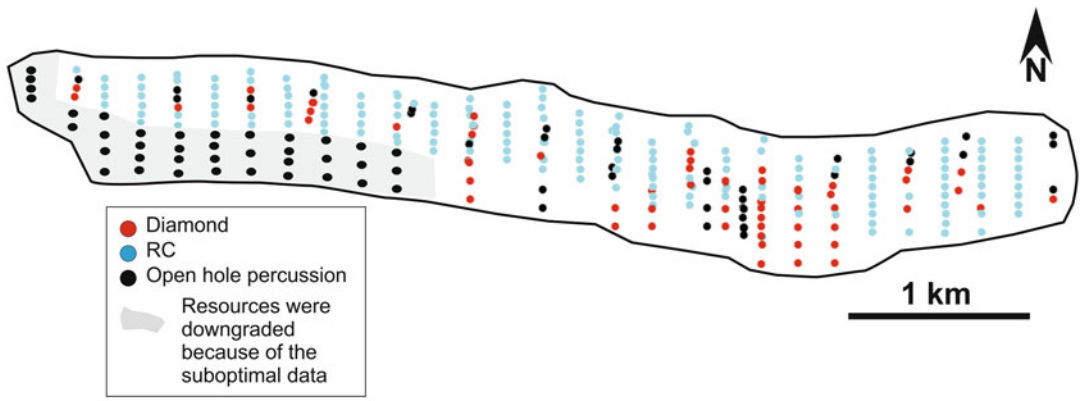

Fig. 15.7 Map showing distribution of the different types of the drill holes, Nammuldi iron-ore deposit, Western Australia

When suboptimal data distributed evenly through the deposit they can be used for resource estimation as an auxiliary information. The auxiliary data are integrated with the better quality data, referred as a target variable, using multivariate geostatistical methods (Abzalov and Pickers 2005).

15.3.2 Data Generations

Exploration of the deposits can take from several years to several decades and include several exploration campaigns. Even if the same drilling method was used through the entire course of exploration the different generations of the data can have different quality therefore it is necessary to analyse data grouping them by exploration campaigns.

All samples should be assigned the date when sample was collected and processed which is used for grouping the data into the data generations (e.g. drilling campaigns). The groups are compared and analysed using conventional EDA tools with an objective to diagnose the potentially invalid data.

The differences between the generations of the data can be enhanced by plotting the data on the maps and comparing them using spider-diagrams (Fig. 15.1). The spider-diagrams can be enhanced by unfolding the ore bodies (Fig. 15.8). Example presented on the Fig. 15.8 is from iron-ore mine in Australia which have experienced production difficulties because of underestimating the Al_2O_3 content of the ore. Analysis of the data by the drilling campaign has identified that the model bias was caused by the biased samples collected in the drill holes drilled in year 2000. Based on this study a mitigation program was developed and implemented which has allowed to overcome the issue.

15.3.3 Grouping Samples by Geological Characteristics

Grouping of the samples by their geological attributes is commonly used when it is expected

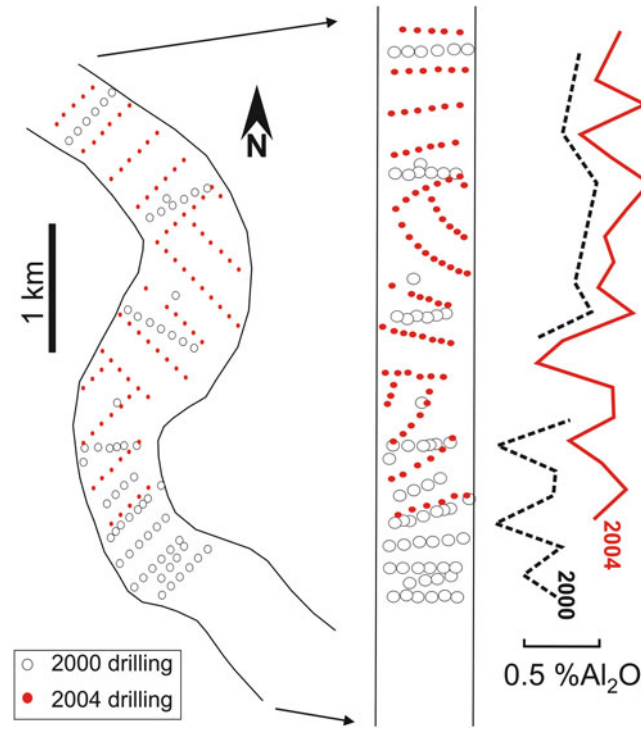

Fig. 15.8 Spider-diagram that has detected bias of 2000 drilling data at the iron ore mine, Australia

that these parameters control mineralisation grade. This approach is also used for estimating average geotechnical or metallurgical characteristics of the rocks, which can differ depending on the rock types, stratigraphy, degree of weathering and structural setting.

Examples of a grouping samples by the rock types includes estimating average dry bulk density of the rocks (Chap. 7 of the book) and their average permeability (Fig.15.6b). Distribution of the mineralisation grade by the rock types or structural settings is also routinely studied and represents one of the objectives of EDA. This analysis helps to reveal a geological control of mineralisation which otherwise could be hidden by a complex geometry of the deposit.

In all cases the most effective techniques for the data analysis are histograms and the boxplot diagrams (Fig.15.6) which are supplemented by analysis of a spatial distribution pattern of a studied variable.

15.4 Statistical Analysis of the Resource Domains

The detailed statistical characteristics of the domains is needed for choosing the geostatistical methods for estimating resources. The following parameters shall be addressed at the EDA study:

- Descriptive statistics of the resource domains (using data declustering if this is needed);
- Assessment of a domain's stationarity;
- Testing of the domains homogeneity;
- Outliers identification;
- Correlation between attributes;
- Spatial trends and discontinuities.

Example on the Fig. 15.9 summarises findings made at the EDA study of the Cliff nickel-sulphide deposit in Western Australia. Mineralisation has been initially constrained by wireframes which were constructed along the geological contacts of the mineralised ultramafic rocks

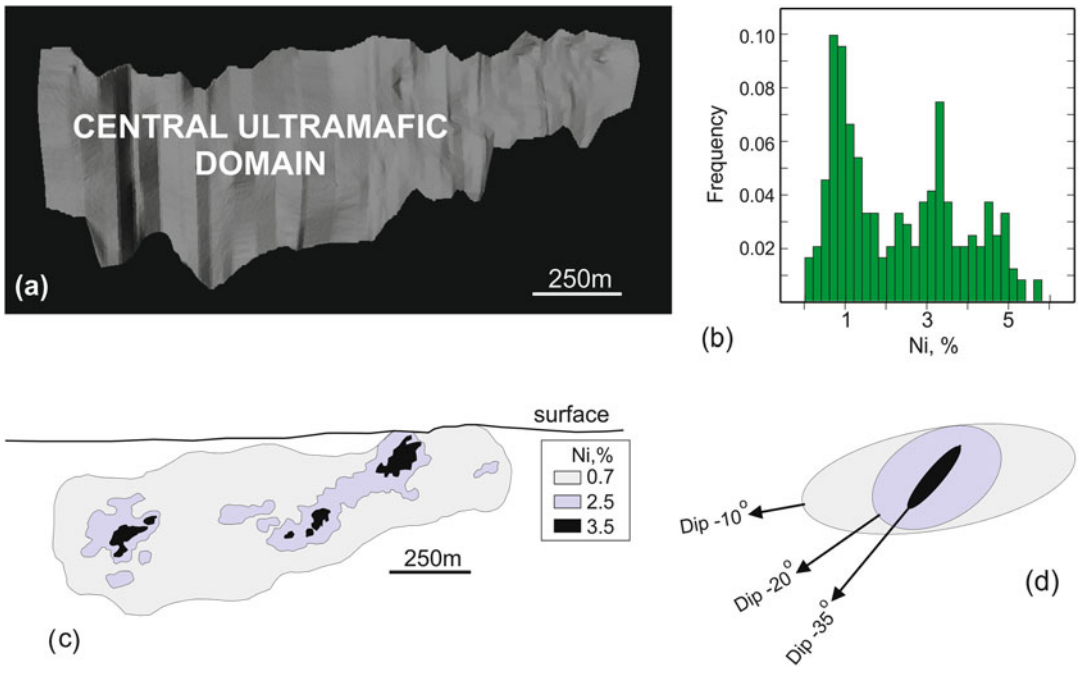

Fig. 15.9 Statistical characterisation of the main ore body (Central Ultramafic Domain) at the Cliff Ni-sulphide deposit, Western Australia: (**a**) 3D image of the wireframe; (**b**) histogram of Ni grades of the composted samples contained in the volume constrained by the wireframe; (**c**) longsection of the domain showing distribution of the Ni grade; (**d**) spatial trends of the different types of mineralisation (grade classes) presented as the continuity ellipses

with the barren gneisses and locally corrected by shifting contact to 0.7 % Ni cut-off grade (Fig. 15.9a). Mineralisation constrained by this wireframe was called Central Ultramafic Domain (Fig.15.9a).

The drill hole samples included into the constrained volume have been selected for EDA analysis. Samples have been composited into 0.5 m long composites and analysed using conventional statistical techniques. Histogram of the composites has multi-modal shape clearly indicating for presence of the different groups of data (Fig. 15.9b). Three statistically homogeneous populations of data, expressed on the histogram as the peaks at 1 %, 3.3 % and 4.8% Ni, have been identified (Fig.15.9b). Analysis of these groups has shown that different grade classes of the samples represent different mineralisation types: disseminated, stringer and massive.

The mineralisation types have different geological settings. Disseminated sulphides are uniformly distributed through the whole Central Ultramafic domain whereas massive mineralisation occurs as a narrow lenses cutting the domain at high angle (Fig. 15.9c). Massive lenses are surrounded by a broad halo of stringer sulphides which spatial distribution approximately coincide with the massive sulphides although their dipping angle is less steep (Fig. 15.9c).

Continuity of mineralisation has been estimated for all three types separately using indicator variograms. Results of the geostatistical analysis are expressed as the continuity ellipses which confirm different orientation of the mineralisation types (Fig. 15.9d).

Based on the EDA results it became obvious that linear estimation methods, ordinary and simple kriging, are suboptimal for this data and choice was made in favour of Multiple Indicator Kriging (MIK). The MIK method is better suited for estimation resources when a studied domain contains several statistically different groups of data which are characterised by the different structural settings and different strike and/or dip orientations (Goovaerts 1997).

Analysis of the univariate distributions should also include estimation of the degree of skewness. Highly skewed statistical distributions can also be suboptimal for estimation resources using linear techniques and may require MIK or similar methods, which are based on modelling the grade indicators. Statistical analysis must always be accompanied by analysis of a spatial distribution of the identified statistical data populations. Even when statistical data analysis suggests a normal (Gaussian) distribution spatial analysis can reveal a strong spatial zoning which may will require application of non-stationary modelling methods (Goovaerts 1997).

Univariate distribution not always reveals peculiarities of the data, therefore the data 'interrogation' need to be continued using auxiliary information. Multivariate analysis of the different chemical elements presented in mineralisation can facilitate definition of the resource domains and also essential for choice of the geostatistical estimation techniques. Commonly used statistical methods of multivariate data analysis are principal component analysis, factor analysis, multi-

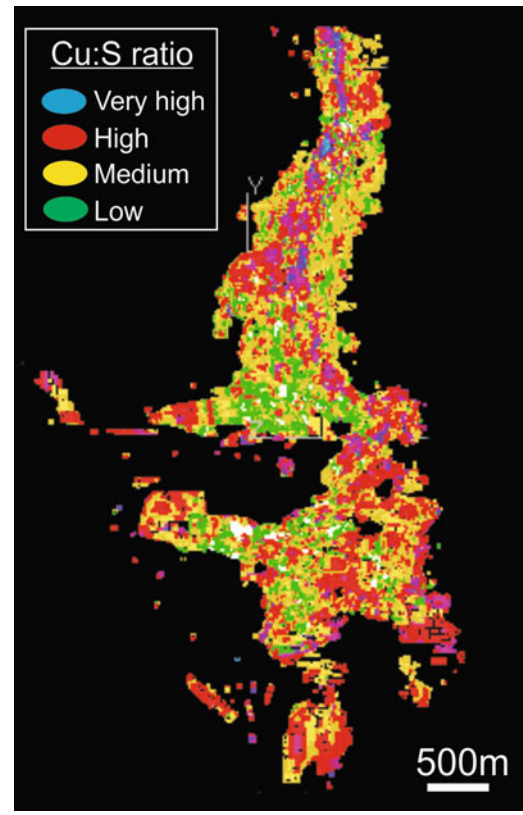

Fig. 15.10 Cu:S ratio at the Olympic Dam deposit, Australia

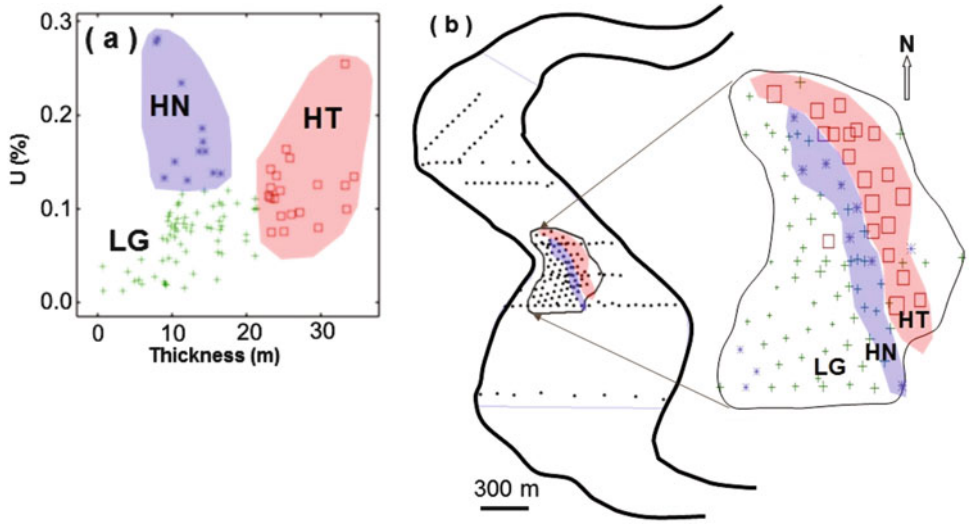

Fig. 15.11 Grouping of the domains by their grade-thickness characteristics and spatial distribution. Roll-type deposit in Shu-Sarysu basin, Kazakhstan (Abzalov 2010). *LG* low grade, *HN* high grade narrow, *HT* high grade thick: (**a**) Grade vs. Thickness diagram of the mineralised intersections; (**b**) map showing spatial distribution of the mineralised intersections

variate regression, discriminant analysis and cluster analysis (Davis 2002).

Application of this approach at the Olympic Dam deposit has revealed a regular change of the Cu:S ratio which imposes additional challenge on using multivariate geostatistical methods for estimation resources (Fig. 15.10).

In the sandstone-type uranium deposits the useful auxiliary information is thickness of the mineralised intersections. Study of the ratio between thickness and grade of the uranium mineralisation at the Budenovskoe deposit has allowed to define three zones of mineralisation. The zones were constrained by wireframes and their resources were estimated as the separate domains (Fig. 15.11).

References

Abzalov MZ (2010) Optimisation of ISL resource models by incorporating algorithms for quantification risks: geostatistical approach. In: Technical meeting on in situ leach (ISL) uranium mining, International Atomic Energy Agency (IAEA), Vienna, Austria, 7–10 June, 2010

Abzalov MZ, Bower J (2014) Geology of bauxite deposits and their resource estimation practices. Appl Earth Sci 123(2):118–134

Abzalov MZ, Pickers N (2005) Integrating different generations of assays using multivariate geostatistics: a case study. Trans Inst Min Metall 114:B23–B32

Abzalov MZ, Menzel B, Wlasenko M, Phillips J (2010) Optimisation of the grade control procedures at the Yandi iron-ore mine, Western Australia: geostatistical approach. Appl Earth Sci 119(3): 132–142

Abzalov MZ, Dumouchel J, Bourque Y, Hees F, Ware C (2011) Drilling techniques for estimation resources of the mineral sands deposits. In: Proceedings of the heavy minerals conference 2011. AusIMM, Melbourne, pp 27–39

Abzalov MZ, Drobov SR, Gorbatenko O, Vershkov AF, Bertoli O, Renard D, Beucher H (2014) Resource estimation of *in-situ* leach uranium projects. Appl Earth Sci 123(2):71–85

Annels AE (1991) Mineral deposit evaluation, a practical approach. Chapman and Hall, London, p 436

Davis JC (2002) Statistics and data analysis in geology, 3rd edn. Wiley, New York, p 638

Deutsch CV, Journel AG (1998) GSLIB: geostatistical software library and user's guide. Oxford University Press, New York, p 340

Goovaerts P (1997) Geostatistics for natural resources evaluation. Oxford University Press, New York, p 483

Isaaks EH, Srivastava RM (1989) An introduction to applied geostatistics. Oxford University Press, New York, p 561

Tukey JW (1977) Exploratory data analysis. Addison – Wesley Longman, Boston, p 688

Resource Estimation Methods

16

Abstract

The chapter reviews the non-geostatistical estimation methods, the most common of them, are polygonal, triangulation, cross-sectional and estimation by the panels (blocking). Another method which also described here is inverse distance weighting (IDW) technique. This is the most advanced technique among the non-geostatistical methods and methodology of its application is explained in details. It is noted, that methodology of IDW technique has many similarities with Ordinary kriging.

Keywords

Polygonal • Triangulation • Cross-sectional • IDW

Estimation mineral resources is one of the main tasks of the geological teams developing and evaluating the mining projects. After mining project has entered into a production stage this task is inherited by the mine geology team who continues delineating the ore bodies. Mine geologists together with mining engineers estimate ore reserves which are deduced from the mineral resource model by adding the modifying factors (mining and metallurgical parameters, environmental, social factors and the project's economics).

Procedure of the resource estimation includes several steps.

1. Raw data are modified and prepared for mineral resource estimation.
2. Data analysed in order to find the optimal resource modelling approach.
3. Mineralisation is delineated and constrained in 3D space.
4. Resources of the constrained areas are estimated by interpolation and extrapolation of the sample assays.
5. Model reviewed and validated against the input data and reconciled against the mine production, when the latter is available.
6. Resource uncertainty is quantitatively estimated and resource categories are defined using the international reporting standards and assigned to the model.

Since 1950th, when mathematical methods of geostatistics have been developed for modelling spatial distributions of the regionalised variables, they have been applied for estimation resources and reserves of the mineral deposits (Krige 1951; Matheron 1963, 1968). Currently this is the main

M. Abzalov, *Applied Mining Geology*, Modern Approaches in Solid Earth Sciences 12,
DOI 10.1007/978-3-319-39264-6_16

estimation approach allowing to construct a robust and accurate 3D models of the ore bodies.

However, non-geostatistical estimation methods, developed and implemented in the mining industry before geostatistics, were not abandoned and still used in parallel with geostatistical techniques. In particular, these methods are useful for preliminary evaluation of the projects before geostatistitians have been engaged. Non-geostatistical methods also commonly applied by the mine geologists for processing of the grade control data and preparing the short term mine production plans.

There are many non-geostatistical estimation methods, called 'classical methods', the most common of them, polygonal, triangulation, cross-sectional and estimation by the panels (blocking). Another method, which also described here is inverse distance weighting (IDW) technique. This is the most advanced technique among the non-geostatistical methods and methodology of its application has many similarities with Ordinary kriging.

16.1 Polygonal Method

This is 2D method applied for estimation tabular deposits. Such deposits can be accurately represented by a mosaic of the polygons of influence drawn on the maps or long sections of the ore bodies (Fig. 16.1a). The method also commonly used for estimation grade of the blast hole pads.

Polygonal estimation method requires construction of the drill hole intersections and estimating the true grade and thickness of the intersections. Each intersection is assigned a polygon of influence and the grade and thickness of an intersection is extrapolated to the area constrained by the polygon of the drill hole influence (Fig. 16.1a).

Average grade of the deposit is estimated by dividing the total contained metal by the sum of the thicknesses, normalised by the polygons of influence (16.1.1). Global tonnage is estimated by adding up the tonnages of the polygons (16.1.2).

$$\text{Mean grade} = \frac{\sum_{i=1}^{N} (\text{Grade i} * \text{Thickness i} * \text{Area of a Polygon i})}{\sum_{i=1}^{N} (\text{Thickness i} * \text{Area of a Polygon i})} \quad (16.1.1)$$

N - number of the polygons (intersections)

$$\text{Tonnage} = \sum_{\text{i}}^{\text{N}} (\text{Thickness i} * \text{Area of a Polygon i} * \text{Tonnage Factor i}) \quad (16.1.2)$$

N - number of the polygons (intersections)

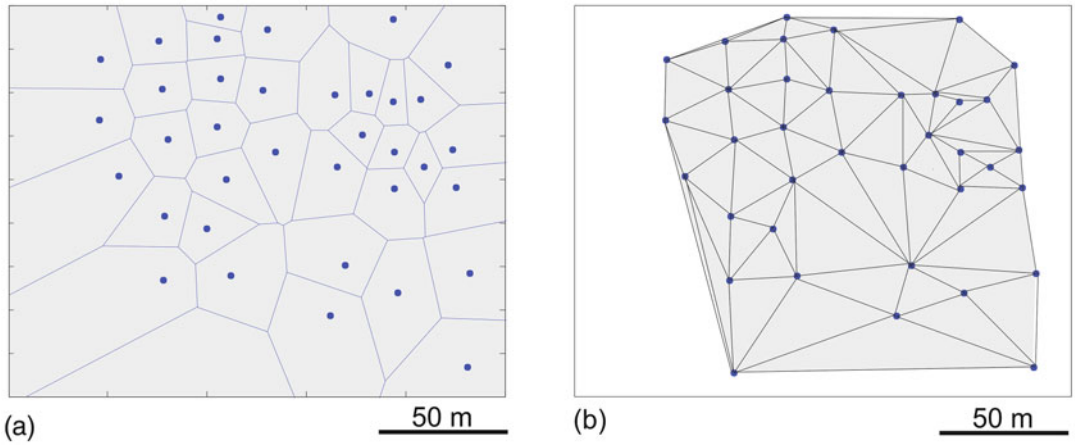

Fig. 16.1 Comparison of the resource estimation methods. *Grey shaded areas* denote the part of the domain where resources were estimation: (**a**) polygonal method; (**b**) estimation by the triangulation

Method has many limitations. One of the most important disadvantages is that resources are estimated at the point support and therefore suboptimal for evaluating mining projects. Extrapolating of a single drill hole intersection to a large area constrained by the polygon of influence can also be source of a significant estimation errors, which are particularly common in a broadly drilled parts of the ore body and along the margins (Fig. 16.1a).

Despite of these limitations the method is still used for estimation resources and reserves (Annels 1991). In particular, it is commonly used for preliminary estimates made before the geostatistitians have been engaged for the project evaluation. However, application of the polygonal method is steadily decreases and replaced by geostatistical resource estimation techniques (Goovaerts 1997).

Another area of this method's application is a grade control at the open pit mines. The method is well suited for estimating reserves of the blast hole pads prepared for mining which is used by the mine geologists as a short term mine production plan.

16.2 Estimation by Triangulation

Triangulation method of resource estimation has a lot of similarities with polygonal method. It is also 2D technique which is preferably applied to the tabular deposits using grade and thickness of the drill hole intersections. The method subdivides the estimated domain on the triangles which are constructed by joining the adjacent drill hole intersections (Fig. 16.1b).

Average grade of the mineralisation constrained by a triangle is estimated as a length weighed average of the drill hole intersections forming the vertices of the studied triangle (16.2.1).

Average thickness of the mineralisation constrained by a triangle is merely an arithmetic mean of the three mineralisation thicknesses deduced from the drill hole intersections forming the vertices of the studied triangle. Tonnage of the mineralisation constrained by a triangle is obtained by multiplying the average thickness by the triangle area and by the tonnage factor.

Global mean grade is estimated as an average grade of the triangles weighed by the triangle areas (16.2.2). The global tonnage is estimated by adding up tonnages of the triangles in the studied domain (16.2.3).

$$\text{GRADE (triangle)} = \frac{\sum_{i=1}^{3} (\text{Grade i} * \text{Thickness i})}{\sum_{i=1}^{3} (\text{Thickness i})}, \tag{16.2.1}$$

$$\text{Mean Grade} = \frac{\sum_{i=1}^{N} (\text{Grade (triangle) i} * \text{Area of a Triangle i})}{\sum_{i=1}^{N} (\text{Area of a Triangle i})}, \tag{16.2.2}$$

N - number of the triangles

$$\text{Tonnage} = \sum_{i=1}^{N} (\text{Thickness of a Triangle i} * \text{Area of a Triangle i}), \tag{16.2.3}$$

N - number of the triangles

Triangulation method partially overcomes limitations of the polygonal method where grade of a single drill hole is extrapolated to the large areas. Triangulation method uses three adjacent drill holes for estimating resources of the area constrained by the triangle with the drill holes at the vertices (Fig. 16.1b). This estimate is more reliable than that is obtained using polygonal method however it also has the significant limitations. The main disadvantages of the triangulation method are as follows:

- estimation results depend on triangulation pattern which is subjectively chosen;

- all drill hole intersections receive the same weight independently of the size and shape of the triangle;
- method is lacking of ability to implement a structural interpretation of the deposit. All three vertices of the triangle receive the same weight independently of their location relative to strike of the ore body. Vertices located along the strike of an ore body receive the same weight as the vertices located in the across the strike direction, which is methodologically incorrect and can possibly lead to serious estimation errors;
- Method also does not allow to estimate the deposit margins (Fig. 16.1b).

The triangulation method has many common features with polygonal and therefore also used for grade control estimations using the blast holes data. Equal size of the blast holes and their distribution as the horizontal layers suites well for using the triangulation method for estimating reserves of the blast hole pads. However, because of the limitations of the triangulation and polygonal techniques, which were explained above, these methods are replaced by geostatistical techniques. The latter produce more accurate grade control estimations and also provide a quantitative estimation of the model uncertainty (Abzalov et al. 2010).

16.3 Cross-Sectional Method

Polygonal and triangulation methods are suboptimal for complex ore bodies whose shape can't be accurately presented on the 2D surfaces. Estimation of such mineralisation is made in 3D usually by constraining mineralisation by the wireframes and estimating grade of the constrained volumes by geostatistical techniques. Alternate approach for estimating the complex mineralisation is by using the cross-sectional method. This is a quasi-3D method presenting the ore body as the stacked cross-sectional blocks (panels).

The method is currently used if the wireframing technologies are not available, usually due to lacking of equipment, or inapplicable, due to extremely complex and irregular shape of the mineralised domains. In particular, it remains one of the main techniques for estimating resources of the roll-type uranium deposits in Kazakhstan (Abzalov et al. 2014).

There are different versions of the cross-sectional method: which are briefly reviewed in this section of the book.

16.3.1 Extrapolation of the Cross-Sections

Estimation procedure using this method is shown schematically on the Fig. 16.2 and explained below.

The method is applied at several steps:

- The cross-sections are drawn through the drilled traverses and the ore body is contoured on each cross-section at the chosen cut-off (Fig. 16.2a);
- Average grade is estimated for each cross-section using the length weighted average technique (16.3.1);
-

$$\text{GRADE (cross-section)} = \frac{\sum_{i=1}^{K} (\text{Grade i} * \text{Length of the sample i})}{\sum_{i=1}^{K} (\text{Length of the sample i})}, \quad (16.3.1)$$

K - number of samples

- The contour of the ore body, interpreted on the cross-section, is extrapolated to the half distance between the drill traverses creating the cross-sectional panel (Fig. 16.2b). The average grade of the cross-section is assigned to the whole panel (Fig. 16.2b). Tonnage of the ore body at the given panel is estimated as a product of the area of the ore body contoured on the cross-section by the distance of extrapolation times the tonnage factor (Fig.16.2b);
- The ore body model is constructed by stacking together all cross-sectional panels forming the quasi-3D model of the ore body (Fig. 16.2c).

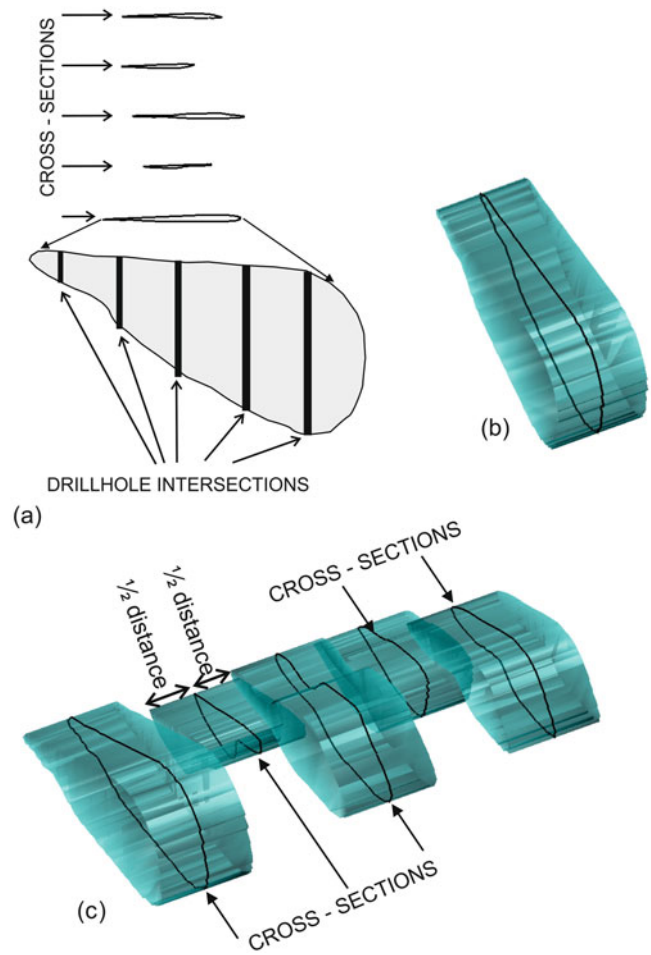

Fig. 16.2 Estimation resources/reserves by extrapolation of the cross-sections: (**a**) sketch showing principles of the ore body delineating by contouring it silhouette on a cross-section; (**b**) extrapolation of the cross-section to a half distance between drill traverses forming the cross-sectional panel; (**c**) construction of a quasi-3D model of the ore body by presenting it as the stacked together cross-sectional panels

Total tonnage is estimated by adding up tonnages of the cross-sectional panels. The average grade is obtained by dividing the global contained metal (sum of the contained metals at the panels) by a total tonnage of ore body constrained by the cross-sectional panels (16.3.2).

$$\text{GRADE (Ore Body)} = \frac{\sum_{i=1}^{N} (\text{Grade (i)} * \text{Tonnage (i)})}{\sum_{i=1}^{N} (\text{Tonnage (i)})}, \quad (16.3.2)$$

N - number of cross-sections

Grade (i) = Length weighted average grade of the samples on the cross-section (i)

Tonnage (i) = Tonnage of a cross-sectional panel (i)
= Area (i) * Distance (i) * Tonnage factor (i)

Area (i) = Area of the ore body contour on the cross-section (i)

Distance (i) = distance of extrapolation of the cross-section (i)

Extrapolation of the shape and grade of the ore body from the cross-sections can be applied only for short distances which can vary between the deposits depending on the mineralisation type and variability. In particular, distance of extrap-

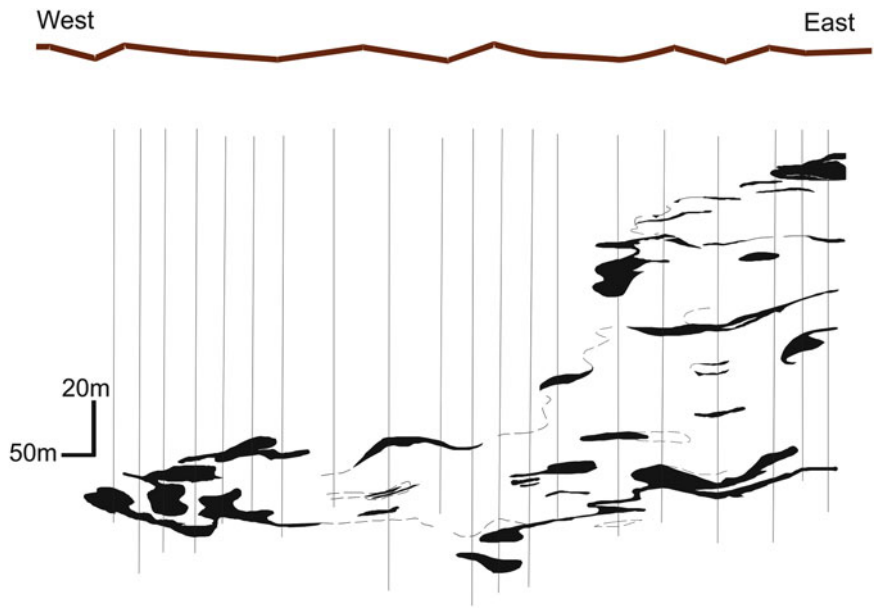

Fig. 16.3 Cross-sections of the Budenovskoe roll-type uranium deposit, Kazakhstan (Abzalov 2010). Mineralisation constrained at 100 ppm U_3O_8

olation should be compliant with spatial continuity of the grade and the ore body thickness. Underestimating the variability of the orebody and extrapolating the cross-sectional estimates to the larger distances can lead to serious estimation errors. Thus, the method is only used if extrapolation distances proved to be appropriate for a given type of deposit and mineralisation style.

Cross-sectional method has found the new applications when wireframing technologies have been implemented for modelling the ore bodies. Extrapolation of the last cross-section is commonly used in order to close the wireframe. This approach is applied when mineralisation is still open and geological interpretation suggests that mineralisation continues beyond the last drilled cross-section.

Extrapolation of the cross-sections is also used when structure of the mineralisation is extremely complex preventing the correlation of the mineralisation contours between cross-sections. Example of such mineralisations was observed at the Budenovskoe roll-front uranium deposit, shown on the Fig. 16.3.

The deposit formed by superimposition of several roll-fronts which has created a highly variable and discontinuous shape of the ore bodies (Abzalov 2010; Abzalov et al. 2014). Accurate correlation between cross-sections was impossible therefore 3D wireframes were constructed by extrapolating the cross-sectional interpretations, like it schematically shown on the Fig. 16.2c. After that wireframes of the cross-sectional panels have been merged together forming a single wireframe which was used for construction the block model and estimating resources of the deposit (Abzalov 2010).

16.3.2 Interpolation Between Cross-Sections

Another approach of the cross-sectional estimation is based on calculating average of the adjacent cross-sections (Fig. 16.4). The volume of the panel constrained by the two adjacent sections is obtained by multiplying the average of their areas $\left(\frac{A1+A2}{2}\right)$ by the separation distance (h) (Fig. 16.4). Global volume is estimated by adding up the panels (16.3.3):

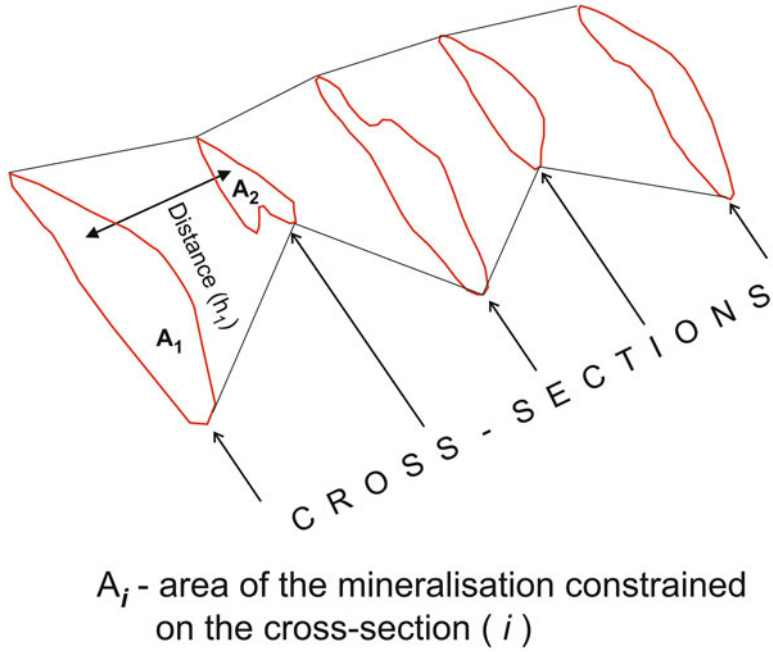

Fig. 16.4 Estimation resources by interpolation of the cross-sections

$$\text{Volume (total)} = \sum_{i=1}^{N-1}\left[\frac{1}{2}(\text{Area (i)} + \text{Area (i+1)}) * \text{h (i)}\right]$$

where N is the number of cross - sections and

h is the distance between cross sections (i) and (i + 1) (16.3.3)

The tonnage is merely a product of volume by the tonnage factor (dry bulk rock density). Average grade of the panel is estimated as average of the two cross-sections weighted by their corresponding areas (16.3.4):

$$\text{Grade (panel 1)} = \left(\frac{\text{Grade 1} * \text{Area 1} + \text{Grade 2} * \text{Area 2}}{2}\right) \quad (16.3.4)$$

where Grade_i is the grade of the cross-section (i) estimated as length weighted average of the samples located on this cross-section (16.3.1).

The overall grade of the deposit is estimated as the average of the panel grades weighted by the panel volumes (16.3.5). In the deposits where rock density is different in the different panels the average grade is estimated as the tonnage weighted average, which requires adding tonnage factor to the Eq. 16.3.5.

$$\text{GRADE (Ore Body)} = \frac{\sum_{i=1}^{N}(\text{Grade (i)} * \text{Tonnage (i)})}{\sum_{i=1}^{N}(\text{Tonnage (i)})} \quad (16.3.5)$$

where N is the number of panels,

Grade (i) is Area weighted average grade of the panel (i) (16.3.2),

Tonnage (i) is Tonnage of a panel (i) = Volume (i) * Tonnage factor (i) and

Volume (i) is Volume of the panel (i) (16.3.3)

This method is commonly used and proved to be very accurate and efficient for production control in the underground mines. It works as follows:

- the ore body and host rocks are systematically mapped and sampled on the advancing faces of the underground ore drives;
- grade and tonnage of the broken ore is estimated for each advance of the ore drive by interpolating the two rock faces, one which was mapped before face was drilled and blasted and the second is the face of the same drive which was exposed after broken ore was hauled.
- The method can also be used for estimation resources and reserves however it is usually replaced by the geostatistical estimations of the ore bodies constrained by the wireframes.

16.4 Estimation by Panels

This method was developed in USSR and officially endorsed by the Russian State's Ore Reserves Committee (GKZ) as a preferred technique for estimating reserves of the tabular ore-bodies. Estimation procedure is as follows:

- Mineralisation is projected onto 2D plan.
- The resource panels, called the resource blocks, according to GKZ nomenclature, are determined and outlined on the 2D plan (Fig. 16.5). The blocks are delineated considering geological continuity and available data. Top and/or bottom of the blocks are commonly constrained by underground drives which are sampled by channel samples (Fig. 16.5). The channel samples are collected through the regular, usually 2 – 3 m, intervals (Fig. 16.5). Sides of the blocks are open at the early stages of exploration. When project matures, in particular at the feasibility stage, the sides of the blocks are delineated by the underground raises. Internal space of the blocks is explored by drilling.
- Resources are estimated for each block by calculating length weighted average grade of the all intersections (16.4.1) and calculating average true thickness of the panel. Tonnage of the block is estimated by multiplying the area of the block on the 2D plan by its average thickness (16.4.2) and by the average dry bulk density of the mineralisation in the block.
- Samples distributed along the block contacts (e.g. drive) are used for estimation of the two blocks, located on the both sides of the given contact (Fig. 16.5)

$$\text{GRADE (Panel)} = \frac{\sum_{i=1}^{K} (G_i * L_i)}{\sum_{i=1}^{K} (L_i)} \quad (16.4.1)$$

K - number of intersections
G - Length weighted grade of intersection
L - True width (length) of intersection

$$\text{THICKNESS (Panel)} = \frac{\sum_{i=1}^{K} (L_i)}{K} \quad (16.4.2)$$

K - number of intersections
L - True width (length) of intersection

The methodology is extremely inefficient, slow, expensive and does not allow to quantify the resource uncertainty and risks. This approach is obsolete and currently is rarely used. It is described here only in order to clarify principles of the resource estimation used in USSR which can be encountered by the project geologists reviewing the old resource estimation reports in the former USSR countries.

16.5 Inverse Distance Weighting Method

The above described techniques assign equal weight to all samples independently of their distance from the estimated point (target). This disadvantage can be overcome by making sample weight inversely proportional to their distance from the point being estimated (Fig. 16.6).

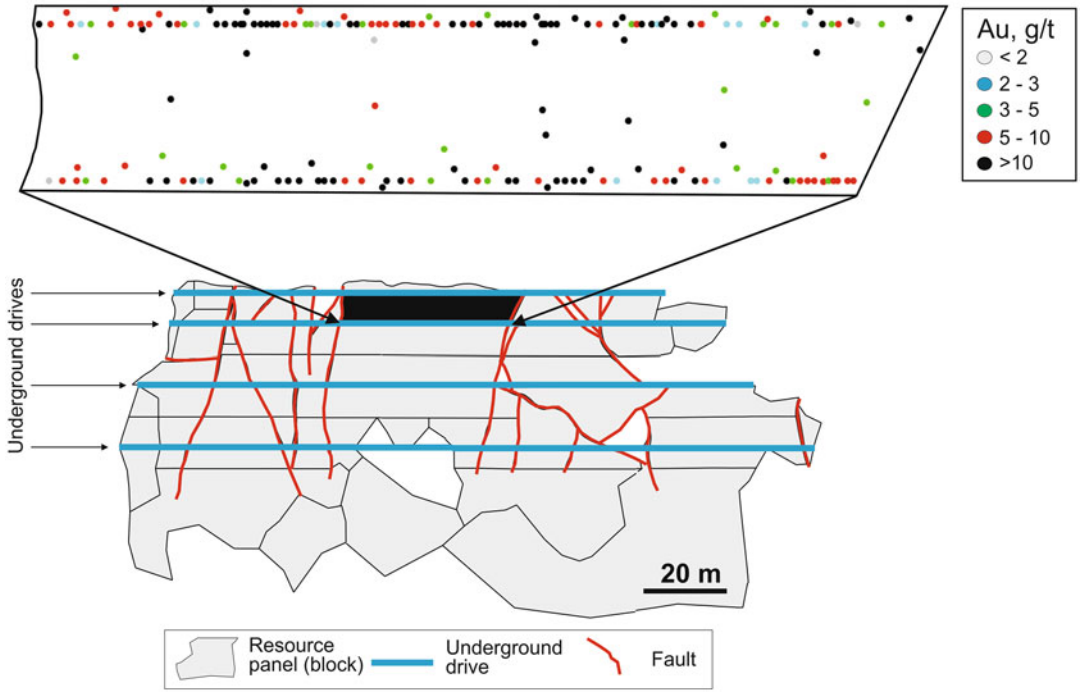

Fig. 16.5 Estimation resources by panels (blocks). Case study of the vein 1 at the Zarmitan deposit, Uzbekistan (Abzalov 2007)

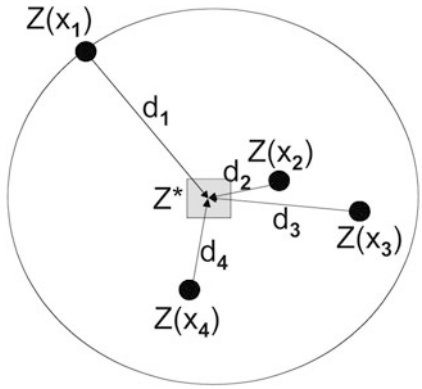

Fig. 16.6 Inverse distance weighting

This approach is used by Inverse Distance Weighing (IDW) method which estimates the sample weight inversely proportionally to a power of the sample distance from the target point (16.5.1 and 16.5.2). When power (α) approaches zero the weights become more similar, and IDW method approaches the arithmetic average of the samples. Large power (α) approaching infinite gives all weight to the closest sample and IDW approaches the polygonal estimate. In practice, the most commonly used inverse distance exponent is 2, however powers of 1 and 3 are also used for estimation mineral resources.

$$\lambda_i^{IDW} = \frac{1/d_i^{\alpha}}{\sum_i^N 1/d_i^{\alpha}}$$

λ_i^{IDW} – sample weight estimated by IDWmethod (Eq.15.5.1) for sample Z (x_i)

d_i - distance of sample Z (x_i) from the target point Z∗ (16.5.1)

α - exponent

N - number of samples included in estimation

$$Z^{*}_{\mathrm{IDW}} = \sum_{i}^{N} \left[\lambda_i^{IDW} Z(x_i)\right]$$

λ_i^{IDW} – sample weights estimated using IDW method (16.5.2)

$Z(x_i)$ - sample (i) at the location (x_i)

N - number of samples included in estimation

References

Abzalov MZ (2007) Granitoid hosted Zarmitan gold deposit, Tian Shan belt, Uzbekistan. Econ Geol 102(3):519–532

Abzalov MZ (2010) Optimisation of ISL resource models by incorporating algorithms for quantification risks: geostatistical approach. In: Technical meeting on in situ leach (ISL) uranium mining, InternationalAtomic Energy Agency (IAEA), Vienna, Austria, 7–10 June, 2010

Abzalov MZ, Menzel B, Wlasenko M, Phillips J (2010) Optimisation of the grade controls procedures at the Yandi iron-ore mine, Western Australia: geostatistical approach. Appl Earth Sci 119(3):132–142

Abzalov MZ, Drobov SR, Gorbatenko O, Vershkov AF, Bertoli O, Renard D, Beucher H (2014) Resource estimation of *in-situ* leach uranium projects. Appl Earth Sci 123(2):71–85

Annels AE (1991) Mineral deposit evaluation, a practical approach. Chapman and Hall, London, p 436

Goovaerts P (1997) Geostatistics for natural resources evaluation. Oxford University Press, New York, p 483

Krige D (1951) A statistical approach to some basic mine valuation problems on the Witwatersrand. J Chem Metall Min Soc S Afr 52:119–139

Matheron G (1963) Principles of geostatistics. Econ Geol 58(8):1246–1266

Matheron G (1968) Osnovy prikladnoi geostatistiki (Basics of applied geostatistics). Mir, Moscow, p 408 (in Russian)

Part IV

Applied Mining Geostatistics

Introduction to Geostatistics

17

Abstract

In the earth sciences in general, and, in particular, in the mineral deposits, the spatial continuity of the geological features, which can be grade of the valuable metals, concentration of the deleterious components or geotechnical characteristics of the rocks, represents natural phenomenon. Accurate estimation of these features in the unsampled location is important for evaluation the mining projects and their cost effectively exploitation.

Geostatistics is a specialised scientific discipline which offers the methodology for modelling the spatial continuity of the regionalised variables. In this chapter, the basic theoretical foundations of geostatistics are introduced to the readers and explained using examples.

Keywords

Geostatistics • Kriging • Regionalised variable • Stationarity

Geostatistics, which was developed in 1950s (Krige 1951; Matheron 1963, 1968), offers the ways of describing and modelling the spatial continuities of the regionalised variables and allows to integrate the inferred continuity parameters into the regression techniques used for their spatial interpolations.

Applications of the geostatistical techniques in mining industry is very broad and ranges from estimation of the mineral resources to assessment of the model uncertainty, quantification of the risks and determining the optimal drilling and sampling grids (David 1977, 1988; Journel and Huijbregts 1978; Isaaks and Srivastava 1989; Rivoirard 1994; Goovaerts 1997; Armstrong 1998; Deutsch and Journel 1998; Chiles and Delfiner 1999; Lantuejoul 2002; Wackernagel 2003; Rossi and Deutsch 2014).

The most commonly used by the mine geologists are the linear univariate geostatistical estimators, Ordinary Kriging (OK) and Simple Kriging (SK). The multivariate techniques, known as methods of the Co-Kriging group (Journel and Huijbregts 1978; David 1988; Goovaerts 1997), allow integrating the different types of data into a single coherent model (Wackernagel 2003; Abzalov and Pickers 2005). These methods include Ordinary co-kriging (COK) and Simple co-kriging (CSK) and their

M. Abzalov, *Applied Mining Geology*, Modern Approaches in Solid Earth Sciences 12,
DOI 10.1007/978-3-319-39264-6_17

variants, such as collocated co-kriging methods (Rivoirard 2001).

A special field represents the Indicator based technologies, in particular Multiple Indicator kriging (MIK) which is in particular effective for modelling spatial distributions and estimating resources of the deposits containing multiple generations of mineralisation showing the different spatial trends (Journel and Huijbregts 1978).

In a non-stationary environment, which for example can be characterised by presence of a drift, the commonly used methods include Kriging with Trend (KT), also called Universal kriging (UK) and more advanced estimators, such as Kriging with External Drift (KED) (Rivoirard 2002; Wackernagel 2003; Abzalov and Pickers 2005).

Geostatistical methods are also used for estimation mining recovery by constructing resource models for different cases of the mining selectivity (Rivoirard 1994; Abzalov 2006). This is made using non-linear geostatistical methods (Lantuejoul 1988). In this book the affine correction (AC) technique, discrete Gaussian change of support (DGCS), Uniform Conditioning (UC) will be presented. A more detailed description is made for Localised Uniform Conditioning (LUC), a novel method developed by Abzalov (2006). The LUC method was implemented in ISATIS (Bleines et al. 2013) and has become one of the common approaches for grade estimation when data spacing is too broad in comparison with the estimated block size (Abzalov 2006, 2014c).

Uncertainty of the geological and resource models are quantified using stochastic methods of geostatistics (Goovaerts 1997; Lantuejoul 2002; Strebelle 2002; Armstrong et al. 2011).

More recently developed stochastic geostatistical algorithms allow to create stochastic models of the geological structures which can be shape of an ore body (Strebelle 2002; Srivastava 2005) or litho-stratigraphic model of a sedimentary basin (Armstrong et al. 2011).

Because of intense using of geostatistical techniques in the mine geology applications the geological personnel working at the operating mines requires a substantially higher degree of training in the applied mining geostatistics then their colleagues from exploration offices. Therefore, a special attention is made here to geostatistics with a focus on the methods most commonly used for mine geology applications. Review of the theoretical background of the geostatistical methods is supported by discussion of the estimation practices coupled with explanation of the methods limitations. Presentation of the geostatistics is facilitated by adding several case studies and exercises.

17.1 Regionalised Variable and Random Function

Information about a particular deposit is typically very fragmentary. Therefore, to draw a conclusion regarding the unsampled locations we need to use a model and the related assumptions defining a spatial distribution of the variable of interest. Quantitative deterministic models, which require a detailed knowledge of the process, are of a little use in geology due to complexity of the geological processes.

Classical statistical methods are not suitable for this purpose because they not differentiate data by their spatial distribution patterns. Limitations of the classic statistics are demonstrated on Fig. 17.1 where shown three different sets of data.

The spatial distribution patterns of these sets of data strongly differ clearly indicating that mine geologist estimating resources of these three hypothetical mineralisations need to consider the different sampling grids and spacing between the data points. However, the histograms and statistical parameters of these three sets are very similar, clearly showing that classic statistic not distinguishing these important differences between them.

Therefore, geostatistics represents the spatially distributed variables, such as metal grades of the deposit, as a random variables fluctuating around a certain value which Matheron (1963) has called ‘drift’.

Geostatistics is based on a concept of a regionalised variable, which is a function z(x) defining

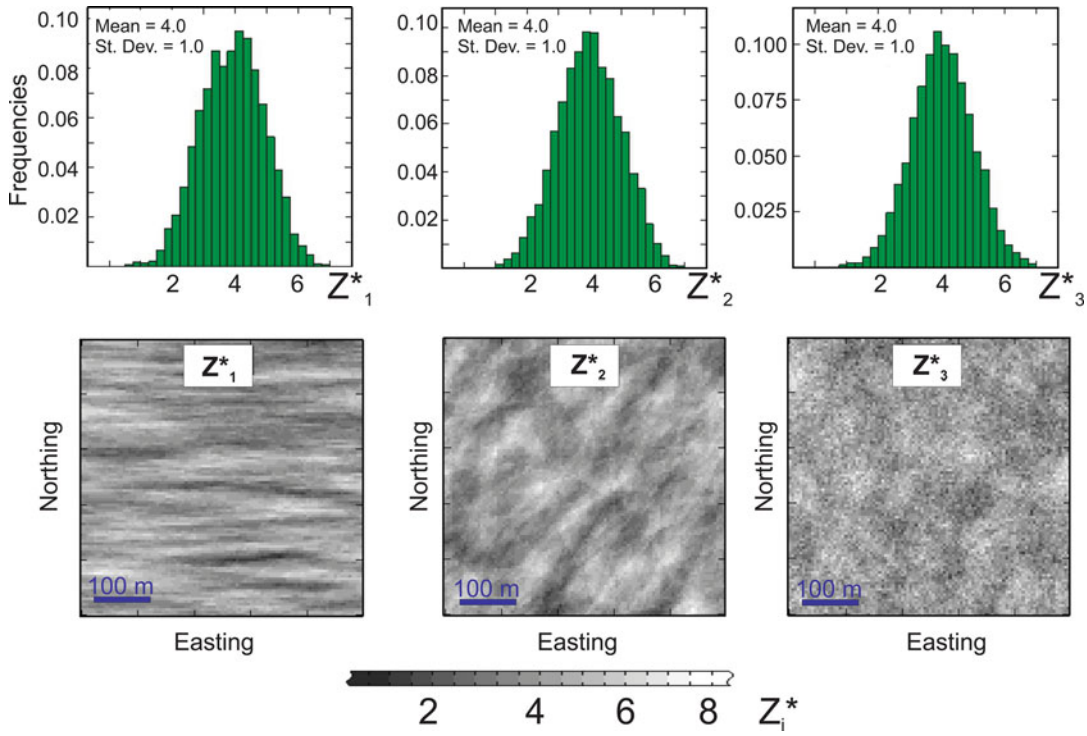

Fig. 17.1 Comparison of the histograms and spatial distribution patterns of the three simulated values

the value of a variable of interest at point (x) distributed in space (R^3). Such function is called a regionalised variable (Matheron 1963).

Distribution of the mineralisation is considered as a particular realisation of the random function Z(x). David (1977) has emphasised that decision taken by geostatisticians to consider such variables like a metal grades of the deposits as a realisation of a random function is merely an epistemological decision, when it is recognised that deterministic methods are of a little use.

Thus, our empirically available grade values distributed in a given deposit from a geostatistical point of view represents one particular realisation of that random function. A challenge faced by the geostatisticians is to find characteristics of the random function Z(x) using the special geostatistical tools, such as variogram or covariance, and integrate these characteristics into regression equations estimating the regionalised variables in the unsampled locations.

17.2 Stationarity and Intrinsic Hypothesis

A variable is considered stationary if its distribution is invariant under translations. Strict stationarity requires that all moments of distribution remain invariant under translations. This condition is very seldom found in the natural world and is difficult to verify from a limited available experimental data. From a practical point of view, the geological phenomena can be considered as a stationary if only the first two moments, mean (17.2.1) and covariance (17.2.2), are constant. This is called 'second order stationarity' and also known as 'weak stationarity' (David 1977; Journel and Huijbregts 1978; Armstrong 1998; Davis 2002).

$$\mathrm{m} = \mathrm{m}(x) = \mathrm{E}\ [\mathrm{Z}(\mathbf{x})] \tag{17.2.1}$$

$$\mathrm{C}(\mathbf{h}) = \mathrm{E}\ \{[\mathrm{Z}(\mathbf{x})\ \mathrm{Z}(\mathbf{x}+\mathbf{h})]\} - \mathrm{m}^2 \tag{17.2.2}$$

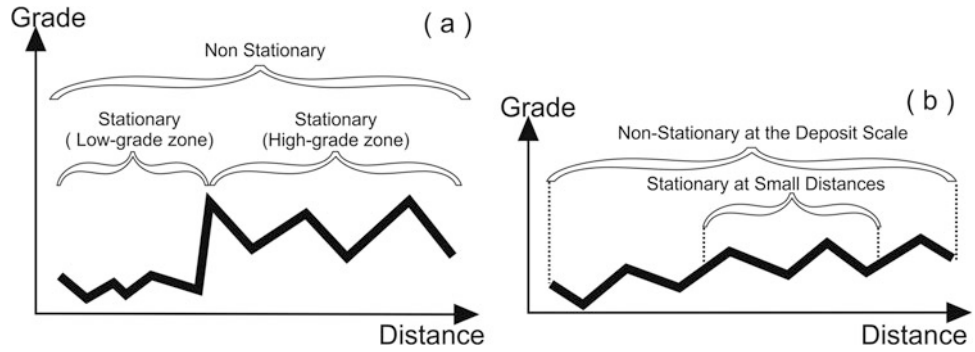

Fig. 17.2 Sketch showing distribution of a hypothetical metal grade along a line. (**a**) Two domains significantly different by their average grade values therefore deposit can not be considered a stationary whereas the high and low-grade domains when analysed separately are satisfying the stationarity conditions; (**b**) Grade distribution is not stationary at the whole deposit scale due to a distinct trend of the grade values. When grade distribution is analysed at a shorter distance it can be considered as being locally stationary

where Z(x) and Z(x + **h**) represents two values of a given variable in the two different points, (x) and (x + **h**).

This approach works well with natural phenomena characterised by non-skewed histograms. However, Krige (1951) has shown that in many deposits a finite grade variance does not exist whereas variation of the grade can be characterised by a constant first two moments. Therefore, if to consider an increment of the function, [Z(x) – Z(x + **h**)], rather than a function itself, a valid assumption regarding constant first two moments of this increment can be made. This assumption of stationarity of the first two moments of the difference between pair of values taken at two different points is known as intrinsic stationarity and leads to notion of variogram which will be discussed in the next chapter.

It is important to note that the stationary regionalised variables always satisfy the intrinsic hypothesis but the converse not always the true, as intrinsic variable can be non-stationary. Practical benefits of using an intrinsic regionalised variable is a broader choice of the possible variogram models in comparison with the cases of a second-order stationarity. In practise a decision on stationarity of a given regionalised variable is made in conjunction with consideration of the uniformity of a given deposit and the scale at which the variable can be considered stationary (Fig. 17.2).

It is very rare that the whole deposit can be considered a stationary domain. More commonly the deposit is subdivided by geologists into several relatively uniform areas (domains), which, when taken separately, satisfy stationarity or at least the intrinsic hypothesis conditions (Fig. 17.2a). Another example, presented in Fig. 17.2b shows the case where grade values exhibit a strong trend therefore are not stationary at the deposit scale. However, at the smaller distances the same variable can be considered as quasi-stationary as trend is negligible at this scale and masked by the data fluctuations (Fig. 17.2b).

References

Abzalov MZ (2006) Localised Uniform Conditioning (LUC): a new approach for direct modelling of small blocks. Math Geol 38(4):393–411

Abzalov MZ (2014) Localised Uniform Conditioning: method and application case studies. J South Afr Inst Min Metall 114(1):1–6

Abzalov MZ, Pickers N (2005) Integrating different generations of assays using multivariate geostatistics: a case study. Trans Inst Min Metall 114:B23–B32

Armstrong M (1998) Basic linear geostatistics. Springer, Berlin, p 153

Armstrong M, Galli A, Beucher H, Le Loc'h G, Renard D, Doligez B, Eschard R, Geffroy F (2011) Plurigaussian simulation in geosciences, 2nd edn. Springer, Berlin, p 149

Bleines C, Bourges M, Deraisme J, Geffroy F, Jeanne N, Lemarchand O, Perseval S, Poisson J, Rambert

F, Renard D, Touffait Y, Wagner L (2013) ISATIS software. Geovariances, Ecole des Mines de Paris, Paris

Chiles J-P, Delfiner P (1999) Geostatistics: modelling spatial uncertainty. Wiley, New York, p 695

David M (1977) Geostatistical ore reserve estimation. Elsevier, Amsterdam, p 364

David M (1988) Handbook of applied advanced geostatistical ore reserve estimation. Elsevier, Amsterdam, p 364

Davis JC (2002) Statistics and data analysis in geology, 3rd edn. Wiley, New York, p 638

Deutsch CV, Journel AG (1998) GSLIB: geostatistical software library and user's guide. Oxford University Press, New York, p 340

Goovaerts P (1997) Geostatistics for natural resources evaluation. Oxford University Press, New York, p 483

Isaaks EH, Srivastava RM (1989) An introduction to applied geostatistics. Oxford University Press, New York, p 561

Journel AG, Huijbregts CJ (1978) Mining geostatistics. Academic, New York, p 600

Krige D (1951) A statistical approach to some basic mine valuation problems on the Witwatersrand. J Chem Metall Min Soc S Afr 52: 119–139

Lantuejoul C (1988) On the importance of choosing a change of support model for global reserves estimation. Math Geol 20(8):1001–1019

Lantuejoul C (2002) Geostatistical simulation: models and algorithms. Springer, Berlin, p 250

Matheron G (1963) Principles of geostatistics. Econ Geol 58(8):1246–1266

Matheron G (1968) Osnovy prikladnoi geostatistiki (Basics of applied geostatistics). Mir, Moscow, p 408 (in Russian)

Rivoirard J (1994) Introduction to disjunctive kriging and non-linear geostatistics. Oxford Press, Claredon, p 181

Rivoirard J (2001) Which models for collocated cokriging? Math Geol 33:117–131

Rivoirard J (2002) On the structural link between variables in kriging with external drift. Math Geol 34:797–808

Rossi ME, Deutsch CV (2014) Mineral resource estimation. Springer, Berlin, p 332

Srivastava RM (2005) Probabilistic modelling of ore lens geometry: an alternative to deterministic wireframes. Math Geol 37(5):513–544

Strebelle S (2002) Conditional simulation of complex geological structures using multiple-point statistics. Math Geol 34(1):1–22

Wackernagel H (2003) Multivariate geostatistics: an introduction with applications, 3rd edn. Springer, Berlin, p 388

Variography

18

Abstract

Geostatistical techniques allow a quantitative assessment of the spatial continuity of the regionalised variable. Most commonly used approach is based on estimating the squared difference between pairs of the data points separated by a vector (**x**). This is a basis of the variogaram, which is a special geostatistical tool applied for modelling the spatial continuity of the studied variables.

Keywords

Measures of continuity • Variogram • Anisotropy • Indicators

18.1 Quantitative Analysis of the Spatial Continuity

A geologist describing a given deposit intuitively uses the concept of continuity. In particular, definition of the strike of mineralisation implies that mineralisation is more continuous in that direction than in other. It is also well known to mine geologists that high-grade gold mineralisation is usually more discontinuous and erratically distributed than lower-grade halo surrounding high-grade shoots. Experienced geologists documenting the geological structures see similarities and differences of the same geological characteristics when they have been observed at the different locations and have a "feelings" regarding how quickly they change in different directions.

Geostatistical techniques allow a quantitative assessment of the spatial continuity of the different attributes of mineralisation which from geostatistical point of view represent the regionalised variables. This section introduces the geostatistical tools used for structural analysis of regionalised variables.

The variogram is the most common geostatistical tools used in mining industry for quantitative definition of the spatial continuities of the various geological attributes such as mineralisation grades, metal accumulations, thicknesses of mineralised zones (Journel and Huijbregts 1978; Goovaerts 1997). This section overviews the theoretical definition of variograms and their properties. The practical problems frequently encountered when calculating the experimental variograms will be discussed in the following

M. Abzalov, *Applied Mining Geology*, Modern Approaches in Solid Earth Sciences 12,
DOI 10.1007/978-3-319-39264-6_18

sections together with case studies showing the different geological applications of variography analysis.

18.2 Intuitive Look at Variogram

The most natural way to compare two values of a given variable, Z(x) and Z(x + **h**), which was collected from two different points, say (x) and (x + **h**) (Fig. 18.1), is to calculate their difference, [Z(x) − Z(x + **h**)]. This typically can be two samples collected from different parts of ore body and assayed for a metal grade. Comparison of just two particular points has little relevance; geologists would be more interested in definition of the general tendency for grades to be similar or dissimilar at a given distance in a given direction. Thus, it is necessary to calculate the average differences between all possible points (x) and (x + **h**). This will provide a reasonable indication of the similarities between data separated by a vector (**h**).

A schematic example presented in Fig. 18.2 shows 10 data points distributed along a line and separated by a regular distance. When we calculate the average difference between all possible data points separated by a distance (h) (Fig. 18.2), we will calculate average of the 8 possible pairs.

Each of the data pairs, Z(x) and Z(x + **h**), separated by a given increment (h), can be plotted on a scatter diagram which allows to visually assess similarities and dissimilarities between the data when they are separated by a given distance (Fig. 18.3). These scatter diagrams of Z(x) vs. Z(x + **h**) are known as h-scatter plots (Isaaks and Srivastava 1989).

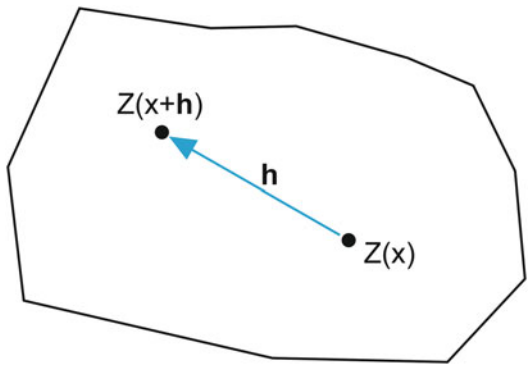

Fig. 18.1 Sketch showing two hypothetical values of the regionalised variable (Z) observed at two different locations (x) and (x + h), which are separated by a vector (h)

It is more convenient to work with positive values which can be easily obtained if the squared differences are calculated. This leads to the formula which is used in most of the geostatistical applications for assessment of the spatial similarity or dissimilarity of regionalised variable values (18.2.1).

$$\gamma(\mathbf{h}) = \frac{1}{2N}\sum_{i=1}^{N}\left\{[Z(x_i + \mathbf{h}) - Z(x_i)]^2\right\} \tag{18.2.1}$$

where (N) is the number of data pairs separated by a vector (**h**). The function [γ (**h**)] defined in equality 18.2.1 is called semivariogram, or variogram for short. Changing the vector (**h**), its size and direction, we can quantify the overall distribution pattern of a given regionalised variable by calculating the variogram values corresponding to a given direction and size of the vector (**h**). As the dissimilarity calculated using equality 18.2.1 is a squared quantity it is independent of a sign of the vector (**h**), therefore the variogram (18.2.1) is symmetric with respect to (**h**).

The values of a variogram calculated along a chosen direction can be plotted against the distance (h). This is a traditional way of presenting the variogram values (Fig. 18.4) when all information is synthesised into a single point per a distance class. Alternative approach is known as plotting the variogram cloud (Chauvet 1982; Armstrong 1998). In this case the squared difference of each data pairs is plotted against the distances (Fig. 18.5).

To assure that variogram cloud is comparable with the variogram the calculated squared differences between data pairs are halved before they are plotted as a variogram cloud (Fig. 18.5). In practise, the experimental variograms are calculated at the regular increments (**h**), called lag of the variogram.

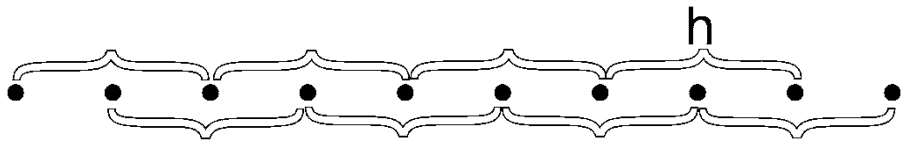

Fig. 18.2 Sketch showing all possible data points separated by the distance (h)

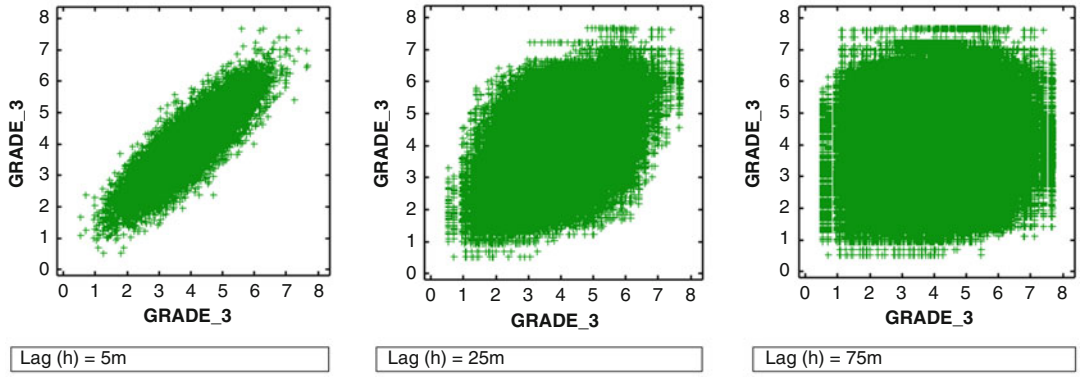

Fig. 18.3 h-scatter plots comparing sample grades at the three different distances (h)

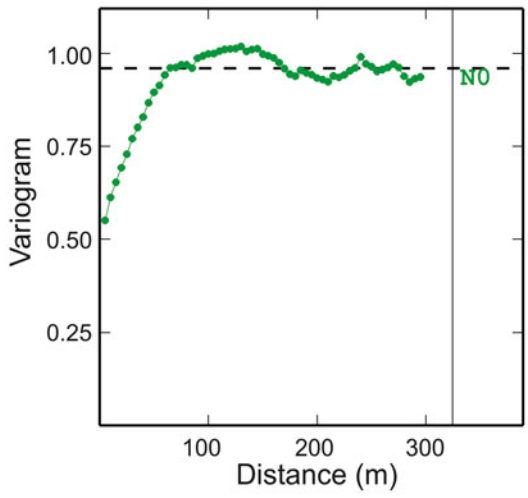

Fig. 18.4 Experimental variogram. *Horizontal dashed line* denotes the sample variance

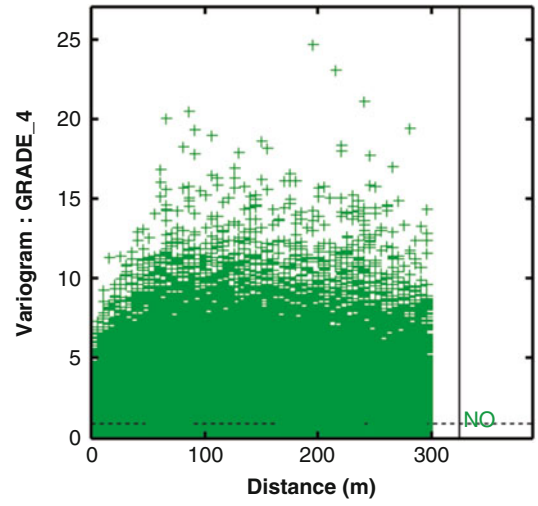

Fig. 18.5 Diagram showing the variogram cloud

18.3 Geostatistical Definition of Variogram

The experimental variogram [γ (**h**)] of the regionalised variable {Z(x)} is a discrete function which describes a spatial continuity of this variable {Z(x)} as a function of direction and distance. In other words, it represents a measure of a spatial dissimilarity between the data points expressed as a function of increasing data separation vector (**h**) and is calculated as half of the squared difference between data points separated by the given vector (**h**).

Theoretical variogram is defined by an intrinsic hypothesis (Journel and Huijbregts 1978;

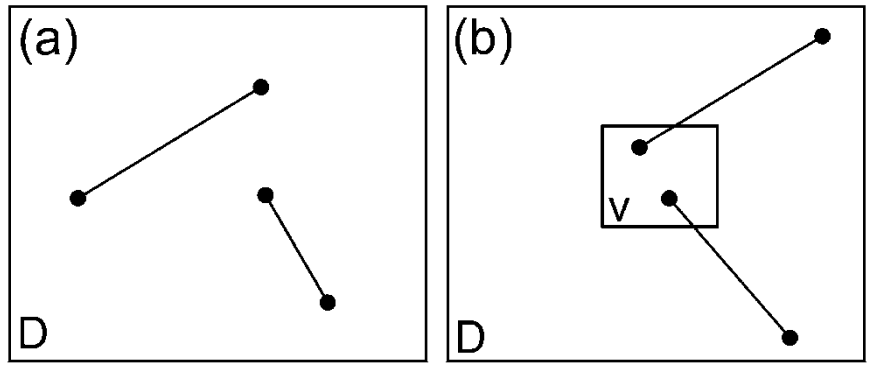

Fig. 18.6 Sketch explaining calculations of the average variograms for the given volumes: (**a**) variogram model averaged over all possible vectors within domain (D); (**b**) the average variogram between two points when one is sweeping inside the block (v) and another is sweeping independently within the domain (D)

Wackernagel 2003). This hypothesis is characterising the type of stationarity and it is based on two assumptions regarding the properties of the increment $[Z(x) - Z(x + \mathbf{h})]$. At first it is assumed that variance of increments has a finite value equal to $[2\gamma(\mathbf{h})]$. This assumption, expressed as equality (18.3.1), defines the variogram as half of variance of the increment $[Z(x) - Z(x + \mathbf{h})]$. Second assumption is that mean of the increment is invariant for any translation of a given vector ($\mathbf{h}$) and is equal to zero (18.3.2).

$$\gamma(\mathbf{h}) = {}^{1}\!/_{2}\ \mathrm{Var}\ [Z(\mathbf{x}) - Z(\mathbf{x} + \mathbf{h})] = {}^{1}\!/_{2}\ \mathrm{E}\left\{[Z(\mathbf{x}) - Z(\mathbf{x} + \mathbf{h})]^2\right\} \tag{18.3.1}$$

$$\mathrm{m}(\mathbf{h}) = \mathrm{E}\ \{[Z(\mathbf{x}) - Z(\mathbf{x} + \mathbf{h})]\} = 0 \tag{18.3.2}$$

18.4 Directional, Omnidirectional and Average Variograms

Variogram can be calculated along a certain direction. In that case it is called a directional variogram. Conversely, if the variogram is calculated between any data points separated by the distance (h) independently of the direction between the data pairs it is called omnidirectional variogram.

The variogram values can be averaged over all possible vectors contained within the given volumes. Two types of the average variograms are presented on the Fig. 18.6. The first type (Fig. 18.6a) when the average variogram value is calculated for all possible vectors contained within the block (D).

The second type of the average variograms is obtained by averaging the variogram values calculated between two points when one is sweeping inside the block (v) and another is sweeping independently within the larger block (D) (Fig. 18.6b).

The average variogram values in a given block (D) are usually denoted as $\overline{\gamma}(D, D)$ or simply $\overline{\gamma}(D)$ and is read a 'gamma-bar of DD'. Second type of the average variogram is denoted as $\overline{\gamma}(v, D)$.

The average variogram values are also known as the auxiliary functions (Journel and Huijbregts 1978). In particular, the variogram model averaged over all possible vectors contained within the block (D) is called F-function.

18.5 Properties of the Variograms

The graphs of the variogram ($\gamma(\mathbf{h})$) values plotted versus the (h) distances generally present the following features. At the origin ($h = 0$) the

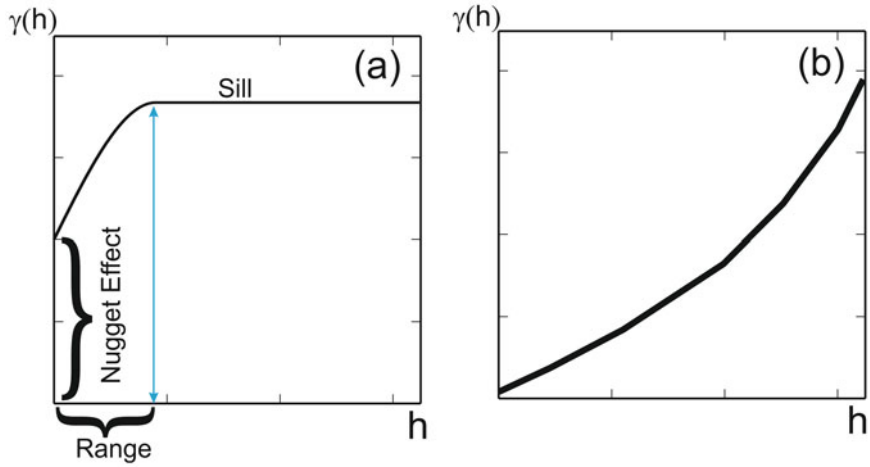

Fig. 18.7 Sketch explaining the variogram types: (**a**) bounded variogram; (**b**) unbounded variogram

variogram value equal zero, however it can be discontinuous just after the origin (Fig. 18.7a). This discontinuity at the origin is called a nugget effect. The graph generally increases with (h). It can continuously increase with the distance (h) increasing or, alternatively, it can stabilise and flatten out at a certain level, called 'sill' (Fig. 18.7a). After variogram has reached its sill it means that there is no correlation between the samples separated by that distance at which variogram has flattened out. Distance at which the variogram reaches its sill is called the range. Therefore, the range gives a precise quantitative meaning to a geological concept of 'zone of influence' of a sample.

Variograms, which reach a sill are called bounded variograms (Fig. 18.7a). Conversely, if the variogram continuous to increase and not flattening it is called unbounded variogram (Fig. 18.7b).

18.5.1 Behaviour Near Origin

Behaviour of the variogram near its origin is one of the most important characteristics of the variograms bearing crucial information regarding spatial continuity of the regionalised variables. The variograms can be subdivided (Journel and Huijbregts 1978; Armstrong 1998) according to their possible behaviour types in four groups (Fig. 18.8): very continuous, moderately continuous, discontinuous and purely random.

Very continuous variables are characterised by a parabolic behaviour of the variogram near its origin (Fig. 18.8a). This feature is indicative of a highly continuous regionalised variable, such as elevation of the water table, characterising by very small variability at a short range. It also can be associated with the presence of a drift.

A linear shape (Fig. 18.8b) of the variogram is a characteristic of a moderately continuous regionalised variable, which is less regular than the variables characterising by parabolic behaviour near origin (Fig. 18.8a). Linear behaviour of the variograms near origin is a common characteristic of the continuous mineralisations such as thicknesses of the sedimentary seams.

Variograms which are discontinuous at origin (Fig. 18.8c) are the most common type found in the studies of the mineral deposits (David 1977; Journel and Huijbregts 1978; Guibal 2001). This discontinuity at the origin, when variogram (γ (**h**)) does not tend to zero with (**h**) approaching zero (Figs. 18.7a and 18.8c), indicates to a highly irregular behaviour of this variable at a short distance. This discontinuity, called 'nugget effect', is caused by sampling errors and also reflects the microstructures, whose continuity is shorter than the smallest distance between the samples.

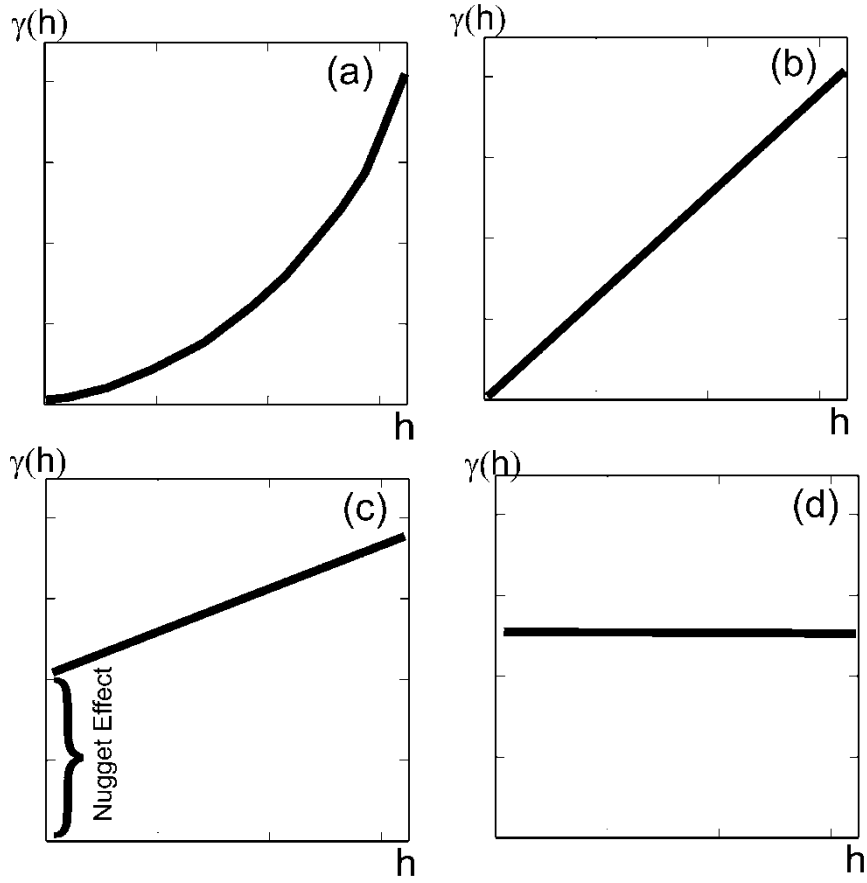

Fig. 18.8 Behaviour of the variogram near origin: (**a**) parabolic shape of highly continuous variable; (**b**) linear shape of a moderately continuous variable; (**c**) discontinuous variable; (**d**) a flat curve indicating a pure random behaviour of the regionalised variable

Some variograms are distributed as flat lines which is indicative of an extremely discontinuous and irregularly distributed variable which is characterised by completely random, chaotic behaviour without any spatial correlation. This type of variogram, which is called a pure nugget effect, is often exhibited by a coarse grained (i.e. nuggetty) gold mineralisation (Bendigo).

18.5.2 Anisotropy

Sill and range of the variogram can vary in the different directions reflecting presence of anisotropy. A very common situation when a regionalised variable is more continuous along one particular direction than in other. This can be the metal grades of a stratiform mineralisation which usually are more continuous in the horizontal directions than vertically (Abzalov and Mazzoni 2004; Abzalov and Bower 2014). Contacts and thicknesses of the sedimentary seams also often appear as anisotropic distributions being more continuous along one preferred direction (Fig. 18.9). Variograms of such variables when calculated in the different directions will reach the same sill however at different ranges (Fig. 18.9). This type of anisotropy is called geometric or elliptical anisotropy as the relationships between the variogram ranges calculated in the different directions satisfy the equation of ellipse (Armstrong 1998).

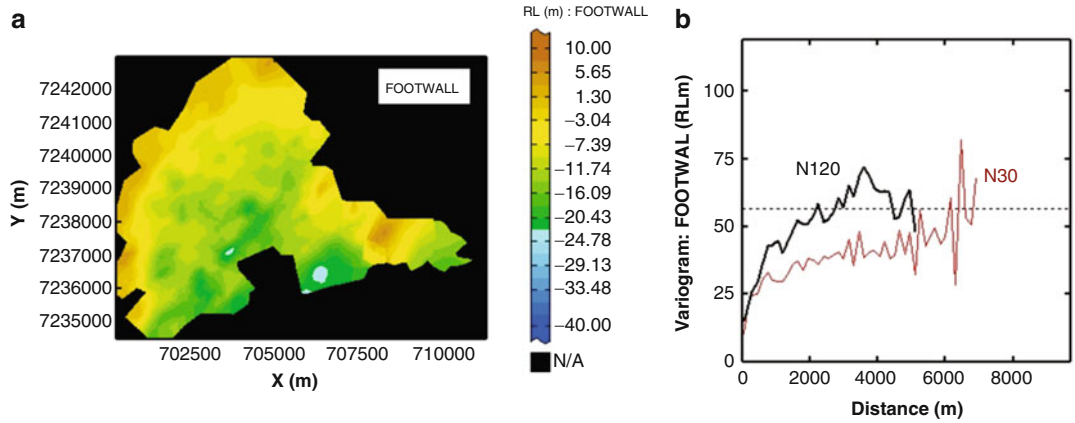

Fig. 18.9 Footwall contact of the Fort Dauphin Ti-rich sands deposit, Madagascar: (**a**) map of the footwall contact; (**b**) experimental directional variograms of the footwall elevation (RLm) calculated along two directions, N30 and N120, exhibiting the geometric anisotropy. N30 (azimuth 030°) represents direction of the long axes of the trough-like basins in the footwall of the mineralised dunes coinciding with the strike of the dunal complexes. Direction N120 (azimuth 120°) is the direction oriented across the strike of the dunes

Definition and quantification of the geometric anisotropy is one of the most important tasks of the variography analysis, having important geological implications (Guibal 2001).

Another type of anisotropy is represented by mineralisation whose variance differs in the different directions. For example, layered mineralisation is often exhibiting more variations between strata than within them. The variogram sills of this type mineralisation differ in the different directions (Fig. 18.10). This anisotropy is called zonal or stratified anisotropy.

18.6 Analysis of the Data Continuity Using a Variogram Map

Variography significantly improves the structural analysis allowing to quantitatively determine the continuities of the regionalised variable in the different directions. This quantification of the spatial anisotropy can be facilitated by presenting it as a special diagram, called the variogram maps (Isaaks and Srivastava 1989). The variogram map is a 2D diagram showing the variogram values calculated along the different directions laying in a given plan, known as a reference plan (Fig. 18.11).

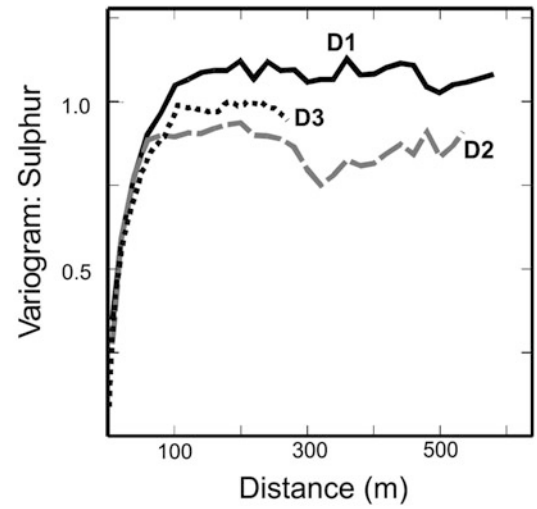

Fig. 18.10 Three experimental directional variograms (D1, D2 and D3) of the sulphur grades in the Australian Cu-deposit. Variograms show a distinct zonal anisotropy (Modified after Abzalov and Pickers (2005))

The reference plan represents a planar structure controlling mineralisation, such as sedimentary strata or shear zone. Variogram map presented on Fig. 18.11 was constructed for footwall elevations shown in the Fig. 18.9.

Centre point of a variogram map represents the variograms origin ($\mathbf{h} = 0$) and directions are determined in the same way as on any geographic

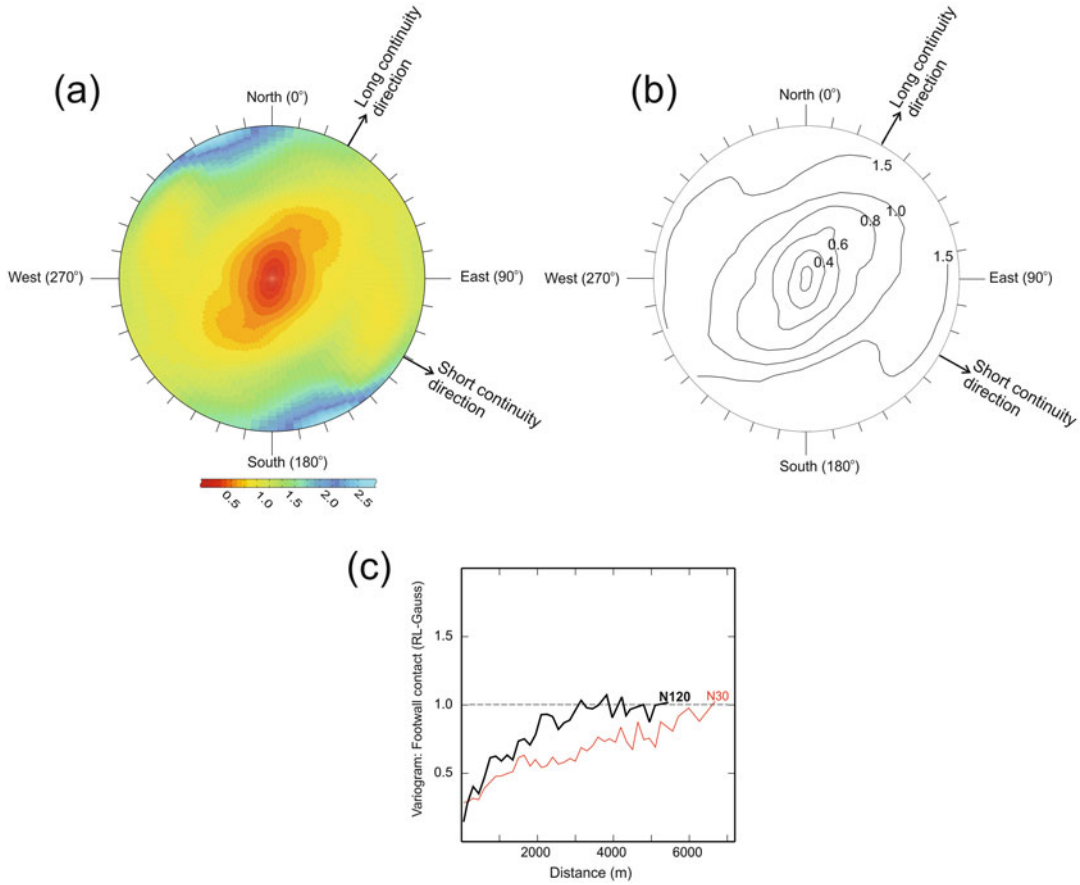

Fig. 18.11 Variogram map of the footwall topography elevation values shown on the Fig. 18.9: (**a**) colour variogram map; (**b**) contour map constructed by drawing isolines through the matching variogram values; (**c**) variograms calculated along the long (Azi 30°) and short (Azi 120°) continuity directions deduced from the variogram map

map, with vertical up direction representing a direction to the North (0°N) and horizontal to the right direction being a direction to the East (90°N) and so on. The variogram values are calculated for the different vectors (**h**) assuring a comprehensive spatial coverage. In practise, the variograms are calculated for 18 or 36 directions, combining data by 20° or 10° sectors respectively. In each directions the variograms are calculated for the different distances. The shortest distance approximately matches a smallest distance between the data points and a largest distance plotted on the variogram map should exceed the longest variogram range obtained for a direction of a highest spatial continuity of a studied variable.

The map is constructed by showing the different variogram values in colours (Fig. 18.11a) or, conversely, by drawing the isolines through the matching values (Fig. 18.11b). Geometric (elliptical) anisotropy is presented on the variogram maps as ellipse which long axis is oriented along the main continuity direction, which commonly is a strike of ore body and short axis is a direction of a highest variability, commonly is a direction across the strike of ore body (Fig. 18.11c).

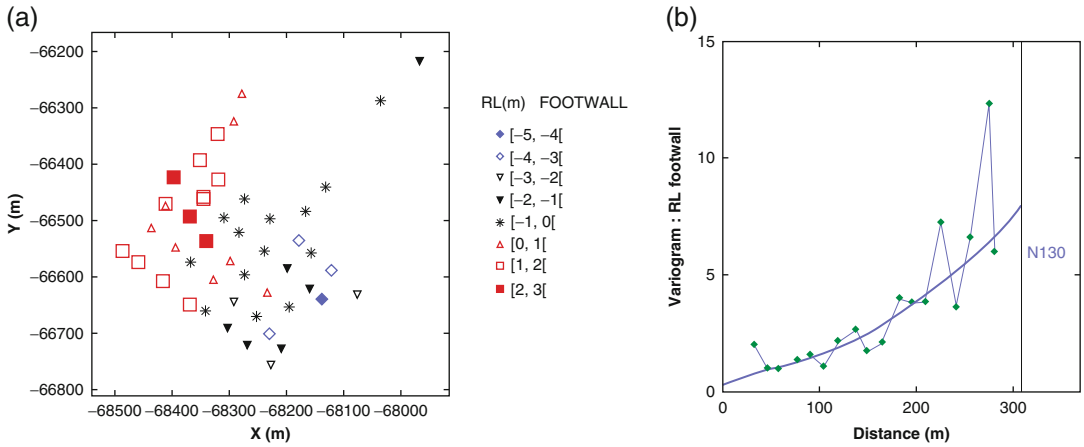

Fig. 18.12 Effect of a data drift on variogram: (**a**) map showing location of the data points; (**b**) variogram of the footwall elevation calculated in the south-eastern direction (azimuth 130°)

In order to obtain a 3D picture of the spatial anisotropy of the given variable the similar maps can be constructed in the three orthogonal plans.

18.7 Presence of Drift

Variogram values can continue to increase with distance. This is a characteristic feature of the unbounded variogram (Fig. 18.7b), however in that cases the variograms at the large lags (h) grow slower than square of the distance. In other words variogram will grow slower than a parabolic function.

In practice, the variograms can grow faster than square of the distance (Fig. 18.12). Such behaviour of the variogram is indicative of a different phenomenon, and namely the presence of the drift expressed as a regular continuous changes of the values of regionalised variable in the certain geographic directions. Example presented in Fig. 18.12a clearly shows a systematic increase of elevation of the footwall contact when we move from the south-eastern margin of the mineralised unit to the north-west. This trend is reflected in the parabolic shape of the variogram at the distances exceeding 100 m.

18.8 Proportional Effect

Local variance of the data can change across the study area. A special case when this local variance is correlated with the local mean is called (Journel and Huijbregts 1978) the 'proportional effect'. It can be direct, when local variance increases with the local mean, and inverse, when higher variance is related to the lower local mean grades. Direct proportional effect is observed in positively skewed data whereas inverse effect often found in the negatively skewed variables.

To test for presence of the proportional effect the local means and variances are calculated by grouping data and estimating local mean and variance. The procedure is shown on the Fig. 18.13. The bauxite deposit is divided on the regular size blocks (Fig. 18.13a) and the local means and variances are calculated within each block and plotted on scatter-diagram (Fig. 18.13b, c).

When proportional effect is combined with data clustering due to preferential sampling of the high-grade areas it can cause distortions of the variograms and complicate their interpretations (Goovaerts 1997). Indeed, closer sampling of the

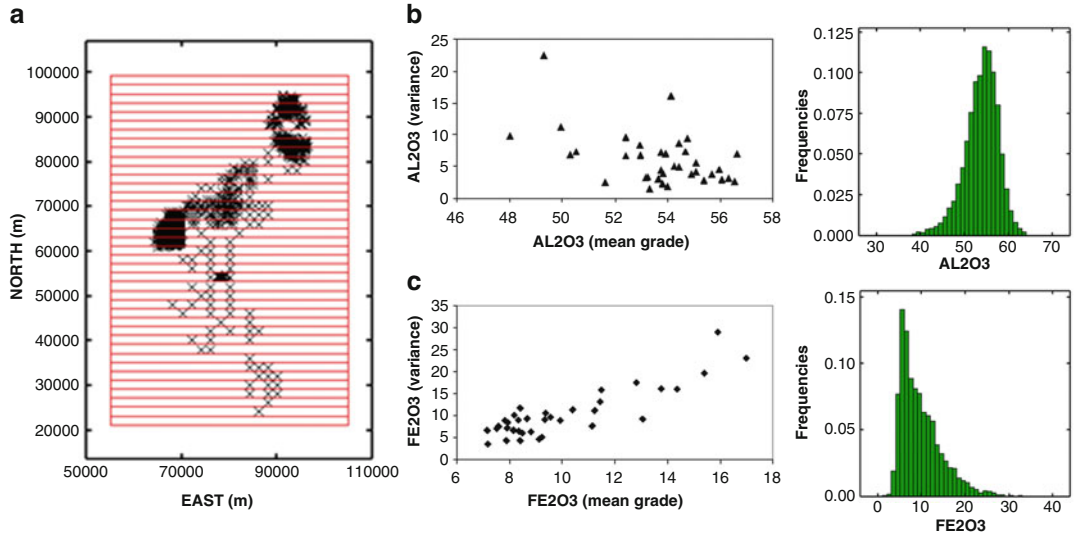

Fig. 18.13 Proportional effect determined at the bauxite deposit, Australia: (**a**) location map. Data are grouped by 2000 m thick panels drawn across the entire deposit; Scatter-diagrams of sample variance vs. mean demonstrating the proportional effect and histograms of the data constructed for (**b**) Al_2O_3 and (**c**) Fe_2O_3

high-grade areas can have the result that the variogram at small lags (**h**) are higher then at the larger lags, as the local variance of these high-grade areas, which are making the main contribution to the variogram values at small lags, is also higher than in other parts of the deposit.

In general, when proportional effect is combined with the data clustering it can lead to overestimation of the relative nugget effect and cause the incorrectly defined short range structures. In the worst cases the combination of the proportional effect and preferential sampling of the high-grade areas can create an uninterpretable variograms resembling that of the spatially uncorrelated variables.

Declustering of the data can improve the variograms of such variables. However, this improvement is coming at the expense of losing an important short range information. Another approach consists of calculating the relative variograms when the variogram values are normalised to the mean values of the data pairs.

18.9 Variogram Sill and the Sample Variance

In the technical literature the variogram plots often contain an additional horizontal line denoting the sample variance (Fig. 18.4). In practise, some resource geologists and geostatistitians try to force the sills of the variogram models to be equal to this value. In particular, David (1977) has stated that 'the sill of the variogram is equal to the variance of the samples in the deposit'.

Relationships between the variogram sills and the sample variances has been studied in details by Barnes (1991) who concluded that expected value of the sample variance is equal to the average variogram value encompassing all (N^2) possible pairs of the (N) available samples distributed in a given volume (V). This relationship is summarised as equality (18.9.1) clearly showing that the expected value of the sample variance $E(\sigma^2)$ depends on the data configuration and entire variogram not just the variogram sill.

$$\mathrm{E}\left(\sigma^2\right) = \overline{\gamma}\left(V, V\right) = \frac{1}{N^2}\sum_{i=1}^{N}\sum_{j=1}^{N}\gamma\left(\mathbf{x}_i, \mathbf{x}_j\right) \tag{18.9.1}$$

When the sides of the block (V) are significantly larger then the variogram ranges, the average value of the variogram $[\overline{\gamma}\,(\mathrm{V}, \mathrm{V})]$ between all possible data points distributed in this block will be the average of the values equal to the sill with a fewer values less than the sill. In this case, the average variogram value is matching the variogram sill (Journel and Huijbregts 1978). In this case the sample variance is a reasonable estimate for the variogram sill (18.9.2)

$$\overline{\gamma}\left(\infty, \infty\right) = \gamma\left(\infty\right) = \sigma^2, \tag{18.9.2}$$

where $[\sigma^2]$ is a point variance of a given regionalised variable $[Var\,(Z\,(\mathbf{x}))]$.

Conversely, if volume (V) is small, being equal or even less than the variogram range then the average variogram value will be the average of many values less than the sill with a few values equal to the sill. In this case the sample variance, which according to equality 18.9.2 is equal to the average value of the variogram, will significantly underestimate the variogram sill. The opposite relationships when the sample variance is larger than the variogram sill are also common (Barnes 1991). In particular, this is frequently observed in the variables exhibiting the direct proportional effect combined with the preferred sampling of the high-grade areas.

In general, it is suggested (Barnes 1991) to use the sill of the experimental variogram as an approximate estimate of the population variance, and that the sample variance should not be used as an estimate of the variogram sill.

18.10 Impact of the Different Support

Regionalised variables such as metal grades distributed in a given deposit can be defined at the different volumes. For example, the drill core samples, whose length varies from 1 to 2 m, are usually composited for resource estimation purposes to a larger composites, often matching a height of the open pit benches, which can be 15 m and larger. Mine planning team uses grades of the blast hole samples and the SMU size blocks estimated using the blast hole data. These different volumes, drill core samples, composites, blast holes and SMUs represent the different volume supports, colloquially referred to as support.

Variograms calculated at the different support noticeably differ by their global sills however are characterised by the similar ranges (Fig. 18.14). Variogram $[\gamma_V(\mathrm{h})]$ calculated at the block (V) support and variogram of the same variable calculated at the point support $[\gamma(\mathrm{h})]$ are related by equation (18.10.1) when distance (h) is large compared to size (V) (Armstrong 1998).

$$\gamma_V\left(\mathbf{h}\right) = \gamma\left(\mathbf{h}\right) - \overline{\gamma}\left(\mathrm{V}, \mathrm{V}\right) \tag{18.10.1}$$

When the block (V) is very small, being smaller than the shortest lag of the variogram the average value of the variogram in such small block (V) will be equal to the nugget effect of the sample variogram $[\gamma(\mathrm{h})]$. In this case, to derive the regularised variograms corresponding to these very small blocks (V) it is sufficient simply to subtract the nugget value from the sample variogram.

18.11 Variogram Models

Variography analysis requires fitting a mathematical function (model) to experimentally calculated variograms. There are several admissible models which can be used for approximating the experimental variograms (Journel and Huijbregts 1978; Goovaerts 1997; Chiles and Delfiner 1999; Wackernagel 2003).

18.11.1 Common Variogram Models

The variogram models most commonly used in the mining industry for mathematically presenting a spatial continuity of the geological fea-

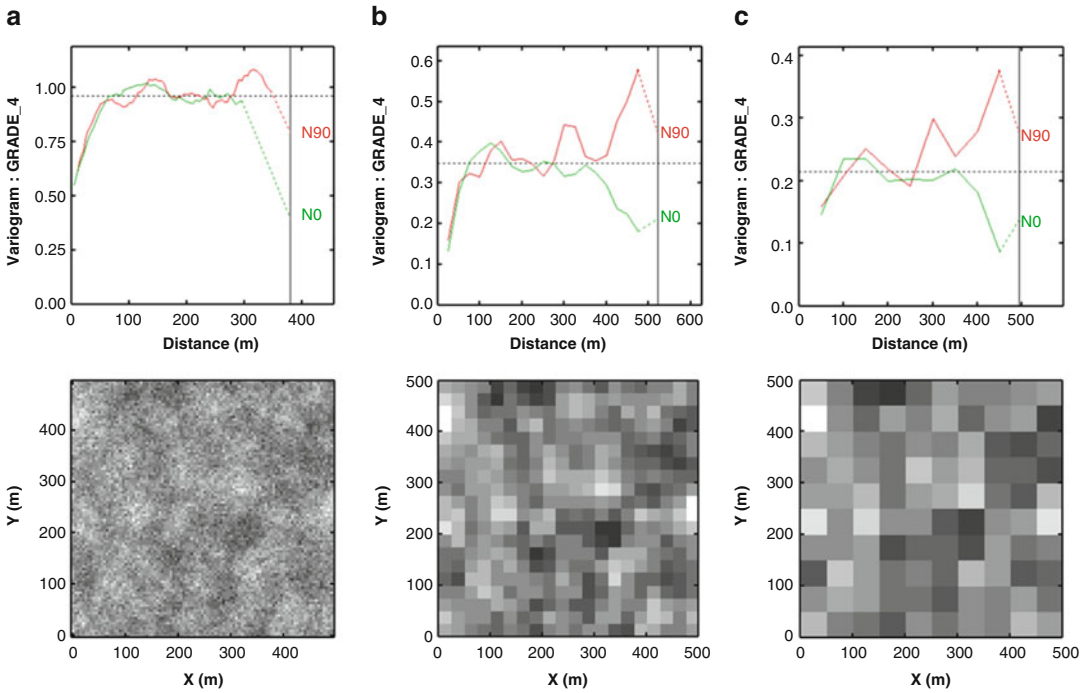

Fig. 18.14 Directional variograms and maps of the simulated variable: (**a**) simulated point data; (**b**) points grouped into 25 m × 25 m blocks; (**c**) points grouped into 50 m × 50 m blocks

tures and metal or mineral grades are nugget effect, spherical, linear, power, exponential and Gaussian models. Mathematical formulation of these models is shown in the equalities (18.11.1, 18.11.2, 18.11.3, 18.11.4, 18.11.5, and 18.11.6).

$$\text{Nugget effect}: \ \gamma(\mathbf{h}) = \begin{cases} 0. & \text{for } |\mathrm{h}| = 0 \\ \mathrm{C}\ (\text{constant}), & \text{for } |\mathrm{h}| > 0 \end{cases} \tag{18.11.1}$$

$$\text{Spherical}: \ \gamma(\mathbf{h}) = \begin{cases} \mathrm{C}\left[\dfrac{3\,|\mathbf{h}|}{2\boldsymbol{a}} + \dfrac{|\mathbf{h}|^3}{2\boldsymbol{a}^3}\right], & \text{for } 0 \le |\mathrm{h}| \le \boldsymbol{a} \\ \mathrm{C}\ (\text{constant}), & \text{for } |\mathrm{h}| > \boldsymbol{a} \end{cases} \tag{18.11.2}$$

where (a) is range of the variogram and (C) is sill.

$$\text{Power}: \ \gamma(\mathbf{h}) = \omega\ |\mathrm{h}|^{\lambda}, \ \text{with} \ \ 0 < \lambda < 2 \tag{18.11.3}$$

$$\text{Linear}: \ \gamma(\mathbf{h}) = \omega\ |\mathrm{h}| \tag{18.11.4}$$

Metal grades are best described by spherical, exponential and linear models (Fig. 18.15) therefore these variograms are most commonly used by geologists for estimating resources of the mineral deposits.

Linear model represents a particular case of a power model when power index (λ) is equal to one. In this case the variogram is simply proportional to the distance (h).

$$\text{Exponential}: \ \gamma(\mathbf{h}) = \mathrm{C}\left[1 - \exp^{\frac{-|\mathrm{h}|}{\mathrm{a}}}\right] \tag{18.11.5}$$

Practical range, at which the exponential variogram reaches the 95 % of sill (C), is equal to (3a).

$$\text{Gaussian}: \ \gamma(\mathbf{h}) = \mathrm{C}\left[1 - \exp^{\frac{-|\mathrm{h}|^2}{\mathrm{a}^2}}\right] \tag{18.11.6}$$

Gaussian model describes the extremely continuous variables such as topography of the gently

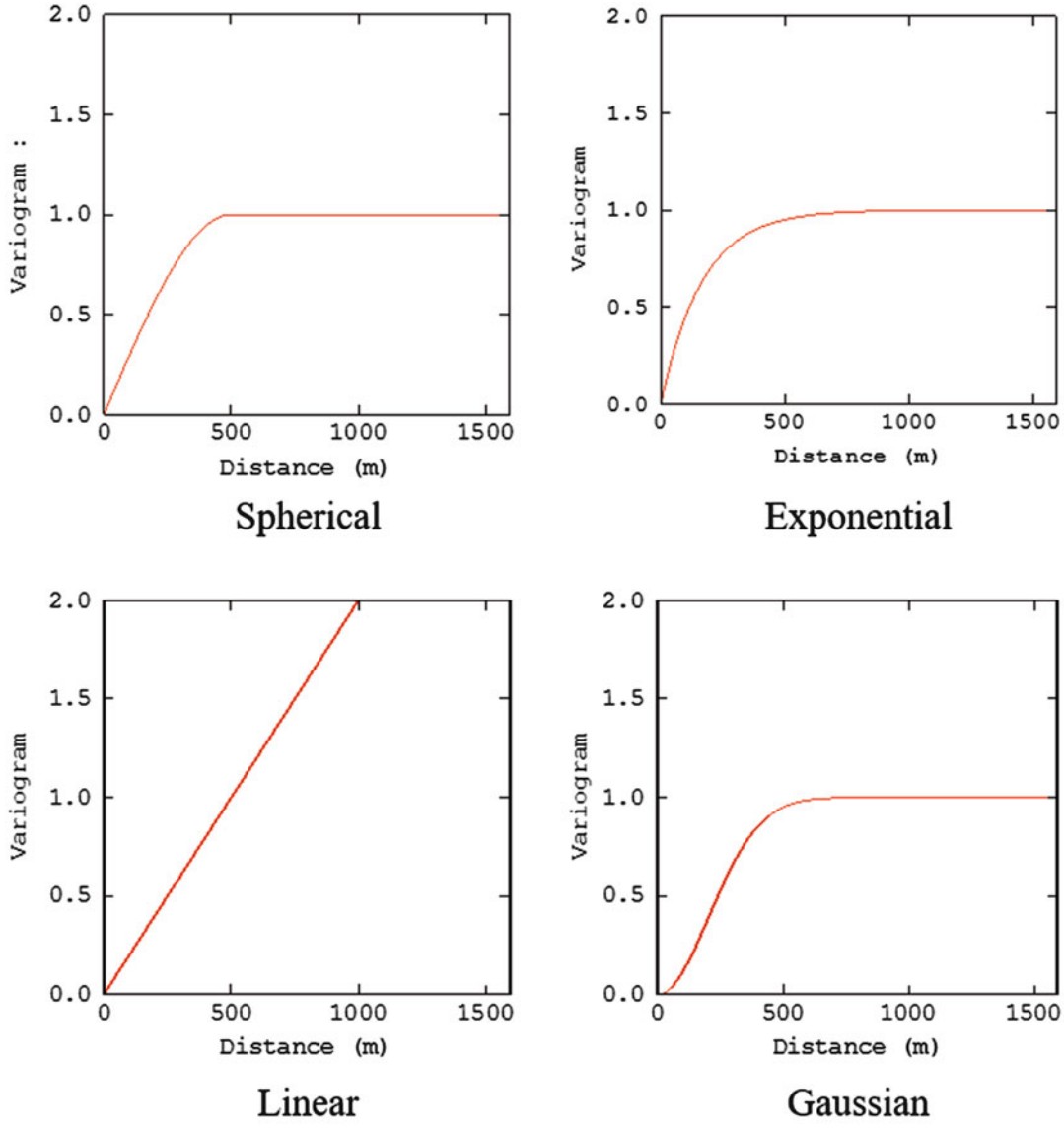

Fig. 18.15 Graphical presentation of the common variogram models

undulating hills (Fig. 18.15). Practical range, at which the variogram reaches the 95 % of sill (C), is equal to (1.73a).

18.11.2 Modelling Geometric Anisotropy

Relationships between variogram model (γ_1) calculated in any given direction (1) coinciding with the coordinate axes, and the overall variogram ($\gamma_2(\mathbf{h})$) in any new direction (2) is defined by equality 18.11.7 (Armstrong 1998).

$$\gamma_2(\mathbf{h}) = \gamma_1 \left\{ \sqrt{\left[(x_1 - x_2)^2 + k^2(y_1 - y_2)^2\right]} \right\} \tag{18.11.7}$$

where (x) and (y) are the coordinates of a vector (**h**) and the $k = \frac{\text{Range 1}}{\text{Range 2}}$. Coefficient (k) is called an anisotropy ratio. In case of a linear variogram

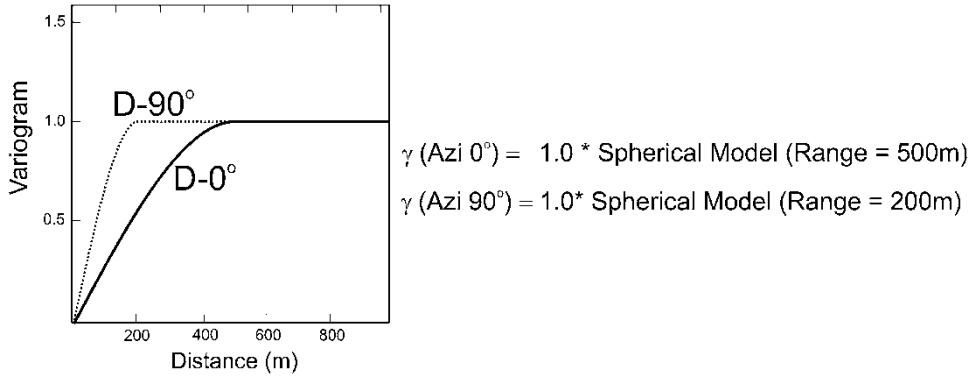

Fig. 18.16 Variogram model describing the geometric anisotropy of the grade distribution

(Fig. 18.15) this coefficient is calculated as ratio of the slopes of the linear variograms (Armstrong 1998).

In practice, the geometric anisotropy is expressed as different ranges of the variograms models calculated along the long and short axis of the variogram's ellipsoid (Fig. 18.16).

18.11.3 Nested Structures

In practise, two or more basic variogram models often need to be combined to optimally fit model to the experimental variograms. Example presented on the Fig. 18.17 is a nested structure, which includes nugget effect, spherical and linear models. Different ranges along 0º and 90° directions (Fig. 18.17a, b) indicate for geometric anisotropy of a studied variable.

The combined model (Fig. 18.17) is called nested because it represents a nested (enclosed) combination of the different structures. The nested structures are the most common type of the variograms models applied for characterisation of the mineral deposit grades.

The nested models are commonly described in a form of a table (Fig. 18.17c). The rows of the table denote the nested structures, including the type of the variogram function, its sill and range (Fig. 18.17c). Columns are used for presenting the variogram ranges determined along the axis of the variogram's ellipse (Fig. 18.17c). The model can also be presented as the formulas which identifies the variograms function for each structure and provides the main parameters, such as sill and range of the variogram (Fig. 18.17d).

However, when fitting the optimal nested model it is important to remember that not all combinations of the permissible models create a permissible nested variogram function (Goovaerts 1997).

18.11.4 Modelling Zonal Anisotropy

Variograms of the zonal anisotropy is built using the nested structures. The modelling procedure is as follows:

- it is necessary to determine direction of the longest continuity which is characterised by the lowest sill of the variogram. In the example of the 2D variogram presented on the Fig. 18.18a this is D-90° direction;
- the next step is to fit the variograms model to this sill;
- after that the zonal anisotropy is modelled. Thus is made by fitting the last structure to the variograms calculated in the short continuity direction (D-0°) which have a higher sill (Fig. 18.18a). In order to assure that the variogram model estimated in the direction D-90° not changed by adding the last structure it is assigned infinite range in this direction (Fig. 18.18b).

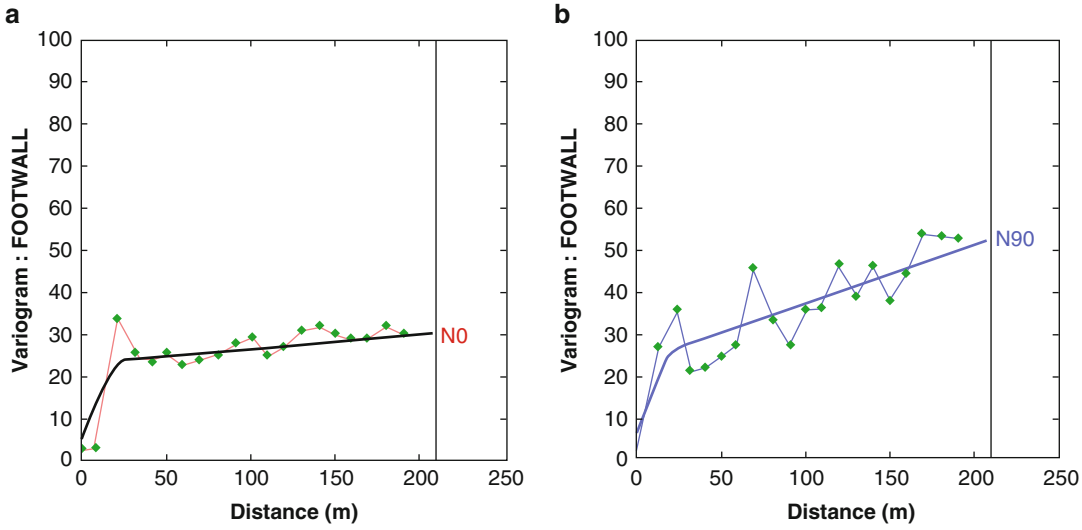

c

Structure	SILL	Ranges (m)	
		Major (N 0)	*Minor (N 90)*
Nugget $_0$	5		
Spherical $_1$	18	35	30
Linear $_2$	35	1000	250

d

γ **(Azi N0°) = 5 *** Nugget + **18 *** Spherical Model **(Range = 35m) + 35 *** Linear Model **(Range = 1000m)**

γ **(Azi N90°) = 5 *** Nugget + **18 *** Spherical Model **(Range = 30m) + 35 *** Linear Model **(Range = 250m)**

Fig. 18.17 Variograms of footwall elevation of the Ti-sands deposit, in the Madagascar, the fitted nested model includes nugget effect, spherical model and linear variograms: (**a**) long continuity direction; (**b**) short continuity direction; (**c**) fitted model presented as table; (**d**) fitted model presented as formulas

18.12 Troublesome Variograms

It is not always possible to calculate the robust experimental variograms of the metal grades. Conventional variograms [γ (**h**)] which are calculated as the average square of the differences between data pairs separated by the distance (h) may fail to reveal a spatial correlation between the data points. The experimental variograms can be erratic and unsuitable for structural analysis. Some most common cases of the troublesome (noisy) variograms and the reasons causing this are discussed in this section.

The noisy variograms in some cases can be improved. The practical approaches allowing to improve the troublesome variograms are shown using the case studies. A special attention is paid to the alternative structural analysis tools which can be used when the conventional variograms

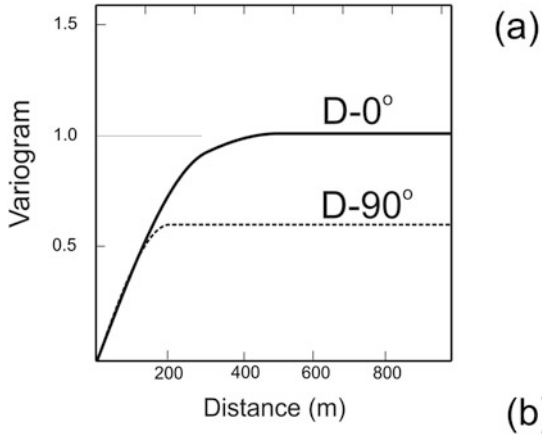

Fig. 18.18 Variogram model describing the zonal anisotropy of the grade distribution: (**a**) graphic presentation of the variogram; (**b**) parameters of the fitted model

have failed to provide a conclusive estimate of the variables' continuity.

18.12.1 Hole Effect

The hole effect is expressed by non-monotonic growth of the variograms which is broken by a sudden decrease and/or increase of the variograms values (Fig. 18.19). This can appear on bounded and non-bounded variograms and is caused commonly by a patchy distribution of the data when two or several groups of samples are separated by a non-sampled intervals (holes).

The hole effect can also be observed on the variograms calculated across a strike of the layered ore body which is composed by intercalation of the two well-differentiated types of mineralisation (Journel and Huijbregts 1978). In the latter case, when the hole effect occurs on the variograms calculated across the strike of a layered sequence, it commonly has a quasi-periodic shape which can be modelled using cardinal sign model (Journel and Huijbregts 1978) (18.12.1).

$$\gamma(\mathbf{h}) = C\left[1 - \frac{\sin\left(\frac{h}{a}\right)}{\frac{h}{a}}\right] \qquad (18.12.1)$$

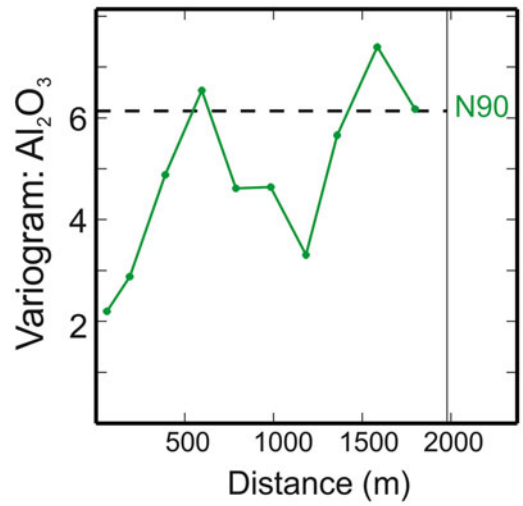

Fig. 18.19 Hole effect displayed by variogram of the Al_2O_3 values at the iron-ore deposit, Australia

18.12.2 Saw-Tooth Shaped and Erratic Variograms

The noisy experimental variograms in some cases exhibit the large amplitude periodic fluctuations called a 'saw-tooth' behaviour. Such behaviour can be caused by incorrectly chosen variogram lag and/or directional tolerance, and the variogram can be improved by increasing the lag.

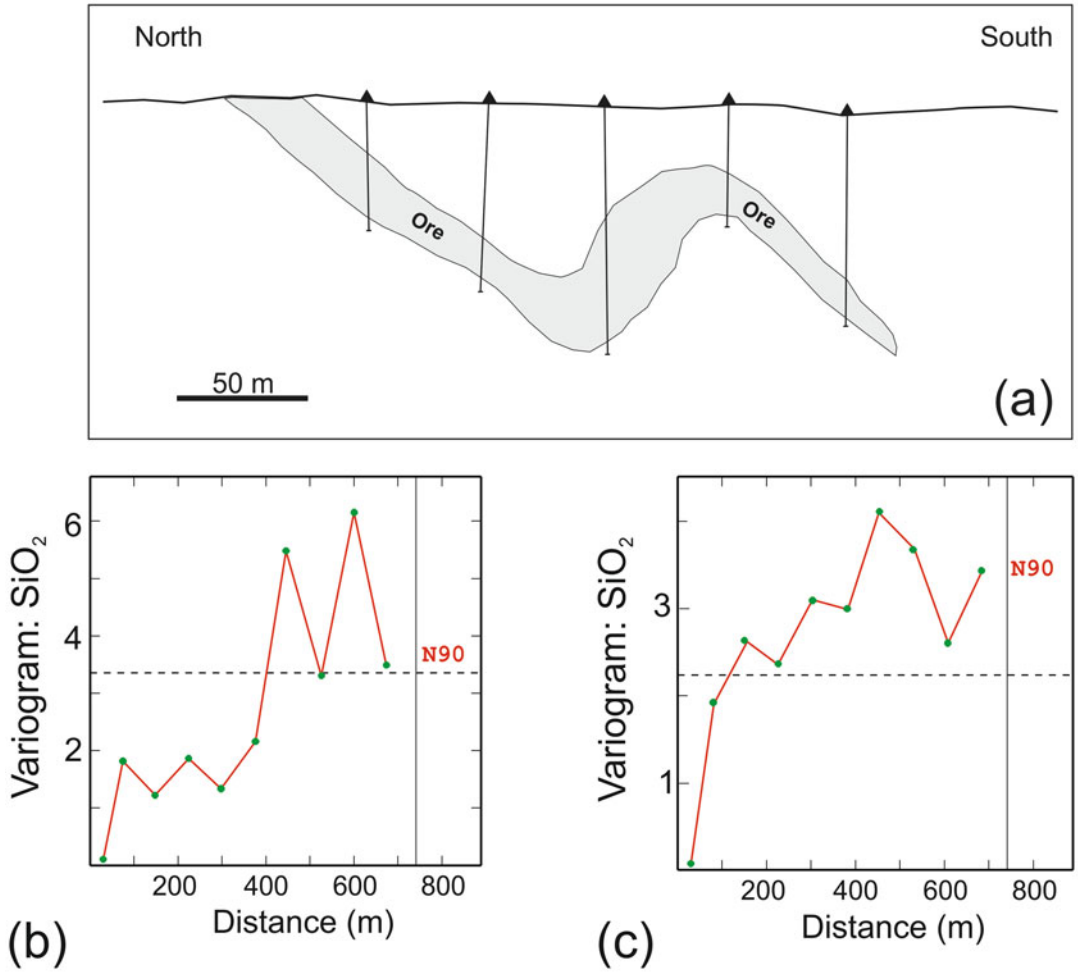

Fig. 18.20 Cross-section and the variograms calculated along the strike (East–West) direction of the folded ore body at the West Angelas iron ore deposit, Australia: (**a**) cross-section of the deposit; (**b**) variogram of SiO_2 calculated in the real coordinates; (**c**) variogram of SiO_2 calculated after ore-body was unfolded

The noisy shape of the variograms can also be caused by a complex geometry of the studied deposit, in particular when ore body is folded (Fig. 18.20a). The variograms of the folded ore bodies are often erratic (Fig. 18.20b), however, they are commonly improved by unfolding of the ore body (Fig. 18.20c).

The experimental variograms are also noisy when the data are strongly skewed, contain outliers, exhibit drift, irregularly distributed or characterised by a proportional effect. Structural analysis of these data may require their transformation or is made using different continuity analysis techniques.

18.13 Alternative Measures of a Spatial Continuity

Some common situations causing an erratic behaviour of the variograms have been discussed in the previous section. This section describes the procedures applied to overcome the noisy behaviour of the variograms, including the data transformation allowing to minimise an impact of outliers and the different structural tools which are applied for structural analysis of a given regionalised variable.

18.13.1 Variograms of the Gaussian Transformed Values

The variograms of the asymmetrically distributed data can be improved by transforming data into standard Gaussian variable with a mean equal to zero and variance equal one. The transformation is called normal score transformation or, alternatively, Gaussian anamorphosis (Olea 1991) and proceeds in three steps:

- the original data are ranked in the ascending order;
- the cumulative distribution frequency (*cdf*) of the original data is estimated;
- the empirical distribution is transformed into Gaussian variable by matching the ranks $\boldsymbol{k}$ of the empirical *cdf* to the corresponding them p_k*-quantiles of the normal standard *cdf* (Fig. 18.21). In practice, the Gaussian anamorphosis are commonly made using Hermite polynomials, which are orthogonal polynomials associated with the standard Gaussian distribution (Chiles and Delfiner 1999; Wackernagel 2003).

The transformed data are used for variography analysis. This includes construction of the experimental variograms using the newly created Gaussian variable and fitting the variogram model. After that the model is back-transformed into a variogram of the original data (Bleines et al. 2013). The back-transformation requires application of the Gaussian anamorphosis algorithm which was used for normal score transformation of the original data (Fig. 18.21) and was saved in the computer. The back-transformed variogram is used to complete the variography analysis and adjusting the variogram model for the original variable.

Effect of the Gaussian anamorphosis on the variogram is presented on the Fig. 18.22. This example is based on the data collected at the CJUP uranium deposit in Jordan (Abzalov et al. 2015). The uranium grade at the deposit is characterised by positively skewed distribution and contains a small proportion of the high grade samples (Fig. 18.22a). Because of a skewed distribution the directional variograms of uranium grade were excessively noisy and was not improved when mineralisation was unfolded (Fig. 18.22a).

In order to improve variograms the assayed uranium grades were transformed to standard Gaussian variable. The transformation was made by iteractive fitting of the Gaussian anamorphosis model using 100 Hermite polynomials.

The transformed data are shown on the Fig. 18.22b. They are characterised by symmetric bell-shaped histogram with a zero mean and variance equal to one (Fig. 18.22b). Variograms of the Gaussian variable is smooth (Fig. 18.22b) and lacking of the erratic fluctuations present on the original (not transformed) variograms (Fig. 18.22a). It is noteworthy, that in both cases shown on the Fig. 18.22, the variograms were calculated using the same estimation parameters.

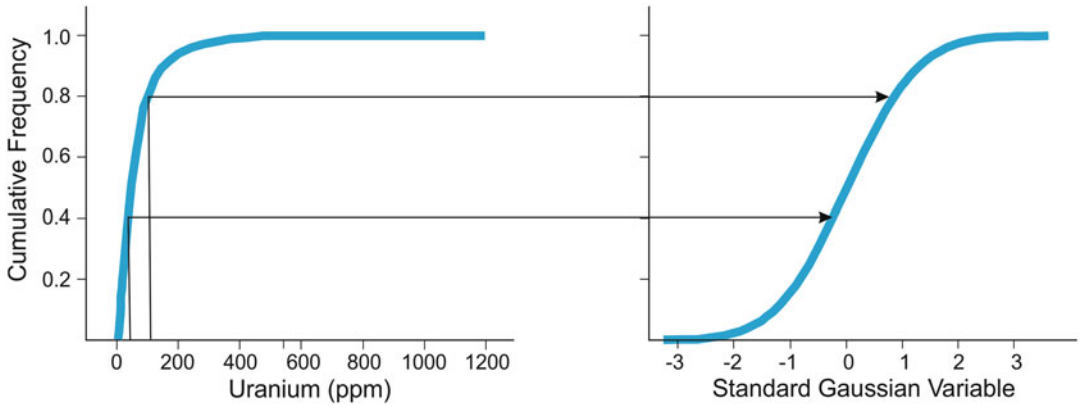

Fig. 18.21 Graphical procedure for transforming the cumulative distribution frequency (cdf) of the studied variable into standard normal distribution

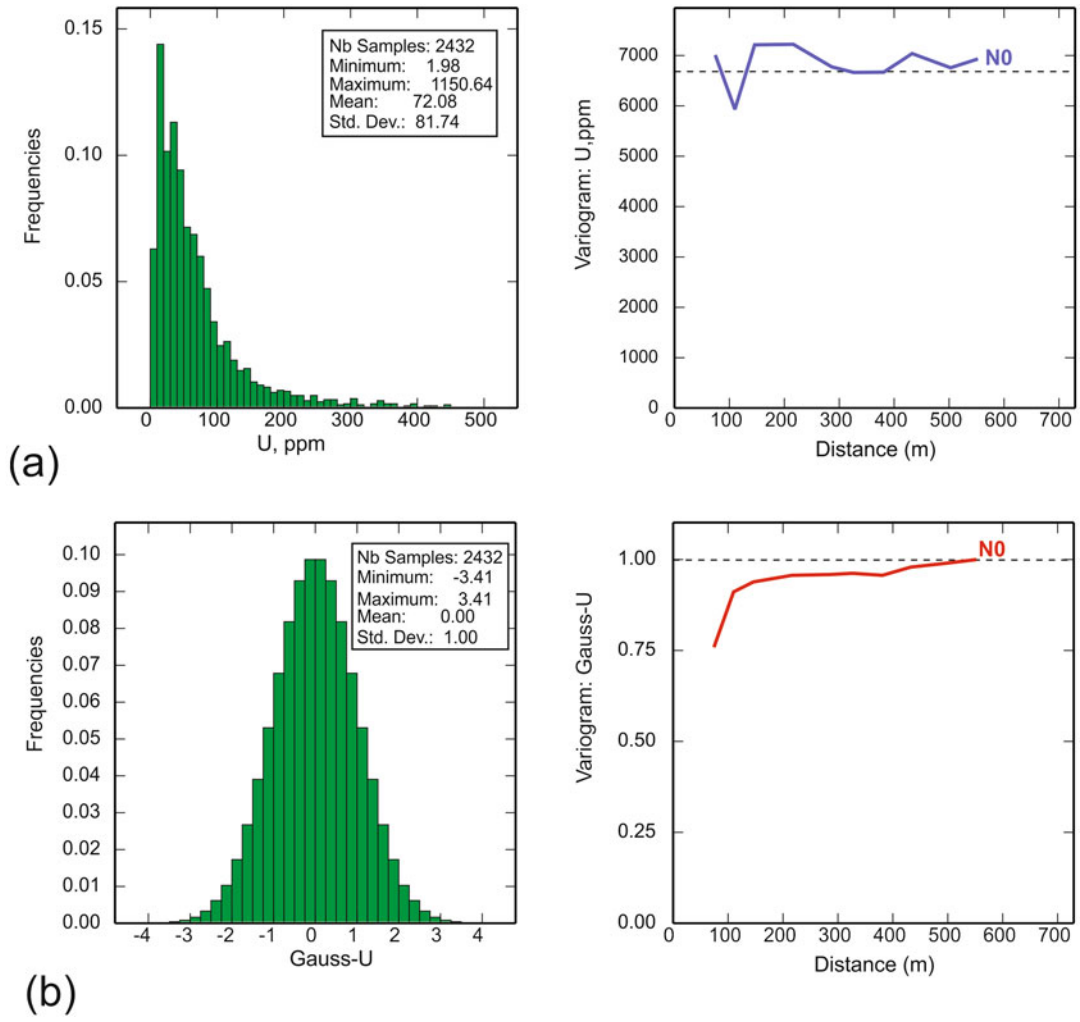

Fig. 18.22 Histograms and the variograms (calculated along north-south direction, azimuth 0°) of the uranium grade at the CJUP deposit, Jordan: (**a**) original data; (**b**) uranium grade transformed to standard Gaussian variable

In other words, Gaussian anamorphosis of the data has significantly improved the variograms.

18.13.2 Relative (Normalised) Variograms

The spatial distribution models can be enhanced by using the relative variograms, which estimate the difference between the data pairs normalised to the data mean. Two types of the relative variograms are most commonly used for mineral resource estimation (Goovaerts 1997; Chiles and Delfiner 1999): the relative variogram obtained by dividing data by the global mean of variable (18.13.1), and the pair-wise relative variogram, which estimates the differences between data pairs relative to the pair mean (18.13.2):

(a) relative variogram

$$\gamma(\mathbf{h}) = \frac{1}{2N}\sum_{i=1}^{N}\frac{[Z(x_i) - Z(x_i + \mathbf{h})]^2}{m^2} \tag{18.13.1}$$

where (m) is mean of the regionalised variable [Z(x)];

(b) pair-wise relative variograms

$$\gamma(\mathbf{h}) = \frac{1}{2N}\sum_{i=1}^{N} \frac{[Z(x_i) - Z(x_i + \mathbf{h})]^2}{\left[\frac{Z(x_i)+Z(x_i+\mathbf{h})}{2}\right]^2} \quad (18.13.2)$$

Another type of the normalised variograms used for the mining geology applications is the non-ergodic relative variogram (18.13.3) which normalises the data by the variogram lags,

$$\gamma(\mathbf{h}) = \frac{1}{2N}\sum_{i=1}^{N} \frac{[Z(x_i) - Z(x_i + \mathbf{h})]^2}{\left[\frac{m_Z^+ + m_Z^-}{2}\right]^2} \quad (18.13.3)$$

where (m_Z^+) and (m_Z^-) are means of the subsets of the variable [Z(x)] corresponding to the heads and tails of the data pairs separated by the lag (**h**).

The relative (normalised) variograms can enhance the spatial continuity of the metal grades and often used for advanced structural analysis of the data. In particular, pair-wise relative variogram is effective and useful for structural analysis of the asymmetrically distributed (skewed) variables (Fig. 18.23).

Another advantage of the pair-wise relative variogram consist in its applicability for estimation of the assay data quality (Abzalov 2014). By comparing the nugget effect of the pair-wise relative variogram with the relative variance of the duplicate samples the contributions of the geological factors into the short range variability of the data can be quantified and separated from the sampling errors (Abzalov 2014).

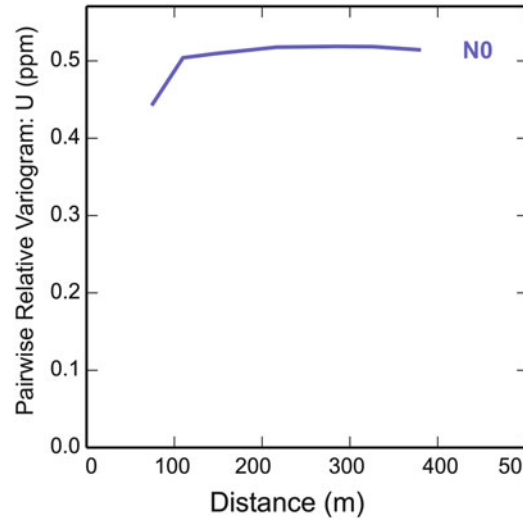

Fig. 18.23 Pair-wise relative variogram of the uranium grade constructed using the data shown on the Fig. 18.22a

18.13.3 Different Structural Tools

Variogram is not the only tool used for analysis of the spatial continuity of the data. The commonly used alternative tools include covariance, correlogram, madogram and rodogram:

(a) Covariance (centred)

$$C(\mathbf{h}) = \frac{1}{N}\sum_{i=1}^{N} \{[Z(x_i) - m]\,[Z(x_i + \mathbf{h}) - m]\} \quad (18.13.4)$$

where (m) is mean of the variable [Z(x)]

The covariance function [C (**h**)] is related to variogram [γ (**h**)] through the following equality (18.13.5)

$$\gamma(\mathbf{h}) = C(0) - C(\mathbf{h}) \quad (18.13.5)$$

where [C(0)] is a covariance at the zero distance which is equal to point variance of a given regionalised variable (18.13.6)

$$C(0) = \sigma^2 = \gamma(\infty) \quad (18.13.6)$$

(b) Covariance (non-centred)

$$C_{NC}(\mathbf{h}) = \frac{1}{N}\sum_{i=1}^{N} [Z(x_i + \mathbf{h})\, Z(x_i)] \quad (18.13.7)$$

(c) Correlogram

$$\rho(\mathbf{h}) = \frac{1}{N}\sum_{i=1}^{N} \frac{\{[Z(x_i) - m][Z(x_i + \mathbf{h}) - m]\}}{\sigma^2} \tag{18.13.8}$$

(d) Madogram (1st order variogram)

$$\tau(\mathbf{h}) = \frac{1}{2N}\sum_{i=1}^{N} |Z(x_i + \mathbf{h}) - Z(x_i)| \tag{18.13.9}$$

(e) Rodogram

$$\tau(\mathbf{h}) = \frac{1}{2N}\sum_{i=1}^{N} \sqrt{|Z(x_i + \mathbf{h}) - Z(x_i)|} \tag{18.13.10}$$

Covariance and correlogram can be used as substitutes for conventional variograms in the kriging systems. Other models, such as madogram, rodogram, are not substitutes for a conventional variogram. However, these functions, representing the robust structural measures, can be used to enhance spatial continuity of the variable of interest and obtain a clearer description of the spatial structures. They define spatial variability of the data as mean absolute deviation to the power 1 (madogram) and 0.5 (rodogram) and therefore less sensitive to the extreme values then conventional variogram, estimating the spatial data variability as half the average squared difference between the data pairs.

18.14 Indicator Variograms

The conventional variogram estimates the average continuity of the studied variable. For example the variogram of a metal grade represents the average continuity of the given metal in the deposit, which is averaging continuities of the high and low grade mineralisation. When continuity of mineralisation significantly differs by the mineralisation types or the grade classes the data transformation into standard Gaussian variable or normalisation relative to the data mean do not overcome limitations of a single variogram. Accurate modelling of such deposits requires several variograms generated for each grade class separately.

In practice, the grade classes are presented as the grade indicators. Transformation of the variable Z(x) into indicators $\boldsymbol{I}(z)$ is made as follows: all Z(x) data are transformed into 1 if they are equal to or less than the indicator (z), otherwise, when Z(x) are larger than the given indicator (z), they are transformed into 0 (18.14.1).

$$I(z) = \begin{cases} 1, & \text{if } Z(x) \le z \\ 0, & \text{otherwise} \end{cases} \tag{18.14.1}$$

The primary objective of the indicator variograms was for estimation resources using Indicator kriging technique (Journel and Huijbregts 1978). However, their application has significantly increased with time and at present the indicator variograms are routinely used as a structural analysis in particular for complex multi-episodic mineralisation (Guibal 2001). The indicator variograms are also useful for constraining mineralisation using geostatistically assisted domaining approach (Abzalov and Humphreys 2002a,b).

18.15 Variograms in the Multivariate Environment

Evaluation of the mining projects requires estimation of the mineralisation grade, by-products, deleterious elements and other non-grade variables of economic significance. In total, this is a common situation when resource estimation includes several variables which are estimated using multivariate geostatistical techniques (Wackernagel 2003; Sommerville et al. 2014; Abzalov and Bower 2014).

18.15.1 Multivariate Geostatistical Functions

Two multivariate functions are most commonly used for resource estimation and the mining geology applications are cross variogram and cross covariance.

Cross-variogram is defined as a half the non-centred covariance between the different regionalised variables $\{z_i(\mathbf{x})$ and $z_j(\mathbf{x})\}$ separated by the vector $\mathbf{h}$

$$\gamma_{ij}(\mathbf{h}) = \frac{1}{2N}\sum_{a=1}^{N}\left[\left(z_i(\mathbf{x_a}) - z_i(\mathbf{x_a}+\mathbf{h})\right) * \left(z_j(\mathbf{x_a}) - z_j(\mathbf{x_a}+\mathbf{h})\right)\right] \quad (18.15.1.)$$

Cross-covariance between variables $\{z_i(\mathbf{x})$ and $z_j(\mathbf{x})\}$ separated by the vector $\mathbf{h}$ is estimated as follows

$$C_{ij}(\mathbf{h}) = \frac{1}{N}\sum_{a=1}^{N}\left[\left(z_i(\mathbf{x_a}) * z_j(\mathbf{x_a}+\mathbf{h})\right) - m_i(-\mathbf{h}) * m_j(+\mathbf{h})\right] \quad (18.15.2)$$

where $m_i(-\mathbf{h})$ and $m_j(+\mathbf{h})$ are the means of tail $z_i(\mathbf{x})$-values and head $z_j(\mathbf{x})$-values:

$$m_i(-\mathbf{h}) = \frac{1}{N}\sum_{a=1}^{N}\left(z_i(\mathbf{x_a})\right)$$

$$m_j(+\mathbf{h}) = \frac{1}{N}\sum_{a=1}^{N}\left(z_j(\mathbf{x_a}+\mathbf{h})\right) \quad (18.15.3)$$

In both cases (18.15.1 and 18.15.2) the N is the number of pairs of data locations separated by a vector $(\mathbf{h})$.

Cross variogram is symmetric in z_i, z_j and $(\mathbf{h}, -\mathbf{h})$; interchanging the variables or changing the vector $(\mathbf{h})$ for opposite $(-\mathbf{h})$ does not make any difference for the variogram value estimated using expression (18.15.1). The cross variogram thus can not detect direction of delay of one variable relative to another.

On the contrary to the cross variogram, cross covariance computed in the different directions are in general different, in other words $C_{ij}(\mathbf{h})$ not equal to $C_{ij}(-\mathbf{h})$. The cross covariance is also changes by interchanging the variables, $C_{ij}(\mathbf{h})$ not equal to $C_{ji}(\mathbf{h})$. This asymmetry of the cross covariance is caused by one variable lagging behind the other, an effect referred to as a lag effect (Journel and Huijbregts 1978).

Capability of the cross covariance to detect delay of one variable relative to another and quantitatively estimate it represents a powerful tool for modelling zoned distributions of the metals. However, the experimental cross covariance can display a pseudo lag effect caused by experimental fluctuations caused by the small numbers of data pairs available (Goovaerts 1997). Therefore, the lag effect which is not backed up by the geological interpretation is better to be ignored.

18.15.2 Linear Model of Coregionalisation

Cross variograms and cross covariances are modelled using the same set of the basic functions which are used in the univariate case (Fig. 18.15). However, the admissible multivariate model must satisfy conditions of the linear model of coregionalisation (Goulard 1989; Goulard and Voltz 1992; Goovaerts 1997; Wackernagel 2003). This model requires that all univariate and cross variogram models should share the same set of basic structures. This condition is expressed as the equality 18.15.4.

$$\gamma_{ij}(\mathbf{h}) = \sum_{K}\left[{}^{K}b_{ij}\,{}^{K}\gamma(\mathbf{h})\right], \quad (18.15.4)$$

where ${}^{K}b_{ij}$ is a coregionalisation matrix of the variogram sills corresponding to the K^{th}-structure of the variogram $\gamma_{ij}(\mathbf{h})$, and ${}^{K}\gamma(\mathbf{h})$ is a model fitted to this structure.

The coregionalisation matrix is estimated for every Kth-structure using the following expression (18.15.5):

$$ {}^{K}b_{ij} = {}^{K}\begin{vmatrix} b_{ii} & b_{ij} \\ b_{ji} & b_{jj} \end{vmatrix} \qquad (18.15.5) $$

The linear model of coregionalisation is permissible if the every coregionalisation matrices ${}^{K}b_{ij}$ are positive semi-definite, which is expressed as

$$ {}^{K}b_{ij} = {}^{K}\begin{vmatrix} b_{ii} & b_{ij} \\ b_{ji} & .b_{jj} \end{vmatrix} \geq 0 \qquad (18.15.6) $$

This condition implies the following constraints

$$ {}^{K}b_{ij} \leq \sqrt{{}^{K}b_{ii} \; {}^{K}b_{jj}} \qquad (18.15.7) $$

The conditions of the linear coregionalisation model are explained using the example of Pb-Zn mineralisation:

$$ \begin{aligned} \gamma_{Pb}(\mathbf{h}) &= 3Nugget + 31\ Spherical\ (h, 40) \\ &\quad + 39\ Spherical\ (h, 200) \\ \gamma_{Zn}(\mathbf{h}) &= 7Nugget + 18\ Spherical\ (h, 40) \\ &\quad + 15\ Spherical\ (h, 200) \\ \gamma_{Pb-Zn}(\mathbf{h}) &= 22\ Spherical\ (h, 40) \\ &\quad + 14\ Spherical\ (h, 200) \end{aligned} $$

$$ {}^{1}b_{Pb-Zn} = {}^{1}\begin{vmatrix} 3 & 0 \\ 0 & .7 \end{vmatrix} = 21 \; {}^{2}b_{Pb-Zn} = {}^{2}\begin{vmatrix} 31 & 22 \\ 22 & .18 \end{vmatrix} = $$

$$ 74 \; {}^{3}b_{Pb-Zn} = {}^{3}\begin{vmatrix} 39 & 14 \\ 14 & 15 \end{vmatrix} = 389 $$

Based on this constraint an envelope of the permissible model can be estimated using the following expression:

$$ \begin{aligned} &-\left({}^{K}\gamma(\mathbf{h})\right)\left(\sum \sqrt{{}^{K}b_{ii} \; {}^{K}b_{jj}}\right) \\ &\leq \left(\gamma_{ij}(\mathbf{h}) = \sum_{K}\left[{}^{K}b_{ij} \; {}^{K}\gamma(\mathbf{h})\right]\right) \\ &\leq {}^{K}\gamma(\mathbf{h})\left(\sum \sqrt{{}^{K}b_{ii} \; {}^{K}b_{jj}}\right) \end{aligned} \qquad (18.15.8) $$

However, application the constraint (18.15.7) becomes very tedious as the number of variables, hence the number of coefficients ${}^{K}b_{ij}$, increases. This is usually overcome by using the iterative computing procedure that fits the linear model of coregionalisation directly under the constraints of positive semi-definiteness of all matrices ${}^{K}b_{ij}$ (Goulard 1989; Goulard and Voltz 1992; Chu 1993).

Exercise 18.15.2 The file Exercise 18.15.2.xls in the Appendix 1 contains coregionalisation matrices for the bivariate case of Pb-Zn mineralisation. Using this file estimate the envelope of a permissible model for the Pb-Zn cross variogram.

References

Abzalov MZ (2014) Geostatistical criteria for choosing optimal ratio between quality and quantity of the samples: method and case studies. In: Mineral resource and Ore Reserves Estimation, AusIMM Monograph 23, 2nd edn. Chapter 2: The resource database. AusIMM, Melbourne, pp 91–96

Abzalov MZ, Bower J (2014) Geology of bauxite deposits and their resource estimation practices. Appl Earth Sci 123(2):118–134

Abzalov MZ, Humphreys M (2002a) Resource estimation of structurally complex and discontinuous mineralisation using non-linear geostatistics: case study of a mesothermal gold deposit in northern Canada. Exp Min Geol J 11(1–4):19–29

Abzalov MZ, Humphreys M (2002b) Geostatistically assisted domaining of structurally complex mineralisation: method and case studies. Geostatistically assisted domaining of structurally complex mineralisation: method and case studies. In: The AusIMM 2002 conference: 150 years of mining, Publication series No 6/02, pp 345–350

Abzalov MZ, Mazzoni P (2004) The use of conditional simulation to assess process risk associated with grade variability at the Corridor Sands detrital ilmenite deposit. In: Dimitrakopoulus R, Ramazan S (eds) Ore body modelling and strategic mine planning: uncertainty and risk management. AusIMM, Melbourne, pp 93–101

Abzalov MZ, Pickers N (2005) Integrating different generations of assays using multivariate geostatistics: a case study. Trans Inst Min Metall 114: B23–B32

Abzalov MZ, van der Heyden A, Saymeh A, Abuqudaira M (2015) Geology and metallogeny of Jordanian uranium deposits. Appl Earth Sci 124(2):63–77

Armstrong M (1998) Basic linear geostatistics. Springer, Berlin, p 153

Barnes R (1991) The variogram sill and the sample variance. Math Geol 23(4):673–678

Bleines C, Bourges M, Deraisme J, Geffroy F, Jeanne N, Lemarchand O, Perseval S, Poisson J, Rambert F, Renard D, Touffait Y, Wagner L (2013) ISATIS software. Geovariances, Ecole des Mines de Paris, Paris

Chauvet P (1982) The variogram cloud. 17th APCOM symposium, pp 757–764

Chiles J-P, Delfiner P (1999) Geostatistics: modelling spatial uncertainty. Wiley, New York, p 695

Chu J (1993) XGAM: a 3D interactive graphic software for modelling variograms and cross variograms under conditions of positive definiteness. In: Stanford Centre for reservoir forecasting, report 6, Stanford, California

David M (1977) Geostatistical ore reserve estimation. Elsevier, Amsterdam, p 364

Goovaerts P (1997) Geostatistics for natural resources evaluation. Oxford University Press, New York, p 483

Goulard M (1989) Inference in a coregionalization model. In: Armstrong M (ed) Geostatistics, vol 1. Kluwer, Dordrecht, pp 397–408

Goulard M, Voltz M (1992) Linear coregionalization model: tools for estimation and choice of cross-variogram matrix. Math Geol 24(3): 269–286

Guibal D (2001) Variography, a tool for the resource geologist. In: Edwards AC (ed) Mineral resource and ore reserve estimation – the AusIMM guide to good practice. AusIMM, Melbourne, pp 85–90

Isaaks EH, Srivastava RM (1989) An introduction to applied geostatistics. Oxford University Press, New York, p 561

Journel AG, Huijbregts CJ (1978) Mining geostatistics. Academic, New York, p 600

Olea RA (ed) (1991) Geostatistical glossary and multilingual dictionary. Oxford University Press, New York, p 177

Sommerville B, Boyle C, Brajkovich N, Savory P, Latscha AA (2014) Mineral resource estimation of the Brockman 4 iron ore deposit in the Pilbara region. Appl Earth Sci 123(2):135–145

Wackernagel H (2003) Multivariate geostatistics: an introduction with applications, 3rd edn. Springer, Berlin, p 388

Methods of the Linear Geostatistics (Kriging)

19

Abstract

Estimation is most commonly made using Ordinary (OK) or Simple (SK) Kriging, which are the variants of the basic linear regression techniques allowing estimation of a single regionalised variable in unsampled locations. Kriging technique imposes the following special constraints on the estimate:

- It minimises an estimation error
- It assures that mathematical expectation of the estimation error is equal to zero.

These characteristics give advantage to kriging in comparison with other linear estimators.

Keywords

Kriging • SK • OK • Kriging variance • Conditional bias

Geostatistical modelling does not describe the physical processes therefore it is of a little use in extrapolative predictions beyond the spatial bounds of the available data. The geostatistical methods are largely based on interpolative predictions based on inferred spatial variability of the available data (i.e. variogram models) and therefore these techniques are broadly used for estimation grade and tonnage of mineral resources and ore reserves.

19.1 Geostatistical Resource Estimation

The whole process of a geostatistical resource modelling can be subdivided on several common steps (Table 19.1) representing a natural methodological sequence of data gathering, analysis and inference. It is important to note that geostatistical estimations are the only

M. Abzalov, *Applied Mining Geology*, Modern Approaches in Solid Earth Sciences 12,
DOI 10.1007/978-3-319-39264-6_19

Table 19.1 General steps in geostatistical resource modelling

Resource estimation steps	Explanation
1. Input samples and measurements	Data collection, testing and quality assurance for data values and locations;
	Definition of the data types and generations;
2. Data processing	Compositing;
	High-grade cut-off;
3. Geological model	Domaining;
	3D constrains (wireframing) of mineralisation and related features (base of oxidation, faults);
	Contacts characterisation;
	Textures of mineralisation (internal dilution, geological control of distribution);
	Spatial distribution characterisation (trends, zoning, high-grade shoots);
4. Structural analysis	Coordinates transformations;
5. Rock density	Measurement techniques and quality assurance;
	Spatial distribution models of the rock densities;
6. Exploratory data analysis (EDA)	Classical descriptive statistics by domains;
	Analysis of stationarity;
	Testing of the populations homogeneity;
	Outliers identification;
	Correlation between attributes;
	Declustering data;
	Spatial trends and discontinuities;
7. Geostatistical analysis (variography)	Analysis of the spatial data autocorrelations
	Enhancing structures using the transformations;
	Testing the basic statistical hypothesis and geostatistical assumptions (multi-Gaussianity, proportional effect, border effect, intrinsic correlation);
8. Estimation methods and parameters	Rational for choosing the geostatistical estimation method;
	Definition of the modelling parameters (search neighbourhoods, block sizes, multiple interpolation passes);
9. Application of the modelling algorithm	Implementation of the algorithm as the computer scripts and macro codes;
	Importing the data to software for resource modelling and testing that file have not been corrupted during data transfer;
10. Model validation	Testing and validation of the estimate, assessing the model's sensitivity to the chosen parameters
11. Classification	Definition of the Mineral resource categories
12. Documentation	Tabulation of the grade and tonnage of the resources
	Reporting results including a comprehensive summary of the data, assumptions made, modelling methods and parameters

one step in the whole process (Table 19.1) therefore a good geostatistical analysis alone is insufficient for obtaining the accurate and reliable estimates of the mineral resources and ore reserves.

19.2 Kriging System

Geostatistical methods have become the main approach applied for estimation grade and tonnage of mineral resources and ore reserves (Krige

1951; Matheron 1963, 1968; David 1977, 1988; Journel and Huijbregts 1978; Cressie 1990; Annels 1991; Goovaerts 1997; Sinclair and Blackwell 2002; Rossi and Deutsch 2014). Most commonly used are the linear estimators known as the kriging system.

Kriging is a variant of the basic linear regression techniques allowing estimation of a single regionalised variable in unsampled locations (Cressie 1990). Besides direct using in the linear estimators, such as Ordinary Kriging (OK) and Simple Kriging (SK), the kriging equations also underly the non-linear estimators and Conditional Simulation techniques (Lantuejoul 2002) which will be reviewed in the following chapters.

The specific feature of a kriging technique is the special conditions imposed on to estimate as a constraining factors. These conditions are as follows:

Kriging estimate minimises an estimation error $\varepsilon = Z_{TRUE} - Z^*_{KRIGING}$;

Kriging approach assures that mathematical expectation of the estimation error is equal to zero $\mathrm{E}(\varepsilon) = \mathrm{E}\left(Z_{TRUE} - Z^*_{KRIGING}\right) = 0$.

These two characteristics give advantage to kriging in comparison with other linear estimators, therefore kriging is commonly referred to as best linear unbiased estimator (Cressie 1990; Annels 1991; Sinclair and Blackwell 2002). It should be remembered that the expressions 'best' and 'un-biased' have purely mathematical meaning and related to mathematical procedures used by kriging. The term 'best' is related to above mentioned condition of a minimal variance of the estimation error, and term 'non-biased' is related to a second condition requiring that mathematical expectation of the estimation error E(ε) was equal to zero. Although these conditions are important for obtaining accurate estimation of the variable Z($\mathbf{x}$) in the unsampled location they alone can not guaranty that obtained results are non-biased.

Quality of the kriging estimate depends on many factors, including parameters which should be determined by a practitioner and entered into the kriging equations, common of them are variogram model, search neighbourhood and model grid dimensions. These are reviewed in this and following sections of the book together with review of the theoretical background of the main variants of kriging and their properties.

19.2.1 Ordinary Kriging

Ordinary kriging (OK) is the most common estimation technique used for mineral resource estimation (Journel and Huijbregts 1978). It is a univariate linear estimator allowing estimate a single regionalised variable in the unsampled locations by inter- and /or extrapolating the known values to the unsampled target node. The OK methodology represents a variant of the basic linear regression estimator, and in a general form it is follows (19.2.1):

$$\begin{cases} Z^*_{OK}(\mathbf{x}) = \sum_i \left[\lambda_i^{OK} Z(\mathbf{x}_i)\right] \\ \sum_i \lambda_i^{OK} = 1 \end{cases} \tag{19.2.1}$$

The OK weights λ_i^{OK} assigned to each datum Z($\mathbf{x}_i$), which are interpreted as a realisation of the regionalised variable of interest Z($\mathbf{x}$), are calculated assuring the minimum estimation variance (estimation error) under the constraint of unbiasedness of the estimator.

The OK system of linear equations which allows to calculate the sample weights in case of the intrinsic distribution model assuring the conditions of optimality and unbiasedness of the estimator is as follows (Journel and Huijbregts 1978; Goovaerts 1997) (19.2.2):

$$\begin{cases} \sum_\beta \lambda_\beta^{\mathrm{OK}} \gamma\left(\mathbf{x}_\beta - \mathbf{x}_\alpha\right) - \mu_{\mathrm{OK}} = \gamma\left(\mathbf{x}_0 - \mathbf{x}_\alpha\right) \\ \sum_\beta \lambda_\beta^{\mathrm{OK}} = 1 \end{cases} \tag{19.2.2}$$

where λ_i^{OK} are the OK weights;

μ_{OK} is the Lagrange multiplier associated with the constraint $\sum_\beta \lambda_\beta^{\mathrm{OK}} = 1$;

$\gamma\left(\mathbf{x}_\beta - \mathbf{x}_\alpha\right)$ are the semi-variograms between data points;

$\gamma\left(\mathbf{x}_0 - \mathbf{x}_\alpha\right)$ is a semi-variogram between each datum and a target node.

The estimation error variance, also known as ordinary kriging variance is calculated as

$$\sigma_{OK}^2(\mathbf{x}) = \sigma_0^2 - \sum_{\alpha} \lambda_{\alpha}^{\mathrm{OK}} \gamma(\mathbf{x}_0 - \mathbf{x}_{\alpha}) - \mu_{\mathrm{OK}}, \tag{19.2.3}$$

where σ_0^2 is the point variance of the regionalised variable Z(**x**).

In the matrix notation the OK system can be represented as follows

$$[\mathrm{W}] * [\lambda] = [\mathrm{B}] \tag{19.2.4}$$

The matrices [W], [λ] and [B] are defined as follows:

$$[\mathrm{W}] = \begin{bmatrix} \gamma(0) & \cdots\cdots & \gamma(\mathbf{x}_1, \mathbf{x}_{\mathrm{N}}) & 1 \\ \cdots\cdots & \gamma(\mathbf{x}_{\alpha}, \mathbf{x}_{\beta}) & \cdots\cdots & 1 \\ \gamma(\mathbf{x}_{\mathrm{N}}, \mathbf{x}_{\beta}) & \cdots\cdots & \gamma(0) & 1 \\ 1 & \cdots\cdots 1 & \cdots\cdots & 0 \end{bmatrix}$$

$$[\lambda] = \begin{bmatrix} \lambda_1 \\ - \\ \lambda_{\mathrm{N}} \\ \mu \end{bmatrix} \text{ and } [\mathrm{B}] = \begin{bmatrix} \gamma(\mathbf{x}_1, \mathbf{x}_0) \\ - - \\ \gamma(\mathbf{x}_{\alpha}, \mathbf{x}_0) \\ - - \\ \gamma(\mathbf{x}_{\mathrm{N}}, \mathbf{x}_0) \\ 1 \end{bmatrix}$$

Sample weights are estimated by solving the Eq. (19.2.4), which can be expressed as $[\lambda] = [\mathrm{B}] * [\mathrm{W}]^{\mathrm{T}}$.

19.2.2 Simple Kriging

Simple kriging is a univariate linear estimator which requires an *a priori* knowledge of the mean value (m) of the variable of interest. This mean value is a part of the SK system (19.2.5) and it is used together with the available data (samples) for estimation the grade at the target node (unsampled location).

$$Z_{SK}^*(\mathbf{x}) = \sum_i \left[\lambda_i^{SK} Z(\mathbf{x}_i)\right] + \mathrm{m}\left(1 - \sum_i \lambda_i^{SK}\right) \tag{19.2.5}$$

SK weights are calculated using SK system of the linear equations such as to minimise the estimation error variance, which is a condition of a kriging unbiasedness. The sum of the SK weights $\lambda_{\beta}^{\mathrm{SK}}$ not equal to one ($\sum_{\beta} \lambda_{\beta}^{\mathrm{SK}} \neq 1$) therefore SK system can not be expressed in terms of variograms (Goovaerts 1997).

The SK system can be written in terms of Z-covariances.

Using covariances the SK system can be written as

$$\sum_b \lambda_b^{\mathrm{SK}} C(\mathbf{x}_a - \mathbf{x}_b) = C(\mathbf{x}_a - \mathbf{x}_b) \tag{19.2.6}$$

The minimum error variance (SK variance) is estimated as

$$\sigma_{SK}^2(\mathbf{x}) = \sigma_0^2 - \sum_{\alpha} \lambda_{\alpha}^{\mathrm{SK}} C(\mathbf{x}_a - \mathbf{x}_0) \tag{19.2.7}$$

where σ_0^2 is the point variance of the regionalised variable Z(**x**).

In the matrix notation the SK system is presented as follows:

$$\left[\mathrm{W}^{\mathrm{SK}}\right] * \left[\lambda^{SK}\right] = \left[\mathrm{B}^{\mathrm{SK}}\right] \tag{19.2.8}$$

where, the $\left[\mathrm{W}^{\mathrm{SK}}\right]$, $[\lambda^{SK}]$ and $\left[\mathrm{B}^{\mathrm{SK}}\right]$ are the matrices of the covariances and the sample weights:

$$\left[\mathrm{W}^{\mathrm{SK}}\right] = \begin{bmatrix} C(\mathbf{x}_1, \mathbf{x}_1) & \cdots\cdots & C(\mathbf{x}_1, \mathbf{x}_{\mathrm{N}}) \\ & - & \\ \cdots\cdots C(\mathbf{x}_{\alpha}, \mathbf{x}_{\beta}) & -- & \cdots\cdots \\ & - & \\ C(\mathbf{x}_{\mathrm{N}}, \mathbf{x}_1) & \cdots\cdots & C(\mathbf{x}_{\mathrm{N}}, \mathbf{x}_N) \end{bmatrix}$$

is the matrix of covariances between the data nodes;

$\left[\lambda^{SK}\right] = \begin{bmatrix} \lambda_1^{SK} \\ - \\ - \\ \lambda_N^{SK} \end{bmatrix}$ is the vector of SK weights;

$\left[\mathrm{B}^{\mathrm{SK}}\right] = \begin{bmatrix} C(\mathbf{x}_1, \mathbf{x}_0) \\ - \\ - \\ C(\mathbf{x}_{\mathrm{N}}, \mathbf{x}_0) \end{bmatrix}$ is the vector of data-to-target node covariances.

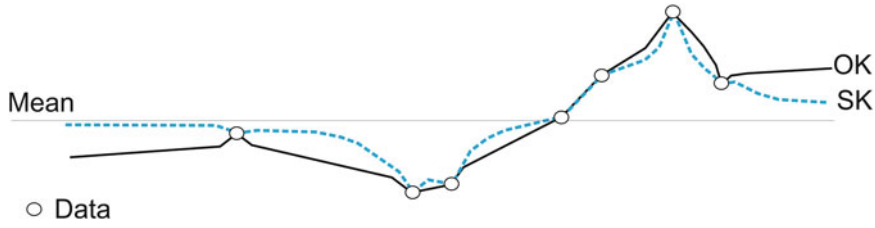

Fig. 19.1 Sketch illustrating difference between Simple (*SK*) and Ordinary (*OK*) kriging estimates

19.2.3 Simple Versus Ordinary Kriging

Estimates obtained by Ordinary (OK) and Simple (SK) kriging differ because of underlying differences in their formulas, 19.2.1 and 19.2.5 correspondingly. Ordinary kriging (OK) system creates a linear combination of the data contained in the search neighbourhood. Simple kriging (SK) together with data also uses mean value of the variable of interest $Z^*_{SK}(\mathbf{x}) = \sum_i \left[\lambda_i^{SK} Z(\mathbf{x}_i)\right] + \mathrm{m}\left(1 - \sum_i \lambda_i^{SK}\right)$. Weight of the mean is usually positive therefore SK estimate can deviate from OK toward the mean of variable (Fig. 19.1). In low-valued areas the OK estimate is lower than SK, and conversely the OK estimate is larger than SK in high-valued areas (Fig. 19.1). The discrepancy between the two estimates $Z^*_{SK}(\mathbf{x})$ and $Z^*_{OK}(\mathbf{x})$ increases when location ($\mathbf{X}$) being estimated gets farther away from data locations (Fig. 19.1). This is a consequence of increasing the weight of the mean $\left(1 - \sum_i \lambda_i^{SK}\right)$ with a distance from the data increase.

Ordinary kriging is usually a preferred method to Simple kriging because it does not require stationarity of the mean over the entire area and better follows fluctuations of the data. Simple kriging is more conservative, however because of this property it can be advantageous for estimating resources in the poorly sampled areas because it decreases the risk of smearing of high or low grade values from a single sample (Fig. 19.1).

19.3 Properties of Kriging

Kriging methodology is the main approach used for estimation mineral resources and ore reserves. Success of this technique is due to its use of a geostatistical distance, which incorporates the actual vector ($\mathbf{h}$) its relation to the spatial continuity of the studied variable introduced through the variogram or covariance models.

Because of use of a spatial continuity model that describes the geostatistical distance between points the methodology is flexible and has an important ability to customise the estimation procedures. Before looking the practice of implementation kriging for resource estimation and other mine geology applications it is necessary to review the main properties of the kriging techniques. It is made in this section of the book with an emphasis on Ordinary kriging.

19.3.1 Exactitude Property of Kriging

Simple and Ordinary kriging are *exact interpolators* (Goovaerts 1997; Wackernagel 2003). This property simply means that when target node coincides with a data point then the estimated value $Z^*(\mathbf{x})$ is identical with the data value at this point.

$$Z*(\mathbf{X}_o) = Z(\mathbf{X}_a), \text{ if } (\mathbf{X}_o) = (\mathbf{X}_a)$$

This is easily to demonstrate using a case with one data point.

In a Simple kriging case weights of the data points are estimated using the set of the linear

equations, which in a matrix notation is expressed as $\left[\mathsf{W}^{\mathsf{SK}}\right] * \left[\lambda^{SK}\right] = \left[\mathsf{B}^{\mathsf{SK}}\right]$.

The matrices $\left[\mathsf{W}^{\mathsf{SK}}\right]$, $[\lambda^{SK}]$ and $\left[\mathsf{B}^{\mathsf{SK}}\right]$ in case of one data point coincident with the target node ($\mathsf{x}_0 = \mathsf{x}_a$) can be defined as follows:

$\left[\mathsf{W}^{\mathsf{SK}}\right] = [C(\mathsf{x}_a, \mathsf{x}_a)]$, $\left[\lambda^{SK}\right] = \left[\lambda_a^{SK}\right]$ and $\left[\mathsf{B}^{\mathsf{SK}}\right] = [C(\mathsf{x}_a, \mathsf{x}_0)]$

However, because x_a coincide with x_0 the covariance $C(\mathsf{x}_a, \mathsf{x}_0)$ is equal to $C(\mathsf{x}_a, \mathsf{x}_a)$, which means that matrix $\left[\mathsf{B}^{\mathsf{SK}}\right]$ which is identical to the matrix $\left[\mathsf{W}^{\mathsf{SK}}\right]$.

Using the SK matrices representing the single sample case which is coincident with location of the target variable, the weight this single sample is estimated, and it is equal to 1:

$$\left[\lambda^{SK}\right] = \left[\mathsf{B}^{\mathsf{SK}}\right] * \left[\mathsf{W}^{\mathsf{SK}}\right]^{\mathrm{T}} = 1$$

The SK Eq. (19.2.5), in one data point case becomes

$$Z^*_{SK}(\mathsf{x}_0) = \lambda_a^{SK} Z(\mathsf{x}_a) + \mathrm{m}\left(1\text{-}\lambda_a^{SK}\right) = 1 * Z(\mathsf{x}_a),$$

if $\mathsf{x}_0 = \mathsf{x}_a$,

Weight assigned to the mean (m) is zero. When more than one data points are used for SK estimation but one of the data coincide with the location of the target note $\mathsf{x}_0 = \mathsf{x}_a$ all other data points will obtain a zero weight.

In the Ordinary kriging case the weights of the data points are estimated using set of the linear equations, which are in the matrix notation are expressed as $[\mathsf{W}] * [\lambda] = [\mathsf{B}]$. The matrixes $[\mathsf{W}]$, $[\lambda]$ and $[\,\mathsf{B}\,]$ for the case of one data point coincident with the target node ($\mathsf{x}_0 = \mathsf{x}_a$) are defined as follows:

$$[\mathsf{W}] = \begin{bmatrix} 0 & 1 \\ 1 & 0 \end{bmatrix} = -1,\ [\lambda] = \begin{bmatrix} \lambda_1 \\ \mu \end{bmatrix},$$

$$\text{and } [\mathsf{B}] = \begin{bmatrix} 0 \\ 1 \end{bmatrix} = -1.$$

The weight of a single sample estimated from this data using the OK equations is equal to 1:

$$[\lambda] = [\mathsf{B}] * [\mathsf{W}]^{\mathrm{T}} = \mathbf{1}$$

The OK Eq. (19.2.1) in one data point case becomes

$Z^*_{OK}(\mathsf{x}_0) = \lambda_a^{OK} Z(\mathsf{x}_a) = 1 * Z(\mathsf{x}_a)$, if $\mathsf{x}_0 = \mathsf{x}_a$,

Therefore, the estimate at the point $\mathbf{X}_0$ which is coincident with location of a single sample $\mathbf{X}_a$ is equal to the value of this sample $Z(\mathsf{x}_a)$.

When OK system has more than one sample but a sample $Z(\mathsf{x}_a)$ is coincident with a target node $\mathbf{X}_0$ the weights λ_i of all other samples and weight of the Lagrange Multiplier μ are zero.

19.3.2 Negative Kriging Weights and Screening Effect

Kriging systems assigns more weights to the samples located close to an estimated point and the weights rapidly decrease with distance from a target point increase (Fig. 19.2). Some samples can receive negative weight which occurs when another sample falls between it and the point being estimated (Fig. 19.2a). This is a specific property of the kriging system called screening effect (Goovaerts 1997).

The negative weights caused by a screening effect allow the kriging estimate to take values outside of the range of data (non-convexity property). In general, this is a desirable property of an estimator because it is unlikely that the sample data set includes the most extreme values and the true values of the studied variable may be beyond the available sample values.

However, there is a risk that negative weights may yield significant errors when they associate with the high grade samples. Such kriging estimates are commonly biased and can significantly underestimate the true value. This is demonstrated in the Table 19.2 showing four kriging estimates obtained by changing value of a sample which has a negative weight in a kriging system. First set (case 1) is the actual drill hole intersections observed at the Meliadine gold deposit (Fig. 19.2). Three other sets are hypothetical, and obtained by changing the value of the data point 4 from 0.6 g/t to 10, 60 and 100 g/t Au. The kriging weights are independent of the actual data point values therefore they not changed and the same weights are used in all four estimates.

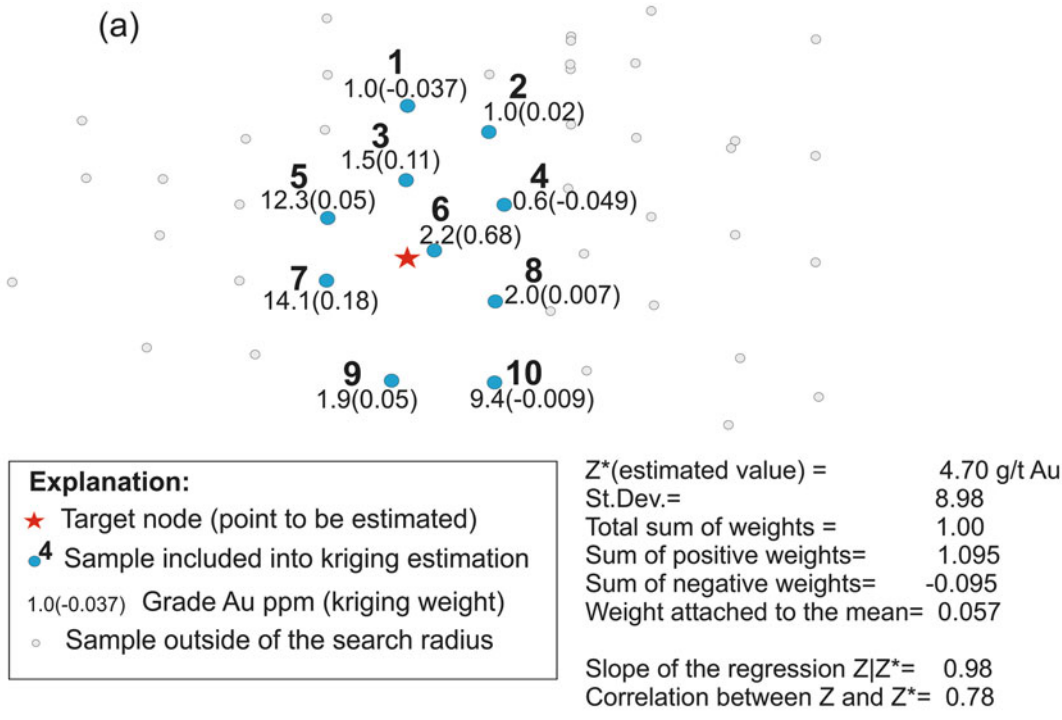

Fig. 19.2 Example of a data configuration displaying the screen effect. Data from the Meliadine gold deposit, Canada (Abzalov and Humphreys 2002a): (**a**) map showing distribution of the data points and their estimated Ordinary kriging weights (Data numbers correspond to Table 19.2; (**b**) variogram model used in the Ordinary kriging estimation)

Table 19.2 Influence of the negative weights on Ordinary kriging estimate

Drill hole number	Ordinary kriging weights	Gold grade (Au, g/t)			
		Case 1 (Fig. 19.2)	Case 2 (hypothetical)	Case 3 (hypothetical)	Case 4 (hypothetical)
1.	−0.037	1.0	1.0	1.0	1.0
2.	0.024	1.0	1.0	1.0	1.0
3.	0.109	1.5	1.5	1.5	1.5
4.	**−0.049**	**0.6**	**10.0**	**60.0**	**100.0**
5.	0.050	12.3	12.3	12.3	12.3
6.	0.676	2.2	2.2	2.2	2.2
7.	0.175	14.0	14.0	14.0	14.0
8.	0.007	2.0	2.0	2.0	2.0
9.	0.054	1.9	1.9	1.9	1.9
10.	−0.009	9.4	9.4	9.4	9.4
Estimate (Z*)		4.71	4.24	1.79	−0.17

Drill hole numbers correspond to Fig. 19.2a

Results, obtained using Ordinary kriging expression show a serious disadvantage of the negative weights (Table 19.2). The increasing value of the data point four yields an opposite effect on the estimated grade, which decreases with drill hole grade increase. The estimated grade becomes negative (−0.17 g/t) when a particularly high grade value associates with a negative weight (Table 19.2).

Because of a risk of a biased results the negative weights are usually removed from the estimates. Because they are caused by a screening effect they can be eliminated or at least their appearance significantly minimised by optimising the search neighbourhood thus that only the data closest to the target node $Z^*(\mathbf{x})$ are used for estimation.

However, changing the search neighbourhood not always produces a desirable result, therefore in order to deal with non-convexity problem the negative weights are commonly excluded from the kriging estimations using one of the mathematical procedures:

- the negative weights are replaced by a 0 and remaining positive weights reset to sum to 1;
- the kriging weights are forced to be positive by adding a constant equal to the modulus of the largest negative weight and then resetting the weights to sum to 1 (Journel and Rao 1996);
- the kriging weights are forced to be positive using statistical transformations (Barnes and Johnson 1984);
- impose constrains on the kriging estimates rather than on the kriging weights. For example, resetting the negative grade values to 0 (Goovaerts 1997).

Removing the negative weights or forcing them to be positive usually improves the estimate although not completely eliminates the bias (Table 19.3). Disadvantage of the removing the negative weights is effectively eliminates the data which associates with them from the kriging estimates and as a consequence, the result remains the same independently of the value of the sample which was removed. This is illustrated in the Table 19.3 where negative weight removing techniques has been applied to the cases 1 and 3. Both cases have identical data configuration, shown on the Fig. 19.2a, and differ only by the value of the data (drill hole) 4, which is 0.6 g/t Au for the case 1 and 60 g/t Au for the case 3. Despite of significant difference of the data, the kriging estimate obtained by applying the negative weight removing techniques, have yielded the identical results.

Because of the drawback of the negative weights estimating of a variable which is characterised by a highly skewed distribution (e.g. gold deposits) a special attention should be made on to optimising the search neighbourhood in order to avoid appearances of the negative weights. Influence of the negative weights is also minimised using Indicator kriging and imposing constraint on the estimates (Goovaerts 1997).

19.3.3 Smoothing Effect

The kriging estimate is commonly lays between largest and smallest value of the input data (Table 19.3). Therefore, kriging estimate decreases variance of the input data. This is shown on the Fig. 19.3 where histogram of the composited samples are plotted against the Ordinary kriging point estimates. Variance of the estimated points decreased by 63 % in comparing with variance of the data points (Fig. 19.3). Reduced variability of estimated value is referred to as smoothing effect of kriging and it is a consequence of combining several samples to form an estimate.

Degree of smoothing can vary depending on the search neighbourhood and variogram model. In particular, kriging smooths distribution of the variable if the search neighbourhood includes samples outside of the variogram range (Fig. 19.4).

Excessively smoothed estimates can lead to incorrectly estimated resources at the given cut-off. This is illustrated on the Fig. 19.4 presenting two block models created using different variogram models and search architecture. The economic resources of this deposit were estimated by applying the 100 ppm U cut-off to the block grades. Excessively smoothed model

Table 19.3 Eliminating the negative weights from the kriging estimate

	Case 1				Case 3			
		Ordinary kriging weights				Ordinary kriging weights		
			Negative weights removed				Negative weights removed	
Drill hole number	Data Au, g/t	Negative weights retained	Method (a)	Method (b)	Data Au, g/t	Negative weights retained	Method (a)	Method (b)
1.	1.0	−0.037		0.008	1.0	−0.037		0.008
2.	1.0	0.024	0.022	0.049	1.0	0.024	0.022	0.049
3.	1.5	0.109	0.100	0.106	1.5	0.109	0.100	0.106
4.	**0.6**	**−0.049**		**0.000**	**60.0**	**−0.049**		**0.000**
5.	12.3	0.050	0.046	0.066	12.3	0.050	0.046	0.066
6.	2.2	0.676	0.617	0.487	2.2	0.676	0.617	0.487
7.	14.0	0.175	0.160	0.150	14.0	0.175	0.160	0.150
8.	2.0	0.007	0.006	0.038	2.0	0.007	0.006	0.038
9.	1.9	0.054	0.049	0.069	1.9	0.054	0.049	0.069
10.	9.4	−0.009		0.027	9.4	−0.009		0.027
Estimate (Z*)		4.71	4.43	4.67		1.79	4.43	4.67

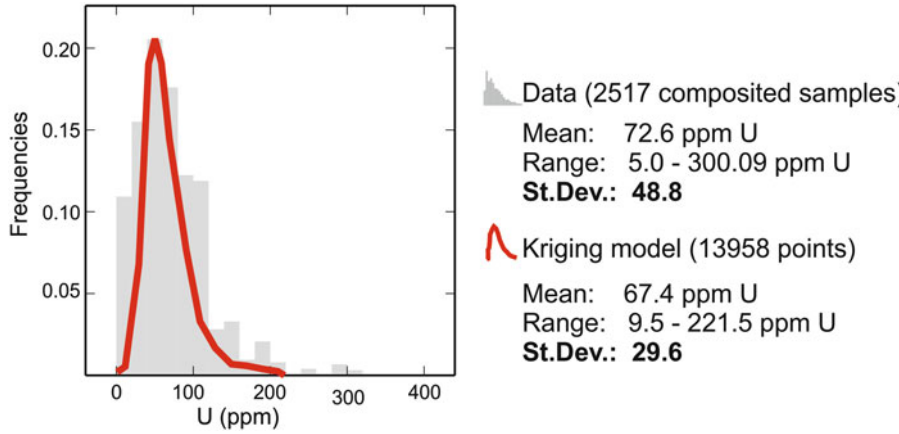

Fig. 19.3 Histograms of the input data and corresponding them Ordinary kriging estimates

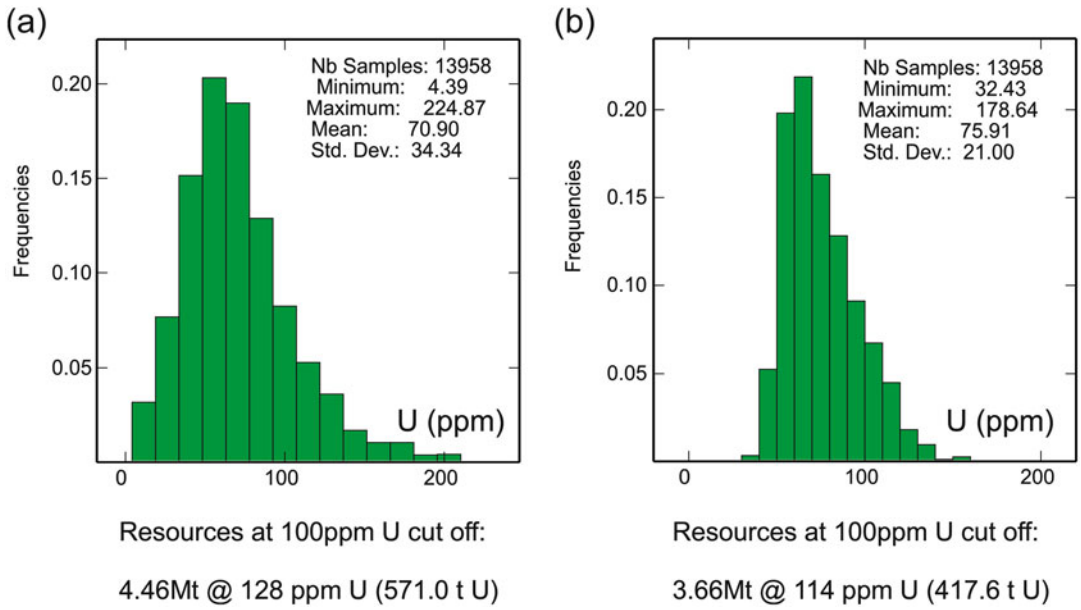

Fig. 19.4 Histograms of the uranium grades estimated using Ordinary kriging. In both cases the isotropic exponential variogram was used and the search neighbourhood was 25 nearest samples: (**a**) 600 m variogram range; (**b**) 60 m variogram range

(Fig. 19.4b) underestimates tonnage and grade of uranium mineralisation in comparison with the less smoothed model (Fig. 19.4a). In total, the contained uranium was underestimated by −27 % (Fig. 19.4).

Another drawback of the kriging's smoothing effect is that it is not uniform and rather depends on the data configuration. Smoothing is minimal in the densely sampled areas, when estimated point is located close to the data locations and increases as the point being estimated gets farther away from the data. As a result of this map of the kriging estimates looks more variable in the densely sampled areas than on the peripheral parts of the studied domain and sparsely sampled areas.

Smoothing effect of kriging increases when it is applied for estimating blocks. This is illustrated on the Fig. 19.5 comparing the point kriging results with the 2D block kriging estimates. In

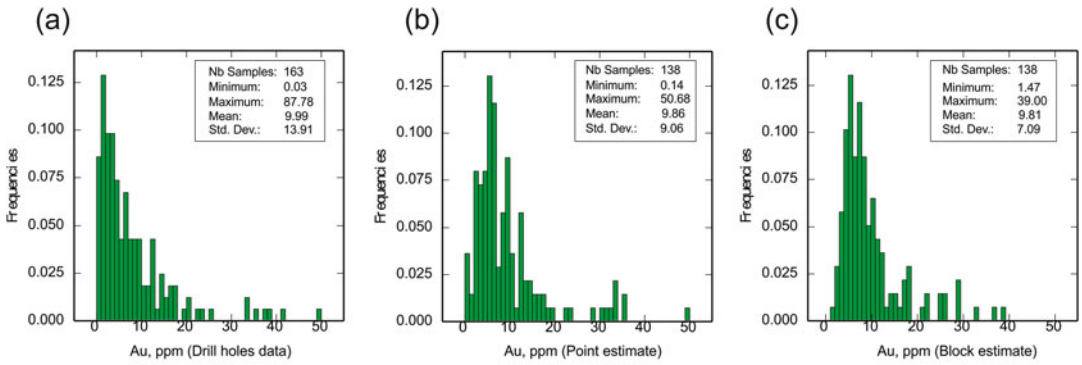

Fig. 19.5 Smoothing effect by point and block kriging: (**a**) point histogram of the drill holes data; (**b**) histogram of the point kriging estimate; (**c**) histogram of the average block grades estimated by the Ordinary block kriging

the both cases the estimation was made using Ordinary kriging method interpolating the sample grades into the 2D grid of 40×40 m. The kriging search neighbourhood was a circle of 200 m radius containing 4–16 data points. The variance of the gold grade changes from 193 Au ppm^2 of the data points (Fig. 19.5a), to 82 Au ppm^2 of the point kriging estimates (Fig. 19.5b) and decreases to 50 Au ppm^2 of the block kriging (Fig. 19.5c).

19.3.4 Kriging Variance

Kriging methodology providing a least-square estimate of the variable Z(**x**) also provides an estimation error, commonly referred to as kriging variance $\sigma^2_{KRIGING}$. This is a very useful parameter of the kriging model allowing to assess uncertainties of the estimates and identify the main risks where a large estimation error associates with a high grade mineralisation. This is illustrated on the Fig. 19.6 showing distribution of the drill holes intersecting gold mineralisation (Fig. 19.6a) and the gold grade estimated by Ordinary kriging (Fig. 19.6b). The kriging estimation errors, which are expressed as the kriging standard deviations, are show on the Fig. 19.6c. Superimposing of the kriging error of 1 standard deviation equal to +/−10 g/t on the grade model (Fig. 19.6b) shows that the many high grade blocks are estimated with an error significantly larger than this threshold.

Kriging variance was also proposed for optimising a search neighbourhood and for classification of the mineral resources (Royle 1977; Diehl and David 1982). However, kriging variance is independent of the value of the data. This can be seen from equalities defining the kriging variance,

$$\sigma^2_{OK}(\mathbf{x}) = \sigma^2_0 - \sum_\alpha \lambda^{\mathrm{OK}}_\alpha \gamma(\mathbf{x}_0 - \mathbf{x}_\alpha) - \mu_{\mathrm{OK}}$$

and

$$\sigma^2_{SK}(\mathbf{x}) = \sigma^2_0 - \sum_\alpha \lambda^{\mathrm{SK}}_\alpha C(\mathbf{x}_a - \mathbf{x}_0),$$

which do not the references to the data values. Because of this peculiarity the kriging system assigns the identical errors to the estimates if their data configurations are identical, and this is independent of the real data values (Fig. 19.6c).

In summary, parameters of the kriging variance are as follows:

- depends on the variogram (covariance) model. The more complex is a spatial variability (e.g. larger nugget effect) the larger estimation error for the same data configurations;
- depends on the data configuration. This is practically most important parameter, allowing to use the kriging variance to choose the optimal drilling grid for classification resources;
- it is independent of the data values. This means that the identical data configurations in a given geostatistical domain (i.e. the same variogram model) would yield the identical

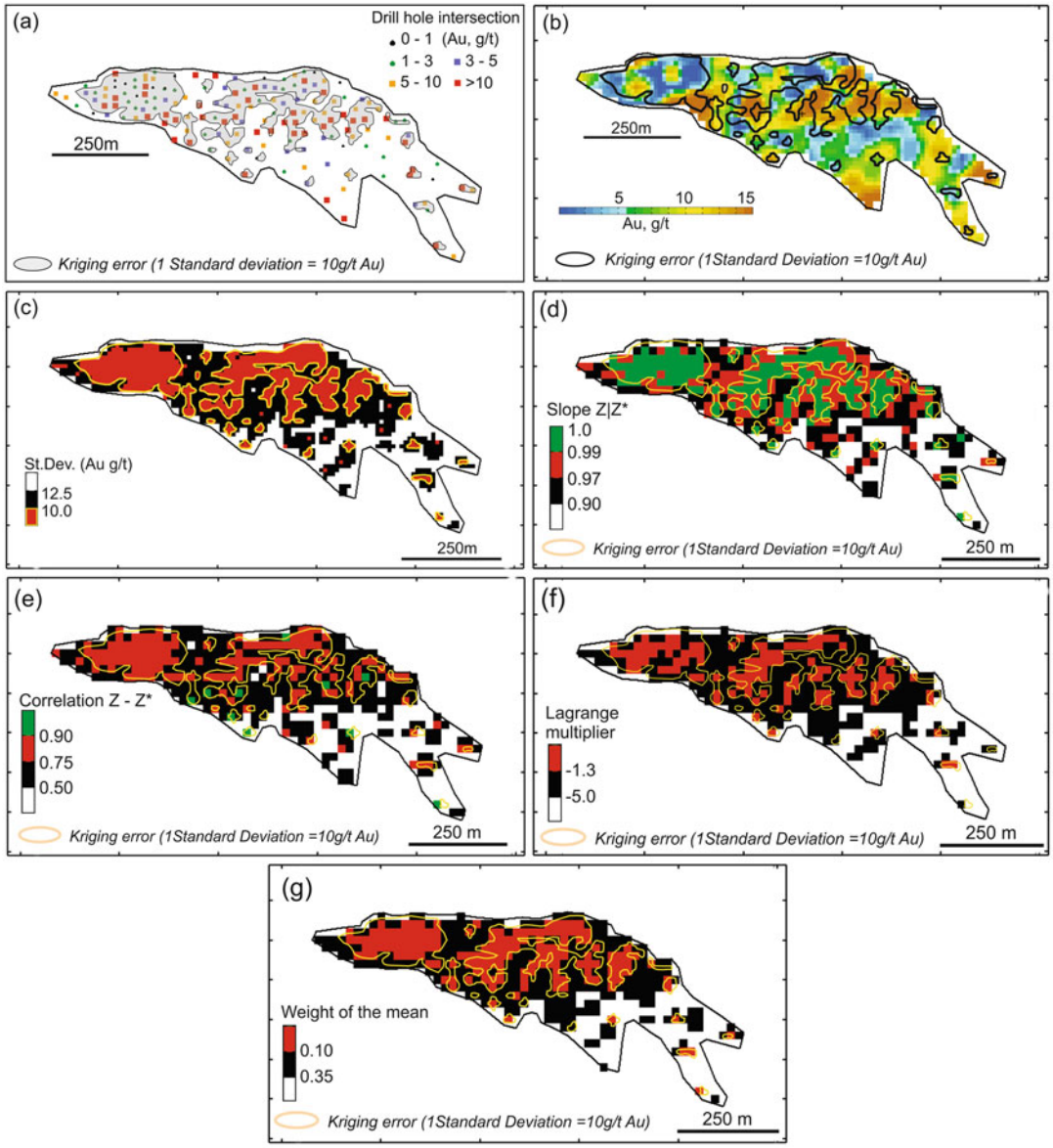

Fig. 19.6 Longsection of the lode 1000 at the Meliadine deposit, Canada (Abzalov and Humphreys 2002a) showing gold grade estimated by 2D Ordinary kriging point model and geostatistical indicators of the kriging efficiency. Contours of the kriging error (1 standard deviation = 10 g/t Au) are shown for the reference: (**a**) data points distribution; (**b**) gold grade; (**c**) kriging estimation error; (**d**) slope of regression of Z|Z*; (**e**) correlation between Z and Z*; (**f**) Lagrange multiplier; (**g**) weight of the mean

kriging variance, no matter what the data values are.

Thus, kriging variance does not provide a true value of estimation error and can be used only as a ranking index of the data geometry.

19.3.5 Conditional Bias

The constraints of the kriging system described in the Sect. 19.2 imply that a kriging approach of interpolating the data is the best and unbiased in the least-square sense because it is obtained

under conditions that estimation error variance is a minimal for a given data configuration and mathematical expectation of the error is equal to 0.

Lacking of the global bias, however, does not guarantee that every local estimate is accurate. In fact, kriging models are commonly biased at the high or low grade intervals, despite of the accurately estimated global mean. This is referred to as conditional bias, because sign and value of the bias depend on the grade class. One of the main causes of a conditional bias is the smoothing effect of kriging, which decreases variability of a studied attribute and this leads to the low grade values are overestimated and the high grades are underestimated.

The conditional bias represents a significant disadvantage of the kriging estimates when their objective was to detect spatial distribution and the actual values of the extreme classes, for example concentration of the metallurgically deleterious components in the ore body or distribution of the environmentally hazardous materials.

19.3.5.1 Slope of the Z|Z* Regression

Conditional bias can be diagnosed and the degree of the bias assessed by plotting the true values Z(**x**) versus corresponding them estimates Z*(**x**). Accurate, non-biased estimates are distributed along bisect (X = Y line) of the diagram of Z vs. Z*. Deviation of the regression line from bisect indicates for a conditional bias, the larger deviation the larger degree of a conditional bias. True value Z(**x**) is usually unknown, unless it is approximated using conditional simulation techniques (Lantuejoul 2002). However, the slope of regression between true, but unknown, value Z(**x**) and the Ordinary kriging estimate $Z^*_{OK}(\mathbf{x})$ can be estimated mathematically (Rivoirard 1987) and used as a non-subjective criteria of efficiency of a kriging search architecture. Ideally, slope of the regression between Z values and it's estimates Z* should be close to 1, in that case the estimated values Z* are plotted close the true but unknown value Z and data points will be distributed along the X = Y line. Slope of regression less than 0.9 indicates that kriging estimates are conditionally biased, which possibly is caused by a suboptimal search neighbourhood.

A simple and intuitively understandable definition of this criteria makes it very popular among resource estimation specialists (Pan 1995; Armstrong 1998). However, application of this criteria without considering the underlying assumptions, imposing a practical limitation on this method, can lead to erroneous results.

Therefore, this section provides a detailed review of geostatistical definition of the slope of regression of the Z on Z^*_{OK} made by Rivoirard (1987). Limitations of this criteria is further discussed and explained using a case study. Procedure of calculation of the slope of regression is as follows.

Weights of λ_i^{OK} and Lagrange multiplier μ_{OK} are calculated from OK system of the linear equations. In the covariance terms they are expressed as

$$\sum_i \left\{\lambda_i^{OK}\,\mathrm{Cov}\left[Z(x_i), Z(x_j)\right]\right\} = \mathrm{Cov}\left[Z(x_0), Z(x_i)\right] + \mu_{OK} \quad (19.3.1)$$

given the $\sum_i \lambda_i^{OK} = 1$ and μ_{OK} is Lagrange multiplier.

Covariance between true but unknown Z(**x**) and estimated $Z^*_{OK}(\mathbf{x})$ is expressed as

$$\begin{aligned}\mathrm{Cov}\left[Z(\mathbf{x}), Z^*_{OK}(\mathbf{x})\right] &= \mathrm{Cov}\left[Z(\mathbf{x}), \sum_i \left[\lambda_i^{OK} Z(\mathbf{x}_i)\right]\right] \\ &= \sum_i \left\{\lambda_i^{OK}\mathrm{Cov}\left[Z(\mathbf{x}), Z(\mathbf{x}_i)\right]\right\} \quad (19.3.2)\end{aligned}$$

The variance of the kriging estimate $Z^*_{OK}(\mathbf{x})$ can be expressed as

$$\begin{aligned}\mathrm{Var}\left[Z^*_{OK}(\mathbf{x})\right] &= \mathrm{Var}\sum_i \left[\lambda_i^{OK} Z(\mathbf{x}_i)\right] \\ &= \sum_i \sum_j \left\{\lambda_i^{OK}\lambda_j^{OK}\mathrm{Cov}\left[Z(\mathbf{x}_i), Z(\mathbf{x}_j)\right]\right\} \quad (19.3.3)\end{aligned}$$

The OK Eq. (19.3.1) can be modified into

$$\sum_i \sum_j \left\{\lambda_i^{\mathrm{OK}} \lambda_j^{\mathrm{OK}} \mathrm{Cov}\left[\mathrm{Z}\left(\mathbf{x}_\mathrm{i}\right), \mathrm{Z}\left(\mathbf{x}_\mathrm{j}\right)\right]\right\} = \sum_j \left\{\lambda_j^{\mathrm{OK}} \mathrm{Cov}\left[\mathrm{Z}\left(\mathbf{x}\right), \mathrm{Z}\left(\mathbf{x}_\mathrm{j}\right)\right]\right\} + \mu_{\mathrm{OK}} \tag{19.3.4}$$

Substituting expressions (19.3.2) and (19.3.3) into (19.3.4) led to the following expression

$$\mathrm{Cov}\left[\mathrm{Z}\left(\mathbf{x}\right), \mathrm{Z}^*_{\mathrm{OK}}\left(\mathbf{x}\right)\right] = \mathrm{Var}\left[\mathrm{Z}^*_{\mathrm{OK}}\left(\mathbf{x}\right)\right] - \mu_{\mathrm{OK}} \tag{19.3.5}$$

Similarly, by substituting expression (19.3.2) into the kriging error variance (19.2.3) it can be expressed as follows:

$$\sigma^2_{OK}\left(\mathbf{x}\right) = \sigma^2_0 - \mathrm{Cov}\left[\mathrm{Z}\left(\mathbf{x}\right), \mathrm{Z}^*_{\mathrm{OK}}\left(\mathbf{x}\right)\right] + \mu_{\mathrm{OK}} \tag{19.3.6}$$

where σ^2_0 is a point variance in the mineralised domain, and σ^2_{OK} is a kriging variance.

Finally, from the expression (19.3.6) covariance between true but unknown value Z(**x**) and estimate Z_{OK}*(**x**) is deduced as follows:

$$\mathrm{Cov}\left[\mathrm{Z}\left(\mathbf{x}\right), \mathrm{Z}^*_{\mathrm{OK}}\left(\mathbf{x}\right)\right] = \sigma^2_0 - \sigma^2_{OK}\left(\mathbf{x}\right) + \mu_{\mathrm{OK}} \tag{19.3.7}$$

The variance of the kriging estimates Z_{OK}*(**x**) is deduced from the expression (19.3.5) by substituting a covariance defined in (19.3.7):

$$\mathrm{Var}\left[\mathrm{Z}^*_{\mathrm{OK}}\left(\mathbf{x}\right)\right] = \sigma^2_0 - \sigma^2_{OK}\left(\mathbf{x}\right) + 2\mu_{\mathrm{OK}} \tag{19.3.8}$$

Slope of regression $\rho\left(\mathrm{Z}\middle|\mathrm{Z}^*_{\mathrm{OK}}\right)$ of true but unknown value Z(**x**) on estimate Z_{OK}*(**x**) can be defined[1] as

$$\rho\left(\mathrm{Z}\middle|\mathrm{Z}^*_{\mathrm{OK}}\right) = \frac{\mathrm{Cov}\left[\mathrm{Z}\left(\mathbf{x}\right), \mathrm{Z}^*_{\mathrm{OK}}\left(\mathbf{x}\right)\right]}{\mathrm{Var}\left[\mathrm{Z}^*_{\mathrm{OK}}\left(\mathbf{x}\right)\right]} = \mathrm{r}_{\mathrm{ZZ}^*_{\mathrm{OK}}} \frac{\sqrt{\sigma^2_0}}{\mathrm{StD}\left[\mathrm{Z}^*_{\mathrm{OK}}\left(\mathbf{x}\right)\right]} \tag{19.3.9}$$

where $r_{ZZ^*_{OK}}$ denotes a correlation coefficient between Z(**x**) and it's estimate Z_{OK}*(**x**),
StD denotes a standard deviation.

Substitution of the expressions (19.3.7) and (19.3.8) into Eq. (19.3.9) allows to finally define a slope of regression of true but unknown value Z(**x**) on the estimate Z_{OK}*(**x**) as follows:

$$\rho\left(\mathrm{Z}\middle|\mathrm{Z}^*_{\mathrm{OK}}\right) = \left[\sigma^2_0 - \sigma^2_{OK}\left(\mathbf{x}\right) + \mu_{\mathrm{OK}}\right] \times \left[\sigma^2_0 - \sigma^2_{OK}\left(\mathbf{x}\right) + 2\mu_{\mathrm{OK}}\right] \tag{19.3.10}$$

where σ^2_0 is a point variance of the estimated variable Z, and σ^2_{OK} is a conventional kriging variance defined in the expression (19.3.6).

By assigning the slope of regression to the kriging estimates they can be classified by the degree of the estimation confidence. In practice, the map showing slope of the regression values is created as a supplement to the map of the krigged values (Fig. 19.6b, d). The areas characterising by the different degrees of a conditional bias are interpreted from the map by applying the thresholds values of the $\rho\left(\mathrm{Z}\middle|\mathrm{Z}^*_{\mathrm{OK}}\right)$. Commonly, if slope of regression is 0.90 and larger (approximately 1.0) the conditions bias is considered insignificant.

[1] Let's consider linear regression: Y* = **ρ** X + b. Residue (i.e. estimation error) can be defined as:

R = Y – Y* = Y – (**ρ**X + b), where Y = true, but unknown value of Y.

Y* is an optimal estimator when error variance [Var(R)] is minimum. Variance of the residue is expressed as follows: Var(R) = Var(Y – **ρ**X – b) = Var(Y) + **ρ**²Var(X) – 2**ρ** Cov(XY).

It's value is minimal when 1st derivative, d/d**ρ** (Var(R)), is equal to zero. In other words:

d/d**ρ** [Var(R)] = d/d**ρ** [Var(Y) + **ρ**²Var(X) – 2**ρ**Cov(XY)] = 0 + 2**ρ**Var(X) – 2Cov(XY) = 0,

which leads to expression for slope of the regression:

ρ = Cov(XY)/Var (X)

The slope of the regression can be expressed through a correlation coefficient, which by definition is r_{XY} = Cov(XY)/[St.Dev (X) * St.D. (Y)]. Where St.D.(X) denotes a standard deviation of variable X. Substituting this to the expression of the slope of the regression yields the following final expression:

ρ (Y|X) = Cov(XY)/Var (X) = r_{XY} * (σ_Y/σ_X).

However, comparing slope of regression with the kriging variance shows that the slope of regression alone is insufficient for diagnostics of the poorly estimated areas. This is illustrated on the Fig. 19.6d where most of the Ordinary kriging estimates are characterised by the $\rho\left(Z\middle|Z^*_{OK}\right)$ values 0.95–1.0 which suggests lack of a conditional bias. However, their kriging estimation error varies in a wide range and often exceeds the threshold of +/−10 g/t indicating for a suboptimal quality of the estimates (Fig.19.6b, d).

Thus, the $\rho\left(Z\middle|Z^*_{OK}\right)$ values of 0.95–1.00 suggesting lacking of a conditional bias can mislead geologists creating them a false impression of the reliable estimates. The slope of regression (Fig. 19.6d) therefore is better to use together with other indicators of the kriging efficiency, in particular kriging variance and correlation coefficient between Z and Z*, for obtaining the more detailed assessment of the kriging model efficiency.

19.3.5.2 Correlation of the Z and Z*

Correlation coefficient of true, but unknown, value Z(**x**) and it's ordinary kriging estimate $Z^*_{OK}(\mathbf{x})$ is a useful criteria of the kriging neighbourhood efficiency (Fig. 19.6e). It is estimated as

$$r_{ZZ^*_{OK}} = \frac{\mathrm{Cov}\left[Z(\mathbf{x}), Z^*_{OK}(\mathbf{x})\right]}{\sigma_0 * \mathrm{StD}\left[Z^*_{OK}(\mathbf{x})\right]} \qquad (19.3.11)$$

Substituting Cov [Z(**x**),Z_{OK}*(**x**)] determined in the 19.3.7 into equality 19.3.11 gives the final expression of a correlation between Z(**x**) and $Z^*_{OK}(\mathbf{x})$:

$$r_{ZZ^*_{OK}} = \frac{\sigma_0^2 - \sigma^2_{OK}(\mathbf{x}) + \mu_{OK}}{\sigma_0 * \mathrm{StD}\left[Z^*_{OK}(\mathbf{x})\right]} \qquad (19.3.12)$$

where σ_0^2 is a point variance of the estimated variable Z, and σ^2_{OK} is a kriging variance.

Coefficient of correlation $r_{ZZ^*_{OK}}$ between Z and Z* (19.3.12) is directly proportional to the slope of regression $\rho\left(Z\middle|Z^*_{OK}\right)$ (19.3.9 and 19.3.10).

Because of similarities of the geostatistical expressions defining the coefficient of correlation $r_{ZZ^*_{OK}}$ (19.3.12) and the slope of regression $\rho\left(Z\middle|Z^*_{OK}\right)$ (19.3.10) these parameters produce the similar results. In particular, map of the coefficient of correlations (Fig. 19.6b) is closely mimicking the map of the slope of regression values (Fig. 19.6a) therefore, in general, these parameters, $r_{ZZ^*_{OK}}$ and $\rho\left(Z\middle|Z^*_{OK}\right)$, can be interchanged.

The slope of regression $\rho\left(Z\middle|Z^*_{OK}\right)$ has an advantage over the coefficient of correlation $r_{ZZ^*_{OK}}$ because it allows to quickly diagnose and quantify the conditional bias of the kriging estimates. A default value of $\rho\left(Z\middle|Z^*_{OK}\right)$ less than 0.90 can be used as a threshold for diagnostics of the conditionally biased estimates.

Correlation coefficient $r_{ZZ^*_{OK}}$ does not allow to directly diagnose if the Ordinary kriging estimates are conditionally biased. However, the histogram of the coefficient of correlation $r_{ZZ^*_{OK}}$ is less skewed than of the slope of regression (Fig. 19.7a) therefore it is more convenient for generating the maps of the kriging efficiency. In particular, when slope of regression lay in the rage of 0.9–1.0 suggesting the accurate and reliable kriging estimates the correlation between Z and Z* can be as low as 0.5 (Fig. 19.7b) clearly showing a poor quality of the kriging estimate.

19.3.5.3 Lagrange Multiplier

Lagrange multiplier present in the expressions defining the slope of regression $\rho\left(Z\middle|Z^*_{OK}\right)$ between Z and Z* (19.3.10) and coefficient of their correlation $r_{ZZ^*_{OK}}$ (19.3.12). This is the main attribute linking the both these parameters, $r_{ZZ^*_{OK}}$ and $\rho\left(Z\middle|Z^*_{OK}\right)$, to the actual distribution of the data (search neighbourhood) therefore it is also can be used for ranking kriging estimates by the degree of confidence. The larger absolute value of the Lagrange multiplier the higher uncertainties of the kriging estimate (Fig. 19.6f). However, a quantitative assessment of the estimation confidence can not be directly obtained from the Lagrange multiplier, and usually made by calibrating them versus the parameters like kriging variance (Fig. 19.6f). It is also more skewed than coefficient of correlation $r_{ZZ^*_{OK}}$ between Z

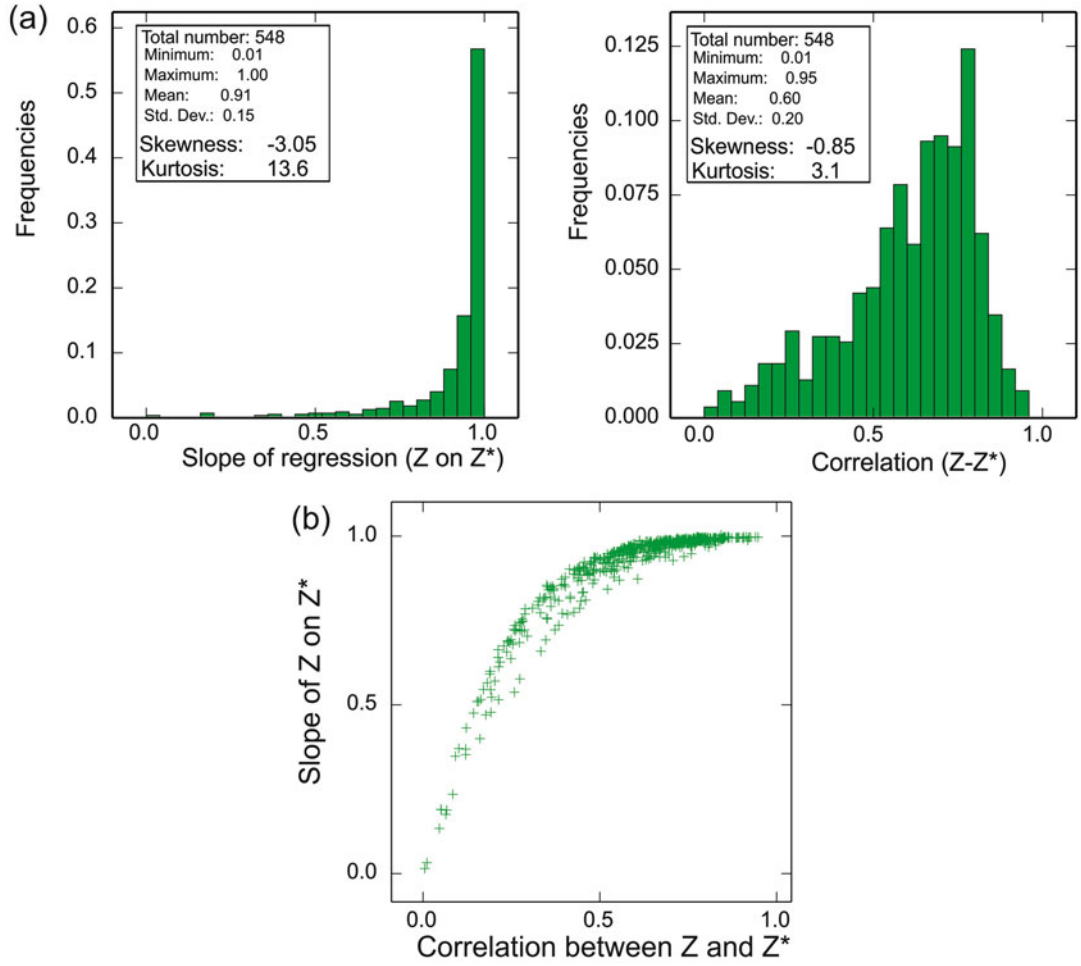

Fig. 19.7 Comparison of the basic statistics of the slope of regression of true but unknown value Z on ordinary kriging estimate Z* and coefficient of correlation between these parameters: (**a**) histograms; (**b**) scatter-diagram

and Z* and therefore is a less sensitive then $r_{ZZ^*_{OK}}$ to changes of the kriging neighbourhood configurations.

19.3.5.4 Weight of the Mean Value

A kriging weight $\left(1-\sum_i \lambda_i^{SK}\right) m$ associated with a mean in the Simple kriging estimator can also be used for comparative analysis of the kriging search neighbourhoods (Rivoirard 1987). The weight of the mean is small in the densely sampled areas, in particular if the estimated point is located close to the data locations and it increases when the data density decrease and the points being estimated gets farther away from the data. This property is commonly used by the resource industry specialists for comparing the different search neighbourhoods and finding the most optimal data configurations when weight of the mean is minimal.

Weight of the mean can also be used for classification resources by the degree of estimation uncertainties. The case presented on the Fig. 19.6g shows that the weight value of 0.10 (i.e. 10 %) closely coincides with the kriging error +/−10 g/t Au (1 standard deviation of the kriging estimate). Therefore, in a practical sense, these two parameters are similar and using weight of the mean does not provide an additional insight into the kriging neighbourhood efficiencies in comparing with the conventional kriging variance (Fig. 19.6c and g).

19.4 Block Kriging

Description of the kriging systems in the Sects. 19.2 and 19.3 were concentrated on the point estimations. Point kriging is a generic term for estimation on a point support. This means that a target can be expressed as a point of coordinate (**x**).

More often, however, it is necessary to estimate the average value of a variable within a volume (**v**) which is made by filling the 3D volumes by the rectangular blocks and estimating the attributes of the blocks. This is referred to a block kriging, which is a generic term for estimation of average value of a variable within the volume (**v**). A kriging model constructed using this approach consists of rectangles (blocks) filling a studied volume and therefore called a block model. This modelling technique is in particular relevant for the mine geology applications where ore bodies are commonly constrained by the wireframes which are filled by the rectangular blocks in order to accurately represent shape and volume of the ore bodies (Fig. 19.8).

19.4.1 Blocks and Point Estimates

One of the most common approaches for obtaining the block estimate is to discretise a block into many points which are estimated using the point kriging approach (Fig. 19.9). Then, the block grade can be obtained by averaging the all individual point estimates within the block (Fig. 19.9). This approach is robust, provides a good results and is used in the most of the computer programmes specialised for the mine geology applications. The main drawback of this technique is the large time required for estimation. When this approach is used every block is estimated by averaging several points estimates which makes estimation of the entire deposit a very time consuming process.

One applying the block kriging needs to find the optimal discretisation pattern which will minimise the computing time without jeopardising the quality of the block estimates. It was suggested (Journel and Huijbregts 1978) to discretise blocks using 4^n points, where n denotes the number of dimensions of the block. This was proposed (Journel and Huijbregts 1978) for using as a rule of thumb discretisation pattern for the block kriging estimates.

More accurately the optimal discretisation grid can be obtained by computing the covariance of the estimates ($\boldsymbol{C}_{vv}$). Choosing location of the discretisation points at random the variability of the $\boldsymbol{C}_{vv}$ can be estimated and plot versus the discretisation grids. This is explained on the Fig. 19.10, which is based on the data from the Meliadine gold deposit (Abzalov and Humphreys 2002a).

The range of approximated $\boldsymbol{C}_{vv}$ values is large when block is discretised using 2×2 points discretisation grid. This is a consequence of a sparse distribution of the discretisation points within the block preventing accurate approximation of the point-to-block and block-to-block covariances. Thus, the excessive variation of the $\boldsymbol{C}_{vv}$ values is indicative that number of discretisation points is insufficient for approximation the volume of a block. Increasing the number of discretisation points decreases variability of the $\boldsymbol{C}_{vv}$ values until a certain value, after which increasing the density of the discretisation points does not significantly change the approximated covariances (Fig. 19.10). The pivot point on the Fig. 19.10 corresponds to the 6×6 discretisation grid after which the $\boldsymbol{C}_{vv}$ values are stabilised. Thus, the grid of 6×6 points was interpreted as the most optimal block discretisation pattern at this deposit.

Block grades can also be estimated directly by using the block kriging equations (Goovaerts 1997). The block kriging system has the following expression in the covariance terms:

$$\begin{cases} \sum\limits_{\beta} \lambda_{\beta}^{\mathrm{OK}} \operatorname{Cov}\left(\mathsf{x}_{\alpha} - \mathsf{x}_{\beta}\right) + \mu_{\mathrm{OK}} = \operatorname{Cov}\left(\mathsf{x}_{\alpha}, V\right) \\ \sum\limits_{\beta} \lambda_{\beta}^{\mathrm{OK}} = 1 \end{cases} \tag{19.4.1}$$

It is identical to the point Ordinary kriging system except for the right-hand side term where point to point covariance $\mathrm{Cov}[\mathrm{Z}(\mathrm{x}_0), \mathrm{Z}(\mathrm{x}_i)]$ is replaced by the point-to-block covariance $\operatorname{Cov}\left(\mathsf{x}_{\alpha}, V\right)$.

Both techniques produce the identical results. Direct block kriging is faster because it doesn't

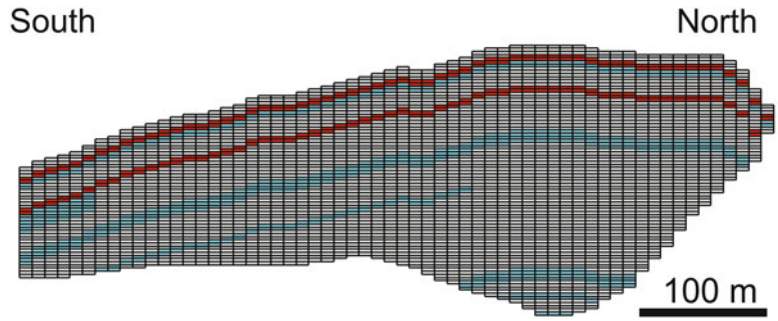

Fig. 19.8 Cross-section through the block model of the Babel nickel-sulphide deposit, Australia. Petrographically different layers within the gabbro-norite intrusion are denoted by the different colours

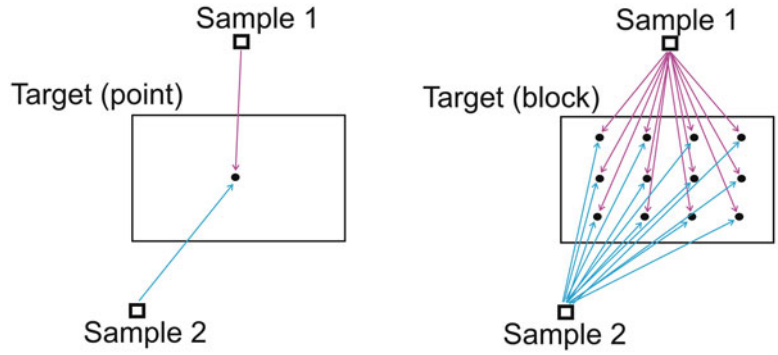

Fig. 19.9 Conceptual presentation of the point and block estimates

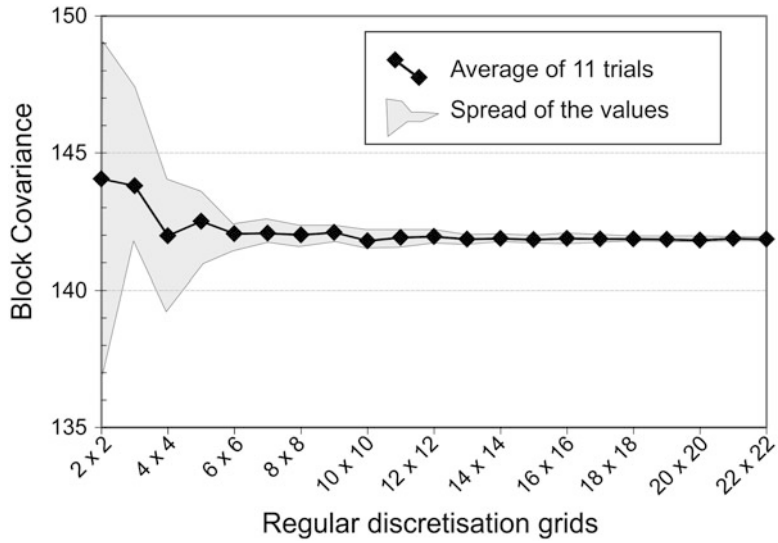

Fig. 19.10 Dependence of the block covariance on the number of discretisation points proposed for the 2D block kriging (Estimated using the data shown on the Fig. 19.2a)

require separate estimation of the discretisation points. However, when the direct kriging is not available in the used computer programmes the block kriging can be performed using a conventional discretisation approach and using the rationale shown on the Fig. 19.10 for finding an optimal discretisation grid.

19.4.2 Kriging of the Small Blocks

Kriging method is suboptimal for estimating grade of the small blocks when data grid is to sparse (Armstrong 1998). Such estimates are commonly conditionally biased due to excessive smoothing of the studied variables (Armstrong

and Champigny 1989). In order to minimise errors the size of the blocks in the resource models are chosen equal to half or quarter of the data grid. However, choice of the block size is made subjectively without quantification of the risks therefore validity of the chosen blocks usually is not known.

The case study presented below investigates dependence of the kriging estimates on the block size and analyses geostatistical criteria which can be used for choosing the optimal size of the kriging blocks. The study is based on the model of the gold deposit represented by the exhaustive set of the data points distributed as 0.5×0.5 m 2D grid (Fig. 19.11a). It was created by conditional simulation of the data from an orogenic gold deposit and retains the main statistical and geostatistical characteristics of a real deposit. The exhaustive set was overlain by a regular 40×40 m grid and the each grid node has been assigned a grade value from the closest point of the exhaustive set. This has produced the subset of the data distributed as a regular 40×40 m grid (Fig. 19.11b). The subset is called samples and it has the same statistical characteristics (Fig. 19.11d) as the exhaustive set (Fig. 19.11c). Experimental variogram estimated from exhaustive set of data and the fitted model are presented on the Fig. 19.11e.

Using the chosen samples (Fig. 19.11b) several Ordinary kriging models have been constructed by changing size of the kriging blocks (Fig. 19.12). All kriging estimates were made using the same search neighbourhood and with the same variogram model (Fig. 19.11e).

The kriging estimates were compared with the exhaustive set which is referred the 'true' data. The 'true' block grades were deduced from the exhaustive set by grouping points into the target blocks and estimating their arithmetic means. Based on this comparison accuracy of the kriging results has been quantified (Fig. 19.13; Table 19.4).

Comparison of the kriging estimates and the true data unequivocally demonstrates that kriging accuracy significantly decreases when blocks are 10×10 m or less (Figs. 19.12 and 19.13). The errors of the kriging estimates generated using small blocks become obvious when economically viable mineralisation was selected by applying cut-off of the 3 g/t Au and compared with the true data (Fig. 19.14). The difference between estimated $Z^*(x)$ and true $Z(x)$ is presented as a relative error by normalising the difference on the true values (19.4.2).

$$\text{Relative error, } \% = 100 \times \frac{Z*(x) - Z(x)}{Z(x)} \tag{19.4.2}$$

Plotting relative error versus the block size (Fig. 19.14) clearly shows that tonnage error is excessively large even when block size matches half a distance between the data points. Magnitude of the tonnage error will lead to serious errors in the estimated mineral resources. According to this study, the only acceptable block size is 40×40 m, which is matching to the data grid (Fig. 19.14).

However, the commonly used geostatistical criteria of the kriging efficiency, in particular slope of regression of the true but unknown Z on the kriging estimate Z* and kriging estimation error, have failed to diagnose the decreased efficiency of the kriging (Table 19.4). Slope of regression of the true but unknown Z on the kriging estimate Z* which (Rivoirard 1987) changes from 0.95 to 0.93, suggesting conditionally non-biased and presumably accurate estimate. Most sensitive geostatistical parameter was correlation coefficient between Z and Z* estimated using 19.3.12 (Table 19.4). Slope of regression between Z and Z* alone is insufficient for assessing validity of the block sizes and the kriging search neighbourhood. In general, the preference should be given to the blocks comparable with the data grid.

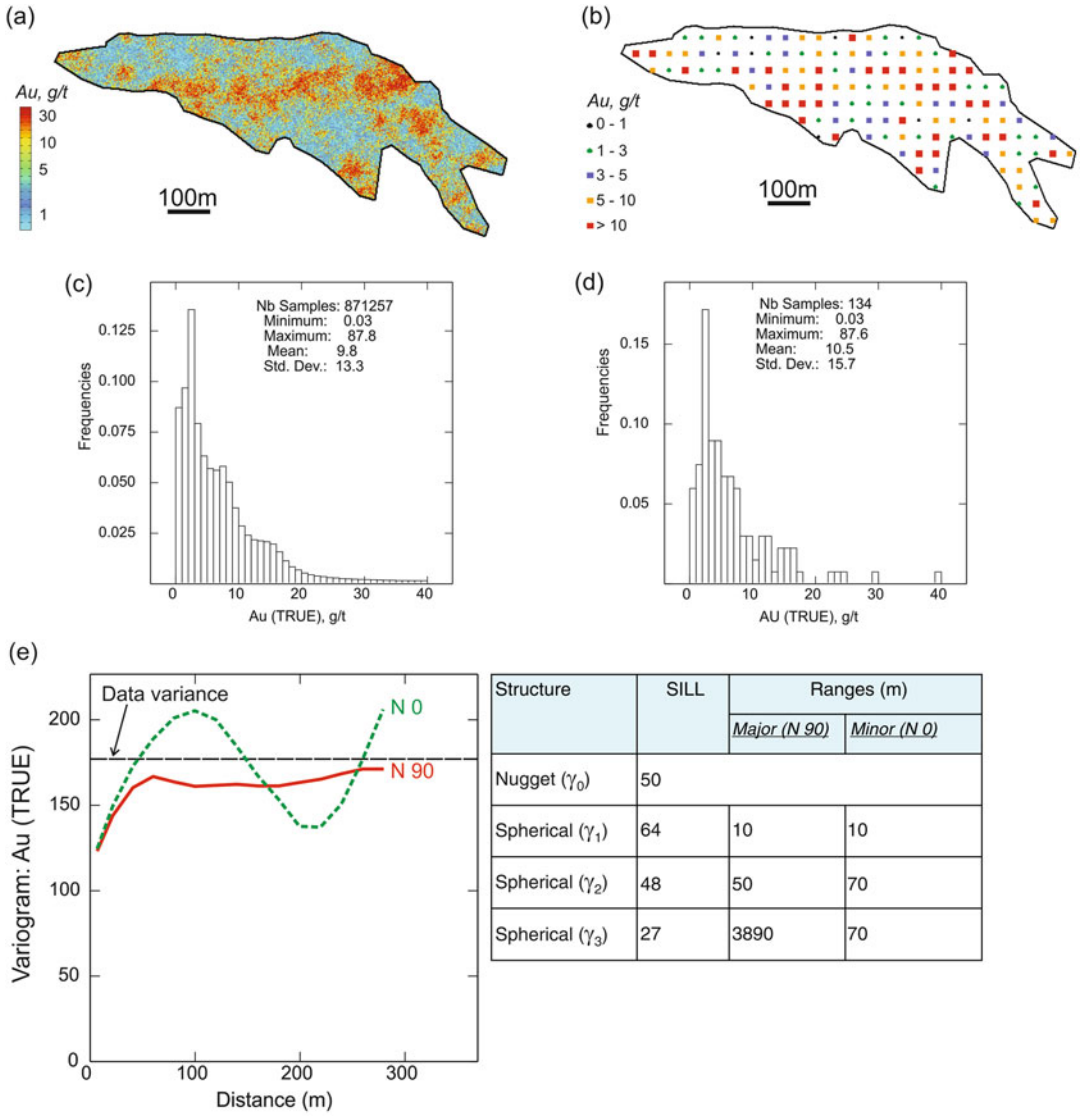

Structure	SILL	Ranges (m)	
		Major (N 90)	*Minor (N 0)*
Nugget (γ_0)	50		
Spherical (γ_1)	64	10	10
Spherical (γ_2)	48	50	70
Spherical (γ_3)	27	3890	70

Fig. 19.11 Model of the gold deposit: (**a**) exhaustive set of points distributed as 0.5×0.5 m 2D grid; (**b**) subset of the data collected at the nodes of the 40×40 m grid and referred as samples; (**c**) histogram of the exhaustive set of data; (**d**) histogram of the samples; (**e**) variogram of the gold grade estimated from exhaustive set

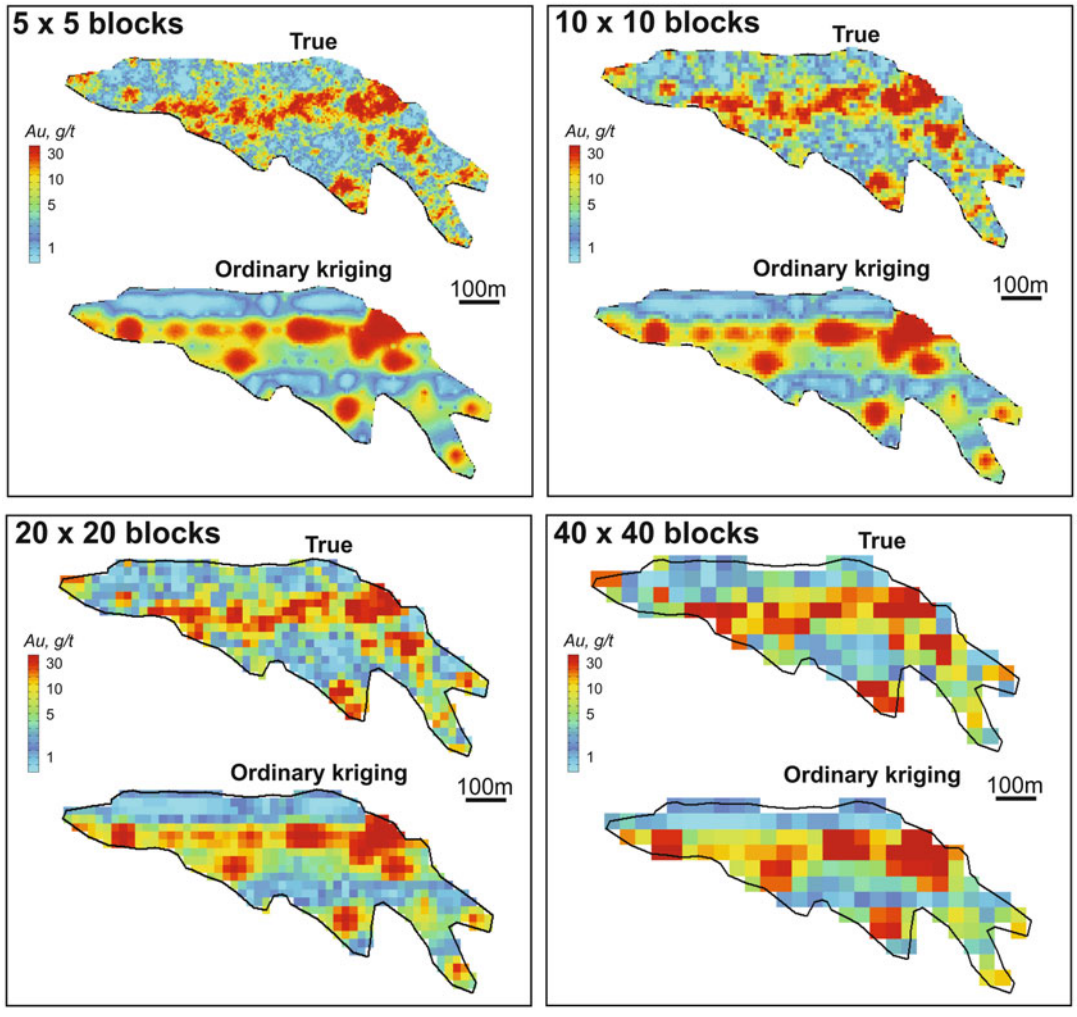

Fig. 19.12 Maps showing distribution of the gold grade estimated by Ordinary kriging and the 'true' block grades

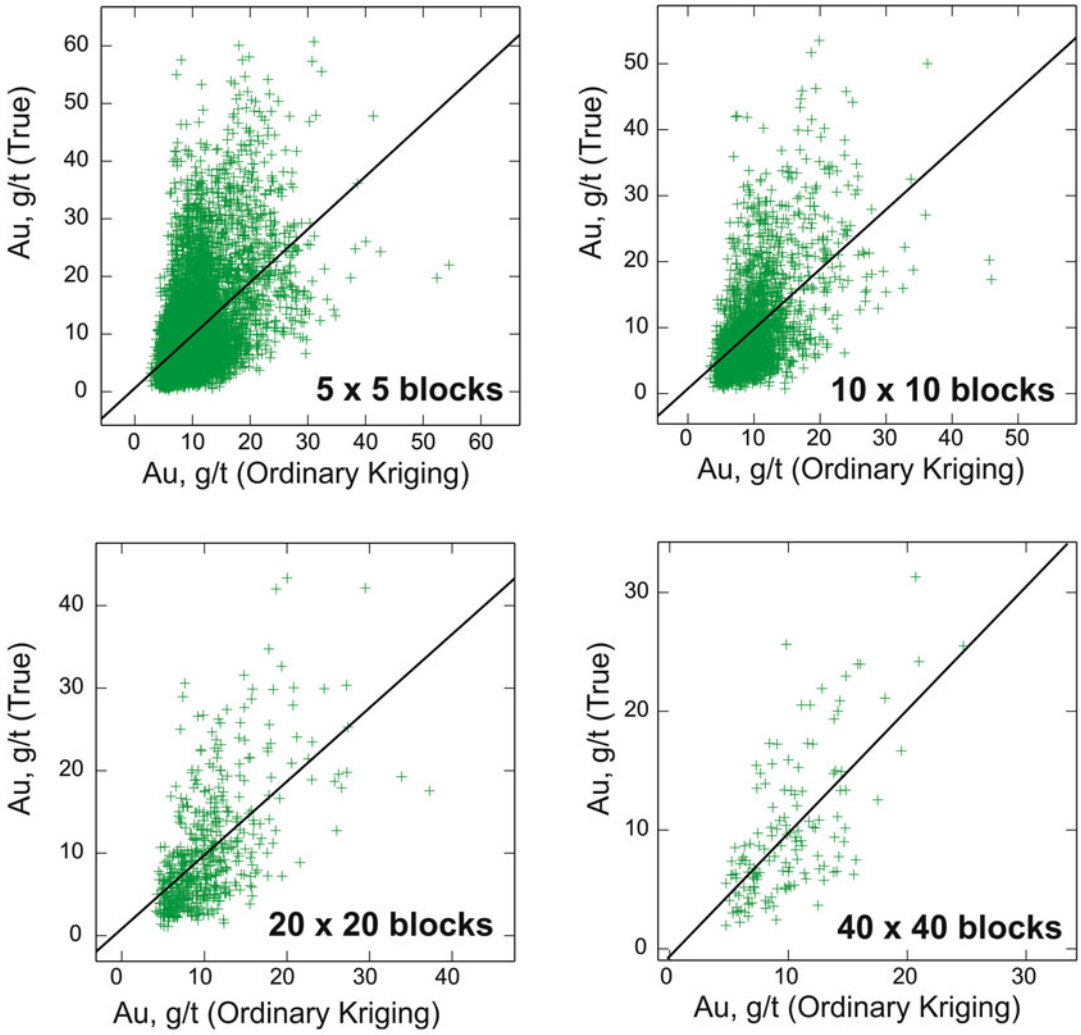

Fig. 19.13 Scatter-diagrams of the block grades estimated by Ordinary kriging. *Straight lines* denote the linear regression of true block grade on their kriging estimates

Table 19.4 Comparative statistical analysis of the Ordinary kriging block estimates with the true data

	True data		Ordinary kriging estimate		True vs. Ordinary kriging estimate			Geostatistical model		
						Regression				
Block size (m)	Mean (Z), g/t	St.D. (Z)	Mean (Z*), g/t	St.D. (Z*)	Correlation	b (tangent)	a (constant)	Kriging error (St.D.)	Slope (Z|Z*)	Rho (Z|Z*)
1 × 1	9.8	10.0	10.0	4.5	0.41	0.92	0.5	5.2	0.95	0.43
5 × 5	9.8	8.1	10.0	4.5	0.51	0.92	0.6	5.2	0.95	0.47
10 × 10	9.8	7.6	10.0	4.5	0.54	0.90	0.7	5.2	0.95	0.52
15 × 15	9.8	7.2	10.0	4.4	0.57	0.93	0.5	5.1	0.95	0.56
20 × 20	9.8	6.9	10.0	4.5	0.58	0.89	0.8	5.1	0.95	0.59
25 × 25	9.8	6.6	10.0	4.2	0.62	0.98	0.0	5.0	0.95	0.61
30 × 30	9.8	6.5	10.0	4.2	0.64	0.98	−0.1	4.9	0.95	0.64
35 × 35	9.7	6.1	10.0	4.0	0.68	1.05	−0.7	4.8	0.94	0.64
40 × 40	9.7	5.9	9.9	3.7	0.65	1.00	−0.6	4.5	0.93	0.62

Kriging error estimated using expression 19.2.3 and expressed here as 1 standard deviation
Slope(Z|Z*) is regression between Z* and Z estimated using Eq. 19.3.10
rho(Z|Z*) is a correlation coefficient between Z* and Z values estimated using Eq. 19.3.12

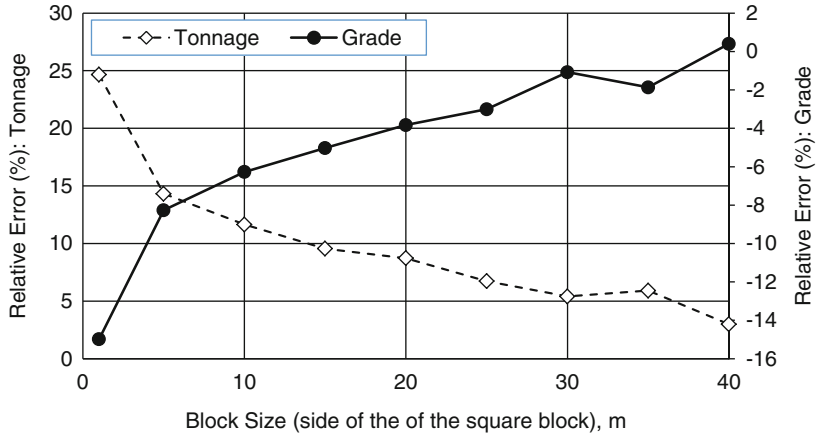

Fig. 19.14 Errors in estimated tonnage (*dashed line*) and grade (*solid line*) of mineralisation plotted versus the kriging block size. The kriging models and true data are compared at the 3 g/t Au cut-off

References

Abzalov MZ, Humphreys M (2002) Resource estimation of structurally complex and discontinuous mineralisation using non-linear geostatistics: case study of a mesothermal gold deposit in northern Canada. Exp Min Geol J 11(1–4):19–29

Annels AE (1991) Mineral deposit evaluation, a practical approach. Chapman and Hall, London, p 436

Armstrong M (1998) Basic linear geostatistics. Springer, Berlin, p 153

Armstrong M, Champigny N (1989) A study on kriging small blocks. CIM Bull 82(923):128–133

Barnes R, Johnson T (1984) Positive kriging. In: Verly G, David M, Journel AG, Marechal A (eds) Geostatistics for natural resources characterisation, vol 1. Reidel, Dordrecht, pp 231–244

Cressie N (1990) The origin of kriging. Math Geol 22(3):239–252

David M (1977) Geostatistical ore reserve estimation. Elsevier, Amsterdam, p 364

David M (1988) Handbook of applied advanced geostatistical ore reserve estimation. Elsevier, Amsterdam, p 364

Dielhl P, David M (1982) Classification of ore reserves/resources based on geostatistical methods. CIM Bull 75(838):127–135

Goovaerts P (1997) Geostatistics for natural resources evaluation. Oxford University Press, New York, p 483

Journel AG, Huijbregts CJ (1978) Mining geostatistics. Academic, New York, p 600

Journel AG, Rao SE (1996) Deriving conditional distributions from ordinary kriging. In: Report 9, Stanford Center for Reservoir Forecasting, Stanford, CA

Krige D (1951) A statistical approach to some basic mine valuation problems on the Witwatersrand. J Chem Metall Min Soc S Afr 52:119–139

Lantuejoul C (2002) Geostatistical simulation: models and algorithms. Springer, Berlin, p 250

Matheron G (1963) Principles of geostatistics. Econ Geol 58(8):1246–1266

Matheron G (1968) Osnovy prikladnoi geostatistiki (Basics of applied geostatistics). Mir, Moscow, pp 408 (in Russian)

Pan G (1995) Practical issues of geostatistical reserve estimation in the mining industry. CIM Bull 88:31–37

Rivoirard J (1987) Two key parameters when choosing the kriging neighborhood. Math Geol 19(8): 851–856

Rossi ME, Deutsch CV (2014) Mineral resource estimation. Springer, Berlin, p 332

Royle AG (1977) How to use geostatistics for ore reserve classification. World Min. February 52–56

Sinclair AJ, Blackwell GH (2002) Applied mineral inventory estimation. Cambridge University Press, Cambridge, p 381

Wackernagel H (2003) Multivariate geostatistics: an introduction with applications, 3rd edn. Springer, Berlin, p 388

Multivariate Geostatistics

20

Abstract

Extension of the kriging system to the multivariate environment allows to simultaneously estimate several variables, for example main metals and the deleterious elements. Methodology, referred as co-kriging, can be applied in isotopic and heterotopic cases.

Properties of the co-kriging systems are analysed and shown that application of the co-kriging in isotopic neighbourhood is limited and depends on spatial correlation between variables. In case of intrinsic correlation, which means that all simple and cross-structures are identical, their co-kriging in isotopic environment produces the same estimate as their direct univariate kriging.

Keywords

Multivariate • Co-kriging • Collocated • External drift

Mine geologists usually work with the several variables. This can be different geochemical characteristics of the ore body, including main metals, economically valuable by-products and metallurgically deleterious components. At the same time mine geologists are dealing with the different types of data, most commonly these are the drill hole samples from the reserve estimation database and the blast hole samples collected for the grade control. At the possession of the mine geologists there are also the bulk samples and production data reported as tonnage and grade of the mined blocks. All these data need to be integrated together in order to generate an accurate mine production plan. The kriging system, Ordinary and Simple kriging, both can be used for simultaneous estimation of the several variables and called co-kriging. They are used for integration of the different data, which can be applied in isotopic and heterotopic cases:

- Isotopic case – all variables are available at the all data points. In geostatistical terms this is referred to all data points are equally informed;
- Heterotopic case – some variables, primary (target) or secondary, are missing at the data nodes. Thus, not all data points are equally informed.

M. Abzalov, *Applied Mining Geology*, Modern Approaches in Solid Earth Sciences 12,
DOI 10.1007/978-3-319-39264-6_20

20.1 Theoretical Background of Multivariate Geostatistics

Mathematical background of the co-kriging methodology is explained using Ordinary co-kriging (COK) system which is supplemented by the brief description of the collocated ordinary co-kriging technique (CCOK).

20.1.1 Ordinary Co-kriging

Ordinary co-kriging (COK) allows simultaneous estimation of the two (i.e. Z_1 and Z_2) or more variables which can be approximated by a joint spatial distribution model (Wackernagel 2003).

In case of the intrinsic hypothesis, the coherent spatial distribution model is a matrix of the semi-variogram functions, including semi-variograms of each variable and their cross-variograms. Thus, extension of the Ordinary kriging system to multivariate environment requires construction of the variogram for each variable and estimating their cross-variograms (Journel and Huijbregts 1978; David 1988; Goovaerts 1997; Wackernagel 2003).

The ordinary co-kriging estimator is written as:

$$Z^*_{1\,COK}(\mathbf{x}) = \sum_{\alpha}\left[\lambda^{COK}_{1\alpha} Z_1(\mathbf{x}_\alpha)\right] + \sum_{\alpha}\left[\lambda^{COK}_{2\alpha} Z_2(\mathbf{x}_\alpha)\right] \tag{20.1.1}$$

Where Z_1 is a target variable and Z_2 is secondary (auxiliary) variable.

COK weights assigned to the primary $\lambda^{COK}_{1\alpha}$ and secondary $\lambda^{COK}_{2\alpha}$ data are calculated solving the COK system of the linear equations:

$$\begin{cases} \sum_{\beta} \lambda^{\mathrm{COK}}_{1\beta}\,\gamma_{11}(\mathbf{x}_\alpha - \mathbf{x}_\beta) + \sum_{\beta} \lambda^{\mathrm{COK}}_{2\beta}\,\gamma_{12}(\mathbf{x}_\alpha - \mathbf{x}_\beta) - \mu^{COK}_1 = \gamma_{11}(\mathbf{x}_0 - \mathbf{x}_\alpha),\ \forall\,\mathbf{x}_\alpha \\ \sum_{\beta} \lambda^{\mathrm{COK}}_{1\beta}\,\gamma_{12}(\mathbf{x}_\alpha - \mathbf{x}_\beta) + \sum_{\beta} \lambda^{\mathrm{COK}}_{2\beta}\,\gamma_{22}(\mathbf{x}_\alpha - \mathbf{x}_\beta) - \mu^{COK}_2 = \gamma_{12}(\mathbf{x}_0 - \mathbf{x}_\alpha),\ \forall\,\mathbf{x}_\alpha \\ \sum_{a} \lambda^{\mathrm{COK}}_{1a} = 1 \\ \sum_{a} \lambda^{\mathrm{COK}}_{2a} = 0 \end{cases} \tag{20.1.2}$$

The variance of the estimation error is written as:

$$\sigma^2_{COK}(\mathbf{x}) = \sigma^2_{Z1} - \sum_{\alpha} \lambda^{\mathrm{COK}}_{1\alpha}\,\gamma_{11}(\mathbf{x}_0 - \mathbf{x}_\alpha) - \sum_{\alpha} \lambda^{\mathrm{COK}}_{2\alpha}\,\gamma_{12}(\mathbf{x}_0 - \mathbf{x}_\alpha) - \mu^{\mathrm{COK}}_1 \tag{20.1.3}$$

where σ^2_{Z1} is the point variance of the target variable $Z_1(\mathbf{x})$

20.1.2 Collocated Co-kriging

Collocated co-kriging is used to model spatial distribution of the target variable of interest considering additional information derived from an exhaustive secondary variable. This means that the data points containing secondary variable are tightly distributed in the study area but target variable is available only at some of the data points. Objective of the method is to estimate value of the target variable in the unsampled locations using secondary variable and applying geostatistically established spatial correlation between secondary and the target variables. Every target node contains secondary variable therefore method referred collocated co-kriging (Rivoirard 2001).

This method uses only part of the secondary data, thus, it is a simplification of the co-kriging model. The most commonly used version of the

collocated co-kriging known as 'multi collocated co-kriging' (CCOK) uses secondary information in the target nodes and at the all data points containing the primary values.

Rivoirard (2001) has studied the models suitable for implementation of the CCOK technique and has concluded that CCOK algorithms equal to COK model in case if residual is spatially uncorrelated with an auxiliary variable and cross-variogram of the target and auxiliary variable is proportional to the variogram of the latter. In other cases CCOK algorithm is close but not equal to COK model as a consequence of the information loss due to simplified (i.e. multi-collocated) neighbourhood.

20.1.3 Properties of the Co-kriging

Co-kriging can be used in isotopic and heterotopic situations. In isotopic neighbourhood adding the secondary variable (Z_2) decreases kriging variance and improves the estimation precision. It also improves consistency between two variables of interest, for example Al_2O_3 and SiO_2 in the bauxite deposits (Abzalov and Bower 2014).

However, application of the co-kriging in isotopic neighbourhood is limited and depends on spatial correlation between variables. In case of intrinsic correlation, which means that all simple and cross-structures are identical, their co-kriging in isotopic environment produces the same estimate as their direct univariate kriging. This is known as self-krigable variables (Wackernagel 2003). Thus, when variables appear intrinsic correlation application of the co-kriging methods is warranted only in the heterotopic neighbourhoods.

Another limitation of the Ordinary co-kriging estimates is the negative weights of the secondary variable. When they associate with large values of the secondary variable (Z_2) it can make negative the estimate of the target variable (Z_1).

20.2 Kriging with External Drift

The kriging with external drift (KED) is another method that used for integrating target variable with exhaustive secondary (external) data. This can be different generations of the assays (Abzalov and Pickers 2005), gamma-logs integrated with PFN data at the uranium deposits (Abzalov et al. 2014) and the different types of samples, in particular the blast hole and the RC drill hole samples (Abzalov et al. 2007, 2010). The KED algorithm models trend exhibited by a smoothly varying external variable $y(\mathbf{x})$. The trend is presented as a linear function.

The system of linear equations assuring minimum error and unbiasedness constraints of the ordinary kriging with external drift model is as follows:

$$\begin{cases} \sum_{\beta} \lambda_{\beta}^{\mathrm{KED}} C_R\left(\mathbf{x}_{\alpha}-\mathbf{x}_{\beta}\right)+\mu_0+\mu_1 y\left(\mathbf{x}_{\alpha}\right) \\ \qquad =C_R\left(\mathbf{x}_0-\mathbf{x}_{\alpha}\right), \ \forall \ \mathbf{x}_{\alpha} \\ \sum_{a} \lambda_{\alpha}^{\mathrm{KED}}=1 \\ \sum_{a} \lambda_{a}^{\mathrm{KED}} y\left(\mathbf{x}_{\alpha}\right)=y\left(\mathbf{x_0}\right) \end{cases} \tag{20.2.1}$$

$$\sigma_{KED}^2(\mathbf{x}) = \sigma_R^2 - \sum_{\alpha} \lambda_{\alpha}^{\mathrm{KED}} C_R\left(\mathbf{x}_0-\mathbf{x}_{\alpha}\right) - \mu_0+\mu_1 y\left(\mathbf{x}_{\alpha}\right) \tag{20.2.2}$$

The most common version of the KED model uses a generalised covariance function (K) instead of a conventional covariance of the residual (C_R). Such modification extends the KED model to non-stationary environments (Bleines et al. 2013).

References

Abzalov MZ, Bower J (2014) Geology of bauxite deposits and their resource estimation practices. Appl Earth Sci 123(2):118–134

Abzalov MZ, Pickers N (2005) Integrating different generations of assays using multivariate geostatistics: a case study. Trans Inst Min Metall 114:B23–B32

Abzalov MZ, Menzel B, Wlasenko M, Phillips J (2007) Grade control at the Yandi iron ore mine, Pilbara region, Western Australia: comparative study of the blastholes and RC holes sampling. In: Proceedings of the iron ore conference 2007. AusIMM, Melbourne, pp 37–43

Abzalov MZ, Menzel B, Wlasenko M, Phillips J (2010) Optimisation of the grade control procedures at the Yandi iron-ore mine, Western Australia: geostatistical approach. Appl Earth Sci 119(3):132–142

Abzalov MZ, Drobov SR, Gorbatenko O, Vershkov AF, Bertoli O, Renard D, Beucher H (2014) Resource estimation of *in-situ* leach uranium projects. Appl Earth Sci 123(2):71–85

Bleines C, Bourges M, Deraisme J, Geffroy F, Jeanne N, Lemarchand O, Perseval S, Poisson J, Rambert F, Renard D, Touffait Y, Wagner L (2013) ISATIS software. Geovariances, Ecole des Mines de Paris, Paris

David M (1988) Handbook of applied advanced geostatistical ore reserve estimation. Elsevier, Amsterdam, p 364

Goovaerts P (1997) Geostatistics for natural resources evaluation. Oxford University Press, New York, p 483

Journel AG, Huijbregts CJ (1978) Mining geostatistics. Academic, New York, p 600

Rivoirard J (2001) Which models for collocated cokriging? Math Geol 33:117–131

Wackernagel H (2003) Multivariate geostatistics: an introduction with applications, 3rd edn. Springer, Berlin, p 388

Multiple Indicator Kriging

21

Abstract

The structural complexity of the deposits containing several generations of the mineralisation exhibiting different spatial trends can be overcome by using the grade indicators:

$$I_i \begin{cases} 1, & \text{if } Z(x) \leq z_i \\ 0, & \text{otherwise.} \end{cases}$$

Spatial distribution of the indicators is estimated using an appropriate kriging algorithm (commonly by Ordinary kriging). Multiple indicator kriging uses different variogram model for each indicator, the approach allowing estimate resources of the deposits formed by several generations of mineralisation occupying the different structural settings.

The estimated indicator probabilities are assembled together into a combined *ccdf* model which is used for determining probability of the estimate being above or below the certain cut-offs.

Keywords

Indicator kriging • Order relation

In the gold deposits the high grade shoots are typically small and the spatial correlation between the high grade values can be observed only at the short distances. On the contrary, the low grade gold mineralisation is significantly more continuous and the low grade samples can be interpolated at the distances of 60–80 m (Abzalov 2007; Abzalov and Humphreys 2002a). Modelling such deposits by a single variogram is impossible when these mineralisation types are superimposed and cannot be separated into different domains.

Using a single variogram is particularly inappropriate when different mineralisation types show the different trends. This is commonly observed in the gold deposits where high grade shoots intersect at the high angle the lower grade mineralisation. Another example is the komatiite-hosted nickel sulphide deposits which commonly contain several types of mineralisation showing

M. Abzalov, *Applied Mining Geology*, Modern Approaches in Solid Earth Sciences 12,
DOI 10.1007/978-3-319-39264-6_21

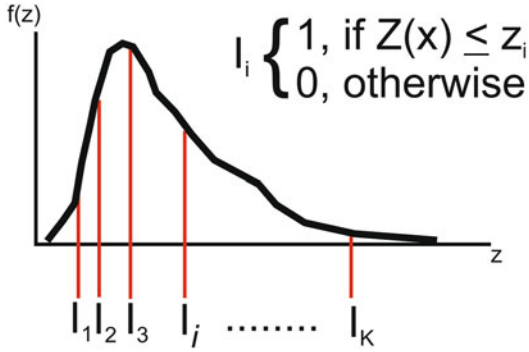

Fig. 21.1 Discretisation of the continuous variable by indicators

elongation in the different directions (Fig. 15.9). Modelling such deposits by a single variogram can overly simplify the actual variability of the deposit and lead to excessive smearing of the high grades.

Resources of such deposits are commonly estimated using the grade indicators which allows to overcome structural complexity of the deposits (Journel 1983; Deutsch and Journel 1998). Resource grade usually estimated using 8–14 indicators, which are distributed regularly through the mineralisation grade (Fig. 21.1). Experience has shown that for variables with a coefficient of variation less than 1.5 eight to ten indicators are sufficient. More skewed distributions, which coefficient of variation exceeds 1.5, ten to fourteen indicators are used

21.1 Methodology of the Multiple Indicator Kriging

Choice of the indicators (thresholds) depends on the grade interval. In the low grade portion of the histogram the thresholds are chosen to create an equal amount of data in each grade class. In the high grade portion this approach is not working and the thresholds are distributed to provide an equal quantity of a metal into each grade class. In order to accurately estimate the resources at the economic cutoff one indicator should be lower than the cutoff value at the studied deposit. A good practice is to also add the indicators representing the natural thresholds of mineralisation which can be recognised from the multi-modal shape of the histograms (Fig. 21.2) or from the spatial distribution pattern of the mineralisation grade (Figs. 15.9 and 21.2). This approach provides a good coverage over the full spectrum of the grade distribution accurately discretising the continuous variable Z(x) into several indicators.

Using indicators and their variogram models the variable Z(x) can be estimated in the unsampled locations. This is made by kriging the indicators I_{Z_i} which provides an estimate of a probability of $Z(\mathbf{x}) \leq z_i \mid (n)$ where (n) is a conditioning information available at the search neighbourhood of the given location (Deutsch and Journel 1998). The estimation is repeated for all indicators and the conditional cumulative distribution function (*ccdf*) is built by assembling the all indicator kriging estimates obtained for the given location.

Indicator kriging (IK) for estimating the *ccdf* can be applied using Ordinary or Simple kriging approaches. However, Ordinary kriging is most commonly used by the geologists because it does not require stationarity of the indicators and also it doesn't need an *apriori* knowledge of the indicators means. Ordinary kriging is implemented in the Multiple Indicator kriging (MIK) technique which uses different variogram model for each indicator. This flexibility makes the MIK in particular well suited for the deposits formed by several generations of mineralisation occupying the different structural settings and, as consequence, requiring different variogram models for each mineralisation type of grade class.

Procedure of using MIK is as follows (Deutsch and Journel 1998).

- Discretise the continuous studied variable Z(**x**) into K indicators and model their variograms (Fig. 21.1). Usually 8–14 indicators (cutoffs) are used for estimating mineral resources.
- Apply OK algorithm for each indicator using the corresponding variogram model.
- Assemble the estimates together into a combined *ccdf* model determining probability of the estimate being above or below the every studied cutoff.

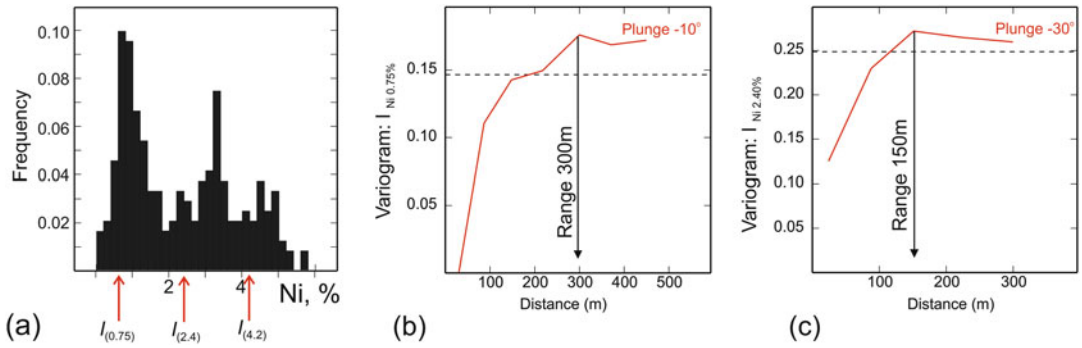

Fig. 21.2 Natural thresholds of the Ni grade and their related indicator variograms, Cliff Ni-sulphide deposit, Australia: (**a**) multimodal histogram of the composited samples showing presence of the different grade classes; (**b**) variogram of the indicator (Ni > 0.75 %) calculated along the main continuity of the nickel mineralisation at this cutoff (plunge −10°); (**c**) indicator (Ni > 2.40 %) variogram calculated along the main continuity of the nickel mineralisation at this cutoff (plunge −30°)

- Estimate probability of each grade class (z_i, z_{i+1}) and the average grade of the samples within the given grade class. This should include $z_0 = z_{min}$ and $z_{K+1} = z_{max}$, which are the minimum and maximum of the data range [Z(**x**)]. This step requires correcting of the raw (obtained by indicator kriging estimate) *ccdf* for the order relations conditions. Average value within each grade class are usually obtained by a linear interpolation of the tabulated bound values. Linear model can also be used for a lower tail of distribution. Estimating within the upper tail (between highest cut-off and the z_{max}) is most challenging. Based on a personal experience the Deutsch and Journel (1998) have suggested to use a hyperbolic function of a power 1.5 which can be used as a general purpose model for processing the upper tail of the indicator kriging results.
- Mean of the *ccdf* is estimated by multiplying probability of the grade class by its mean and adding up all products obtained for the location (**x**) (21.1.1). This is called the E-type estimate (Deutsch and Journel 1998):

$$z^*_{MIK}(\mathbf{x}) = \sum_{i=1}^{K+1} z_i^{\text{GRADE CLASS}} \left\{ \text{Prob}^*[Z(\mathbf{x}) \le z_i] - \text{Prob}^*[Z(\mathbf{x}) \le z_{i-1}] \right\} \Big| (n) \quad (21.1.1.)$$

where z_i ($i = 1, \ldots, K$) is the K cut-offs;

$z_i^{\text{GRADE CLASS}}$ is the conditioning mean estimated for each grade class (z_i, z_{i+1}) of the entire range of Z variable, including $z_0 = z_{min}$ and $z_{K+1} = z_{max}$;

(n) denotes the conditioning information available in the search neighbourhood of the location (**x**).

- Estimate z^*_{MIK} can be corrected for the different volume (volume support) using one of the non-linear geostatistical techniques (Deutsch and Journel 1998).

21.2 Practical Notes on the Indicators Post-Processing

Conditional probabilities estimated by kriging of the indicator values may not comply with the order relations conditions (Fig. 21.3). Deviation from the order relation is caused by the negative kriging weights and lack of data in some grade classes and it is very common in the MIK estimates which estimates *ccdf* using several variogram models. This is the main drawback of the indicator based estimates, however it is usually overweighted by flexibility of the approach allowing to accurately model structurally complex deposits.

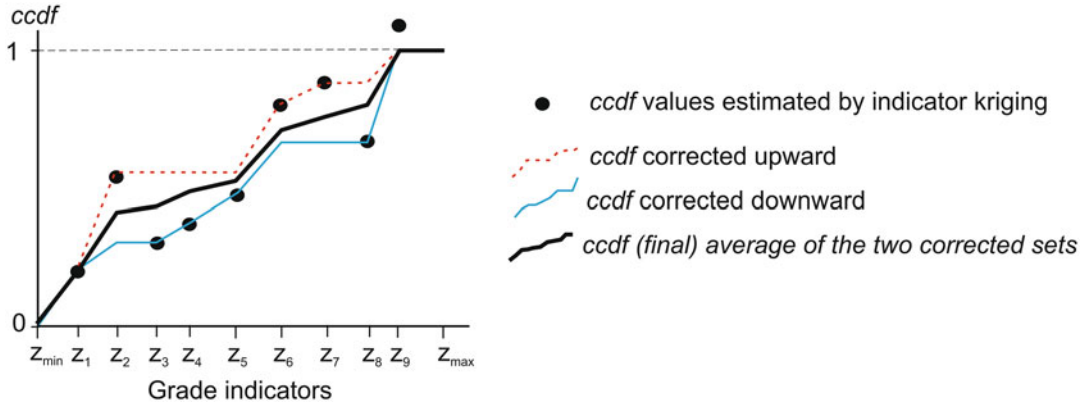

Fig. 21.3 Order relation problems and their correction

The number of deviations can be partially reduced by using the same search neighbourhood for all indicators however this does not entirely eliminate the order relation problem. Thus, the *ccdf* after it as obtained by kriging of the indicators needs to be corrected for order relation. A common procedure for post-processing of the indicator kriging results includes upward and downward correction of the raw *ccdf* values and averaging the two sets of the corrected *ccdf's* (Fig. 21.3).

References

Abzalov MZ (2007) Granitoid hosted Zarmitan gold deposit, Tian Shan belt, Uzbekistan. Econ Geol 102(3):519–532

Abzalov MZ, Humphreys M (2002) Resource estimation of structurally complex and discontinuous mineralisation using non-linear geostatistics: case study of a mesothermal gold deposit in northern Canada. Exp Min Geol J 11(1–4):19–29

Deutsch CV, Journel AG (1998) GSLIB: geostatistical software library and user's guide. Oxford University Press, New York, p 340

Journel AG (1983) Non-parametric estimation of spatial distribution. Math Geol 15(3):445–468

Estimation of the Recoverable Resources

22

Abstract

Estimation of the recoverable resources are made using non-linear geostatistical methods allowing to model the grade-tonnage relations corresponding to the mining selectivity, in other words, to a certain volume (support).

The methods have practical importance for the mine geologists, who commonly involved in estimating recoverable resources and converting them to ore reserves, therefore the change-of-support techniques are explained in sufficient details for their practical application by the geologists. A special attention is made to the novel technique, known as Localised Uniform Conditioning (LUC), allowing estimating grade into small blocks.

Keywords

Volume-variance • Change of support • Uniform conditioning • LUC

In the mining industry it is well understood that mineralisation distributed in a given deposit can not be extracted completely due to economic and technical reasons. Economic reasons are reflected in existence of a certain economic threshold, known as cutoff value (z_c), below which extraction of the ore becomes uneconomic. Technical reasons, such as mining techniques and equipment size, define the mining selectivity. The experienced mine geologists know that tonnage and average grade of ore which can be profitably recovered from a given deposit depends on how selectively the given deposit is mined. In other words, correct prediction of the tonnage and grade of recoverable resources requires consideration of the dimensions of selectively minable units (SMU) representing the smallest blocks at which ore will be separated from waste during mining. The portion of mineralisation which can be profitably extracted from a given deposit is traditionally called the recoverable resources (Marechal 1984; Buxton 1984; Demange et al. 1987; Rossi and Parker 1994; Rossi and Deutsch 2014).

Impact of the chosen volume support on the data statistics is shown on the Fig. 22.1 which shows an impact of the chosen sizes of the blocks for reported resources of the deposit. This example highlights a practical importance of considering the support effect for correct prediction of the grade distribution profiles of the recoverable resources. It is obvious that applying cut-off on

M. Abzalov, *Applied Mining Geology*, Modern Approaches in Solid Earth Sciences 12,
DOI 10.1007/978-3-319-39264-6_22

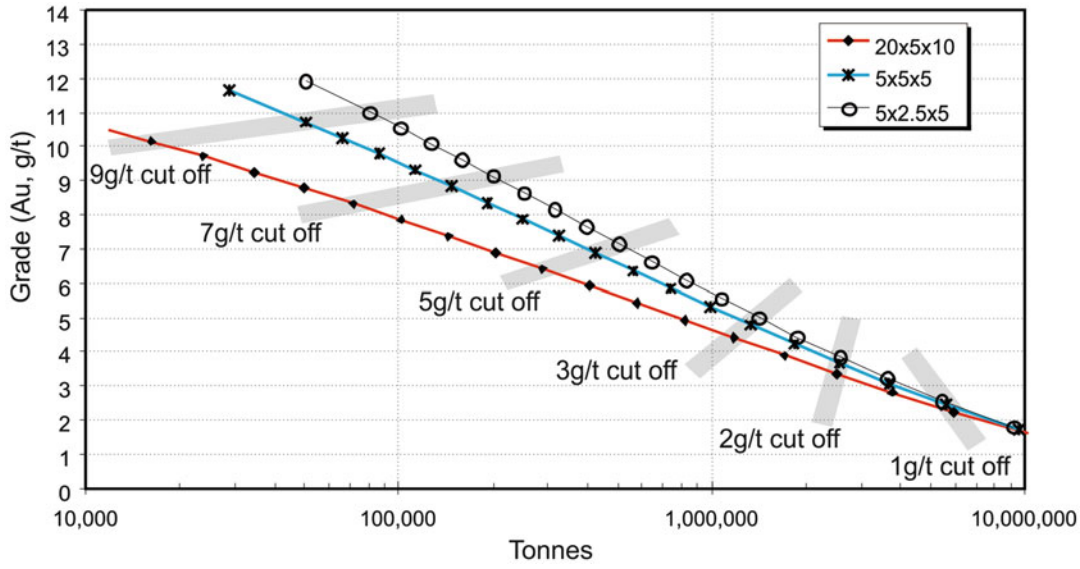

Fig. 22.1 Grade – tonnage relationships at the different block size, Meliadine gold deposit, Canada (Abzalov and Humphreys 2002a)

one support will give very different results than applying the same cut-off on another support (Fig. 22.1), hence, the recoverable resources have to be reported at the support which is matching to the mining selectivity.

22.1 Change of Support Concept

Estimation of the recoverable resources are made using non-linear geostatistical methods, commonly known as change of support techniques, allowing to model the grade-tonnage relations corresponding to the mining selectivity (Journel and Huijbregts 1978; Lantuejoul 1988; David 1988; Isaaks and Srivastava 1989; Rivoirard 1994; Goovaerts 1997; Chiles and Delfiner 1999; Wackernagel 2003; Abzalov 2006, 2014c).

The non-linear geostatistical methods which are used for estimation of recoverable resources are based on conversion of the sample (quasi-point) distributions to distribution at the given SMU volume. This can be made using several methods which are broadly subdivided on the global and local estimates. The global change-of-support methods by their definition do not determine a spatial location of the identified recoverable resources. The local change of support techniques, on the contrary to the global methods, allow to approximately localise the spatial position of the identified grade classes (Abzalov 2006).

It is important to stress that these techniques require use of the data sets representative of the given ore bodies. David (1972) has emphasised that no matter how complex is a mathematical treatment which has been applied to the data, its not increasing the quantity of basic information the data (samples) contain and therefore the resultant grade-tonnage curves can be no more representative of the ore body than are the samples.

Another correction of the experimentally estimated grade-tonnage relationships includes correction for insufficient information, known as 'Information Effect'. The 'Information Effect' correction is applied to further improve a given change-of-support model (Bleines et al. 2013; Wackernagel 2003).

22.1.1 Dispersion Variance

Dispersion variance $\sigma^2(v|D)$ is a variance of the grades defined on one support (v) distributed within a larger volume of support (D). This can be

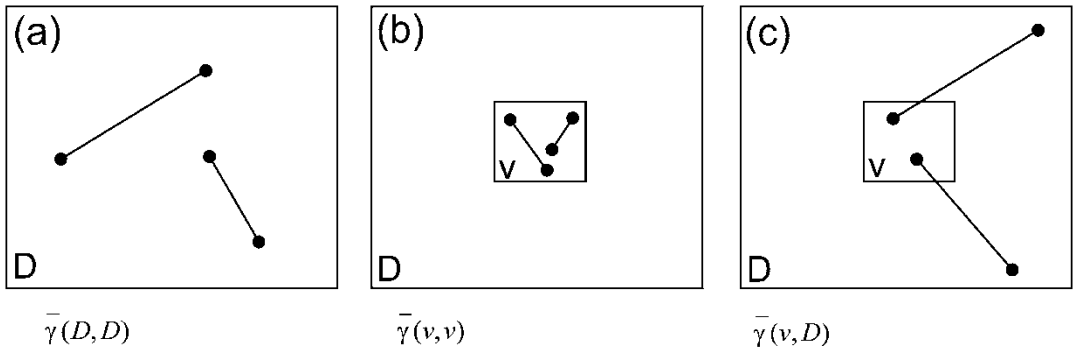

Fig. 22.2 Average variograms: (**a**) variogram model averaged over all possible vectors within domain (D); (**b**) variogram model averaged over all possible vectors within block (v); (**c**) the average variogram between two points when one is sweeping inside the block (v) and another is sweeping independently within the domain (D)

variance of composited samples within a deposit, or variance of the SMU grades within bench of the open pit.

Dispersion variance of point values distributed within any volume can be estimated from the variogram model (Fig. 22.2). In particular, dispersion variance of a point value within the domain (D) equal to the average variogram value when the end points are sweeping independently inside the given domain (D) (Fig. 22.2a). The dispersion variance of the point values within the blocks (v) is equal to the variogram model averaged over all possible vectors contained within this block (v) (Fig. 22.2b). Finally, dispersion variance of support (v) within a larger support of size (D) is equal to the average variogram between two points when one is sweeping inside the block (v) and another is sweeping independently within the (D) (Fig. 22.2c).

The average variogram values in a given volume (V) are usually denoted as $\overline{\gamma}(V,V)$ or simply $\overline{\gamma}(V)$ and is read a 'gamma-bar of VV'. The average variogram values are also known as the auxiliary functions (Journel and Huijbregts 1978). In particular, the variogram model averaged over all possible vectors contained within the block (V) is called F-function.

The relationships between dispersion variances and average variogram values are as follows:

$$\begin{aligned}\sigma^2\left(\mathrm{o}\middle|v\right) &= \overline{\gamma}(v) = \mathrm{F}\left(\mathrm{v}\right)\\ \sigma^2\left(\mathrm{o}\middle|D\right) &= \overline{\gamma}\left(\mathrm{D}\right) = \mathrm{F}\left(\mathrm{D}\right)\end{aligned} \qquad (22.1.1)$$

22.1.2 Volume Variance Relations

The regular relationships between the variances and the volumes (supports) at which this variable was evaluated are known as a volume-variance relationship. The volume-variance relationships are traditionally expressed through the dispersion variances (22.1.2)

$$\begin{aligned}\sigma^2\left(v\middle|D\right) &= \sigma^2\left(0\middle|D\right) - \sigma^2\left(\mathrm{o}\middle|v\right)\\ &= \sigma^2\left(0\middle|D\right) - \overline{\gamma}(v)\end{aligned} \qquad (22.1.2)$$

where $\sigma^2\left(v\middle|D\right)$ is dispersion variance of the blocks of size (v) distributed in the domain (D), $\sigma^2\left(0\middle|D\right)$ is variance of points distributed in the domain (D), $\sigma^2\left(\mathrm{o}\middle|v\right)$ is variance of points distributed in the small blocks of size (v) which is equal to the average variogram $\overline{\gamma}(v)$ in the block (v).

Equality (22.1.2) is known as Krige's additivity relationship and it represents one of the main theoretical basis of the change-of-support techniques.

22.1.3 Conditions for Change-of-Support Models

Three conditions necessary for change of support model (Rivoirard 1994).

The expected mean grade is independent of the support.

$$\mathrm{E}[\mathrm{Z}(\mathrm{x})] = \mathrm{E}[\mathrm{Z}(v)] = \mathrm{m} \tag{22.1.3}$$

Relationships between volume and variance must be consistent with Krige's relationship (22.1.2).

Cartier's relation (22.1.4), which states that that the expected grade of any point (x) randomly chosen in a block (v) is the block grade, must be satisfied.

$$\mathrm{E}\left[\mathrm{Z}(\underline{\mathrm{x}}) \middle| \mathrm{Z}(v)\right] = [\mathrm{Z}(v)] \tag{22.1.4}$$

22.2 Global Change of Support Methods

The global change of support methods allow to infer from the sample data the grade-tonnage relationships of mineralisation distributed as small rectangular blocks of size (v) in a large stationary domain of size (D). The blocks of size (v) represent the selectively minable units (SMU) which were introduced in the previous section.

Tonnage $[\mathrm{T}_v(\mathrm{z_C})]$, contained metal $[\mathrm{Q}_v(\mathrm{z_C})]$, and grade $[\mathrm{M}_v(\mathrm{z_C})]$, of mineralisation recovered above the given cut-off $(\mathrm{z_C})$ when mined as the blocks of size (v) can be conceptually expressed as follows:

$$T_v(z_c) = T * E[I_{Z_v \geq z_C}] = \mathrm{T} * \mathrm{F}(\mathrm{z_c})$$

$$Q_v(z_c) = T * E[Z_v * I_{Z_v \geq z_C}]$$

$$= T * \int_{z_c}^{\infty} Z_v * F(dz)$$

$$M_v(z_c) = \frac{Q_v}{T_v}$$

where $\mathrm{F}(\mathrm{z_c}) = p[Z_v \geq z_c]$

and T is total tonnage of ore body.

These global grade-tonnage relationships at a given volume support can be deduced from the point (i.e. sample) recovery functions using a suitable geostatistical change-of-support technique. The most common methods in mining industry are affine correction, indirect lognormal change of support, lognormal short cut and discrete Gaussian change of support (DGCS).

Affine correction (Lantuejoul 1988; David 1988; Isaaks and Shrivastava 1989) is a simplest among these methods. Application of the affine correction technique is limited to non-skewed or weekly skewed data due to theoretical and practical constraints.

Lognormal short cut technique has been designed (Isaaks and Srivastava 1989) for change of support correction of skewed data, which distribution can be approximated by lognormal distribution low. In particular, this method has been successfully applied to Cu-porphyry style mineralisation.

Discrete Gaussian change of support (Lantuejoul 1988) is a most advanced technique applicable to any uni-modal monotonously distributed variable and does not constrained by a particular distribution law.

22.2.1 Affine Correction

This change of support method uses an assumption that changing of the volume support of the data changes a variance of the data distribution but does not change the shape of the histogram (Lantuejoul 1988; David 1988; Isaaks and Shrivastava 1989). This assumption, known as permanence of the distribution shape, leads to the following equality (22.2.1):

$$\frac{z_v - m}{\sigma_{(v|D)}} = \frac{z - m}{\sigma_{(0|D)}} \tag{22.2.1}$$

where (v) is SMU-sized rectangular cell in the larger domain (D), (m) is the mean value of distribution, (z) sample grades, $(\sigma_{(0|D)})$ standard deviation of the sample (quasi point) grades, (z_v) grade of the SMU of support (v), and $(\sigma_{(v|D)})$ is

the standard deviation of SMU grades distributed in the domain (D).

It is obvious that this assumption of permanence of the histogram shape imposes a strong constrain on application of the affine correction technique which is limited to non-skewed data whose histograms can be approximated by normal distribution.

22.2.1.1 Recovered Grade

Recovered grade (z_v) is calculated from the sample grades (z) using the equality (22.2.2), which is obtained by a simple transformations of the above introduced relation (22.2.1).

$$z_v = (z - m)\frac{\sigma_{(v|D)}}{\sigma_{(o||D)}} + m \qquad (22.2.2)$$

22.2.1.2 Recovered Tonnage

Recovered tonnage represents a proportion of mineralisation which grade is equal or exceeds the given cut-off (z_c). It can be expressed as probability $p[Z_v \geq z_c]$ that at any point the block grade (z_v) can exceed the given cut-off (z_c).

$$T_v = p[Z_v \geq z_C] \qquad (22.2.3)$$

If the block grade (z_v) is a normally distributed variable with zero mean and unit variance ($z_v = y$, where y N 0,1) the required proportion can be estimated as

$$T_v = p[Z_v \geq z_C] = 1 - G(y_C), \qquad (22.2.4)$$

where (G) is cumulative distribution function (cdf) of a normally distributed grade values (z_v), representing an area under the standard normal curve (Fig. 22.3).

The formula (22.2.4) is used for estimating recoverable tonnage which is deduced from the statistical tables presenting the (G) values of the standard normal distributions (Appendix 2). In practise, application of the equality 22.2.4 requires conversion of the actual sample grades (z) to the corresponding them block grades (z_v) and then standardising these new grades to obtain a standard Gaussian variable (y).

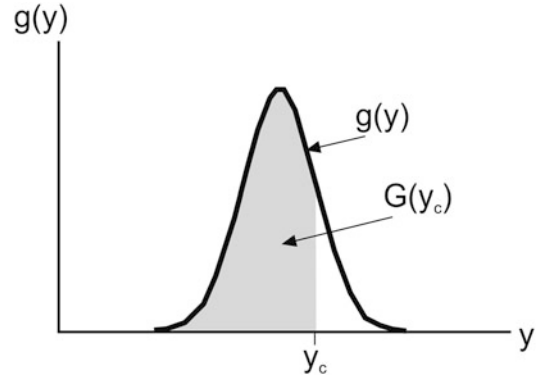

Fig. 22.3 Probabilistic [i.e. $p[Y > yc] = 1 - G(yc)$] definition of a proportion of the normally distributed values (y) which are equal or exceed a given threshold (yc). Where g(y) – probability density function and G(y) – cumulative distribution function of a standard normal variable (y)

22.2.1.3 Recovered Metal

Recovered metal is estimated using the formula

$$Q_v = T_v * m_v = mT_0\left(1 - \frac{\sigma_{(v|D)}}{\sigma_{(o|D)}}\right) + \frac{\sigma_{(v|D)}}{\sigma_{(o|D)}}Q_0 \qquad (22.2.5)$$

where T_0 – recovered tonnage and Q_0 – recovered metal at the sample (point) support.

The metal-tonnage curve (Q_v) obtained for a block of size (v) by applying an affine correction represents a weighted average between metal vs. tonnage curves at the point support (Q_0) and that of the curve ($Q_\infty = mT$), where (Q_∞) corresponds to a metal recovered as the blocks of infinite size.

Practical procedure of applying affine correction to the sample grades includes the following steps (David 1988).

- Estimate the variogram model.
- Apply the data declustering algorithm and estimate the mean (m) and variance (σ_0^2) of the declustered samples.
- Calculate the average value of variogram $\overline{\gamma}(v)$ in the block of size (v).

- Compute dispersion variance $\sigma^2_{(v|D)}$ of blocks of size (v) distributed in the larger domain (D). This is obtained using an above introduced Krige's relationship (22.1.2).
- Applying affine correction (22.2.2) technique convert the sample grades to corresponding them grades of the blocks of size (v). The array of (z_v) values arranged in increasing order represents a disjunctive coding of distribution function of the grade values estimated at the support of the SMU size blocks (David 1988). This array of (z_v) values is finally used to construct the grade-tonnage relationships for a given support (v).
- Recovered tonnage is finally estimated by ordering the block (v) grades obtained by affine correction algorithm in their grade increasing order and then calculating the proportion of blocks whose grade is equal or exceeds the given cut-off value. This proportion represents an empirically estimated tonnage of mineralisation recoverable at a block of SMU size (v).
- Recovered metal (Q_v) represents the sum of the products of the grades (z_v) of the economically recovered blocks $(z_v \geq z_C)$ multiplied by their tonnages $(Q_v = \sum_1^N z_v * 1/N)$, where 1/N represents tonnage of a block (v) expressed as a proportion of the total tonnage.
- Recovered grade is simply calculated by dividing a recovered metal (Q_v) by a recovered tonnage (T_v). Alternatively, it can be empirically calculated as average grade (z_v) of the economically recoverable blocks (i.e. $z_v \geq z_C$).

22.2.2 Discrete Gaussian Change of Support

Discrete Gaussian change of support (DGCS) method is most advanced technique which can be applied to skewed distributions independently of the data distribution law (Lantuejoul 1988; David 1988; Rivoirard 1994; Goovaerts 1997; Chiles and Delfiner 1999).

The DGCS technique expresses distribution of the SMU *(v)* grades using a Hermite polynomial expansion

$$Z(v) = \varphi\ vY(v) \quad = \sum_{k=1}^{\infty} \frac{\phi_k}{k!}\, r^k\, H_k\,(Y(v)) \tag{22.2.6}$$

where k are coefficients established in the normal score transformation (Gaussian anamorphosis), *Y(v)* is the Gaussian variable with mean 0 and variance 1 and *r* is the point-to-block correction coefficient. An applicability of the Gaussian-based algorithms, such as DGCS, requires diffusive type boundaries between the different grade classes. Such grade distribution model is known as the border effect and it is characterised by a distinctly zoned distribution of the different grade classes. One of the most common methods is calculation of the ratio between indicators cross-variograms to indicator variograms (Abzalov and Humphreys 2002a, b). If these ratios are regularly changes with the distance, which is indicative of a gradational changes of the grade values across the boundaries of the grade classes, then Gaussian-based models are applicable.

Underlying assumption of the above equality that pairs of Gaussian transformed values *Y(**x**)* (point anamorphosis) and *Y(**v**)* (block anamorphosis) are bi-Gaussian linearly correlated values with a correlation coefficient of ***r***. This coefficient is unknown and needs to be calculated. Procedure of computing of the point-to-block correction coefficient *r* is as follows.

1. The first step is to compute a point anamorphosis $(Z(x) = \varphi\ (Y(x)))$.
2. The next step is to calculate an empirical variogram $\gamma(\mathbf{h})$ using the available point data $Z(\mathbf{x})$ (samples) and fit an appropriate model.
3. The point-to-block correction coefficient (r) of the block *(v)* can be calculated using the following geostatistical relationship between the variance of *Z(v)* and the block anamorphosis function:

$$Var\,[Z(v)] = Var\ [\varphi\ vY(v)] \quad = \sum_{k=1}^{\infty} \frac{\phi_k^2}{k!}\, r^{2k} \tag{22.2.7}$$

The variance of Z(v) is equal to a block covariance $\overline{C}(v, v)$ which can be easily calculated from the variogram model.

$$\text{Var}(Z(\mathbf{v})) = \overline{C}(\mathbf{v}) = \gamma(\infty) - \overline{\gamma}(\mathbf{v}) \quad (22.2.8)$$

Therefore, using the above relationships the final equation for calculating the point-to-block correction coefficient $\boldsymbol{r}$ can be expressed as follows

$$[\gamma(\infty) - \overline{\gamma}(\mathbf{v})] = \sum_{k=1}^{\infty} \frac{\phi_k^2}{k!} r^{2k} \quad (22.2.9)$$

22.3 Local Change of Support Methods

Linear estimators of a kriging system are not suitable for estimating small block if data spacing is to sparse. However, estimating grade of the large blocks (panels) whose size is adequate to a given data spacing is impractical for technical and financial valuation of a mining project because it is necessary to estimate tonnage (T_v) and grade (Z_v) of mineralisation above a given economic cut-off (z_C) taking into account a proposed mining selectivity (v). Therefore, the local change of support methods have been developed allowing to estimate recoverable resources within each panel (Abzalov 2006).

22.3.1 Uniform Conditioning

Uniform conditioning (UC) (Rivoirard 1994; Chiles and Delfiner 1999; Wackernagel 2003) is a non-linear geostatistical technique of calculating tonnage (T_v) and mean grade (M_v) of recoverable resources distributed in a large panel (V) as the small blocks of size (v) representing a partitioning of this panel (Fig. 22.4). These small blocks of support (v) represent selectively minable units (SMU) which can be selectively extracted from a panel (Z_V). They are classified as 'ore' if the SMU grade z(v) is equal to or exceeds the cut-off value $z_C(v)$ and is a 'waste' otherwise.

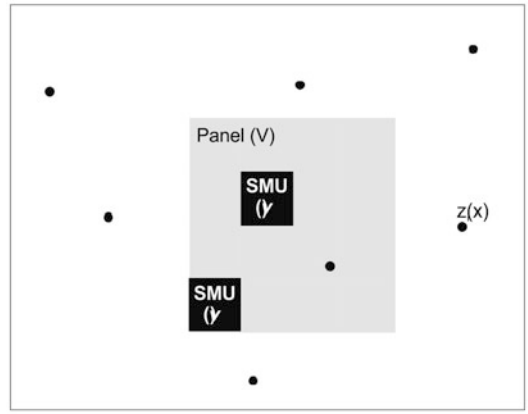

Fig. 22.4 Distribution of the selective mining units (SMU) of support (v) in the panel (V). Data nodes Z(x) are denoted as *black dots*

In geostatistical terms the UC technique (Rivoirard 1994; Wackernagel 2003) involves calculating a conditional expectation of a non-linear function $\Psi(Z(v))$ of the blocks (v) with respect to the corresponding panel grade Z(V). The method requires diffusive type boundaries between the different grade classes which is tested by calculation of the ratio between indicators cross-variograms to indicator variograms (Abzalov and Humphreys 2002a). Another underlying assumption of the UC method is that the grade of the panel Z(V) is known. In practise, as the true panel grades Z(V) are not available they are substituted in the UC models by the Z(V)* panel grades estimated by Ordinary kriging.

Estimation of a non-linear function $\Psi(Z(v))$ from the available data (samples) $Z(\mathbf{x})$ is made by applying the DGCS method (Lantuejoul 1988; Rivoirard 1994; Wackernagel 2003) for calculating a point-to-SMU (v) anamorphosis (22.3.1) and a point-to-panel (V) anamorphosis (22.3.2).

$$Z(v) = \varphi\, v\,(Y(v)) \;=\; \sum_{k=1}^{\infty} \frac{\phi_k}{k!} r^k H_k(Y(v)) \quad (22.3.1)$$

$$Z(V) = \varphi_V\ (Y(V)) \ = \ \sum_{k=1}^{\infty} \frac{\phi_k}{k!}\, s^k\, H_k\left(Y^*(V)\right) \tag{22.3.2}$$

These models are further used for calculation of recoverable tonnage (T) (22.3.3).

$$T_v\,(z_C) = E\left[I_{Z(v)\geq z_C}\,|Z^*(V)\right]$$
$$= E\left[I_{Y_v\geq y_C}\,\middle|\,Y_V^*\right] = 1 - G\left\{\frac{y_C - \frac{s}{r}Y_V^*}{\sqrt{1-\left(\frac{s}{r}\right)^2}}\right\} \tag{22.3.3}$$

and contained metal (Q) (22.3.4)

$$Q_v\,(z_C) = E\left[Z(v)I_{Z(v)\geq z_C}\,|Z^*(V)\right]$$
$$= \sum_{k=1}^{N}\left(\frac{s}{r}\right)^k H_k\left(Y_V^*\right)\sum_{j=1}^{N}\phi_j r^j \int_{y_C}^{+\infty} H_k(y)H_j(y)g(y)dy \tag{22.3.4}$$

where $Y_V{}^* = \varphi_V^{-1}\,(Z^*(V))$ and $y_C = \varphi_v^{-1}\,(z_C)$

Finally, the mean grade (M) of the recovered mineralisation whose SMU grades are above a given cut-off z_C is estimated as

$$M_v\,(z_C) = \frac{Q_v\,(z_C)}{T_v\,(z_C)} \tag{22.3.5}$$

22.3.2 Localised Uniform Conditioning

The conventional UC method estimates tonnage and grade of mineralisation which can be extracted as small selectively minable blocks (SMU) from the large blocks (panels) whose grade is modelled by Ordinary kriging. Recoverable mineralisation is presented by UC technique as proportions of the panels without specifying the actual locations of the SMU. This inability to predict a spatial location of the economically extractable SMU blocks is the main disadvantage of the conventional UC method.

A new approach, called Localised Uniform Conditioning (LUC), has been developed in 2006 (Abzalov 2006) to overcome limitation of the conventional UC technique. The LUC method converts the grade-tonnage relationships estimated by a conventional UC technique for each panel to the grades of the actual SMU size blocks, representing partitioning of the given panel. It is based on ranking of the SMU blocks in their grade increasing order and then assigning the mean grade of a grade class to the SMU blocks whose ranks match to a grade class. An approximate ranking of the SMU blocks can be made by their direct kriging from the sparse data grid. Accuracy of the SMU ranking can be further improved by using additional information, such as high-resolution geophysical data.

Procedure of applying LUC technique is as follows (Abzalov 2006, 2014c). Conventional UC method estimates a tonnage and grade of mineralisation which can be recovered using SMU of size (v) at the chosen cut-off value. A set of grade tonnage distributions is constructed for each studied panel by applying several cut-off values (zc_N).

The LUC algorithm estimates the mean grades of the grade classes in each panel at the given SMU support. The grade class is the portion of the panel whose grade is higher then a given cut-off (zc_i) but lower than the next cut-off (zc_{i+1}). The next step is to rank the SMU blocks distributed in each panel in their grade increasing order. Finally, the mean grades of the grade class which have been deduced from the UC model are assigned to the SMU blocks whose rank matches the grade class. Thus, the key features of the LUC approach are the ability to calculate the mean grade of the grade class and assign these means grades to the SMU size blocks which have been ranked in each panel in increasing order of their grade.

The procedure of calculating the mean grade for each grade class and assigning these grades to the corresponding SMU blocks is shown schematically on the process map (Fig. 22.5). Firstly, the UC method is used to estimate the grade-tonnage relationships of recoverable

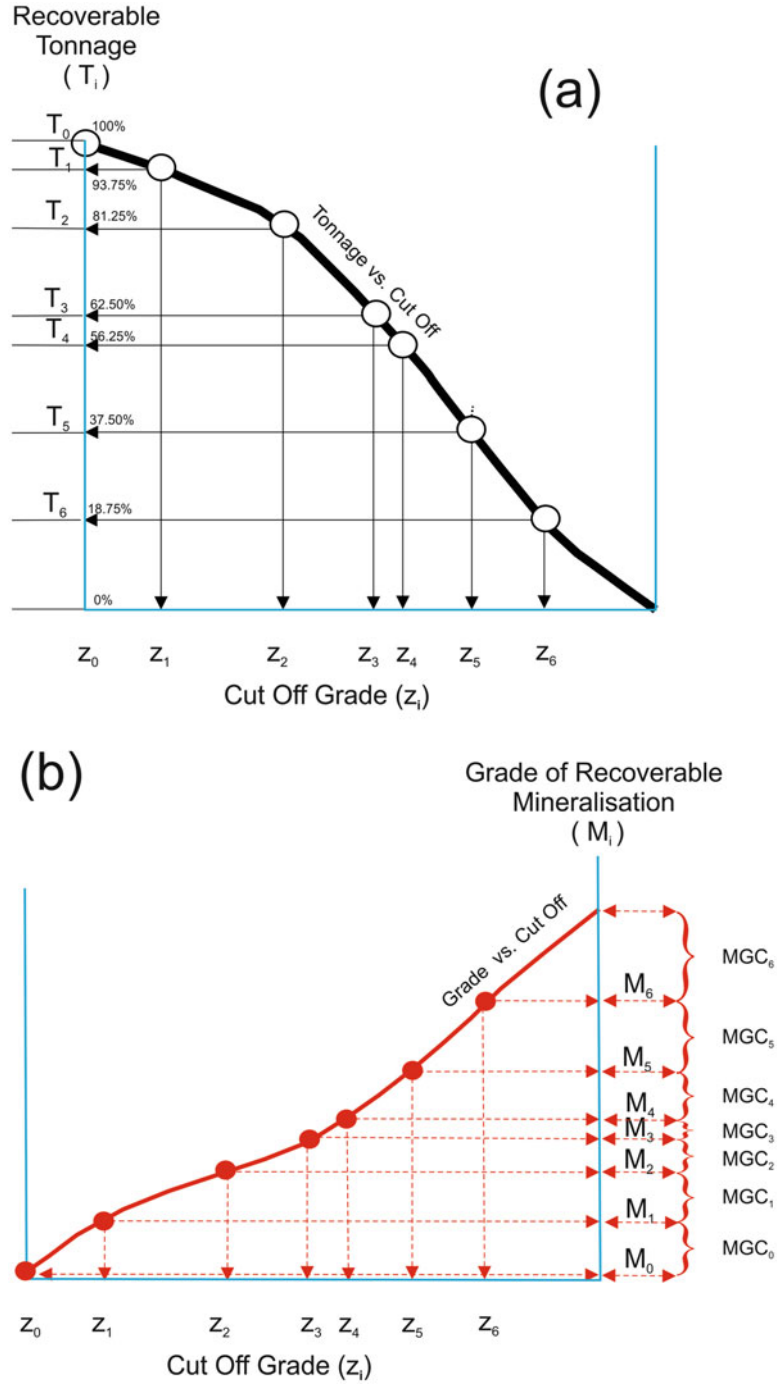

Fig. 22.5 Definition of the grade classes and assigning the grade to the SMU blocks. The example uses 16 SMU blocks in a panel and 6 cut-off values used in the UC model. (**a**) Definition of the grade classes from UC results. Grade class (GC) represents a portion of mineralisation distributed in the panel as the SMU size blocks which grade lies within the range of Zi and Zi + 1 cut-off values, Ti – tonnage of mineralisation above the cut-off Zi expressed as proportion (%) of the panel; (**b**) definition of the mean grades (MGCi) of the grade class; (**c**) assigning the grade class indexes (TGCi) to the SMU blocks falling within the range from Ti to Ti + 1; (**d**) assigning the mean grades (MGCi) of the grade class (GCi) to the SMU blocks whose index (TGCi) matches the grade class

resources distributed as SMU of size (v) in the panels (V). Then, the 3D panels need to be split (partitioned) on sub-cells whose size are equal to that of the chosen SMU size. All SMU size blocks distributed in a panel are ranked in increasing order of their grade. Ranking procedure is explained further in the next section.

The next step is to define the grade classes using relationships between the tonnage of recoverable mineralisation (T_v) and the cut-off grade

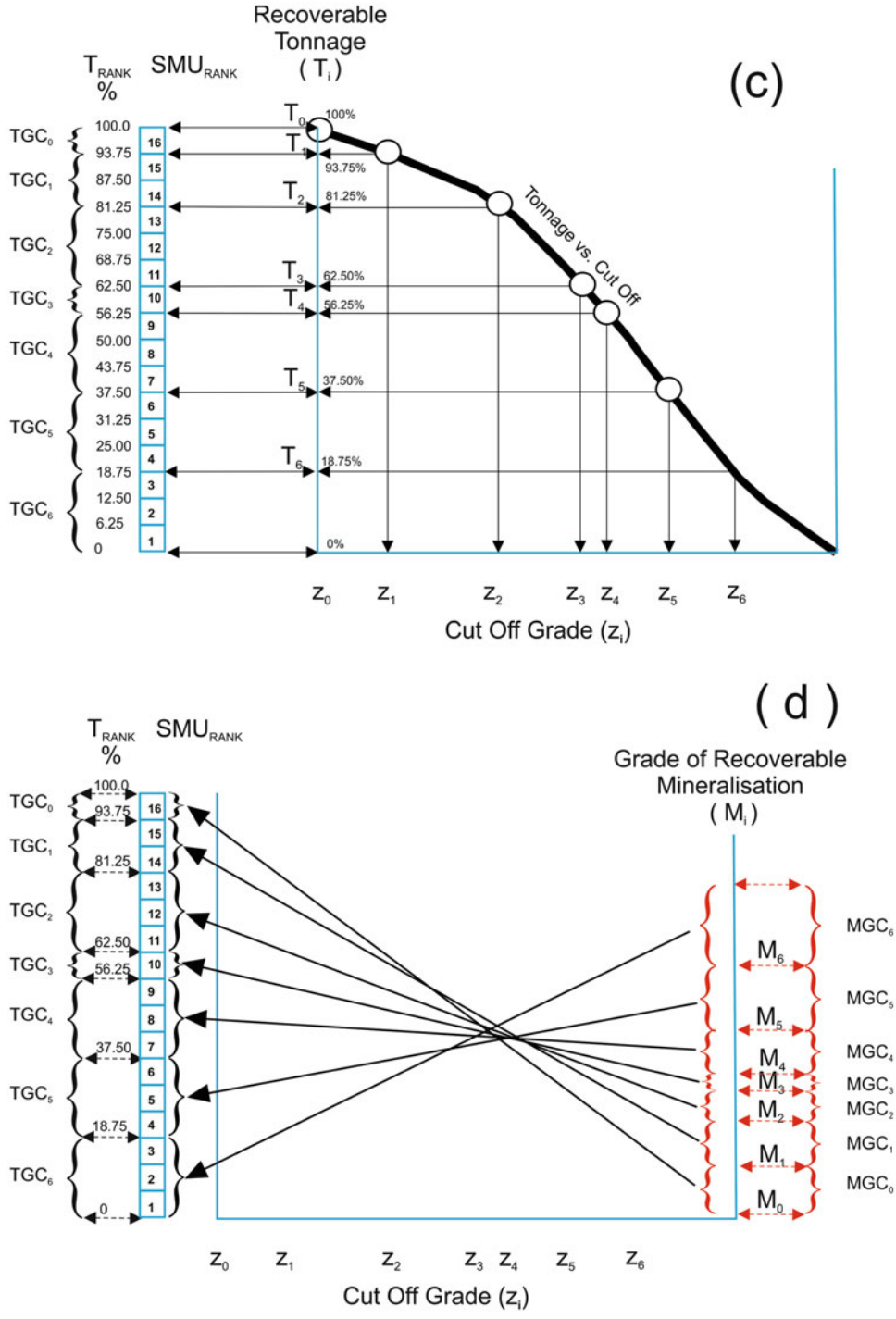

Fig. 22.5 (continued)

(zc) estimated by UC technique for each panel (Fig. 22.5a). The grade class (GC_i) represents a proportion of a panel whose grade is above the given cut-off (zc_i) and less than the next cut-off value (zc_{i+1}). Each grade class is defined by its lower (zc_i) and upper (zc_{i+1}) cut-off values and by corresponding $T_i(zc_i)$ and $T_{i+1}(zc_{i+1})$ values representing a recoverable tonnage at lower and upper cut-offs defining the given grade class. In other words

$$GC_i \subset \{T_i(zc_i), T_{i+1}(zc_{i+1})\},$$

$$\text{and } GC_i \subset \{zc_i,\ zc_{i+1}\},$$

where T_i (zc_i) is recoverable tonnage at cut-off (zc_i) and T_{i+1} (zc_{i+1}) is recoverable tonnage at cut-off (zc_{i+1}).

Then the SMU ranks need to be converted to the grade classes (Fig. 22.5a). This is achieved by defining the SMU ranks as proportions of the panel tonnage T_v.

$$SMU_k \subset (T_K,\ T_{K+1}),$$

where SMU_K is the SMU of a rank (k), T_K is the proportion of the panel tonnage distributed in SMU blocks whose rank is equal or lower than (k), and T_{K+1} is the proportion of the panel distributed in SMU blocks having higher rank.

The grade class can be determined for each SMU_K by comparing its (T_K, T_{K+1}) intervals with the intervals of the grade classes $\{T_i(zc_i), T_{i+1}(zc_{i+1})\}$ (Fig. 22.5a). SMU_K will be assigned grade class (GC_i) if $(T_K - T_{K+1}) \subset (T_i - T_{i+1})$

The next step is to calculate the mean grades (M_i) of the grade classes (MGC_i) in the panels using the UC model (Fig. 22.5b). The mean grades (M_i) of the grade classes can be transferred to the SMU blocks by matching their rank with the grade class. To do so it is necessary to convert SMU ranks to the grade classes (Fig. 22.5c). Finally, a mean grade of each class is assigned to the SMU blocks by matching their grade class indexes (MGC_i and TGC_i) (Fig. 22.5d).

The above explained procedure of assigning the grade values to the SMU blocks (Fig. 22.5) assumes an exact match between grade class intervals $\{T_i(zc_i), T_{i+1}(zc_{i+1})\}$ and intervals of SMU bocks (T_K, T_{K+1}).

Researchers designing the computerised scripts for implementation of the LUC approach need to consider the cases when the range of SMU ($T_{RANK} - T_{RANK+1}$) does not precisely matches that of the grade classes ($T_i - T_{i+1}$). The problem can be partially overcome if to use large number of the grade classes. Personal experience shows that a good match between grade – tonnage relationships estimated by conventional UC method and by the LUC approach is achieved when 50 grade classes are used. Further improvement can be achieved if the mean SMU grade is estimated by weighting grades of the classes to their proportions of the SMU. This approach was used by the author in the case studies (Abzalov 2006, 2014c).

The underlying concept of the LUC method is an ability to rank the SMU blocks in increasing order of their grade (Fig. 22.6). Accurate rankings would require high density information. However, in some cases reasonably accurate ranks of the SMU blocks in the panels can be deduced from the spatial distribution patterns of the grade values, such as zoning or grade trends. The latter approach is particularly relevant for continuous mineralisation, characterised by a low nugget effect, such as disseminated base-metal sulphides, bauxites and iron-oxide deposits. Spatial grade distribution patterns are often recognised by geoscientists in such deposits even when drill spacing is still too broad for direct accurate modelling of small block grades, but sufficient for identification of the major distribution trends.

The global distribution features of the grade variables exhibiting a strong continuity can be reconstructed by interpolating available data nodes using a conventional linear interpolator, such as OK. In other words, it is suggested that direct kriging of the small blocks can be used for their approximate ranking in grade increasing order in the panels even when drill spacing is too broad to avoid a smoothed SMU grade estimation.

The validity of the obtained grade ranks depends on complexity of the grade distribution patterns. At this stage it is assumed that the above assumption is applicable to grade variables whose spatial distribution satisfies a border effect

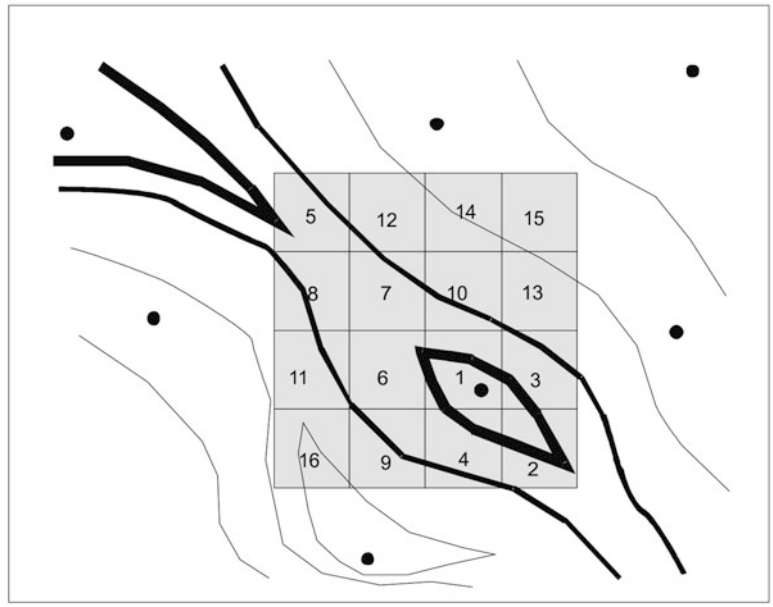

Fig. 22.6 Estimation of the SMU grade ranks from the sparsely distributed data

condition and which are also characterised by a low nugget effect and exhibit good continuity at their variogram origins and also where the available data grid is not too sparse or remote from the panel.

Applying LUC method to various mineral deposits have shown that the LUC model closely reproduces the actual histogram of the SMU supported grades it provides a significantly better estimate of the recoverable resources at the given economic cut-offs than direct kriging of the SMU grades from the sparse data grid (Abzalov 2006, 2014c). These findings suggest that LUC method is a very useful tool at the early stages of exploration and mining project evaluation when sparsely distributed data is usually the only available information.

Exercise 22.3.2
Application of the LUC technique for estimation of the SMU blocks grade. The panels, estimated using UC method, and the block model, containing the SMU blocks ranked within each panel, are available in the file Exercise 22.3.2.zip (Appendix 1). The task is to complete the LUC estimate of the SMU grades using the Fortran code (Exercise 22.3.2.zip).

22.3.3 Application of the LUC Method to the Iron Ore Deposit

The LUC method was used for estimating resources of the pisolitic iron-oxide mineralisation in the eastern Pilbara, Western Australia (Abzalov 2014c). Resources of the deposit are defined by drilling using the grids as follows:

Measured: 100×50 m
Indicated: 200×100 m
Inferred: 300×200 m

However, it has been recognised that use of large blocks, such as $100 \times 50 \times 10$ m, for definition of Measured resources and Proved reserves can lead to a substantial underestimation of the actual variability of the ore-body, which is mined with a selectivity of approximately $25 \times 25 \times 10$ m (Abzalov et al. 2007, 2010). As a consequence, using the large blocks for the reserve model can cause incorrect estimation of the recoverable mineralisation. For example, if it is suggested that $\leq 2.6\,\%$ Al_2O_3 is a metallurgically acceptable threshold for the Al_2O_3 content in the iron-ore then modelling grade distribution as $100 \times 50 \times 10$ m

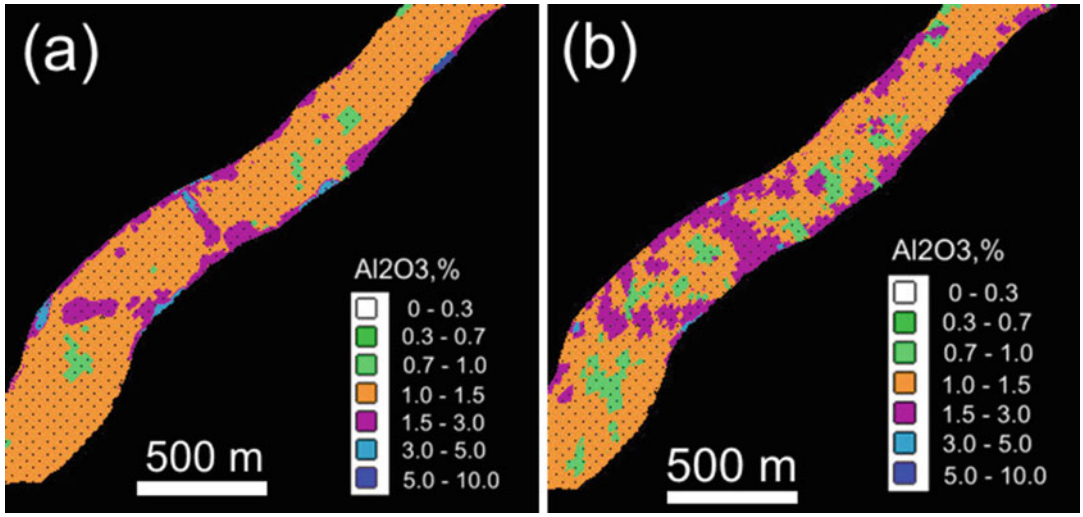

Fig. 22.7 Block models constructed using the drill holes distributed as 100 × 50 m grid: (**a**) OK model; (**b**) LUC model

blocks would overestimate tonnage of the recoverable ore by 3.7 % in comparison with the model estimated as 25 × 25 × 10 m blocks, which matches the mining selectivity (Abzalov 2014c).

Direct estimation of the small blocks by kriging is not feasible because of the large distances between the drill holes. Therefore, in order to obtain more accurate estimation of the recoverable resources it was decided to use LUC method.

Initially a LUC method was tested on a detailed study area which was drilled at 50 × 50 m centres and contains 8121 samples. The drill data has been sampled, in order to create a more sparsely distributed subset, with the drill holes distributed at 100 × 50 m centres, which matches a drill grid used for definition Measured Resources. The subset contains 4801 samples. It has been used to generate block models through application of the LUC technique applied to estimate the Al_2O_3 grade distributed as the SMU blocks of 25 × 25 × 10 m in size (Fig. 22.7). For comparison, Al_2O_3 grades of the same blocks have been estimated by Ordinary kriging (OK) applied to the same subset of the data, distributed as 100 × 50 m centres (Fig. 22.7).

The LUC model exhibits significantly higher resolution than OK model constructed using the same data (Fig. 22.7). Resolution of the LUC method is matching the mining selectivity and therefore is suited for detailed production planning at this project.

References

Abzalov MZ (2006) Localised Uniform Conditioning (LUC): a new approach for direct modelling of small blocks. Math Geol 38(4):393–411

Abzalov MZ (2014) Localised Uniform Conditioning: method and application case studies. J South Afr Inst Min Metall 114(1):1–6

Abzalov MZ, Humphreys M (2002a) Resource estimation of structurally complex and discontinuous mineralisation using non-linear geostatistics: case study of a mesothermal gold deposit in northern Canada. Exp Min Geol J 11(1–4):19–29

Abzalov MZ, Humphreys M (2002b) Geostatistically assisted domaining of structurally complex mineralisation: method and case studies. Geostatistically assisted domaining of structurally complex mineralisation: method and case studies. In: The AusIMM 2002 conference: 150 years of mining, Publication series No 6/02, AusIMM, Melbourne pp 345–350

Abzalov MZ, Menzel B, Wlasenko M, Phillips J (2007) Grade control at the Yandi iron ore mine, Pilbara region, Western Australia: comparative study of the blastholes and RC holes sampling. In: Proceedings of the iron ore conference 2007. AusIMM, Melbourne, pp 37–43

Abzalov MZ, Menzel B, Wlasenko M, Phillips J (2010) Optimisation of the grade control procedures at the Yandi iron-ore mine, Western Australia: geostatistical approach. Appl Earth Sci 119(3):132–142

Bleines C, Bourges M, Deraisme J, Geffroy F, Jeanne N, Lemarchand O, Perseval S, Poisson J, Rambert F, Renard D, Touffait Y, Wagner L (2013) ISATIS software. Geovariances, Ecole des Mines de Paris, Paris

Buxton BE (1984) Estimation variance of global recoverable reserve estimates. In: Verly G et al (eds) Geostatistics for natural resources characterisation, Part 1. Reidel, Dordrecht, pp 165–183

Chiles J-P, Delfiner P (1999) Geostatistics: modelling spatial uncertainty. Wiley, New York, p 695

David M (1972) Grade-tonnage curve: use and misuse in ore-reserve estimation. Trans Inst Min Metall 81:A129–A132

David M (1988) Handbook of applied advanced geostatistical ore reserve estimation. Elsevier, Amsterdam, p 364

Demange C, Lajaunie C, Lantuejoul C, Rivoirard J (1987) Global recoverable reserves: testing various changes of support models on uranium data. In: Armstrong M (ed) Geostatistical case studies. Reidel, Dordrecht, pp 187–208

Goovaerts P (1997) Geostatistics for natural resources evaluation. Oxford University Press, New York, p 483

Isaaks EH, Srivastava RM (1989) An introduction to applied geostatistics. Oxford University Press, New York, p 561

Journel AG, Huijbregts CJ (1978) Mining geostatistics. Academic, New York, p 600

Lantuejoul C (1988) On the importance of choosing a change of support model for global reserves estimation. Math Geol 20(8):1001–1019

Marechal A (1984) Recovery estimation: a review of models and methods. In: Verly G (ed) Geostatistics for natural resources characterisation, Part 1. Reidel, Dordrecht, pp 385–420

Rivoirard J (1994) Introduction to disjunctive kriging and non-linear geostatistics. Oxford Press, Claredon, p 181

Rossi ME, Deutsch CV (2014) Mineral resource estimation. Springer, Berlin, p 332

Rossi ME, Parker HM (1994) Estimating recoverable reserves: is it hopeless? In: Dimitrakopoulos R (ed) Geostatistics for the next century. Kluwer, Dordrecht, pp 259–276

Wackernagel H (2003) Multivariate geostatistics: an introduction with applications, 3rd edn. Springer, Berlin, p 388

Model Review and Validation 23

Abstract

Geostatistically estimated mineral resource block model has to be validated before it is released for the mine projects evaluation and the production planning tasks. Validating procedures should be comprehensive and allowing to assess validity of the global and local estimates. Degree of smoothing in the model must be estimated and its impact on recovered resources quantified. The most commonly used techniques for validating the mineral resource estimates includes application of the spider-diagrams comparing the estimates with the input data and the cross-validation techniques.

Keywords

Block model • Cross-validation • DGCS • Spider-diagram

23.1 Validating of the Global Estimates

Geologists commonly compare the histograms of the estimated block grades with the data in order to verify that their global means are identical. This allows to check for presence of the global biases of the estimates. However, comparison of the histograms is insufficient for validating the estimates because the globally unbiased results can be conditionally biased. This is illustrated on the Fig. 23.1 comparing grades of the samples and the blocks estimated by Ordinary kriging. One of the compared models uses blocks of 5×5 m which are too small for the given data distributed as 40×40 m grid and, therefore, produces incorrect results (Figs. 19.12 and 19.14). However, conditional bias of that model can not be diagnosed from the histogram (Fig. 23.1). Thus, the validating of the geostatistical estimates must include assessment of the degree of their smoothing.

Degree of smoothing can be approximately assessed by comparing the grade-tonnage diagram deduced from the kriging block model with the discrete Gaussian change-of-support (DGCS) model (Fig. 23.2). The latter estimates relationship between tonnage and grade in accordance with a volume – variance relationship principle. Deviation of the kriging estimates from the DGCS model is usually indicates that kriging model is not compliant with the volume support condition. This is presented on the Fig. 23.2a,

M. Abzalov, *Applied Mining Geology*, Modern Approaches in Solid Earth Sciences 12,
DOI 10.1007/978-3-319-39264-6_23

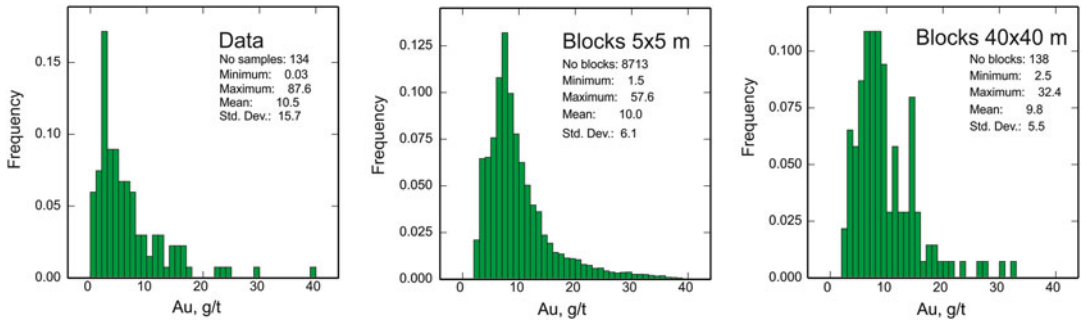

Fig. 23.1 Histograms of the samples and the block grades estimated by Ordinary kriging (based on the data presented in the Sect. 19.4.2)

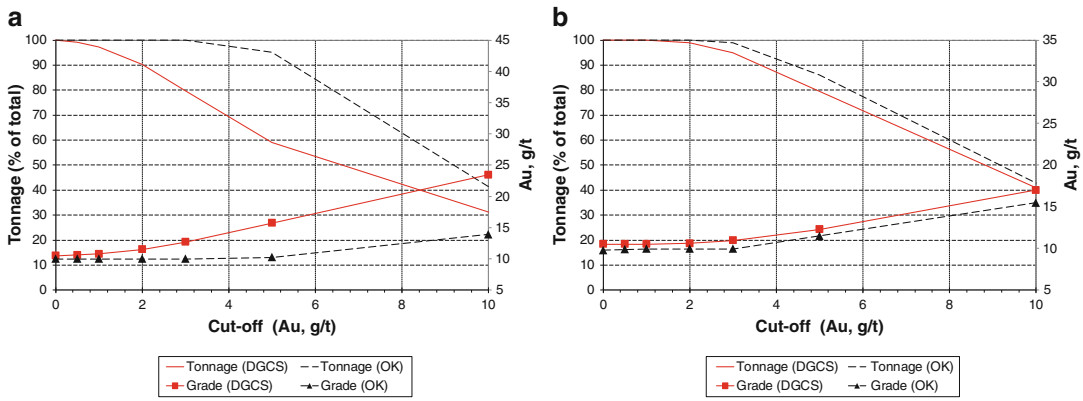

Fig. 23.2 Grade-tonnage relationships based on the Ordinary kriging (OK) and the discrete Gaussian change of support (DGCS) estimates. Both models were created using data points distributed as 40×40 m grid: (**a**) blocks are 5×5 m; (**b**) blocks 40×40 m

where significant deviation of the OK model from the DGCS estimates is caused by using 5×5 m blocks which were too small given the distance between the data points was 40×40 m. Estimating grade into larger blocks, 40×40 m, has improved the estimate (Fig. 23.2b).

23.2 Validating of the Local Estimates

Accurate estimation of the grade in the unsampled locations is the most challenging task in geostatistics and resource estimation practices. Accuracy of the local estimates largely depends on the density of the data distribution. At the early exploration stage, when samples are collected along the broad grid, local accuracy of the block model is limited to the large blocks (panels). With maturing the mining project, in particular when grade control data has become available, the accurately grade can be accurately estimated into SMU size blocks. Thus, planning the validation of the local estimates it is necessary realistically assess the spatial distribution of the data and its impact onto the resolution of the kriging block model.

23.2.1 Validating of the Local Mean

A standard procedure of validating of the locally estimated grade is based on grouping estimated blocks and corresponding them data (samples) by the large panels drawn across the entire ore body (Fig. 23.3). In other words, the proposed approach estimates the local mean of the data which is compared with the mean of the estimated

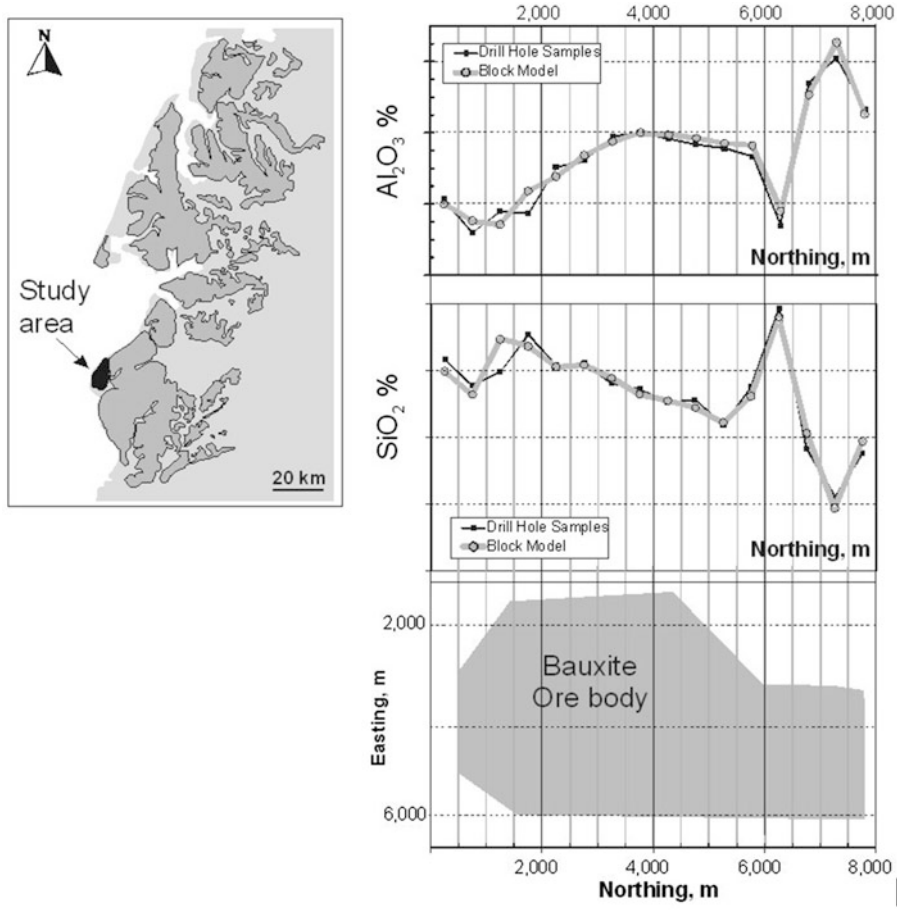

Fig. 23.3 Validation of the bauxite resources using the spider-diagrams (Abzalov and Bower 2014). Estimated Al_2O_3 and SiO_2 grades are averaged by 500 m thick panels, sliced across the domain, and compared with their corresponding sample grades

blocks confined to the same panel. Size of the panel depends on the data distribution. It should be large enough and to contain sufficient amount of the data then the principle of the permanence of a mean becomes applicable for the local means.

Usually, the panels are drawn along the strike of ore body (mineralised domain) and includes a space encompassing one or two drill traverses (Abzalov and Bower 2014; Abzalov et al. 2014). Using two orthogonal directions for validating the local means, commonly along strike and vertical, provides more reliable results and should be always considered if data permits to do so.

Average grades are calculated for each panel using all samples within the panel and compared to the average grade of this panel estimated from the block model. Estimated average grades are plotted on a diagram against coordinates denoting the centre of the panel (Fig. 23.3). The diagram is usually referred to as a spider diagram. Deviation of the block grades from the mean of the corresponding data indicates for the local bias of the estimates. The commonly observed distributions are when mean of the block grades are consistently lower then mean of the samples in the high grade panels and, on the contrary, systematically higher then mean of the samples in the low grade panels. This indicate for excessive smoothing of the estimates, which most likely is caused by incorrectly chosen search neighbourhood.

23.2.2 Validating by the Drill Hole Intersections

Degree of smoothing can be assessed by comparing the drill hole intersections with corresponding them kriged blocks (Fig. 23.4). The method works in particular well at the tabular ore bodies, including bauxite, iron ore and stratiform base metal mineralisation. Despite of the apparent simplicity of this approach, which is colloquially referred to validating by the drill hole intersections, it is a powerful tool allowing to diagnose if the kriging model is excessively smoothed.

Application of this technique is illustrated on the Fig. 23.5 showing two models validated by the drill hole intersections. The first model was estimated using Ordinary kriging (OK) (Fig. 23.5a), second, using Localised Uniform Conditioning (LUC) (Fig. 23.5b). When average grades of the block model intersections were plotted against corresponding them drill holes a moderate conditional bias was found in the OK estimate. This is expressed in deviation of the Reduced Major Axis (RMA) from the first bisect (Fig. 23.5a). Application of the LUC method has improved the accuracy of the estimate and eliminated the conditional bias where slope of the data distribution on the diagram is equal to 1 (Fig. 23.5b). Another useful criteria is the relative scatter of the data points around the RMA line (Fig. 23.5).

23.2.3 Cross Validation Technique

This method is based on successively removing a point data from the data array and estimating the given location, which has become unsampled, using the remaining data (Davis 1987). The procedure is repeated many times with the different data points and the estimates are compared with the sample which has been removed. Plotting the estimates values against the true (sample) values allows to diagnose and quantify the global and conditional biases.

The method is popular among the resource geologists and is widely used for validating mineral resource estimation. The procedure of cross validation is in particular useful for comparing results by several estimation methods, which can be ranked by the degree of their conditional biases (Sinclair and Blackwell 2002). The more the slope departs from unity the greater is the conditional bias of the estimate.

23.3 Validating of the Tonnage

Most of the above discussed validation procedures are dealing with grade of mineralisation. The tonnage, another economically important measure of the resources and reserves, is not fully addressed by the above described techniques. Accuracy of a tonnage estimation largely depends on validity of the geological interpretation and

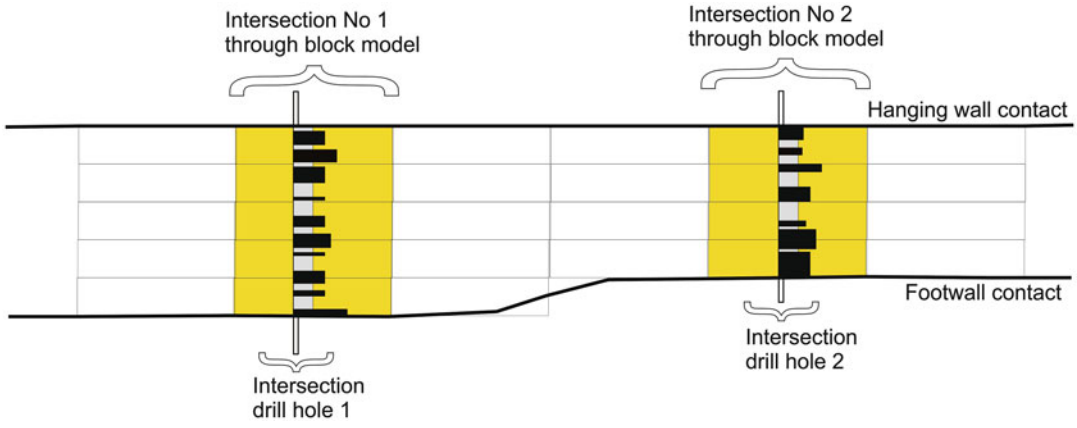

Fig. 23.4 Explanation of the technique of validating by the drill hole intersections

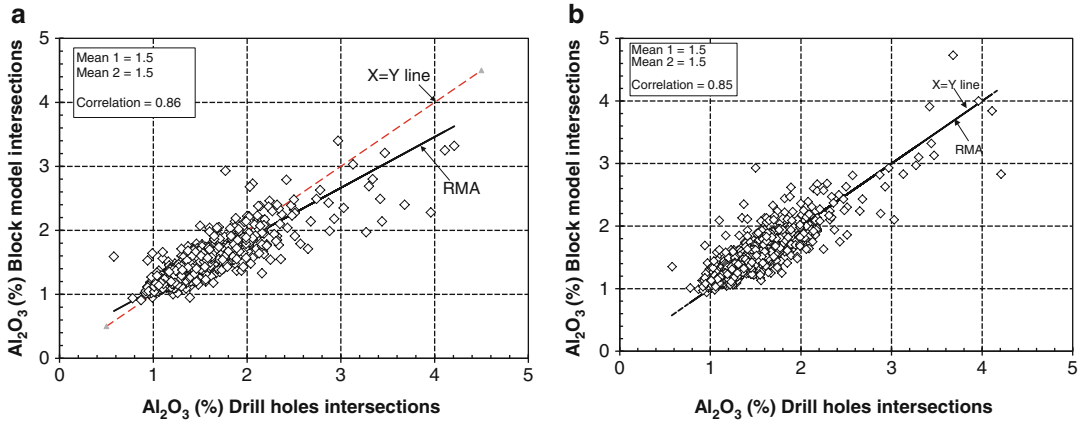

Fig. 23.5 Validation of the resources of the iron-oxide deposit by comparative analysis of the mineralised intersections. RMA – reduced major axis (Abzalov 2008): (**a**) estimated by OK; (**b**) estimated by LUC after unfolding of the data

accuracy of its implementation in the wireframes constraining the mineralised domains therefore validating of the tonnage should be based on auditing and confirmation of the validity of geological interpretations. This should include the next attributes:

- validity of the chosen geometry of mineralisation;
- contact analysis and assessment of the accuracy of the contact position in the unsampled locations;
- presence of the waste blocks within the ore body;
- validity of extrapolating the mineralisation to unsampled locations.

The uncertainties of the geological models can be estimated using conditional simulation techniques which are discussed in the Part 5 of the book. However, the validation of the geological interpretations commonly become possible only after the mine mapping data have become available. Therefore, mapping of the mines remains the main technique for accurate reconciliation of the ore reserves tonnages which is essential for achieving a high efficiency of a mining operation. Thus, mapping of the mine workings cannot be replaced by mathematical procedures and should be considered as a necessary technique for the ore reserves validation and their reconciliation with the mine production.

References

Abzalov MZ (2008) Quality control of assay data: a review of procedures for measuring and monitoring precision and accuracy. Exp Min Geol J 17(3–4):131–144

Abzalov MZ, Bower J (2014) Geology of bauxite deposits and their resource estimation practices. Appl Earth Sci 123(2):118–134

Abzalov MZ, Drobov SR, Gorbatenko O, Vershkov AF, Bertoli O, Renard D, Beucher H (2014) Resource estimation of *in-situ* leach uranium projects. Appl Earth Sci 123(2):71–85

Davis BM (1987) Uses and abuses of cross-validation in geostatistics. Math Geol 19(3): 241–248

Sinclair AJ, Blackwell GH (2002) Applied mineral inventory estimation. Cambridge University Press, Cambridge, p 381

Reconciliation with New Data

24

Abstract

Validation of the model should be continued through the entire duration of the mining project and repeated each time when the new data become available. This can be next phase of the infill drilling providing the more detailed geological information and higher density of sampling allowing to better model spatial continuity of the grade and deleterious elements. Commencement of production provides the grade control data, which because of their high density of a spatial distribution provides a unique opportunity for validating the ore reserves and the underlying resource estimate. Eventually, the mine and the plant production data provides an ultimate opportunity to reconcile the ore reserves.

Keywords

Reconciliation • Ore grade control • Mine production

24.1 Validating Using the Infill Drilling Data

Development of the mineral resources is made at several stages including consecutive infilling of the drilling grids which is needed for upgrading the resource categories. The procedure of the staged development of the resources is explained on the Fig. 24.1 showing the block-1 of the CJUP uranium deposit in Jordan (Abzalov et al. 2015).

The first phase of exploration was made by drilling and trenching with the data distributed as 200×200 m grid (Fig. 24.1b). This phase of exploration was culminated by estimation of the Inferred resources (Fig. 24.1c). It was followed by the next phase of exploration when the previous data grid was infilled into the 100×100 m grid of trenching (Fig. 24.1b). The resources were estimated again, and classified as Indicated resource (Fig. 24.1d). This is a common approach of upgrading the resource category by infilling the exploration data into tighter grids. However, unfortunately its often overlooked that the infill data present an excellent opportunity for reviewing accuracy of the previously estimated resources, which need to be made routinely each time when the new exploration data become available.

Procedure of validating resources using infill drilling results is as follows (Figs. 24.1, 24.2 and 24.3).

M. Abzalov, *Applied Mining Geology*, Modern Approaches in Solid Earth Sciences 12,
DOI 10.1007/978-3-319-39264-6_24

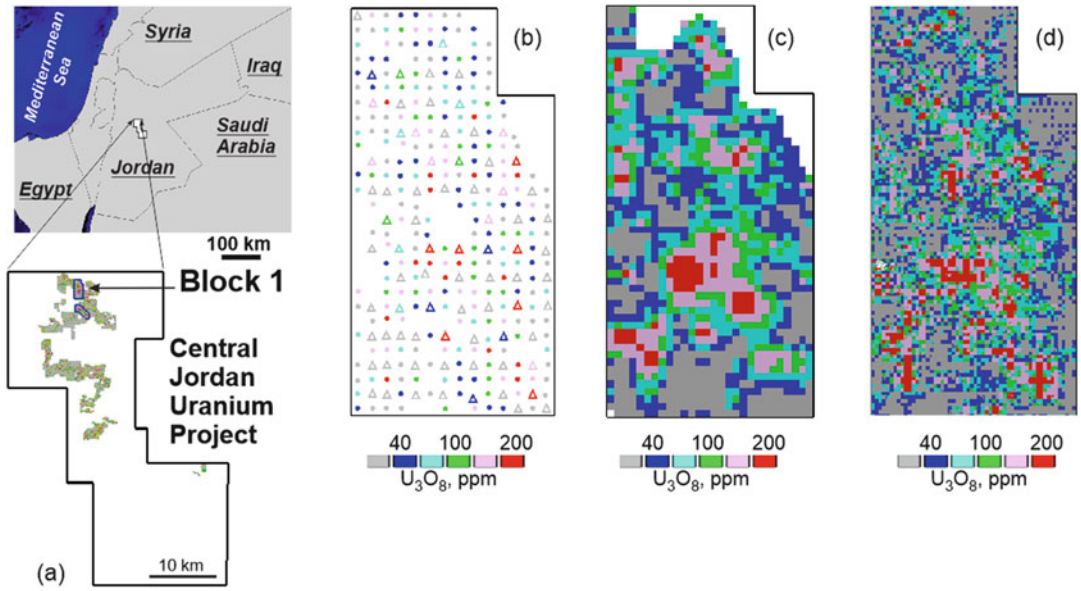

Fig. 24.1 Validating resources of the block-1 in central Jordanian uranium project (Abzalov et al. 2015) using infill sampling data: (**a**) map showing location of the project; (**b**) distribution of the exploration trenches: triangles – 200×200 m grid, dots-100×100 m grid; (**c**) Inferred resources estimated using 200×200 m data; (**d**) Indicated resources estimated using 100×100 m data

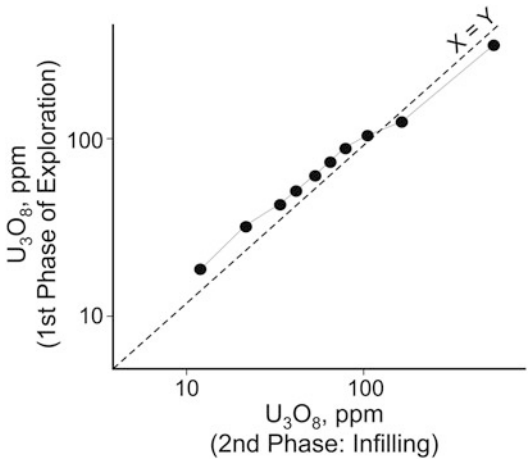

Fig. 24.2 Q-Q plot comparing two generations of the exploration samples

The first step is to compare the different generations of the exploration data. The conventional approach for comparative analysis of the data includes construction of the histograms, spider-diagrams and the Q-Q plots (Fig. 24.2).

After quality of the infill data has been confirmed they can be used for validating the resource model which was constructed before the infill data has become available (Fig. 24.1c). This is made by comparison of the block model grades with the corresponding them samples from the infill drill holes. The samples and the resource model blocks are grouped into large panels and the average grade of the samples estimated and compared with the corresponding average of the resource model. A common approach is to use panels drawn across the strike of the studied domain and plotting the average grades into spider-diagrams (Fig. 24.3). However, the panels corresponding to the monthly and quarterly production of the ore can also be used for this purpose. Depending on the findings of the comparative analysis the resource estimation parameters can be revised and the changes will be implemented during the next phase of the resource estimation.

Eventually, after quality of the infill drilling data has been confirmed and the past resource model has been validated the new resource estimation can be made using all available data (Fig. 24.1b). Methodology of the resource estimation is changed in accordance with the findings of the resource validation using the infill drilling

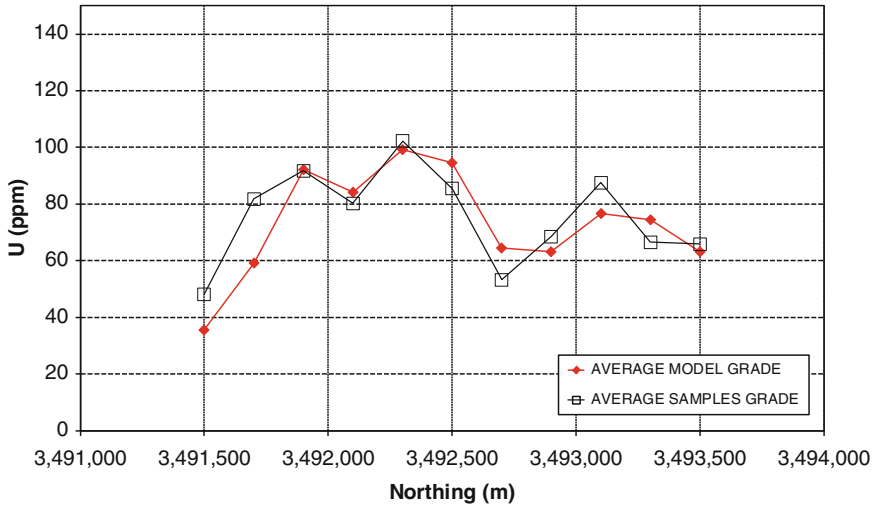

Fig. 24.3 Spider-diagram comparing the estimated resource block grades with the exploration trenches infilling the first grid. All data are grouped by 200 m panels drawn across the block-1

data. The new estimate is based on larger amount of data distributed as a tighter exploration grid and therefore are commonly classified into higher category of resources (Figs. 24.1c, d).

The final step is to compare the new resource model (Fig. 24.1d) with the previous estimate (Fig. 24.1c). This step is important because infill drilling commonly reveals the new structural features, including new high grade shoots or internal waste and, as a result, the tonnage and grade of the earlier estimated domains changes after more drill holes are drilled. Therefore, the good practice is to estimate these changes and report them as a resource categories conversion rates.

24.2 Reconciliation with the Mine Production Data

Procedure of reconciliation with a mine production has several steps:

- the produced blocks should be accurately surveyed in order to estimate the actual volume of ore which has been excavated during the period of time of interest (e.g. monthly production);
- the produced ore is accurately weighed therefore tonnage of the excavated ore can be used for reconciliation;
- grade of the excavated ore is measured using the group of samples collected from the conveyer belt transporting the crushed ore;
- produced metal as it is recorded at the plant is reconciled with the assayed tailings in order to construct the full metal balance in the plant;
- using the surveyed coordinates of the mined volume extract the corresponding volume from the ore block model and estimate its tonnage and grade as it is presented in the ore model;
- compare the actual production numbers with that which were derived from the ore block model, estimate and report reconciliation as percentage of production.

It should be remembered that mine production is uncertain by its nature (Schofield 2001b) partially because of mining dilution which not always accurately estimated due to surveying errors. Losses at the process plant and miscalculated metal recovery can further complicates reconciliation procedures. In addition, the extensive use of stockpiling can significantly affect the ability to relate process plant data to specific ore location. Therefore, reconciliation of reserves with a mine production must be used strictly together with reconciliation with the grade control data.

24.3 Ore Grade Control

Main purpose of grade control at the mines is for accurate definition of the contact between ore and waste and determining grade of the mined ore. Where applicable, the grade control objective can also include accurate estimation of the main by-product metals and deleterious components. The latter is in particular important if mining operation requires blending ore derived from the different sources in order to obtain the optimal physical and chemical characteristics of the ore for processing at the given plant.

Grade control is usually performed before commencing production from the given part of the deposit when access to ore body has been obtained for a short period of time. Sizes of the blocks that are characterised by grade control procedures should correspond to actual mining selectivity therefore their accurate characterisation requires large amount of additional samples usually taken at the distances of 5×5 m to 20×20 m (Pevely 2001; Blackwell 2000; Abzalov et al. 2010).

Because of high density of spatial distribution of the grade control samples this data provide a unique opportunity for validation of the estimated resources and reserves, because this is the last and the most detailed sampling data available for evaluation of the ore body before it was mined.

Thus, grade control at the operating mines has two main purposes, it provides a detailed information for accurate characterisation of the mined rocks into ore and waste types and also is the final test of the ore reserves validity before they were mined.

24.3.1 Grade Control at the Open Pit Mine

In the open pit mines the ore grade is controlled by sampling blastholes or additional infill drilling (Pevely 2001; Blackwell 2000; Abzalov et al. 2007, 2010). Sampling methods currently used for sampling of the blasthole cones are briefly summarised in the Table 24.1.

Grade control drilling is usually made by using RC or open hole percussion drill rigs (Abzalov et al. 2010). The preference to these methods is made because of the limited time available for drilling and necessity to collect large amount of representative samples. The constraints imposed by the mine logistics dictate the needs of choosing the low cost drilling techniques characterised by a high drilling rates, which can be achieved without compromising the samples quality. Auger drilling can also be used for grade control if ground is soft which permitting using the auger drilling (Abzalov and Bower 2014).

Another approach includes direct sampling from the mine faces or using shallow trenches and winzes. This was broadly used in the past however is currently replaced by the grade control drilling.

High density of the grade control data distribution allows to obtain the most accurate location of the ore body contacts and to delineate contours of internal waste. Conventional processing of the grade control data is as follows:

- The ore body contacts are conventionally drawn through the blastholes by applying the cut-off value used at the given mine for separating ore from waste (Fig. 24.4);
- The defined contacts are then marked on the open pit benches by the mine geologists, usually using the marking tapes;
- Average grade of the ore prepared for mining is estimated by averaging the grades of all blasthole samples collected from the delineated ore body polygons.

This procedure is currently replaced by geostatistical modelling of the data allowing more accurately estimate grade of the delineated ore body blocks. Most commonly this is made by Ordinary kriging method although Indicator kriging is also used at some gold mines. Depending on a mineralisation style, mine geologist is making decision if a soft or hard boundary approach is used for the grade estimation.

The kriging estimate is compared with the ore reserve model and based on this comparison the validity of the ore reserve estimate is quantified. The differences between the ore reserve and the

Table 24.1 Grade control methods at the selected open pit mines

Mine	Country	Commodity	Grade control method	Sampling grid	Description of the method
Yandi	Australia	Iron ore	Blast holes sampling	7 × 9 m	Approximately 5 kg sample is collected from a blast hole cone. Sample is collected by shovel from two spots located at 90° to each other
West Angelas	Australia	Iron ore	RC drilling	12.5 × 12.5 m	Conventional RC drillholes sampled at 1 m intervals
Rossing	Namibia	Uranium	Blast holes sampling	6 × 6 m	Approximately 4 kg sample is collected from the four spots randomly distributed around the blast hole cone. This is coupled with radiometric tests using hand-held radiometer
Tarkwa	Ghana	Gold	In-pit trenching	10–12.5 m distance between trenches	Dug by dozer ripper
Taparko	Burkina Faso	Gold	Blast holes sampling	3.5 × 3.5 m	
Geita	Tanzania	Gold	RC drilling	10 × 5 m	Conventional RC drillholes sampled at 1 m intervals
Sangaredi	Guinea	Bauxite	Auger drilling	10 × 5 m	Sampling made using radial cannels approach
Voisey's Bay	Canada	Nickel	Blast holes sampling	5 × 5 m	Sample is collected by a scoop from the four points randomly distributed around the blasthole cone
Escondida	Chile	Copper	Blast holes sampling	7 × 7 m	Approximately 10 kg sample is collected from 8 spots regularly distributed around the blasthole cone. Sampling made by using spear, piercing it through the entire sector of a cone

grade control models can be further quantified using conditional simulation techniques, which also is used for comparing different grade control methods and quantifying their corresponding errors (Fig. 24.4).

24.3.2 Grade Control at the Underground Mines

Grade control procedures at the underground mines differ depending on the mining method. At the mines where ore is selectively mined using cut-and-fill or shrinkage stoping methods the grade control is largely made by mapping and sampling of the ore drive faces (Zarmitan, Uzbekistan). At the bulk mining underground operations the grade control is usually made by additional infill drilling, using diamond core (Olympic Dam, Australia) or, percussion (Rocky's Reward, Australia) techniques. Percussion drilling is commonly made by Jumbo-rigs which can be located on the footwall drives. The drilling has to be coupled with mapping and sampling of mineralisation exposed in the underground workings, including ore drives faces and backs and the side walls of the cross-cuts (Perseverance, Australia). If the procedure is systematically applied with a due rigour it provides a good quality information with the level of the details sufficient for accurate design of the mining stopes.

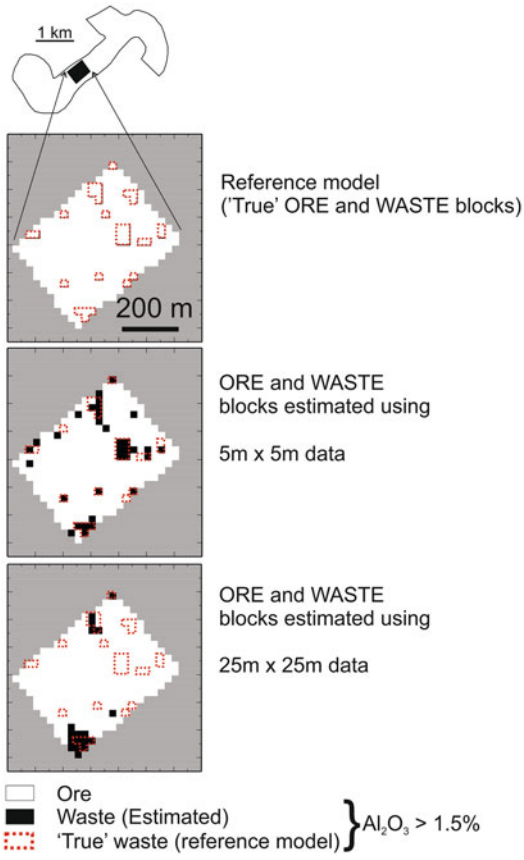

Fig. 24.4 Distribution of the ore and waste within the detailed study block at the Yandi iron ore mine (Abzalov et al. 2007)

High density of spatial distribution the grade control samples allows to accurately estimate grade of the ore in the stope which are compared with the corresponding parts of the resource and reserve block models for their verification.

In some instances, the grade control samples are collected from the draw points of the underground stopes (Fig. 5.5). This is in particular common procedure at the block cave (Northparkes, Australia) mines. However, validity of such grade control samples is seriously questionable and this data cannot be used for verification reserves.

References

Abzalov MZ, Bower J (2014) Geology of bauxite deposits and their resource estimation practices. Appl Earth Sci 123(2):118–134

Abzalov MZ, Menzel B, Wlasenko M, Phillips J (2007) Grade control at the Yandi iron ore mine, Pilbara region, Western Australia: comparative study of the blastholes and RC holes sampling. In: Proceedings of the iron ore conference 2007. AusIMM, Melbourne, pp 37–43

Abzalov MZ, Menzel B, Wlasenko M, Phillips J (2010) Optimisation of the grade control procedures at the Yandi iron-ore mine, Western Australia: geostatistical approach. Appl Earth Sci 119(3): 132–142

Abzalov MZ, van der Heyden A, Saymeh A, Abuqudaira M (2015) Geology and metallogeny of Jordanian uranium deposits. Appl Earth Sci 124(2):63–77

Blackwell GH (2000) Open pit mine planning with simulated gold grades. CIM Bull 93: 31–37

Pevely S (2001) Ore reserve, grade control and mine/mill reconciliation practices at McArthur River mine, NT. In: Edwards AC (ed) Mineral resource and ore reserves estimation – the AusIMM guide to good practice. AusIMM, Melbourne, pp 567–578

Schofield NA (2001b) The myth of mine reconciliation. In: Edwards AC (ed) Mineral resource and ore reserves estimation – the AusIMM guide to good practice. AusIMM, Melbourne, pp 601–610

Part V

Estimating Uncertainty

Grade Uncertainty

25

Abstract

Uncertainty of the mineral resource and ore reserve models are estimated using stochastic simulation techniques. The approach is referred to as conditional simulation and represents application of the Monte Carlo simulation principles to the regionalised variables.

Conditional simulation generates unlimited number of equiprobable models (realisations) of the studied geological body. All realisations honour statistical and geostatistical characteristics of the constraining data however differ in details. Thus, by statistical analysis of the differences between simulated realisations the uncertainty of the geostatistical model can be accurately quantified.

Keywords

Stochastic • Conditional simulation • TB • SGS • SIS • Corridor sands

Developing of the mining projects is a high risk endeavour, therefore technical and financial risks need to be quantitatively estimated. This includes quantification of the geological uncertainty, degree of the grade and the deleterious components variability and quantification errors in the estimated geotechnical parameters. These estimates are usually made by stochastic simulation using the Monte Carlo algorithms extended to the regionalised variables. The approach is referred to as conditional simulation because the simulated models are adjusted (conditioned) to the actual data (samples).

Conditional simulation generates quantitative models of the ore body reproducing the data histogram and their spatial variability. However, because the conditional simulation techniques are based on the Monte Carlo stochastic algorithm it generates unlimited number of equiprobable models (realisations) of the ore body. All realisations honour statistical and geostatistical characteristics of the constraining data however differ in details. The higher variability of the data and less samples available for constraining the models the larger degree of the differences between realisations. Thus, by statistical analysis of the differences between simulated realisations the uncertainty of the geostatistical model can be accurately quantified.

M. Abzalov, *Applied Mining Geology*, Modern Approaches in Solid Earth Sciences 12,
DOI 10.1007/978-3-319-39264-6_25

25.1 Methods of Conditional Simulation

The methods of conditional simulation are subdivided onto three groups, depending on the nature of the variable to be simulated.

- Simulation of the continuous variables including chemical composition of mineralisation, thickness, geotechnical parameters and deleterious components;
- Simulation of the categorical variables. These are lithofacies, geological structures and tectonic faults;
- Object based simulation. Objects are defined by their shape, location and orientation.

The main conditional simulation methods in use in the mining industry are introduced in this chapter. The description of the stochastic simulation methods is not overloaded by explanation of their mathematical principles and is primarily focused on their application in the mine geology. The comprehensive mathematical analysis of these techniques can be found in the geostatistical textbooks (Chiles and Delfiner 1999; Lantuejoul 2002; Wackernagel 2003) and in the special papers which are references where appropriate in the following chapters.

Most common application of the conditional simulation techniques is for quantification of uncertainty in estimated grade. Methodology is based on generating several equiprobable models (realisations) of spatial distribution of the studied grade (Fig. 25.1). The obtained realisations are compared and their differences statistically analysed which allows to quantify a degree of the estimated grade uncertainty. Usually 25–50 realisations is needed in order to obtain a statistically valid results.

The uncertainty in the estimated ore grade is commonly used for quantification the mine production risks. In particular, this is often incorporated into the mine designs (Blackwell 2000) and also can be used for assessment of the metallurgical processing risks (Abzalov and Mazzoni 2004).

Another common application of this methodology is for classification of the mineral resources into the categories, Measured, Indicated and Inferred (Abzalov and Bower 2009).

Estimation of grade uncertainties is usually made by one of the three conditional simulation techniques: Turning Bands, Sequential Gaussian Simulation or Sequential Indicator Simulation (Chiles and Delfiner 1999; Lantuejoul 2002; Wackernagel 2003). The former two methods are Gaussian based, which require transformation of the data into standard Gaussian variable, with a zero mean and unit variance. The transformations are usually made using Hermite polynomials (Rivoirard 1994). The simulated Gaussian variable is then transformed back to original data space. Sequential Indicator Simulation requires transformation of the data into Indicator variables (Deutsch and Journel 1998).

The Gaussian based methods, Turning Bands and Sequential Gaussian Simulation, assume a multi-Gaussian property of the studied regionalised variable which is also should be coupled with its diffusive distribution model. These two conditions need to be tested prior to application of the modelling methodology. Border effect indicating for diffusive distribution is usually tested by calculating the ratios between cross-variograms of the indicators and indicator variograms (Abzalov and Humphreys 2002a, b). Multi-Gaussianity can be tested by calculating variograms of indicators calculated for the chosen data percentiles and comparing them with indicator variograms calculated for the same percentiles of the Gaussian transformed data (Goovaerts 1997).

25.1.1 Turning Bands

Turning Bands (TB) is one-dimensional simulation technique carried along the lines regularly spaced within the studied volume (Journel 1974). A coherent 3D model of mineralisation is obtained by projecting of the simulated values into unestimated nodes (points) located between the lines and averaging the projected

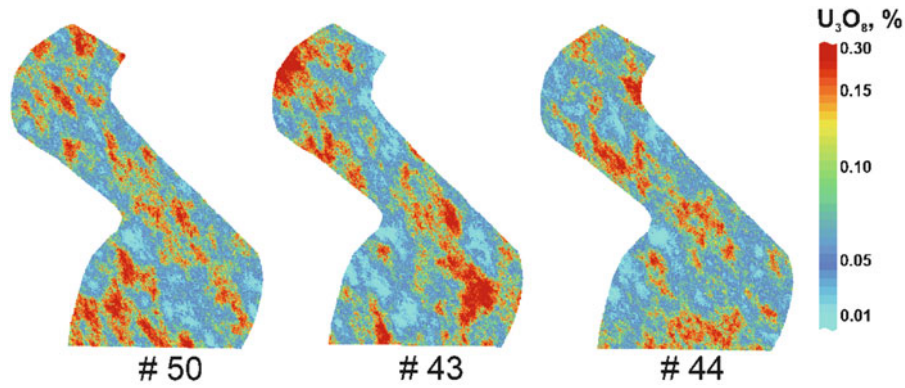

Fig. 25.1 Three equiprobable models (realisations) of the average uranium grade at the sandstone hosted deposit in Kazakhstan (Abzalov 2010)

values. Conditioning is obtained by kriging of the data points together with simulated nodes. Procedure of conditioning is as follows:

- non-conditional simulations at all target points and all sample points
- kriging the samples (data) into all nodes
- kriging simulated values into all nodes
- combine kriged values using formula 25.1.1.

$$Z^*_{\text{Turning Bands}} = \text{Estimate 2} + (\text{Estimate 1} - \text{Estimate 3}) \quad (25.1.1)$$

25.1.2 Sequential Gaussian Simulation

Sequential Gaussian simulation (SGS) is a Gaussian-based method of conditional simulation (Goovaerts 1997; Chilès and Delfiner 1999). This method uses data transformed to a Gaussian distribution with a zero mean and a unit variance (Gaussian anamorphosis), which is then used to simulate spatial distribution of the variable of interest.

Simulated realisation is achieved by defining a random path through the grid nodes including the conditioning data, which has been migrated to the nearest grid nodes and considered as hard data. A sequential neighbourhood of the target node is established, which includes hard data (original data) and already simulated nodes (soft data). The combination of the hard and soft data is used to calculate a local conditioning distribution and derive a simulated value at the target node. The simulated value determined as (25.1.2):

$$Z^*_{SGS} = Z^*_{SK} + \sigma_K\,(U) \quad (25.1.2)$$

where,
Z^*_{SGS} is SGS simulated value
Z^*_{SK} simple kriging estimate
σ_K standard deviation of the kriging estimate
(U) is a random normal function.

The method is effectively used for modelling the metal grades at the different deposit types and the mineralisation styles (Abzalov and Bower 2009; Abzalov and Mazzoni 2004). The main practical limitation of the technique is multi-Gaussianity condition which not always met, in particular when studied variable is characterised by highly skewed distribution aggravated by presence of anomalously high values.

25.1.3 Sequential Indicator Simulation

Sequential Indicator Simulation represents an extension of the sequential stochastic simulation algorithms to Indicator variables. The technique allows to reproduce the cumulative conditional distribution functions generated conditioning

them to spatial distribution of the data points (Deutsch and Journel 1998).

Sequential Indicator Simulation (SIS) is applied for characterising spatial distribution of the highly skewed variables, in particular grade of the gold and uranium deposits (Journel and Isaaks 1984). Such variables are containing the extreme values are not suitable for modelling using the multi-Gaussian approach and are better represented by simulating as a set of categorical variables (indicators).

Procedure of Sequential Indicator Simulation is as follows:

- A random path is defined through the grid nodes to be simulated (target nodes). The part also includes the data points (data nodes);
- Discretise the data into several (k) indicators using (k) cut-offs (thresholds). The procedure is the same as was used for Multiple Indicator Kriging;
- Determine (k) conditional cumulative distribution function (*ccdf*) using an indicator kriging algorithm;
- Correct for order relations and build a complete *ccdf* model;
- Draw a simulation value from the corrected *ccdf*;
- Add the simulated value to the conditioning data set;
- Proceed to the next node on the random path and repeat the above steps.

A main difficulty of the SIS method is the order relation problem (Blackwell 2000; Deutsch and Journel 1998). This is the same problem as was observed with Multiple Indicator Kriging. Distortion of the order relation is minimised by using the same search neighbourhood for all indicators and is further corrected using upward and downward changes of the raw *ccdf* values and then averaging the two sets of the corrected *ccdf's*.

The technique allows to overcome a problem of excessively skewed distributions and in particular well suited for gold and uranium deposits where different grade classes of mineralisation commonly occupy the different structural settings.

25.2 Application of the Conditional Simulation in the Corridor Sands Project

In this section, practice of the Conditional Simulation is explained using a case study of the Corridor Sands project in Mozambique where SGS technique was applied for estimation of the metallurgical risks (Abzalov and Mazzoni 2004).

At this project it was recognised, that while the resource model for deposit carries a high degree of confidence, the drilling density is such that there will be uncertainty on the predictability of local variations of the ore grade and metallurgically deleterious components on a daily or weekly production basis. Thus, there was a risk that the tolerance limits of the metallurgical concentrator can be exceeded due to excessive local variability of the ore composition. In order to examine the possible risk at the front end of the plant for local grade variability to exceed the primary concentrator tolerance limits a conditional simulation study was conducted.

25.2.1 Project Background

The Corridor Sands district of ilmenite bearing heavy mineral sands is located in southern Mozambique (Fig. 25.2), approximately 20–60 km from the Indian Ocean. It contains several deposits, discovered in 1997 during exploration of Pleistocene dunes along the east coast of Africa. The district represents the largest known resource of ilmenite with total endowment assessed as being in the order of 16.5 billion tonnes at 5 % total heavy minerals (Abzalov and Mazzoni 2004). The largest and the best explored is Deposit 1, which alone contains measured and indicated resources of 2.7 billion tonnes at 4 %

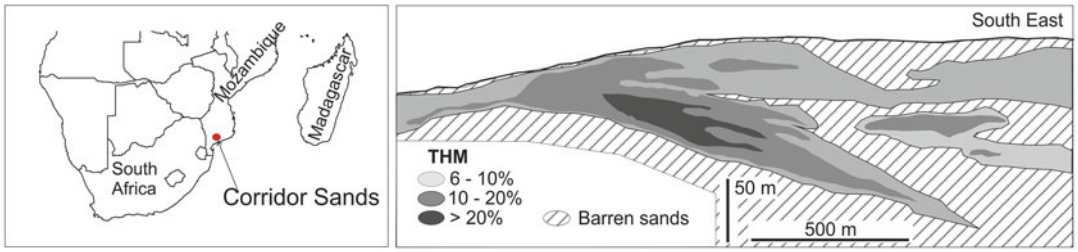

Fig. 25.2 Typical cross-section of the Corridor Sands deposit, Mozambique (Generalised after (Abzalov and Mazzoni 2004))

ilmenite (Abzalov and Mazzoni 2004). Resources of the Deposit 1 have been defined using air core drilling. Inferred category of the resources is based on drilling along 1 km spaced traverses. Indicated and Measured categories have been defined by infill drilling on 250 m × 125 m grid, including the initial mining area which was drilled on 100 m × 100 m and some smaller parts drilled on 25 m and 50 m grids (Abzalov and Mazzoni 2004). Quality of the aircore drilling was tested by twinning them with diamond holes, drilled using a triple tube core drilling technology (Abzalov et al. 2011). A bankable feasibility study of the project was based on approximately 1200 holes with total length of about 80,000 m.

Drilling has delineated a titanium rich sands that extend in north-east direction for more than 6 km dipping to south-east and thickening south eastwards to over 140 m (Fig. 25.2).

The mineralised stratigraphy is subdivided into six geological domains (Abzalov and Mazzoni 2004). These represent stratigraphic units formed as a result of superimposition of the different depositional facies and post-depositional pedogenic weathering processes. Domains are different by colour, clay content, grain size and grade of the total heavy minerals. The contacts between the domains are gently undulating rather than planar and characterised by presence of irregular trough and pot-holes, which are visible in the trial pit. Contacts are usually sharp and supported by textural differences between the stratigraphic units. The depositional breaks are sometimes accompanied by evidence of soil forming processes, including induration on the contacts.

The mineralogy and chemistry can be considered in terms of mineralised sand comprising silt (<45 μm), oversize material (>1 mm), light sand and total heavy minerals (THM). The THM component comprises varying proportions of magnetite, ilmenite, altered ilmenite, hematite, goethite, leucoxene, chromite, rutile, anatase, epidote, pyroxene, amphibole, andalusite, staurolite, zircon, sphene, monazite, garnet and kyanite. The valuable heavy minerals are ilmenite, rutile, leucoxene and zircon. They are generally finer grained than the other minerals.

The heavy minerals are subdivided into magnetic fractions. Magnetite, ilmenite, altered ilmenite, and chromite make up the bulk of the 'magnetic' and 'crude ilmenite' fractions. Rutile, zircon and andalusite are essentially confined to the 'non-magnetic' fraction. The remaining heavy minerals make up the bulk of the 'magnetic-others' fraction. The mineralogy of the 'crude ilmenite', and that of the 'non-magnetic' fractions, which contain the rutile and zircon, are the important aspects for the recovery processes.

The Project envisages the establishment of a fully integrated heavy mineral sands mining, mineral processing and beneficiation operation together with its associated infrastructure, including an export facility for shipment of final products. An open pit mine is planned as a conventional truck and shovel operation delivering ore from free digging faces to a two-stage mineral processing plant. The primary concentrating plant will utilise trommels and desliming cyclones to remove the oversize and silt (<45 μm) fraction. Heavy minerals are recovered from the remaining sand by wet gravity spirals.

The magnetite is stripped off magnetically to produce a heavy mineral concentrate. The valuable heavy minerals, ilmenite, zircon, rutile and leucoxene are then separated in the mineral separation plant. A smelting complex located adjacent to the mining and mineral processing operations will upgrade the ilmenite to a titanium dioxide slag containing about 85 % titanium dioxide, together with a high purity foundry iron product. Sale of slag to pigment producers and iron to foundries will provide the bulk of the project revenue.

25.2.2 Scope of the Conditional Simulation Study

A distinct feature of the deposit is the presence of an abundant <45 μm silt fraction, representing fine weathering products of the original mineralised sand. The primary concentrating plant is designed to run continuously at up to 25 % silt and 15 % THM grades. In case if the silt concentration exceeds 25 %, this can lead to loss of process efficiency and additional process cost, such as excessive flocculant consumption. Silt grade of 3 m drill samples occasionally exceeds the threshold of 25 %, which suggests that average silt grade of small volumes of ore, such as selective mining units (SMU), can exceed the primary concentrator tolerance limits.

To assess the risk of delivering ore with composition exceeding the primary concentrator tolerance level, spatial distribution of the ore grade has been modelled using the SGS algorithm. The study was focused on a local variability of silt and total heavy minerals (THM) grade as the two variables of greatest concern to the primary concentrator.

Three mutually related tasks have been studied using the SGS technique.

1. The SGS method has been primarily applied to assess the short-range grade fluctuations in the resource. This was made by simulating the grade into the SMU size blocks. The several sizes of the SMU blocks ($5 \times 5 \times 3$, $10 \times 10 \times 12$, $25 \times 25 \times 12$ and $125 \times 62.5 \times 3$ m) were tested in order to assess dependence of the recovered grade on the mining selectivity.
2. Based on the estimated short-range variability of the ore grade the risk of delivering ore with silt and THM grades exceeding the plant tolerance thresholds has been quantified. Based on these results the optimal parameters of the primary concentrator plant have been chosen.
3. Additional outcome of the work was a validation of the Ordinary kriging estimates by their comparison with the SGS model.

25.2.3 Implementation of the SGS Technique

The study was based on the drill hole samples collected from the initial mining area at the Corridor Sands project (Abzalov and Mazzoni 2004). The area was drilled on 100 m × 100 m centres and locally on 25 m crosses. All holes were sampled at regular 3 m intervals and assayed for silt and THM contents. The study database includes 1246 silt assays and 1244 THM assays (Fig. 25.3).

Before applying of the SGS methodology the distribution of the THM and silt was tested to assure that the variables comply with a multi-Gaussianity condition and also exhibit a diffusive distribution model required for accurate application of the Gaussian based simulation techniques (Goovaerts 1997; Abzalov and Humphreys 2002a, b).

Next step is to prepare data for SGS study. In this study the data had to be declustered in order to remove bias associated with clustering of the holes around high-grade areas. The declustering was made using a cell declustering method. The optimal declustering results have been obtained using $150 \times 150 \times 3$ m moving 'window'. Statistical distribution characteristics of the raw and declustered assays are summarised in the Table 25.1.

Declustered data have been transformed to standard Gaussian variable by applying the Hermite polynomials expansion technique (Goovaerts 1997). In particular, a frequency

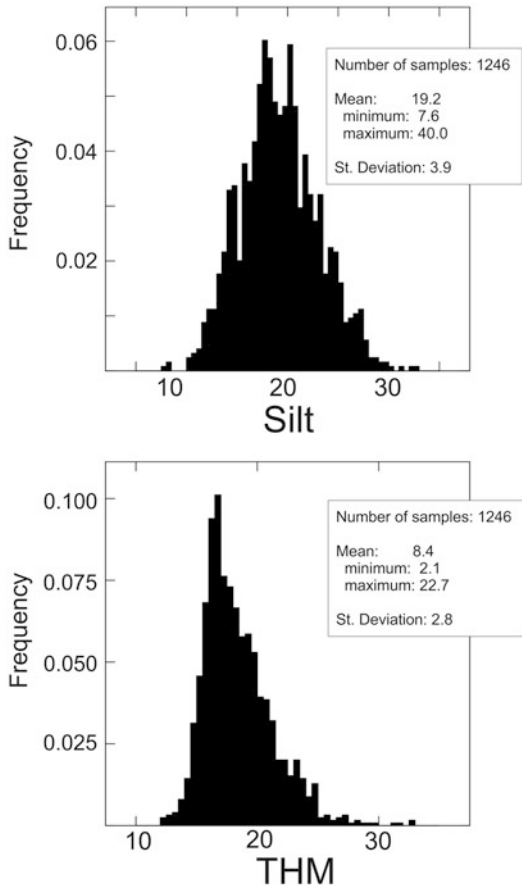

Fig. 25.3 Histograms (non-declustered data) of the THM and silt grades of the 3 m drill hole samples. SGS study database, Corridor Sands project (Reprinted from (Abzalov and Mazzoni 2004) with permission of Australasian Institute of Mining and Metalllurgy)

inversion method (Bleines et al. 2013) was utilised for Gaussian transformations of the declustered data.

Grade continuity has been analysed by calculating variograms of the silt and THM grades and their Gaussian transformed values. Directional variograms of the Gaussian variables and their models are presented in Fig. 25.4. These variograms show a noticeable anisotropy with a major anisotropy axis oriented at 100° south-east. Indicator variography, which was used to enhance the grade distribution patterns, accords well with the variography of the Gaussian transformed data.

SGS methodology was applied for modelling grade distribution into the blocks of $5 \times 5 \times \times 3$ m. Simulation was made using sequential search neighbourhood containing 35 samples and 27 simulated nodes. Simulated results have been combined to the larger blocks, $10 \times 10 \times 12$, $25 \times 25 \times 12$ and $125 \times 62.5 \times 3$ m, representing the proposed selective mining unit (SMU) sizes.

25.2.4 Results and Discussion

Spatial distributions of simulated THM and silt values are shown on the bench plans (Fig. 25.5a). The simulation results show a significant heterogeneity of the silt distribution (Fig. 25.5b). THM grade is more continuous then silt and, in general, is distributed more compactly (Fig. 25.5c).

25.2.4.1 Recoverable Resources

The resources recoverable at the given SMU sizes estimated using SGS methodology are presented as grade-tonnage diagrams (Fig. 25.6). These results suggest that recoverable silt grade is highly sensitive to the chosen size of SMU (Fig. 25.6a). In particular, if the Corridor Sands deposit was mined using $10 \times 10 \times 12$ m SMU sizes, 5 % of the mined blocks would have silt grade exceeding 23 %. THM grade is less sensitive to changing the SMU size than silt (Fig. 25.6b).

25.2.4.2 Risk of Exceeding Plant Tolerance Thresholds

Risk of exceeding the plant tolerance limits (20 % or 25 % silt) was deduced from the SGS model by estimating the probability of the SMU grades to exceed a given threshold (Fig. 25.7). Probability diagrams presented on the Fig. 25.7 show that risk of delivery high-silt ore (silt >25 %) from the initial mining area rapidly increases if the actual tolerance of the plant is lower than 25 % silt. Thus, approximately one third of the total $10 \times 10 \times 12$ m blocks are characterised by a very high probability (0.75) of exceeding 20 % silt grade (Fig. 25.7). These findings have helped to choose the plant design assuring that a silt tolerance is set to 25 % silt.

Table 25.1 Comparison of declustered and non-declustered (raw) assays

		Non-declustered data	Declustered data
Total heavy minerals (THM)	Mean	8.36	7.89
	Standard deviation	2.85	2.52
Silt	Mean	19.16	18.82
	Standard deviation	3.9	3.90

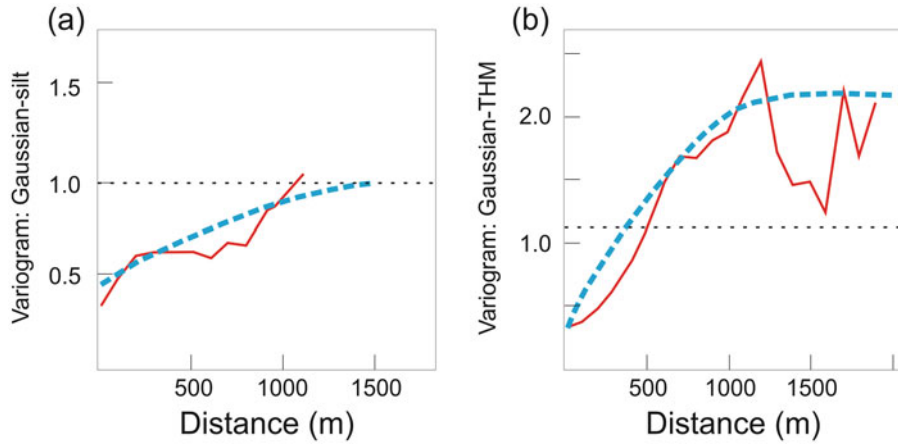

Fig. 25.4 Experimental variograms (*solid lines*) and fitted models (*dashed lines*) calculated along the major anisotropy axis (azimuth 100° south-east). Gaussian transformed silt (**a**) and THM (**b**) values (Reprinted from (Abzalov and Mazzoni 2004) with permission of Australasian Institute of Mining and Metalllurgy)

Study of the THM distribution shows that risk of exceeding the plant threshold of 15 % THM is negligible, as conditional simulation results shows that less than one per cent of $10 \times 10 \times 10$ m SMU blocks will contain THM grades higher than 15 % (Fig. 25.6b).

25.2.4.3 Comparison of the SGS and OK Results

The simulated silt and THM values of the $125 \times 62.5 \times 3$ m blocks have been compared with their grades obtained by Ordinary kriging. The average SGS grade of the blocks was estimated by grouping realisations into $125 \times 62.5 \times 3$ m blocks and calculating the arithmetic mean of the SGS realisations. The obtained value is compared with the corresponding Ordinary kriging estimate. Comparison of the two values is usually made by plotting them on the scatter diagram. In a more general form the two independent estimates can be compared by estimating the average grade of the mineralised domain, like it is shown in the Table 25.2. Comparison of the estimated means show that both methods have produced identical results (Table 25.2). Differences in the mean grades obtained by the two methods are statistically insignificant. Thus, the SGS model supports the validity of the Ordinary kriging estimates.

In summary, the work demonstrated that for a smallest mining unit (SMU) size of 10 m × 10 m × 12 m, there will be no issues with the plant ability to handle silt variability at the designed maximum tolerance limit of 25 % silt. At a lower plant feed tolerance of 20 % silt then about one in three SMU could be expected to exceed this. In-pit blending with ore from domains with lower silt content would be required to control the plant feed composition.

The average grade of the $125 \times 62.5 \times 3$ m blocks estimated from the SGS model is similar to the grade of these blocks estimated by

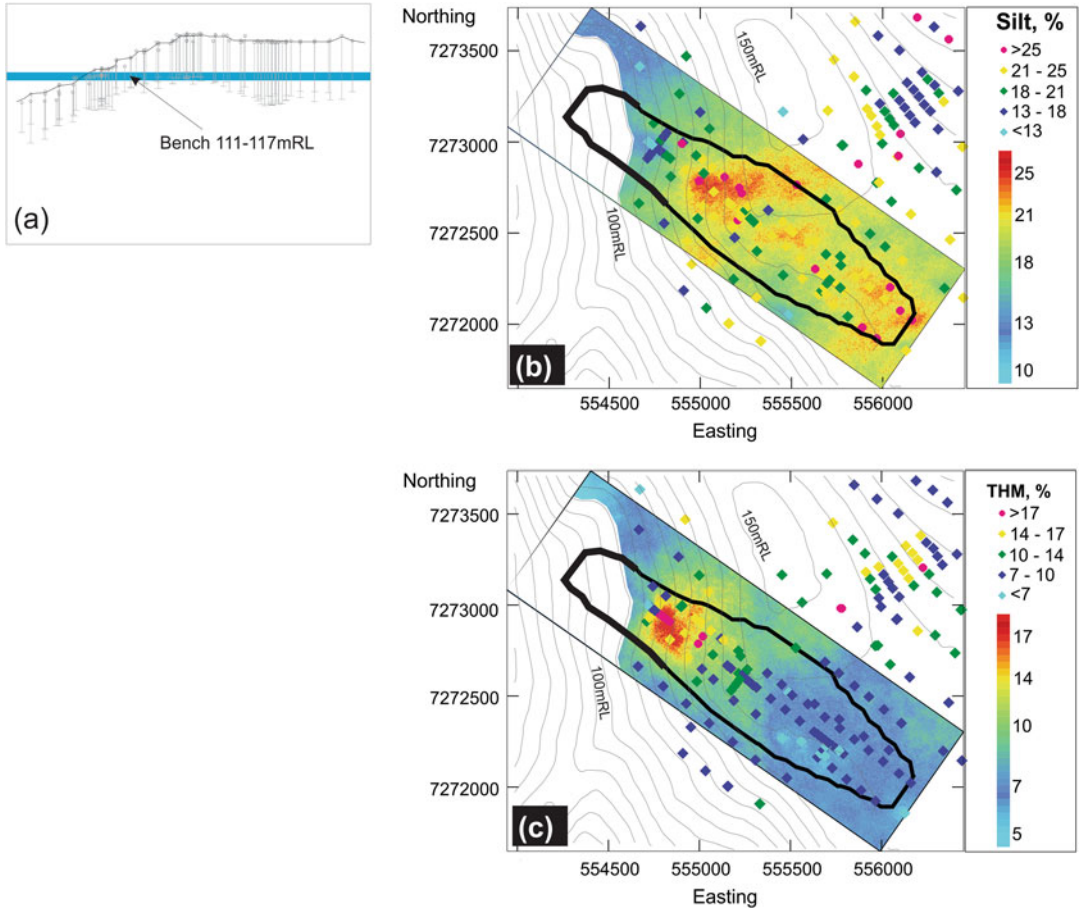

Fig. 25.5 Simulated grade values (background) and drill hole data (symbols). Bench 111–117 m RL of the Corridor Sands deposit (Reprinted from (Abzalov and Mazzoni 2004) with permission of Australasian Institute of Mining and Metalllurgy: (**a**) bench location; (**b**) silt; (**c**) THM)

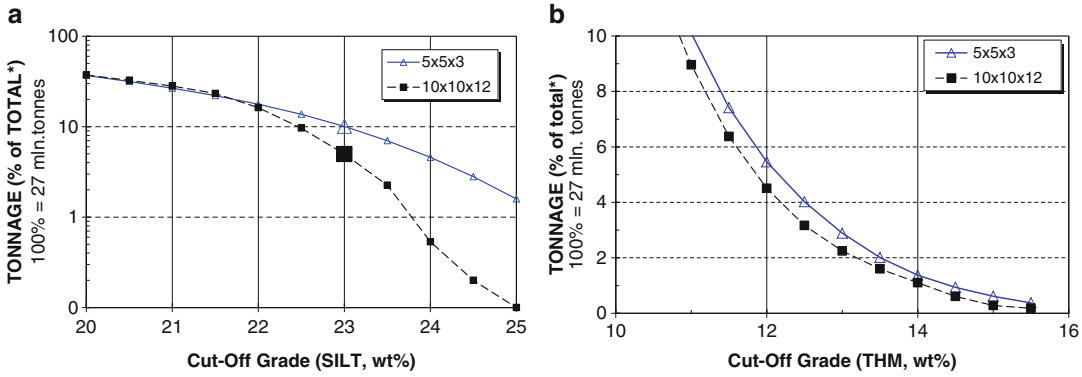

Fig. 25.6 Grade–tonnage curves calculated for different SMUs from the corresponding SGS models: (**a**) silt; (**b**) THM

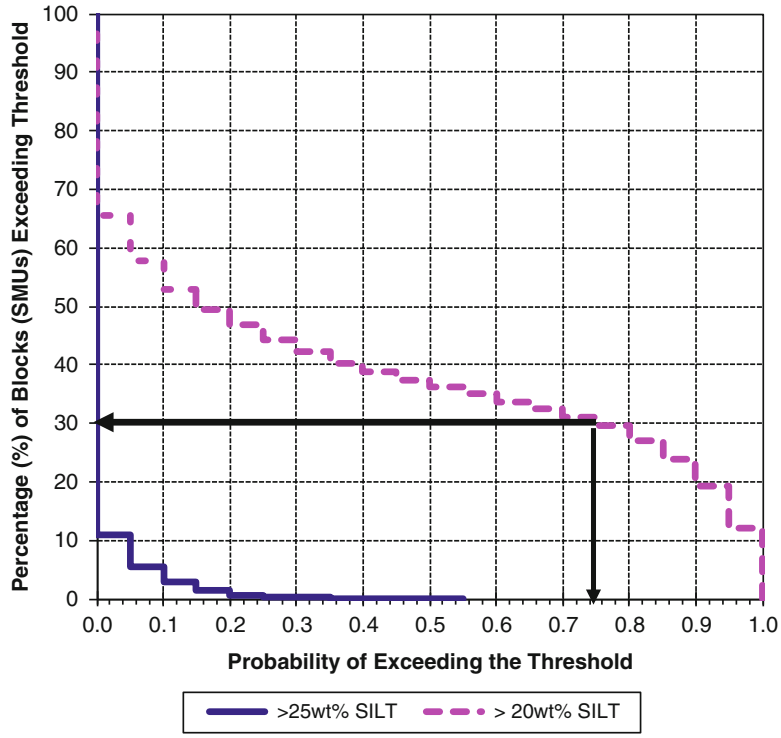

Fig. 25.7 Risk of exceeding the tolerance thresholds (20 % and 25 % silt). Mining selectivity is 10 × 10 × 12 m blocks

Table 25.2 Comparison of ordinary kriging estimates with SGS model

	SILT ±	2st.dev.	THM ±	2st.dev.
Ordinary kriging	19.0 ±	5.12	7.9 ±	3.84
SGS	19.1 ±	5.38	8.2 ±	3.94
Difference	−0.1		−0.2	
Correlation coefficient	0.9		1.0	

Corridor sands deposit (Abzalov and Mazzoni 2004)

Ordinary kriging (Table 25.2). Thus, the SGS model supports the validity of the Ordinary kriging results.

References

Abzalov MZ (2010) Optimisation of ISL resource models by incorporating algorithms for quantification risks: geostatistical approach. In: Technical meeting on in situ leach (ISL) uranium mining, International Atomic Energy Agency (IAEA), Vienna, Austria, 7–10 June, 2010

Abzalov MZ, Humphreys M (2002a) Resource estimation of structurally complex and discontinuous mineralisation using non-linear geostatistics: case study of a mesothermal gold deposit in northern Canada. Exp Min Geol J 11(1–4):19–29

Abzalov MZ, Humphreys M (2002b) Geostatistically assisted domaining of structurally complex mineralisation: method and case studies. Geostatistically assisted domaining of structurally complex mineralisation: method and case studies. In: The AusIMM 2002 conference: 150 years of mining, Publication series No 6/02, AusIMM, Melbourne, pp 345–350

Abzalov MZ, Mazzoni P (2004) The use of conditional simulation to assess process risk associated with grade variability at the Corridor Sands detrital ilmenite deposit. In: Dimitrakopoulus R, Ramazan S (eds) Ore body modelling and strategic mine planning: uncertainty and risk management. AusIMM, Melbourne, pp 93–101

Abzalov MZ, Bower J (2009) Optimisation of the drill grid at the Weipa bauxite deposit using conditional simulation. In: Seventh international mining geology conference, AusIMM, Melbourne, pp 247–251

Abzalov MZ, Dumouchel J, Bourque Y, Hees F, Ware C (2011) Drilling techniques for estimation resources of the mineral sands deposits. In: Proceedings of the heavy minerals conference 2011. AusIMM, Melbourne, pp 27–39

Blackwell GH (2000) Open pit mine planning with simulated gold grades. CIM Bull 93:31–37

Bleines C, Bourges M, Deraisme J, Geffroy F, Jeanne N, Lemarchand O, Perseval S, Poisson J, Rambert F, Renard D, Touffait Y, Wagner L (2013) ISATIS software. Geovariances, Ecole des Mines de Paris, Paris

Chiles J-P, Delfiner P (1999) Geostatistics: modelling spatial uncertainty. Wiley, New York, p 695

Deutsch CV, Journel AG (1998) GSLIB: geostatistical software library and user's guide. Oxford University Press, New York, p 340

Goovaerts P (1997) Geostatistics for natural resources evaluation. Oxford University Press, New York, p 483

Journel AG (1974) Geostatistics for conditional simulation of ore bodies. Econ Geol 69(5):673–687

Journel AG, Isaaks EH (1984) Conditional indicator simulation: application to a Saskatchewan uranium deposit. Math Geol 16(7):685–718

Lantuejoul C (2002) Geostatistical simulation: models and algorithms. Springer, Berlin, p 250

Rivoirard J (1994) Introduction to disjunctive kriging and non-linear geostatistics. Oxford Press, Clarendon, p 181

Wackernagel H (2003) Multivariate geostatistics: an introduction with applications, 3rd edn. Springer, Berlin, p 388

Quantitative Geological Models

26

Abstract

The 3D geological models are the basis for delineating the mineralised domains which underline the whole process of the mineral resource estimation and also serves as a key parameter for selection of the mining methods and eventual conversion of the resources to reserves. Degree of the geological model's uncertainty need to be estimated during the project evaluation studies and the risks of a project's failure caused by incorrectly interpreted geology quantified and incorporated into classification of the mineral resources and ore reserves

Keywords

Stochastic models • Pluri-Gaussian • Indicator • Domaining

26.1 Geological Models

Success of a mining project to a large degree depends on accuracy of the geological interpretation and, in particular, it depends on accuracy of 3D quantitative geological model used. Before commencing modelling of the geological features it is necessary to clearly identify which characteristics are relevant for estimation of the mineral resources and ore reserves. For example, the questions related to genesis of mineralisation, metallogeny of the provinces have direct implication in developing exploration strategy and optimising the exploration techniques but often not related to the mine geology needs.

The relevance of geological characteristics changes depending on commodity and mineralisation style. For example, the detailed knowledge of the ore mineralogy is not the critical parameter for estimation resources of the nickel-sulphide deposits but this is one of the main parameters for rare-earth bearing pegmatite deposits. Thus, before constructing the quantitative geological model of the deposit it is necessary to identify geological parameters relevant for estimation resources at the given deposit. Most common geological parameters addressed in details during mining projects evaluation are:

- Geometry of the ore body;
- Characterisation of the contacts, sharp or gradational, straight or irregular;
- Internal structure of the ore body, in particular geochemical and mineralogical zoning and layering;

M. Abzalov, *Applied Mining Geology*, Modern Approaches in Solid Earth Sciences 12,
DOI 10.1007/978-3-319-39264-6_26

- Presence of the multiple generations of mineralisation and differences of their structural controls;
- Presence of the internal waste within the ore body;
- Distribution of the weathered and oxidised rocks affecting the stabilities of the pit walls or underground workings;
- Faults, dykes and pegmatite veins representing the geotechnical hazards and also internal waste within the pre body.

Accurate mapping of the above listed features requires high density of the data points which usually becomes available only after the ore body is exposed by mine workings. At the beginning of the project, when geological information is almost entirely represented by the drill holes data, creating an accurate 3D geological model of a deposit may not be possible. Thus, the geological model created by the project development team for selection of the mining and processing methods may be inaccurate incorrectly representing geometry or internal structure of the ore body (Fig. 26.1).

There are several stochastic methods allowing to model geometry of the geological domains and their internal structures. One of the most common techniques is truncated Plurigaussian simulation (Armstrong et al. 2011) which is used for stochastic modelling of the sedimentary basins. The technique applies set of multiple thresholds which truncates a simulated Gaussian variable. A similar methodology of truncating a continuous variable by a spatially varying set of thresholds is used by indicator P-field simulation which was proposed for probabilistic modelling of ore lens geometry (Srivastava 2005).

The more complex geological structures can be modelled using conditional simulation method based on multiple point statistics (Strebelle 2002). The method usually referred to as Snesim (Strebelle 2002). It allows to model the highly irregular shapes of the geological domains, including braded channels of the paleo-placer deposits and multiply folded gold lodes.

Use of the fractals methodology is becoming more popular among the resource estimation specialists since powerful computers has become the routine tools in the mining industry. The fractals based simulation is particularly useful for stochastic modelling of a fracture network (Chiles 1988) including the complex geometric patterns of the tectonic faults and the anastomosing shear zones. The technique can also be used for improving delineation of the ore body lenses.

All these methods require good geological knowledge of the deposit including in details understanding of the domain's structure and relationships between rocks. Thus, the techniques are usually applied by geostatistitians in a close collaboration with the geologists, which provide a detailed geological information of the deposit. This is demonstrated in the next sections, where an examples of the indicator assisted domaining and the Plurigaussian simulation are presented.

26.2 Indicator Assisted Domaining

One of the techniques commonly used for construction of the quantitative 3D geological models is a method based on the grade indicators. The technique was initially proposed (Abzalov and Humphreys 2002a, b) for delineating the re-

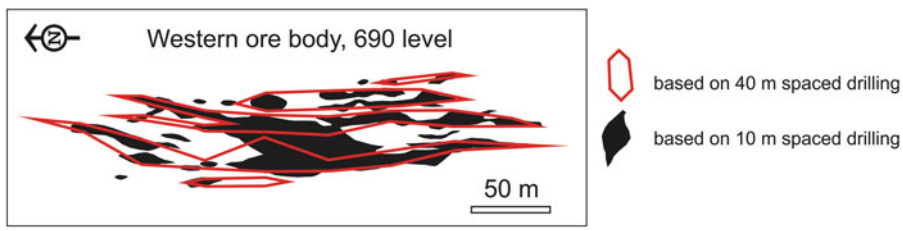

Fig. 26.1 Reserve domains of the CSA mine, Australia outlined at 1 % Cu cut-off from 40 to 10 m spaced drilling (Stegman 2001)

source domains of the structurally complex gold-lodes and stock-works occurring as a mixture of high and low-grade areas intermingled with waste and characterised by complex geometry and poor grade continuity. This type deposits often contain several generations of mineralisation which are characterised by different spatial trends.

The structural complexity of mineralisation together with the heterogeneous nature of the mineralised zones prevents unambiguous application of the conventional deterministic methodology for 3D constraining of the mineralised domains. Therefore it was suggested (Abzalov and Humphreys 2002a, b) to use probabilistic approach for definition domains. The proposed technique defines domains geostatistically using the indicator probability model.

This methodology has been successfully tested on a number of deposits including copper deposits, structurally complex turbidite-hosted gold mineralisation, Ni-sulphide deposits and uranium roll-fronts.

26.2.1 Indicator Probability Model

An indicator probability map is generated by creating the block model of the deposit and estimating the probability of each block grade to exceed the given threshold value (Fig. 26.2). The threshold is usually chosen equal to the lower cut-off boundary of the economic mineralisation. One indicator is usually sufficient to delineate the mineralisation. In case if the mineralisation contains the meaningful high- and low-grade domains they are further subdivided using second indicator, usually chosen at the lower cut-off boundary of the high-grade shoots (Abzalov and Humphreys 2002a). Using more than two indicators is usually impractical as this introduces a substantial risk of over-domaining which can compromise the integrity of the grade distribution.

The spatial distribution of the chosen indicators is modelled by estimating their variograms and the probability of exceeding the given grade threshold is estimated by Ordinary kriging for each modelled block. The key parameters controlling the probabilistically defined structure of the mineralisation are the block size, indicator threshold value, indicator variography parameters and the accepted level of probability to exceed threshold for contouring the high-grade blocks.

The size of the blocks is largely controlled by the drilling density, spatial distribution pattern of the samples and the grade continuity. In general, block size is chosen as equal to half a distance between the drill holes. More accurate assessment of the appropriate block sizes can be made using special geostatistical criteria, such as weight of the mean in the simple kriging system, kriging variance, correlation between the true grade but unknown grade (Z) and the estimated grade (Z*) and the value of the regression slope of Z|Z*.

Spatial distribution of the threshold indicator is further modelled by applying the Ordinary kriging algorithm. The resulting indicator probability map needs to be reviewed and assessed against the distribution patterns of the original assays and the geological interpretation of the mineralised structures. This comparative analysis of the indicator probability map with geological data facilitates the choice of the indicator probability value that (a) has the spatial distribution most consistent with geological interpretation and (b) best fits the spatial distribution pattern of the mineralised domains.

It is obvious that study of the best drilled parts of the mineralised zones provides a less subjective choice of the indicator probability value which is most optimal for definition of the domains. The chosen value can then be used as a threshold to subdivide the whole mineralised zone, including it's poorly tested parts, on the domains.

The probability value chosen as a threshold for domaining of the zone can be different in the various projects as it depends on many factors, including block size, search neighbourhood and the indicator value. In the case presented on the Fig. 26.2 the probability values of 0.2–0.3 for the 1 g/t Au indicator were used to subdivide the gold stock-work of the Meliadine deposit into high- and low-grade domains (Abzalov and Humphreys 2002a).

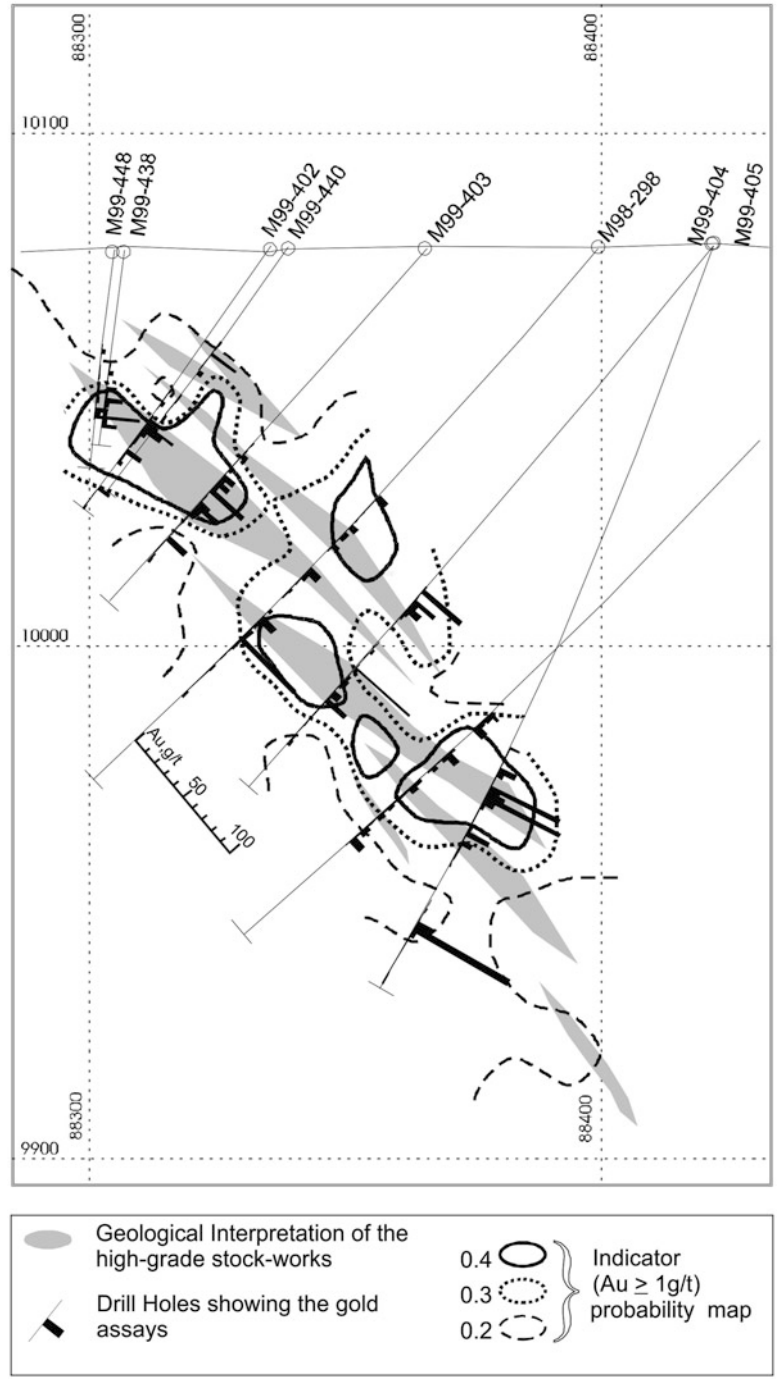

Fig. 26.2 Cross-section of the Meliadine gold deposit, Canada. Geological interpretation of the high-grade shoots and kriged Au > 1 g/t indicator probability contours (Abzalov and Humphreys 2002a,b)

The 3D volume of the domain is obtained by grouping the blocks according to their probability of exceeding the threshold and creating a continuous closed volume (domain) (Fig. 26.3). Application of higher threshold values will lead to over-domaining of mineralisation by generating an excessive amount of small high-grade subzones. Thus, the probability level was chosen

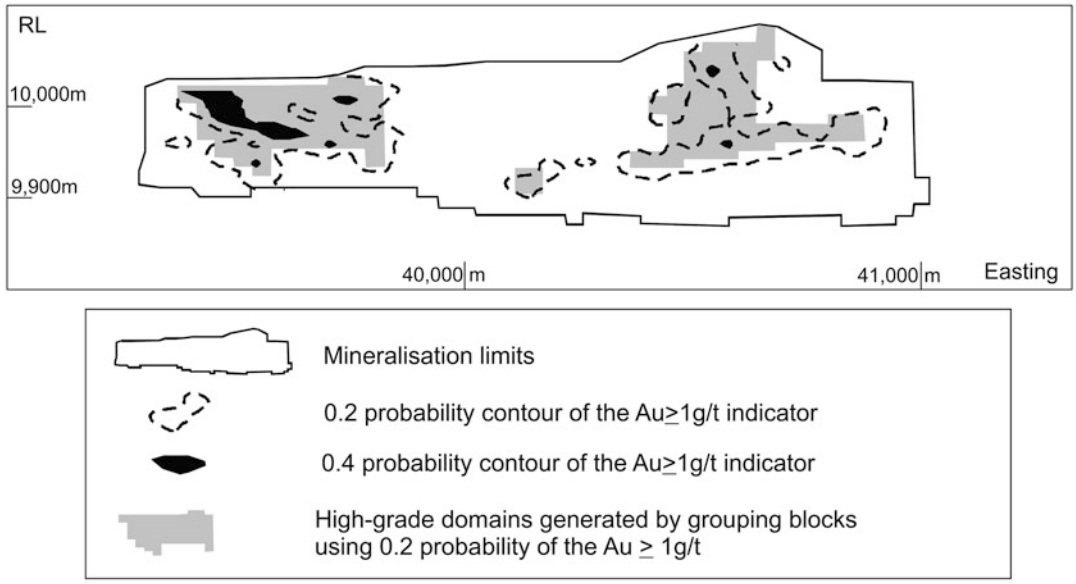

Fig. 26.3 Long-section of the stock-work zone, Meliadine deposit, Canada, showing distribution of geostatistically defined domains (Abzalov and Humphreys 2002a, b)

by fitting to local geological knowledge of the orebody.

26.2.2 Structural Interpretation

The probabilistically defined high-grade areas usually represent irregularly distributed clusters of the blocks that need to be coalesced together to generate the domains. This can be achieved by filling the gaps between the defined blocks using mathematical procedures known as morphological dilation and erosion (Bleines et al. 2013). Degree of the blocks merging should be compliant with the mineralisation style and the structural model of the deposit (Fig. 26.4). In general, the tolerance of one block is sufficient for closing the gaps between the kriged blocks for the most of the studied deposits, which have included gold lodes (Abzalov and Humphreys 2002a), uranium rolls (Abzalov 2010; Abzalov et al. 2014), copper porphyries and the komatiite-hosted nickel-sulphide deposits (Abzalov and Humphreys 2002b).

26.2.3 Boundary Conditions

Boundary conditions need to be imposed on the geostatistically defined domains in a manner similar to those of conventional wireframing. Hard domain boundaries will not permit interpolation of the grades across the boundaries. Soft domain boundaries, including their different versions such as one-way soft boundaries and partly soft boundaries, allow, to various degrees, the data from the other side of the boundary to be used in the grade interpolation. A decision regarding the use of hard or soft boundaries depends on the geological characteristics of mineralisation

26.3 Stochastic Modelling of the Geological Structures

One of the biggest challenges faced by geologist estimating mineral resources is an uncertainty of the geological interpretations. Shape and volume of the ore body can significantly differ depending

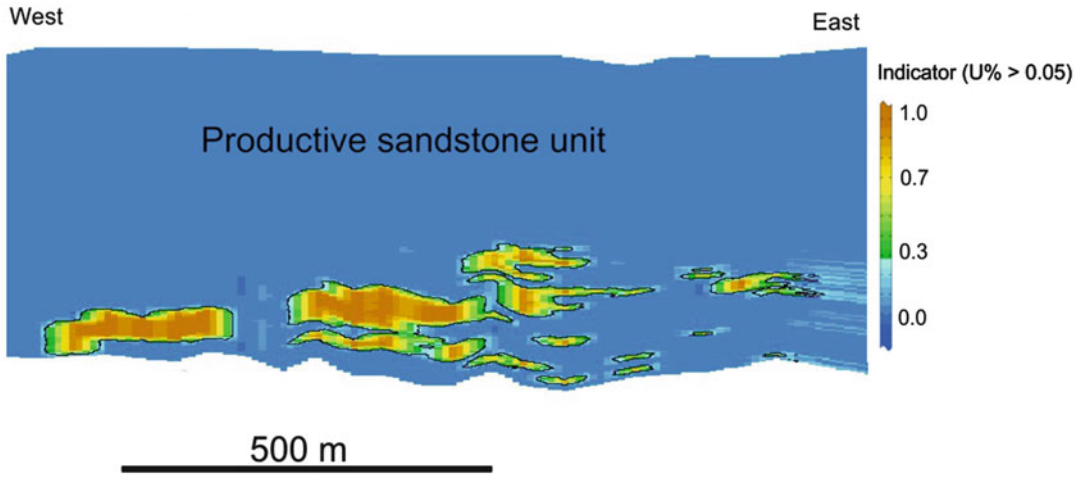

Fig. 26.4 Cross-section of the uranium roll-front generated using indicator assisted domaining approach (Abzalov 2010; Abzalov et al. 2014)

on geological interpretation (Fig. 26.1) resulting in serious errors in the estimated resource tonnages. Srivastava (2005) has emphasised that the failure to incorporate the uncertainty in the shape of the geological domains can lead to a gross underestimation of the uncertainty in the resource estimates. Thus, geologist must quantify the degree of uncertainty of the ore body geometry.

26.3.1 Plurigaussian Conditional Simulation: Case Study

The scope of the study was to create a probabilistic 3D model of the stratigraphic sequence that hosts uranium rolls at the sandstone-type uranium deposit in Kazakhstan (Abzalov 2010; Abzalov et al. 2014). The litho-stratigraphic model was further used for creating a 3D model of the permeability of the host sequence and quantitatively estimating its uncertainty.

Uranium mineralisation at the studied deposit is located at the depth of 500–600 m below surface (Fig. 26.5). It is distributed in the productive unit of the Tertiary age, which is approximately 100–150 m thick and composed by weakly consolidated sands intercalated with gravel and shales. It also contains small lenses of the carbonate rocks, mainly limestone. The productive unit is overlaid by thick sequence of barren sediments of Late Tertiary and Quaternary ages.

Uranium mineralisation is distributed preferably along the footwall contact of the productive unit, denoted as Lower contact on the Fig. 26.5. However, the uranium concentrations do not show any relationship with the rock types (Fig. 26.5).

26.3.1.1 Methodology of Plurigaussian Simulation

Current study uses Plurigaussian (PGS) simulation method (Armstrong et al. 2011) for modelling spatial distribution of the sedimentary rocks (lithotypes) in the productive unit (Fig. 26.5). The PGS method transforms the categorical variables, such as the lithotype numbers into continuous variable. This is made by a series of mathematical transformations, firstly by a Gaussian transformation and, then, generating the indicator variables by applying the thresholds to the Gaussian variables. Construction of the PGS model requires four main components.

1. The ‘Proportions of the lithotypes’. This is a model describing proportions of the different lithotypes forming thesedimentary sequence.

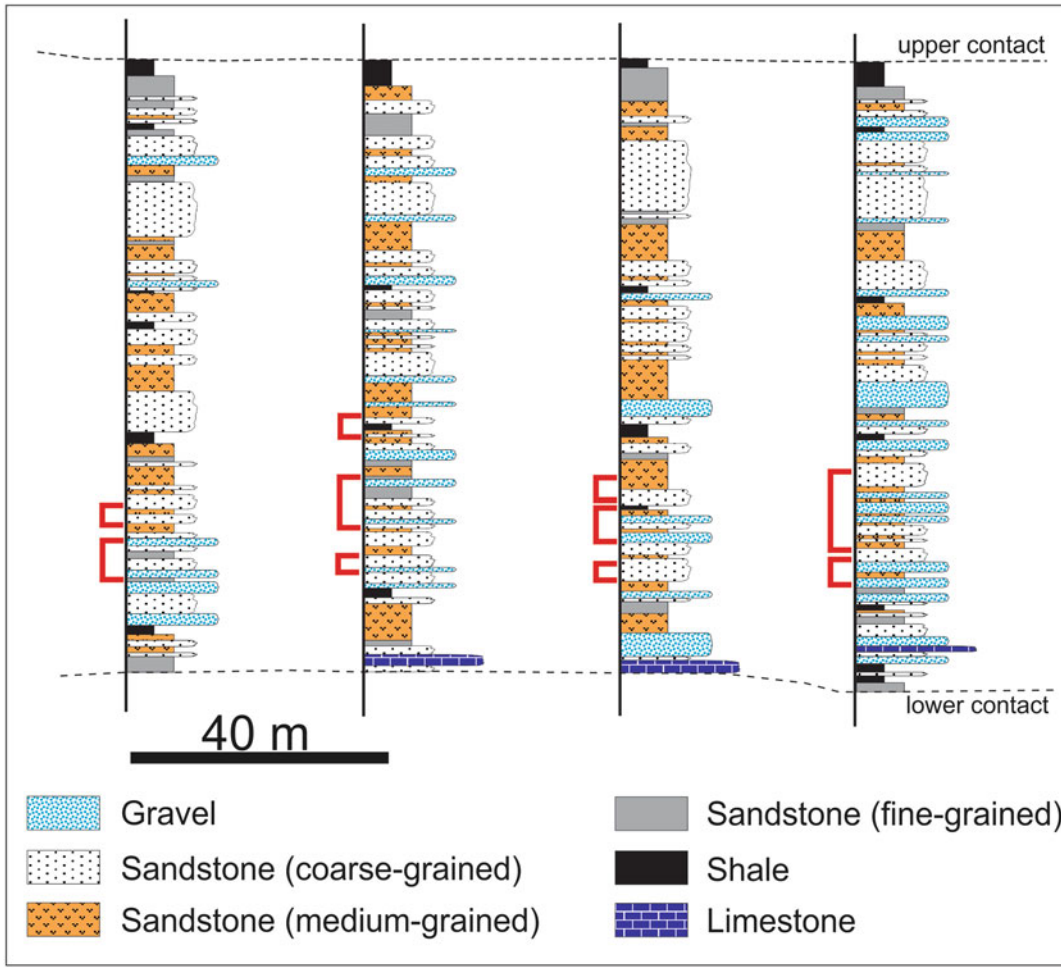

Fig. 26.5 Cross-section of the uranium roll-front deposit showing rock types and uranium grade (*red bars*) (Abzalov 2010; Abzalov et al. 2014)

The proportions are estimated globally for the entire project area and locally, if the proportions changes in the different parts of the project as a result of geological zoning;

2. The 'Lithotype rule'. This is a model describing the geological relationships between lithotypes, such as sequence of the lithotypes distribution, stratigraphic contacts, cross-cutting relationships;
3. The variogram models of the underlying Gaussian functions. The variograms quantify spatial relationships between lithotypes, in particular a degree of the spatial continuity of the lithotypes. The model controls dimensions and the shapes of the simulated lithotypes;
4. The thresholds which applied for truncating the estimated Gaussian variable. The truncating procedure allows to back-transform the Gaussian variable into lithotypes. The thresholds are deduced from the lithotype proportions in the drill holes.

The PGS model uses Upper and Lower contacts (Fig. 26.5) which were created before the PGS simulation has started and needed for constraining the PGS model's top and bottom.

26.3.1.2 Estimating of the Lithotypes Proportions

Proportions of the lithotypes were estimated for each drill hole (Fig. 26.6). Using this data the global proportion curve was estimated for the entire project (Fig. 26.7).

Distribution of the lithotypes on the global proportion curve (Fig. 26.7) shows that proportion of conglomerates is higher in the lower part of the unit. It is highest, approximately 0.25 of the total thickness, in the narrow interval from the Lower contact to approximately 30 m above it, after that proportion of conglomerates gradually decreases. Proportions of the coarse-grained sandstones change periodically suggesting that productive unit can be subdivided on 4 sub-units, representing sedimentary cycles (Fig. 26.7). Sub-units 1 and 2 can be combined into lower member (U-1) of the Productive unit, and sub-units 3 and 4 are combined into upper member (U-2) (Fig. 26.7).

However, review of the lithotype proportions by the drill holes (Fig. 26.6) clearly shows their non-stationary distribution. In particular, fine grained sands are more common in the northern part of the deposit and shales are more common in the southern part. In the non-stationary geological environments the global proportion curve shown on the Fig. 26.7 can not be used for modelling of the spatial distribution of the lithotypes. To overcome the problem of non-stationarity the study area is subdivided onto stationary domains and the vertical lithotype proportion curves have been calculated for each domain.

The proportions were averaged by estimating them into the large blocks (panels) of 500×350 m (Fig. 26.8). The map of the estimated by kriging lithotypes clearly shows spatial trends of the lithotype proportions. The differences of the proportion curves of the panels reflect zoned distribution of the lithotypes. However, the main stratigraphic boundary diagnosed on the global proportion curve (Fig. 26.7), which subdivides the productive unit onto U-1 and U-2 members, can also be observed on the diagrams of the panels (Fig. 26.8).

26.3.1.3 Applying of the 'Lithotype Rule'

'Lithotype rule' is a stratigraphic model summarising relationships between the rock types. The chosen rule should meet three criteria:

- the chosen model should meet the relationships between rocks observed in the drill holes (Fig. 26.5);
- the frequency of the contacts between lithotypes, estimated along the drill hole lines (Table 26.1), should be honoured by the chosen 'lithotype rule';
- the chosen 'Lithotype rule' should be consistent with the Plurigaussian variograms. Therefore 'Lithotype rule' is chosen and optimised iteratively by changing the distribution pattern of the lithotypes and testing it by estimating the Plurigaussian variograms.

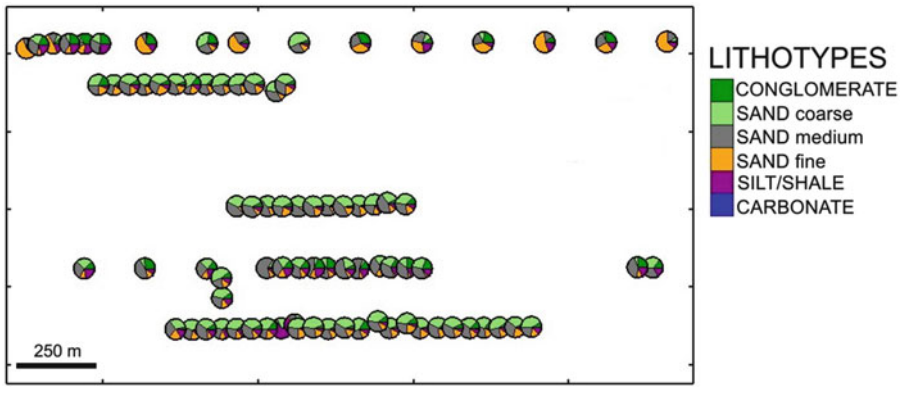

Fig. 26.6 Proportion of the lithotypes estimated by the drill holes

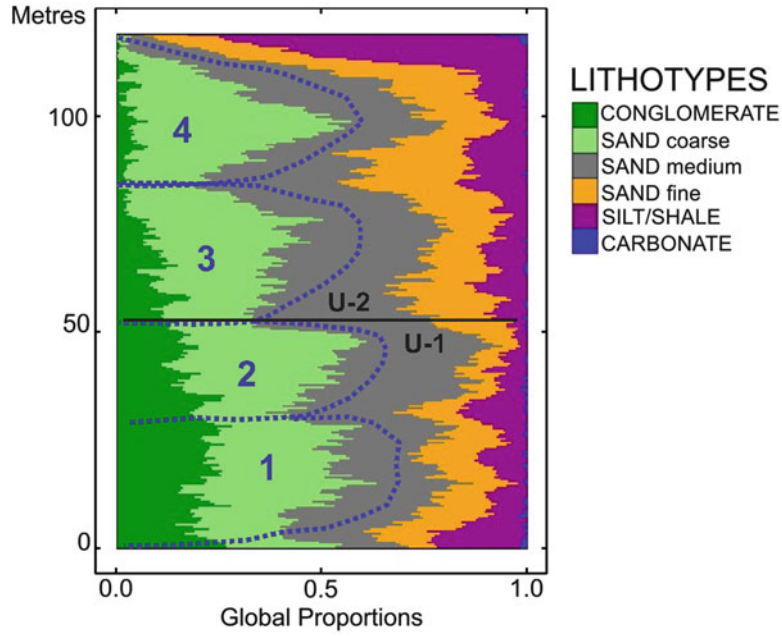

Fig. 26.7 Global proportion of the lithotypes

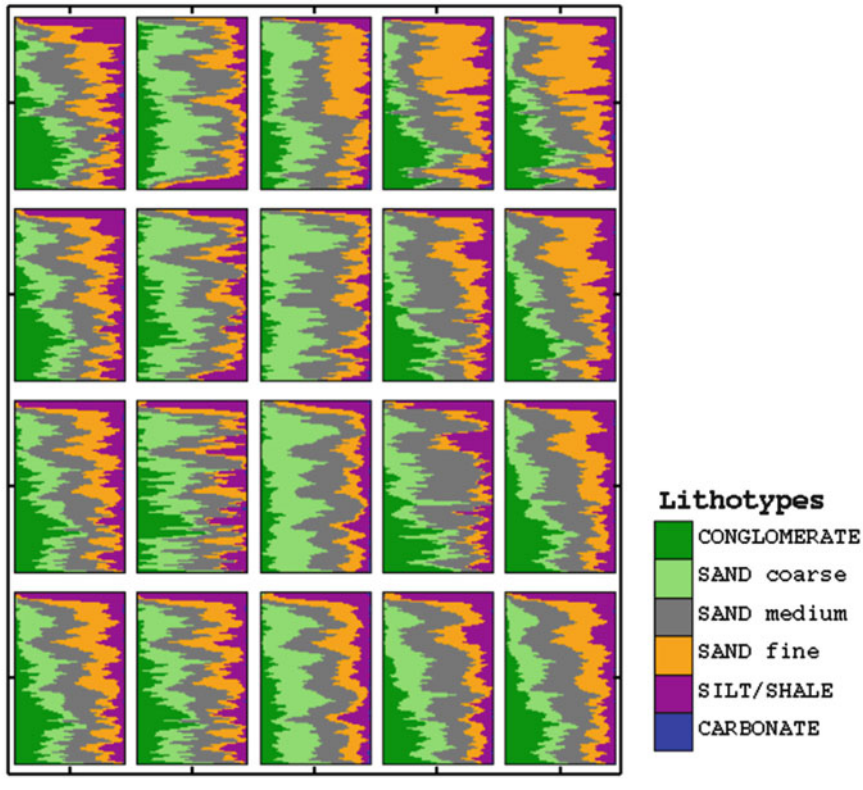

Fig. 26.8 Map showing lithotype proportions estimated by the panels of 500(X) × 350(Y) m

Table 26.1 Transition matrix showing relationships between lithotypes calculated along the drill holes

Downward probability matrix							
	Number	L1	L2	L3	L4	L5	L6
L1	2343	0.708	0.101	0.109	0.050	0.029	0.004
L2	5623	0.053	0.769	0.114	0.042	0.020	0.001
L3	6144	0.042	0.117	0.757	0.055	0.028	0.001
L4	3226	0.031	0.087	0.118	0.710	0.051	0.002
L5	2466	0.020	0.031	0.090	0.094	0.764	0.001
L6	41	0.073	0.098	0.146	0.171	0.439	0.073
Upward probability matrix							
	Number	L1	L2	L3	L4	L5	L6
L1	2366	0.701	0.126	0.109	0.043	0.021	0.001
L2	5643	0.042	0.767	0.127	0.050	0.013	0.001
L3	6156	0.041	0.104	0.756	0.062	0.036	0.001
L4	3223	0.036	0.074	0.105	0.711	0.072	0.002
L5	2420	0.028	0.048	0.070	0.068	0.779	0.007
L6	35	0.257	0.200	0.171	0.229	0.057	0.086

Explanation: *L1* conglomerate, *L2* coarse grained sandstone, *L3* medium grained sandstone, *L4* file grained sandstone, *L5* siltstone, *L6* carbonate

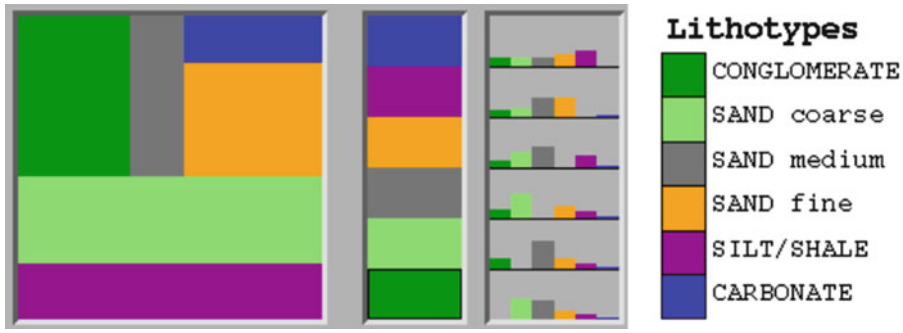

Fig. 26.9 Stratigraphic model ('lithotype rule') describing relationships between rock types in the productive unit of the project

Final 'lithotype rule' which was chosen and optimised using the three criteria is shown on the Fig. 26.9.

26.3.1.4 Plurigaussian Variograms

Plurigaussian variograms have been calculated for two Gaussian functions, by applying search parameters summarised in the Table 26.2. Estimated experimental variograms and their models are shown on the Figs. 26.10 and 26.11 and the model parameters are summarised in the Table 26.3.

Table 26.2 Calculation parameters of the Plurigaussian variograms

	N00	N90	Vertical
Lag	250	75	0.5
Number of lags	20	20	50
Angular tolerance	45	45	10

26.3.1.5 Results and Discussion

Ten equiprobable realisations of the Plurigaussian model have been created. Each of the realisations represents equiprobable model of distri-

bution the rock types in the productive unit. Three of the simulated realisations are shown on the Fig. 26.12.

The model realistically conveys the complex and highly irregular intercalations of the different sedimentary rocks. Stratigraphic sequence generated by Plurigaussian method accords well with relationships between sedimentary rocks observed in the drill holes.

Patterns of the rock distributions differ in the different realisations (Fig. 26.12) are indicative of a degree of uncertainty in the lithotype model which increases in the less drilled parts of the deposit. The high variability of the host sedimentary sequence clearly shows that deterministic interpretation of the cross-sections, commonly used by geologists, is suboptimal approach because the interpreted cross-sections are overly simplistic and don't show the actual complexity of the sedimentary sequences that host uranium mineralisation.

Uncertainty of the stratigraphic model is estimated by statistical analysis of the Plurigaussian simulation results (Fig. 26.12).

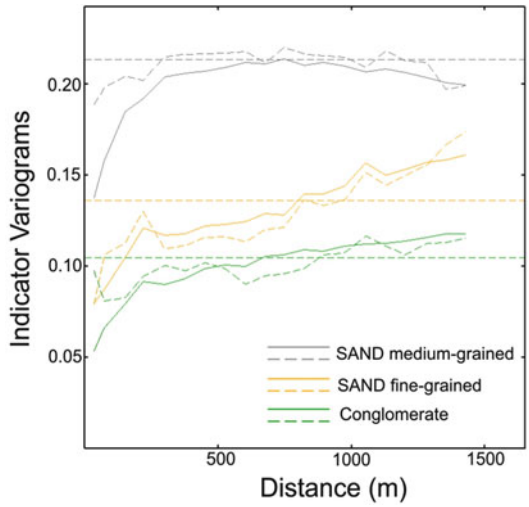

Fig. 26.10 Variograms of the Indicators of Gaussian function #1 calculated horizontally along the N90 direction

Table 26.3 Models of the Gaussian variograms

Function	Model	Sill	N00	N90	Vertical
Gaussian #1	Exponential	1	400	400	7
Gaussian #2	Cubic	0.3	50	50	4.5
	Spherical	0.7	300	300	15

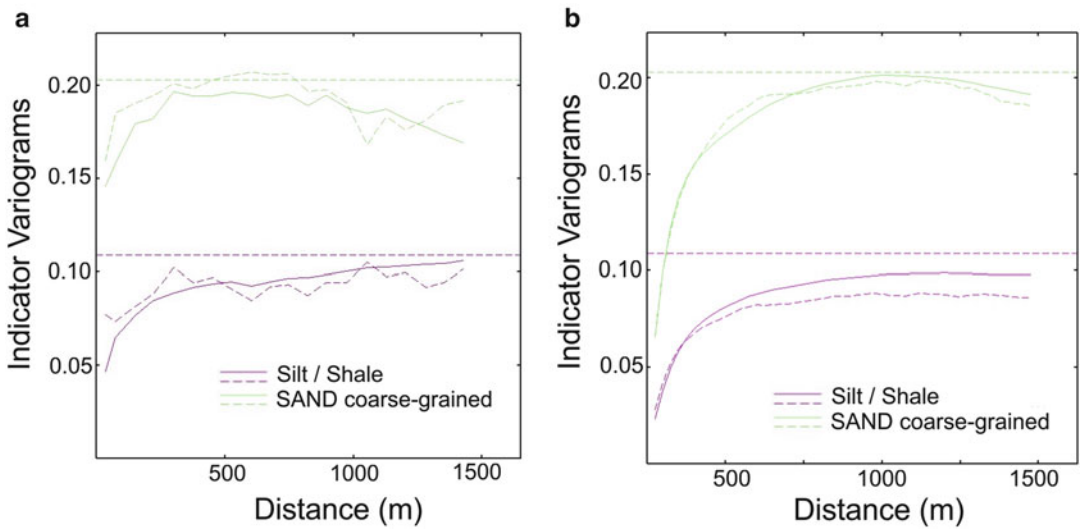

Fig. 26.11 Variograms of the Indicators of Gaussian function #2 calculated (**a**) horizontally along the N90 direction and (**b**) vertically

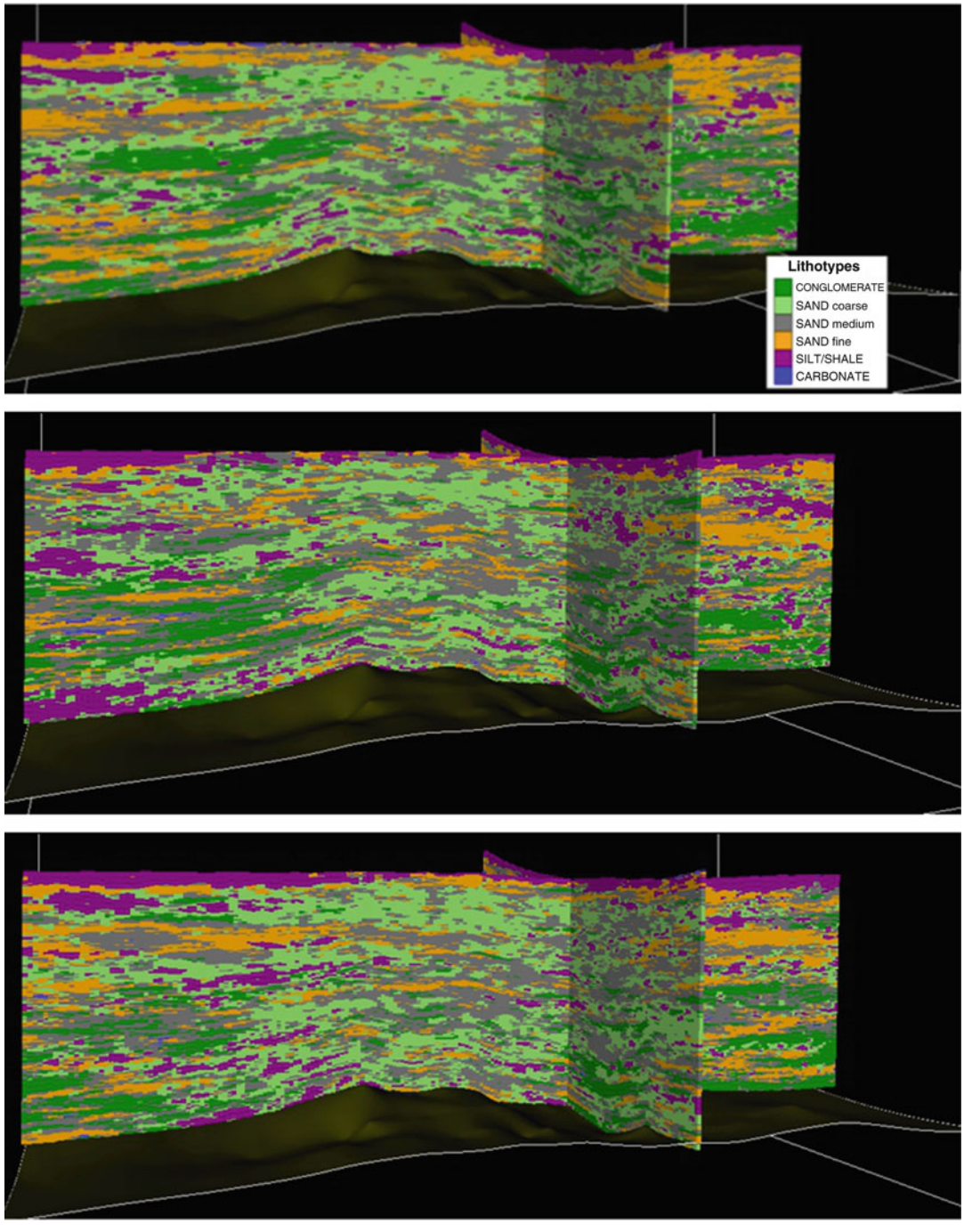

Fig. 26.12 Three interpretations of the sedimentary sequence distributed in the Productive unit representing equiprobable realisations (#1, #3 and #6) of the Plurigaussian model

References

Abzalov MZ (2010) Optimisation of ISL resource models by incorporating algorithms for quantification risks: geostatistical approach. In: Technical meeting on in situ leach (ISL) uranium mining. International Atomic Energy Agency (IAEA), Vienna, Austria, 7–10 June, 2010

Abzalov MZ, Humphreys M (2002a) Resource estimation of structurally complex and discontinuous mineralisation using non-linear geostatistics: case study of a mesothermal gold deposit in northern Canada. Exp Min Geol J 11(1–4):19–29

Abzalov MZ, Humphreys M (2002b) Geostatistically assisted domaining of structurally complex mineralisation: method and case studies. Geostatistically assisted domaining of structurally complex mineralisation: method and case studies. In: The AusIMM 2002 conference: 150 years of mining, Publication series No 6/02, pp 345–350

Abzalov MZ, Drobov SR, Gorbatenko O, Vershkov AF, Bertoli O, Renard D, Beucher H (2014) Resource estimation of *in-situ* leach uranium projects. Appl Earth Sci 123(2):71–85

Armstrong M, Galli A, Beucher H, Le Loc'h G, Renard D, Doligez B, Eschard R, Geffroy F (2011) Plurigaussian simulation in geosciences, 2nd edn. Springer, Berlin, p 149

Bleines C, Bourges M, Deraisme J, Geffroy F, Jeanne N, Lemarchand O, Perseval S, Poisson J, Rambert F, Renard D, Touffait Y, Wagner L (2013) ISATIS software. Geovariances, Ecole des Mines de Paris, Paris

Chiles J-P (1988) Fractals and geostatistical methods for modelling of a fracture network. Math Geol 20(6):631–654

Srivastava RM (2005) Probabilistic modelling of ore lens geometry: an alternative to deterministic wireframes. Math Geol 37(5):513–544

Stegman CL (2001) How domain envelopes impact on the resource estimate – case studies from the Cobar gold filed, NSW, Australia. In: Edwards AC (ed) Mineral resource and ore reserves estimation – the AusIMM guide to good practice. AusIMM, Melbourne, pp 221–236

Strebelle S (2002) Conditional simulation of complex geological structures using multiple-point statistics. Math Geol 34(1):1–22

Part VI

Classification

Principles of Classification 27

Abstract

Technical and economic evaluation of the mining projects requires classification of the mineralisation into mineral resources and ore reserves. These two classes of estimated mineral endowment differ by the relevance to the actual mine plans. Mineral resources are estimated mainly using geoscientific information with a limited amount of the technical studies. The ore reserves, on the contrary to mineral resources, are derived from the mine designs or mine plans and require rigorous technical and economic analysis of the mining project. Both classes are subdivided onto several categories by the confidence of the estimate.

Keywords

Mineral resource • Ore reserve

27.1 International Reporting Systems

Necessity for international reporting systems have been recognised in early 1970s when investors in the mining industry have become greatly concerned that lacking of the reporting standards causes multibillion losses.

In 1971 the Joint Ore Reserves Committee (JORC) was established in Australia and in 1989 the JORC Code was first published. Since 1989 the JORC Code has been incorporated into the Listing Rules of the Australian and New Zealand Stock Exchanges, making compliance mandatory for publically listed companies in Australia and New Zealand.

Similar reporting systems have been created in South Africa (SAMREC Code), Canada (NI 43–101) and other countries.

27.2 Mineral Resources and Ore Reserves

Fundamental principle of the proposed reporting systems is subdivision of the mineral endowment into three types: exploration results, mineral resources and ore reserves, which reflects the details of exploration and depth of the technical and economic evaluation of the mining project. Classification principles are presented on the Fig. 27.1 which sets a framework for classifying tonnage and grade estimates into the different categories

M. Abzalov, *Applied Mining Geology*, Modern Approaches in Solid Earth Sciences 12,
DOI 10.1007/978-3-319-39264-6_27

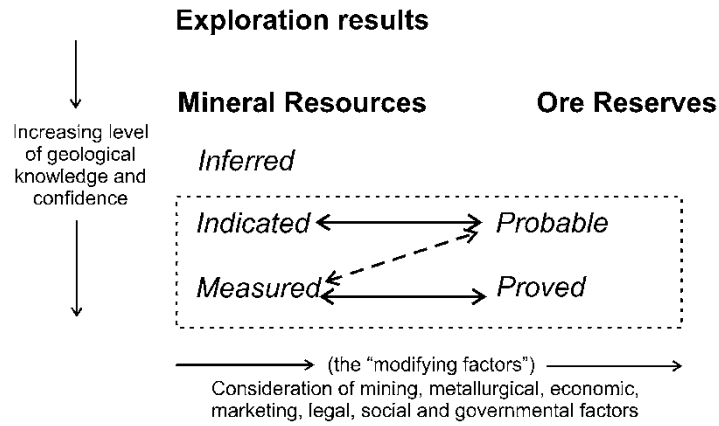

Fig. 27.1 General relation between exploration results, mineral resources and ore reserves (JORC 2012)

of the mineral resources and ore reserves reflecting the different degrees in the estimation confidence and the different levels of technical and economic evaluation studies.

At the early stage of exploration the generated data are insufficient for estimation of mineral resources and ore reserves however it might be of use to investors therefore it is reported as 'Exploration Results'. These usually include results of outcrop sampling, assays of drill hole intersections, geochemical exploration data and geophysical survey results. In general, if a company reports the 'Exploration Results' then estimates of tonnages and average grade usually are not assigned to the mineralisation. Alternatively, if the company has chosen to discuss and report the 'Exploration Results' in terms of a size of the exploration target it should be quoted as a range of tonnes and a range of grade (JORC 2012).

When exploration matures the more data becomes available for estimation allowing to classify the mineral endowment as mineral resource and ore reserves.

Clause 20 of the JORC Code (2012) defines the 'Mineral Resources' as follows:

- "A Mineral Resource is a concentration or occurrence of solid material of economic interest in or on the Earth's crust in such form, grade (or quality), and quantity that there are reasonable prospects for eventual economic extraction. The location, quantity, grade (or quality), continuity and other geological characteristics of a mineral resource are known, estimated or interpreted from specific geological evidence and knowledge, including sampling. Mineral resources are sub-divided, in order of increasing geological confidence, into Inferred, Indicated and Measured categories".

Thus, subdivision of the resources onto categories reflects a confidence in the estimated tonnage and grade of the mineralisation and also depends on a reliability of the geological interpretations.

Not all mineralisation estimated and classified as a mineral resource can be mined (Fig. 27.2). Some parts of the mineralised bodies are not recovered, representing the mining losses, and at the same time the recovered mineralisation is commonly diluted therefore grade of the recovered ore differs from the corresponding them mineral resources. Thus, tonnage and grade of the ore reserves are estimated by correcting the mineral resources for mining dilution and losses. Application of dilution factor to the recovered ore and estimation of the mining losses require good understanding of a spatial distribution of mineralisation therefore only Measured and Indicated resources can be converted to reserves (Fig. 27.1).

Degree of the resource dilution and the mining losses depends on selectivity of the mining method used. The higher selectivity of a mining method the better recovery of the resources is achieved with a minimal dilution rates. This is

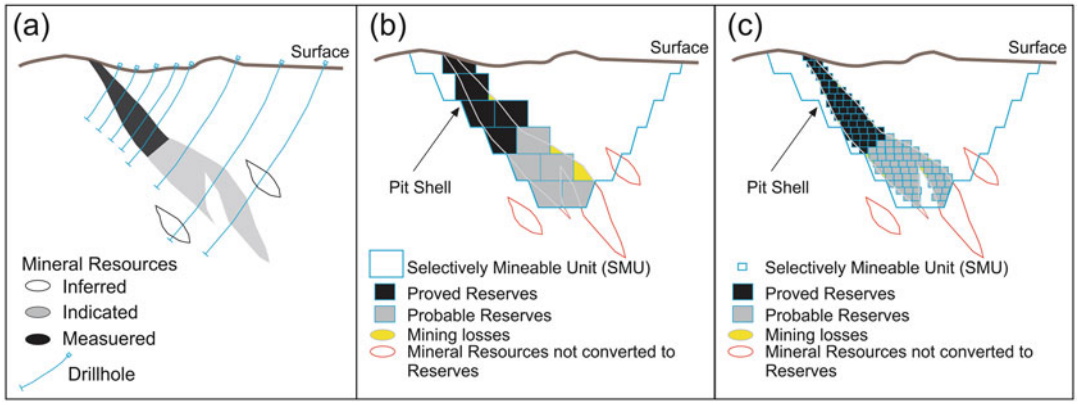

Fig. 27.2 Sketch showing impact of the mining selectivity onto the ore reserves: (**a**) mineral resource model; (**b**) ore reserves corresponding to non-selective mining; (**c**) ore reserves corresponding to a highly-selective mining

schematically shown on the Fig. 27.2, presenting two different ore reserves models (Fig. 27.2b, c) generated from a single resource model. In both cases the pit shell is the same therefore the ore reserves are obtained from the same part of the resource model falling into the proposed open pit (Fig. 27.2b, c). However, the obtained reserve models are different suggesting the different tonnage and grade of the ore reserves (Fig. 27.2b, c). The differences are caused by the different mining selectivity of the two compared method. First case, shown on the Fig. 27.2b, assumes a relatively non-selective bulk mining option. Second case, shown on the Fig. 27.2c, is, on a contrary, presents a highly selective mining method. Because of the different size of their corresponding SMU blocks geometry of the ore reserve models is different indicating for different tonnage and grade of the reserves. Thus, estimation and reporting of the ore reserves should be made in a strict accordance with the proposed mining method and accurately estimated size of the SMU blocks (Fig. 27.2b, c).

Resources falling outside of the pit shells are not be converted to the reserves because they are not economically mineable at the economic and technical parameters used for construction the pit models (Fig. 27.2). However, these are still can be reported as mineral resource in case if they pass the requirement for "reasonable prospects for eventual economic extraction" (JORC 2012). The same is related to Inferred resources which can not be converted to ore reserves because of a low confidence in their tonnage and grade.

In addition to adding the mining losses and the grade dilution conversion of the resources to reserves should also include all possible constraints that can be imposed by the metallurgical technologies and also legal, environmental, social and marketing factors (Fig. 27.1). Thus, the ore reserve is a part of the mineral resources which can be economically mined in a given economic environment and under all other constraining factors. Definition of the ore reserve proposed by the JORC Code (2012) is as follows:

- "An Ore Reserve is the economically mineable part of a Measured and/or Indicated Mineral Resource. It includes diluting materials and allowances for losses, which may occur when the material is mined or extracted and is defined by studies at pre-feasibility or feasibility level as appropriate that include application of Modifying Factors. Such studies demonstrate that, at the time of reporting, extraction could reasonably be justified. The reference point at which Reserves are defined, usually the point where the ore is delivered to the processing plant, must be stated. It is important that,

in all situations where the reference point is different, such as for a saleable product, a clarifying statement is included to ensure that the reader is fully informed as to what is being reported".

Reference

JORC Code (2012) Australaisian code for reporting of exploration results, mineral resources and ore reserves. AusIMM, Melbourne, p 44

Methodology of the Mineral Resource Classification

28

Abstract

The quantitative classification techniques are based on geostatistically quantified uncertainties in the estimated resource and reserve values. This should include estimation of the uncertainties in grade, volume (which is largely controlled by the geological interpretation and constraints), samples quality and tonnage factor. The quantitative classification methods were traditionally focused on the grades estimation uncertainties which are discussed in this chapter. The most commonly used methods include estimation variance approximately estimated using auxiliary geostatistical functions (e.g. F-function) and empirically estimated resource uncertainties, obtained using conditional simulation methods. The most efficient way of using the estimation errors for classification resources is by relating them to the production rates, including the annual, quarterly and monthly productions.

These methods allow to quantify the quality of the estimate but doesn't address issues such as the data quality and robustness of the underlying geological model. If there are any significant uncertainties in either of these two items then the final classification should reflect this.

Keywords

Mineral resource • Ore reserve • Geostatistics • Gove mine

28.1 Geostatistical Classification Methods

International reporting systems set the classification frameworks, however do not specify the procedures and methodology of classification (JORC 2012). As a consequence, the classification techniques currently used in industry vary widely depending on experience of the specialists responsible for classification. Traditional classification approaches, such as a distance to the nearest sample or number of samples in the search neighbourhood, are qualitative and based on subjectively chosen classification criteria, therefore rational of resource classification is ill defined. The limitation of the conventional classification principles is recognised by the modern report-

M. Abzalov, *Applied Mining Geology*, Modern Approaches in Solid Earth Sciences 12,
DOI 10.1007/978-3-319-39264-6_28

ing systems which, although don't specify the definition of the levels of confidence, encourage use of quantitative geostatistical criteria for non-subjective and consistent definition of the resource categories (JORC 2012).

The geostatistical approach of the resource classification was used since 1970s (Royle 1977; Dielhl and David 1982) and has become in particular common in 2000s (Blackwell 1998; Arik 1999; Sinclair and Blackwell 2000; Snowden 2001; Schofield 2001; Dimitrakopoulos 2002; Abzalov and Bower 2009; Abzalov 2010). Using of the geostatistical criteria allows to obtain a quantitative measure of the resource estimation uncertainty which are used to define the resource category.

There are many different geostatistical methods which have been used for classification resources and reserves which differ by degree of rigour of the geostatistical studies. Commonly used geostatistical criteria of the resource classification are as follows:

- Kriging variance (Royle 1977; Blackwell 1998);
- Various mathematical formulas combining several geostatistical parameters (Krige 1996; Arik 1999; Snowden 2001);
- Estimation variance of the mining stopes obtained using conditional simulation (Dimitrakopoulos 2002);
- Probability that mining stope grade exceeds the certain threshold (Davis 1992; Schofield 2001; Dimitrakopoulos 2002);
- Geostatistical auxiliary functions (Annels 1991);
- Classification relating resource uncertainty to the mine production plan.

At present there is no single and universally accepted methodology for estimating a resource uncertainty and there is no agreement between specialists regarding what classification criteria and levels of precision error to use for definition of the resource categories. In particular, Royle (1977) has suggested to classify resources according to estimation precision of the single kriged blocks. Alternative approach advocated by many practitioners (Dielhl and David 1982; Davis 1992), suggest to classify the resource categories by applying geostatistical criteria to the large panels representing the several months of production.

Level of acceptable precision errors used for classification resources and reserves also differ. Thus, Diehl and David (1982) have suggested to use different levels of errors for the different categories. They use +/−10 % as error tolerance for proved reserves, +/−20 % for probable, +/−40 % for Indicated resources and +/−60 % for Inferred. Alternative approach is to use the same level of error for all categories but differentiate them by the size of the estimated panels (Davis 1992). This approach has evolved into the classification technique which relates the resource uncertainty with the mine production plans.

28.2 Classification Related to the Mine Production Plans

This approach was developed in late 1990s (M.Belanger, personal communication) and currently it is one of the most commonly used methods of resource classification. The technique relates the resource categories to the mine production plans and as a consequence the defined categories of the resources and reserves are customised to the technical and economic characteristics of the studied project. This approach has advantage in comparison with more general classification systems because it allows to quantify the resource and reserve uncertainties specifically for the given project.

28.2.1 Classification Criteria

Underlying principle of the method is quantification of uncertainties in estimated tonnage and grade of the ore blocks which size is determined from the mine production plans. Most commonly these are annual and quarterly production volumes which are used as the reference points for classification resources into Indicated and Measured resources. Classification using this method is made at several steps (Abzalov and Bower 2009).

1. Deposit is subdivided on the blocks (panels) matching the annual and quarterly production plans of the mine.
2. Next step is to create the data sets distributed following the grids proposed for resource definition. These sets can be sampled from available drill holes, if their distribution is tighter then the smallest grid proposed for definition resources. However, in practice distribution of the exploration drill holes is too broad and not suitable for subsampling therefore sets of experimental data are usually created using conditional simulation of the drill holes and sampling one of the realisations.
3. Conditional simulation models of the deposit are generated for each generated sets of data. The models usually include 30–50 realisations and should cover entire deposit or, at least, its representative part including several years of production. However, in some cases a good result can be obtained using only 10 realisations in the model (Rossi and Camacho 2004). The number of simulated realisations in a model is mostly a practical consideration, representing a compromise between the level of details to which the uncertainty model should be estimated, from one side, and the time and budget constrains for the project, from another.
4. Point model results of conditional simulation are grouped into the delineated panels and the average panel grades are estimated for each realisations separately.
5. Estimation uncertainty is deduced for every studied drill grid by statistical analysis of the simulated panel grades and tonnages.
6. An optimal resource definition grids are chosen by comparing obtained errors with the classification thresholds. Most commonly used classification criteria are as follows:

   (a) mineralisation is defined as Measured resource if the volume of the deposit, representing the quarterly production (3 months), is estimated with an error ±15 % at the 90 % confidence level

   (b) Indicated resources include mineralisation corresponding to the annual production plan and estimated with precision of ±15 % (or ±30 %) at the 90 % confidence level.

This methodology was tested at the different mining projects encompassing different commodities and mineralisation types (Abzalov and Bower 2009; Abzalov 2010, 2013). In general, the methodology was found robust and suitable to provide non-subjective classification of the mineral resources and ore reserves customising it to technical and economic characteristics of the studied project. However, the tests have also revealed that the classification parameters can vary at the different projects. For example, the Measured resources can be defined using the volume of the deposit representing 1 month of the mine production (Rocky's Reward, Australia).

The level of the estimation uncertainty which is used as a threshold for classification resources also varies. For example, at the bauxite deposits in Australia, threshold for classification is ±10 % at the 95 % confidence level (i.e., 2 standard deviations) (Abzalov and Bower 2014). In general, using +/−15 % error can be too loose because profit margin of the mining operations is rarely exceeding 15 % and in many operations is less then it.

Tolerance of plants to variation of metal grades and deleterious components usually varies within the range of 10–20 % (Abzalov and Mazzoni 2004) therefore definition reserves with +/−15 % error imposes risk that significant portion of the mineralisation will be sterilised and excluded from reserves, like it happened at Phosphate Hill operation of the WMC Resources.

Even larger uncertainty exists regarding the criteria of definition of the Inferred resources, which are commonly defined without considering their relevance to a project's characteristics. The current author suggests an alternative approach which relates Inferred resources to the project economics. It is suggested that a minimum amount of a greenfield project's resources should not be less than that needed to payback

the capital cost. At the early stages of the project evaluation the accurate estimates of the project costs and the mine production rates are not available therefore these parameters are usually inferred from another project exploiting a similar type of the deposit.

Level of acceptable precision error should be deduced from the estimated profit margin. In the highly profitable projects the tolerance to the error is larger than at the operations where head grade of the mined ore is close to the break-even grade. However, an error of +/−15 % estimated with a confidence of 95 % (2 standard deviations) can be used as a default threshold for definition of the Inferred resources if more accurately determined levels of the acceptable errors are not available. This approach was implemented for classification Inferred resources at the Australian bauxite deposits (Abzalov and Bower 2014) and at the CJUP deposit in Jordan (Abzalov et al. 2015).

28.2.2 Classification Procedures

Procedures of resource classification by relating the estimation errors to mine production rates are explained in this section of the book using as an example a case study carried at Gove bauxite deposit and supporting it by the similar studies undertaken at the Weipa deposit in Australia (Abzalov and Bower 2009, 2014).

The Gove deposit is located on the Gove peninsula close to the coast of the Gulf of Carpentaria (Fig. 28.1). It was explored during 1955–1968 and mined from 1971 until present. Continuing exploration have evoked a necessity to review the validity of the drill grids currently used at the Gove plateaus for definition bauxite resources. The was made using the methodology of classification relating the resource uncertainty to the production plans and was based on a representative part of the deposit chosen as a special study area (Fig. 28.1).

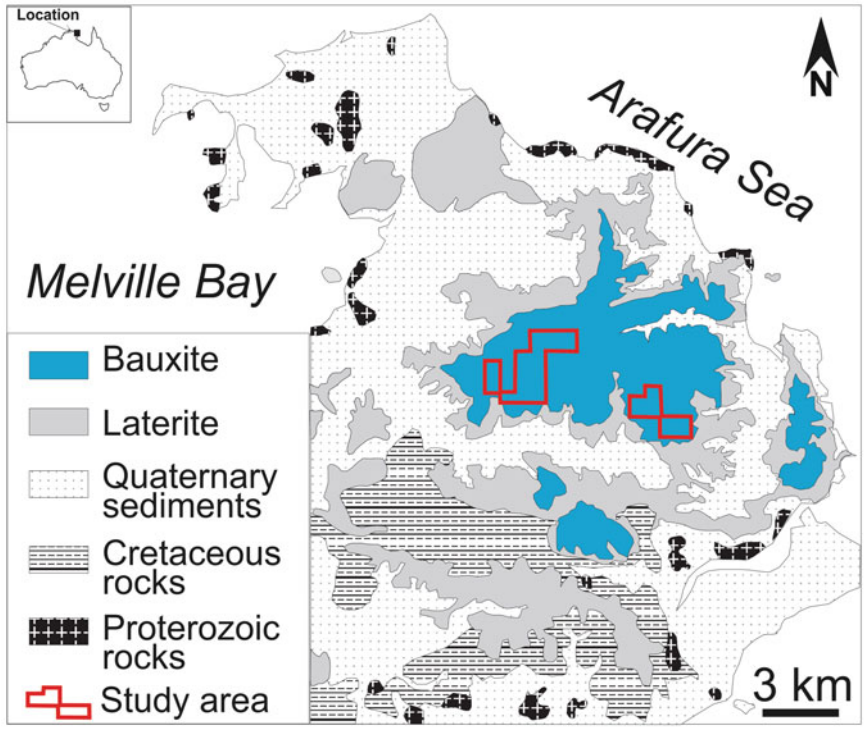

Fig. 28.1 Geological map of the Gove deposit (generalised after Ferenczi 2001) showing the study areas chosen for definition of the resource categories

The study area was subdivided onto panels, representing annual, quarterly and monthly production volumes. It contains 21 annual production blocks, 69 blocks matching to the quarterly production plans and 185 blocks each equal to the monthly production plans.

The study area was systematically drilled following the grid of 50 × 50 m. This drill holes database was sampled in order to create the experimental sets of data. In total six grids were created by sampling the exploration database, this includes 50×50, 70×70. 100×100, 150×150, 200×200 and 300×300 m.

One more grid, 20×20 m, was needed to estimate uncertainties of the blocks equal to the monthly production volumes. This grid is smaller then actual spacing between drill holes, which is approximately 50×50 m, therefore the experimental set of 20×20 m had to be created using conditional simulation techniques (Abzalov and Bower 2009). This was made by applying Sequential Gaussian (SGS) conditional simulation methodology in order to model drill hole data to the grid of 20×20 m and choosing a single realisation of this model which was used as an experimental data set.

Two grade variables have been chosen for estimation of the resource uncertainty, Al_2O_3 and SiO_2. Seven SGS models of the deposit have been created for each variable, each corresponding to one of the chosen data grids. The models include 15 equiprobable realisations built on the grid of $10 \times 10 \times 0.5$ m (Fig. 28.2). This grid produces a model characterised by a quasi-point support and therefore the SGS results can be grouped to the larger blocks, including mine stopes, pit benches, and any other volumes of interest. In our case, these are the panels matching to the mine production plans, annual, quarterly and monthly. Examples of the SGS realisations grouped to the panels of $230 \times 450 \times 3.5$ m which are equal to the monthly production volumes are shown on the Fig. 28.3.

Thus, every realisation of the SGS model creates one estimate of the panels grade. In total, 15 values were obtained for each panel. These values are equiprobable and therefore can be used for statistical quantification of the panels' grade uncertainties.

The uncertainty (estimation error) is usually estimated as a relative variance of the grade values (28.2.1) or as coefficient of variation (COV) expressed as percentage (28.2.2). The latter estimate is more convenient because the value of 2COV quantifies the error with a confidence level of 95 % (Abzalov 2008; Abzalov and Bower 2009).

$$\text{Relative Variance} = \frac{\text{Variace of the Block Grade}}{(\text{Mean Grade})^2} \tag{28.2.1}$$

Fig. 28.2 Two equiprobable realisations (#01 and #15) of the SGS model showing spatial distribution of the SiO_2 (%) grade. The model was built using the data distributed as 200×200 m grid which were interpolated to the quasi-point grid of $10 \times 10 \times 0.5$ m

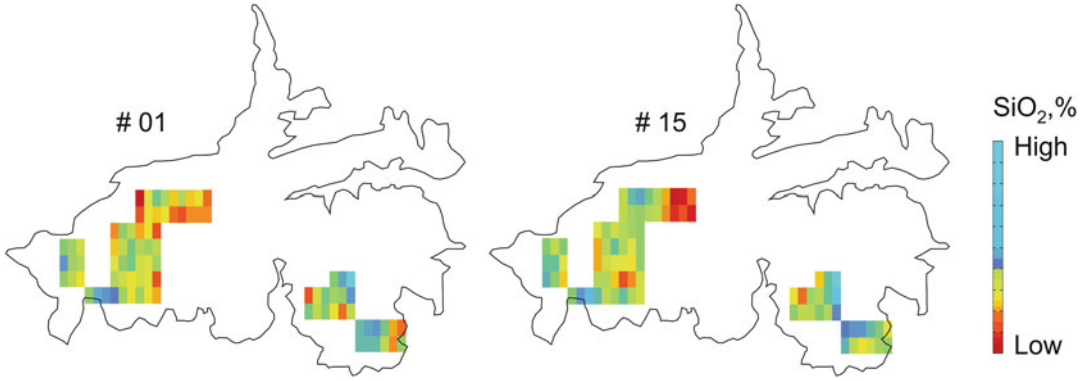

Fig. 28.3 Two equiprobable realisations (#01 and #15) of the SGS model of the SiO_2 (%) grade built using 200 × 200 m data and averaged to the panels of 230 × 450 × 3.5 m. Panel's size is equal to the monthly production plans

$$\text{Coefficient of Variation } (\%) = 100\% \times \frac{\sqrt{\text{Variace of the Block Grade}}}{\text{Mean Grade}} \quad (28.2.2)$$

The estimated uncertainties allow to compare the studied grids and chose the optimal for definition the resource categories (Fig. 28.4).

A common practice is to estimate the average level of uncertainty for each grid and to plot the obtained values versus the studied grids. The optimal grid is chosen by finding the largest grid where the average uncertainty is less or equal to a designated threshold (Rossi and Camacho 2004; Abzalov and Bower 2009).

In the current study it was suggested to classify resources of the deposit using the following criteria.

- Measured resources are defined by estimating uncertainty of the parts of the deposit equal to the quarterly production volumes. The resources are classified as Measured if they are estimated with an error of +/−10 % at 95 % confidence limits.
- Indicated resources are defined by estimating uncertainty of the parts of the deposit equal to the annual production volumes. It should be estimated with +/−10 % error at 95 % confidence limits.
- Inferred Resources include mineralisation for which global tonnage and grade are estimated with 30 % uncertainty at 95 % confidence limits.

Application of these criteria is shown of the Fig. 28.5. According to the proposed method an accurate estimation of the silica contents can be obtained for monthly production plans if the data grid will be approximately 30 × 30 m (Fig. 28.5). Similar graphs are created for the panels representing quaternary and annual production volumes which are used as a basis for choosing the optimal grids for the resource classification as Measured and Indicated (Abzalov and Bower 2009, 2014).

28.2.3 Classification Using Auxiliary Geostatistical Functions

The approach described in the previous section is methodologically robust and provides accurate results, however, it can be excessively time consuming and requires full access to the original data which often not available at the early stages of the mining project's evaluation. Alternatively, estimation errors can be deduced using auxiliary geostatistical functions. In particular, estimation errors of the metal grades, thicknesses of the seams and rock densities can be deduced from their Gamma-bar parameters (Journel and Huijbregts 1978, Annels 1991). This parameter, also known in geostatistics as auxiliary F-function (Annels 1991; Olea 1991), represents the mean

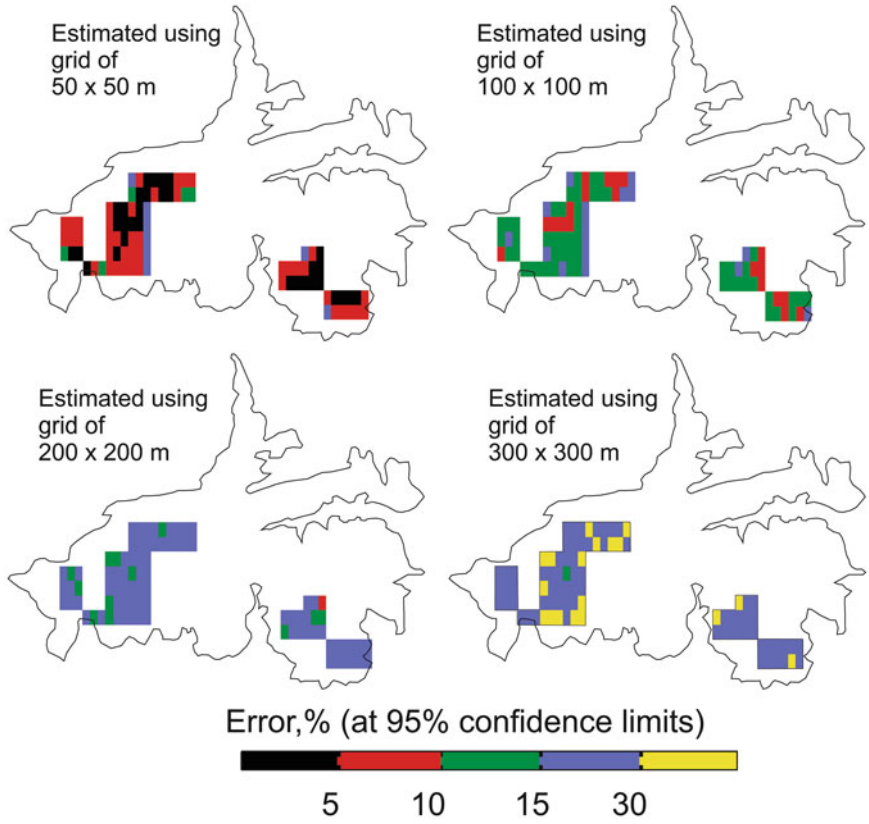

Fig. 28.4 Uncertainty of the SiO_2 grades of the monthly production volumes estimated using different data grids

variogram $\overline{\gamma}$ (V, V) averaged over all possible vectors contained within a rectangular block (V) (28.2.3).

$$\mathrm{F}\ (\mathrm{V}) = \overline{\gamma}\ (\mathrm{V}, \mathrm{V}) \tag{28.2.3}$$

An important property of the F-function is that it is equal to dispersion variance (D) of a point support within a rectangular block (V) (Olea 1991). In other words, mean variogram over rectangular block (V) is equal to the extension variance that results from forecasting the average property in the block (V) using the value defined over point (o) which can take any position within the block (V).

$$\mathrm{F}\ (\mathrm{V}) = \overline{\gamma}\ (\mathrm{V}, \mathrm{V}) = \mathrm{D}\left(\mathrm{o}\middle|\mathrm{V}\right) \tag{28.2.4}$$

where,

F(V) – the value of F-function estimated for the rectangular block of size (V);

$\overline{\gamma}$ (V, V) – mean of the variograms estimated over all possible vectors within a rectangular block (V);

D $\left(\mathrm{o}\middle|\mathrm{V}\right)$ – dispersion variance of a point support (o) within a rectangular block of size (V).

This property of Eq. 28.2.4 links the variogram model with the estimation error and allows the use of the F-function as a measure of resource estimation uncertainty. The F-function is applicable when the drilling grid is quasi-regular, implying that every studied rectangular block contains a sample; however, a sample can take any position within the block (i.e. 'floating' at random) (Fig. 28.6). Such distribution of data points is usually referred to as a random stratified grid (Journel and Huijbregts 1978, Annels 1991) and is one of the most common types of drilling patterns used for estimating mineral resources therefore the F-function is the most appropriate geostatistical criteria for estimating the resource uncertainties.

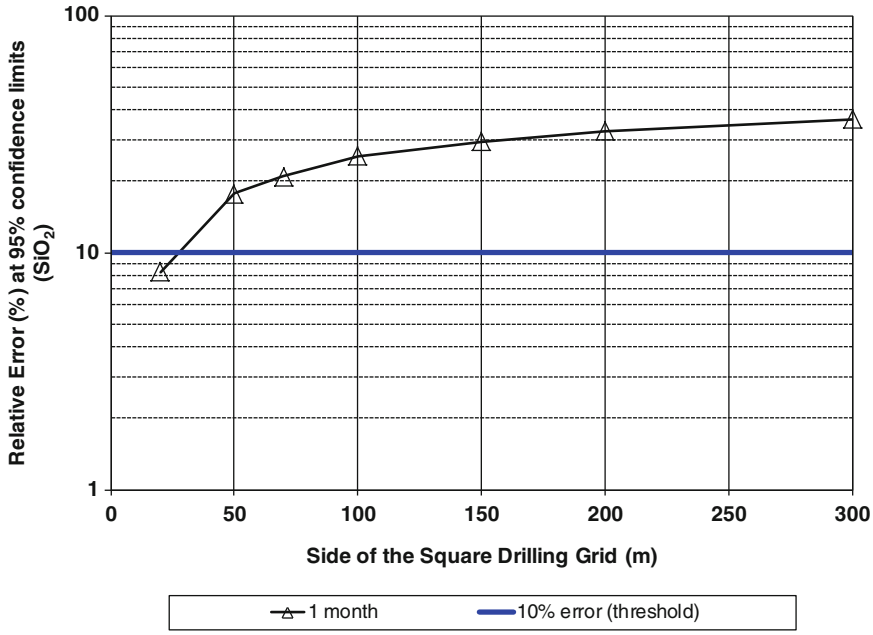

Fig. 28.5 Average estimation error of the SiO_2 grades of the monthly production panels vs. data grids

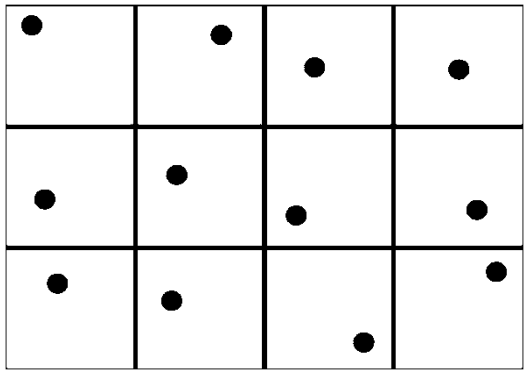

Fig. 28.6 Random stratified grid

The calculation procedure includes the construction of experimental variograms of the studied variable, fitting of a variogram model, and then estimation of the average of the variogram over the rectangular block of interest. The size of the rectangular block chosen for calculation of the F-functions should match the dimensions of the sampling grids proposed for the definition of mineral resources.

In practice, the F-function values corresponding to the blocks of interest are usually deduced from special geostatistical diagrams, which have calibrated the F-function values depending on the variogram model and ratios of the variogram ranges to the dimensions of the investigated drill grids.

The diagrams of the geostatistical auxiliary functions can be found in many geostatistical textbooks (Annels 1991). An alternative approach for estimating the F-function value is by using a computer programs. In that case, all possible vectors in the studied rectangular block are approximated by discretising it and presenting as a matrix of data points. Usually, discretisation to a matrix of 10(X) ×10(Y) × 10(Z) points produces an accurate result. The variogram model, which was deduced from the samples, is applied for calculation of the variograms over all possible vectors between discretisation points contained within a studied rectangular block. The estimated variograms are then averaged to obtain a mean variogram value (i.e. F-function).

The methodology is applied as follows:

- Initially, the experimental variograms and their models are estimated for main metals. At

some deposits the definition of their mineral resources and ore reserves requires an accurate estimation of the deleterious components. In particular, these are the contents of SiO_2 and Al_2O_3 at iron ore deposits (Abzalov et al. 2010), and the contents of SiO_2 and Fe_2O_3 at bauxite deposits (Abzalov and Bower 2009);
- The F(V) values have to be calculated for blocks of size (V) corresponding to the drill grids used for estimation Measured and Indicated resources;
- The uncertainties of the estimated mineral resources (estimation errors) are calculated by dividing the obtained F(V) value by the numbers of the (V) size blocks contained at the ore volumes representing the annual (for Indicated resources) or quarterly (for Measured resources) production;
- Finally, the optimal distribution grids are determined by finding spatial distribution patterns at which the estimation errors match the precision of the estimated metal grades.

References

Abzalov MZ (2008) Quality control of assay data: a review of procedures for measuring and monitoring precision and accuracy. Exp Min Geol J 17(3–4):131–144

Abzalov MZ (2010) Optimisation of ISL resource models by incorporating algorithms for quantification risks: geostatistical approach. In: Technical meeting on in situ leach (ISL) uranium mining, International Atomic Energy Agency (IAEA), Vienna, Austria, 7–10 June, 2010

Abzalov MZ (2013) Measuring and modelling of the dry bulk density for estimation mineral resources. Appl Earth Sci 122(1):16–29

Abzalov MZ, Mazzoni P (2004) The use of conditional simulation to assess process risk associated with grade variability at the corridor sands detrital ilmenite deposit. In: Dimitrakopoulus R, Ramazan S (eds) Ore body modelling and strategic mine planning: uncertainty and risk management. AusIMM, Melbourne, pp 93–101

Abzalov MZ, Bower J (2009) Optimisation of the drill grid at the Weipa bauxite deposit using conditional simulation. In: Seventh international mining geology conference, AusIMM, Melbourne, pp 247–251

Abzalov MZ, Bower J (2014) Geology of bauxite deposits and their resource estimation practices. Appl Earth Sci 123(2):118–134

Abzalov MZ, Menzel B, Wlasenko M, Phillips J (2010) Optimisation of the grade control procedures at the Yandi iron-ore mine, Western Australia: geostatistical approach. Appl Earth Sci 119(3):132–142

Abzalov MZ, van der Heyden A, Saymeh A, Abuqudaira M (2015) Geology and metallogeny of Jordanian uranium deposits. Appl Earth Sci 124(2):63–77

Annels AE (1991) Mineral deposit evaluation, a practical approach. Chapman and Hall, London, p 436

Arik A (1999) An alternative approach to resource classification. In: Proceedings of the 1999 computer applications in the mineral industries (APCOM) symposium, Colorado School of Mines, Colorado, pp 45–53

Blackwell G (1998) Relative kriging error – a basis for mineral resource classification. Exp Min Geol 7(1–2):99–105

Davis B (1992) Confidence interval estimation for minable reserves. SME Preprint 92–39:7

Dielhl P, David M (1982) Classification of ore reserves/resources based on geostatistical methods. CIM Bull 75(838):127–135

Dimitrakopoulos R (2002) Orebody uncertainty, risk assessment and profitability in recoverable reserves, ore selection and mine planning: workshop course. BRC, The University of Queensland, p 304

Ferenczi PA (2001) Iron ore, manganese and bauxite deposits of the Northern Territory. Northern Territory Geological Survey Report 13. Darwin, Government Printer of the Northern Territory, p 113

JORC Code (2012) Australaisian code for reporting of exploration results, mineral resources and ore reserves. AusIMM, Melbourne, p 44

Journel AG, Huijbregts CJ (1978) Mining geostatistics. Academic Press, New York, p 600

Krige D (1996) A practical analysis of the effects of spatial structure and of data available and accessed, on conditional biases in ordinary kriging. In: Geostatistics, Wollongong '96, v2, pp 799–810

Olea RA (ed) (1991) Geostatistical glossary and multilingual dictionary. Oxford University Press, New York, p 177

Rossi ME, Camacho JE (2004) Application of conditional simulation to resource classification scheme. CIM Bull 97(1079):62–68

Royle AG (1977) How to use geostatistics for ore reserve classification. World Min 30:52–56

Schofield NA (2001) Determining optimal drilling densities for near mine resources. In: Edwards AC (ed) Mineral resource and ore reserves estimation – the AusIMM guide to good practice. AusIMM, Melbourne, pp 293–298

Sinclair AJ, Blackwell GH (2000) Resource/reserve classification and the qualified person. CIM Bull 93(1038):29–35

Snowden DV (2001) Practical interpretation of mineral resource and ore reserve classification guidelines. In: Edwards AC (ed) Mineral resource and ore reserve estimation – the AusIMM guide to good practice. AusIMM, Melbourne, pp 643–652

Conversion Resources to Reserves

29

Abstract

Assessment of the project's feasibility involves conversion of the mineral resources to ore reserves which is undertaken with a strong input from the geologists into estimation of the mining and metallurgical factors. In particular, geologists may be responsible for metallurgical characterisation of the ore types assuring that bulk samples are representative and sufficient for conclusive tests.

A novel approach to confirm their representativeness is proposed in this chapter. The bulk samples are considered to be representative of the entirety of the studied deposit if they provide good spatial coverage of the deposit, and their composition matches every fifth percentile or, at least, fifth, twenty-fifth, fiftieth, seventy-fifth and ninety-fifth percentiles, of the selective mining unit (SMU) compositions. The compositional representativeness of bulk samples is checked by plotting against histograms of SMU blocks, including comparisons of metal grades and metallurgically deleterious elements.

Keywords

Mineral resource • Ore reserves • SMU • Bulk samples • Economics • NPV

Classification of the estimated mineral endowment as mineral resource requires only "reasonable prospects for eventual economic extraction". Thus, mineral resources can include material which extraction is not economically viable at the time of reporting. Ore reserves, on the contrary, are strictly related to the mine plans and include only that material which is amenable for economic extraction at the time of reporting. For example, the JORC Code defines ore reserves as a modified sub-set of economically mineable Indicated and Measured resources, emphasising that ore reserves should be defined by studies at least at a Pre-Feasibility level.

Thus, estimation of the ore reserves requires additional studies encompassing a wide range of the disciplines addressing all factors, technical, social, legal, economic, environmental and financial, that can potentially restrict the economic extraction of the metals of interest. Geological

M. Abzalov, *Applied Mining Geology*, Modern Approaches in Solid Earth Sciences 12,
DOI 10.1007/978-3-319-39264-6_29

team contributes to the ore reserves definition by participating in most of the technical and economic studies. However, the strongest demand for input from the mine geologists exists at the evaluation of the mining and metallurgical factors. These two factors set the production rates and costs, which constitute a basis for economic evaluation of the mining project including determining the economically viable cut-off value for a project which is also briefly discussed here.

29.1 Mining Factors

By definition, the reserves should be derived from the mine designs or mine plans and cannot be obtained by simple factoring of the mineral resources (JORC Code 2012). Therefore, estimation of the ore reserves requires various inputs from a mining engineer who is a key member of the ore reserves estimating team. However, without a strong geological understanding of the ore body and, in particular, sound knowledge of the deposit's structure and composition estimation of the ore reserves can become a futile exercise. It is important that the geologists providing input to the ore reserves models should have a solid experience in the mining technologies suggested at the studied mining project or applied if mine is operating. Good understanding of the mining technologies by the mine geologists facilitates their communication with the mining engineers.

Reserves are usually estimated from a block model consisting of the regular blocks which size is equal to a smallest selectively mineable unit (SMU). Mineralised bodies smaller than the SMU cannot be mined selectively and therefore the SMUs containing this mineralisation are diluted by the waste material. Degree of dilution depends on a mining method. Some parts of mineralisation cannot be extracted because of constraints imposed by the mining technologies. For example, these can be pillars left in the underground mines. Unrecoverable mineralisation is considered as mining losses and not included to the reported ore reserves.

Considering these mining factors the ore reserves are estimated by applying the economic cut-off criteria to the diluted grade of the SMU blocks located in the designed pit shells or underground stope. All resources which are located outside of the mine design are not converted to reserves and therefore should continue to be reported as mineral resources.

29.2 Metallurgical Factors

Mine plans are traditionally based upon the ore grade. It is well known, however, that grade is not the only characteristic that can be taken into account to maximise performance at the processing plant and many other parameters need to be taken into account, including ore and gangue mineralogy, ore texture, grindability, concentration of the metallurgically deleterious components and other properties characterising the ore.

Metallurgical characteristics of mineralisations are rarely uniform through the entirety of the deposit and therefore their spatial distribution should be accurately mapped by geologists and implemented in the 3D model of the deposit and integrate this data in a mine plan. The approach is commonly referred as geometallurgical modelling and involve a cross-discipline team with an important role played by the mine geologists (Coward et al. 2009; Richmond and Shaw 2009).

Geological team assists the project metallurgists in developing the processing technologies and optimising them specifically for the ore bodies at the studied project. Geologists have to collect all required geological, mineralogical and geochemical data needed for metallurgical characterisation of mineralisation. This may also include a detailed textural characteristics of the mineralised bodies or a detailed mineralogical mapping which can be necessary for their accurate metallurgical classification. In case if two or more metallurgically different types of mineralisation are identified their spatial distribution should be studied and incorporated into the ore reserve model of the deposit.

29.2.1 Metallurgical Systematics of the Ore Reserves

Geometallurgical variables include the rock properties that have an impact on the metallurgical behaviour of the ore. Most commonly used geometallurgical variables include (Richmond and Shaw 2009):

- ore mineralogy, including by-product metals;
- gangue mineralogy;
- textures and the ore liberation;
- grindability;
- deleterious components geochemistry and mineralogy;
- acid production sulphides in the waste and tailing;
- rock weathering;
- power and water consumption.

The geometallurgical variables have been subdivided onto primary and response variables (Coward et al. 2009).

Primary variables include the attributes of rock that can be directly measured. The most obvious example of the primary variables is a concentration of the deleterious elements. Response variable include the attributes of rock that describe the response of the rock to a process. Examples of this type variables includes metallurgical recovery of the metals and ore grindability.

29.2.2 Representativity of the Bulk Samples

The metallurgical characteristics of the mineralisation are determined by the series of tests performed on bulk samples, which form the main source of empirical data for the optimisation of ore processing technologies. This testing enable estimation of metallurgical recovery and the quantification of the factors that control the metallurgical behaviour of the ore, thereby assisting in the estimation of processing costs.

Metallurgical testings usually require large volumes of ore, from several hundred kilograms to several tens of tonnes for a single bulk sample, and can be followed up by additional studies at the scale of a pilot production. Large volumes of the bulk samples meant that only a limited number of individual samples can be used during metallurgical testwork. Thus, the effectiveness of metallurgical testing is limited by the degree to which these samples are representative of the orebody as a whole and by the appropriateness of the metallurgical testing methodology used during this characterisation. Location of the sites for collecting of the bulk samples is determined by the project geologists who must ensure their representativity for the project because validity of metallurgical tests depends on the representativeness of the bulk samples used.

Here, a novel approach of estimating bulk samples representativeness is briefly described together with example of the bulk sampling programme undertaken at the project in Jordan (Abzalov and Allaboun 2015). The approach requires two studies: firstly, analysis of the spatial distribution of the bulk samples assuring that they cover the whole deposit, and, secondly, analysis of statistical data to assure that the composition of the bulk samples are statistically representative of the entirety of the deposit.

The locations used for bulk sampling should cover the entire deposit and all types of mineralised material within the deposit in order to be considered as representative for the entirety of deposit. This means that the bulk samples have to be chosen from different locations representing the different parts of the deposit (Fig. 29.1a, b, c). Samples should be evenly spread over the entire deposit and should not be clustered in small areas that may represent preferential samples from the more accessible parts of a deposit (Fig. 29.1d).

If data quantity permits the construction of variograms, then the spatial continuity of the metallurgical characteristics can be geostatistically estimated and used to create a metallurgical model for the deposit. In particular, if a robust spatial correlation has been found between ore body characteristics (metal grades, mineralogy, textures) and metallurgical recovery, the test work results can be extrapolated to all blocks in the model using multivariate geostatistical techniques.

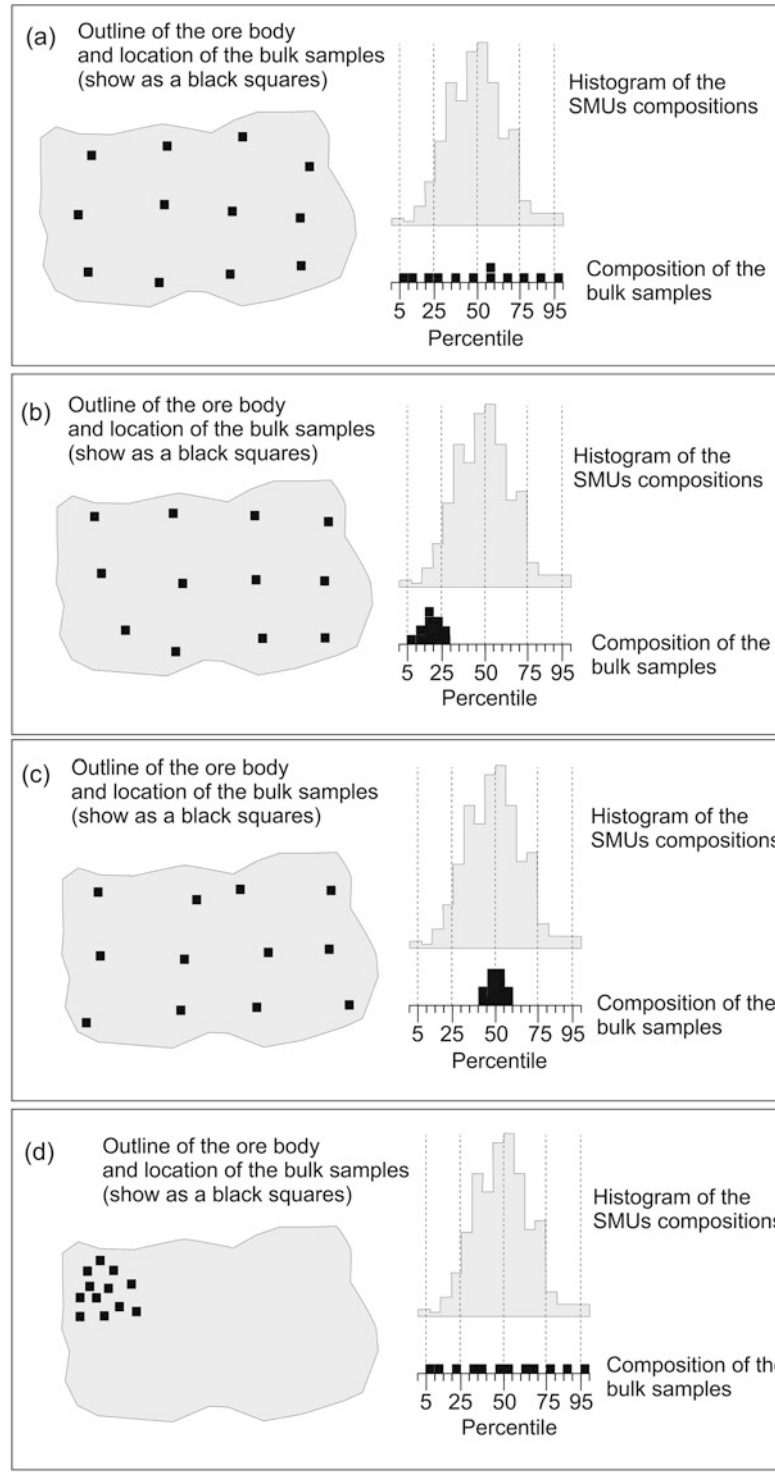

Fig. 29.1 Sketch showing representative and non-representative bulk sample configurations: (**a**) representative bulk samples; (**b**) spatial distribution of samples representative but compositions are biased toward low-grade mineralisation; (**c**) representative spatial distribution of samples but their compositions are non-representative as the sampling did not include both low and high-grade mineralisation; (**d**) samples are statistically representative statistically but spatial distribution is non-representative

The approach used during this study checks the representativeness of bulk samples compositions by plotting bulk samples versus histograms of the blocks whose size is equal to a smallest selectively mineable unit (SMU) at the given project (Fig. 29.1). The comparison should not be limited to mineralisation grade, but should also include metallurgically deleterious elements. If the quantitative mineralogical composition was systematically analysed through entire deposit the histograms of the metallurgically important minerals should be also created for the SMU size blocks and compared with the mineralogical composition of the bulk samples.

The histogram of the SMU blocks is created by geostatistically adjusting the resource block model to the proposed mining selectivity at the studied project, meaning that the blocks are regularised to the size of the selectively mineable units. This adjustment is made using non-linear geostatistical methods such as Localised Uniform Conditioning (LUC) (Abzalov 2006).

The bulk samples are considered to be representative of the deposit characteristics if their grade, concentration of the deleterious elements and other non-grade variables of economic significance are representative of the deposit (Abzalov and Allaboun 2015). Comparison of the arithmetic means of these two sets of data is insufficient to assure the representativeness of bulk samples because equal mean values are no guarantee that the spread of the bulk sample compositions encompasses the entire range of the ore grade classes within the deposit (Fig. 29.1c). Therefore, it was suggested to validate representativity of the bulk samples by comparing their statistical distribution with the histograms of the SMU grades (Abzalov and Allaboun 2015). The bulk samples are considered representative if their compositions encompass the entire range of the SMU compositions.

The best practice is to conduct testing using the bulk samples that approximately correspond to every 5th percentile of the SMU histograms (Fig. 29.1a). However, if the number of samples is less than ten, they should match at least the 5th, 25th, 50th, 75th and 95th percentiles of the SMU compositions.

This criterion is used to select locations for bulk sampling, which are deduced from a deposit's block model. In a situation where a deposit contains several metallurgically different domains, for example gold deposit containing oxidised ore, free milling sulphide ore and refractory ore, every metallurgically different domain should be studied considering them as a separate ore body. Results obtained at one domain (eg oxidised gold mineralisation) can be absolutely different, and therefore inapplicable to another part of the mineralisation (eg sulphide associated gold lode).

After the bulk samples have been processed, their representativeness is checked again by plotting them vs. the histograms of the SMUs (Fig. 29.1). This stage is necessary because the actual grade of a bulk sample may differ from the model due to geostatistical estimation errors.

The results obtained from individual bulk samples are used to infer the dependence of the metallurgical characteristics of the studied mineralisation on the variations of both metal grades and deleterious components.

This methodology was successfully implemented at the uranium project in Jordan (Abzalov and Allaboun 2015; Abzalov et al. 2015). The metallurgical tests at this project were focused on two small domains within the CJUP deposit, Khan Azabib and Siwaqa, which were considered as the most likely sites for proposed initial mining (Fig. 29.2). Sampling locations were chosen from the CJUP resource model ensuring that their spatial distribution is representative for the domains (Fig. 29.2) and compositions of the collected bulk samples cover the majority of the SMU block histograms (Fig. 29.3).

Assays of the bulk samples have shown that they contain between 81 and 289 ppm uranium, indicating a good coverage of SMU block grades (Fig. 29.3). Mineralisation containing less than 80 ppm U was excluded from metallurgical testing because this material is considered uneconomic (Abzalov et al. 2015). In addition to the estimated uranium grade, each block was also characterised by the contained amount of the deleterious components; this group of elements and oxides include sulphur, phosphorous and clay

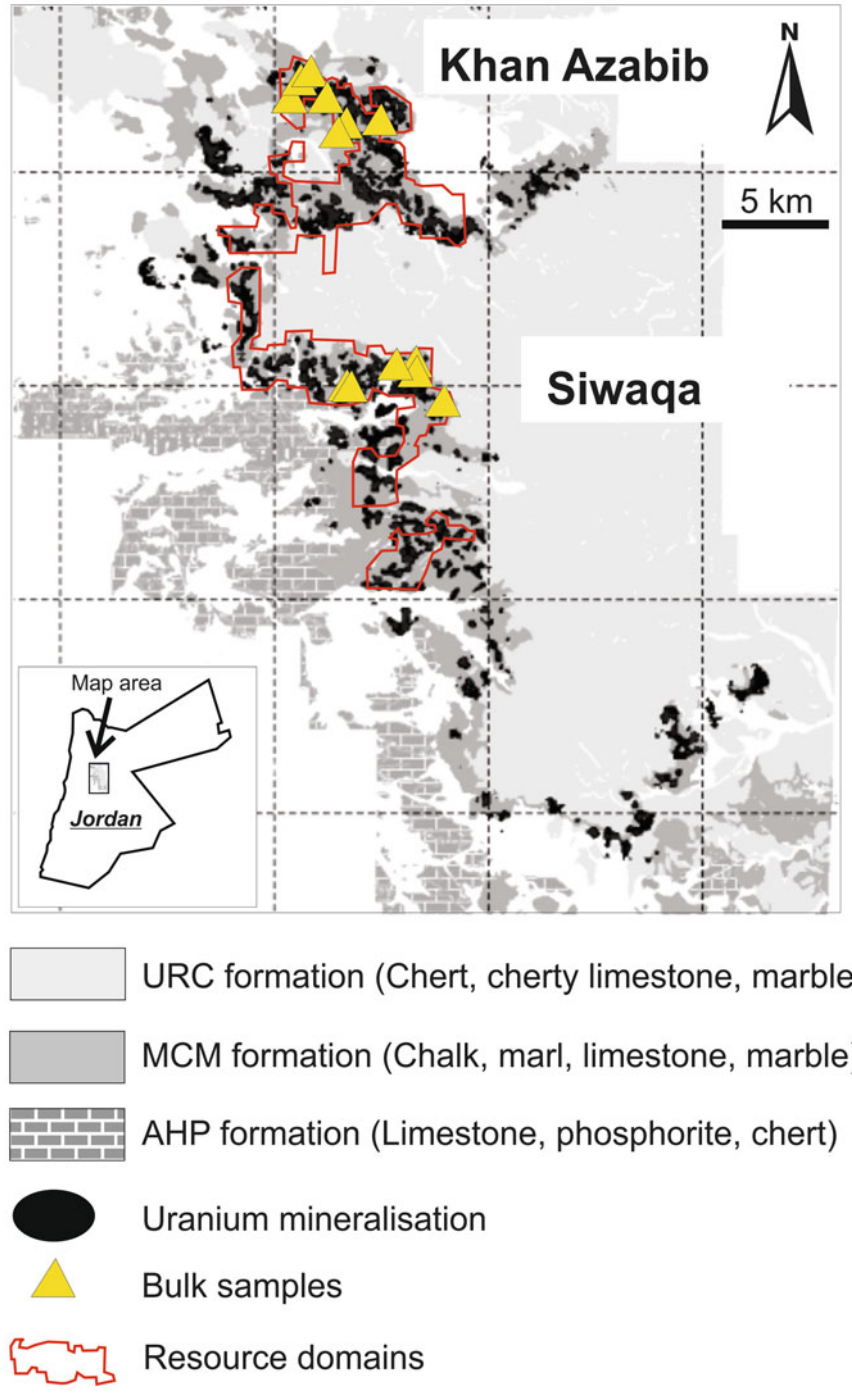

Fig. 29.2 Geological map showing spatial distribution of the bulk samples within the CJUP deposit (Reprinted from (Abzalov and Allaboun 2015) with permission of Taylor-Francis Group)

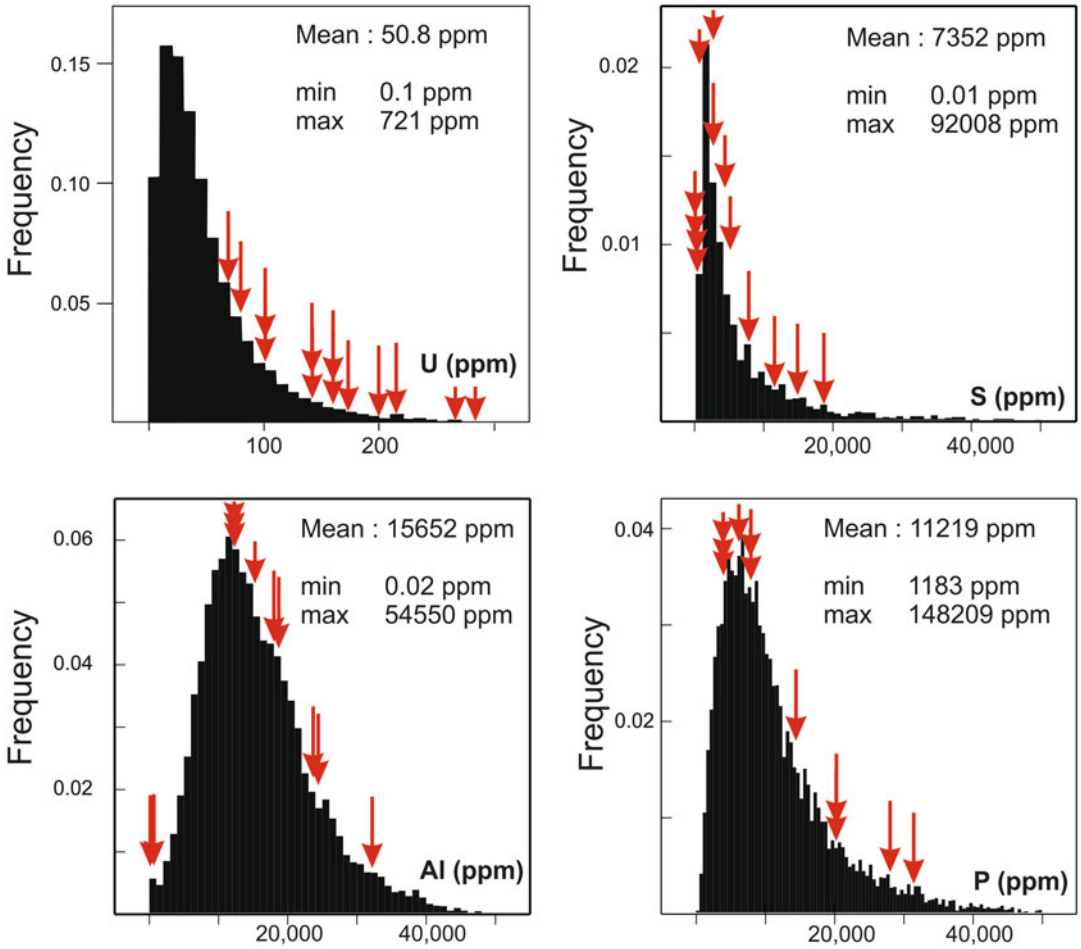

Fig. 29.3 Composition of bulk samples (*red arrows*) plotted on the histograms of SMU block ($50 \times 50 \times 0.5$ m) compositions, with resources are reported using an 80 ppm U cut-off (Abzalov and Allaboun 2015)

(Abzalov et al. 2015). Alumina concentrations were used to determine the clay concentrations in bulk samples and within SMU blocks, primarily as the clay minerals within the CJUP deposit are dominated by alumina.

In general, the principles of representativeness of the bulk samples composition (as shown in Fig. 29.1a) were correctly implemented at the CJUP project, as bulk samples compositions are close to 5th, 25th, 50th and 75th percentiles of the SMU block compositions. However, the material with highest concentrations of deleterious components (95th percentile) was not present in the bulk samples analysed during this testing (Fig. 29.3). In particular, the processed bulk samples contain less than 2 wt% sulphur (Fig. 29.3) therefore additional samples containing 4–6 wt% of sulphur will be collected and processed during the next phase of metallurgical tests.

29.3 Project Economics

Conversion resources to ore reserves requires determining of economically viable cut-off grade. This is an economic threshold which is used for delineating (constraining) of the ore bodies.

Estimation of the economic cut-off is a complex economic problem (Lane 2015) which is beyond the scope of a mine geologist

responsibilities and therefore only a brief overview of the concept is presented in this book. A common practice is to deduce economic cut-off using one of the breakeven formulae with reference to production costs, metal prices and operation capacities (29.3.1).

$$\mathrm{g\ (cut-off)} = \frac{\mathrm{OC}}{\mathrm{p}} \tag{29.3.1}$$

where

OC = operating costs (mining and processing) per tonne milled
p = realised metal price per unit of grade

Despite of simplicity of this formula (29.3.1) it is often used by the mine personnel to reviewer the cut-offs at the operational level and allow to analyse the impact of changed metal prices and recoveries on the selection of the economic cut-offs.

The economic cut-off can also be optimised to the cash flow however the estimates are commonly made independently of the actual variation of the grade within the mineralised body being mined (Lane 2015).

Using selected cut-offs and the costs a cash flow can be estimated for the proposed production rates and used for economic valuation of the mining projects. Two main parameters which are commonly estimated and reported as economic characteristics of the project are net present value (29.3.2) and internal rate of return (29.3.3) (Wellmer 1989).

$$NPV_{TOTAL} = \sum_{t=1}^{n} \left(\frac{\mathrm{CF_t}}{(1+K)^t} \right) - \mathrm{CAPEX} \tag{29.3.2}$$

where

NPV = Net Present Value
$\mathrm{CF_t}$ = cash flow for period (t)
K = discount rate
n = total project life (number of years)
CAPEX is initial capital expenditure.

Internal rate of return (IRR) is a discount rate (K) value which satisfies the equality 29.3.3.

$$0 = \sum_{t=1}^{n} \left(\frac{\mathrm{CF_t}}{(1+K)^t} \right) \tag{29.3.3}$$

References

Abzalov MZ (2006) Localised Uniform Conditioning (LUC): a new approach for direct modelling of small blocks. Math Geol 38(4):393–411

Abzalov MZ, Allaboun H (2015) Bulk samples testing for metallurgical characterisation of surficial uranium mineralisation at the Central Jordan Uranium Project. Appl Earth Sci 124(2):129–134

Abzalov MZ, van der Heyden A, Saymeh A, Abuqudaira M (2015) Geology and metallogeny of Jordanian uranium deposits. Appl Earth Sci 124(2):63–77

Coward S, Vann J, Dunham S, Stewart M (2009) The primary-response framework for geometallurgical variables. In: Dominy S (ed) Proceedings – seventh international mining geology conference 2009. AusIMM, Melbourne, pp 109–113

JORC Code (2012) Australaisian code for reporting of exploration results, mineral resources and ore reserves. AusIMM, Melbourne, p 44

Lane KF (2015) The economic definition of ore. Cut-off grade in theory and practice, 4th edn. Comet strategy, Brisbane, p 147

Richmond A, Shaw WJ (2009) Geometallurgical modelling – Quo Vadis. In: Dominy S (ed) Proceedings – seventh international mining geology conference 2009. AusIMM, Melbourne, pp 115–118

Wellmer F-W (1989) Economic evaluations in exploration. Springer, Berlin, p 163

Balance Between Quantity and Quality of Samples

30

Abstract

Evaluation of the mining project and exploitation of the mines depends on quality and quantity of analytical data which are usually obtained by assaying drill hole samples distributed on regular grids. Uncertainty of the estimated grades, depends on the assays precision (i.e. repeatability), on the spatial distribution (i.e. spacing of the drill holes) and also on a spatial continuity of the studied variables. A novel approach suggested for determining an optimal ratio between samples quality and the drill holes spacing by comparing relative variance of the samples duplicates and the nugget effect of the pair-wise relative variogram.

Keywords

Optimal sampling • CV% • Grade control

30.1 Introduction to a Problem

The current study presents a new approach for optimisation of sampling grids. It is based on quantitative estimation of the spatial continuity of the studied variable and comparing it with sampling error. Quantification of both parameters allows definition of an optimal and a cost effective trade-off between drill hole spacing and sampling protocol (Abzalov 2014).

Geostatistically deduced uncertainty (error) in mineral resources and ore reserves (Abzalov and Bower 2009; Blackwell 1998; Journel and Huijbregts 1978; Annels 1991) is largely dependent on the nugget effect of the studied variable. As an example, the relationship between a model uncertainty and the value of the nugget effect is shown on the Fig. 30.1.

Three grade distribution models (Fig. 30.1) have been generated from a single set of data (Abzalov 2010) by applying variograms models which differed by their nugget effect. Geostatistical nugget effect, which is a discontinuity of variogram at the origin (Olea 1991), is caused by sampling error and spatial discontinuity of the studied variable over short distances. The latter is referred to as a geological factor, because it largely depends on a mineralisation style and the structure of the deposit.

M. Abzalov, *Applied Mining Geology*, Modern Approaches in Solid Earth Sciences 12,
DOI 10.1007/978-3-319-39264-6_30

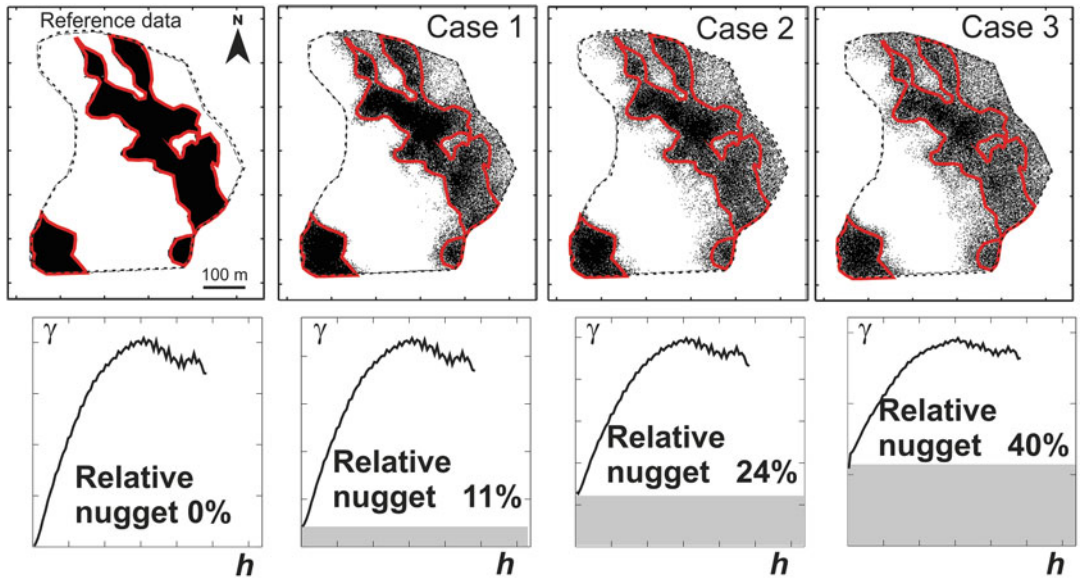

Fig. 30.1 Map of the modelled uranium grade showing effect of the nugget effect on model uncertainty (Reprinted from (Abzalov 2014) with permission of Australasian Institute of mining and metalllurgy)

30.2 Geological Factor and Sampling Error

Contributions of the geological and sampling factors to the nugget effect can be quantified by using the approach based on estimating the pair-wise relative variogram of the data. This technique can be used as a measurer of a spatial continuity of the data and, at the same time, is applicable for estimating the samples precision error (Abzalov 2014).

The pair-wise relative variogram is calculated by dividing (normalising) the variogram by the arithmetic means of the corresponding pairs of samples (30.2.1).

$$\gamma_{PWR}\ (\mathbf{h}) = \frac{2}{N}\sum_{i=1}^{N}\frac{[Z(x_i) - Z(x_i + \mathbf{h})]^2}{[Z(x_i) + Z(x_i + \mathbf{h})]^2} \quad (30.2.1)$$

where,

$Z(x_i)$ – the studied regionalised variable (Z) at the location (x_i);

$Z(x_i + \mathbf{h})$ – the studied regionalised variable (Z) at the location $(x_i + \mathbf{h})$, where $(\mathbf{h})$ is a vector separating two data points.

The same approach is used for estimating the samples precision error, which is calculated as an average coefficient of variation of the duplicated samples (Abzalov 2008) (30.2.2 and 30.2.3).

$$CV\% = 100\% \sqrt{\frac{2}{N}\sum_{i=1}^{N}\left(\frac{(a_i - b_i)^2}{(a_i + b_i)^2}\right)} \quad (30.2.2)$$

where N is number of sample pairs, and a_i is the original and b_i the duplicate of the *ith* sample pair.

The CV% (30.2.2) can be easily transferred into relative variance σ^2_{RSV}

$$\sigma^2_{RSV} = CV^2 = \frac{2}{N}\sum_{i=1}^{N}\left(\frac{(a_i - b_i)^2}{(a_i + b_i)^2}\right) \quad (30.2.3)$$

Thus, the pair-wise relative variogram technique allows to compare the assay data variance with

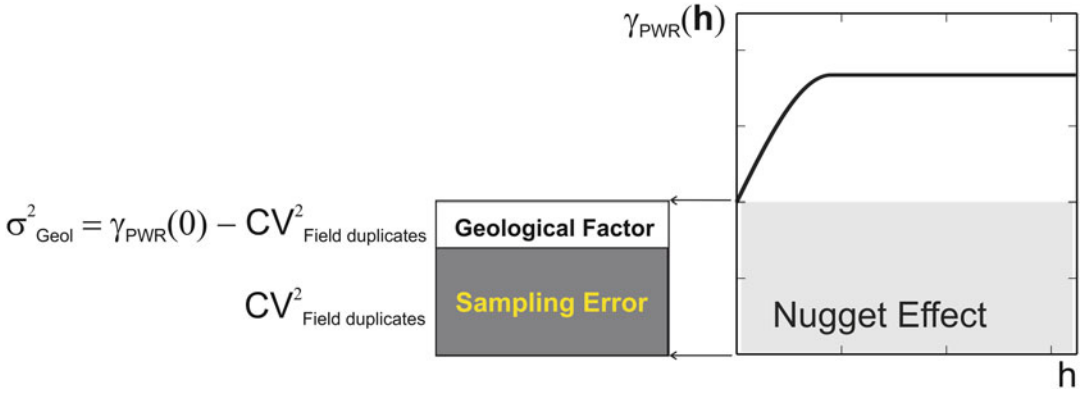

Fig. 30.2 Sketch explaining contribution to the nugget effect of a geological and sampling factors (Reprinted from (Abzalov 2014) with permission of Australasian Institute of mining and metalllurgy)

spatial variability of the studied variable. The nugget effect [γ_{PWR} **(0)**] inferred from the pair-wise relative variogram model represents the combination of sampling precision errors and geological discontinuity over short distances (Fig. 30.2). However, Eq. 30.2.3 estimates only the contribution to the nugget effect made by the sampling precision error (σ^2_{RSV}). Therefore, the difference between these two values can be considered as the contribution to the nugget effect made by geological factors (Fig. 30.2).

Thus, both factors causing the nugget effect of the pair-wise relative variogram can be quantified and by comparing the two contributions an optimal approach can be found for decreasing the overall estimation error (Abzalov 2014). For example, when sampling error constitutes most of the nugget effect, improving quality of the resource estimates and reliability of the results can be achieved by updating the sampling protocols. This is likely to be more cost effective than additional infill drilling with shorter distances between holes.

Alternatively, if the comparison shows that the nugget effect is largely caused by geological factors, investing in updating sampling procedures will add little if anything to improvement of the quality of the resource estimates, and attention should be focus on optimising the drill spacing.

At the grade control stage the proposed methodology can be further enhanced by adding economic parameters, such as the costs of lost and recovered ore, cost of ore dilution by the waste material incorrectly classified as ore and the costs of the grade control drilling and sampling. Economic benefits of the changed sampling protocols are calculated as a difference between additional amount of recovered ore, plus savings from the minimised dilution and minus the increased grade control drilling and sampling costs (Abzalov et al. 2010). The grade control costs are in turn minimised by applying, the proposed in the current paper, geostatistical approach to find an optimal trade-off between drill hole spacing and sampling protocol.

References

Abzalov MZ (2008) Quality control of assay data: a review of procedures for measuring and monitoring precision and accuracy. Explor Min Geol J 17(3–4):131–144

Abzalov MZ (2010) Optimisation of ISL resource models by incorporating algorithms for quantification risks: geostatistical approach. In: Technical meeting on in situ leach (ISL) uranium mining, International Atomic Energy Agency (IAEA), Vienna, Austria, 7–10 June 2010

Abzalov MZ (2014) Geostatistical criteria for choosing optimal ratio between quality and quantity of the samples: method and case studies. In: Mineral resource and ore reserves estimation, AusIMM monograph 23, 2nd edn. Chapter 2: The resource database. AusIMM, Melbourne, pp 91–96

Abzalov MZ, Bower J (2009) Optimisation of the drill grid at the Weipa bauxite deposit using conditional simulation. In: Seventh international mining geology conference. AusIMM, Melbourne, pp 247–251

Abzalov MZ, Menzel B, Wlasenko M, Phillips J (2010) Optimisation of the grade control procedures at the Yandi iron-ore mine, Western Australia: geostatistical approach. Appl Earth Sci 119(3):132–142

Annels AE (1991) Mineral deposit evaluation, a practical approach. Chapman and Hall, London, p 436

Blackwell G (1998) Relative kriging error – a basis for mineral resource classification. Explor Min Geol 7(1–2):99–105

Journel AG, Huijbregts CJ (1978) Mining geostatistics. Academic, New York, p 600

Olea RA (ed) (1991) Geostatistical glossary and multilingual dictionary. Oxford University Press, New York, p 177

Part VII

Mineral Deposit Types

Lode Gold Deposits

31

Abstract

Brief description of the several orogenic gold deposits is provided together with the basic principles of the gold projects evaluation. Emphasis is made on methodology of the gold deposits sampling, geological interpretation and estimation resources.

Common problems encountered when evaluating of the gold deposits are as follows:

- sample size (mass) is not representative (small) for a given mineralisation
- laboratory sampling protocols reduce sample mass at too coarse particle size
- analytical techniques are suboptimal for a given mineralisation
- strongly skewed statistical distribution of gold require using special techniques for preventing smearing of the high-grade values
- because of a strong variability of the grade at the short distances evaluation of these type deposits requires high density of drilling, up to 20 × 20 m grids, which is commonly supported by collection of the bulk samples.

Keywords

Gold deposits • Orogenic • Mineral resource

Gold deposits occur in a wide range of the geological environments and significantly differ by the mineralisation styles, host rocks, deposit structures and the ore mineralogy (Heald et al. 1987; Goldfarb et al. 2001). Size of the deposits and mineralisation grade also vary in a very wide range therefore methodologies of the projects evaluation significantly changes depending on the proposed mining methods.

Because of complexity of this group the review of the gold deposits was limited to the several orogenic type lode-gold deposits (Fig. 31.1), including Zarmitan (Abzalov 2007), Meliadine (Abzalov and Humphreys 2002a), Natalka (Eremin et al. 1994; Abzalov 1999), Norseman (Thomas et al. 1990), Ballarat (Phillips and Hughes 1996) and several projects in the Birimian greenstone belt (Milesi et al. 1992).

M. Abzalov, *Applied Mining Geology*, Modern Approaches in Solid Earth Sciences 12,
DOI 10.1007/978-3-319-39264-6_31

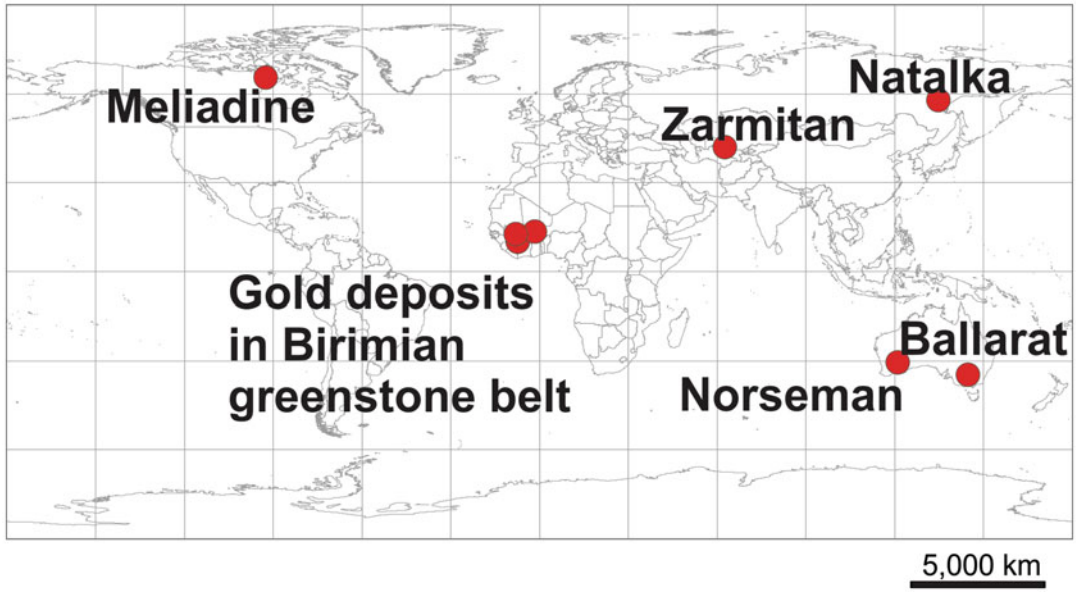

Fig. 31.1 World map showing location of the main gold deposits included in the current review

The chosen deposits encompass different geological environments (Table 31.1) and therefore, despite of the limited number of the case studies used, the given selection provides a good picture of the gold projects evaluation procedures. The chosen deposits allow to understand the main difficulties in evaluation of the gold deposits and the causes of errors. Additional information, in particular mining and ore processing aspects of the gold projects evaluation, is available in Vallee et al. (1992).

31.1 Geology of the Orogenic Gold Deposits

Orogenic gold deposits usually have a complex structure formed by the numerous lodes, which often are oriented in the different directions and intensely branching (Fig. 31.2). This creates the complexly interlocking structural patterns of the orogenic gold deposits. Most complex geometry of mineralisation is observed at the shear-hosted gold deposits, however, vein type deposits can also exhibit a significant structural complexity. Lodes can be discontinuous along the strike and their grade and thickness significantly change at the short distances (Fig. 31.2c) which aggravates the structural complexities of these type deposits.

Contacts of the lodes are usually sharp and the gold content can rapidly change from zero at the host rocks to the high grade values immediately after passing the contact (Fig. 31.3). In order to prevent smearing of the high grade values the mineralisation is constrained by wireframes and grade is estimated using a hard boundary approach. Accurate definition of the contacts is particularly important because even small inaccuracy in the contacts location can lead to the serious errors in estimated resources.

Alternative approach for constraining gold lodes is based on using the grade indicators (Abzalov and Humphreys 2002a, b). In general, because of the structural complexity of the gold deposits and highly variable thicknesses of the lodes their delineation can be extremely difficult task requiring high density of drilling (Vallee et al.1992).

Gold deposits commonly contain several generations of mineralisation which can differ by the mineral and chemical compositions. Their spatial distribution is commonly controlled by the different structures and as a result of this spatial orientation of the gold mineralisation changes

Table 31.1 Geological characteristics of the selected gold deposits

Deposit	Country	Geological province, belt	Host rocks	Mineralisation style	Metamorphism	Alteration	References
Meliadine	Canada	Rankin Inlet greenstone belt of the Western Churchill province	Mafic volcanics intercalated with siliciclastic rocks (turbidite) and banded iron formation	Shear-hosted quartz-ankerite vein network and replacement style mineralisation	Epidote-amphibolite	Cryptic silica alteration together with sulphides, chlorite and biotite-sericite	Abzalov and Humphreys (2002a)
Zarmitan	Uzbekistan	South-Tianshan orogenic belt	Granite intrusion and turbidite	Ribbon-textured quartz veins and shear hosted linear stockworks	Sub-greenschist	Albite, K-feldspar and chlorite. Lodes hosted by sedimentary rocks are surrounded by halo of sulphides	Abzalov (2007)
Natalka	Russia	Yana-Kolyma belt	Turbidite	Sulphide disseminated turbidite hosted lodes	Sub-greenschist	Silica alteration with sulphides and sericite with minor chlorite and carbonate	Eremin et al. (1994), Abzalov (1999)
Yanfolila	Mali	Birimian	Turbidite	Shear hosted lodes	Epidote-amphibolite		Milesi et al. (1992)
Ballarat	Australia	Lahlan fold belt	Interbedded greywacke and mudstone	Fault controlled quartz reefs	Greenshist	Weak halo of silica, carbonate, chlorite and sericite	Phillips and Hughes (1996)
Norseman	Australia	Norseman-Wiluna greenstone belt	Pillow basalt	Quartz veins	Greenschist	Chlorite bearing assemblage developed in the mafic dykes and biotite occurs in the basalts	Thomas et al. (1990)

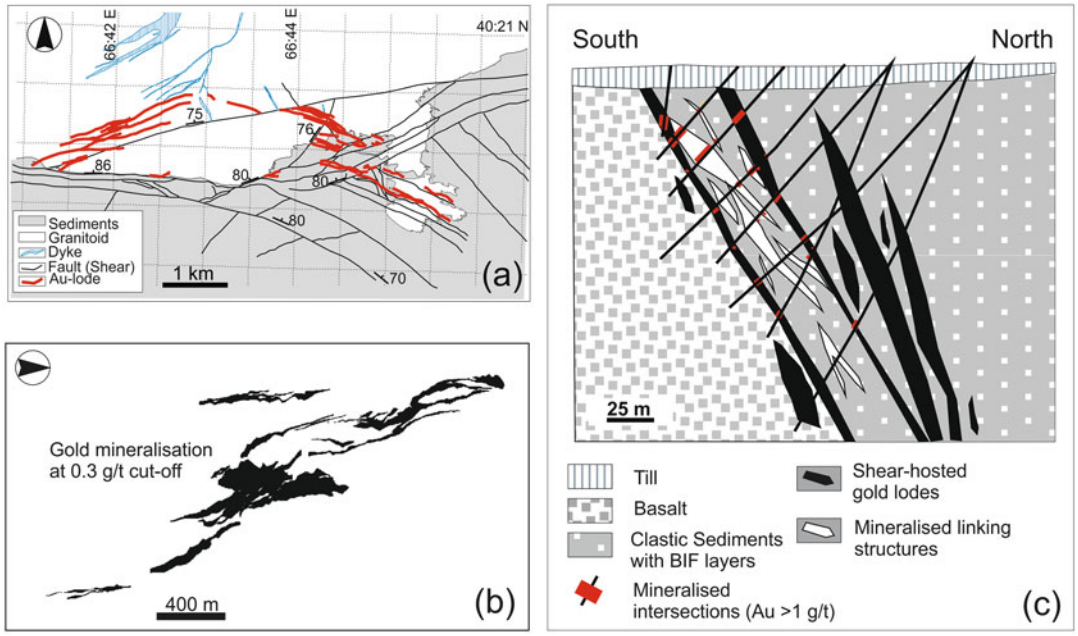

Fig. 31.2 Geometry of the gold lodes: (**a**) Zarmitan mine, Uzbekistan (Abzalov 2007); (**b**) Sissingue project, Cote d'Ivoire; (**c**) Meliadine project, Canada (Abzalov and Humphreys 2002a)

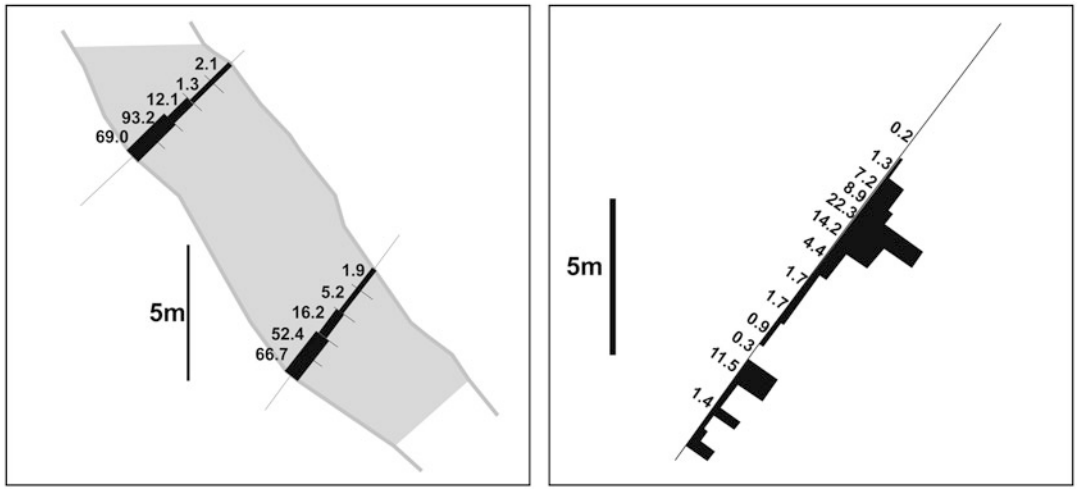

Fig. 31.3 Grade distribution profiles of the gold lodes at the Meliadine deposit, Canada (Abzalov 2009; Abzalov and Humphreys 2002a)

depending on composition and grade. In particular, the high grade shoots often are distributed discordantly to the lower grade mineralisation. This structural feature, coupled with presence of the small very high grade (bonanza) shoots, presents a serious challenge for estimation resources of the gold deposits. Using a single variogram is not always plausible choice because it can lead to excessive smearing of the high grade mineralisation. This problem can be overcome by using Multiple Indicator kriging technique for estimating resources of the orogenic gold deposits.

31.2 Sampling and Assaying of the Gold Deposits

Evaluation of the orogenic gold deposits is commonly made using diamond and reverse circulation (RC) drilling (Table 31.2). Diamond drilling gives a good indication of the deposits geology allowing to accurately interpret geometry of the mineralised domains, thickness of the lodes and is essential for understanding the structural control of mineralisation (Long 1998; Sketchley 1998; Vallee 1998). Quality of the sample assays depends on a core size and sample recovery. Preference is usually given to the largest diameter of a drill core, not less than NQ size, which allows to decrease the samples variance. Core recovery depends on the rock types drilled and the drilling procedures. In the fractured rocks core recovery is commonly low. Recovery is also decreases in weathered rocks and intensely foliated shear zones where mechanical competency of the rocks significantly decreased causing selective core loss (Long 1998).

RC drilling produces samples that are less representative than core samples and require extra care in supervising sampling at a drill site. In the coarse gold environment RC drilling is commonly unreliable due to selective sample loss, segregation of the gold grains in the reverse circulation system and cross-contamination leading to the samples bias. Therefore, face-sampling hummer is a preferred RC technique in the gold deposits. Samples contamination can be reduced by using short sampling intervals, therefore RC drill holes are commonly sampled at intervals less than 1 m.

Mineralisation hosted by weathered rocks can be estimated using air-core (AC) and rotary air-blast (RAB) drilling techniques, which are sampled at 0.5–1.5 m intervals. These techniques are commonly used in the Western Australia and Africa (Table 31.2).

Drilling of the gold lodes can be supported by channel sampling of the exploration shafts and on the surface, using exploration trenches (Table 31.2). This technique provides a detailed geological information and allows to collect representative samples (Vallee 1998). Domini et al. (2000) suggest to use channel sampling of the underground workings as the main resource definition technique for the coarse gold deposits (Domini et al. 2000). Its application, unfortunately, is constrained by high costs and therefore is commonly restricted to collecting of the bulk samples.

31.2.1 Samples Preparation

Gold deposits are characterised by highly skewed statistical distribution of the gold grade which can be coupled with presence of the coarse gold grains creating excessive heterogeneity of mineralisation, colloquially referred to as ‘nuggetty’ (Domini et al. 2000). In practice this means that even small rock fragments can significantly differ by the gold contents. As a consequence of the gold grade complexity and the ‘nuggetty’ style of mineralisation at the orogenic gold lodes their sampling and assaying is especially challenging task. Not surprisingly, that repeatability of the gold assays is usually lower than that of the base metals and other commodities (Abzalov 2008).

Common problems encountered at sampling programs that lead to collection of poor quality data are as follows (Sketchley 1998):

- sample size (mass) is not representative (small) for a given mineralisation;
- laboratory sampling protocols reduce sample mass at too coarse particle size;
- analytical techniques are suboptimal for a given mineralisation.

The sample variance can be reduced by taking lager samples, which are crushed and pulverised in its entirety to a nominal 95 % passing 75 μm. This decreases precision error leading to significant improvement of the gold assays repeatability. However, processing of the large samples is an expensive option, therefore, in practice, samples are prepared by their consecutive comminution and sub-sampling.

Sampling protocols are optimised for a given deposit using detailed screen tests of the gold grains distribution by the size classes.

Table 31.2 Resource estimation data at the selected gold deposits

Deposit	Resource estimation data		Number of samples	Average length of the samples	Sampling grid (metres) by resource categories		
	Exploration method	Available data			Measured	Indicated	Inferred
Meliadine	Diamond core, mainly NQ size	327 drill holes, total length 70.3 thousand metres	27,184 drill core	Drill core – 1 m	20 × 20 (?)	40 × 40	80 × 80
Natalka	Diamond core, NQ and HQ size, and RC drilling. Channel sampling of the exploration trenches and in the underground workings	206.6 thousand metres of underground developments; 693.7 thousand metres of trenching; 210.7 thousand metres of diamond core drilling	117,601 drill core; 68,182 channel samples	Drill core – 1.6 m; channel samples – 2.3 m	50 × 50	200–100 × 40	200 × 80–100
Norseman (Gladstone domain)	Diamond core and RC drilling	887 drill holes, total length 47.1 thousand metres	30,338 drill hole samples	1.3 m	20 × 20	40 × 40	100 × 50
Yanfolila	Diamond core, RC, AC and RAB drilling	7922 drill holes	10,337 drill core; 146,960 – RC; 90,351 – AC; 15,024 – RAB	Drill core – 1 m; RC – 1 m; AC – 2.4 m; RAB – 3 m		30 × 20	60 × 60
Zarmitan	Diamond core, NQ and HQ size. Channel sampling of the exploration trenches and in the underground workings	134.97 thousand metres of underground developments; 100.4 thousand metres of trenching; 884.3 thousand metres of diamond core drilling	267,726 drill core; 116,967 channel samples	Drill core – 0.8 m; channel samples – 0.7 m	Not available		

This information and empirically estimated sampling constants are used for construction of the sampling control charts (nomograms) (Pitard 1993; Francois-Bongarcon 1993, 2005). Francois-Bongarcon (1993) has suggested to use as a default values the K-constant equal to 470 and α -constant equal to 1.5 in the projects when calibrated values of the sampling constants are not available. These values can be used for construction of the preliminary sampling protocols however a great care should be taken as the default parameters can significantly differ from the actual values.

Sketchley (1998) has suggested to classify gold ores into three categories of sampling difficulties using sampling constants. First category includes fine grained gold which characterised by K-constant values within the range to 1–100. Second category includes medium grained deposits; the K-constant values are in the range of 100–500. Last group includes coarse grained deposits; the K-constant values exceed 500 (Sketchley 1998).

31.2.2 Gold Assays

Traditional method of gold analysis is fire assay (Hoffman et al. 1998). The basic procedure for fire assay includes mixing a 30 g or 50 g aliquot of powdered sample with a flux containing of sodium carbonate (soda ash), borax, litharge (PbO), flour and silica. The mixed material is fired at temperatures approximately 1000–1200 °C achieving a full melting and then its poured into a mold. When cool, the Pb button is separated from slag and placed into special cupel where gold is finely recovered into bead.

Final determination of the gold is made by weighing the gold recovered from the fire assay bead. The technique is called gravimetric finish (Hoffman et al. 1998) and applied to high grade samples (Fig. 31.4). Low-grade samples analysed using modern analytical finishes. The entire bead is dissolved in acid and assayed by flame atomic absorption spectroscopy (AA) or, less commonly, using inductively coupled plasma-mass spectrometry (ICP-MS) or direct current plasma emission spectrometry (Fig. 31.4). Lowest detection limits are obtained by assaying the bead using instrumental neutron activation analysis (INAA).

A variation of the fire assay technique is known as metallic screen assay (Hoffman et al. 1998). The method is used for samples containing coarse gold and involves crushing and sieving out coarse fraction (100 or 150 μm). Oversize fraction is assayed in the entirety including the nylon screen. Undersize fraction is reduced and analysed using conventional fire assay. Normally two aliquots of 50 g each are used for analysis of every undersize fraction. Sample grade is estimated using formula 31.2.1.

$$\text{Grade} = \frac{(\text{Ms} - \text{Mc})\,\frac{A_1 + A_2}{2} + (\text{Mc})\,A_3}{\text{Ms}} \tag{31.2.1}$$

where

Ms – original sample weight
Mc – weight of the coarse fraction
A_1 and A_2 – grade of the undersize fraction assayed twice
A_3 – grade of the oversize fraction.

For mineralisation containing extremely coarse gold grains two screens are used, 110 and 550 μm (Dominy et al. 2000).

Fire assaying remains the standard procedure in the mining industry and when methodology is rigorously performed it produces accurate closely repeatable results. The main sources of errors at the fire assaying methodology are as follows (Hoffman et al. 1998):

- using of unmarked crucibles can result in sample mix-ups;
- re-using crucibles in the laboratory is a source of potential contamination of the samples;
- high sulphide content requires special treatment of samples, usually roasting. Assayed values of the not treated samples can be seriously biased;
- some laboratories decrease fusion time in order to increase throughput of samples. This creates a risk of a not total gold recoveries;

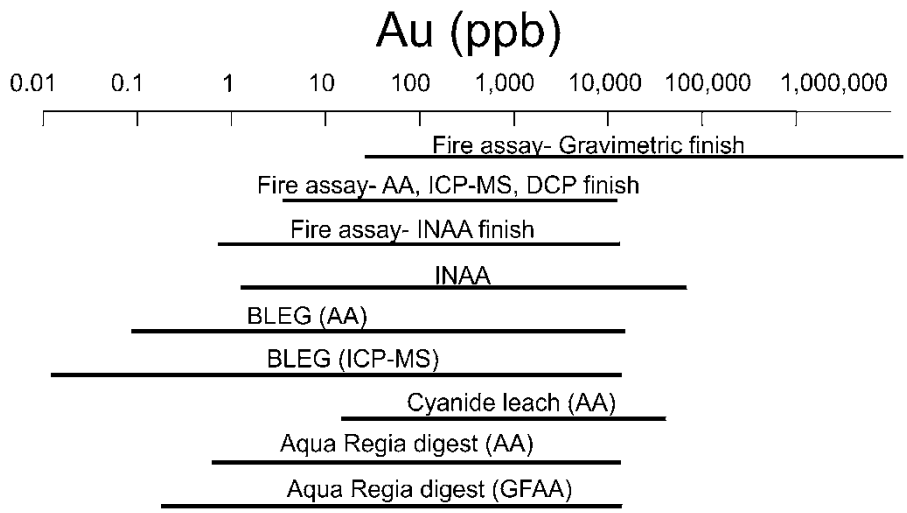

Fig. 31.4 Comparison of the effective ranges of the gold assay methods, generalised after Hoffman et al. (1998). Abbreviations are explained in the text

Another commonly used technique is bulk leachable extractable gold (BLEG). The method involves grinding a large sample, 1–5 kg, and placing it into a polyethylene bottle where gold is dissolved in the cyanide solution (0.25–1 % NaCN) by agitating (bottle rolling) (Hoffman et al. 1998). Leaching time can take from several hours to several days. Special catalysts, such as LeachWELL 60X, accelerates the rate of cyanidation significantly decreasing the time needed for dissolving the samples.

Performance of the BLEG method depends on mineralogy and geochemistry of the samples and must be specified by the project team. A special attention should be paid to sample weight and size of the fraction encapsulated in the polyethylene bottle, strength of the NaCN solution and agitation time.

Cyanide solution is analysed for gold using atomic absorption (AA) or graphite furnace-atomic absorption (GFAA) methods. This is made by extraction of gold into organic solvent, which is needed to avoid Fe interference. Direct analysis of the cyanide leach by AA method can be significantly overestimate gold grade. The problem can be overcome by using by ICP-MS method, which can be directly applied to the cyanide leach without extraction of the gold into organic solvent. The ICP-MS finish of the BLEG method has the best detection limit, approximately 0.05 ppb Au (Fig. 31.4). Residue of the bottle-roll leaching should be analysed for undissolved gold by a conventional fire assay method.

The main disadvantages of the method summarised by Hoffman et al. (1998) are as follows:

- presence of carbonates and/or sulphides can cause excessive cyanide consumption;
- gold can be lost from the cyanide leach by absorption onto carbonaceous material;
- re-use of the bottles can lead to samples contamination.

Another two methods, which are used for determining the gold concentration in the rock samples includes instrumental neutron activation analysis (INAA) of the pulverised samples and Aqua Regia dissolution of the pulverised samples with subsequent instrumental analysis of the acid solution (Fig. 31.4). INAA method is rarely used in the mining industry due to rarity of the nuclear reactors suitable to perform commercial INAA. Aqua Regia dissolution is widely used in Australia for grade control at the mines. However, the commonly reported disadvantage of this method is underestimating the gold grade in comparison with fire assay technique. Variation

of this method is four-acid digest, allowing to obtain more complete dissolution of a gold. Gold, reported by four-acid digest method is comparable with the results of the conventional fire assay.

31.2.3 Samples Quality Control

The errors can be introduced at the any stages of the analytical data collection, from drilling of the deposits through all phases of the samples preparation and assaying to eventual reporting of the analytical results into the project's database (Sketchley 1998; Abzalov 2008, 2011, 2014).

Several methods are available to ensure the quality of the assayed data (Valle 1998; Long 1998; Sketchley 1998; Dominy et al. 2000; Abzalov 2008, 2009):

- drilling of the twin holes;
- duplicate samples study;
- sieve tests of the sample comminution products;
- using blank samples;
- using certified standards;
- verification assaying results using external laboratory.

Control of the samples quality at the gold deposits is a labour intense and should be performed with an extra care, in particular if the studied mineralisation contains the coarse gold. When RC drilling is used for evaluation of the projects or grade control at the operating mines the samples should be thoroughly investigated for cross contamination. In some cases contamination of the samples can be recognised by a systematic decrease of the gold grade in the down-the-hole direction, which is indicative of the down-the-hole smearing of the gold grade caused by the samples contamination. However, contamination of the samples not always can be recognised from the grade distribution profiles therefore twinning of the RC holes by the diamond core drill holes should be systematically used as a routine quality control technique.

Repeatability of the analysis is controlled by duplicate samples. Every stage of sub-sampling should be monitored using duplicate samples analysis, however, the main attention should be paid to the field duplicates and to the first split in laboratory (Abzalov 2008). Statistical analysis of the duplicate samples allows to estimate the precision error (quantitative assessment of the degree of samples repeatability). The size of the estimated error allows to identify the steps contributing the largest variance and based on these findings to modify the samples preparation procedures (Abzalov 2011).

Duplicate analysis can be also used for validation of the sampling protocols. Inappropriate sampling protocols are commonly manifested by most sample grades being lower than the true gold content and a several results being significantly higher. This is expressed in a poor repeatability of the gold assays by the duplicate samples. When this problem is encountered the sampling protocol mast be reviewed and optimised. Abzalov (2008) has shown that samples precision error can be kept below 40 % even in a coarse gold environment if the right protocol and equipment are used.

High malleability creates the serious problems for pulverisation of the gold ore samples. Gold grains often not disintegrated to a nominal screen size because of their high malleability. Small gold particles can be aggregated and rolled into larger grains, having cigar-like or disk shapes. In order to prevent samples contamination, the grinder and pulveriser must be cleaned after each sample using compressed air and the barren quartz flush. Blank samples must be added to every sample batch, preferably placing them after the high grade ore samples.

31.3 Dry Bulk Density

Density of the gold mineralisation and their host rocks at the studied gold deposits were measured using the drill core samples (Table 31.3). Measurements are made using conventional techniques, most commonly by a water

Table 31.3 Dry bulk density (DBD) of the gold mineralisation

Deposit (country)	Gold assaying			Density measurements			Ratio: assay samples per 1 density measurement	Reference
	Number of assay samples	Average (Au, g/t)	COV	Number of samples for the rock density measurements	Average (t/m^3)	COV		
Meliadine (Canada)	27,184	1.5	6.4	2535	2.83	0.03	11	Abzalov and Humphreys (2002a), Abzalov (2013)
Natalka (Russia)	273,690	1.4	4.8	5612	2.68	0.08	49	Markevich, pers. communication
Yanfolila (Mali)	262,672	Not available	4.7	8468	1.8–3.03	0.03–0.07	31	Project geologists, pers. communication
Zarmitan (Uzbekistan)	384,693	1.3	1.2	11,021	2.73	0.05	35	Abzalov (2007)

COV (Coefficient of Variation) = standard deviation/mean

displacement method applied to a wax coated samples (Abzalov 2013). A vacuum sealing of the friable materials in polymer bags can be used as an alternative to a wax coating.

Frequency of the DBD measurements vary from 1 per 11 assay samples to 1 per 49 assay samples (Table 31.3). In general, DBD measurements at the orogenic gold deposits are made with a rate of 1 DBD sample per approximately 30 assay samples (Table 31.3).

31.4 Estimation of Resources and Reserves

Conventional approach of estimating gold resources is based on constraining mineralisation in 3D by wireframes and estimating grade using geostatistical techniques. Less commonly the lodes are delineated using indicator based techniques (Abzalov and Humphreys 2002b).

Narrow gold veins can be estimated in 2D (Dagbert 2001). The approach is robust and was successfully used in the past when computer based 3D technologies were not routinely available in the mining industry (e.g. Zarmitan mine). At present, it is usually replaced by 3D based technologies, however, using it as alternative estimate is fully warranted.

Gold grade is usually interpolated using Ordinary kriging or Multiple Indicator kriging. When data characteristics (nuggetty, strongly skewed) or their spatial distribution (highly irregular shape of the domains) or quantity of the samples did not allow to construct a meaningful variogram model the kriging estimation systems are commonly replaced by Inverse Distance method.

31.4.1 Top Cut

In order to prevent excessive smearing of the high grade values they are truncated, the procedure is commonly referred as high grade capping or top cut. The cutting of the high grade values is applied to the composited data, therefore before applying the top cut it is necessary to ensure that all samples have the same volume support.

Optimisation of the high grade cut-off procedures is made empirically by reconciling the estimated models against the grade control and production data. When these data not available

Table 31.4 Examples of the cut-off grades for reporting of the gold resources

Deposit (country)	Open pit reserves	Underground reserves	Material type
Meliadine (Canada)	1.0	3.0	Free milling
Natalka (Russia)	0.4	4.0	Free milling
Yanfolila (Mali)	0.6		Oxidised mineralisation
Zarmitan (Uzbekistan)	1.0	3.0	Free milling
	3.0	5.0	Refractory

the high grade values are usually truncated to the 95 percentile of the cumulative frequency diagram (Vallee et al. 1992). Alternatively, the high gold grades are cut to one of the following values:

- sum of the data mean and twice of the standard deviation;
- four times of the mean value;
- the point where the ragged tail starts on a grade histogram.

31.4.2 Classification

Summarising the resource definition approaches at the studied deposits the following drill grids can be suggested as a guideline for planning resource definition drilling at the orogenic gold deposits:

- Measured: 20–30 × 20–30 m
- Indicated: 40–60 × 40–60 m
- Inferred: 80–120 × 60–80 m.

Cut off values for reporting resources varies from 0.4 to 3 g/t for open pit and from 3 to 5 g/t underground mines (Table 31.4).

References

Abzalov MZ (1999) Gold deposits of the Russian North East (the Northern Circum Pacific): metallogenic overview. In: Proceedings of the PACRIM '99 symposium. AusIMM, Melbourne, pp 701–714

Abzalov MZ (2007) Granitoid hosted Zarmitan gold deposit, Tian Shan belt, Uzbekistan. Econ Geol 102(3):519–532

Abzalov MZ (2008) Quality control of assay data: a review of procedures for measuring and monitoring precision and accuracy. Explor Min Geol J 17(3–4):131–144

Abzalov MZ (2009) Use of twinned drill – holes in mineral resource estimation. Explor Min Geol J 18(1–4):13–23

Abzalov MZ (2011) Sampling errors and control of assay data quality in exploration and mining geology. In: Ivanov O (ed) Application and experience of quality control. InTECH, Vienna, pp 611–644

Abzalov MZ (2013) Measuring and modelling of the dry bulk density for estimation mineral resources. Appl Earth Sci 122(1):16–29

Abzalov MZ (2014) Design principles of relational databases and management of dataflow for resource estimation. In: Mineral resource and ore reserves estimation, AusIMM monograph 23, 2nd edn. Chapter 2: The resource database. AusIMM, Melbourne, pp 47–52

Abzalov MZ, Humphreys M (2002a) Resource estimation of structurally complex and discontinuous mineralisation using non-linear geostatistics: case study of a mesothermal gold deposit in Northern Canada. Explor Min Geol J 11(1–4):19–29

Abzalov MZ, Humphreys M (2002b) Geostatistically assisted domaining of structurally complex mineralisation: method and case studies. Geostatistically assisted domaining of structurally complex mineralisation: method and case studies. In: The AusIMM 2002 conference: 150 years of mining, Publication series no 6/02. AusIMM, Melbourne, pp 345–350

Dagbert M (2001) Comments on "The estimation of mineralised veins: a comparative study of direct and indirect approaches", by D.Marcotte and A.Boucher. Explor Min Geol J 10(3):243–244

Dominy SC, Annels AE, Johansen GF, Cuffley BW (2000) General considerations of sampling and assaying in a coarse gold environment. Trans Inst Min Metall 109:B145–B167

Eremin RA, Voroshin SV, Sidorov VA, Shakhtyrov VG, Pristavko VA (1994) Geology and genesis of the Natalka gold deposit, Northeast Russia. Int Geol Rev 36:1113–1138

Francois-Bongarcon D (1993) The practise of the sampling theory of broken ore. CIM Bull 86(970):75–81

Francois-Bongarcon D (2005) Modelling of the liberation factor and its calibration. In: Proceedings second world conference on sampling and blending. AusIMM, Melbourne, pp 11–13

Goldfarb RJ, Groves DI, Gardoll S (2001) Orogenic gold deposits and geological time: a global synthesis. Ore Geol Rev 18(1):1–7

Heald P, Foley NK, Hayba DO (1987) Comparative anatomy of volcanic hosted epithermal deposits: acid-sulphate and adularia-sericite type. Econ Geol 82(1):1–26

Hoffman EL, Clark JR, Yeager JR (1998) Gold analysis – fire assays and alternative methods. Explor Min Geol J 7(1–2):155–160

Long S (1998) Practical quality control procedures in mineral inventory estimation. Explor Min Geol 7(1–2):117–127

Milesi J-P, Lendru P, Feybesse J-L, Dommanget A, Marcoux E (1992) Early proterozoic ore deposits and tectonics of the Birimian orogenic belt, West Africa. Precambrian Res 58: 305–344

Phillips GN, Hughes MJ (1996) The geology and gold deposits of the Victorian gold province. Ore Geol Rev 11:255–302

Pitard FF (1993) Pierre Gy's sampling theory and sampling practise, 2nd edn. CRC Press, New York, p 488

Sketchley DA (1998) Gold deposits: establishing sampling protocols and monitoring quality control. Explor Min Geol 7(1–2):129–138

Thomas A, Johnson K, MacGeehan PJ (1990) Norseman gold deposits. In: Hughes FE (ed) Geology of the mineral deposits of Australia and Papua New Guinea. AusIMM, Melbourne, pp 493–504

Vallee M (1998) Quality assurance, continuous quality improvement and standards. Explor Min Geol 7(1–2):1–15

Vallee M, David M, Dagbert M, Desrochers C (1992) Guide to the evaluation of gold deposits: geological society of CIM, Special vol. 45. CIM, Montreal, p 299

Uranium Deposits (In-Situ Leach Projects)

32

Abstract

Sandstone-type uranium deposits are commonly located below the water table in weakly lithified or non-consolidated sands, and therefore they can be exploited using *In-Situ Leach* (ISL) technology. Such technology is based on dissolving uranium minerals directly in their host rocks (*in-situ*) by reactive solutions that are injected through drill holes, and then pumping the dissolved solution to the surface through some discharge drill holes.

Estimation and reporting of uranium resources for ISL projects differ from hard rock mining projects. Uranium grade is determined by down-hole geophysics, in particular the gamma-logging and the prompt fission neutrons logging coupled with sampling and assaying of the drill core. The main parameters which need to be considered are as follows:

- grade and geometry of mineralisation are estimated with accuracy sufficient for supporting the remote mining
- if grade is estimated using the gamma-logging technique secular disequilibrium should be studied and reported
- hydrogeological confinement of the mineralised horizon
- permeability of the mineralised horizon
- composition of the host rocks, in particular the carbonate content, in order to estimate if uranium mineralisation is amenable to dissolution by acid or alkaline solutions
- groundwater flow
- aquifer salinity
- rate of the *in-situ* dissolution of the uranium minerals.

M. Abzalov, *Applied Mining Geology*, Modern Approaches in Solid Earth Sciences 12,
DOI 10.1007/978-3-319-39264-6_32

Hydrogeological and geotechnical information is obtained by testing the drill core samples and by using the pump tests and the downhole piezometers. Modifying factors for conversion resources to reserves are verified and corrected using field leach tests of uranium.

Keywords
Uranium • Sandstone-type • Roll-front • ISL • Mineral resource • Shu-Sarysu

The current review is focused on sandstone hosted uranium deposits (Fig. 32.1). Globally, this is most abundant type of uranium deposits, containing approximately 28 % of the world uranium resources (Abzalov 2012). Depending on their depositional environments and structural characteristics, the sandstone uranium deposits are subdivided into four main groups: roll-type, also known as rollfront; tabular; basal channel; and structurally controlled (Dahlkamp 1993; Abzalov 2012).

This type deposits are characterised by difficult geotechnical conditions caused by the presence of aquifers in the poorly consolidated sands that host these deposits. As a consequence, this type deposits are exploited using a special technology, known as *In-Situ* Leach (ISL), which is based on dissolving uranium minerals directly in their host rocks (*in-situ*) by reactive solutions injected through drill holes (Abzalov 2012). Special geological characteristics of the sandstone-type uranium deposits and their highly specific exploitation techniques based on ISL technology have led to the development of special procedures for resource estimation which are described in this chapter.

The current review uses information collected from several deposits in Kazakhstan, USA and Australia (Table 32.1). The studied deposits include Inkai and Budenovskoe, both of which are located in the Shu-Sarysu basin (Fig. 32.1b). Rollfronts were additionally studied at the Akdala (Shu Sarysu basin) and Kharasan (Syrdaria basin) deposits in central Kazakhstan (Fig. 32.1b). Several roll-type deposits were studied in the Great Divide basin, Wyoming, USA (Abzalov and Paulson 2012) (Fig. 32.1c). The review of the basal-channel type mineralisation is based mainly on the deposits of the Callabonna sub-basin in Australia (Fig. 32.1d).

The studied deposits differ in their depositional environments and structural characteristics (Table 32.1). However, the methodology of estimation of resources is similar within the studied group and so they are described together.

32.1 Sandstone Hosted Uranium Deposits

Sandstone-type uranium mineralisation is formed by low temperature hydrothermal solutions depositing uranium in permeable sedimentary strata. As a consequence of a given depositional environment, the mineralisation geometry is highly irregular (Fig. 32.2). In plan view, mineralised zones can form meandering ribbons up to several tens of kilometres long (Fig. 32.1b), or, can be represented by a swarm of discontinuous lenses. This is common for basal channel type deposits where uranium is distributed along braided palaeo-channels (Figs. 14.13d and 32.1d).

On the cross-section the mineralisation occurs as roll-shaped bodies (Fig. 32.2c) or, more commonly, as the complex bodies of amoeba-like shapes formed by several vertically stacked mineralised zones (Fig. 32.2a). Tabular ore bodies also present (Fig. 32.2b) although they are less common for roll-front and palaeochannel deposit types.

The main uranium minerals of the sandstone-type uranium deposits are pitchblende and

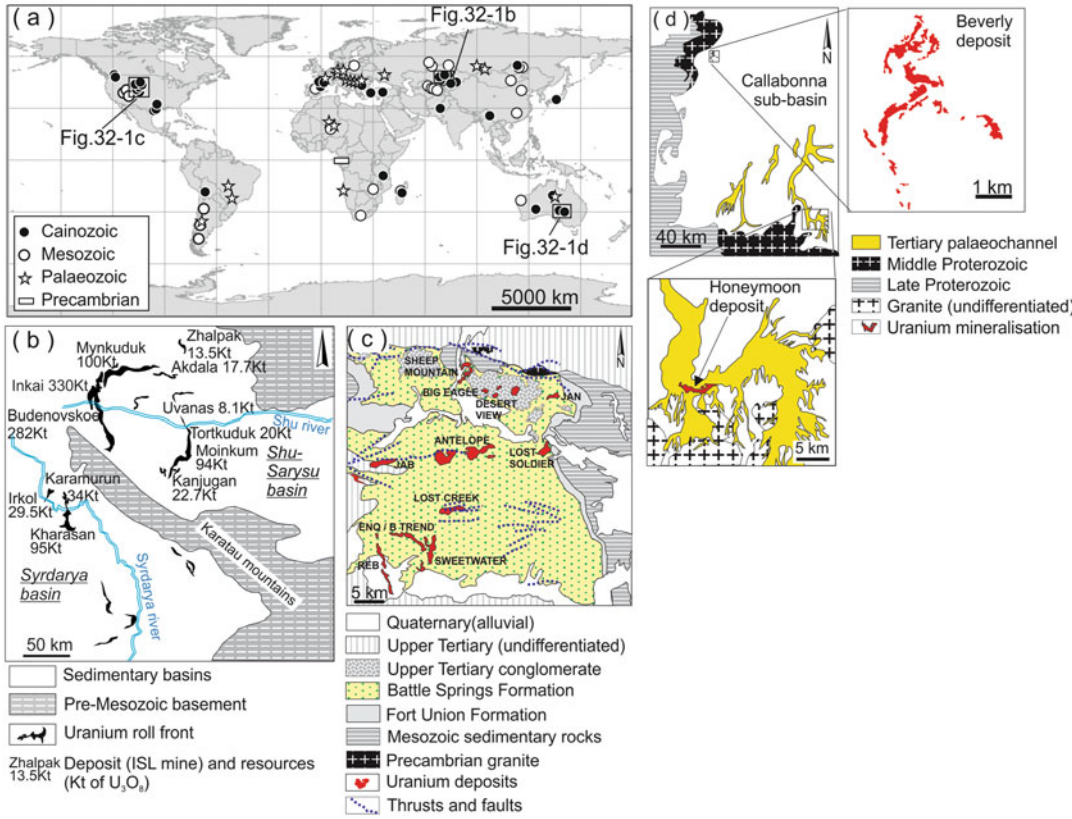

Fig. 32.1 (**a**) Map showing distribution of the sandstone-type uranium deposits and the studied basins (Reprinted from (Abzalov et al. 2014) with permission of Taylor-Francis Group); (**b**) Syrdarja and Shu-Sarysu basins in Kazakhstan; (**c**) Great Divide basin, Wyoming; (**d**) Callabonna sub-basin, South Australia

coffinite (Abzalov 2012) which are easily recovered from host rocks by sulphuric acid or alkaline leach.

32.2 Resource Definition Drilling

Exploration for sandstone-type uranium deposits is entirely based on drilling and usually commences as a series of widely spaced drill fences distributed along a redox front with the drill fences oriented at a right angle to the front. The distance between drill traverses at this stage is several kilometres. The quality of drilling and recovery of representative samples is important from the early stage of the project and progressively increases as the project matures and approaches the resource estimation stage. In order to minimise core losses, triple-tube diamond drilling is routinely used. Shallow deposits can be drilled using Sonic methods which are successfully used for exploration of the mineral sands deposits (Abzalov et al. 2011).

In Kazakhstan, the exploration traverses are distributed at 6–12 km spacing. The distance between drill holes on the traverse is usually 200 m. When mineralisation is encountered the drilling spacing is progressively reduced. Depending on mineralisation style, the final resource definition grid at the feasibility study stage can be 50 × 25 m (Table 32.1).

In the Great Divide Basin, USA, a similarly staged drilling approach was used for estimation resources, although, some deposits in the region have been infilled to 30 × 30 m (Abzalov and Paulson 2012).

Table 32.1 Characteristics of the studied uranium deposits

Deposit	Deposit type	Country, basin	Depth below surface (metres)	Resources and past production			Drilling grid by resource[a] categories			Uranium recovery (%)	Acid consumption (acid tonnes per 1 tonne of uranium)	Rock density (t/m^3)	Reference
				Tonnage (Mt)	Grade								
					U_3O_8 %	Cut off (U_3O_8 %)	Inferred	Indicated	Measured				
Kharasan	Rolls	Kazakhstan, Syrdarya	560–680	38.6	0.11	0.010	400 × 50	200 × 50	50 × 50 – 25	93	90–140	1.70	Pool and Wallis (2006c), Petrov et al. (2008), and Abzalov (2012)
Akdala	Rolls	Kazakhstan, Shu-Sarysu	200–250	30.3	0.069	0.010	400 × 50	200 × 50	50 × 50–25	90	35	1.70	Pool and Wallis (2006b), Petrov et al. (2008), and Abzalov (2012)
Inkai	Tabular and Rolls	Kazakhstan, Shu-Sarysu	350–510	32.7	0.051	0.010	400 × 50	200 × 50	50 × 50–25	90	50	1.70	Pool and Wallis (2006a), Petrov et al. (2008), and Abzalov (2012)
Budenovskoe	Tabular and Rolls	Kazakhstan, Shu-Sarysu	630–680	250–275	0.089	0.010	400 × 50	200 × 50	50×50–25	80–90	45	1.70	Petrov et al. (2008)
Honeymoon	Basal channel	Australia, Callabonna	100–200	15.23	0.081	0.020	200−120 ×60	80×40	40×40 −20	70	7.7	1.90	Bush (2000), McKay et al. (2007), and Penny (2012)
Billeroo	Basal channel	Australia, Callabonna	100–200	Not avaiable	0.053	0.020	200−120 ×60	80 × 40	40×40 −20			1.90	
Beverly	Basal channel	Australia, Callabonna	100–120	11.7	0.18	0.015 m%			35 × 35	68 (sand), 36 (silty sand)	7.7	1.70	Penny (2012) and Abzalov et al. (2014)
Four Miles	Basal channel	Australia, Callabonna	180–250	9.8	0.33	0.015 m%			35 × 35			1.70	Penney (2012)
Sheep Mountain	Tabular and Rolls	USA, Great Divide	20–300	12.9	0.12				30 × 30				Abzalov and Paulson (2012)
REB	Rolls	USA, Great Divide	30–200	10–14	0.04–0.05	0.025		60 × 60				2.30	Abzalov and Paulson (2012)

Modified after Abzalov et al. (2014)

[a]Resources of the Kazakhstan deposits were reported using the Kazakhstan State Reporting System (usually referred as GKZ). Their conversion to the JORC categories are approximate and was made by the current authors

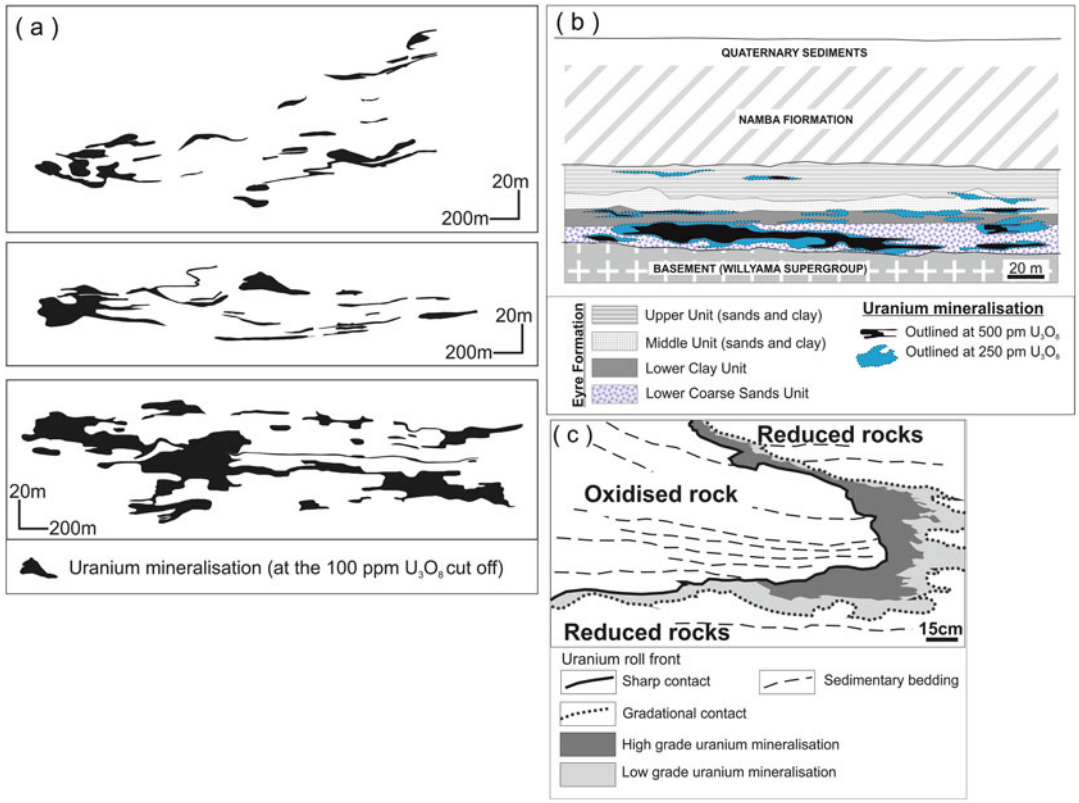

Fig. 32.2 Cross-sections of the sandstone-hosted uranium deposits: (**a**) complex shape of the rolls formed by several mineralised zones which are vertically stacked forming amoeba-shaped bodies, Shu-Sarysu basin, Kazakhstan; (**b**) tabular shape of uranium mineralisation at the Honeymoon deposit, Australia; (**c**) rollfront at the Shirley basin in Wyoming, USA (interpreted from the outcrop photo)

Resources of the sandstone-type uranium deposits in Australia (e.g. Beverly and Honeymoon) are estimated using drillholes distributed as a square grid with 25–30 m centres (McKay et al. 2007).

As an approximate guideline the following drilling grids can be considered for preliminary estimation of the drilling budget (Abzalov 2010):

- Measured resources, range from 50−40 × 25 m;
- Indicated resources, range from 80 × 40 m;
- Inferred resources, range from 160−120 × 40 m.

The geometry of basal channel type mineralisation is usually more complex and therefore requires tighter drilling than commonly used for uranium rolls. In contrast, tabular mineralisation is characterised by a simple geometry and good spatial continuity of the uranium grade, meaning that resources can be estimated using fewer drill holes.

32.3 Geophysical Logging of the Drillholes

Two geophysical methods are currently used for the estimation of uranium grade, gamma-log and prompt fission neutrons (PFN). The methods are fast, inexpensive and allow logging of mineralised intersections at 5–15 cm intervals. However, application of the geophysical methods, in particular the gamma – logging technique, re-

quires special study of the radioactive isotope systems ensuring that methodology is applicable at the given deposit.

32.3.1 Gamma Logging

The most common technique for *in-situ* measuring of the uranium grade in the drill holes is based on measuring gamma radiation, which is recorded as counts per second and recalculated to uranium content. However, most of the gamma rays are generated by radioactive isotopes ^{214}Bi and ^{214}Pb representing the daughter products of the ^{238}U radioactive decay. ^{238}U itself does not generate significant gamma ray energy, therefore, the gamma logging is only an indirect estimation method deducing the uranium content from the daughter isotopes.

Accurate estimation by this method is possible if there is a strict relationship between uranium and its daughter products, but this is not always the case. The daughter isotopes have different geochemical characteristics to ^{238}U and therefore can be removed from uranium ore, as is commonly observed in young sandstone type uranium deposits where uranium often is not in equilibrium with its decay products, which may have been removed by the ground water. As a result of this, the gamma intensity may not match the concentration of uranium and gamma logs can underestimate or overestimate the actual uranium grade. Intensity and type of disequilibrium can change over short distances within the same ore body, which makes it impossible to calibrate gamma logs for resource estimation. Disequilibrium can also cause a spatial offset of the daughter products displacing the gamma anomalies from the actual location of the uranium ore body. Therefore, isotopic relationships in the uranium decay system need to be studied before gamma logging technique are applied for resource estimation.

The use of gamma log is warranted when a stable relationship between parent and daughter isotopes has been confirmed for a domain. Uranium content is estimated from the gamma counts by correcting them for hole and probe diameters, logging intervals, K-factor (conversion factor), drill mud factor and dead time, and is commonly referred to as eU_3O_8. The K-factor is obtained by calibration of the gamma probe from a known drillhole in a specially constructed test pit, that are typically located at government nuclear testing facilities. Additional calibration should be run at the project site and should be a regular part of a gamma logging process. This is usually made by keeping one hole at the project site open through the course of the project and using it for internal control.

Quality control of the gamma probe also requires re-logging of approximately 10 % of the drillholes to ensure repeatability of the results. Estimated eU_3O_8 values need to be calibrated against the chemical assays of the drill core samples. Because gamma logs and chemically assayed samples represent different volumes of rocks their direct comparison is difficult and requires a large amount of samples for statistically valid results. For example, at one of the studied projects, 107 drill holes were used for calibration of eU_3O_8 data.

32.3.2 Prompt Fission Neutron (PFN) Analyser

A PFN is a geophysical technique which overcomes the gamma-ray technology gap for disequilibrium (Penny et al. 2012). The PFN method uses a pulsed neutron source for emitting high energy neutrons to the rocks and it records the ratio of generated epithermal neutrons to thermal neutrons. This ratio is proportional to the U^{235} content in the rocks which allows direct measurement of uranium content and does not require equilibrium between uranium decay products (Penney et al. 2012). The uranium content determined by the PFN method is commonly denoted as pU_3O_8 instead of the eU_3O_8 used for uranium contents deduced from the gamma logs.

Currently the PFN is the main method for estimating uranium grade in the Australian ISL uranium projects (Penny et al. 2012), and is also

widely used in USA and in the former USSR. In particular, in Kazakhstan, no less than 20 % of the uranium resource estimation drill holes have to be logged using the PFN[1] technique.

Disadvantage of the PFN instruments is a high detection limit, approximately in the range of 0.01–0.025 % U_3O_8. However, this is improved at the 3rd generation of PFN instruments which reportedly have detection limit in the range of 0.005–0.008 % U_3O_8 (Drobov, personal communication).

PFN instruments need to be calibrated against known standards including consideration of the moisture content and salinity of water (Penney et al. 2012). PFN quality control includes weekly calibration and reconciliation of PFN grades against XRF core assays. Repeat runs of the PFN tool in the drill holes are used for estimation precision error (repeatability) of the PFN results. Both gamma-log and PFN require accurate measurement of the drill hole diameter for correction of the down-hole geophysical measurements.

32.3.3 Supplementary Geophysical Techniques

Application of the geophysical methods for estimating uranium grade requires knowledge of the drillhole diameter, which is measured by routinely using the down-hole calliper survey. Drill hole locations are also surveyed if holes are deeper than 100 m. Studies at the Beverly mine in Australia have shown that vertical drill holes drilled using mud rotary drilling technology deviate on average 10 m at a depth of 100 m (mine geologists, personal comm.). In Kazakhstan, surveying drillholes deeper than 100 m is mandatory.

[1]In USSR a different version of the prompt fission neutron logging technique was developed in early 1980s, called 'KND' and widely used in Russia, Uzbekistan and Kazakhstan for the estimation uranium resources in ISL projects

32.4 Drillhole Sample Assays

Sampling of the drill holes and chemical analysis of samples are necessary for accurate estimation resources of the ISL projects. In Kazakhstan, it is compulsory to collect and assay drill core samples through all mineralised intervals of the ISL projects. This is prescribed by the resource reporting guidelines in Kazakhstan. Representative samples are obtained by using triple tube diamond drilling technique. Drill hole samples are assayed for uranium and Th, Se, V, Mo, Sc, Re and As and organic carbon (C_{org}).

Carbonate content is assayed from the drill core samples and reported as CO_2 (wt%). This is the deleterious component for acid leach ISL method and the assay is used for estimating the acid consumption at the ISL operations. The CO_2 content is accurately estimated and reported for every mineralised domain.

The distribution of the drill core samples should be representative for the deposit covering the entire ore body. In Kazakhstan carbonate contents is determined using the 400 × 50 m sampling grid. However, the grid varies depending on complexity of the deposit. The entire intersection of the ore-bearing aquifer is sampled. The samples are also used for detailed geotechnical, petrographic and mineralogical study of the uranium mineralisation and their host rocks. In particular, the mineralised rocks need to be categorised by the grain size distribution profiles and porosity.

32.5 Data Quality and Mineral Resource Categories

In order to standardise reporting of the ISL uranium projects McKay et al. (2007) have suggested classifying resources depending on type and quality of data:

- Mineralisation in which grade is estimated using poorly calibrated 'historical' gamma ray data not corrected for disequilibrium can be classified as Inferred resources at best;

- Indicated resources are assigned if the gamma ray probe data are properly calibrated using PFN and supported by adequate allowance for disequilibrium;
- Measured resource status is assigned to mineralisation which is estimated by properly calibrated PFN data, hydrological and geotechnical characteristics are accurately estimated.

These criteria only address data quality. Drill spacing optimal for estimation of resources should be estimated for each deposit separately depending on geological and grade variability.

32.6 Geological and Geotechnical Logging of the Drillholes

32.6.1 Lithology

Feasibility of the ISL projects depends on permeability of the host rocks, which significantly varies depending on the rock types, facies and the oxidation state of the system. Thus, detailed lithological logging of the drill holes is very important and usually precedes the modelling of spatial distribution of the uranium grade. Lithological characteristics of the ore-bearing strata are deduced from the down hole electric survey logs. Two methods that are commonly used are apparent resistivity and self-potential, with electro-magnetic techniques used in highly saline conditions. Emphasis of the lithological interpretation is made on the following parameters:

- Grain sizes of the clastic sediments;
- Degree of the diagenetic lithification;
- Diagnostic and accurate location of the clay beds;
- Diagnostic and accurate locations of the carbonate beds, and;
- Oxidised state of the rocks.

The geophysical logs are supported by conventional petrographic logging of the drill cuttings, which includes the lithofacies and documentation of their colours. Colour of the rock chips assists in identification of the oxidation state. More detailed petrographic studies are made using drillhole samples.

Geophysical data and petrographic logs are used for cross-section interpretations and construction of the litho-stratigraphic model of the deposit.

32.6.2 Hydrogeology

Hydrogeological data used in ISL resource estimation include chemical composition of the ground waters, its pressure at the mineralised aquifers and ground water flow directions. In Kazakhstan, ground water temperature is also measured using down hole thermometry and monitored during production. High temperatures, exceeding 20°C (Zhalpak deposit, Kazakhstan) are a favourable factor for ISL project.

Water pressure within aquifers is estimated by systematic piezometer measurements made in the test drillholes distributed through the entire deposit. These techniques, together with pumping test run for estimating the permeability of the rocks, are at the core of the hydrogeological studies and were used systematically at all of the studied ISL projects. Distribution of the hydrogeological drillholes varies depending on complexity of the hydrogeological conditions of the deposit. In Kazakhstan, every uraniferous aquifer is studied by at least 3–5 hydrogeological drillholes, distributed at a distance of 1–5 km. Additionally 2–3 drillholes are drilled outside of the studied resource domain for estimation of ground water flow direction and velocity.

The chemical composition of the ground water controls the in-situ uranium recovery rates. For example, high chlorine contents can potentially lower uranium recovery. In Kazakhstan, aquifers hosted by Palaeogene sediments and all deposits in the Syrdarya basin are characterised by low salinity waters, concentration of the dissolved mineralisation is 0.3–1.0 g/l. Aquifers in the Shu-Sarysu basin hosted in Upper Cretaceous sediments is more saline, and concentration of mineralisation is in the range of 1.5–6 g/l.

32.6.3 Permeability

Permeability of the host strata is determined separately for all main lithological types of rocks. Example of filtration coefficient determined in the host rocks of the Budenovskoe deposit in Kazakhstan is shown in the Fig. 15.6b. Average filtration coefficients change from 9.8 m/day in conglomerates to 6.6 m/day in fine grained sands and drop to less than 1 m/day in the silty clay beds.

Permeability is determined initially by testing the drill core samples and, when a project matures, by using drill hole pump tests. The drill core samples are collected from all lithological types of rocks in the studied aquifer and should include samples from barren sediments outside of mineralised units. ISL mining is favoured when the permeability of mineralisation is higher than that of the enclosing sediments. Opposite relationships lead to excessive losses and/or dilution of leach solutions, significantly decreasing the economic efficiency of the ISL operation.

The samples are collected from specially drilled holes, which are distributed along the strike of mineralisation at a distance of 800–1600 m. Samples are collected every 3–5 m in uranium mineralisation and 3–10 m in overlying and underlying waste rocks. Two types of samples are studied, solid unbroken samples where sedimentary textures are well preserved and broken rocks, allowing a realistic estimation of the permeability ranges to be obtained for every lithotype.

Mature projects use down hole pump tests. These tests require estimation of speed and degree of dropping of the water level at the studied aquifer and the time needed for its restoration. The duration of the pumping tests differs depending on hydrogeological characteristics of the deposit. In Kazakhstan, pumping tests for aquifers hosted in Palaeogenic rocks last 1 to 3 days with pump tests for aquifers hosted in Upper Cretaceous rocks lasting up to 4 days.

These tests in addition to characterisation physical parameters of the studied aquifers that also provide water samples for chemical characterisation.

32.6.4 Porosity and Rock Density

The dry bulk density of the rocks is determined indirectly through geophysically estimated porosity of the host sediments and composition of the sand grains. The latest generation of PFN tools (generation 3) measure the porosity of the rock together with the uranium grade (Penny et al. 2012). The density can also be measured directly using core samples collected by Sonic drilling (Abzalov et al. 2011) or using triple tube diamond drilling. Rock densities of the sandstone uranium deposits are commonly varying within the range of 1.70–1.90 t/m^3.

32.7 Resource Estimation

Estimation resources of the sandstone-type deposits starts with construction of a litho-stratigraphic model of the deposit. These data are used for guiding correlation of the uranium intersections between drillholes when a 3D model of uranium mineralisation is constructed. The litho-stratigraphic model is also used as a background for the hydrogeological characterisation of the deposit.

32.7.1 Geological Model

Two approaches are currently used for construction of litho-stratigraphic models, conventional cross-sectional interpretations and geostatistical 3D modelling using plurigaussian method (Armstrong et al. 2011). Conventional geological cross-sections are subjective and their uncertainty cannot be quantified, which is the main limitation of this technique. Plurigaussian stochastic simulation method allows to generate multiple realisations of the litho-stratigraphic model, and to select the model with the highest likelihood (Fig. 26.12).

Table 32.2 Examples of cut-offs used for definition uranium resources

Deposit	Cut-off U_3O_8 (wt.%)
ISL mine/project	
Budenovskoe, Kazakhstan	0.010
Honeymoon, Australia	0.025
Open pit mine/project	
Rossing, Namibia	0.015
Ranger, Australia	0.020
Langer Heinrich, Namibia	0.025
Trekkopje, Namibia	0.010
Polymetallic underground operations	
Olympic Dam, Australia	30–70 US$/t

32.7.2 Estimation of Uranium Grade

Construction of uranium bodies can be made using 2D seam models (e.g. Beverly mine), or in 3D, constraining mineralisation by wireframes (e.g. deposits at the Great Divide basin). In both cases the mineralised intersections have to be defined at the every drillhole using a cut-off grade established for the given project (Table 32.2) and this is used for cross-sectional interpretation of the deposit (Fig. 32.2).

An alternative approach, which uses geostatistical criteria for constraining the mineralised domains, was tested at the Budenovskoe deposit (Abzalov et al. 2014). The method, which is based on constraining mineralisation using grade indictors, was initially proposed for orogenic gold deposits (Abzalov and Humphreys 2002a, b) and has not been applied before to sandstone type uranium mineralisation. Results of application of the method to the Budenovskoe deposit are highly encouraging, showing that rollfront structures can be reproduced in great detail using this technique.

For resource estimation purposes the constrained domains can be grouped together, ensuring that the created groups are geologically related and geostatistically stationary. Grouping of the domains was used by Abzalov (2010) for estimating resources of the complex uranium rollfront formed by multiple hydrothermal episodes. At this deposit, located in the Shu-Sarysu basin, the domains have been grouped using grade-thickness relationships of the mineralised intersections (Fig. 32.3). Thin lenses of high grade uranium were combined into an HN group (Fig. 32.3a) and separated from the second group containing thick layers of high grade uranium. The second group is referred as the HT group (Fig.32.3a). Third group includes low grade mineralisation (LG) that usually present as narrow and discontinuous lenses. These groups occupy different parts of the rollfront forming three separate ribbon-like bodies elongated in the north-south direction along the strike of the rollfront (Fig. 32.3b). The spatial distribution of the domains combined together into the HN, HT and LG groups (Fig. 32.3b) is in good accordance with their grade-thickness characteristics (Fig. 32.3a) and confirms the validity of the defined groups.

32.7.3 Geostatistical Resource Estimation

Sandstone-type uranium mineralisation is characterised by a positively skewed statistical distribution of U_3O_8 grades with coefficient of skewness commonly exceeding 25. Two typical histograms of the uranium grades (Fig. 32.4) shows long tails created by the small numbers of high grade samples. This represents an additional challenge for estimation resources of the sandstone-type deposits, which together with extremely complex geometry of this type deposits makes their resource estimation a highly challenging process. Conventional variograms of U_3O_8 grades are usually very noisy therefore they are commonly modelled by transforming data to Gaussian distributed variables or using grade indicators (Goovaerts 1997; Chiles and Delfiner 1999). Both of these approaches can be used and usually improve the variograms (Fig. 32.5). Further improvement can be achieved if the geometry of the uranium rolls is simplified by straightening them using one of the available unfolding algorithms which are available within the majority of commercially available mining software packages.

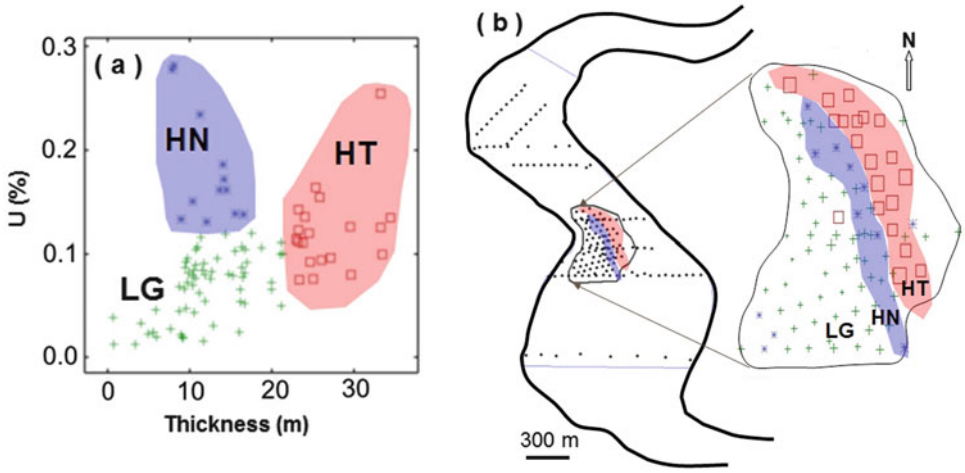

Fig. 32.3 Grouping of the domains by their grade-thickness characteristics and spatial distribution. Roll-type deposit in Shu-Sarysu basin, Kazakhstan (Abzalov 2010; Abzalov et al. 2014). *LG* low grade, *HN* high grade narrow, *HT* high grade thick: (**a**) grade vs. thickness diagram of the mineralised intersections; (**b**) map showing spatial distribution of the mineralised intersections

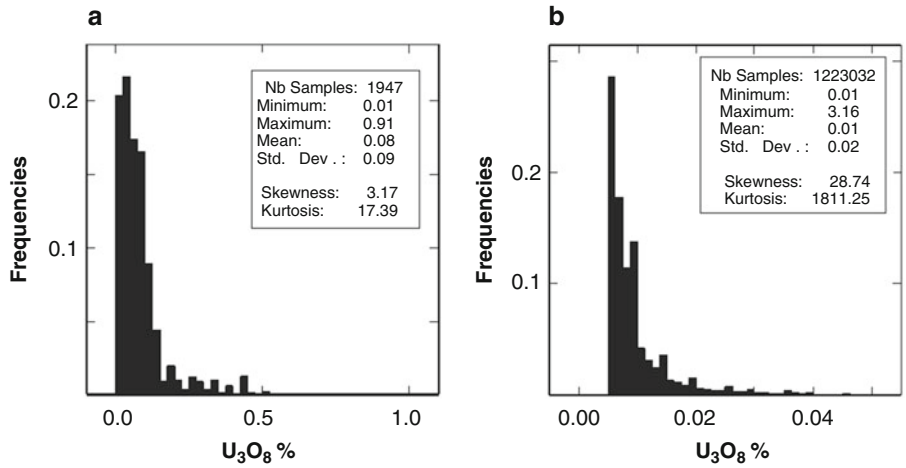

Fig. 32.4 Histograms of the uranium grades (Abzalov et al. 2014): (**a**) Budenovskoe deposit, Shu-Sarysu basin, Kazakhstan. Composite length is 0.5 m; (**b**) deposit in Great Divide basin, USA. Composite length is 0.6 m

Sandstone-type uranium mineralisation is characterised by strong variability of the uranium grade at short distances. In general, variography analysis suggests that 60–80 % of the global variance at the studied sandstone-type uranium deposits occurs at distances of 30–80 m between data points (Fig. 32.5). This observation accords well with the common practice of estimating Measured resources of the ISL uranium projects using tight drilling, commonly 25−50 × 25 m.

32.8 Viability of the Resources

The final stage of definition of resources of the ISL uranium projects is construction of the blocks which have reasonable prospects for eventual economic extraction (JORC 2012). This requires integration of the litho-stratigraphic model with the uranium grade model and implementing geological, hydrogeological, geotechnical and eco-

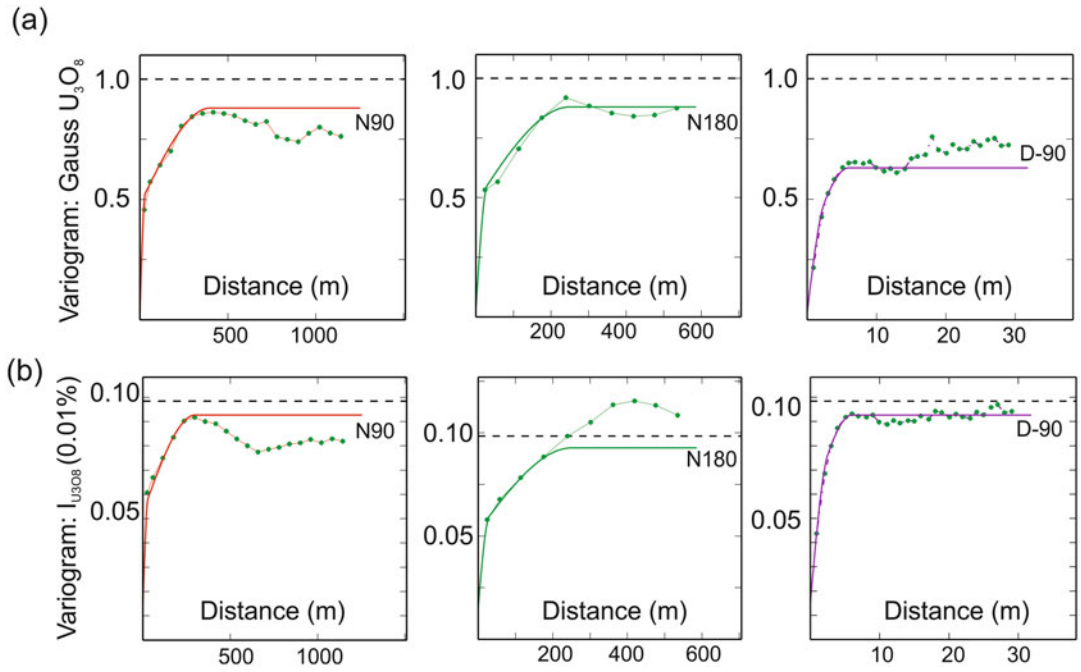

Fig. 32.5 Variograms (experimental and model) of transformed U_3O_8 grade at the rollfront uranium deposit in Great Divide basin, USA. N90 is a direction along the strike of the roll, N180 across the strike, D-90 vertical (Abzalov et al. 2014): (**a**) Gaussian transformed; (**b**) Indicator variable ($U_3O_8 > 0.01\,\%$)

nomic parameters for constraining the potentially mineable blocks. The parameters commonly used for constraining resource blocks are overall contained metal (product of grade by thickness), thickness of the mineralised intersection, thickness of the waste rocks in the constrained domains, thickness of the impermeable strata in the block and the concentration of the carbonates (Table 32.3). Contained metal is used for initial definition of the resource blocks. At the Kazakhstan deposits, the economic mineralisation is delineated at a 0.06 m*%U_3O_8 cut off value.

The constrained mineable block is further checked and corrected for internal waste and thickness of the enclosed impermeable layers, assuring that overall permeability of the rocks in the constrained block should is not less than 1.0 m/day (Table 32.3). Mineralisation which does not meet the criteria shown in the Table 32.3 is reported as a low grade non-economic resource.

Concentration of carbonates is the main parameter for metallurgical characterisation of the ISL uranium resources, which requires determining a leaching system. Two chemical leaching systems are used: acid and alkali (Bush 2000; IAEA 2001). Acid leaching is faster and produces better recovery of uranium than alkaline leach. At the Honeymoon mine, Australia, direct comparison of the two approaches has shown that acid leach achieves 80 % recovery of the in situ resources approximately four times faster than using alkaline leach method (Bush 2000). Acid leaching also allows recovery of some by-product metals (Karimov et al. 1996). However, the acid leaching approach becomes inefficient when the host rocks contain carbonates because of excessively high acid consumption. In general, when the CO_2 content of the host rocks exceeds 2 %, acid leaching becomes economically non-viable for exploitation of the deposit using acid leach ISL technology.

An alternative approach is alkaline (sodium carbonate) leaching, which has been successfully used for sandstone deposits containing carbonates. The alkaline leach method is characterised by a high selectivity for uranium with a minimal attack on most gangue minerals, therefore, in

Table 32.3 Parameters applied for constraining economic mineralisation of uranium-ISL projects in Kazakhstan

Category	Parameters
The cut-off grade	0.01 % U
Total metal content per drill hole intersection (grade × thickness)	The constrained interval should contain not less than 0.060 m% U per drill hole
Total metal content per resource block	The constrained resource block (domain) should contain not less than 0.1 m% U
Internal dilution	The maximum thickness of internal waste within the mineralised envelops is 1 m
	Overall thickness of internal waste intervals included in resource block (domain) should not exceed 6 m
	The minimum mineralisation-to-barren ratio is 0.75. This is a ratio between the number of economic resource holes to the total number of holes within the outline of a resource block
Selectively minable units	The minimum area of an isolated resource block is 40,000 m^2, maximum size is 300,000 m^2
Permeability	Minimum permeability of host strata is 1.0 m/day
	The content of silt and clay material (<0.05 mm) per mineralisation thickness is not to exceed 20 % of mineralised intersection
Metallurgical constrains for acid leach	Carbonate content for acid leaching should be low, $CO_2 < 2$ %
	Where CO_2 content exceeds 2 % alkaline leach technology is a preferred option

general, this method is less corrosive than sulphuric acid leach. These characteristics partially compensate for lower kinetics, less aggressiveness and the higher energy consumption of the alkaline leach method.

The parameters presented in Table 32.3 are the basis for developing modifying factors for conversion resources to reserves and, in general, can be used as an approximate guide for planning resource estimation programmes at the uranium ISL projects. However, it should be remembered that these parameters are project specific and can vary depending on mineralisation depth, composition and permeability of the host rocks and aquifer characteristics. Thus, the accurate values of the modifying factors are developed empirically, by using field leach tests. The pilot production of uranium is a strict requirement for feasibility studies of the ISL uranium projects.

32.9 Reconciliation of the Resources

Publicly available data on reconciliation of the ISL uranium resources are very limited. In Kazakhstan the reported recovery is approximately 90 %, although lower than expected recovery was reported at the Budenovskoe project, albeit in an early stage of production meaning that recovery rates can improve. Reported recovery rates at the Australian ISL uranium operations are significantly lower at 60–70 %.

References

Abzalov MZ (2010) Optimisation of ISL resource models by incorporating algorithms for quantification risks: geostatistical approach. In: Technical meeting on in situ leach (ISL) uranium mining, International Atomic Energy Agency (IAEA), Vienna, 7–10 June 2010

Abzalov MZ (2012) Sandstone hosted uranium deposits amenable for exploitation by in-situ leaching technologies. Appl Earth Sci 121(2):55–64

Abzalov MZ, Humphreys M (2002a) Resource estimation of structurally complex and discontinuous mineralisation using non-linear geostatistics: case study of a mesothermal gold deposit in Northern Canada. Explor Min Geol J 11(1–4):19–29

Abzalov MZ, Humphreys M (2002b) Geostatistically assisted domaining of structurally complex mineralisation: method and case studies. Geostatistically assisted domaining of structurally complex mineralisation: method and case studies. In: The AusIMM 2002

conference: 150 years of mining, Publication series no 6/02, pp 345–350
Abzalov MZ, Paulson O (2012) Uranium deposits of the great divide Basin, Wyoming, USA. Appl Earth Sci 121(2):76–83
Abzalov MZ, Dumouchel J, Bourque Y, Hees F, Ware C (2011) Drilling techniques for estimation resources of the mineral sands deposits. In: Proceedings of the heavy minerals conference 2011, AusIMM, Melbourne, pp 27–39
Abzalov MZ, Drobov SR, Gorbatenko O, Vershkov AF, Bertoli O, Renard D, Beucher H (2014) Resource estimation of *in-situ* leach uranium projects. Appl Earth Sci 123(2):71–85
Armstrong M, Galli A, Beucher H, Le Loc'h G, Renard D, Doligez B, Eschard R, Geffroy F (2011) Plurigaussian simulation in geosciences, 2nd edn. Springer, Berlin, p 149
Bush PD (2000) Development considerations for the Honeymoon ISL uranium project. CIM Bull 93(1045):65–73
Chiles J-P, Delfiner P (1999) Geostatistics: modelling spatial uncertainty. Wiley, New York, p 695
Dahlkamp FJ (1993) Geology of the uranium deposits. Springer, Berlin, p 460
Goovaerts P (1997) Geostatistics for natural resources evaluation. Oxford University Press, New York, p 483
IAEA (2001) Manual of acid in situ leach uranium technology, TECDOC-1239. International Atomic Energy Agency, Vienna, p 283
JORC Code (2012) Australaisian code for reporting of exploration results, mineral resources and ore reserves. AusIMM, Melbourne, p 44
Karimov KhK, Bobonorov NS, Brovin KG, Goldshtein RI, Korsakov YuF, Mazurkevich AP, Natalchenko BI, Tolstov EA, Shmariovich EP (1996) Uranium deposits of the Uchkuduk type in the Republic of Uzbekistan. FAN, Tashkent, Uzbekistan, p335 (in Russian)
McKay AD, Stoker P, Bampton KF, Lambert IB (2007) Resource estimation for *in-situ* leach uranium projects and reporting under the JORC Code. In: Uranium reporting workshop, Uranium and the JORC Code. AusIMM, Adelaide branch, Adelaide, Australia
Penney R (2012) Australian sandstone-hosted uranium deposits. Appl Earth Sci 121(2):65–75
Penney R, Ames C, Quinn D, Ross A (2012) Determining uranium concentration in boreholes using wireline logging techniques: comparison of gamma logging with prompt fission neutron technology (PFN). Appl Earth Sci 121(2):55–64
Petrov NN, Berikbolov BR, Aubakirov KhB, Vershkov AF, Lukhtin VF, Plekhanov VN, Cherniakov VM, Yazikov VG (2008) Uranium deposits of Kazakhstan (exogenic), 2nd edn. Volkovgeologiia, Almaty, Kazakhstan, p 318 (in Russian)
Pool TC, Wallis CS (2006a) Technical report on the South Inkai uranium project, Kazakhstan. Prepared for Urasia Energy (BVI) Ltd. Roscoe Postle Associates Inc, Toronto, Canada
Pool TC, Wallis CS (2006b) Technical report on the Akdala uranium mine, Kazakhstan. Prepared for Urasia Energy (BVI) Ltd. Roscoe Postle Associates Inc, Toronto, Canada
Pool TC, Wallis CS (2006c) Technical report on the North Kharasan uranium project, Kazakhstan. Prepared for Urasia Energy (BVI) Ltd. Roscoe Postle Associates Inc, Toronto, Canada

Iron-Oxide Deposits

33

Abstract

Project evaluation procedures described in this chapter are mainly based on examples from the Hamersley Province in the Western Australia containing deposits associated with the banded iron-formation and the goethitic palaeochannel deposits.

Iron-oxide deposits are evaluated using large diameter (HQ and larger) diamond drill core drilling and RC drilling. Proportions between these techniques differ at the studied projects. Distances between drill holes vary from 25 × 25 m used for definition Measured resources at the West Angelas deposit to 300 × 200 m, which was used for definition Inferred resources of the Yandi deposit.

Rock density at the iron ore deposits can change at the short distance from 1.5 to 4 t/m^3 depending on contents of the iron-oxide minerals and presence of the cavities. Accurate estimation of the tonnage factor requires systematic measurement of the rock density along the drill holes which is commonly determined using the down-hole gamma-gamma logging which are verified by laboratory measurements.

Samples are assayed by conventional XRF analysis for Fe, Si, Al, Ti, Mn, Ca, P, S, Mg, K, Zn, Pb and Cu which are estimated into resource block model by Ordinary kriging. In addition to these elements, loss on ignition (LOI) is determined using 2 and 5 g pulverised sub-sample placed into a ceramic crucible and ignited to 1050 °C for 45 min.

Keywords

Hamersley province • Iron-ore • Mineral resource • Ore reserves

33.1 Geological Constraints of the Resource Models

Project evaluation procedures described in this chapter are mainly based on examples from the Hamersley Province in the Western Australia (Fig. 33.1, Table 33.1) (Abzalov et al. 2007, 2010; Sommerville et al. 2014). The province contains numerous iron ore deposits associated with the banded iron-formation (BIF) occurring in Brockman and Marra Mamba Iron Formations which are characterised by extensive

M. Abzalov, *Applied Mining Geology*, Modern Approaches in Solid Earth Sciences 12,
DOI 10.1007/978-3-319-39264-6_33

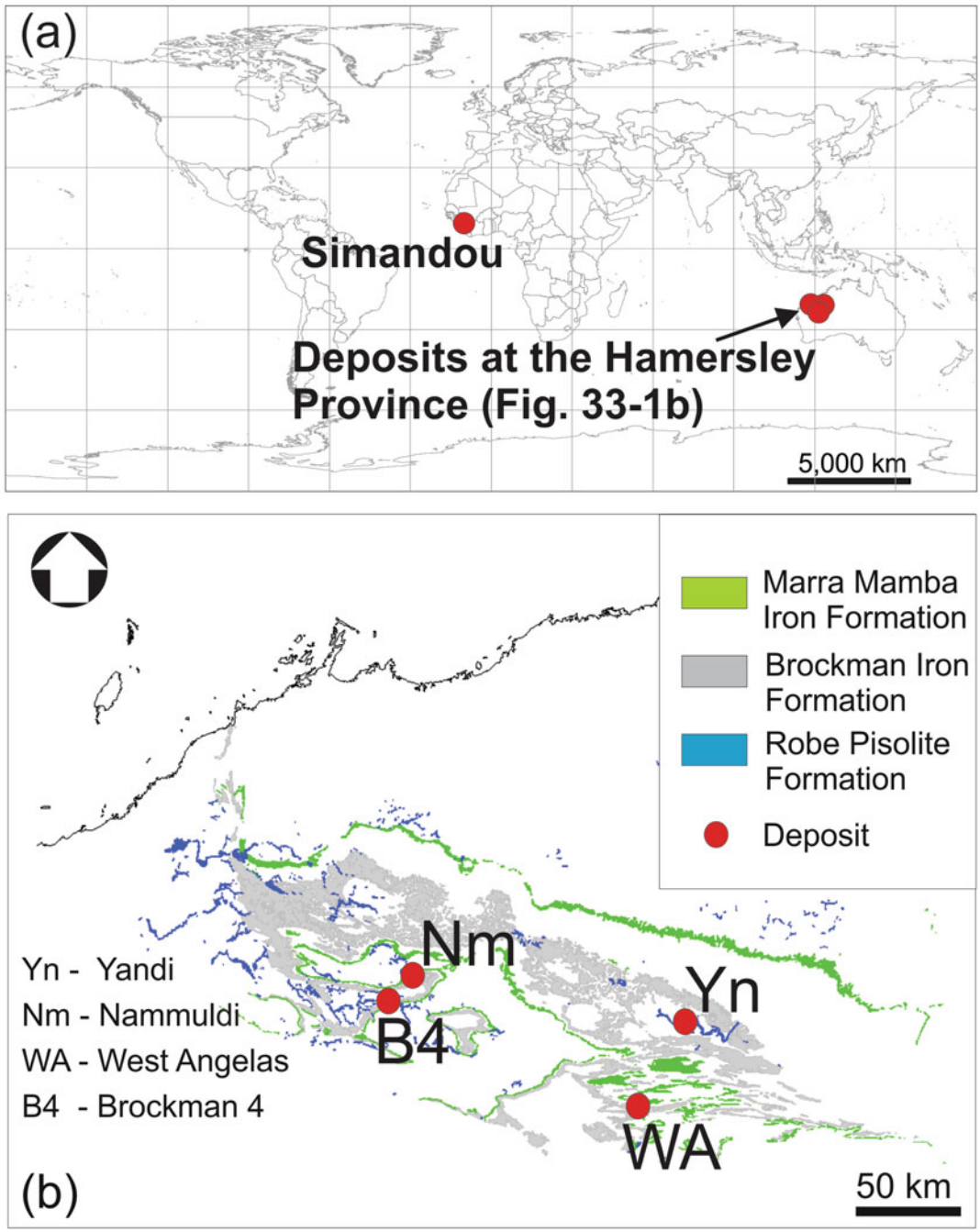

Fig. 33.1 (**a**) World map showing location of the studied iron-ore deposits; (**b**) Generalised geological map of the *Hamersley Province*

concentration of high grade iron ore (Harmsworth et al. 2001). The province also contains goethitic palaeochannel deposits, usually referred as Channel Iron Deposit (CID-type), emphasising that their host structure is the course of an ancient river (Harmsworth et al. 2001, Ramanaidou et al. 2003). These deposits are found mainly in the Robe River and Yandicoogina Creek palaeo-drainage systems (Harmsworth et al. 1990).

Table 33.1 Resource estimation data at the selected deposits

Deposit name	Type	Resource and past production		Drilling grids by resource categories		
		Tonnage (million tonnes)	Grade (Fe, %)	Inferred	Indicated	Measured
West Angelas	BIF-derived	440	62.1	200 × 50	50 × 50	25 × 25
Nammuldi	BIF-derived	250	62.3	200 × 50	100 × 50	50 × 50
Brockman 4	BIF-derived	47	62.3	200 × 100	100 × 100	50 × 50
Simandou	BIF-derived	>2000	64.0	200 × 200	100 × 100	50 × 50
Yandi	CID	930	58.0	300 × 200	200 × 100	100 × 50

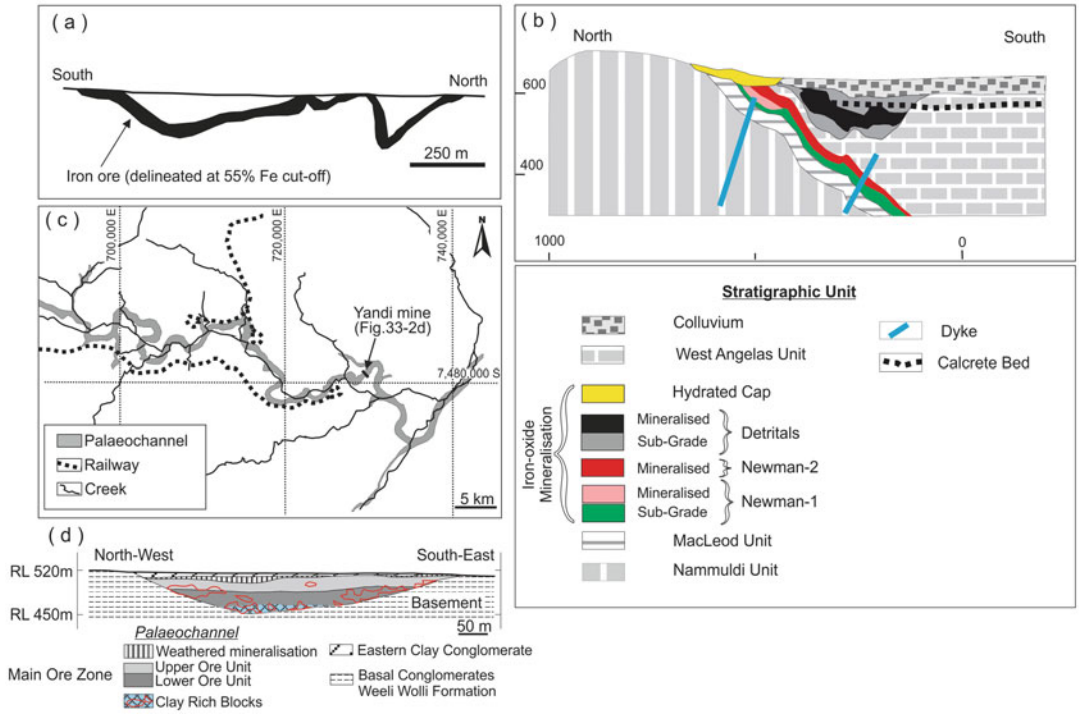

Fig. 33.2 Geology of the iron-ore deposits in the Hamersley basin. Location of the deposits is shown on the Fig. 33.1: (**a**) Cross-section of the West Angelas BIF-derived deposit; (**b**) Cross-section of the BIF-derived Nammuldi deposit showing distribution of the different types of mineralisation; (**c**) Yandicoogina palaeochannel that hosts Yandi deposit; (**d**) Cross-section of the Yandi deposit

Evaluation procedures developed at the Hamersley basin (Abzalov et al. 2010; Sommerville et al. 2014) have been implemented at the Simandou project in Guinea, also representing a BIF-derived high grade iron-oxide (haematite) deposit (Fig. 33.1, Table 33.1).

A BIF-derived iron-ore deposit in the Hamersley basin have been developed as a result of remobilisation of the iron-oxides from Precambrian banded iron formation (Harmsworth et al. 2001, Ramanaidou et al. 2003; Morris and Kneeshaw 2011). As a consequence the iron-oxide mineralisation is essentially a stratiform inheriting the stratified structure of the host sequences (Fig. 33.2a, b).

Contacts between stratigraphic units and mineralisation are usually distinct and in places are marked by shale bands (Fig. 33.3). Iron-oxide mineralisation occurs as the continuous layers which exhibit normal stratigraphic relationships with the host sedimentary sequence (Fig. 33.3),

however grade often unevenly distributed within the ore-bearing layer (Fig. 33.4).

Intense weathering of these deposits creates a supergene alteration zone which is commonly referred as a 'hydrated cap'. A specific feature of the rocks distributed in the 'hydrated cap' is their vuggy textures with the voids locally filled by kaolinite and silica. This zone is characterised by an erratic iron grade distribution, presence of numerous clay pods and zones of supergene silica enrichment. Footwall contact of the 'hydrated cap' is very irregular as it is complicated by steeply dipping structures which locally control penetration of the supergene alterations to a significant depth.

Palaeochannel deposits (CID-type) are second commercially most important type of the iron-oxide accumulations in the Hamersley province. The deposits occur in meandering palaeochannels filled with pisolitic goethite-hematite iron mineralisation (Fig. 33.2c). The pisoliths (pea-stone) generally range in diameter from 1 to 5 mm, with most less than 2 mm. They typically have haematitic cores surrounded by several goethitic rims (cortices). The pisoliths are cemented by a goethitic matrix to form a hard, brittle rock.

When viewed at the mining bench scale the CID ore is jointed, locally cavernous and vuggy. The joints and cavities are commonly infilled with clay and/or goethite (Fig. 33.2d). Quality of the iron ore at the CID deposits is better in the centre of the palaeochannels, where ore has lower levels of SiO_2 and Al_2O_3 than at the edges.

Detrital mineralisation represents a transported regolith developed as a palaeochannel over the West Angelas shales (Fig. 33.2b). It also contains clay pods with dimensions varying from several metres to several tens of metres.

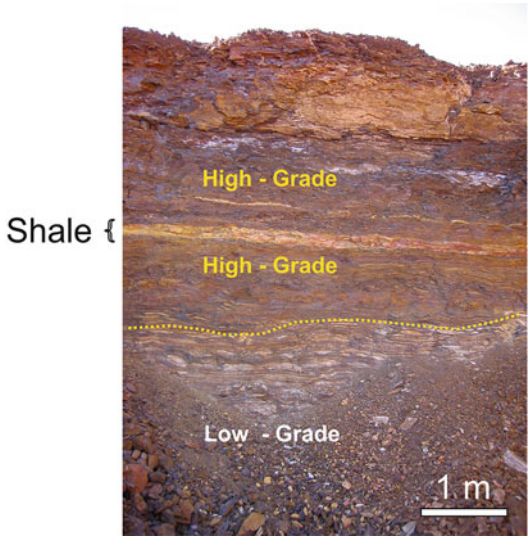

Fig. 33.3 Contacts between stratigraphic units exposed at the Nammuldi open pit

33.2 Resource Estimation Drilling

Iron-oxide deposits are evaluated using large diameter (HQ and larger) diamond drill core drilling and RC drilling. Proportions between these techniques differ at the studied projects. At Brockman 4 resources were estimated mainly

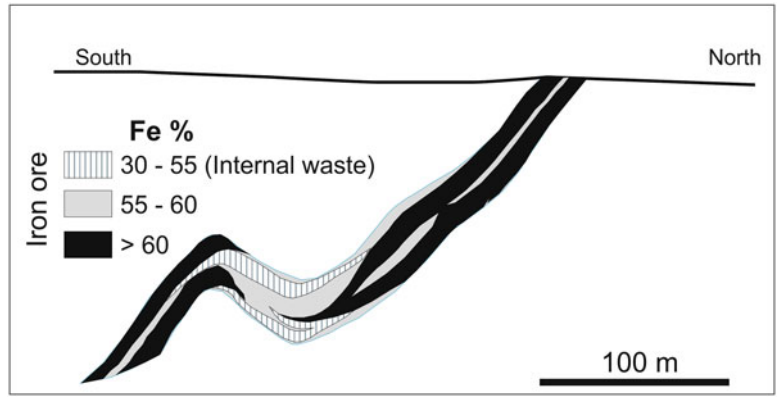

Fig. 33.4 Cross-section of the Nammuldi deposit showing distribution of the iron grade

by RC drilling (3673 RC holes and 5 HQ size diamond drill holes) (Sommerville et al. 2014). For comparison, resources of the E-F lenses of the Nammuldi deposit were estimated using 872 RC drill holes and 70 diamond core drill holes.

Distances between drill holes vary from 25 × 25 m used for definition Measured resources at the West Angelas deposit to 300 × 200 m, which was used for definition Inferred resources of the Yandi deposit (Table 33.1).

33.3 Sampling and Assaying

Example of the sampling protocol used at the West Angelas deposit is as follows:

- 2–3 kg sample split down to a sub-sample of 1 kg;
- Sub-sample is dried and then pulverised to 160 μm (95 % passing);
- 0.75 g aliquot is collected from the of pulverised material and fused into a glass disk at 1050 °C;
- Fused disk of sample is assayed by conventional wave-length dispersive XRF analysis for Fe, Si, Al, Ti, Mn, Ca, P, S, Mg, K, Zn, Pb, and Cu;
- LOI (loss on ignition) analysis was done using 2 g and 5 g pulverised sub-sample, weighed then placed into a ceramic crucible and ignited to 1050 °C for 45 min, weight loss measured and LOI calculated.

The protocol is robust and allows to obtain good quality assay data. When protocol rigorously followed the precision error of the assayed Fe, Al_2O_3, SiO_2 and LOI values lies in the range from 2 to 8 CV % (Abzalov 2008).

33.4 Dry Bulk Density of the Rocks

Rock density at the iron ore deposits can change at the short distance from 1.5 to 4 t/m^3 depending on contents of the iron-oxide minerals and presence of the cavities (Fig. 33.5).

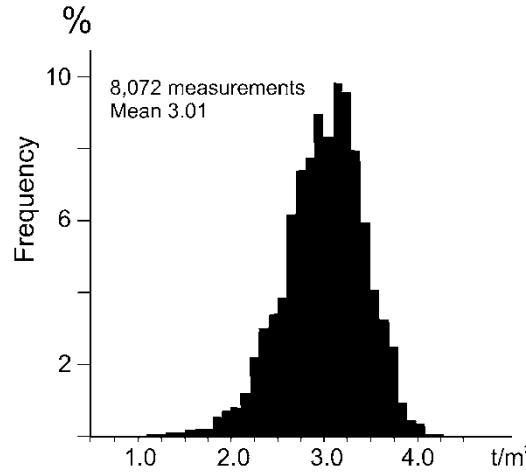

Fig. 33.5 Histogram of the rocks density (DBD) at the Nammuldi deposit

Accurate estimation of the tonnage factor requires systematic measurement of the rock density along the drill holes through assuring the good coverage of the entire deposit. In the Hamersley basin the rock densities are primarily determined using the down-hole gamma-gamma logging which are verified by laboratory measurements made on the drill core samples.

33.5 Estimation Resources and Reserves

Variables which are estimated into the resource block model of the iron ore deposits at the Hamersley province include Fe, Si, Al, P, Mn, S, TiO_2, CaO, MgO, LOI and density. The estimation is commonly made using Ordinary kriging (OK) or co-kriging (COK) methods. The general principles of estimation are as follows (Sommerville et al. 2010):

- The same kriging search neighbourhood is used for all estimates of chemical variables in the same domain. This is necessary to assure that sum of the oxides lie within the range of 98 to 102 %;
- Density is estimated independently of chemical variables;

- Estimation is made using hard boundaries approach;
- Unfolding is used for estimation resources of the stratified mineralisation;
- Special attention is made to drill hole samples which have high manganese values to reduce their smearing in the block model.

References

Abzalov MZ (2008) Quality control of assay data: a review of procedures for measuring and monitoring precision and accuracy. Explor Min Geol J 17(3–4):131–144

Abzalov MZ, Menzel B, Wlasenko M, Phillips J (2007) Grade control at the Yandi iron ore mine, Pilbara region, Western Australia: comparative study of the blastholes and RC holes sampling. In: Proceedings of the iron ore conference 2007, AusIMM, Melbourne, pp 37–43

Abzalov MZ, Menzel B, Wlasenko M, Phillips J (2010) Optimisation of the grade control procedures at the Yandi iron-ore mine, Western Australia: geostatistical approach. Appl Earth Sci 119(3):132–142

Harmsworth RA, Kneeshaw M, Morris RC, Robinson CJ, Shrivastava PK (2001) BIF-derived iron ores of the Hamersley Province. In: Hughes FE (ed) Geology of the mineral deposits of Australia and Papua New Guinea. AusIMM, Melbourne, pp 617–642

Morris RC, Kneeshaw M (2011) Genesis modelling for the Hamersley BIF-hosted iron ores of Western Australia: a critical review. Aust J Earth Sci 58: 417–451

Ramanaidou ER, Morris RC, Horwitz RC (2003) Channel iron deposits of the Hamersley Province, Western Australia. Aust J Earth Sci 50:669–690

Sommerville B, Boyle C, Brajkovich N, Savory P, Latscha AA (2014) Mineral resource estimation of the Brockman 4 iron ore deposit in the Pilbara region. Appl Earth Sci 123(2):135–145

Bauxite Deposits

34

Abstract

The procedures used for bauxite resource estimation are summarised using examples from Australia, Africa, South America and Asia. In the all studied cases the bauxite resources were estimated by drilling and sampling drill holes at 0.25–0.5 m intervals. Short sampling intervals are necessary for accurate estimation of the mineralisation contacts. Samples of the non-consolidated bauxites usually beneficiated by sieving and removing the barren fine grained material prior to chemical assays. Consolidated bauxites are not beneficiated and processed in a conventional manner. Bauxites density is preferably measured using the sand replacement method which is a formally certified technique for measuring bauxite density at the Australian deposits.

Bauxites grade is estimated using conventional geostatistical techniques, which are commonly applied after geometry of the bauxite seam is flattened using 'equal thickness unfolding' method, or, in some cases, using 'top flattening' approach. Conversion resources to the ore reserves requires the following mining and processing conditions to be taken into considerations:

- Haulage distance;
- A vertical mining selectivity of 0.25–0.5 m;
- Pre-production infill drilling is usually used for grade control purposes;
- Grindability of the bauxites and quantification of the Bond Work Index;
- Optimal mesh size for bauxite beneficiation;
- Detailed chemical and mineralogical characterisation of the crude bauxite, including deleterious components, in particular iron and silica;
- Characterisation of the pre-desilication behaviour of the bauxite;
- Characterisation of the alumina extraction;
- The refinery parameters, including recovered alumina, refinery caustic consumption and red mud loading;

M. Abzalov, *Applied Mining Geology*, Modern Approaches in Solid Earth Sciences 12,
DOI 10.1007/978-3-319-39264-6_34

- Presence of the organic carbon, oxalate formation rate and carbonate formation rate;
- The mud settling rate, mud compaction and overflow clarity.

Keywords
Bauxite • Resource • Reserves • Pisolite • Weipa • Gove • Sangaredi • Amargosa

The procedures used for bauxite resource estimation are summarised using several representative deposits in Australia, Africa, South America and Asia (Fig. 34.1; Table 34.1). Most of the studied deposits are mined by large-scale open pit methods typically producing several million tonnes of bauxite a year over a mine life of 20–40 years (Bardossy and Aleva 1990).

The data presented include different types of bauxites, varying from non-consolidated pisolitic mineralisation (Weipa) to intensely lithified bauxites beds (Sangaredi) and buried paleo plateaus (Az Zabira) (Fig. 34.1, Table 34.1). Studied deposits also include examples of a complexly zoned bauxite strata, represented by irregular intercalation of the different types of sediments (Fig. 34.2).

34.1 Geological Constraints of the Resource Models

34.1.1 Shape of the Bauxite Plateaus

Accurate estimation of bauxite tonnage is a very challenging task because of the irregular geometry of the bauxite plateaus which are strongly dissected by erosional troughs and creeks making the plateau edges extremely irregular. Delineation of the boundaries of such plateaus by drilling is inefficient and is excessively time consuming, expensive and inaccurate. An alternative approach commonly used in the past was based on the interpretation of satellite images. The modern practice is to delineate plateau edges using airborne surveying techniques which are significantly more accurate than satellite images. The technology includes airborne radar survey or airborne laser survey. The radar survey used at the Trombetos deposit in Brazil has a resolution of 2.5 m per pixel which produces accurate edges of the bauxite plateaus. This technique also simultaneously generates the digital terrain model, which accurately represents the topographic surface even in presence of dense vegetation because the wave length can be adjusted to ensure that signals are penetrate to ground.

At the Gove deposit the plateau edges are currently delineated by airborne laser survey which also produces noticeable improvement in the interpreted geometry of the bauxite ore bodies.

34.1.2 Contacts

Bauxite seam contacts are usually sharp but can be highly irregular. Special geostatistical studies undertaken at the Weipa and Andoom deposits have shown that the geometry of the footwall contact is characterised by a large uncertainty exceeding that of the bauxite alumina grade, content of the deleterious components, and thickness of mineralisation (Abzalov and Bower 2009, 2014).

The procedure of constraining the bauxite seams are as follows. First, it is necessary to study the vertical profiles of the laterite sequence with an emphasis on changes of the chemistry through the bauxite contacts. When contacts are sharp, the bauxite grade is modelled and estimated using a hard-boundary approach, without diluting the mineralised samples by the low-grade samples located outside of the contacts.

Sharp contacts are characterised by a rapid change in chemistry between the bauxite and

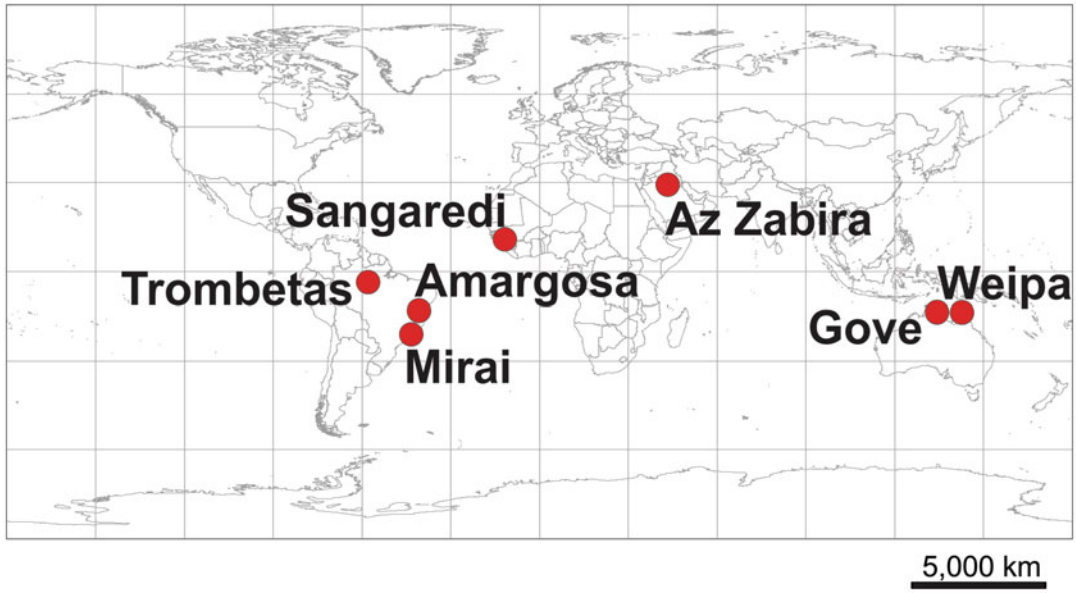

Fig. 34.1 World map showing location of the studied bauxite deposits

their host strata (Fig. 34.3). This is the most common type of bauxite contacts observed at most of the studied deposits Alternatively, when contacts are gradational, the laterite changes gradually produce a gentle slope of the curve on the diagram depicting the average composition of the drill hole samples. Such contacts are less common at the studied bauxite deposits. When they are encountered, the grade of the bauxites is modelled and estimated using a soft-boundary approach.

Second, contact surfaces are delineated geostatistically. Based on personal experience the author suggests delineating bauxite contacts using Ordinary co-kriging. For the upper contact the drill hole piercing points are used as a target (i.e. main) variable. The auxiliary variable is a topographic surface derived from the digital terrane model. The footwall contact is modelled by Ordinary co-kriging using bauxite thickness as a target variable and the upper contact as an auxiliary variable (Goovaerts 1997; Chiles and Delfiner 1999).

The same approach can be used when a bauxite seam includes several different units which need to be modelled separately. However, it is important not to over complicate the geological model because this increases resource model uncertainty and risks of estimation errors.

34.1.3 Vertical Profile of the Bauxite Seams

Bauxite seams often exhibit strong vertical zoning (Fig. 34.2) which complicates the estimation of their resources. Two of the most common types of the vertical bauxite seam profiles are shown in Fig. 34.4.

Gradational zoning is characterised by a gradual decrease in Al_2O_3 and an increase in SiO_2 towards the upper and lower contacts of the bauxite seam (Fig. 34.4a). This type of zoning is best expressed at the deposits of the Weipa plateau. Definition of ore grade and classification of the bauxite products depends on their overall chemistry, therefore resource models of the bauxite deposits need to accurately reproduce the vertical profiles of Al_2O_3 and SiO_2. This is usually achieved by applying a special unfolding algorithm, referred to as the 'equal thickness unfolding' method. This algorithm flattens geological strata and equalises its thickness by changing the vertical coordinates of the drill hole

Table 34.1 Geological characteristics of the bauxite deposits

Deposit	Resources and past-production			Average thickness (m)	Density of bauxites (t/m^3)	Bauxite textures	Bauxite mineralogy	Mineralisation age	Protolith	References
	Tonnage (million tonnes)	Grade								
		Al_2O_3 %	SiO_2 %							
Weipa	3440	55.1	4.3	2.1	1.60	Loose pisolite (4–9 mm); Blocky bauxite (30–300 mm)	Gibbsite; Boehmite; Quartz; Goethite; Kaolinite; Hydro-Haematite; Maghemite; Anatase	Tertiary	Bulimba sediments of tertiary age	Schaap (1990) and Abzalov and Bower (2009)
Gove	252	50.4	5.0	3.7	1.79[a]	Loose pisolite; Cemented pisolite; Tubular bauxite	Gibbsite; Boehmite; Quartz; Kaolinite; Goethite; Leucoxene; Rutile	Tertiary	Arkozic and quarzose sandstones of Yirkkala formation, Late Albian	Lillehagen (1979) and Ferenczi (2001)
Sangaredi (Halco lease)	990.6 (4212.4)	50.9 (48.9)	1.9 (2.1)	25	1.87[b]	Cemented pisolite; Fine grained massive bauxite (white bauxite); In situ lateritic bauxite	Gibbsite; Quartz; Kaolinite; Goethite	Tertiary	Schists and sandstones of devonian age intruded by dolerite	
Trombetos	Not available			4.3	1.70	In situ lateritic bauxite; minor loose pisolite	Gibbsite constitute 81 % of ore; boehmite <1 %; Kaolinite; Ilmenite	Tertiary	Basal conglomerates of the barreiras series in which diorite and quartzite pebbles are predominant	Grubb (1979)
Az Zabira	Not available			6.8	2.03	Cemented pisolite	Gibbsite; Boehmite; Quartz; Goethite; Haematite	Early cretaceous	Intercalation of jurassic sandstone and kaolinitic claystone	

[a]Density varies from 1.54 t/m^3 of loose pisolite layer to 1.89 t/m^3 of cemented soft bauxite layer
[b]1.87 t/m^3 is used as average density for the bauxite located above 190 m RL. Residual basal bauxite has density of 2.00 t/m^3

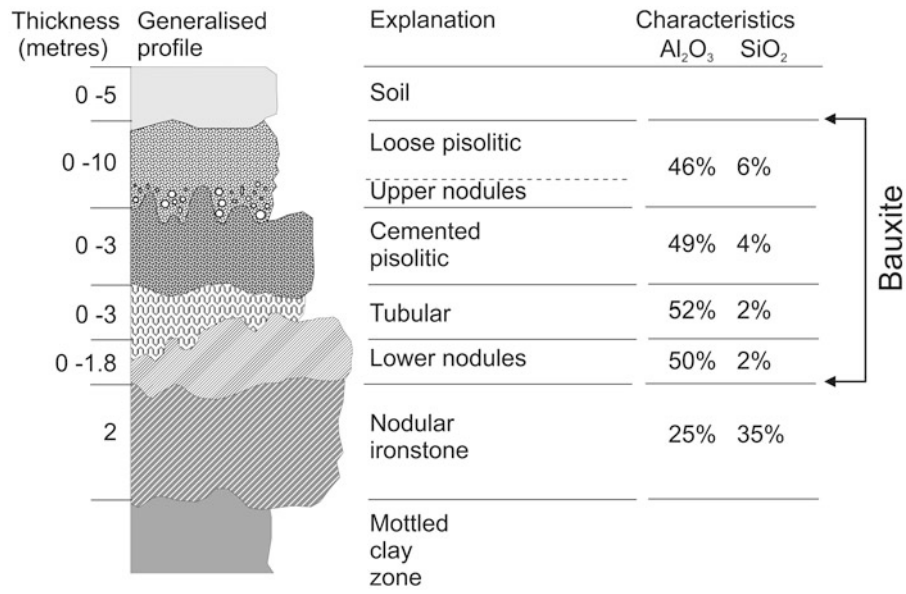

Fig. 34.2 Bauxite profile of the Gove deposits (Modified after Lillehagen (1979), Ferenczi (2001), Abzalov and Bower (2014))

samples, hence normalising the thickness. The same transformation is made to the block model.

Another type of zoning is represented by irregular intercalation of the different types of sediments, including high grade and low grade bauxites and barren rocks, which are usually lenses of clay or discontinuous beds of shales (Fig. 34.4b). It is also modelled using the 'equal thickness unfolding' method or, alternatively, it can be modelled using a 'top flattening' method. The latter is particularly efficient when the bauxite seam contains erosional channels which make 'equal thickness unfolding' unsuitable for accurate representation of the bauxite structure (Abzalov and Bower 2014).

Deposits which have experienced several episodes of weathering and diagenetic reworking (Gove, Az Zabira) have a stratified structure formed by the stratigraphic succession of the different bauxites layers (Fig. 34.2). Separating layers for their independent modelling is inefficient for resource estimation. The layers are discontinuous and characterised by rapid thickness changes over short distances and have highly irregular contact geometries. An additional challenge is to represent the presence of erosional channels cutting the entire bauxite profile and the gradational zoning observed within some layers (Abzalov and Bower 2014).

34.1.4 Domains

Estimation of mineral resource requires subdividing mineralisation into geostatistically uniform parts, referred to as stationary domains (Goovaerts 1997; Chiles and Delfiner 1999). However, the bauxite plateaus are usually zoned laterally (Abzalov and Bower 2014). Thickness of mineralisation is larger and Al_2O_3 grade higher in their central parts gradually decreasing toward the plateau margins and accompanied by a reverse change in SiO_2 content. The same zoned pattern can be repeated in different plateaus, e.g. Gove deposit (Abzalov and Bower 2014). Conversely, a single zoning can be observed across the entire belt or the part of the belt, encompassing several plateaus, e.g. Sangaredi deposit (Abzalov and Bower 2014).

The strongly zoned structure of bauxite deposits means that defining geostatistically stationary domains is a particularly challenging task.

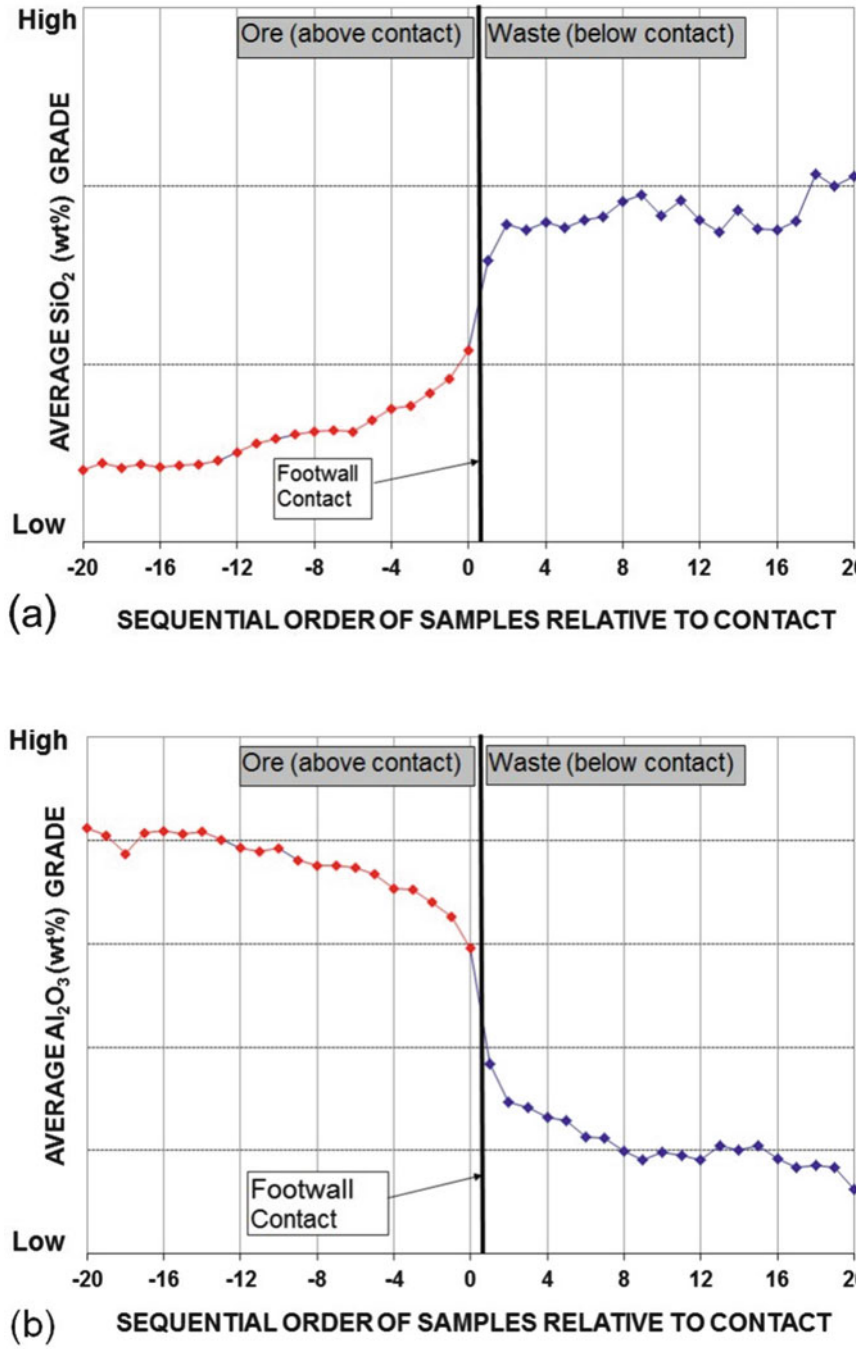

Fig. 34.3 Changes in the laterite chemistry through the footwall contact of the bauxite seam. Average of 350 drill holes (Abzalov and Bower 2014): (**a**) Distribution of SiO_2; (**b**) Distribution of Al_2O_3

A common approach is to define each zoned plateau as a separate domain and model them independently (Gove). Alternatively, a group of plateaus can be modelled as a single domain if the grade continues across the plateau margins. In the more complicated cases, when the spatial distribution of the estimated variables exhibit a strong non-stationarity, accurate estimation of the

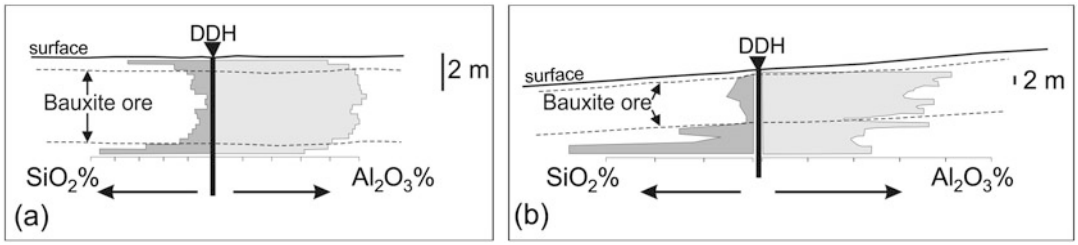

Fig. 34.4 Distribution of the SiO_2 and Al_2O_3 along the vertical profiles of the bauxite seams: (**a**) Gradational zoning of the bauxites at the Weipa deposit; (**b**) Intercalation of high and low grade bauxites and clay lenses at the Sangaredi deposit

bauxite resources may require the application of non-stationary geostatistical techniques, such as Universal Kriging or Kriging with External Drift (Goovaerts 1997; Chiles and Delfiner 1999).

There are also cases when a single plateau is subdivided into several domains, which are modelled separately. In particular, at the Amargosa deposit bauxites formed on anorthosites are modelled separately from the bauxites developed on charnokites and gneisses in order to prevent excessive smoothing of the high grade of the anorthositic bauxites (Abzalov and Bower 2014).

34.2 Drilling

Bauxite deposits are usually large, and can cover areas of several hundred to several thousand square kilometres, therefore the estimation of bauxite resources requires thousands of drill holes (Table 34.2). The total metres drilled varies from several thousand metres, to several hundred thousand metres.

Due to high drilling costs from large meterage and the significant number of drill holes needed for accurate bauxite resource estimation, it is preferable to use cheaper drilling methods such as RC and auger (Table 34.2). Diamond drilling, which is more expensive, is used when other drilling methods are thought to be suboptimal for accurate categorisation of the bauxite types and estimation of their resources.

Auger drilling, which is the main drilling method at the Sangaredi deposits (Table 34.2), tends to overestimate the thickness of the bauxite seam because of down hole sample contamination. Therefore, when using auger drilling the results need to be verified and if necessary corrected using diamond drilling. Alternatively, Sonic drilling, which routinely used for estimating the resources of mineral sands (Abzalov et al. 2011), can be used for the verification of auger drill results at the bauxite deposits.

Drilling grids suitable for the definition of bauxite resources at the studied deposits are shown in the Table 34.2. The differences in the drilling grids chosen for defining resource categories reflect differences of the deposit complexities. In particular, this is the difference in spatial variability of deleterious components and the uncertainty of the footwall contact topography or the presence of internal waste (Abzalov and Bower 2009).

Based on the studied deposits (Table 34.2) the following guideline drill grids can be used for planning drilling for bauxite resource estimation:

- Measured: average 125 × 125 m (range from 50 × 50 to 200 × 200 m);
- Indicated: average 250 × 250 m (range from 100 × 100 to 400 × 400 m);
- Inferred: average 500 × 500 m (range from 200 × 200 to 900 × 900 m).

Some operations drill additional holes at the production stage infilling their resource definition drill grids. In particular, at the Sangaredi mine, Probable reserves are developed by infilling the 150 × 150 m drill grid used for Indicated resources to 75 × 75 m. Proved reserves are defined by infilling the grid to 37.5 × 37.5 m.

Table 34.2 Resource estimation data at the selected bauxite deposits (Abzalov and Bower 2014)

Deposit	Drilling method	Number of holes	Total metres drilled	Drilling depth (metres)			Sample size (m)	Drilling grid by resource categories (metres)		
				Min	Max	Average		Measured	Indicated	Inferred
Weipa	RC	96,653	>400,000	0.5	21.5	4.06	0.25	150 × 150	300 × 300	900 × 900
Gove	Diamond core	17,816	75,268	0.25	14.5	4.22	0.25	75 × 75	150 × 150	500 × 500
Sangaredi[a]	Augur and Diamond core (PQ size)	63,350[b]	469,765	1	41.2	10.4	1.0 and 0.5	50 × 50	150 × 150	150 − 600 × 150 − 600

RC – Reverse Circulation drilling

[a]only data on Initial Territory of Sangaredi deposit

[b]2882 holes were diamond core drilling; other 60,468 holes were drilled by mechanised auger method

34.3 Sampling and Logging Holes

It is common practice to sample bauxite deposits at short intervals, usually at 0.25 or 0.5 m (Table 34.2). Small samples are needed for the accurate definition of the footwall contact to prevent dilution of the bauxite by footwall material, which is usually characterised by high content of the deleterious components, in particular silica and iron (Fig. 34.2). They also necessary for construction of the accurate reserves models of the bauxite deposits which are commonly mined selectivity at 0.5 m benches

Logging of the drill hole samples includes a description of the bauxite types, most common of which are: loose pisolitic, cemented pisolitic, tubular, nodular, blocky bauxite and earthy bauxite. It is also a common practise to document the type and distribution of the iron oxides and hydroxides present as impurities in the bauxite, e.g. ironstone pisolites or fine grained earthy material where goethite and limonite are mixed with clay minerals. The latter is reflected in the bauxite colour, which is classified using a standard palette.

Silica, iron and titanium minerals need to be identified and recorded in all geological logs. Silica is commonly presented as quartz (SiO_2) and hydrated aluminium silicate clays (e.g. kaolinite – $Al_2O_3*2SiO_2*2H_2O$ and halloysite – $Al_2O_3*2SiO_2*3H_2O$). Titanium usually is present as ilmenite ($FeTiO_3$), rutile (TiO_2) and anatase (TiO_2). These minerals and iron oxides are typical for bauxites developed on anorthosites.

Geotechnical characterisation of bauxite includes the following standard parameters:

- Rock density;
- Hardness;
- Moisture.

At some Brazilian operations it also includes documentation of plants and rock boulders intersected by the drill holes. They can be serious obstacles for the transportation of bauxites by conveyor belts, and can also cause a disruption of the bauxite beneficiation at a metallurgical plant.

34.4 Sample Preparation and Assaying

The sample preparation procedures are different for non-cemented and cemented bauxites.

34.4.1 Sample Preparation

Non-cemented bauxites are upgraded (beneficiated) by sieving and washing away the fine fraction which mostly contains clay and silica rich minerals (Table 34.3). The sieve fraction is determined empirically and can be different at different deposits or at the different parts of the same deposit depending on their grade vs. size fraction profile. Examples of the sieve size used for beneficiation of the bauxites are as follows:

- Deposit 1: −10 mesh (−1.7 mm) discarded, +10 mesh (+1.7 mm) is retained;
- Deposit 2: −28 mesh (−0.6 mm) discarded, +28 mesh (+0.6 mm) is retained;
- Deposit 3: −48 mesh (−0.3 mm) discarded, +48 mesh (+0.3 mm) is retained.

Beneficiation is measured as the ratio of the weights of the recovered (beneficiated) bauxite to the weight of sample before processing. This ratio is referred to as the ‘yield’ and expressed as a percentage. Beneficiated bauxites are dried and then ground and pulverised, usually to 200 mesh (0.074 mm) for analysis using ICP-MS and XRF methods. An example of a sample preparation protocol is shown in Table 34.3.

Cemented bauxites are not beneficiated therefore samples are processed in a conventional manner, by drying the sample followed by crushing, grinding and pulverisation. Sample preparation protocols are commonly optimised by estimating the Fundamental Sampling Error and constructing sampling nomograms according to the Theory of Sampling (Gy 1979; Francois-Bongarcon and Gy 2001).

Table 34.3 Example of the sample preparation and quality control protocol (Abzalov and Bower 2014)

Samples quality control	Comminution / Subsampling
	Initial sample, approximately 10–12 kg in weight, brought from drill site to the lab, weighed and air dried;
	Sample dried (at 105 °C) and crushed to 25–13 mm;
At this stage Coarse duplicates are collected. Duplicates are taken from a 70 % portion that is prepared for beneficiation (washing). Duplicates are taken at the rate of 1:20	(Split 1) Sample split by cone and quarter method and 70 % of material (6–9 kg) is collected for washing
	Washed samples are sieved using two screens (20 and 150 mesh sizes). − 150 mesh is rejected and the rest is collected for further study
	+20 mesh material is ground to 95 % passing 2.36 mm sieve
Interim duplicates are collected at the rate of 1:20	(Split 2) The sample is split by riffle splitter and 350 g collected for further assays, the remaining material is retained for auditing purpose.
	350 g pulverised to −100 mesh (0.149 mm);
Pulp duplicates are collected at the rate of 1:20	(Split 3) 30 g aliquots are collected from the 350 g pulp for assaying
Standards inserted at the rate of approximately 1:10 to 1:20	Assays. Two analytical techniques are used:
	Total Available Alumina (TAA), Loss on Ignition (LOI) and reactive silica (R-SiO2) are assayed by wet chemistry technique;
	The full suite of elements assayed by XRF

34.4.2 Analytical Techniques

When processing includes beneficiation of bauxites the weight of rejected and retained material is reported for all samples. The retained samples are assayed for Al_2O_3 and all deleterious components. Main deleterious components in the bauxite deposits are: SiO_2, TiO_2, Fe_2O_3, Mn, Zn, Ca, and P_2O_5 (Abzalov and Bower 2014).

These are usually assayed by conventional XRF. However, the special analytical techniques are often used in order to more accurately determine metallurgical characteristics of the bauxites. In particular, when silica is present in different minerals additional assays are made for the accurate estimation of concentration of reactive silica which can be a serious hazard for alumina production from bauxites by the Bayer process. Loss on Ignition (LOI) should be recorded for all assayed samples. This is an important check of the assay quality as the sum of the oxide weights and LOI should be close to 100 wt%. It is also needed for recalculating the chemical composition of samples to their mineralogical composition using stoichiometric mineral formulas. This is used at some operations (Weipa) for the mineralogical classification of bauxite products. In addition to the oxides and LOI measurements, the following are determined on a project basis:

- Quartz. The percentage of quartz in a sample is determined through a wet chemical technique, whereby a strong acid dissolves the silica. This process is both costly and time consuming and poses significant health and safety risks to the laboratory analyst. Other methods are currently being evaluated for this determination;
- Kaolinite. The amount of kaolinite in a sample, total silica minus the quartz content, is calculated as the difference between assayed SiO_2 content and the amount of quartz;
- Organic carbon. This variable is used in orebody models. Organic carbon is measured using a commercial carbon analyser. This technology is both proven and simple;
- Alumina species, Tri-hydrate (THA) and monohydrate (MHA). These are traditionally determined through a “bomb digest”. This

process replicates the conditions in the digestion train in an alumina refinery and allows the concentration of both high temperature digestible alumina (MHA) and low temperature digestible alumina (THA) to be determined.

34.4.3 Sample Quality Control

Sample quality control at bauxite projects is similar to conventional QAQC procedures in the mining industry (Abzalov 2008). The frequency of collecting duplicate samples at the bauxite projects is usually 1:10 to 1:20 (Table 34.3). The duplicates are used for estimating sample precision which is reported as CV% (Abzalov 2008). Examples of precision errors at the bauxite deposits are shown in Table 34.4.

Standard samples are used to check the laboratory analytical accuracy and inserted at rates of 1:20, similar to other types of metallic deposits (Abzalov 2008).

It is noted that QAQC procedures at the bauxite deposits have specific features caused by drilling and sampling of soft, non-consolidated sediments including:

- Recovery of drill hole samples is usually limited to measuring their weights which is often insufficient for assuring sample quality and representativity;
- Using blanks is impractical for controlling sample contamination in the laboratory.

The above mentioned difficulties are partially overcome by drilling twin holes which are commonly used at bauxite projects as a routine method of data quality control, and for verification of historic data (Abzalov 2009).

34.5 Dry Bulk Density of the Rocks

The techniques used for measuring the dry bulk density (DBD) of bauxite are:

- Sand replacement method (Weipa, Gove);
- Diamond core drilling (Gove, Sangaredi);
- PVC tube (Trombetos);
- Sonic drilling (Amargosa).

The sand replacement method is a most common method which is formally certified for measuring dry bulk density (DBD) of the rocks at the Australian deposits (Table 34.5). When thickness of the bauxite seam reaches several metres the sand replacement technique will require digging of exploration pits therefore a modern practice

Table 34.4 Common ranges of the precision errors (CV%)* estimated at the pisolitic bauxites using duplicate samples

	XRF analysis			
	Al_2O_3	SiO_2	Fe_2O_3	Loss on ignition (LOI)
Coarse duplicates (171 duplicate samples)	3–6	7–10	5–8	6–10
Pulp duplicates (141 duplicate samples)	1–2	3–6	1–2	2–4

*Calculation of CV% is explained elsewhere (Abzalov 2008)

Table 34.5 Dry bulk density (DBD) of the bauxites (Abzalov and Bower 2014)

Deposits	Deposit type	Dry bulk density (DBD) t/m^3	
		Average	Range by rock types and domains
Weipa, Australia	Non-consolidated pisolitic bauxite	1.60	1.47–1.67
Gove, Australia	Loose pisolitic bauxite;	1.79	1.54–1.89
	Cemented pisolitic bauxite;		
	Cemented tubular bauxite		
Sangaredi, Guinea	Lithified massive and oolitic bauxite	2.00	1.84–2.62
Az Zabira, Saudi Arabia	Buried palaeo plateaus	2.05	Density of the waste rocks is 1.9
Brazilian deposits	Non-consolidated pisolitic bauxite	1.50–1.70	

is to use Sonic drilling for accurate DBD measurement (Abzalov et al. 2011; Abzalov 2013; Abzalov and Bower 2014).

Assigning rock density values to a block model is usually made by calculating average DBD values for each domain and the material types which are constrained by a geological model (Table 34.5). Interpolation of the DBD data using geostatistical algorithms, as practised with base metal deposits (Abzalov 2013), is usually inapplicable at the bauxite deposits due to insufficient DBD data. Some sites (e.g. Sangaredi) deduce DBD values for each modelled block from their chemical compositions. This approach requires thorough calibration of relationships between density and chemical composition of the bauxites.

34.6 Estimation Bauxite Grade

Bauxite resources are estimated using Ordinary kriging which is commonly supported by conditional simulation techniques applied to the bauxite grade and thickness for quantification of the resource model uncertainties and risks (Abzalov and Bower 2009). Lateral dimension of the kriging blocks are usually half the distance between drill holes, vertical dimension match the sample size (0.25 or 0.5 m).

Construction and modelling of the variograms is usually made after the mineralisation geometry is simplified using unfolding algorithms. In the unfolded environments most of the studied variables produce robust 3D variograms. Typical variogram models are presented in Table 34.6.

Both main metals, Al_2O_3 and SiO_2, commonly exhibit good spatial continuity (Fig. 34.5a, c) which accords well with the estimated variogram ranges exceeding several hundred metres (Table 34.6). Zoned distribution of the alumina and silica is usually coupled with zoned structure of the plateau thicknesses (Fig. 34.5b).

34.7 Classification

Bauxite mineralisation is classified as a resource if chemical and mineralogical compositions meet project specific cut-off criteria. The most commonly used cut-off is 30–50 % of Al_2O_3. Bauxite also should be low in SiO_2 usually less than 10 %.

34.7.1 Mineral Resources

The drilling grids which are used for classification of the bauxite resources by confidence categories are summarised in Table 34.2. In the past, the grids have been chosen empirically, based on general resource estimation practices and reconciliation of reserves by production. However, at present, many sites have reviewed their historical drill grids using geostatistical classification criteria (Abzalov and Bower 2009). Variables which are commonly modelled using conditional simulation techniques for estimating the resource uncertainty and their classification into the categories include:

- Al_2O_3, which is the main metal setting the economic value of the bauxites;
- SiO_2, the main metallurgically deleterious component controlling the product types;
- Bauxite thickness, the variable controlling volume and tonnage of the ore;
- Footwall contact topography, its accurate modelling is important for correct estimation of the bauxite dilution.

34.7.2 Conversion to Ore Reserves

Conversion of mineral resource to ore reserves requires consideration of the following factors.

34.7.2.1 Mining Parameters

Bauxite mining has particular considerations arising from the unique features of the bauxite deposits. They are mined by open pits method which are commonly shallow but cover large areas, up to several hundred square kilometres. The open pits are often operated using a free digging approach (Weipa) because bauxites are usually hosted in soft non-consolidated lateritic sequences. Thus, conversion bauxite resources to

Table 34.6 Examples of the Al_2O_3 and SiO_2 variogram models from bauxite deposits (Abzalov and Bower 2014)

Modelled variable	Deposit	Nested structure	Sill	Range			Comments
			normalised to 1.0	Major axis (Azi 0)	Minor axis (Azi 90)	Vertical (D-90)	
Al_2O_3, %	Weipa – Area 1	Nugget	0.02				Nugget effect
		Spherical – 1	0.50	300	250	1.4	Local component
		Spherical – 2	0.48	4000	3000	3.2	Regional component
Al_2O_3, %	Gove (2D variogram is used)	Nugget	0.30				Nugget effect
		Spherical – 1	0.26	130	130		Local component
		Spherical – 2	0.20	445	445		
		Spherical – 3	0.24	1500	1500		Regional component
SiO_2, %	Weipa – Area 1	Nugget	0.30				Nugget effect
		Spherical – 1	0.15	500	900	3.0	Local component
		Spherical – 2	0.20	2000	2000	25.0	
		Spherical – 3	0.40	Infinite	9500	30.0	Regional component
SiO_2, %	Weipa – Area 2	Nugget	0.05				Nugget effect
		Spherical – 1	0.45	200	200	3.3	Local component
		Spherical – 2	0.50	3600	4000	3.3	Regional component

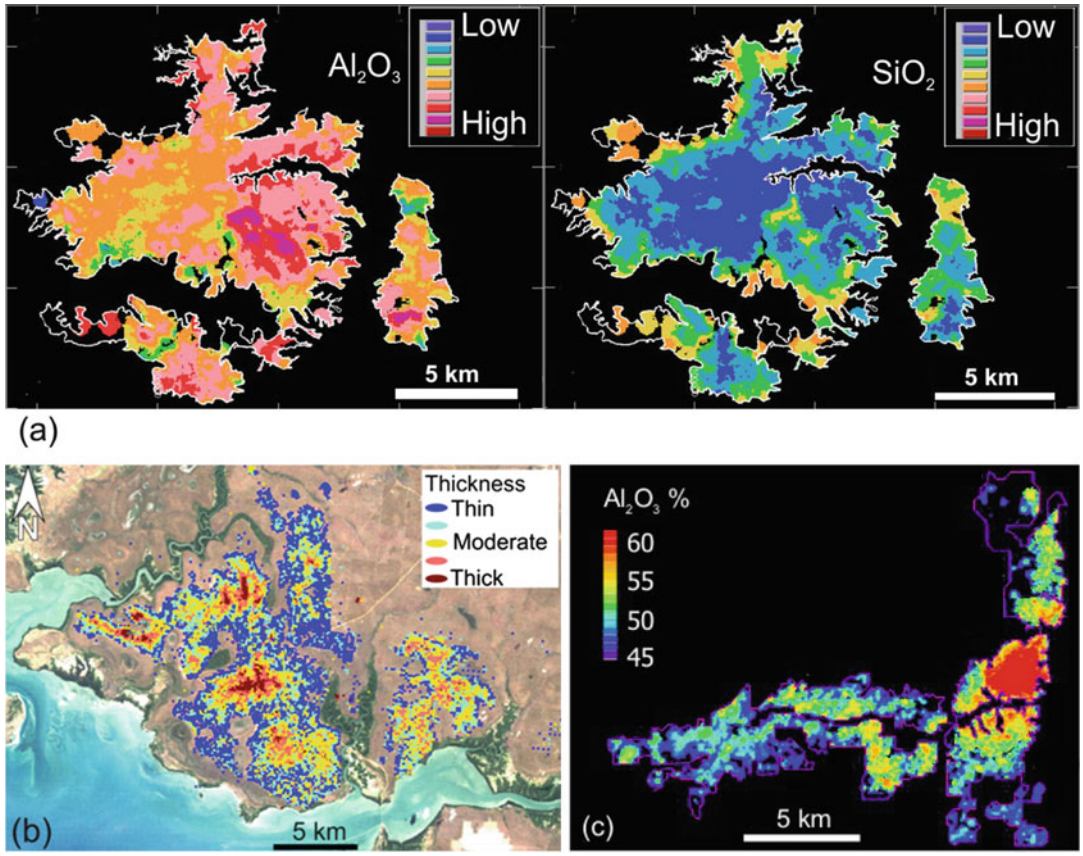

Fig. 34.5 Zoned structure of the bauxite deposits (Reprinted from (Abzalov and Bower 2014) with permission of Taylor-Francis Group: (**a**) Gove; (**b**) Weipa; (**c**) Sangaredi)

reserves, requires the following mining conditions to be taken into considerations:

- Haulage of bauxites represents one of the main mining costs therefore the choice of the optimal mining fleet and optimisation of haulage routes are crucial aspects of mine planning;
- Despite the large mining areas and production rates exceeding 10Mt/year, bauxites are mined at a vertical selectivity of 0.25–0.5 m which is needed to control the dilution by footwall material;
- Grade control at the production stage may not be practical therefore pre-production infill drilling is usually used for grade control purposes and should be budgeted as an operational cost;
- Pit slope stability is rarely an issue for bauxite mines.

34.7.2.2 Metallurgical Factors

In early exploration stage, bauxite characterisation is made using drillhole samples. These tests, although preliminary in nature, allow a basic characterisation of the metallurgical properties of the bauxites, and the construction of predictive models of their behaviour in the refinery.

When project matures, usually at the prefeasibility and feasibility stages, specialised refinery characterisation testwork is undertaken, focussing on the behaviour of the bauxite in a given refinery. This type of work is generally done with the representative bulk sample, which is tailored for a particular refinery. Representative nature of the bulk samples should be ensured regarding their spatial distribution and composition (Abzalov and Allaboun 2015). Refinery characterisation of bauxites includes the following tests:

- Chemical and mineralogical characterisation of the crude bauxite;
- Estimation of the bauxite grindability and quantification of the Bond Work Index;
- Estimation of the particle size distribution with an objective to determine the optimal mesh size for bauxite beneficiation;
- Characterisation of the pre-desilication behaviour of the bauxite by silica dissolution and DSP precipitation;
- Characterisation of the alumina extraction and impact of the deleterious components, in particular iron and silica;
- Characterisation of the bauxite behaviour at the refinery, and the estimation of refinery parameters, including recovered alumina, refinery caustic consumption and red mud loading;
- A special study is made to characterise extractable organic carbon, oxalate formation rate and carbonate formation rate;
- The settling behaviour is studied by estimating the mud settling rate, mud compaction and overflow clarity;
- Simulation of the entire bauxite processing flowsheet at the given plant conditions.

References

Abzalov MZ (2008) Quality control of assay data: a review of procedures for measuring and monitoring precision and accuracy. Explor Min Geol J 17(3–4):131–144

Abzalov MZ (2009) Use of twinned drill – holes in mineral resource estimation. Explor Min Geol J 18(1–4):13–23

Abzalov MZ (2013) Measuring and modelling of the dry bulk density for estimation mineral resources. Appl Earth Sci 122(1):16–29

Abzalov MZ, Allaboun H (2015) Bulk samples testing for metallurgical characterisation of surficial uranium mineralisation at the Central Jordan Uranium Project. Appl Earth Sci 124(2):129–134

Abzalov MZ, Bower J (2009) Optimisation of the drill grid at the Weipa bauxite deposit using conditional simulation. In: Seventh international mining geology conference. AusIMM, Melbourne, pp 247–251

Abzalov MZ, Bower J (2014) Geology of bauxite deposits and their resource estimation practices. Appl Earth Sci 123(2):118–134

Abzalov MZ, Dumouchel J, Bourque Y, Hees F, Ware C (2011) Drilling techniques for estimation resources of the mineral sands deposits. In: Proceedings of the heavy minerals conference 2011. AusIMM, Melbourne, pp 27–39

Bardossy G, Aleva GJ (1990) Lateritic bauxites, vol 27, Developments in economic geology. Elsevier, Amsterdam

Chiles J-P, Delfiner P (1999) Geostatistics: modelling spatial uncertainty. Wiley, New York, p 695

Ferenczi PA (2001) Iron ore, manganese and bauxite deposits of the Northern Territory, Northern Territory Geological Survey report 13. Government Printer of the Northern Territory, Darwin, p 113

Francois-Bongarcon D, Gy P (2001) The most common error in applying 'Gy's formula' in the theory of mineral sampling, and the history of the liberation factor. In: Edwards A (ed) Mineral resources and ore reserve estimation – The AusIMM guide to good practise. AusIMM, Melbourne, pp 67–72

Goovaerts P (1997) Geostatistics for natural resources evaluation. Oxford University Press, New York, p 483

Grubb PLC (1979) Genesis of bauxite deposits in the lower Amazon basin and Guianas coastal plain. Econ Geol 74(4):735–750

Gy P (1979) Sampling of particulate materials, theory and practice, vol 4, Developments in geomathematics. Elsevier, Amsterdam, p 431

Lillehagen NB (1979) The estimation and mining of Gove bauxite reserves. In: Estimation and statement of mineral reserves. AusIMM Sydney Branch, Sydney, pp 19–32

Schaap AD (1990) Weipa kaolin and bauxite deposits. In: Hughes FE (ed) Geology of the mineral deposits of Australia and Papua New Guinea. AusIMM, Melbourne, pp 1669–1673

Mineral Sands

35

Abstract

Mineral sand deposits fall into three main deposit styles, palaeo marine placers, aeolian (dunal) sands and alluvial deposits. Two types are included into the current review. These are palaeo marine placers, Fort Dauphin located in Madagascar and Corridor Sands in Mozambique, and Richards Bay deposit in South Africa, which is aeolian type mineral sands deposit. The main challenges in evaluating of the mineral sands deposits are as follows:

- mineral sands deposits comprise non-consolidated to semi-consolidated sands hosting valuable heavy minerals, mainly ilmenite, rutile, leucoxene and zircon. The large difference in the mineral densities can result in the heavy minerals segregation in the drilling rods causing a biased composition of the recovered samples;
- the mineral sands deposits are commonly mined using dredging technologies. The heterogeneous nature and highly variable geotechnical characteristics, including presence of the hard pan lenses within non-consolidated sediments, imposes an additional challenge on the drilling and mining equipment;
- the product costs depend on mineralogy of the heavy fraction, therefore mineral composition of the heavy fraction needs to be accurately estimated into the block model.

Keywords

Mineral sands • Placer • Aeolian • Resource • Dredging • Richards Bay • Fort Dauphin • Corridor Sands

Mineral sand deposits being economically exploited around the world fall into three main deposit styles, palaeo marine placers, aeolian (dunal) sands and alluvial deposits. Resource estimation for mineral sands, in general, follows standard estimation principles as applied to commodities throughout the mineral resource sector. There are, however, characteristics of the mineral

M. Abzalov, *Applied Mining Geology*, Modern Approaches in Solid Earth Sciences 12,
DOI 10.1007/978-3-319-39264-6_35

sands that differ them from other commodities and require special attention when these deposits are studied.

The main challenges in evaluating of the mineral sands deposits are as follows (Abzalov and Mazzoni 2004, Abzalov et al. 2011, Jones and O'Brien 2014):

- Mineral sands deposits comprise non-consolidated to semi-consolidated sands hosting valuable heavy minerals, mainly ilmenite, rutile, leucoxene and zircon. The total content of the economic heavy minerals is usually in the order of several percent and are unevenly distributed in a matrix of gangue quartz and feldspar. The heavy minerals have an average density of 4.6 g/cm^3 and are significantly heavier than the sand matrix (density 2.6 g/cm^3). The large difference in the mineral densities can result in the heavy minerals segregation in the drilling rods and sample capturing devices causing a biased composition of the recovered samples;
- Other challenges include the presence of hard pan lenses, concretions and clay beds, hosted within non-consolidated sediments;
- The mineral sands deposits are commonly mined using dredging technologies. The heterogeneous nature and highly variable geotechnical characteristics, in particular presence of the hard pan lenses within non-consolidated sediments imposes an additional challenge on the drilling and mining equipment;
- The product costs depend on mineralogy of the heavy fraction, therefore mineral composition of the heavy fraction needs to be accurately estimated into the block model, especially for construction of the ore reserves model.

35.1 Geology of the Selected Deposits

Current review includes three deposits located on the Atlantic coast of southern Africa (Fig. 35.1). Two deposits, Fort Dauphin located in Madagascar (Fig. 35.1b, c) and Corridor Sands in Mozambique (Fig. 35.1d) are palaeo marine placers. Richards Bay deposit in South Africa is aeolian type mineral sands deposit (Fig. 35.1e).

35.1.1 Fort Dauphin

Fort Dauphin deposit is located on the south-eastern coast of Madagascar (Fig. 35.1b). It occupies an area of approximately 45 km^2 and contains 575 million tonnes of the titanium rich sands with an average THM (total heavy minerals) grade of approximately 4.7 %. Mineralisation was intensely explored in late 70th through to 1980s and additional drilling was undertaken in 2004 mainly for verification of the previous results. In total, the resource definition database contains 1523 drill holes and 17,807 sample analyses. The holes were drilled at 400×200 m grid which then was infilled to 200×100 m spacing.

The mineralised sands of the Fort Dauphin deposit are subdivided into three units (Fig. 35.1c): Upper Mineralised Sands (UMS), Transitional sands (TS) and Lower Mineralised Sands (LMS). They are resting on laterite, marine clays, usually referred as Clay Floor unit (CF), footwall slimes and in places directly on the bedrocks.

UMS unit represents the top part of the prograding beach sand complexes in which heavy minerals have been sorted and concentrated by removing the barren sands by wind action. Sands often exhibit laminar textures formed by the bands of the heavy minerals. TS unit marks the transition between Upper (UMS) and Lower (LMS) mineralised units. It is characterised by lower heavy minerals contents (THM 1–2 %) grades and has a relatively constant thickness of 3–6 m. The TS sands are coarser grained and more poorly sorted than the overlying them UMS unit. Heavy minerals banding, and cross-bedding, presence of the slump and erosional features are indicative of accumulation of the TS sands in a relatively high energy environment. The lowermost mineralised unit (LMS) consists of the foreshore sand facies which are typified by fine to medium grained sands with abundant

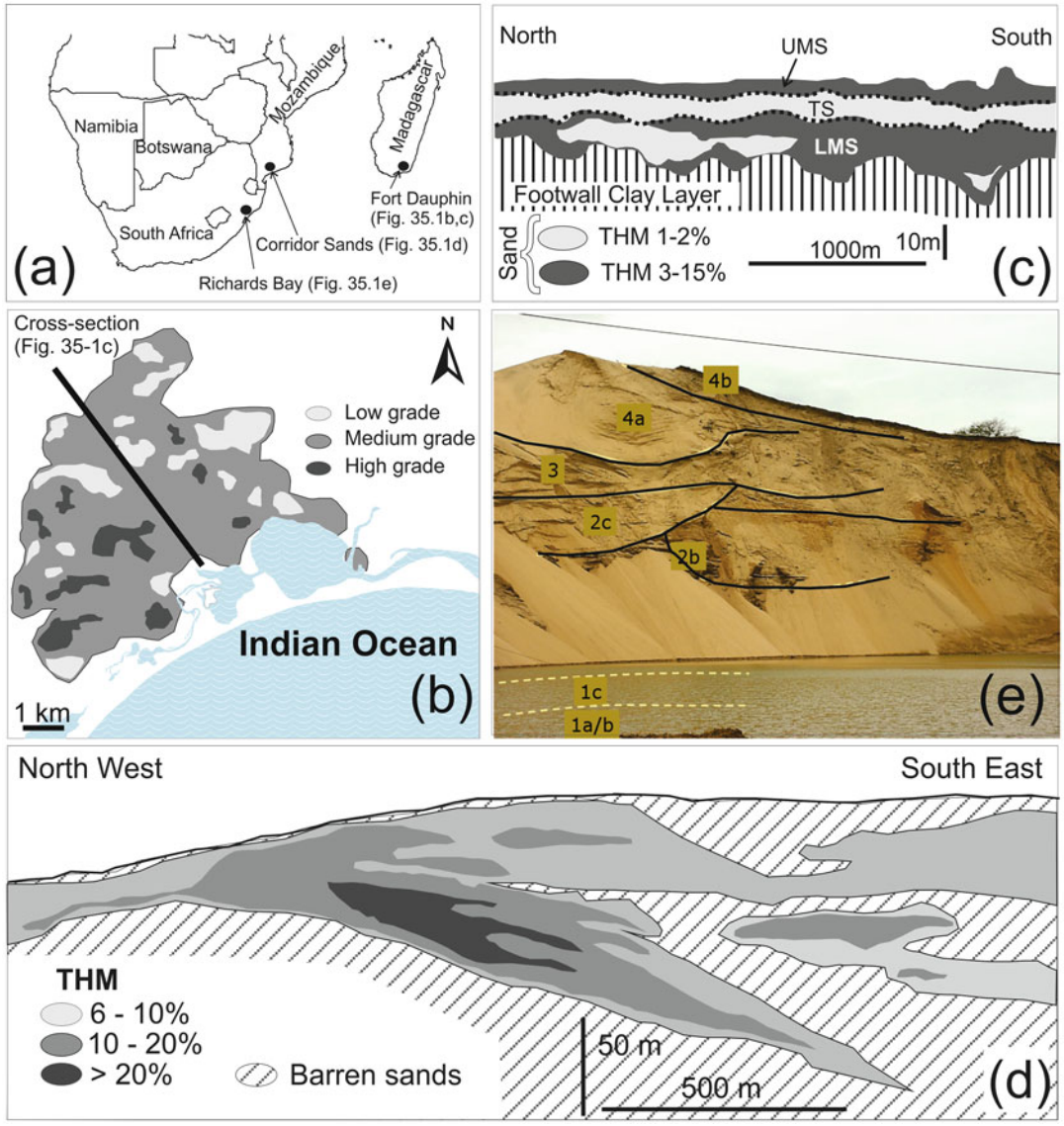

Fig. 35.1 Geological characteristics of the studied deposits (Abzalov et al. 2011): (**a**) map showing location of the studied deposits; (**b**) generalised map showing distribution of the heavy minerals at the Fort Dauphin deposit, Madagascar; (**c**) cross-section of the Fort Dauphin deposit (the location is shown on the map (**b**). *Dotted lines* denote the contacts of the stratigraphic units: *UMS* Upper Mineralised Unit, *TS* Transitional Unit, *LMS* Lower Mineralised Unit (**d**) typical cross-section of the Corridor Sands deposit, Mozambique. Generalised after (Abzalov and Mazzoni 2004); (**e**) sequence of the coastal dunes exposed at the wall of the dredge pond, Richards Bay deposit, Republic of South Africa

heavy mineral laminations. The base of the unit can contain the soils. Sands at the top of the unit often are strongly indurated. Sediments forming the base of the deposit include marine clays, silts and sands deposited as offshore facies.

35.1.2 Corridor Sands

The Corridor Sands district of ilmenite bearing heavy mineral sands is located in southern Mozambique (Fig. 35.1d), approximately 20–60 km from the Indian Ocean. The district

represents the largest known resource of ilmenite with total endowment assessed as being in the order of 16.5 billion tonnes at 5 % total heavy minerals (Abzalov and Mazzoni 2004).

The largest and the best explored is Deposit 1, which is a type deposit for entire Corridor Sands district (Abzalov and Mazzoni 2004). Resources of the Deposit 1 have been defined using air core drilling. Inferred category of the resources is based on drilling along 1 km spaced N-S traverses. Indicated and Measured categories have been defined by infill drilling on 250 m × 125 m grid, including the initial mining area which was drilled on 100 m × 100 m and some smaller parts drilled on 25 m and 50 m grids (Abzalov and Mazzoni 2004). Quality of the aircore drilling was tested by twinning them with diamond holes, drilled using a triple tube core drilling technology. A bankable feasibility study of the project was based on approximately 1200 holes with total length of about 80,000 m.

Drilling has delineated a titanium rich sands that extend in north-east direction for more than 6 km dipping to south-east and thickening south eastwards to over 140 m (Fig. 35.1d). The mineralised stratigraphy is subdivided into six geological domains (Abzalov and Mazzoni 2004). These represent stratigraphic units formed as a result of superimposition of the different depositional facies and post-depositional pedogenic weathering processes. Domains are different by colour, clay content, grain size and grade of the total heavy minerals (THM). In gross morphology terms, the individual sand bodies that represent each of the domains are sheet-like with lens, prism (wedge) or ribbon geometries (Fig. 35.1d). The contacts between the domains are gently undulating rather than planar and characterised by presence of irregular trough and pot-holes. Contacts are usually sharp and supported by textural differences between the stratigraphic units. The depositional breaks are sometimes accompanied by evidence of soil forming processes, including induration on the contacts.

The valuable heavy minerals are ilmenite, rutile, sphene, leucoxene and zircon. Heavy minerals fraction also contains hematite, goethite, leucoxene, chromite, rutile, anatase, epidote, pyroxene, amphibole, andalusite, staurolite, monazite, garnet and kyanite. They are generally coarser grained than the valuable heavy minerals.

35.1.3 Richard's Bay

The coastal dunes of the Richards Bay area are aeolian in origin and belong to the upper three formations (Kosi Bay, Kwambonambi and Sibayi respectively) of the Quaternary Maputaland Group (Botha 1997). These comprise unconsolidated to semi-consolidated sediments which were deposited unconformably onto the consolidated calc-arenites of the Port Durnford Formation or Cretaceous arenites (inland) in response to sea-level fluctuations during the period from the mid to late Pleistocene to the present day (Botha 1997, Ware and Whitmore 2007). These formations have subsequently been modified by weathering processes, which have resulted in the formation of calcrete and ferricrete discontinuous lenses throughout the deposit (Ware and Whitmore 2007). Only the Kwambonambi and Sibayi Formations are suitably mineralised and have informally being further subdivided into 10 distinct units for mining purposes (Fig. 35.1e).

Heavy mineral distribution (specific gravity above 2.9 g/cm^3) follows the south-south-west direction of the dunes. Some differential occurs between high and low dunes, the greatest concentration of minerals being in the lower areas. Surface enrichment parallel to the dune direction tends to occur. The heavy mineral suite of the deposit is made up of sub-angular to well-rounded grains of ilmenite, rutile, zircon and other trace heavy minerals.

Economic concentrations of heavy minerals in the Richards Bay area have been being exploited by Richards Bay Minerals since 1976 with the Zulti North lease currently being exploited. This lease contains a further 1.6 billion tonnes of mineralised sands. The Zulti South lease is currently under prefeasibility study and it is expected to contain approximately 480 million tonnes of mineralised sands. Titaniferous sands of the Zulti North deposit encompass an area of 20 km along the strike and 3 km across. The Zulti South lease

is approximately half the size of the Zulti North lease.

Resources of the Zulti North were originally defined by air core drilling. In total, 8731 air core holes were drilled which were subsequently verified by 751 Sonic drilling holes. Measured resources were established by air core drilling at a 50 × 50 m grid, Indicated resources by broader spaced drilling, usually at 800 × 100 m grid. Similarly, measure resource for Sonic were established on a 200 × 100 m grid and indicated on a 400 × 400 m grid. Resources of the Zulti South are mainly developed by Sonic drilling. In total, 283 Sonic holes were drilled at a grid spacing of 200 × 200 m.

35.2 Drilling

Definition of the mineral sands resources usually requires several thousand drill holes which total length can be of the order of 80,000 m (Table 35.1). The most common techniques currently used for appraisal of mineral sands deposits hosted in weekly lithified or non-consolidated sediments include non-core drilling methods based on percussion technologies, in particular the techniques which use a reverse circulation approach (Chugh 1985, Abzalov et al. 2011, Jones and O'Brien 2014). This is usually referred as air-core reverse circulation drilling or simply air-core.

Another common technique which is applied for estimation resources of the mineral sands is Sonic drilling (Oothoudt 1999). A variation of this method, known as vibrocore, was the main method for development resources of the Fort Dauphin deposit in Madagascar.

Triple tube diamond core drilling is also used in the mineral sands industry (Chugh 1985, Cumming and Wicklund 1980, Hartley 1994). This technique is mainly used for verification of the historic drilling results.

Methods such as auger and tricon drilling have been used in the past as routine techniques for exploration of the heavy mineral sands, however they are less common in the modern industry.

Air-core (AC) is relatively cheap drilling method allowing for extensive exploration and resource definition drill-out. However, it is the authors' experience that AC drilling can generate biased results by systematically underestimating the THM (total heavy minerals) grades of the mineral sands (Abzalov et al. 2011). At the Richards Bay deposit twinning of the AC holes by Sonic holes has found that AC drilling underestimates the THM grades by 30–50 % (Abzalov 2009, Abzalov et al. 2011). Other important finding of that study was that AC drilling incorrectly estimated thickness of the heavy mineral sands and position of the footwall contact (Abzalov 2009).

At the Corridor Sands deposit the AC drilling have been verified by twinning them using a triple tube diamond core drilling technique (Abzalov 2009). Comparison of the twin holes has shown that air core samples underestimate THM grade

Table 35.1 Resource estimation data

Deposit	Drilling method	Number of holes	Total length (metres)	Drilling grid by resource categories (metres)			References
				Measured	Indicated	Inferred	
Fort Dauphin	Vibra core	31,151	17,986	200 × 100	400 × 200	400 × 200	Abzalov et al. (2011)
Corridor Sands	Air Core	~1200	>80,000	100–250 × 100–125		1000 × 200	Abzalov and Mazzoni (2004)
Richards Bay	Air core	8731		50 × 50	800 × 100		Abzalov et al. (2011)
	Sonic	1034		200 × 100	400 × 400		

by 10–30 % and the bias increases when sampled units are located below the water table.

Thus, the modern practice is to verify the AC drilling results of the mineral sands deposits by the alternative drilling techniques, usually Sonic or triple tube diamond core drilling. This approach was applied at the all of discussed in the current review heavy mineral sands projects.

35.3 Sample Processing and Assaying

Mineral sands differ from other commodities with respect to the determination of the valuable components of mineralised orebodies. Primary assaying is focused on determining the percentage of the total heavy minerals contained in a given sample. This is determined by separating heavy minerals fraction using heavy liquids, commonly 2.85 g/cm^3 (Jones and O'Brien 2014). Other results of interest from the primary assay include clay fines and slimes (material generally less than 45 μm to 75 μm), sand (generally 45 μm or 75 μm to 500 μm or 2.0 mm) and oversize (generally greater than 500 μm or 2.0 mm) (Abzalov and Mazzoni 2004). Assay of primary material sizes is not standardised across the industry. In particular, the size ranges can change depending on the process metallurgy requirements.

After total heavy minerals are extracted the secondary assay is undertaken. The heavy minerals fraction is further subdivided using magnetic separator and analysed to determine percentage of key valuable minerals such as ilmenite, zircon, rutile and leucoxene. Percentage of the deleterious minerals also reported at the second level of assaying.

A tertiary level of analysis occasionally is carried out on individual mineral species in order to determine quality characteristics. These may include assaying of the trace elemental contamination, commonly uranium, thorium, chrome, manganese and silica.

35.4 Samples Quality Control Procedures

Quality control procedures in the mineral sands industry include conventional set of techniques, mainly using reference standards, duplicate samples analysis and drilling the twin holes. Precision error (CV%) of the THM grade varies at the reviewed deposits from 8 to 18 % (Abzalov 2008).

Notably that the fines material is lost during assaying and only the heavy minerals content within the retained sand fraction can be reassayed which necessitates constant monitoring of standard results to detect any issues that may arise.

35.5 Dry Bulk Density of the Rocks

Density of the mineral sands is usually determined using physical samples obtained using Sonic drilling (Abzalov et al. 2011) or in the trial pits (Corridor Sands). Alternatively, it can be measured in the drill holes using nuclear densometric tool (Jones and O'Brien 2014).

35.6 Estimation and Reporting Resources

The resource models of the mineral sands are estimated constraining mineralisation by wireframes which honours the geological characteristics of the deposits. The most common geological features implemented into the mineral sands resource models are the palaeo-shorelines of the marine placers (Fig. 35.1b) and the palaeochannels and the local sedimentary basins of the lacustrine and alluvial deposits (Jones and O'Brien 2014).

Stratigraphic control is used for subdividing deposit onto domains by the host litho-stratotypes (Fig. 35.1c, d). Mineralisation distributed in the aeolian sands often occurs as a single continuous

body distributed along the footwall of the dunes therefore stratigraphic and lithological control should be implied to resource model only after detailed paleo-facial interpretation of the sand complexes.

Main difficulty in estimating mineral sands resources is to obtain an accurate estimation of the minerals, ilmenite, rutile, zircon and leucoxene, because the product costs significantly vary depending on the dominant minerals:

Ilmenite	100–200 $/t
Leucoxene	300 $/t
Rutile	700 $/t
Zircon	1500 $/t

The common practice is to estimate initially the total heavy minerals (THM) and silt/slime contents (Abzalov and Mazzoni 2004). These are estimated using conventional methodology applying Ordinary kriging or Inverse distance techniques.

Estimation of the mineral species into the block model is more challenging, because the estimate of the mineral needs to take into account distribution of the THM grade. This is made by recalculating the mineral contents in THM into their overall content in a sample and then estimating mineral grade into blocks using univariant estimation techniques. Alternatively, minerals can be estimated together using co-kriging. Multivariate estimate is benefited if THM grade is used as auxiliary information.

Notably, that estimation parameters used for the different styles of mineral sand orebodies can be quite different and therefore they are assessed on a case-by-case basis (Abzalov and Mazzoni 2004).

References

Abzalov MZ (2008) Quality control of assay data: a review of procedures for measuring and monitoring precision and accuracy. Exp Min Geol J 17(3–4):131–144

Abzalov MZ (2009) Use of twinned drill – holes in mineral resource estimation. Exp Min Geol J 18(1–4):13–23

Abzalov MZ, Mazzoni P (2004) The use of conditional simulation to assess process risk associated with grade variability at the Corridor Sands detrital ilmenite deposit. In: Dimitrakopoulus R, Ramazan S (eds) Ore body modelling and strategic mine planning: uncertainty and risk management. AusIMM, Melbourne, pp 93–101

Abzalov MZ, Dumouchel J, Bourque Y, Hees F, Ware C (2011) Drilling techniques for estimation resources of the mineral sands deposits. In: Proceedings of the heavy minerals conference 2011. AusIMM, Melbourne, pp 27–39

Botha GA (1997) The Maputaland group: a provisional lithostratigraphy for coastal KwaZulu-Natal. In: Maputaland focus on the quaternary evolution of the south-east African coastal plain. International union for quaternary research workshop abstracts. Council for Geoscience: Pretoria, South Africa, pp 21–26

Chugh CP (1985) Manual of drilling technology. Balkema, Rotterdam, p 567

Cumming JD, Wicklund AP (1980) Diamond drill handbook, 3rd edn. Smit, Toronto, p 547

Hartley JS (1994) Drilling: tools and programme management. Balkema, Rotterdam, p 150

Jones G, O'Brien V (2014) Aspects of resource estimation for mineral sands deposits. App Earth Sci 123(2):86–94

Oothoudt T (1999) The benefits of sonic core drilling to the mining industry. In: Tailing and mine waste '99: proceedings of the sixth international conference on tailings and mine waste '99, Fort Collins, Colorado, USA, 24–27 January, pp 3–12

Ware CI, Whitmore G (2007) Weathering of coastal dunes in northern KwaZulu-Natal, South Africa. J Coast Res 23(3):630–646

Appendices

Appendix 1: List of the Exercises and Electronic Files with the Solutions

Chapter	Section	Exercise reference number	Explanation	File
Chapter 9	9.2.2	9.2.2.a	Sampling tree experiment	Exercise 9.2.2.a.xls
Chapter 9	9.2.2	9.2.2.b	30 piece experiment	Exercise 9.2.2.b.xls
Chapter 9	9.2.3	9.2.3.a	Construct nomogram	Exercise 9.2.3.a.xls
Chapter 10	10.1.1	10.1.1.a	Statistical test of the standard samples	
Chapter 10	10.1.1	10.1.1.b	Statistical test of the standard samples	
Chapter 10	10.1.1	10.1.1.c	Statistical test of the standard samples	
Chapter 10	10.1.1	10.1.1.d	Statistical test of the standard samples	
Chapter 10	10.1.1	10.1.1.e	Statistical test of the standard samples	
Chapter 10	10.1.3	10.1.3.	Standard samples diagnostic diagram	Exercise 10.1.3.xls
Chapter 10	10.2.2	10.2.2.a	Thompson – Howarth test	Exercise 10.2.2.a.xls
Chapter 10	10.2.2	10.2.2.b	RMA diagram	Exercise 10.2.2.b-c-d.xls
Chapter 10	10.2.2	10.2.2.c	RDP diagram	Exercise 10.2.2.b-c-d.xls
Chapter 10	10.2.2	10.2.2.d	CV% method	Exercise 10.2.2.b-c-d.xls
Chapter 14	14.2.1	14.2.1	Contact profile	Exercise 14.2.1.ZIP
Chapter 14	14.3.1	14.3.1	Unfolding	Exercise 14.3.1.ZIP
Chapter 18	18.5.2	18.5.2	Linear model of coregionalisation	Exercise 18.5.2.xls
Chapter 22	22.3.2	22.3.2	LUC method	Exercise 22.3.2.ZIP

Appendix 2: Mathematical Background

Normal Distribution

Data distribution is called normal if probability density function (pdf) f(z) is determined as follows:

$$f(z) = \frac{1}{\sigma\sqrt{2\pi}} e^{-\frac{1}{2}\left(\frac{z-m}{\sigma}\right)^2}, \quad for -\infty < z < +\infty$$

Mean (m) and variance (s^2) of the normal distribution are determined as follows:

Electronic supplementary material The online version of this chapter (doi: 10.1007/978-3-319-39264-6) contains supplementary material, which is available to authorized users.

M. Abzalov, *Applied Mining Geology*, Modern Approaches in Solid Earth Sciences 12,
DOI 10.1007/978-3-319-39264-6

$$m = E(z) = \frac{1}{N}\sum_{i=1}^{N} z_i$$

$$\sigma^2 = Var(z) = E\left(z^2\right) - [E(z)]^2 = \frac{1}{N}\left(\sum_{i=1}^{N} z_i^2\right) - m^2$$

$$= \frac{1}{N}\sum_{i=1}^{N} (z_i - m)^2$$

A normal distribution with a zero mean (m = 0) and unit variance ($s^2 = 0$) represents a special case of a centred and standardised distribution which is usually called a Standard Gaussian distribution. Density function of such distribution is determined as follows:

$$f(z) = \frac{1}{\sqrt{2\pi}} e^{-\frac{1}{2}z^2},\ for -\infty < z < +\infty$$

Normally distributed variable can be easily converted to standard Gaussian variable by simple normalising of the (z) values applying the following formula:

$$Y = \frac{Z - m}{\sigma},$$

where (z) is a normally distributed variable with mean equal (m) and variance equal (σ^2) and the variable (Y), is a Standard Gaussian variable, with zero mean and unit variance.

Confidence Limits

Mean +/− 1.0 standard deviation (68.27 % probability)
Mean +/− 1.645 standard deviation (90 % probability)
Mean +/− 1.96 standard deviation (95 % probability)
Mean +/−2.0 standard deviation (95.45 % probability or 95 % if rounded for simplicity)
Mean +/− 2.57 standard deviation (99 % probability)
Mean +/− 3.0 standard deviation (99.73 %)

Lognormal Distribution

Lognormal distribution is encountered when a random variable is such, that it's natural logarithm [ln(z)] has a normal distribution.

The probability density function (pdf) f(z) is determined as follows:

$$f(z) = \frac{1}{\sigma\sqrt{2\pi}} z^{-1}\ e^{-\frac{1}{2}(\ln(z-\omega))^2/\beta^2},$$

$$for\ all\ z > 0,\ \beta > 0$$

Lognormally distributed variable (z) can be transformed to the Gaussian variable (y) with zero mean and unit variance through the following expression

$$z = e^{(\beta\ Y\ +\ \omega)}$$

Taking logarithms of the above expression leads to the following formula:

$$\ln(z) = \beta Y + \omega$$

In other words, lognormal random variable (z) is related to the Gaussian variable (y) through two constants (β and ω) this is why it is called a two-parameter lognormal variable.

The constants (β) and (ω) represent distribution parameters of Lognormally transformed data. In particular, (ω) is mean and (β^2) is variance of Lognormally transformed data

$$\omega = E[\ln(z)] = \frac{1}{N}\sum_{i=1}^{N} [\ln(z_i)]$$

$$\beta^2 = Var[\ln(z)] = \frac{1}{N}\sum_{i=1}^{N} [\ln(z_i) - \omega]^2$$

Mean (m) and variance (σ^2) of the lognormal distribution are determined as follows:

$$m = E(z) = e^{\left(\omega + \frac{\beta^2}{2}\right)}$$

$$\sigma^2 = Var(z) = e^{(2\omega + \beta^2)}\ \left(e^{\beta^2} - 1\right)$$

Important properties of the lognormal distribution are as follows:

$$E[\exp(aU)] = \exp\left(a^2/2\right),\ \text{where U} \sim (0, 1)$$

$$z = e^{\omega}\ e^{\beta Y} = m\ \exp\left(\beta Y - \beta^2/2\right)$$

$$Var(z) = m^2\ \left(e^{\beta^2} - 1\right)$$

$$E\left(z^2\right) = m^2\ \exp\left(\beta^2\right)$$

$$E\left(e^{\lambda Y} I_{y \geq y_C}\right) = e^{\lambda^2/2}\ [1 - G(y_C - \lambda)]$$

References

Abzalov MZ (1998) Chrome-spinels in gabbro-wehrlite intrusions of the Pechenga area, Kola Peninsula, Russia: emphasis on alteration features. Lithos 43(3):109–134

Abzalov MZ (1999) Gold deposits of the Russian North East (the Northern Circum Pacific): metallogenic overview. In: Proceedings of the PACRIM'99 symposium. AusIMM, Melbourne, pp 701–714

Abzalov MZ (2006) Localised Uniform Conditioning (LUC): a new approach for direct modelling of small blocks. Math Geol 38(4):393–411

Abzalov MZ (2007) Granitoid hosted Zarmitan gold deposit, Tian Shan belt, Uzbekistan. Econ Geol 102(3):519–532

Abzalov MZ (2008) Quality control of assay data: a review of procedures for measuring and monitoring precision and accuracy. Exp Min Geol J 17(3–4): 131–144

Abzalov MZ (2009) Use of twinned drill – holes in mineral resource estimation. Exp Min Geol J 18(1–4):13–23

Abzalov MZ (2010) Optimisation of ISL resource models by incorporating algorithms for quantification risks: geostatistical approach. In: Technical meeting on in situ leach (ISL) uranium mining, International Atomic Energy Agency (IAEA), Vienna, Austria, 7–10 June, 2010

Abzalov MZ (2011) Sampling errors and control of assay data quality in exploration and mining geology. In: Ivanov O (ed) Application and experience of quality control. InTECH, Vienna, pp 611–644

Abzalov MZ (2012) Sandstone hosted uranium deposits amenable for exploitation by in-situ leaching technologies. App Earth Sci 121(2):55–64

Abzalov MZ (2013) Measuring and modelling of the dry bulk density for estimation mineral resources. App Earth Sci 122(1):16–29

Abzalov MZ (2014a) Design principles of relational databases and management of dataflow for resource estimation. In: Mineral resource and ore reserves estimation, AusIMM Monograph 23, 2nd edn, Chap. 2: The resource database. AusIMM, Melbourne, pp 47–52

Abzalov MZ (2014b) Geostatistical criteria for choosing optimal ratio between quality and quantity of the samples: method and case studies. In: Mineral resource and ore reserves estimation, AusIMM Monograph 23, 2nd edn, Chap. 2: The resource database. AusIMM, Melbourne, pp 91–96

Abzalov MZ (2014c) Localised uniform conditioning: method and application case studies. J South Afr Inst Min Metall 114(1):1–6

Abzalov MZ, Allaboun H (2015) Bulk samples testing for metallurgical characterisation of surficial uranium mineralisation at the Central Jordan Uranium Project. App Earth Sci 124(2):129–134

Abzalov MZ, Both RA (1997) The Pechenga Ni-Cu deposits, Russia: data on PGE and Au distribution and sulphur isotope compositions. Min Petrol 61(1–4):119–143

Abzalov MZ, Bower J (2009) Optimisation of the drill grid at the Weipa bauxite deposit using conditional simulation. In: Seventh International Mining Geology Conference, AusIMM, Melbourne, pp 247–251

Abzalov MZ, Bower J (2014) Geology of bauxite deposits and their resource estimation practices. App Earth Sci 123(2):118–134

Abzalov MZ, Humphreys M (2002a) Resource estimation of structurally complex and discontinuous mineralisation using non-linear geostatistics: case study of a mesothermal gold deposit in northern Canada. Exp Min Geol J 11(1–4):19–29

Abzalov MZ, Humphreys M (2002b) Geostatistically assisted domaining of structurally complex mineralisation: method and case studies. Geostatistically assisted domaining of structurally complex mineralisation: method and case studies. In: The AusIMM 2002 Conference: 150 years of mining, Publication series No 6/02, pp 345–350

Abzalov MZ, Mazzoni P (2004) The use of conditional simulation to assess process risk associated with grade variability at the Corridor Sands detrital ilmenite deposit. In: Dimitrakopoulus R, Ramazan S (eds) Ore body modelling and strategic mine planning: uncertainty and risk management. AusIMM, Melbourne, pp 93–101

M. Abzalov, *Applied Mining Geology*, Modern Approaches in Solid Earth Sciences 12,
DOI 10.1007/978-3-319-39264-6

Abzalov MZ, Paulson O (2012) Uranium deposits of the Great Divide Basin, Wyoming, USA. App Earth Sci 121(2):76–83

Abzalov MZ, Pickers N (2005) Integrating different generations of assays using multivariate geostatistics: a case study. Trans Inst Min Metall 114:B23–B32

Abzalov MZ, Brewer TS, Polezhaeva LI (1997) Chemistry and distribution of accessory Ni, Co, Fe arsenic minerals in the Pechenga Ni-Cu deposits, Kola Peninsula, Russia. Miner Petrol 61(1–4):145–161

Abzalov MZ, Menzel B, Wlasenko M, Phillips J (2007) Grade control at the Yandi iron ore mine, Pilbara region, Western Australia: comparative study of the blastholes and RC holes sampling. In: Proceedings of the iron ore conference 2007. AusIMM, Melbourne, pp 37–43

Abzalov MZ, Menzel B, Wlasenko M, Phillips J (2010) Optimisation of the grade control procedures at the Yandi iron-ore mine, Western Australia: geostatistical approach. App Earth Sci 119(3):132–142

Abzalov MZ, Dumouchel J, Bourque Y, Hees F, Ware C (2011) Drilling techniques for estimation resources of the mineral sands deposits. In: Proceedings of the heavy minerals conference 2011. AusIMM, Melbourne, pp 27–39

Abzalov MZ, Drobov SR, Gorbatenko O, Vershkov AF, Bertoli O, Renard D, Beucher H (2014) Resource estimation of *in-situ* leach uranium projects. App Earth Sci 123(2):71–85

Abzalov MZ, van der Heyden A, Saymeh A, Abuqudaira M (2015) Geology and metallogeny of Jordanian uranium deposits. App Earth Sci 124(2):63–77

Annels AE (1991) Mineral deposit evaluation, a practical approach. Chapman and Hall, London, p 436

Annels AE, Hellewell EG (1988) The orientation of bedding, veins and joints in core: a new method and case history. Int J Min Geol Eng 5(3):307–320

Arik A (1999) An alternative approach to resource classification. In: Proceedings of the 1999 Computer Applications in the Mineral Industries (APCOM) symposium. Colorado School of Mines, Colorado, pp 45–53

Armstrong M (1984) Improving the estimation and modelling of the variogram. In: Verly G et al (eds) Geostatistics for natural resources characterisation, part 1. Reidel, Dordrecht, pp 1–19

Armstrong M (1998) Basic linear geostatistics. Springer, Berlin, p 153

Armstrong M, Champigny N (1989) A study on kriging small blocks. CIM Bull 82(923):128–133

Armstrong M, Galli A, Beucher H, Le Loc'h G, Renard D, Doligez B, Eschard R, Geffroy F (2011) Plurigaussian simulation in geosciences, 2nd edn. Springer, Berlin, p 149

AS1289.5.3.1 (2004) Australian standard, methods of testing soils for engineering purposes. Method 5.3.1: soils compaction and density tests – determination of the field density of a soil – sand replacement method using a sand-cone pouring apparatus. Standards Australia International, Sydney, Australia, p 12

AS2891.9.1 (2005) Australian standard, methods of sampling and testing asphalt. Method 9.1: determination of bulk density of compacted asphalt – waxing procedure. Standards Australia International, Sydney, Australia, p 8

Atkinson KB (1996) Close range photogrammetry and machine vision. Whittles, Latheronwheel, p 384

Bardossy G, Aleva GJ (1990) Lateritic bauxites: developments in economic geology 27. Elsevier, Amsterdam

Barnes R (1991) The variogram sill and the sample variance. Math Geol 23(4):673–678

Barnes R, Johnson T (1984) Positive kriging. In: Verly G, David M, Journel AG, Marechal A (eds) Geostatistics for natural resources characterisation, vol 1. Reidel, Dordrecht, pp 231–244

Bartlett HE, Viljoen R (2002) Variance relationships between masses, grades, and particle sizes for gold ores from Witwatersrand. J South Afr Inst Min Metall 102(8):491–500

Barton N, Lien R, Lunde J (1974) Engineering classification of rock masses for the design of tunnel support, Rock mechanics. Mathisen & Halvorsen, Oslo, pp 189–236

Bevan PA (1994) The weighing of assays and the importance of both grade and specific gravity. CIM Bull 86(970):88–90

Bieniawski ZT (1973) Engineering classification of jointed rock masses. Trans S Afr Inst Civ Eng 15(12):335–344

Bieniawski ZT (1993) Classification of rock mass for engineering: the RMR system and future trends. In: Hudson J (ed) Comprehensive rock engineering, vol 3. Pergamon, Oxford, pp 553–573

Birch JC (2006) Using 3 DM analyst mine mapping suite for rock face characterisation. In: Tonon E, Kottenstette J (eds) Laser and photogrammetric methods for rock face characterisation. Colorado School of Mines, Golden, Colorado

Blackwell G (1998) Relative kriging error – a basis for mineral resource classification. Exp Min Geol 7(1–2):99–105

Blackwell GH (2000) Open pit mine planning with simulated gold grades. CIM Bull 93:31–37

Bleines C, Bourges M, Deraisme J, Geffroy F, Jeanne N, Lemarchand O, Perseval S, Poisson J, Rambert F, Renard D, Touffait Y, Wagner L (2013) ISATIS software. Geovariances, Ecole des Mines de Paris, Paris

Botha GA (1997) The Maputaland group: a provisional lithostratigraphy for coastal KwaZulu-Natal. In: Maputaland focus on the quaternary evolution of the south-east African coastal plain. International Union for Quaternary Research Workshop abstracts. Council for Geoscience, Pretoria, pp 21–26

Brady BHG, Brown ET (2004) Rock mechanics for underground mining. Kluwer Academic Publishing, New York, p 628

Bumstead ED (1984) Some comments on the precision and accuracy of gold analysis in exploration. Proc AusIMM 289:71–78

Bush PD (2000) Development considerations for the Honeymoon ISL uranium project. CIM Bull 93(1045):65–73

Butt CRM, Lintern MG, Anand RR (2000) Evolution of regolith and landscapes in deeply weathered terrain – implications for geochemical exploration. Ore Geol Rev 16:167–183

Buxton BE (1984) Estimation variance of global recoverable reserve estimates. In: Verly G et al (eds) Geostatistics for natural resources characterisation, part 1. Reidel, Dordrecht, pp 165–183

CANMET (1998) Assessment of laboratory performance with certified reference materials. CANMET Canadian Certified Reference Materials Project Bulletin, p 5

Chauvet P (1982) The variogram cloud. 17th APCOM symposium, pp 757–764

Chiles JP (1988) Fractals and geostatistical methods for modelling of a fracture network. Math Geol 20(6):631–654

Chiles JP, Delfiner P (1999) Geostatistics: modelling spatial uncertainty. Wiley, New York, p 695

Chu J (1993) XGAM: A 3D interactive graphic software for modelling variograms and cross variograms under conditions of positive definiteness. In: Stanford Centre for Reservoir Forecasting, report 6, Stanford, California

Chugh CP (1985) Manual of drilling technology. Balkema, Rotterdam, p 567

Codd EF (1990) The relational model for database management, 2nd edn. Addison – Wesley Longman, Boston, p 567

Coward S, Vann J, Dunham S, Stewart M (2009) The primary-response framework for geometallurgical variables. In: Dominy S (ed) Proceedings – seventh international mining geology conference 2009. AusIMM, Melbourne, pp 109–113

Cressie N (1990) The origin of kriging. Math Geol 22(3):239–252

Cumming JD, Wicklund AP (1980) Diamond drill handbook, 3rd edn. Smit, Toronto, p 547

Dagbert M (2001) Comments on "The estimation of mineralised veins: a comparative study of direct and indirect approaches", by D. Marcotte and A. Boucher. Exp Min Geol J 10(3):243–244

Dahlkamp FJ (1993) Geology of the uranium deposits. Springer, Berlin, p 460

David M (1972) Grade-tonnage curve: use and misuse in ore-reserve estimation. Trans Inst Min Metall 81:A129–A132

David M (1977) Geostatistical ore reserve estimation. Elsevier, Amsterdam, p 364

David M (1988) Handbook of applied advanced geostatistical ore reserve estimation. Elsevier, Amsterdam, p 364

Davis BM (1987) Uses and abuses of cross-validation in geostatistics. Math Geol 19(3):241–248

Davis B (1992) Confidence interval estimation for minable reserves. SME preprint 92–39, p 7

Davis JC (2002) Statistics and data analysis in geology, 3rd edn. Wiley, New York, p 638

De Castilho MV, Mazzoni PKM, Francois-Bongarcon D (2005) Calibration of parameters for estimating sampling variance. In: Proceedings – Second World Conference on Sampling and Blending. AusIMM, Melbourne, pp 3–8

Deere DU (1964) Technical description of rock cores for engineering purposes. Rock Mech Rock Eng 1(1):17–22

Deere DU (1968) Geological considerations. In: Stagg KG, Zienkiewicz OC (eds) Rock mechanics in engineering practice. Wiley, London, pp 1–20

Demange C, Lajaunie C, Lantuejoul C, Rivoirard J (1987) Global recoverable reserves: testing various changes of support models on uranium data. In: Armstrong M, Matheron G (eds) Geostatistical case studies. Reidel, Dordrecht, pp 187–208

Deutsch CV, Journel AG (1998) GSLIB: geostatistical software library and user's guide. Oxford University Press, New York, p 340

Dielhl P, David M (1982) Classification of ore reserves/resources based on geostatistical methods. CIM Bull 75(838):127–135

Dimitrakopoulos R (2002) Orebody uncertainty, risk assessment and profitability in recoverable reserves, ore selection and mine planning: Workshop course. BRC, The University of Queensland, p 304

Dominy SC, Annels AE, Johansen GF, Cuffley BW (2000) General considerations of sampling and assaying in a coarse gold environment. Trans Inst Min Metall 109:B145–B167

Eggington HF (ed) (1985) Australian drillers guide, 2nd edn. Australian Drilling Industry Training Committee Ltd, Sydney, p 572

Eremeev AN, Ostroumov GV, Anosov VV, Berenshtein LE, Korolev VP, Samonov IZ (1982) Instruction on internal, external and arbitrary quality control of the exploration samples assayed in the laboratories of the Ministry of Geology of the USSR. VIMS, Moscow, p 106 (in Russian)

Eremin RA, Voroshin SV, Sidorov VA, Shakhtyrov VG, Pristavko VA (1994) Geology and genesis of the Natalka gold deposit, Northeast Russia. Int Geol Rev 36:1113–1138

Ferenczi PA (2001) Iron ore, manganese and bauxite deposits of the Northern Territory. Northern Territory Geological Survey Report 13. Darwin, Government Printer of the Northern Territory, p 113

Francois-Bongarcon D (1991) Geostatistical determination of sample variance in the sampling of broken ore. CIM Bull 84(950):46–57

Francois-Bongarcon D (1993) The practise of the sampling theory of broken ore. CIM Bull 86(970): 75–81

Francois-Bongarcon D (1998) Error variance information from paired data: application to sampling theory. Exp Min Geol J 7(1–2):161–165

Francois-Bongarcon D (2005) Modelling of the liberation factor and its calibration. In: Proceedings second world conference on sampling and blending. AusIMM, Melbourne, pp 11–13

Francois-Bongarcon D, Gy P (2001) The most common error in applying 'Gy's formula' in the theory of mineral sampling, and the history of the liberation factor. In: Edwards A (ed) Mineral resources and ore reserve estimation – the AusIMM guide to good practise. AusIMM, Melbourne, pp 67–72

Garrett RG (1969) The determination of sampling and analytical errors in exploration geochemistry. Econ Geol 64(5):568–569

Gilfillan JF (1998) Testing the data—the role of technical due diligence. In: Ore reserves and finance seminar, Sydney, 15 June, 1998. AusIMM, Melbourne, pp 33–42

Goldfarb RJ, Groves DI, Gardoll S (2001) Orogenic gold deposits and geological time: a global synthesis. Ore Geol Rev 18(1):1–7

Goovaerts P (1997) Geostatistics for natural resources evaluation. Oxford University Press, New York, p 483

Goulard M (1989) Inference in a coregionalization model. In: Armstrong M (ed) Geostatistics, vol 1. Kluwer, Dordrecht, pp 397–408

Goulard M, Voltz M (1992) Linear coregionalization model: tools for estimation and choice of cross-variogram matrix. Math Geol 24(3):269–286

Grimstad E, Barton N (1993) Updating the Q-system for NMT. In: Kompen R, Opsahl OA, Berg KR (eds) Proceedings International conference sprayed concrete – modern use of wet mix sprayed concrete for underground support. Norwegian Concrete Association, Oslo, pp 46–66

Grubb PLC (1979) Genesis of bauxite deposits in the lower Amazon basin and Guianas coastal plain. Econ Geol 74(4):735–750

Guibal D (2001) Variography, a tool for the resource geologist. In: Edwards AC (ed) Mineral resource and ore reserve estimation – the AusIMM guide to good practice. AusIMM, Melbourne, pp 85–90

Gy P (1979) Sampling of particulate materials, theory and practice, Developments in Geomathematics 4. Elsevier, Amsterdam, p 431

Hamrin H (1982) Choosing an underground mining method. In: Hustrulid WA (ed) Underground mining methods handbook. AIME, New York, pp 88–112

Hamrin H (2001) Underground mining methods and applications. In: Hustrulid WA, Bullock RL (eds) Underground mining methods: engineering fundamentals and international case studies. Society for Mining Metallurgy and Exploration, Littleton, Colorado, pp 3–14

Harmsworth RA, Kneeshaw M, Morris RC, Robinson CJ, Shrivastava PK (2001) BIF-derived iron ores of the Hamersley Province. In: Hughes FE (ed) Geology of the mineral deposits of Australia and Papua New Guinea. AusIMM, Melbourne, pp 617–642

Hartley JS (1994) Drilling: tools and programme management. Balkema, Rotterdam, p 150

Heald P, Foley NK, Hayba DO (1987) Comparative anatomy of volcanic hosted epithermal deposits: acid-sulphate and adularia-sericite type. Econ Geol 82(1):1–26

Hoffman EL, Clark JR, Yeager JR (1998) Gold analysis – fire assays and alternative methods. Exp Min Geol J 7(1–2):155–160

Howarth R, Thompson M (1976) Duplicate analysis in geochemical practice: part 2, examination of proposed method and examples of its use. Analyst 101:699–709

Hudson JA, Harrison JP (1997) Engineering rock mechanics. An introduction to the principles. Pergamon, Amsterdam, p 444

IAEA (2001) Manual of acid in situ leach uranium technology, TECDOC-1239. International Atomic Energy Agency, Vienna, p 283

Isaaks EH, Srivastava RM (1989) An introduction to applied geostatistics. Oxford University Press, New York, p 561

ISO Guide 33 (1989) Uses of certified reference materials. Standards Council of Canada, p 12

Jones G, O'Brien V (2014) Aspects of resource estimation for mineral sands deposits. App Earth Sci 123(2): 86–94

JORC Code (2012) Australaisian code for reporting of exploration results, mineral resources and ore reserves. AusIMM, Melbourne, p 44

Journel AG (1974) Geostatistics for conditional simulation of ore bodies. Econ Geol 69(5):673–687

Journel AG (1983) Non-parametric estimation of spatial distribution. Math Geol 15(3):445–468

Journel AG, Huijbregts CJ (1978) Mining geostatistics. Academic, New York, p 600

Journel AG, Isaaks EH (1984) Conditional indicator simulation: application to a Saskatchewan uranium deposit. Math Geol 16(7):685–718

Journel AG, Rao SE (1996) Deriving conditional distributions from ordinary kriging. In: Report 9, Stanford Center for Reservoir Forecasting, Stanford, CA

Kane JS (1992) Reference samples for use in analytical geochemistry: their availability preparation and appropriate use. J Geochem Exp 44:37–63

Karimov KK, Bobonorov NS, Brovin KG, Goldshtein RI, Korsakov YF, Mazurkevich AP, Natalchenko BI, Tolstov EA, Shmariovich EP (1996) Uranium deposits of the Uchkuduk type in the Republic of Uzbekistan. FAN, Tashkent, p 335 (in Russian)

Kemeny J, Mofya E, Handy J (2003) The use of digital imaging and laser scanning technologies for field rock fracture characterisation. In: Culligan J, Einstein H, White A (eds) Proceedings of soil and rock America 2003 – 12th Pan American conference on soil mechanics and geotechnical engineering and the 39th US rock mechanics symposium. Massachusetts Institute of Technology, Cambridge, pp 117–122

Kemeny J, Turner K, Norton B (2006) LIDAR for rock mass characterisation: hardware, software, accuracy and best practices. In: Tonon F, Kottenstette J (eds) Laser and photogrammetric methods for rock face characterisation. Colorado School of Mines, Golden, Colorado

Krige D (1951) A statistical approach to some basic mine valuation problems on the Witwatersrand. J Chem Metall Min Soc S Afr 52:119–139

Krige D (1996) A practical analysis of the effects of spatial structure and of data available and accessed, on conditional biases in ordinary kriging. In: Geostatistics, Wollongong'96, v2, pp 799–810

Lane KF (2015) The economic definition of ore. Cut-off grade in theory and practice, 4th edn. Comet strategy, Brisbane, p 147

Lantuejoul C (1988) On the importance of choosing a change of support model for global reserves estimation. Math Geol 20(8):1001–1019

Lantuejoul C (2002) Geostatistical simulation: models and algorithms. Springer, Berlin, p 250

Lawrence MJ (1997) Behind Busang, the Bre-X scandal: could it happen in Australia? Aus J Min 12(134):33–50

Leaver ME, Sketchley DA, Bowman WS (1997) The benefits of the use of CCRMP's custom reference materials. Canadian Certified Reference Materials Project. In: Society of Mineral Analysts Conference. MSL No 637, p 16

Lewis RW (2001) Resource database: now and in the future. In: Edwards AC (ed) Mineral resource and ore reserve estimation – the AusIMM guide to good practice. AusIMM, Melbourne, pp 43–48

Lillehagen NB (1979) The estimation and mining of Gove bauxite reserves. In: Estimation and statement of mineral reserves. AusIMM Sydney branch, Sydney, pp 19–32

Lipton IT (2001) Measurement of bulk density for resource estimation. In: Edwards AC (ed) Mineral resource and ore reserve estimation – the AusIMM guide to good practice. AusIMM, Melbourne, pp 57–66

Long S (1998) Practical quality control procedures in mineral inventory estimation. Exp Min Geol 7(1–2):117–127

Magri EJ, McKenna P (1986) A geostatistical study of diamond-saw sampling versus chip sampling. J South Afr Inst Min Metall 86(8):335–347

Marcotte D, Boucher A (2001) The estimation of mineralised veins: a comparative study of direct and indirect approaches. Exp Min Geol 10(3):235–242

Marechal A (1984) Recovery estimation: a review of models and methods. In: Verly G (ed) Geostatistics for natural resources characterisation, part 1. Reidel, Dordrecht, pp 385–420

Marjoribanks RW (2007) Structural logging of drill core, Handbook 5. Australian Institute of Geoscientists, Perth, p 68

Matheron G (1963) Principles of geostatistics. Econ Geol 58(8):1246–1266

Matheron G (1968) Osnovy prikladnoi geostatistiki (Basics of applied geostatistics). Mir, Moscow, p 408 (in Russian)

McGlone C (ed) (2004) Manual of photogrammetry, 5th edn. American Society for Photogrammetry and Remote Sensing, p 1168

McKay AD, Stoker P, Bampton KF, Lambert IB (2007) Resource estimation for *in-situ* leach uranium projects and reporting under the JORC Code. In: Uranium reporting workshop, Uranium and the JORC Code. AusIMM, Adelaide Branch, Adelaide

Milesi J-P, Lendru P, Feybesse J-L, Dommanget A, Marcoux E (1992) Early proterozoic ore deposits and tectonics of the Birimian orogenic belt, West Africa. Precambrian Res 58:305–344

Minkkinen P, Paakkunainen M (2005) Direct estimation of sampling variance from time series measurements – comparison to variographic analysis. In: Proceedings – second world conference on sampling and blending, AusIMM, Melbourne, pp 39–44

Minnitt RCA, Rice PM, Spangenberg C (2007) Part 2: experimental calibration of sampling parameters K and alfa for Gy's formula by the sampling tree method. J South Afr Min Metall 107: 513–518

Morris RC, Kneeshaw M (2011) Genesis modelling for the Hamersley BIF-hosted iron ores of Western Australia: a critical review. Aust J Earth Sci 58: 417–451

Nordin W (2009) The effect of downhole survey uncertainty on modelled volume. In: 7th international mining geology conference. AusIMM, Melbourne, pp 81–84

Olea RA (ed) (1991) Geostatistical glossary and multilingual dictionary. Oxford University Press, New York, p 177

Oothoudt T (1999) The benefits of sonic core drilling to the mining industry. In: Tailing and mine waste'99: Proceedings of the sixth international conference on tailings and mine waste'99, Fort Collins, Colorado, USA, 24–27 January, pp 3–12

Pan G (1995) Practical issues of geostatistical reserve estimation in the mining industry. CIM Bull 88:31–37

Penney R (2012) Australian sandstone-hosted uranium deposits. App Earth Sci 121(2):65–75

Penney R, Ames C, Quinn D, Ross A (2012) Determining uranium concentration in boreholes using wireline logging techniques: comparison of gamma logging with prompt fission neutron technology (PFN). App Earth Sci 121(2):55–64

Peters WC (1987) Exploration and mining geology, 2nd edn. Wiley, New York, p 706

Petrov NN, Berikbolov BR, Aubakirov KB, Vershkov AF, Lukhtin VF, Plekhanov VN, Cherniakov VM, Yazikov VG (2008) Uranium deposits of Kazakhstan (exogenic), 2nd edn. Volkovgeologiia, Almaty, p 318 (in Russian)

Pevely S (2001) Ore reserve, grade control and mine/mill reconciliation practices at McArthur River mine, NT. In: Edwards AC (ed) Mineral resource and ore reserves estimation – the AusIMM guide to good practice. AusIMM, Melbourne, pp 567–578

Phillips GN, Hughes MJ (1996) The geology and gold deposits of the Victorian gold province. Ore Geol Rev 11:255–302

Pitard FF (1993) Pierre Gy's sampling theory and sampling practise, 2nd edn. CRC Press, New York, p 488

Pitard FF (1998) A strategy to minimise ore grade reconciliation problems between the mine and the mill. In: Mine to mill. AusIMM, Melbourne, pp 77–82

Pitard FF (2005) Sampling correctness – comprehensive guidelines. In: Proceedings – second world conference on sampling and blending, AusIMM, Melbourne, pp 55–66

Poboline FF (2005) 3D laser scanner hardware and software surveys. http://www.poboline.com/FILES/HTML/ProductSurveys/

Pool TC, Wallis CS (2006a) Technical report on the South Inkai uranium project, Kazakhstan. Prepared for Urasia Energy (BVI) Ltd. Roscoe Postle Associates Inc, Toronto, Canada

Pool TC, Wallis CS (2006b) Technical report on the Akdala uranium mine, Kazakhstan. Prepared for Urasia Energy (BVI) Ltd. Roscoe Postle Associates Inc, Toronto, Canada

Pool TC, Wallis CS (2006c) Technical report on the North Kharasan uranium project, Kazakhstan. Prepared for Urasia Energy (BVI) Ltd. Roscoe Postle Associates Inc, Toronto, Canada

Preston KB, Sanders RH (1993) Estimating the *in situ* relative density of coal. In: Australian coal geology, vol 9. AusIMM, Melbourne, pp 22–26

Priest SD, Hudson JA (1981) Estimation of discontinuity spacing and trace length using scanline surveys. Int J Rock Mech Min Sci Geomech Abstr 18(3): 183–197

Ramanaidou ER, Morris RC, Horwitz RC (2003) Channel iron deposits of the Hamersley Province, Western Australia. Aus J Earth Sci 50:669–690

Richmond A, Shaw WJ (2009) Geometallurgical modelling – Quo Vadis. In: Dominy S (ed) Proceedings – seventh international mining geology conference 2009. AusIMM, Melbourne, pp 115–118

Rivoirard J (1987) Two key parameters when choosing the kriging neighborhood. Math Geol 19(8): 851–856

Rivoirard J (1994) Introduction to disjunctive kriging and non-linear geostatistics. Oxford Press, Claredon, p 181

Rivoirard J (2001) Which models for collocated cokriging? Math Geol 33:117–131

Rivoirard J (2002) On the structural link between variables in kriging with external drift. Math Geol 34:797–808

Roden S, Smith T (2001) Sampling and analysis protocols and their role in mineral exploration and new resource development. In: Edwards A (ed) Mineral resources and ore reserve estimation – the AusIMM guide to good practise. AusIMM, Melbourne, pp 73–78

Rossi ME, Camacho JE (2004) Application of conditional simulation to resource classification scheme. CIM Bull 97(1079):62–68

Rossi ME, Deutsch CV (2014) Mineral resource estimation. Springer, Berlin, p 332

Rossi ME, Parker HM (1994) Estimating recoverable reserves: is it hopeless? In: Dimitrakopoulos R (ed) Geostatistics for the next century. Kluwer, Dordrecht, pp 259–276

Royle AG (1977) How to use geostatistics for ore reserve classification. World Min (February):52–56

Schaap AD (1990) Weipa kaolin and bauxite deposits. In: Hughes FE (ed) Geology of the mineral deposits of Australia and Papua New Guinea. AusIMM, Melbourne, pp 1669–1673

Schofield NA (2001a) Determining optimal drilling densities for near mine resources. In: Edwards AC (ed) Mineral resource and ore reserves estimation – the AusIMM guide to good practice. AusIMM, Melbourne, pp 293–298

Schofield NA (2001b) The myth of mine reconciliation. In: Edwards AC (ed) Mineral resource and ore reserves estimation – the AusIMM guide to good practice. AusIMM, Melbourne, pp 601–610

Schwann BB (1987) The application of Ditch Witch sampling in oxidized open cut gold mines. In: Equipment in minerals industry, Proceedings of exploration, mining and processing conference. AusIMM, Kalgoorlie Branch, Kalgoorlie, Australia, pp 25–31

Shaw WJ (1997) Validation of sampling and assaying quality for bankable feasibility studies. In: The resource database towards 2000. AusIMM Illawara Branch, Wollongong, pp 69–79

Sinclair AJ, Bentzen A (1998) Evaluation of errors in paired analytical data by a linear model. Exp Min Geol 7(1–2):167–173

Sinclair AJ, Blackwell GH (2000) Resource/reserve classification and the qualified person. CIM Bull 93(1038):29–35

Sinclair AJ, Blackwell GH (2002) Applied mineral inventory estimation. Cambridge University Press, Cambridge, p 381

Sketchley DA (1998) Gold deposits: establishing sampling protocols and monitoring quality control. Exp Min Geol 7(1–2):129–138

Snowden DV (2001) Practical interpretation of mineral resource and ore reserve classification guidelines. In: Edwards AC (ed) Mineral resource and ore reserve estimation – the AusIMM guide to good practice. AusIMM, Melbourne, pp 643–652

Sommerville B, Boyle C, Brajkovich N, Savory P, Latscha AA (2014) Mineral resource estimation of the Brockman 4 iron ore deposit in the Pilbara region. App Earth Sci 123(2):135–145

Srivastava RM (2005) Probabilistic modelling of ore lens geometry: an alternative to deterministic wireframes. Math Geol 37(5):513–544

Stanley CR (2006) On the special application of Thompson-Howarth error analysis to geochemical variables exhibiting a nugget effect. Geochem: Explor Environ Anal 6:357–368

Stanley CR, Lawie D (2007a) Average relative error in geochemical determinations: clarification, calculation and a plea for consistency. Exp Min Geol 16:265–274

Stanley CR, Lawie D (2007b) Thompson-Howarth error analysis: unbiased alternatives to the large-sample method for assessing non-normally distributed measurement error in geochemical samples. Geochem: Explor Environ Anal 7:1–10

Stegman CL (2001) How domain envelopes impact on the resource estimate – case studies from the Cobar Gold Filed, NSW, Australia. In: Edwards AC (ed) Mineral resource and ore reserves estimation – the AusIMM

guide to good practice. AusIMM, Melbourne, pp 221–236
Strebelle S (2002) Conditional simulation of complex geological structures using multiple-point statistics. Math Geol 34(1):1–22
Taylor JK (1987) Quality assurance of chemical measurements. Lewis Publishers, Michigan, p 135
Thomas A, Johnson K, MacGeehan PJ (1990) Norseman gold deposits. In: Hughes FE (ed) Geology of the mineral deposits of Australia and Papua New Guinea. AusIMM, Melbourne, pp 493–504
Thompson M, Howarth R (1973) The rapid estimation and control of precision by duplicate determinations. Analyst 98(1164):153–160
Thompson M, Howarth R (1976) Duplicate analysis in geochemical practice: part 1. Theoretical approach and estimation of analytical reproducibility. Analyst 101:690–698
Thompson M, Howarth R (1978) A new approach to the estimation of analytical precision. J Geochem Exp 9(1):23–30
Tukey JW (1977) Exploratory data analysis. Addison – Wesley Longman, Boston, p 688
Vallee M (1998) Quality assurance, continuous quality improvement and standards. Exp Min Geol 7(1–2):1–15
Vallee M, David M, Dagbert M, Desrochers C (1992) Guide to the evaluation of gold deposits: Geological society of CIM, Special volume 45, p 299
Vutukuri VS, Lama RD, Saluja SS (1974) Handbook on mechanical properties of rocks: series on rock and soil mechanics, v2, n1. Trans Tech Publication, Bay Village, Ohio, USA, p 280
Wackernagel H (2003) Multivariate geostatistics: an introduction with applications, 3rd edn. Springer, Berlin, p 388
Ware CI, Whitmore G (2007) Weathering of coastal dunes in northern KwaZulu-Natal, South Africa. J Coast Res 23(3):630–646
Wellmer F-W (1989) Economic evaluations in exploration. Springer, Berlin, p 163
Zimmer PW (1963) Orientation of small diameter core. Econ Geol 58(8):1313–1325

Index

M. Abzalov, *Applied Mining Geology*, Modern Approaches in Solid Earth Sciences 12,
DOI 10.1007/978-3-319-39264-6